METHODS IN MOLECULAR MEDICINE™

# Prostate Cancer Methods and Protocols

Edited by

Pamela J. Russell
Paul Jackson
Elizabeth A. Kingsley

HUMANA PRESS

# 1

# Epidemiological Investigation of Prostate Cancer

**Graham G. Giles**

## 1. Introduction

Prostate cancer is the most common male cancer diagnosed in Western populations. Autopsy studies have shown that with increasing age, the majority of men will develop microscopic foci of cancer (often termed "latent" prostate cancer) and that this is true in populations that are at both high and low risk for the invasive form of the disease ***(1)***. However, only a small percentage of men will develop invasive prostate cancer. The prevalence of prostate cancer is, thus, very common; but to most men, prostate cancer will be only incidental to their health and death.

Although much progress has been made in recent years in identifying risk factors for prostate cancer, much more epidemiological research needs to be conducted combining molecular biology and genetics in population studies. We still need to answer the question, *what causes a minority of the common microscopic prostate cancers to grow and spread?* ***(2)***. Until we have this answer, we can do nothing to prevent life-threatening prostate cancer from occurring, and many men will continue to be treated for prostate cancer, perhaps unnecessarily.

A major problem with past epidemiological studies of prostate cancer has been a lack of disease specificity—most epidemiological studies combine all diagnoses of prostate cancer as if they are the same disease. Given the low metastatic and lethal potential of most prostate cancers, the arbitrary grouping of all prostate cancers is destined to produce weak and inconsistent findings, and such has been the history of prostate cancer epidemiology ***(2)***. Since the 1990s, the problem of disease specificity has worsened with the advent of prostate-specific antigen (PSA) testing and the detection of thousands of prostate cancers, many of which probably would never have manifested as

From: *Methods in Molecular Medicine, Vol. 81: Prostate Cancer Methods and Protocols*
Edited by: P. J. Russell, P. Jackson, and E. A. Kingsley © Humana Press Inc., Totowa, NJ

invasive prostate cancer *(3)*. Therefore, it is essential that future epidemiological studies take this biological and diagnostic heterogeneity into account and attempt to stratify analyses of prostate tumors based on biomarkers and relevant aspects of clinical presentation.

### 1.1. Epidemiological Methods

Epidemiology is the science that deals with the distribution, occurrence, and determinants of disease in populations. The first two items require some form of monitoring mechanism, such as a cancer or death registry that provides population-based incidence and mortality data. Data that are obtained from these sources are commonly used to give group information, e.g., to estimate the community burden of prostate cancer and to describe its trends over time and by age, region, race, occupation, and so on. Population-based time trends in incidence and mortality rates can be used to evaluate interventions focused on prevention, early detection, or treatment. In regard to prostate cancer, there have been huge increases in incidence in Australia and elsewhere *(3)* because of early detection. Whether this trend will eventually impact on mortality rates is unclear.

To investigate the determinants of a disease, such as prostate cancer, requires the collection of detailed risk exposure data at the level of the individual so that comparisons can be drawn between men who have prostate cancer and those who do not. There are two principal research designs: the case-control study and the cohort study; a comprehensive treatment of these designs can be obtained from the standard references of Breslow and Day *(4,5)*. Briefly, case-control studies start by selecting a series of affected case subjects and a series of unaffected control subjects, commonly a few hundred cases and age-matched controls. All subjects are then interviewed in regard to past exposures to particular risk factors.

The selection of appropriate controls is one of the most difficult aspects of this design. Theoretically, cases and controls should be sampled from the same population base. It follows, therefore, that if cases have been ascertained from a population-based cancer registry, controls need to be sampled from the same population that gave rise to the cases. Comprehensive registers of the general population for this purpose often do not exist or are not accessible to researchers. Various alternative methods of control sampling are available, including random household surveys (similar to a census) and random-digit dialing. Although imperfect, the Electoral Register has been used to select controls for studies in Australia, and in this instance, cases have to be limited to subjects enrolled on the Register to use the same reference population.

Because of their retrospective nature and the fact that affected subjects may be more interested in the research and respond more carefully to questions than

would unaffected controls, case-control studies are prone to bias. The estimate of risk obtained from a case-control study is the odds ratio (OR), and ORs of up to 2 or more can be produced by biases in the study. The value of case-control studies is that they are relatively cheap and quick especially for rare outcomes. They are of most use when estimating fairly substantive risks (ORs > 4), where obvious confounding variables, such as smoking, are well controlled.

Cohort studies, on the other hand, start by recruiting large numbers (tens to hundreds of thousands) of unaffected subjects and measuring individual exposures to various risk factors before disease occurrence. The cohort is then observed over time and when sufficient diagnoses have been made, the incidence of the disease in the exposed group is compared with the incidence of disease in the unexposed group. This comparison yields a relative risk (RR), which is approximated by the OR estimates from case-control studies. Because of its prospective design, the cohort study is less prone to biases than a case-control study. However, their large size and their requirement for lengthy follow-up make them very expensive compared with case-control studies. Cohort studies are particularly useful for estimating unbiased risks of moderate size (RRs < 4). They are also useful with respect to exposures that are difficult to recall or for those that require data or substrates to be collected before disease occurrence. For example, most modern cohorts include the collection of biospecimens, particularly blood, at the time of recruitment.

Ultimately, the risk factors identified from case-control and cohort designs need to be confirmed before expensive public health interventions are initiated. Interventions should usually be tested in randomized controlled trials similarly to those used for clinical trials of new pharmaceutical products or a new screening test. Intervention trials are like cohort studies. In a simple intervention, eligible subjects are randomized to receive either the active intervention or a placebo and, after sufficient time has elapsed, the incidence of the endpoint is compared between the two groups.

In critically appraising epidemiological literature, it is important to keep the study design in mind. Generally speaking, intervention trials give better evidence than cohort studies that, in turn, give better evidence than case-control studies. It is equally important, however, to examine whether the findings from a variety of studies are consistent. Often the quality of individual studies must also be taken into account. With respect to case-control studies, questions that need to be addressed include the following: was the case series adequately described, was the control selection appropriate, was the sample size adequate to detect the desired effect, were the response rates adequate, were the exposures measured accurately, was the analysis appropriate, e.g., were the known confounders controlled for? With respect to cohort studies, an additional question to be asked concerns the degree of loss to follow-up.

Ultimately, the principal outcome of interest is an estimate of risk. The most important aspects of this estimate are its size and its confidence interval. An OR or RR of 10 or more after adjusting for other factors is a strong risk, especially if it has a narrow 95% confidence interval. A risk of this size is likely to be involved in a causal pathway, especially if a dose–response relationship can also be demonstrated. Risk estimates less than 2 are weak and may result from uncontrolled confounding or bias, especially in case-control studies. Estimates between these extremes require careful interpretation and replication in other studies. Risk estimates can often be attenuated by poor exposure measurement, and an observed OR of 4 may reflect an underlying risk of far greater magnitude. This becomes a substantive problem in nutritional epidemiology, where the measurement of dietary intake is known to be poor. In studies of genetic polymorphisms and dietary variables, for example, although the polymorphism can be measured accurately, the observed association between polymorphism status and a given diet variable will be attenuated because of the error associated with dietary measurement.

## 2. Trends

Prostate cancer is one of the most age-dependent cancers—rare before the age of 50, it increases at an exponential rate thereafter. As in many other Western industrialized countries, prostate cancer is the most common male cancer diagnosed in Australia. In 1997, there were 9725 diagnoses and 2449 deaths. The age-standardized incidence rate (adjusted to the world standard population) was 74.5 per 100,000, and the death rate was 16.5 per 100,000 ***(6)***. The age-standardized incidence rate per 100,000 in Australia was in the low 40s during the late 1980s. As in many other parts of the world, including the United States, the incidence of prostate cancer in Australia has increased dramatically in the last decade of the twentieth century as a result of widespread testing with PSA. Rates are now declining from a peak reached in 1994, but the continued growth in PSA testing means that rates are unlikely to fall to the earlier levels ***(3)***.

In the latest international data, available from the seventh edition of *Cancer Incidence in Five Continents* ***(7)***, which covers the period of 1988 to 1992, Australia's incidence patterns, compared with the rest of the world, are intermediate to those of North America (high) and Asia (low). Selected age-standardized (world population) incidence rates per 100,000 were as follows: United States "Surveillance Epidemiology and End Results" registries (SEER) *blacks* (137), United States SEER whites (101), Australia, Victoria (48), Italy, Varese registry (28), England and Wales (28), Japan, Miyagi registry (9). In ethnic subgroups of the Australian population—migrants to Australia from the countries of southern Europe and Asia—the incidence is half that of Australian-

born men ***(8)***. These differences are also seen in mortality data where Australian-born men have a higher age-standardized mortality rate (17.4 per 100,000) compared with Italian (10.9) and Greek (10.3) migrants ***(9)***. An increase in prostate cancer incidence for migrants from low- to high-risk populations has been taken as evidence of the importance of environmental (lifestyle) exposures in modulating prostate cancer risk. For example, Japanese Americans have rates intermediate to those of SEER whites and native Japanese shown above (Hawaii 64, Los Angeles 47) ***(7)***. This reduced migrant incidence is important because it points to what might protect against prostate cancer rather than increase the risk.

## 3. Risk Factors

The causes of prostate cancer have been investigated in numerous case-control studies and a few prospective cohort studies. Recent reviews ***(10–12)*** are major reference sources, but much of the historical literature is uninformative. Apart from the problem identified earlier with respect to lack of disease specificity, there are many other problems with epidemiological studies of prostate cancer particularly in regard to small sample sizes, poor statistical power, poor exposure measurement, and inappropriate study designs. The best available evidence is obtained from a handful of large well-controlled case-control studies and a few cohort studies. After age, the strongest risk factors for prostate cancer (identified from case-control studies) are having a family history of prostate cancer and having a high dietary fat intake. During the 1990s, large prospective studies identified that specific fatty acids, antioxidant vitamins, carotenoids, and phytoestrogens may alter prostate cancer risk. They also showed that changes in plasma levels of key hormones and associated molecules and naturally occurring variants in genes (polymorphisms) of the androgen, vitamin D, and insulin-like growth factor 1 (IGF-1) prostate cell growth regulatory pathways might alter prostate cancer risk and that dietary factors may affect prostate cancer risk by interacting with these pathways. Nevertheless, the causes of prostate cancer remain unclear, and much research remains to be conducted.

### *3.1. Family History and Genetics*

On a population basis, prostate cancer is a familial disease. The increased risk to a first-degree relative of a man with prostate cancer is on average about 2–3-fold ***(13)*** and is greater the younger the age at diagnosis of the case. In theory, the established environmental risk factors for prostate cancer that can be measured and are familial, such as some components of diet, would explain only a small proportion of familial aggregation of the disease ***(14)***. Of course, one cannot attribute all the residual familial aggregation to genetic factors, as

there may be other environmental and or familial factors not yet identified, and the difficulties in measuring diet mean that their familial effects will be underestimated ***(15)***. Nevertheless, even if a 1.5-fold increased risk associated with having an affected first-degree relative was because of genetic factors, the combined effects of those genetic factors would have a large effect on disease risk equivalent to an interquartile risk ratio of 20–100-fold or more ***(15)***. Furthermore, it needs to be recognized that the same degree of familial aggregation can be not only a consequence of a rare high-risk mutation but also a consequence of a common low-risk polymorphism.

With recent advances in the Human Genome Project, there has been an increasing interest in the role of genetic factors in one's susceptibility to prostate cancer. This has been fueled by a number of linkage analyses based on genome scans of families that contain several men with prostate cancer, usually with early-onset disease. These have led to the identification of at least six chromosomal regions that might contain genes which, when mutated, confer a high lifetime risk of prostate cancer ***(16)***. The autosomal genes are presumed to confer a dominantly inherited risk, and there is also evidence for at least one prostate cancer-susceptibility locus on the X chromosome. As discussed in a recent review, convincing replications have been rare, and heterogeneity analyses suggest that if any one of these regions contains a major prostate cancer gene, mutations in that gene will explain only a small proportion of multiple-case prostate cancer families, presumably because of their rarity ***(16)***. Therefore, as for breast and colorectal cancers, there may be several "high-risk" genes. On the other hand, there have been reports of more modest risks of prostate cancer associated with common variants (polymorphisms) in candidate genes, such as those that encode the androgen receptor (AR), PSA, 5α-reductase type 2 (SRD5A2), cytochrome P450 (CYP3A4), vitamin D receptor (VDR), glutathione-S-transferase, and HPC2/ELAC2 ***(17–23)***. If true, the modest risks associated with common polymorphisms might explain—in an epidemiological sense—a far greater proportion of disease than the high risks associated with rare mutations. Some of these common polymorphisms are discussed more fully below.

### 3.2. Hormones and Other Growth Factors

Growth and maintenance of normal prostate epithelium is regulated by the androgen and vitamin D pathways. These usually affect prostate cell growth in opposing ways, with androgens stimulating and vitamin D metabolites inhibiting cell proliferation ***(24)***. The androgen and vitamin D pathways interact at various levels, with one endpoint of both being the IGF-1 axis ***(24)***. Perturbations of the androgen, vitamin D, and IGF-1 pathways have been associated with prostate cancer ***(24)***.

### *3.2.1. Androgen Signaling Pathway*

Cell division in the prostate is controlled by testosterone (T) ***(25)***. T diffuses freely into prostate cells, where it is irreversibly reduced to its more active form 5α-dihydrotestosterone (DHT) by the enzyme 5α-reductase type 2 ***(25)***. DHT binds to AR to induce a conformational change in the receptor, receptor dimerization, and binding to androgen response elements of target genes to regulate their transcription ***(25)***. The observation that most advanced prostate tumors respond, at least initially, to androgen ablation and that alterations in the androgen signaling axis, including for example somatic mutations in the AR gene, contribute to the development of androgen-independent growth of human prostate tumors ***(26)***, point to an androgen requirement for prostate cancer cell growth. Consistent with these observations, allelic variants of SRD5A2 (49T, 89V), which are thought to increase the activity of the 5α-reductase type 2, have been associated with an increased risk of prostate cancer ***(27)***. Short alleles of the AR CAG microsatellite (where a CAG trinucleotide is subject to a varying number of repeats) have also been associated with increased risk of prostate cancer and with cancers of aggressive phenotype ***(27)***. AR genes with short CAG regions are more highly expressed compared with AR genes with longer CAG regions ***(28,29)***. Other polymorphisms have been identified in genes encoding androgen biosynthetic and catabolic enzymes (e.g., CYP17, HSD3B2, and HSD17B3), but their association with prostate cancer has not been determined ***(28,30)***. Consistent with the hypothesis that increased AR activity increases the risk of prostate cancer, prospective risk studies of androgen plasma/serum measurements suggest that a high plasma T to DHT ratio, high circulating levels of T, low levels of the sulfated or unsulfated adrenal androgen dehydroepiandrosterone (DHEA), or low levels of sex hormone-binding globulin (SHBG), which binds to T thereby decreasing its bioavailability, may elevate risk ***(11)***.

### *3.2.2. Vitamin D Pathway*

Vitamin D is a component of homeostatic mechanisms that ensure normal plasma concentration of calcium and phosphorus. It is primarily formed in the skin through sunlight-stimulated conversion from 7-dehydrocholesterol and derived to a lesser extent from diet. Much like the AR, the VDR translocates to the nucleus, where it regulates transcription of VDR-responsive genes upon binding its most active metabolite, 1α,25-hydroxyvitamin D3 (1,25$D_3$). Whereas androgens stimulate prostate cell proliferation, 1,25$D_3$ inhibits cell growth ***(31)***. If vitamin D does play a role in prostate cancer, alterations in the VDR gene that affect the activity of the receptor would be relevant to prostate cancer susceptibility. Three restriction fragment length polymorphisms (RFLP) with *Bsm*I, *Apa*I, and *Taq*I, as well as a polymorphism in the translation initia-

tion site of the VDR gene, and a poly A length polymorphism have been identified in the VDR gene ***(32,33)***. It is not clear whether any of these affect VDR function. However, a small study showed that a single long poly A allele of VDR was associated with a 4–5-fold increased risk of prostate cancer compared with carriers of the short allele ***(33)***. Furthermore, an independent study found that individuals homozygous for the *Taq*I site appeared to have one-third the risk of developing prostate cancer of heterozygous men or men lacking the site on both alleles ***(34)***. Although these preliminary studies implicate the poly A and the *Taq*I polymorphisms as strong determinants of prostate cancer risk, they need to be replicated. Although two small nested case-control studies provide evidence that high levels of $1,25D_3$ in prediagnostic sera are associated with lower risk of prostate cancer, particularly for advanced disease among older men, serum measurements of $1,25D_3$ and $25D_3$ have been confounded by seasonal variations ***(35)***. Homozygosity for the Taq1 restriction site has been significantly associated with higher serum $1,25D_3$ levels compared with other genotypes at this locus; thus, it may be an alternative marker for serum $1,25D_3$ levels ***(34)***.

### 3.2.3. IGF-1 Pathway

Both the AR and the VDR are thought to produce some of their respective growth effects via the IGF-1 pathway. IGF-1 is a polypeptide insulin-like growth factor that regulates cell growth predominantly by interacting with the cell surface IGF-1 receptor (IGF-1R). In the prostate, bioavailability of IGF-1 is regulated by at least six binding proteins (IGF-BP2-7) ***(24)***. Expression of the major circulating IGF-BP (IGF-BP3) is regulated by opposing actions of the androgen and vitamin D pathways. On one hand, androgens inhibit expression of IGF-BP3, presumably by upregulating the IGF-BP3-specific protease PSA, thus releasing IGF-1 ***(24)***. On the other hand, an analog of $1,25D_3$ has been shown to upregulate the expression of IGF-BP3, thus precluding the association of IGF-1 with its receptor ***(36)***. In addition, some evidence would suggest that IGF-BP3 induces IGF-independent apoptosis, possibly by binding to the putative IGF-BP3 receptor ***(36)***. Two case-control studies found an association between circulating IGF-1 levels and prostate cancer risk ***(10,11)***. This was confirmed in a prospective study that showed an approximate doubling of risk per 100 ng/mL increase in serum IGF-1 in samples collected before subsequent development of prostate cancer ***(11)***. The association was stronger when IGFBP-3 was controlled for, presumably because IGF-BP3 binding renders IGF-1 unavailable ***(11)***. To date, IGF-1 is one of the strongest risk factors identified for prostate cancer. Although a number of RFLPs and a CA dinucleotide repeat length polymorphism upstream of the IGF-1 transcriptional start site have been identified ***(37,38)***, direct association of these with prostate cancer risk has yet to be evaluated. It seems highly probable, however, that the CA

polymorphism will affect prostate cancer risk because it has been shown that Caucasians homozygous for the (CA) 19 alleles have significantly lower IGF-1 serum levels than other genotypes ***(39)***.

### *3.3. Diet and Nutrition*

#### *3.3.1. Fats*

Fats have been consistently linked with prostate cancer, particularly advanced disease. Recent cohort studies have found positive associations between prostate cancer and red meat consumption, total animal fat consumption, and intake of fatty animal foods ***(9–12)***. In regard to specific fats, intakes of α-linolenic acid, saturated fat, and monounsaturated fat have been associated with increased risk of advanced prostate cancer, whereas linoleic acid has not. It has been proposed that fatty acids may modulate prostate cancer risk by affecting serum sex hormone levels. Other ways in which fatty acids may influence prostate cancer include synthesizing eicosanoids, which affect tumor cell proliferation, immune response, invasion, and metastasis; altering the composition of cell membrane phospholipids (thus affecting membrane permeability and receptor activity); affecting 5α-reductase type I activity ***(40)***; forming free radicals from fatty acid peroxidation; and decreasing $1,25D_3$ levels or by increasing IGF-1 levels ***(10,11)***. Evidence suggests that increased biosynthesis by prostate cancer cells of arachidonic acid-derived prostaglandins and hydroxy-acid eicosanoids via cyclooxygenase type 2 (COX-2) and lipoxygenase (LOX) enzyme pathways results in enhanced cancer cell proliferation and invasive and metastatic behavior. This mechanism is consistent with the findings of increased levels of enzyme expression and eicosanoid biosynthesis recently reported by laboratory studies of prostate cancer. Dietary polyunsaturated fatty acid (PUFA) subgroups (n-6 and long-chain n-3 PUFAs) may modify eicosanoid biosynthesis and prostate cancer risk as a result of competitive inhibition of COX and LOX enzymes. Regulation of the expression of COX-2 and LOX enzymes may be brought about by cytokines, pro-antioxidant states, and hormonal factors, the actions of which may be modified by dietary factors such as antioxidants derived from fruit and vegetables. The COX enzyme may be directly inhibited by nonsteroidal anti-inflammatory drugs ***(41–44)***.

#### *3.3.2. Vitamins and Carotenoids*

Studies have not supported a protective effect of vitamin A on prostate cancer; in fact, some have shown that retinol increases risk ***(10–12,45)***. Similarly, there is mixed evidence on the effects of dietary β carotene. Although some case-control studies suggest a protective effect, no benefit was seen in large prospective studies. Vitamin E (α-tocopherol) is a lipid-soluble antioxidant. In the Alpha Tocopherol Beta Carotene trial, male smokers randomized to take

50 mg of α-tocopherol supplement had a statistically significant 32% decrease in clinical prostate cancer incidence and a significant 41% reduction in prostate cancer mortality compared with the placebo group ***(10–12)***. Evidence of an effect from amounts of vitamin E consumed from dietary sources, however, is weak.

Vitamin D is thought to protect against prostate cancer. The consistent positive association between prostate cancer and dairy products, which are rich in vitamin D, may be explained by the high calcium content in dairy foods that suppresses formation and circulating levels of $1,25D_3$. Indeed, two studies found strong positive associations of calcium intakes with prostate cancer ***(10,11)***. Associations of fructose intake (negative) and meat intake (positive) with prostate cancer risk could be partly explained by effects on $1,25D_3$ levels.

Tomatoes and foods that contain concentrated tomato products cooked with oil have been shown to be protective against prostate cancer. Lycopene, a fat-soluble carotenoid principally found in tomatoes, is an efficient singlet oxygen quencher and has been shown to be unusually concentrated in the prostate gland ***(46)***. In the Health Professionals Follow Up Study, high lycopene intake was related to a 21% lower risk of prostate cancer ($p < 0.05$). This relationship between lycopene intake and lower risk of prostate cancer was stronger for advanced cases ***(10,11)***. In the Physicians Health Study, where prediagnostic plasma lycopene levels among 578 cases were compared with those among 1294 controls, men with higher plasma lycopene levels had a 25% reduction in overall prostate cancer risk and a 44% (statistically significant) reduction in risk of aggressive cancer.

### 3.3.3. Phytoestrogens

Phytoestrogens are produced by plants or by bacterial fermentation of plant compounds in the gut and include two groups of hormone-like diphenolic compounds, isoflavonoids and lignins. At the ecological level, their consumption has been proposed as a contributing factor to the low levels of prostate and breast cancers in societies consuming high levels of soy products and other legumes. Consistent with this observation, phytoestrogens have been shown to inhibit in vivo and in vitro prostate tumor model systems ***(47)***. Although the biological function of these agents is not fully understood, they have been reported to inhibit 5α-reductase types I and II, 17β-hydroxysteroid dehydrogenase and the aromatase enzymes, and to stimulate the synthesis of SHBG and of UDP-glucuronyltransferase (which catalyzes the excretion of steroids), suggesting that they may act in part by decreasing the biologically available fraction of androgens ***(47)***. The isoflavanoid genistein is also a potent inhibitor of protein tyrosine kinase that activates various growth factor

receptors, including the IGF-1 receptor by phosphorylation ***(47)***. Some phytoestrogens have also been shown to act as antiestrogens, as weak estrogens, and as antioxidants ***(47)***.

### *3.3.4. Energy Intake, Body Size, and Body Composition*

There is some evidence that energy intake might be associated with prostate cancer and that this might be via an effect on IGF-1 levels ***(48)***. Energy intake and energy balance also are associated with body adiposity. Two-thirds of plasma estrogen (E) in men is derived from the conversion of the adrenal steroid DHEA and androstenedione by the aromatase enzyme system in adipose and muscle. Thus, body composition affects the proportion of circulating E and T. Prostate cells are sensitive not only to T but also to E because they express both the α and β form of the E receptor ***(49)***. Exposure of the male mouse fetus to a 50% physiologic increase in E has been shown to induce a sixfold increase in expression of the AR relative to controls and resulted in the development of an enlarged adult prostate gland ***(49)***. Taken together, these findings suggest that at any time in life, an increased exposure to E can affect prostate cell growth and may thus also impact on prostate growth regulatory dysfunction. To date, associations between body mass index (BMI) and prostate cancer have been inconsistent, perhaps reflecting the inadequacy of BMI as a measure of body composition.

### *3.3.5. Physical Activity and Obesity*

Physical activity can reduce plasma T levels and, therefore, theoretically could reduce the risk of prostate cancer. The evidence from epidemiological studies is inconsistent but suggestive of a protective effect ***(11)*** possibly restricted to high physical activity levels. For example, two recent prospective cohort studies in the United States ***(50,51)*** showed no evidence of an association with physical activity, whereas another ***(52)*** showed that physically inactive men were at increased risk compared with very active men, but this association was limited to Black Americans and was not statistically significant in Caucasian Americans. A cohort study of 22,895 Norwegian men gave a RR of 0.8 (0.62–1.03) for high vs low activity ***(53)***.

Physical activity and obesity are negatively correlated and yet both are negatively correlated with testosterone levels. There is only inconsistent evidence that obesity (as measured by BMI) is associated with prostate cancer. BMI is a problematic measure in this regard because it combines both adiposity and lean body mass, the two components having different hormonal associations, with the latter being under the influence of androgens and IGF-1. This question will

only be resolved by cohort studies that include separate estimates of lean and fat body mass ***(54)***.

### 3.4. Other Lifestyle Factors

#### 3.4.1. Sexuality

As already noted, it has long been known that both normal and malignant prostate growth is related to the action of androgens. The idea that prostate cancer risk, therefore, might be related to variation in the androgen milieu of men and be manifested by differences in sexual activity has been pursued in several studies, most of which were reviewed in the mid-1990s ***(12)***. There have been a few published since ***(55–58)***. Again, these studies have resulted in weak and inconsistent findings. Many focused on reports of sexually transmitted disease (STD) and behaviors that would be associated with increased risk of infection, such as intercourse with prostitutes, having sex without condoms, and having multiple sex partners. Apart from a history of STDs, the most consistent finding is that married men are at increased risk. A recent study has implicated human papillomavirus infection in prostate carcinogenesis ***(59)***.

In regard specifically to sexual activity, the literature is once again very inconsistent, with some studies limited to sexual intercourse, others including all episodes leading to ejaculation. Rotkin ***(60)*** proposed as far back as 1977 that reduced ejaculatory frequency in normal men increased the risk of prostate cancer by some as yet unknown mechanism. This idea is supported by a case-control study ***(61)***, which reported an OR of 4.05 (2.99–5.48) for men who had had an (undefined) period of interrupted sexual activity. Added to this is the observation that Roman Catholic priests, celibates who presumably have a low ejaculatory output, have an above-average risk of dying from prostate cancer ***(62)***.

#### 3.4.2. Tobacco

A scientific consensus meeting in 1996 ***(63)*** concluded that smoking was probably not associated with the incidence of prostate cancer but that there was some evidence that smoking might be positively associated with mortality from this cancer. Since this meeting, there have been other reports that have examined the issue, including a review ***(64)*** that summarized the weak and inconsistent findings of all previous case-control and cohort studies. More recent cohort studies, such as those of US physicians and health professionals ***(65,66)***, have given similar estimates; close to unity for associations between the incidence of all prostate cancer and either current or past smoking and modest positive associations with respect to fatal prostate cancer (RRs between 1.3 and 2).

### *3.4.3. Alcohol*

A review of alcohol and prostate cancer that included studies published before 1997 concluded that there was no association between low to moderate alcohol consumption and prostate cancer, but the authors could not exclude the possibility of an association with heavy drinking and the possibility of population subgroups defined by genetic markers and family history in which effects of alcohol on prostate cancer might be observed ***(67)***. Since this review was published, a US case-control study found no association between alcohol and prostate cancer even at the highest levels of alcohol consumption ***(68)***. A Canadian case-control study found a slightly protective effect (OR 0.89) consistent with the known estrogenic effects of alcohol consumption ***(69)***. The Netherlands Cohort Study ***(70)*** also found no substantive association with alcohol consumption.

### *3.4.4. Occupation*

The occupational associations with prostate cancer are weak and inconsistent ***(12)***. Such as exist may be the result of uncontrolled confounding with social class. For example, professional men may be more likely to seek medical attention and thus to have prostate cancer diagnosed than men of lower education and social status. Cadmium exposure has had a long history of suspicion but there is little evidence of an effect. A number of studies have looked at farming, pesticide exposure in particular, but most exposures have not been measured at the level of the individual. If pesticide residues in the body act like estrogens—as has been suggested in studies of breast cancer—they would be expected to reduce prostate cancer risk. Prostate cancer is also unusual among malignancies in that there is no evidence that it is increased after exposure to ionizing radiation ***(11)***.

## 4. Conclusions

The established risk factors for prostate cancer are few: advancing age and having a family history of prostate cancer. During the last decade, case-control and cohort studies have identified a number of new risk factors for prostate cancer, and more research is now required to confirm their effects, both individually and in concert with other factors. There can, however, be little justification for conducting further case-control studies of prostate cancer, particularly since the widespread use of PSA testing, and much more attention will have to be paid in future epidemiological studies to prostate tumor subclassification in terms of method of detection, markers of biological "aggressiveness" and genetic changes.

Many of these new leads involve the possible influence of polymorphisms in key genes involved in important physiological processes in the prostate such as

the androgen, VDR, and IGF pathways. To fully explore, and to control for, the complexity of interrelationships between the several elements in these pathways requires very large prospective cohort studies in which blood has been sampled before diagnosis. Such studies will be important for identifying which modifiable aspects of lifestyle (diet, alcohol, tobacco, physical activity, etc.) might be targeted for intervention to reduce risk.

The detection of early prostate cancers by PSA-testing relatives of men with prostate cancer is going to affect the prevalence and meaningfulness of multiple-case prostate cancer families. Because multiple-case families form the substrate for linkage analysis and gene hunting, and also the clientele of genetic counseling services, this phenomenon is going to cause considerable confusion and wasted effort. Presently, men with a family history of prostate cancer can be given little by way of advice for preventive action. It is likely that one or more genetic mutations associated with a high-risk for prostate cancer will be identified in the next 5 yr. Even so, the risks will probably be similar to those for mutations in the first two breast cancer genes, and will only be informative in a very small proportion of families. Unfortunately, it is difficult to foresee, when prostate cancer gene mutation carriers are identified in the future, what advice they might be offered—prophylactic prostatectomies? The issue becomes even more complicated when considering the appropriate advice that might be given to men in a possible future scenario where they may be given a genetic risk profile based on their polymorphism status for several genes. Hopefully, such genetic screening will only occur after its efficacy has been established, when we have a better understanding of tumor heterogeneity and prognosis, and when there are improved treatment options available.

Naturally, it would be better to prevent prostate cancer than to treat it. We have some interesting leads from epidemiology, but these require more research before widespread public health initiatives will be possible. Some agents may be appropriate for pharmaceutical development, such as COX-2 inhibitors and compounds that alter IGF-1 activity. Potential agents for prostate cancer chemoprevention via dietary supplementation include vitamin E, selenium, and lycopene, and these substances are already being trialed. To end with a cautionary tale, it is important that chemoprevention trials are followed up for sufficient time and that other endpoints are also captured, as the supplementation of diets with super-physiological doses of individual micronutrients has sometimes met with unexpected and unwanted results. For example, an unexpected 40% decrease in prostate cancers in the α-tocopherol arm was offset by an 18% increase in lung cancers observed in the β-carotene arm of the ATBC trial ***(45)***.

## References


1. Yatani, R., Chigusa, I., Akazaki, K., Stemmermann, G. N., Welsh, R. A., and Correa, P. (1982) Geographic pathology of latent prostatic carcinoma. *Int. J. Cancer* **29,** 611–616.
2. Giles, G. G. and Ireland, P. (1997) Diet, nutrition and prostate cancer. *Int. J. Cancer* **74,** 1–5.
3. Smith, D. P. and Armstrong, B. K. (1998) Prostate-specific antigen testing in Australia and association with prostate cancer incidence in New South Wales. *Med. J. Aust.* **169,** 17–20.
4. Breslow, N. E. and Day, N. E. (1980) *Statistical Methods in Cancer Research: Vol 1. The Analysis of Case-Control Studies.* International Agency for Research on Cancer, Lyon, IARC Scientific Publications No. 32.
5. Breslow, N. E. and Day, NE. (1987) *Statistical Methods in Cancer Research: Vol 2. The Design and Analysis of Cohort Studies.* International Agency for Research on Cancer, Lyon, IARC Scientific Publications No. 82.
6. Australian Institute of Health & Welfare and Australasian Association of Cancer Registries. (1997) *Cancer in Australia.* Australian Institute of Health & Welfare, Canberra, 2000.
7. Parkin, D. M., Muir, C., Waterhouse, J., Mack, T., Powell, J., and Whelan, S. (eds.) (1992) *Cancer Incidence in Five Continents, Vol. VI.* International Agency for Research on Cancer, Lyon, IARC Scientific Publications No. 120.
8. Minami, Y. Staples, M., and Giles, G. G. (1993) Cancer in Italian migrants to Victoria. *Eur. J. Cancer* **29,** 1735–1740.
9. Giles, G. G., Jelfs, P., and Kliewer, E. (1995) *Cancer Mortality in Migrants to Australia.* Australian Institute of Health and Welfare: Cancer Series No. 4, Australian Institute of Health and Welfare, Canberra.
10. Clinton, S. K. and Giovannucci, E. (1998) Diet, nutrition, and prostate cancer. *Ann. Rev. Nutr.* **18,** 413–440.
11. Chan, J. M., Stampfer, M. J., and Giovannucci, E. L. (1998) What causes prostate cancer? A brief summary of the epidemiology. *Semin. Cancer Biol.* **8,** 263–273.
12. Ross, R. K. and Schottenfeld, D. (1996) Prostate cancer, in *Cancer Epidemiology and Prevention, 2nd ed.* (Schottenfeld, D. and Fraumeni, J. F., eds.), Oxford University Press, New York, pp. 1180–1206.
13. Lesko, S. M., Rosenberg, L., and Shapiro, S. (1996) Family history and prostate cancer risk. *Am. J. Epidemiol.* **144,** 1041–1047.
14. Hopper, J. L. and Carlin, J. B. (1992) Familial aggregation of a disease consequent upon correlation between relatives in a risk factor measured on a continuous scale. *Am. J. Epidemiol.* **136,** 1138–1147.
15. Peto, J. (1980) Genetic predisposition to cancer, in *Cancer Incidence in Defined Populations,* Banbury Report no. 4 (Cairns, J., Lyon, J. L., and Skolnick, M., eds.), Cold Spring Harbor Laboratory, Cold Spring Harbor, NY, pp. 203–213.
16. Ostrander, E. A. and Stanford, J. L. (2000) Genetics of prostate cancer: too many loci, too few genes. *Am. J. Hum. Genet.* **67,** 1367–1375.

17. Ingles, S. A., Ross, R. K., Yu, M. C., Irvine, R. A., La Pera, G., Haile, R. W., et al. (1997) Association of prostate cancer risk with genetic polymorphisms in vitamin D receptor and androgen receptor. *J. Natl. Cancer Inst.* **89,** 166–170.
18. Xue, W., Irvine, R. A., Yu, M. C., Ross, R. K., Coetzee, G. A., and Ingles, S. A. (2000) Susceptibility to prostate cancer: Interaction between genotypes at the androgen receptor and prostate specific antigen loci. *Cancer Res.* **60,** 839–841.
19. Jaffe, J. M., Malkowicz, S. B., Walker, A. H., MacBride, S., Peschel, R., Tomaszewski, J., et al. (2000) Association of SRD5A2 genotype and pathological characteristics of prostate tumors. *Cancer Res.* **60,** 1626–1630.
20. Walker, A. H., Jaffe, J. M., Gunasegaram, S., Cummings, S. A., Huang, C. S., Chern, H. D., et al. (1998) Characterization of an allelic variant in the nifedipine-specific element of CYP3A4: Ethnic distribution and implications for prostate cancer risk. *Hum. Mutat.* **12,** 289–295.
21. Ma, J., Stampfer, M. J., Gann, P. H., Hough, H. L., Giovannucci, E., Kelsey, K. T., et al. (1998) Vitamin D receptor polymorphisms, circulating vitamin D metabolites, and risk of prostate cancer in US physicians. *Cancer Epidemiol. Biomarkers Prev.* **242,** 467–473.
22. Kelada, S. N., Kardia, S. L. R, Walker, A. H., Wein, A. J., Malkowicz, S. B., and Rebbeck, T. R. (2000) The glutathione S-transferase-mu and -theta genotypes in the etiology of prostate cancer: Genotype-environment interactions with smoking. *Cancer Epidemiol. Biomarkers Prev.* **9,** 1329–1334.
23. Rebbeck, T. R., Walker, A. H., Zeigler-Johnson, C., Weisberg, S., Martin, A. M., Nathanson, K. L., et al. (2000) Association of HPC2/ELAC2 genotypes and prostate cancer. *Am. J. Hum. Genet.* **67,** 1014–1019.
24. Russell, P. J., Bennett, S., and Stricker, P. (1998) Growth factor involvement in progression of prostate cancer. *Clin. Chem.* **44,** 705–723.
25. Santen, R. J. (1992) Endocrine treatment of prostate cancer. *J. Clin. Endocrinol. Metab.* **75,** 685–689.
26. Bentel, J. M. and Tilley, W. D. (1996) Androgen receptors in prostate cancer. *J. Endocrinol.* **151,** 1–11.
27. Ross, R. K., Pike, M. C., Coetzee, G. A., Reichardt, J. K. V., Mimi, C. Y., Feigelson, H., et al. (1998) Androgen metabolism and prostate cancer: establishing a model of genetic susceptibility. *Cancer Res.* **58,** 4497–4504.
28. Choong, C. S., Kemppainen, J. A., Zhou, Z. X., and Wilson, E. M. (1996) Reduced androgen receptor gene expression with first exon CAG repeat expansion. *Mol. Endocrinol.* **10,** 1527–1535.
29. Chamberlain, N. L., Driver, E. D., and Miesfeld, R. L. (1994) The length and location of CAG trinucleotide repeats in the androgen receptor N-terminal domain affect transactivation function. *Nucleic Acids Res.* **22,** 3181–3186.
30. Moghrabi, N., Hughes, E., Dunaif, A., and Andersson, S. (1998) Deleterious missense mutations and silent polymorphism in the human 17b-hydroxysteroid dehydrogenase 3 gene (HSD17B3). *J. Clin. Endocrinol. Metab.* **83,** 2855–2860.
31. Issa, L. L., Leong, G. M., and Eisman, J. A. (1998) Molecular mechanism of vitamin D receptor action. *Inflamm. Res.* **47,** 451–475.

32. Morrison, N. A., Qi, J. C., Tokita, A., Kelly, P. J., Crofts, L., Nguyen, T. V., et al. (1994) Prediction of bone density from vitamin D receptor alleles. *Nature* **367,** 284–287.
33. Ingles, S. A., Ross, R. K., Yu, M. C., Irvine, R. A., La Pera, G., Haile, R. W., et al. (1997) Association of prostate cancer risk with genetic polymorphisms in Vitamin D receptor and Androgen Receptor. *J. Natl. Cancer Inst.* **89,** 166–171.
34. Taylor, J. A., Hirvonen, A., Watson, M., Pittman, G., Mohler, J. L., and Bell, D. A. (1996) Association of prostate cancer with vitamin D receptor gene polymorphism. *Cancer Res.* **56,** 4108–4110.
35. Corder, E. H., Friedman, G. D., Vogelman, J. H., and Orentreich, N. (1995) Seasonal variation in Vitamin D, Vitamin D-binding protein, and dehydroepiandrosterone: Risk of prostate cancer in black and white men. *Cancer Epidemiol. Biomarkers Prev.* **4,** 655–659.
36. Nickerson, T. and Huynh, H. (1999) Vitamin D analogue EB1089-induced prostate regression is associated with increased gene expression of insulin-like growth factor binding proteins. *J. Endocrinol.* **160,** 223–229.
37. Miyao, M., Hosoi, T., Inoue, S., Hoshino, S., Shiraki, M., Orimo, H., et al. (1998) Polymorphism of insulin-like growth factor I gene and bone mineral density. *Calcified Tissue Int.* **63,** 306–311.
38. Mullis, P. E., Patel, M. S., Brickell, P. M., and Brook, C. G. (1991) Constitutionally short stature: analysis of the insulin-like growth factor-I gene and the human growth hormone gene cluster. *Pediatr. Res.* **29,** 412–415.
39. Rosen, C. J., Kurland, E. S., Vereault, D., Adler, R. A., Rackoff, P. J., Craig, W. Y., et al. (1998) Association between IGF I and a simple sequence repeat in the IGF I gene: Implications for genetic studies of bone mineral density. *J. Clin. Endocrinol. Metab.* **83,** 2286–2290.
40. Liang, T. and Liao, S. (1992) Inhibition of steroid 5 a reductase by specific aliphatic unsaturated fatty acids. *Biochem. J.* **285,** 557–562.
41. Zhou, J. R. and Blackburn, G. L. (1997) Bridging animal and human studies: What are the missing segments in dietary fat and prostate cancer? *Am. J. Clin. Nutr.* **66,** 1572S–1580S
42. Norrish, A. E., Jackson, R. T., and McRae, C. U. (1998) Non-steroidal anti-inflammatory drugs and prostate cancer progression. *Int. J. Cancer* **77,** 511–515.
43. Ghoshi, J. and Myers, C. (1998) Arachidonic acid metabolism and cancer of the prostate. *Nutrition* **14,** 48–49.
44. Cesano, A., Visonneau, S., Scimeca, J. A., Kritchevsky, D., and Santoli, D. (1998) Opposite effects of linoleic acid and conjugated linoleic acid on human prostatic cancer in SCID mice. *Anticancer Res.* **18,** 833–838.
45. Rautalahti, M., Albanes, D., Virtamo, J., Taylor, P. R., Huttunen, J. K., and Heinonen, O. P. (1997) Beta-carotene did not work: aftermath of the ATBC study. *Cancer Lett.* **114,** 235–236.
46. Clinton, S. K., Emenhiser, C., Schwartz, S.J., Bostwick, D. G., Williams, A. W., Moore, B. J., et al. (1996) Cis-trans lycopene isomers, carotenoids, and retinol in the human prostate cancer. *Cancer Epidemiol. Biomarkers Prev.* **5,** 823–833.

47. Griffiths, K., Denis, L., Turkes, A., and Morton, M. S. (1998) Possible relationship between dietary factors and pathogenesis of prostate cancer. *Int. J. Urol.* **5,** 195–213.
48. Wolk, A., Mantzoros, C. S., Andersson, S. O., Bergstrom, R., Signorello, L. B., Lagiou, P., et al. (1998) Insulin-like growth factor 1 and prostate cancer risk: a population-based case-control study. *J. Natl. Cancer Inst.* **90,** 911–915.
49. vom Saal, F. S., Timms, B. G., Montano, M. M., Palanza, P., Thayer, K. A., Nagel, S. C., et al. (1997) Prostate enlargement in mice due to fetal exposure to low doses of estradiol or diethylstilbestrol and opposite effects at high doses. *Proc. Natl. Acad. Sci. USA* **94,** 2056–2061.
50. Putnam, S. D., Cerhan, J. R., Parker, A. S., Bianchi, G. D., Wallace, R. B., Cantor, K. P., et al. (2000) Lifestyle and anthropometric risk factors for prostate cancer in a cohort of Iowa men. *Ann. Epidemiol.* **10,** 361–369.
51. Liu, S., Lee, I. M., Linson, P., Ajani, U. Buring, J. E., and Hennekens, C. H. (2000) A prospective study of physical activity and risk of prostate cancer in US physicians. *Int. J. Epidemiol.* **29,** 29–35.
52. Clarke, G. and Whittemore, A. S. (2000) Prostate cancer risk in relation to anthropometry and physical activity: Tthe National Health and Nutrition Examination Survey Epidemiological Follow-Up Study. *Cancer Epidemiol. Biomarkers Prev.* **9,** 875–881.
53. Lund-Nilsen, T. I., Johnsen, R., and Vatten, L. J. (2000) Socio-economic and lifestyle factors associated with the risk of prostate cancer. *Br. J. Cancer* **82,** 1358–1363.
54. Severson, R. K., Grove, J. S., Nomura, A. M. Y., and Stemmerman, G. N. (1988) Body mass and prostate cancer: a prospective study. *Br. Med. J.* **297,** 713–715.
55. Ewings, P. and Bowie, C. (1996) A case-control study of cancer of the prostate in Somerset and east Devon. *Br. J. Cancer* **74,** 661–666.
56. Hayes, R. B., Pottern, L. M., Strickler, H., Rabkin, C., Pope, V., Swanson, G. M., et al. (2000) Sexual behaviour, STDs and risks for prostate cancer. *Br. J. Cancer* **82,** 718–725.
57. Andersson, S. O., Baron, J., Bergstrom, R., Lindgren, C., Wolk, A., and Adami, H. O. (1996) Lifestyle factors and prostate cancer risk: A case-control study in Sweden. *Cancer Epidemiol. Biomarkers Prev.* **5,** 509–513.
58. Hsieh, C. C., Thanos, A., Mitropoulos, D., Deliveliotis, C., Mantzoros, C. S., and Trichopoulos, D. (1999) Risk factors for prostate cancer: A case-control study in Greece. *Int. J. Cancer* **80,** 699–703.
59. Dillner, J., Knekt, P., Boman, J., Lehtinen, M., Af Geijersstam, V., Sapp, M., et al. (1998) Sero-epidemiological association between human-papillomavirus infection and risk of prostate cancer. *Int. J. Cancer* **75,** 564–567.
60. Rotkin, I. D. (1977) Studies in the epidemiology of prostatic cancer: expanded sampling. *Cancer Treatment Reports* **61,** 173–180.
61. Fincham, S. M., Hill, G. B., Hanson, J., and Wijayasinghe, C. (1990) Epidemiology of prostatic cancer: A case-control study. *Prostate* **17,** 189–206.

62. Ross, R. K., Deapen, D. M., Casagrande, J. T., Paganini-Hill, A., and Henderson, B. E. (1981) A cohort study of mortality from cancer of the prostate in Catholic priests. *Br. J. Cancer* **43,** 233–235.
63. Colditz, G. (1996) Consensus conference: smoking and prostate cancer. *Cancer Causes Control* **7,** 560–562.
64. Lumey, L. H. (1996) Prostate cancer and smoking: A review of case-control and cohort studies. *Prostate* **29,** 249–260.
65. Giovannucci, E., Rimm, E. B., Ascherio, A., Colditz, G. A., Spiegelman, D., Stampfer, M. J., et al. (1999) Smoking and risk of total and fatal prostate cancer in United States health professionals. *Cancer Epidemiol. Biomarkers Prev.* **8,** 277–282.
66. Lotufo, P. A., Lee, I. M., Ajani, U. A., Hennekens, C. H., and Manson, J. E. (2000) Cigarette smoking and risk of prostate cancer in the Physicians' Health Study. *Int. J. Cancer* **87,** 141–144.
67. Breslow, R. A. and Weed, D. L. (1998) Review of epidemiologic studies of alcohol and prostate cancer: 1971–1996. *Nutr. Cancer* **30,** 1–13.
68. Lumey, L. H., Pittman, B., and Wynder, E. L. (1998) Alcohol use and prostate cancer in U.S. whites: No association in a confirmatory study. *Prostate* **36,** 250–255.
69. Villeneuve, P. J., Johnson, K. C., Krieger, N., and Mao, Y. (1999) Risk factors for prostate cancer: results from the Canadian National Enhanced Cancer Surveillance System. The Canadian Cancer Registries Epidemiology Research Group. *Cancer Causes Control* **10,** 355–367.
70. Schuurman, A. G., Goldbohm, R. A., and van den Brandt, P. A. (1999) A prospective study on consumption of alcoholic beverages in relation to prostate cancer incidence (The Netherlands). *Cancer Causes Control* **10,** 597–605.

# 2

# Human Prostate Cancer Cell Lines

**Pamela J. Russell and Elizabeth A. Kingsley**

## 1. Introduction

Prostate cancer affects many men in the West but rarely occurs in Japan or China. Some epidemiological factors that may be important in this are described elsewhere in this volume. Prostate cancer has become the most common malignancy and the second highest cause of cancer death in Western society. The disease is very heterogeneous in terms of grade, genetics, ploidy, and oncogene/tumor suppressor gene expression, and its biological, hormonal, and molecular characteristics are extremely complex. Growth of early prostate cancer requires 5α-dihydrotestosterone produced from testosterone by the 5α-reductase enzyme system; such prostate cells are described as androgen dependent (AD). Subsequently, the prostate cancer cells may respond to androgen but do not require it for growth; these cells are androgen sensitive (AS). Because of the requirement for androgen for growth of prostate cancer, patients whose tumors are not suitable for surgical intervention or radiotherapy may be treated by hormonal intervention, either continuous or intermittent, to prevent prostate cancer cell growth ***(1–3)***. This leads to periods of remission from disease, but almost invariably, the prostate cancer recurs, by which time the prostate cancer cells have become androgen-independent (AI) ***(4,5)***. This may be accompanied by changes in the androgen receptor (AR), which may undergo mutation ***(6,7)***, amplification ***(8)***, or loss ***(9)***. Prostate cancer cells metastasize to various organs but particularly to local lymph nodes and to skeletal bone. Important antigens expressed by prostate cancer cells include prostate-specific antigen (PSA), which has been used both for screening for prostate cancer and for management of patients with the disease ***(10,11)***. Prostate-specific membrane antigen (PSMA) is produced in two forms that differ in the normal prostate, benign hyperplasia of the prostate, and prostate cancer ***(12)***. PSMA is upregulated in prostate cancer compared with normal cells

From: *Methods in Molecular Medicine, Vol. 81: Prostate Cancer Methods and Protocols*
Edited by: P. J. Russell, P. Jackson, and E. A. Kingsley © Humana Press Inc., Totowa, NJ

and is found in cells in increased concentration once they become AI ***(13,14)***. Interactions between epithelial cells and stroma appear to be very important in allowing prostate cells to grow and form tumors, partly because of paracrine pathways that exist in this tissue ***(15,16)***. Prostate cancer rarely arises spontaneously in animals, and the human cancer cells are particularly difficult to grow in culture as long-term cell lines ***(17)***. Elsewhere in this book, methods for growing primary cultures of the prostate, for immortalizing prostate cells, and for isolating prostate stem cells are described. This chapter describes the commonly used prostate cancer cell lines, their preferred media for growth, and some of their important uses, including inoculation into mice to produce bony metastases.

## 2. Lines Derived from Human Tumors

A listing of the major human prostate cell lines and their media requirements may be found in **Tables 1** and **2;** more specialized media for the establishment and growth of prostate cells are described elsewhere in this volume. The characteristics of a number of prostate cell lines are summarized in **Table 3**.

Most human prostate cancer cell lines have been established from metastatic deposits with the exception of PC-93 ***(18)***, which is grown from an AD primary tumor. However, PC-93 and other widely used lines, including PC-3 ***(19)***, DU-145 ***(20)***, and TSU-Pr1 ***(21)***, are all AI; all lack androgen receptors (with the possible exception of PC-93), PSA, and 5α-reductase; and all produce poorly differentiated tumors if inoculated into nude mice. Until very recently, the paucity of AD cell lines has made studies of the early progression of prostate cancer using human materials very difficult. However, metastatic sublines of PC-3 have been developed by injecting cells into nude mice via different routes, especially orthotopically ***(22)***, and this process can be readily followed by using PC-3 cells expressing luciferase ***(23)***.

Until recently, the LNCaP cell line, established from a metastatic deposit in a lymph node ***(24)***, was the only human prostate cancer cell line to demonstrate androgen sensitivity. After its initial characterization, several laboratories found LNCaP cells to be poorly tumorigenic in nude mice unless coinoculated with tissue-specific mesenchymal or stromal cells ***(25,26)*** or Matrigel™ ***(27)***, emphasizing the importance of extracellular matrix and paracrine-mediated growth factors in prostate cancer growth and site-specific metastasis ***(28)***. New lines were obtained by culturing LNCaP cells that had been grown in castrated mice ***(29)***. The C-4 LNCaP line is AI, produces PSA and a factor that stimulates PSA production, and the C4-2 and C4-2B lines metastasize to lymph nodes and bone after subcutaneous or orthotopic inoculation ***(29,30)***. Others have also selected more highly metastatic cells ***(22)*** by serial reinjection into the prostate of prostate cancer cell lines or by growing

**Table 1**
**Profile of Established Human Prostate Cancer and Immortalized Cell Lines**

| Cell line | Source | Media requirements[a] | References |
|---|---|---|---|
| PC-93 | AD primary prostate cancer | A | ***18, 86*** |
| PC-3 | Lumbar metastasis | B or D (ATCC[b] recommendation) | ***19*** |
| DU-145 | Central nervous system metastasis | B or E (ATCC recommendation) | ***20*** |
| TSU-Pr1[c] | Cervival lymph node metastasis in Japanese male | B or F | ***21*** |
| LNCaP | Lymph node metastasis in Caucasian male | G or B | ***24, 87, 88, 89*** |
| LNCaP-FGC[d] | Clonal derivative of LNCaP | B | ***24, 87*** |
| LNCaP-LN-3 | Metastatic subline of LNCaP cells derived by orthotopic implantation | H or I | ***22*** |
| LNCaP-C4 | Metastatic subline of LNCaP, derived after coinoculation of LNCaP and fibroblasts | G | ***29, 30*** |
| LNCaP-C4B | Metastatic subline derived from LNCaP-C4 after reinoculation into castrated mice | G | ***29, 30*** |
| MDA PCa 2a | AI bone metastasis from African-American male | J or K | ***34, 35*** |
| MDA PCa 2b | AI bone metastasis from African-American male | J or K | ***34, 35*** |
| ALVA-101 | Bone metastasis | L | ***36*** |
| ALVA-31[e] | Well-differentiated adenocarcinoma | M | ***38*** |
| ALVA-41[e] | Bone metastasis | L | ***42*** |
| 22Rv1 | Derived from CWR22R, an androgen-dependent prostate cancer xenograft line | B | ***43*** |
| ARCaP | Derived from ascitic fluid from a patient with metastatic disease | G | ***44*** |
| PPC-1[e] | Poorly differentiated adenocarcinoma | B | ***45*** |

*(Table continues)*

**Table 1**
***(Continued)***

| Cell line | Source | Media requirements[a] | References |
|---|---|---|---|
| LAPC3 | Derived from xenograft established from specimen obtained via transurethral resection of the prostate | N | ***47*** |
| LAPC4 | Derived from xenograft established from a lymph node metastasis | N | ***47*** |
| P69SV40T | Immortalized cell line derived by transfection of adult prostate epithelial cells with the SV40 large T antigen gene | O | ***58*** |
| RWPE-2 | Immortalized cell line initially derived by transfection of adult (Caucasian) prostatic epithelial cells with human papillomavirus 18, then made tumorigenic by infection with v-K-ras | P | ***59*** |
| CA-HPV-10 | Immortalized cell line derived by human papilloma virus 18 transfection of prostatic epithelia cells from a high-grade adenocarcinoma | Q | ***60*** |
| PZ-HPV-7 | Immortalized cell line derived by human papilloma virus 18 transfection of normal prostatic peripheral zone epithelial cells | Q | ***60*** |

[a]*See* **Table 2** for details of cell line media requirements.
[b]ATCC: American Type Culture Collection (http://www.atcc.org).
[c]The nature of this cell line has recently been questioned; *see* **ref. *90***.
[d]LNCaP-FGC: LNCaP clone, Fast Growing Colony; available from the ATTC.
[e]The nature of this cell line has recently been questioned; *see* **ref. *91***.

**Table 2**
**Media Requirements of Human Prostate Cancer and Immortalized Cell Lines**

| Designation | Components |
|---|---|
| A | Eagle's minimum essential medium (MEM) supplemented with 10% FBS and 2 m*M* L-glutamine |
| B | Roswell Park Memorial Institute (RPMI) 1640 medium, supplemented with 10% fetal bovine serum (FBS) |
| C | Dulbecco's modified Eagle medium (DMEM), supplemented with 10% FBS |
| D | Kaighn's modification of Ham's F-12 medium (F-12K), supplemented with 10% FBS and 2 m*M* L-glutamine, and adjusted to contain 1.5 g/L sodium bicarbonate |
| E | MEM supplemented with 10% FBS, 2 m*M* L-glutamine and Earle's balanced salt solution (BSS) adjusted to contain 1.5 g/L sodium bicarbonate, 0.1 m*M* nonessential amino acids and 1.0 m*M* sodium pyruvate |
| F | RPMI supplemented with 5% FBS |
| G | "T-medium": DMEM:F-12K, 4:1, supplemented with 5% FBS, 3 g/L sodium bicarbonate, 5 µg/mL insulin, 13.6 pg/mL triiodothyronine, 5 µg/mL transferrin, 0.25 µg/mL biotin, 25 µg/mL adenine ***(88,89)*** |
| H | Medium "B" supplemented with sodium pyruvate, nonessential amino acids and vitamins |
| I | RPMI:F-12K, 1:1, supplemented with 10% FBS |
| J | BRFF HPC1 medium (Biological Research Faculty and Facility, Inc., Jamesville, MD) supplemented with 15% FBS |
| K | F-12K supplemented with 20% FBS, 10 mg/mL epidermal growth factor, 100 ng/mL hydrocortisone, 5 µg/mL insulin, 25 ng/mL cholera toxin, $5 \times 10^{-6}$ *M* phosphoethanolamine, $3 \times 10^{-8}$ *M* sodium selenite |
| L | RPMI supplemented with 5% FBS, 2 m*M* L-glutamine, and 1 m*M* sodium pyruvate |
| M | RPMI supplemented with 10% FBS, 1% L-glutamine, 1% sodium pyruvate, buffered to pH 7.4 with 7.5% (w/v) sodium bicarbonate |
| N | Iscove's modified Dulbecco's medium (IMDM) supplemented with 10% FBS and 10 n*M* R1881 synthetic steroid |
| O | Serum-free RPMI supplemented with 10 ng/mL epidermal growth factor, 5 µg/mL insulin, 5 µg/mL transferrin, 5 ng/mL selenium, and 0.1 µ*M* dexamethasone |
| P | Keratinocyte serum-free medium (KSFM) supplemented with 50 µg/mL bovine pituitary extract and 5 ng/mL epidermal growth factor |
| Q | Keratinocyte serum-free medium (KSFM) supplemented with 50 µg/mL bovine pituitary extract |

**Table 3**
**Characteristics of Human Prostate Cancer and Immortalized Cell Lines**

| Cell line | Androgen receptor | Androgen sensitivity | 5α-Reductase |
|---|---|---|---|
| PC-93 | ? | AI | – |
| PC-3 | – | AI | – |
| DU-145 | – | AI | – |
| TSU-Pr1 | – | AI | NR |
| LNCaP | +<br>Mutated | AS | – |
| Sublines: | | | |
| C4 | | AI | ++ |
| C4-2 | AI + mets | +++ | + |
| C4-2B | AI + mets | +++ | + |
| P104-R2 | Stimulated by finasteride | | |
| LN3 | | Less sensitive than LNCaP | +++ |
| MDA PCa 2a | + | AS | |
| MDA PCa 2b | + | AS | |
| ALVA101 | + | AS | + |
| 22Rv1 | Grown from an AI xenograft | AS | NR |
| ARCaP | + | Androgen repressed | NR |
| LACP-4 | + | AS | NR |
| P69SV40T | NR | NR | NR |
| RWPE-2 | + | + | NR |
| CA-HPV-10 | NR | NR | NR |

[a]NR, not reported.

| PSA | PAMA | p53/other features | References |
|---|---|---|---|
| – | NR[a] | NR | ***18*** |
| – | – | Deletion mutation of *p53* | ***19,92*** |
| – | – | Mutated *p53*, pro to leu codon 223; val to phe codon 274 | ***20,93*** |
| | | Has mutated p16 codon 84 | ***50*** |
| – | NR | Mutated *p53* (has mutated H-ras) | ***21,92*** |
| + | + | Silent mutation of *p53* | ***24,92*** |
| + | | | ***29*** |
| | | Low levels of functional *p53* | ***30*** |
| | | | ***30*** |
| | | | ***32*** |
| ++ | | | ***22*** |
| + | NR | NR | ***34,35*** |
| + | NR | NR | ***34,35*** |
| + | NR | NR | ***36*** |
| + | NR | – | ***43*** |
| + | NR | NR | ***44*** |
| + | NR | AI sublines express high levels of HER/2-neu | ***47,48*** |
| NR | NR | Express EGFR and TGFα | ***58*** |
| + | NR | Express HPV-18 E7 protein; mutated *Ki-ras* | ***59*** |
| NR | NR | Cytogenetic abnormalities | ***61*** |

the cells in the prostate of SCID mice ***(31)***. The LN3 cell line derived from the LNCaP line by this method is more metastatic to liver, less sensitive to androgen, and its cells produce high levels of both PSA and PSMA ***(22)***. The LNCaP line expresses a mutated AR. Some mutations of the AR are associated with stimulation of the cells by antiandrogens, causing concern over the use of drugs, such as finasteride for the treatment of late-stage prostate cancer. The subline LNCaP 104-R2 manifests this phenomenon ***(32)***. Using a subline, LNCaP-abl, produced by growing LNCaP cells in androgen-depleted medium for 87 passages, bicalutamide was shown to acquire agonistic properties that were not related to changes in AR activity or with amplification of the AR gene in these cells ***(33)***. Recently, new androgen responsive lines have been established. The MDA PCa 2a and MDA PCa 2b lines were both isolated from a single bone metastasis from an African American male who had AI prostate cancer ***(34)***. They both express PSA (MDA PCa 2a produces 0.43 and MDA PCa 2b produces 0.67 ng/mL of PSA/g of tumor), ARs, and are AS and both grow in nude mice; they differ in their morphology in vitro and in their karyotypes and are thought to represent distinct clones from the same tumor ***(34,35)***. Despite their androgen sensitivity, these cells show intact p53 and Bcl-2, Rb, and p16, reflecting a common subset of human AI prostate cancer ***(35)***. The ALVA-101 ***(36)*** line is also AS; these cells respond to 5α-DHT by upregulating an autocrine loop involving epidermal growth factor receptors and their ligand, transforming growth factor-α (TGFα) ***(37)***. The tumor induction and take rates of the ALVA-31 cell line are similar in female and castrated male nude mice; however, an increased growth rate in intact male mice suggests a degree of androgen responsiveness ***(38)***. The line is positive for both PSA and PAP, and expresses the highest level of vitamin D receptor of all established prostate cancer cell lines ***(39)***. However, it lacks α-catenin ***(40)***, and expresses only low levels of AR, p21, and p27 ***(41)*** The ALVA-41 line expresses AR with a binding capacity similar to that of LNCaP, and the line is androgen responsive ***(42)***; it expresses PAP but not PSA.

A new prostate cancer cell line, 22Rv1, has been derived from the xenograft line, CWR22R: it expresses PSA, is slightly stimulated by DHT, and expresses an AR. Its growth is stimulated by epidermal growth factor but is not inhibited by transforming growth factor-beta 1 ***(43)***.

An unusual cell line, ARCaP ***(44)***, was derived from prostate cancer cells in ascites fluid of a man with metastatic disease and exhibits androgen- and estrogen-repressed growth and tumor formation in hormone-deficient or castrated mice. These cells express low levels of AR and PSA and are highly metastatic when inoculated orthotopically. Androgen-repressed prostate cancers are thought to occur only very late in the progression of the disease.

The PPC-1 cell line was established from a primary prostatic tumor site, a poorly differentiated adenocarcinoma ***(45)***. It is hormone insensitive ***(45)***, tumorigenic, and spontaneously metastasizes to the lungs and lymph nodes after sc inoculation in nude mice ***(46)***.

Two cell lines established from xenografted prostate cancer tissue, LAPC-3 and LAPC-4, showed chromosomal abnormalities and expressed wild-type ARs ***(47)***. LAPC-3 is AI, whereas LAPC-4 is AS. The LAPC-4 xenograft has been propagated as a continuous cell line that retains its hormone-responsive characteristics, but the xenografted line can progress to AI when grown in female or castrated male mice. In this model, the AI sublines express higher levels of HER-2/neu than the AS cells. Forced overexpression of HER-2/neu in AD cells allowed ligand-independent growth. HER-2/neu activated the AR pathway in the absence of ligand and synergized with low levels of androgen to superactivate the pathway ***(48)***.

Molecular analyses have shown that many of the cell lines contain *p53* mutations (*see* **Table 3**), consistent with the finding that *p53* mutations commonly occur in late-stage prostate cancer. When *p53* mutation occurs in early stage disease, however, it predisposes to cancer progression ***(49)***. In some cases, alterations of other oncogenes/suppressor genes have been observed. The DU-145 line shows a mutation in the *p16* gene, involved in cell cycle control ***(50)***. Relatively few of the lines express PSA or PSMA, which has been shown to be overexpressed in late-stage prostate cancers in man ***(51)***. Loss of the tumor suppressor gene, *PTEN/MMAC1*, which maps to 10q23.3, occurs commonly in prostate cancer. Several cell lines and xenograft lines show homozygous deletions of the *PTEN* gene or parts thereof (PC-3, PC133, PCEW, PC295, and PC324), and others contain nonsense mutations (PC82 and PC346) or frameshift mutations (LNCaP and PC374) ***(52)***. *PTEN/MMAC1* acts as a negative regulator of the phosphoinositide 3-kinase (P13-kinase)/Akt pathway and inactivation of the *PTEN/MMAC1* gene leads to constitutive activation of either P13-kinase or Akt, which can induce cellular transformation ***(53)***.

Cell–cell adhesion may be mediated through calcium-dependent, homotypic cadherin-catenin interactions ***(54)***; α-catenin, in turn, bridges the cadherin–catenin complex to the actin filaments of the cytoskeleton. Dysfunction of the cadherin pathway by gene deletions, gene promoter hypermethylation, and loss of heterozygosity (LOH) ***(54)*** is involved in tumor invasiveness and disease progression. E-cadherin is a prognostic marker for prostate cancer, based on a correlation of grade and aberrant E-cadherin staining, whereas P-cadherin is lost in all prostatic cancers, possibly because it is only expressed in basal cells. Expression of α-catenin, which binds to E-cadherin at the cytoplasmic domain, may also be reduced in prostatic tumors; α-catenin is not

expressed in PC-3 cells (that are E-cadherin positive) because of a homozygous deletion on chromosome 5q ***(55)***. Microcell transfer of chromosome 5 into PC-3 cells resulted in cell–cell adhesion and loss of tumorigenicity when the cells were implanted in nude mice. Similarly, the ALVA-31 line lacks α-catenin but is E-cadherin positive ***(40)***, whereas TSU-Pr1 cells express α-catenin but are E-cadherin negative ***(56)***. Expression of different cadherins and catenins in seven prostate cancer cell lines is described elsewhere ***(56)***. Expression of novel cadherins, such as N-cadherin and cadherin-11 (also called OB-cadherin) ***(56)***, may also play an important role in prostate cancer progression. A splice variant of cadherin-11 may act as a dominant-negative regulator of cell adhesion ***(57)***.

## 3. Immortalized Cell Lines

Several new immortalized nontumorigenic as well as tumorigenic adult human prostatic epithelial cell lines, which express functional characteristics of prostatic epithelial cells, provide additional in vitro cell models for studies on prostatic neoplasia. (These are described in more detail elsewhere in this volume.) Researchers have immortalized cells (*see* **Tables 1** and **3**) by transfection with an SV40 construct containing the SV40 large-T antigen gene ***(58)*** or by transfection with plasmids containing a single copy of the human papillomavirus (HPV) 18 genome ***(59–61)***. In each case, the viral proteins used interact with *p53,* indicating that loss of p53 function may be extremely important for the growth of prostate cancer cells. The use of HPVs for immortalization is based on observations that around 40% of prostate cancers contain DNA from either HPV-16, -18, or -33 ***(62,63)***, suggesting a possible role for HPV in prostate cancer. Further transformation of immortalized cells with the *Ki-ras,* based on observations of *Ki-ras* mutations in prostate cancer ***(63)***, was performed to make the cells tumorigenic ***(59)***, providing models for the study of genes involved in progression of prostate cancer, for example by comparative genomic hybridization ***(64)***. In addition, a stromal myofibroblast line has been established for studies of epithelial–stromal interactions. This line, WPMY-1, immortalized with SV40 large T antigen, expresses smooth muscle alpha-actin and vimentin, is positive for AR and large-T Ag, heterogeneous for p53 and pRb, and grows in serum-free medium ***(65)***. Conditioned medium from WPMY-1 cells causes marked inhibition of growth of WPE1-10 epithelial cells, immortalized from the same prostate. Other lines immortalized using HPV-18 include PZ-HPV-7 (normal prostate) and CA-HPV-10 (primary prostate cancer) ***(61)***, which show multiple cytogenetic changes. E6 and E7 transforming proteins of HPV-16 have been used to establish 14 immortal benign or malignant prostate epithelial cell cultures from primary adenocarcinomas ***(66)***, and these lines have been used to study allelic LOH. LOH at chro-

mosome 8p was seen in tumor-derived lines but not those from autologous benign prostatic epithelium.

In a similar fashion, normal rat prostate epithelial cells immortalized with SV-40 large T antigen have been used to study the progression to AI and malignancy in Copenhagen rats ***(67)***. The immortalized cells were transfected with *v*-H-*ras* and *c*-*myc* to create invasive cancer lines.

## 4. Primary Cultures

Stromal–epithelial interactions are pivotal in many aspects of prostatic biology. The investigation of factors that regulate these interactions and the growth and differentiation of human prostatic cells has been performed using defined and experimental culture systems for both epithelial and stromal cells from primary prostate cancers ***(68,69)***. Using such systems, fibroblastic or smooth muscle cells can be promoted, maintained, and investigated in a defined manner ***(70)***. The methods for developing primary cultures are described in Chapter 3.

## 5. Models for Bony Metastases

Prostate cancer is unique in that it is osteogenic, resulting in the formation of dense sclerotic bone with high levels of osteoblastic activity. A potential regulator of the tropism of prostate cancer to bone is a family of proteins that belong to the transforming growth factor β (TGF-β) family called bone morphogenetic protein (BMP), which are involved in stimulating bone formation in vivo. Some BMPs and their receptors are expressed on prostate cancer cells. These receptors are regulated by androgen and can differentially modulate prostate cancer cell growth in response to BMP under different hormonal conditions ***(71)***. Because xenografts grown subcutaneously in nude mice rarely metastasize, special methods have been developed to study bony metastases from human prostate cancers in experimental models. As mentioned previously, the C4-2 and C4-2B sublines that were developed from LNCaP cells by coinoculation with tissue-specific or bone-derived mesenchymal or stromal cells in castrated mice metastasize to lymph nodes and bone after subcutaneous or orthotopic inoculation ***(29,30)***. Intrafemoral injection has been used to establish osteoblastic bone lesions of PC-3, LNCaP, C4-2, and C4-2B4 in athymic ***(72)*** and SCID/bg mice. In the latter, osteoblastic tumors occurred in the bone marrow space within 3 to 5 wk, and serum PSA showed a stepwise elevation with tumor growth ***(73)***. The growth of PC-3 in the femur of nude mice was significantly inhibited by treatment with systemic interleukin-2, which caused vascular damage and infiltration of polymorphonuclear cells and lymphocytes in the tumor as well as in necrotic areas with apoptotic cells ***(74)***.

In a related model system, humanized SCID mice have been used to test the ability of prostate cancer cells to "home" to bone ***(75)***. C57.17 SCID-hu mice

were implanted with macroscopic fragments of human fetal bone, lung, or intestine or mouse bone subcutaneously and injected 4 wk later with human prostate cancer cells given via the tail vein or implanted transdermally. PC-3, DU-145, and LNCaP cells colonized implanted human bone fragments with osteolytic lesions in the case of PC-3 and DU-145 and osteoblastic and osteolytic lesions from LNCaP cells. Each cell line formed tumors in implanted human lung tissue, but these were very small. Similar studies were performed using humanized nonobese diabetic/severe combined immunodeficient (NOD/SCID-hu) mice engrafted with human adult bone or lung ***(76)***. In this study, a much higher take rate was shown by the LNCaP cells, which formed osteoblastic metastases (65% of LNCaP) than PC-3 cells that caused oesteolytic lesions (3% of PC-3) in the human bone but not in mouse bone.

## 6. Hormone Therapy

Prostate cancer cell lines have been used to study various treatment strategies. One of the mainstays of treatment for prostate cancer is androgen ablation, which can inhibit tumor growth when the cancer is AD or AS. However, prostate tumors can adapt to an environment with low androgen supply by using a hyperactive AR; the mechanisms involve mutations of the AR, generating receptors with broadened activation spectra, increased receptor expression, and activation by interaction with other signaling pathways ***(6,77)***. For these reasons, prostate cancer models have been widely used to study a variety of experimental hormonal manipulations, including those possibly suitable for AI disease. Intermittent use of hormone ablation in the LNCaP model prolonged the time until AI PSA production began ***(78)***. In LNCaP cells, an interaction occurs between the DNA- and ligand-binding domains of AR and the leucine zipper region of *c-Jun*. This association provides a link between the transcription factor, AP-1, and AR signal transduction pathways in the regulation of the *PSA* gene ***(78)***. Both luteinizing hormone-releasing hormone (LH-RH) and growth hormone-releasing hormone analogs have proved useful for treating PC-3 or DU-145 AI xenografts and both appear to invoke increased expression of mRNA for insulin-like growth factor II (IGF-II) in the tumors ***(79–82)***. LH-RH vaccines have also been used to induce atrophy of the prostate in rat models ***(83)*** and may provide an inexpensive alternative to the use of LH-RH analogs. Photodynamic therapy given in vitro was more effective in LNCaP cells when they were pretreated with 5α-dihydrotestosterone, suggesting an androgen-modulated effect on both uptake and phototoxicity ***(84)***. This effect was not observed in AI PC-3 cells in vitro. However, subsequent studies in vivo using R3327-MatLyLu Dunning cells grown orthotopically in the ventral prostate indicated that benzoporphyrin derivative monoacid ring A, combined with surgery, could inhibit both local primary tumor growth as well as reduce distant metastases ***(85)***.

Other modalities, including antibody-based therapy, gene therapy, and new chemotherapeutic drugs ***(86)***, have also been extensively tested at a preclinical level using human prostate cancer cell lines, either in vitro or grown as xenografts in various locations (orthotopic, in the femur) of nude or SCID mice. Such treatments are outside the scope of this chapter.

## References


1. Paul, R. and Breul, J. (2000) Antiandrogen withdrawal syndrome associated with prostate cancer therapies: Incidence and clinical significance. *Drug Safety* **23,** 381–390.
2. Rambeaud, J. J. (1999) Intermittent complete androgen blockade in metastatic prostate cancer. *Eur. Urol.* **35 (Suppl 1),** 32–36.
3. Sciarra, A., Casale, P., Colella, D., Di Chiro, C., and Di Silverio, F. (1999) Hormone-refractory prostate cancer? Anti-androgen withdrawal and intermittent hormone therapy. *Scand. J. Urol. Nephrol.* **33,** 211–216.
4. Laufer, M., Denmeade, S. R., Sinibaldi, V. J., Carbucci, M. A., and Eisenberger, M. A. (2000) Complete androgen blockade for prostate cancer: What went wrong? *J. Urol.* **164,** 3–9.
5. Lara, P. N., Jr and Meyers, F. J. (1999) Treatment options in androgen-independent prostate cancer. *Cancer Invest.* **17,** 137–144.
6. Culig, Z., Hobisch, A., Hittmair, A., Peterziel, H., Cato, A. C., Bartsch, G., et al. (1998) Expression, structure and function of androgen receptor in advanced prostatic carcinoma. *Prostate* **35,** 63–70.
7. Wang, C. and Uchida, T. (1997) Androgen receptor gene mutations in prostate cancer. *Jpn. J. Urol.* **88,** 550–556.
8. Henshall, S. M., Quinn, D. I., Lee, C. S., Head, D. R., Golovsky, D., Brenner, P. C., et al. (2001) Altered expression of androgen receptor in the malignant epithelium and adjacent stroma is associated with early relapse in prostate cancer. *Cancer Res.* **61,** 423–427.
9. Kinoshita, H., Shi, Y., Sandefur, C., Meisner, L. F., Chang, C., Choon, A., et al. (2000) Methylation of the androgen receptor minimal promoter silences transcription in human prostate cancer. *Cancer Res.* **60,** 3623–3630.
10. Polascik, T. J., Oesterling, J. E., and Partin, A. W. (1999) Prostate specific antigen: A decade of discovery—what have we learned and where are we going. *J. Urol.* **162,** 293–306.
11. Peehl, D. M. (1995) Prostate specific antigen role and function. *Cancer Suppl.* **75,** 2021–2026.
12. Su, S. L., Huang, I. P., Fair, W. R., Powell, C. T., and Heston, W. D. W. (1995) Alternatively spliced variants of prostate-specific membrane antigen RNA: Ratio of expression as a potential measurement of progression. *Cancer Res.* **55,** 1441–1443.
13. O'Keefe, D. S., Uchida, A., Bacich, D. J., Watt, F. B., Martorana, A., Molloy, P. L., et al. (2000) Prostate-specific suicide gene therapy using the prostate-specific membrane antigen promoter and enhancer. *Prostate* **45,** 149–157.

14. Chang, S. S., Reuter, V. E., Heston, W. D. W., Hutchinson, B. Grauer, L. S., and Gaudin, P. B. (2000) Short term neoadjuvant therapy does not affect prostate specific membrane antigen expression in prostate tissues. *Cancer* **88,** 407–415.
15. Cuhna, G. R., Fujii, H., Neubauer, B. L., Shannon, J. M., Sawyer, L., and Reese, B. A. (1983) Epithelial-mesenchymal interactions in prostate development. I. Morphological bservations of prostatic induction by urogenital sinus mesenchyme in epithelium of the adult rodent urinary bladder. *J. Cell Biol.* **96,** 1662–1670.
16. Russell, P. J., Bennett, S., and Stricker, P. (1998) Growth factor involvement in progression of prostate cancer. *Clin. Chem.* **44,** 705–723.
17. Bosland, M. C., Chung, L. W. K., Greenberg, N. M., Ho, S-M., Isaacs, J. T., Lane, K., et al. (1996) Recent advances in the development of animal and cell culture models for prostate cancer research. A minireview. *Urol. Oncol.* **2,** 99–128.
18. Claas, F. H. J. and van Steenbrugge, G. J. (1983) Expression of HLA-like structures on a permanent human tumor line PC-93. *Tissue Antigens* **21,** 227–232.
19. Kaighn, M. E., Narayan, K. S., Ohnuki, Y., Lechner, J. F., and Jones, L. W. (1979) Establishment and characterization of a human prostatic carcinoma cell line (PC-3). *Invest. Urol.* **17,** 16–23.
20. Stone, K. R., Mickey, D. D., Wunderli, H., Mickey, G. H., and Paulson, D. F. (1978) Isolation of a human prostate carcinoma cell line (DU 145). *Int. J. Cancer* **21,** 274–281.
21. Iizumi, T., Yazaki, T., Kanoh, S., Kondo, I., and Koiso, K. (1987) Establishment of a new prostatic carcinoma cell (TSU-Pr1). *J. Urol.* **137,** 1304–1306.
22. Pettaway, C. A., Pathak, S., Greene, G., Ramirez, E., Wilson, M. R., Killion, J. J., et al. (1996) Selection of highly metastatic variants of different human prostatic carcinomas using orthotopic implantation in nude mice. *Clin. Cancer Res.* **2,** 1627–1636.
23. Rubio, N., Villacampa, M. M., and Blanco, J. (1998) Traffic to lymph nodes of PC-3 prostate tumor cells in nude mice visualized using the luciferase gene as a tumor cell marker. *Lab. Invest.* **78,** 1315–1325.
24. Horoszewicz, J. S., Leong, S. S., Chu, T. M., Wajsman, Z. L., Friedman, M., Papsidero, et al. (1980) The LNCaP cell line: A new model for studies on human prostatic carcinoma. *Prog. Clin. Biol. Res.* **37,** 115–132.
25. Gleave, M., Hsieh, J. T., Gao, C. A., von Eschenbach, A. C., and Chung, L. W. K. (1991) Acceleration of human prostate cancer growth in vivo by factors produced by prostate and bone fibroblasts. *Cancer Res.* **51,** 3753–3761.
26. Gleave, M. E., Hsieh, J. T., von Eschenbach, A. C., and Chung, L. W. K. (1992) Prostate and bone fibroblasts induce human prostate cancer growth in vivo: implications for bidirectional tumor-stromal interaction in prostate carcinoma growth and metastasis. *J. Urol.* **147,** 1151–1159.
27. Lim, D. J., Liu, X. L., Sutkowski, D. M., Braun, E. J., Lee, C., and Kozlowski, J. M. (1993) Growth of an androgen-sensitive human prostate cancer cell line, LNCaP, in nude mice. *Prostate* **22,** 109–118.
28. Chung, L. W. K., Gleave, M. E., Hsieh, J. T., Hong, S. J., and Zhau, H. E. (1991) Reciprocal mesenchymal-epithelial interaction affecting prostate cancer tumour growth and hormonal responsiveness. *Cancer Surv.* **11,** 91–121.

29. Wu, H.-C., Hsieh, J. T., Gleave, M. E., Brown, N. M., Pathak, S., and Chung, L. W. K. (1994) Derivation of androgen-independent LNCaP prostatic cancer cell sublines: Role of bone stromal cells. *Int. J. Cancer* **57,** 406–412.
30. Thalmann, G. N., Anezinis, P. E., Chang, S. M., Zhau, H. E., Kim, E. E., Hopwood, V. L., et al. (1994) Androgen-independent cancer progression and bone metastasis in the LNCaP model of human prostate cancer. *Cancer Res.* **54,** 2577–2581.
31. Sato, N., Gleave, M. E., Bruchovsky, N., Rennie, P. S., Beraldi, E., and Sullivan, L. D. (1997) A metastatic and androgen-sensitive human prostate cancer model using intraprostatic inoculation of LNCaP cells in SCID mice. *Cancer Res.* **57,** 1584–1589.
32. Umekita, Y., Hiipakka, R. A., Kokontis, J. M., and Liao, S. (1996) Human prostate tumor growth in athymic mice: inhibition by androgens and stimulation by finasteride. *Proc. Natl. Acad. Sci. USA* **93,** 11802–11807.
33. Culig, Z., Hoffmann, J., Erdel, M., Eder, I. E., Hobisch, A., Hittmair, A., et al. (1999) Switch from antagonist to agonist of the androgen receptor bicalutamide is associated with prostate tumour progression in a new model system. *Br. J. Cancer* **81,** 242–251.
34. Navone, N. M., Olive, M., Ozen, M., Davis, R., Troncoso, P., Tu, S. M., et al. (1997) Establishment of two human prostate cancer cell lines derived from a single bone metastasis. *Clin. Cancer Res.* **3,** 2493–2500.
35. Navone, N. M., Rodriquez-Vargas, M. C., Benedict, W. F., Troncoso, P., McDonnell, T. J., Zhou, J. H., Luthra, R., et al. (2000) TabBO: A model reflecting common molecular features of androgen-independent prostate cancer. *Clin. Cancer Res.* **6,** 1190–1197.
36. Plymate, S. R., Loop, S. M., Hoop, R. C., Wiren, K. M., Ostenson, R., Hryb, D. J., et al. (1991) Effects of sex hormone binding globulin (SHBG) on human prostatic carcinoma. *J. Steroid Biochem. Mol. Biol.* **40,** 833–839.
37. Liu, X. H., Wiley, H. S., and Meikle, A. W. (1993) Androgens regulate proliferation of human prostate cancer cells in culture by increasing transforming growth factor-α (TGF-α) and epidermal growth factor (EGF)/TGF-α receptor. *J. Clin. Endocrinol. Metab.* **77,** 1472–1478.
38. Loop, S. M., Rozanski, T. A., and Ostenson, R. C. (1993) Human primary prostate tumor cell line, ALVA-31: A new model for studying the hormonal regulation of prostate tumor cell growth. *Prostate* **22,** 93–108.
39. Zhuang, S. H., Schwartz, G. G., Cameron, D., and Burnstein, K. L. (1997) Vitamin D receptor content and transcriptional activity do not fully predict antiproliferative effects of vitamin D in human prostate cancer cell lines. *Mol. Cell. Endocrinol.* **126,** 83–90.
40. Tomita, K., van Bokhoven, A., Jansen, C. F., Bussemakers, M. J., and Schalken, J. A. (2000) Coordinate recruitment of E-cadherin and ALCAM to cell-cell contacts by alpha-catenin. *Biochem. Biophys. Res. Commun.* **267,** 870–874.
41. Yang, E. S., Maiorino, C. A., Roos, B. A., Knight, S. R., and Burnstein, K. L. (2002) Vitamin D-mediated growth inhibition of an androgen-ablated LNCaP cell line model of human prostate cancer. *Mol. Cell. Endocrinol.* **186,** 69–79.

42. Nakhla, A. M. and Rosner, W. (1994) Characterization of ALVA-41 cells, a new human prostatic cancer cell line. *Steroids* **59,** 586–589.
43. Sramkoski, R. M., Pretlow, T. G. II, Giaconia, J. M., Pretlow, T. P., Schwartz, S., Sy, M. S., et al. (1999) A new human prostate carcinoma cell line, 22Rv1. *In Vitro Cell Dev. Biol. Anim.* **35,** 403–409.
44. Zhau, H. Y., Chang, S. M., Chen, B. Q., Wang, Y., Zhang, H., Kao, C., et al. (1996) Androgen-repressed phenotype in human prostate cancer. *Proc. Natl. Acad. Sci. USA* **93,** 15152–15157.
45. Brothman, A. R., Lesho, L. J., Somers, K. D., Wright, G. L. Jr., and Merchant, D. J. (1989) Phenotypic and cytogenetic characterization of a cell line derived from primary prostatic carcinoma. *Int. J. Cancer* **44,** 898–903.
46. Brothman, A. R., Wilkins, P. C., Sales, E. W., and Somers, K. D. (1991) Metastatic properties of the human prostatic cell line, PPC-1, in athymic nude mice. *J. Urol.* **145,** 1088–1091.
47. Klein, K. A., Reiter, R. E., Redula, J., Moradi, H., Zhu, X. L., Brothman, A. R., et al. (1997) Progression of metastatic human prostate cancer to androgen independence in immunodeficient SCID mice. *Nat, Med.* **3,** 402–408.
48. Craft, N., Shostak, Y., Carey, M., and Sawyers, C. L. (1999) A mechanism for hormone-independent prostate cancer through modulation of androgen receptor signaling by the HER-2/neu tyrosine kinase. *Nat. Med.* **5,** 280–285.
49. Downing, S. R., Jackson P., and Russell P. J. (2002) Mutations within the tumour suppressor gene p53 are not confined to a late event in prostate cancer progression: A review of the evidence. *Urol. Oncol.* **6,** 103–110.
50. Gaddipatti, J. P., McLeod, D. G., Sesterhenn, I. A., Hussussian, C. J., Tong, Y. A., Seth, P., et al. (1997) Mutations of the p16 gene product are rare in prostate cancer. *Prostate* **30,** 188–194.
51. Wright, G. L. Jr, Grob, B. M., Haley, C. Grossman, K., Newhall, K., Petrylak, D., et al. (1996) Upregulation of prostate-specific membrane antigen after androgen-deprivation therapy. *Urology* **48,** 326–334.
52. Vlietstra, R. J., van Alewijk, D. C., Hermans, K. G., van Steenbrugge, G. J., and Trapman, J. (1998) Frequent inactivation of PTEN in prostate cancer cell lines and xenografts. *Cancer Res.* **58,** 2720–2723.
53. Wu, X., Senechal, K., Neshat, M. S., Whang, Y. E., and Sawyers, C. L. (1998) The PTEN/MMAC1 tumor suppressor phosphatase functions as a negative regulator of the phosphoinositide 3-kinase/Akt pathway. *Proc. Natl. Acad. Sci. USA* **95,** 15587–15591.
54. Paul, R., Ewing, C. M., Jarrard, D. F., and Isaacs, W. B. (1997) The cadherin cell-cell adhesion pathway in prostate cancer progression. *Br. J. Urol.* **79(Suppl. 1),** 37–43.
55. Ewing, C. M., Ru, N., Morton, R. A., Robinson, J. C., Wheelock, M. J., Johnson, K. R., et al. (1995) Chromosome 5 suppresses tumorigenicity of PC3 prostate cancer cells: Correlation with re-expression of alpha-catenin and restoration of E-cadherin function. *Cancer Res.* **55,** 4813–4817.
56. Bussemakers, M. J., Van Bokhoven, A., Tomita, K., Jansen, C. F., and Schalken, J. A. (2000) Complex cadherin expression in human prostate cancer cells. *Int. J. Cancer* **85,** 446–450.

57. Okazaki, M., Takeshita, S., Kawai, S., Kikuno, R., Tsujimura, A., Kudo, A., et al. (1994) Molecular cloning and characterization of OB-cadherin, a new member of cadherin family expressed in osteoblasts. *J. Biol. Chem.* **269,** 12092–12098.
58. Bae, V. L., Jackson-Cook, C. K., Brothman, A. R., Maygarden, S. J., and Ware, J. L. (1994) Tumorigenicity of SV40 T antigen immortalized human prostate epithelial cells: Association with decreased epidermal growth factor receptor expression. *Int. J. Cancer* **58,** 721–729.
59. Bello, D., Webber, M. M., Kleinman, H. K., Wartinger, D. D., and Rhim, J. S. (1997) Androgen responsive adult human prostatic epithelial cell lines immortalized by human papillomavirus 18. *Carcinogenesis* **18,** 1215–1223.
60. Rhim, J. S., Webber, M. M., Bello, D., Lee, M. S., Arnstein, P., Chen, L. S., et al. (1994) Stepwise immortalization and transformation of adult human prostate epithelial cells by a combination of HPV-18 and v-Ki-ras. *Proc. Natl. Acad. Sci. USA* **91,** 11874–11878.
61. Weijerman, P. C., van Drunen, E., Konig, J. J., Teubel, W., Romijn, J. C., Schroder, F. H., et al. (1997) Specific cytogenetic aberrations in two novel human prostatic cell lines immortalized by human papillomavirus type 18 DNA. *Cancer Genet. Cytogenet.* **99,** 108–115.
62. McNicol, P. J. and Dodd, J. G. (1991) High prevalence of human papillomavirus in prostate tissues. *J. Urol.* **145,** 850–853.
63. Anwar, K., Nakakuki, K., Shiraishi, T., Naiki, H., Yatani, R., and Inuzuka, M. (1992) Presence of ras oncogene mutations and human papillomavirus DNA in human prostate carcinomas. *Cancer Res.* **52,** 5991–5996.
64. Hukku, B., Mally, M., Cher, M. L., Peehl, D. M., Kung, H., and Rhim, J. S. (2000) Stepwise genetic changes associated with progression of nontumorigenic HPV-18 immortalized human prostate cancer-derived cell line to a malignant phenotype. *Cancer Genet. Cytogenet.* **120,** 117–126.
65. Webber, M. M., Trakul, N., Thraves, P. S., Bello-DeOcampo, D., Chu, W. W., Storto, P. D., et al. (1999) A human prostatic stromal myofibroblast cell line WPMY-1: A model for stromal-epithelial interactions in prostatic neoplasia. *Carcinogenesis* **20,** 1185–1192.
66. Bright, R. K., Vocke, C. D., Emmert-Buck, M. R., Duray, P. H., Solomon, D., Fetsch, P., et al. (1997) Generation and genetic characterization of immortal human prostate epithelial cell lines derived from primary cancer specimens. *Cancer Res.* **57,** 995–1002.
67. Lehr, J. E., Pienta, K. J., Yamazaki, K., and Pilat, M. J. (1998) A model to study c-myc and v-H-ras induced prostate cancer progression in the Copenhagen rat. *Cell. Mol. Biol.* **44,** 949–959.
68. Peehl, D. M., Sellers, R. G., and Wong, S. T. (1998) Defined medium for normal adult human prostatic stromal cells. *In Vitro Cell Development Biol. Anim.* **34,** 555–560.
69. Planz, B., Kirley, S. D., Wang, Q. F., Tabatabaei, S., Aretz, H. T., and Mcdougal, W. C. (1999) Characterization of a stromal cell model of the benign and malignant prostate from explant culture. *J. Urol.* **161,** 1329–1336.

70. Peehl, D. M. and Sellers, R. G. (1998) Basic FGF, EGF and PDGF modify TGF-beta-induction of smooth muscle cell phenotype in human prostatic stromal cells. *Prostate* **35,** 125–134.
71. Ide, H., Yoshida, T., Matsumoto, N., Aoki, K., Osada, Y., Sugimura, T., et al. (1997) Growth regulation of human prostate cancer cells by bone morphogenetic protein-2. *Cancer Res.* **57,** 5022–5027.
72. Soos, G., Jones, R. F., Haas, G. P., and Wang, C. Y. (1997) Comparative intraosseal growth of human prostate cancer cell lines LNCaP and PC-3 in the nude mouse. *Anticancer Res.* **17,** 4253–4258.
73. Wu, T. T., Sikes, R. A., Ciu, Q., Thalmann, G. N., Kao, C., Murphy, C. F., et al. (1998) Establishing human prostate cancer cell xenografts in bone: induction of osteoblastic reaction by prostate-specific antigen-producing tumors in athymic and SCID/bg mice using LNCaP and lineage-derived metastatic sublines. *Int. J. Cancer* **77,** 887–894.
74. Kocheril, S. V., Grignon, D. J., Wang, C. Y., Maughan, R. L., Montecillo, E. J., Talati, B., et al. (1999) Responsiveness of human prostate carcinoma bone tumors to interleukin-2 therapy in a mouse xenograft tumor model. *Cancer Detect. Prev.* **23,** 408–416.
75. Nemeth, J. A., Harb, J. F., Barroso, U. Jr., He, Z., Grignon, D. J., and Cher, M. L. (1999) Severe combined immunodeficient-hu model of human prostate cancer metastasis to human bone. *Cancer Res.* **59,** 1987–1993.
76. Yonou, H., Yokose, T., Kamijo, T., Kanomata, N., Hasebe, T., Nagai, K., et al. (2001) Establishment of a novel species- and tissue-specific metastasis model of human prostate cancer in humanized non-obese diabetic/severe combined immunodeficient mice engrafted with human adult lung and bone. *Cancer Res.* **61,** 2177–2182.
77. Gleave, M., Santo, N., Rennie, P. S., Goldenberg, S. L., Bruchovsky, N., and Sullivan, L. D. (1996) Hormone release and intermittent hormonal therapy in the LNCaP model of human prostate cancer. *Prog. Urol.* **6,** 375–385.
78. Sato, N., Sadar, M. D., Bruchovsky, N., Saatcioglu, F., Rennie, P. S., Sato, S., et al. (1997) Androgenic induction of prostate-specific antigen gene is repressed by protein-protein interaction between the androgen receptor and AP-1/c-Jun in the human prostate cancer cell line LNCaP. *J. Biol. Chem.* **272,** 17485–17494.
79. Jungwirth, A., Galvan, G., Pinski, J., Halmos, G., Szepeshazi, K., Cai, R. Z., et al. (1997) Luteinizing hormone-releasing hormone antagonist Cetrorelix (SB-75) and bombesin antagonist RC-3940-II inhibit the growth of androgen-independent PC-3 prostate cancer in nude mice. *Prostate* **32,** 164–172.
80. Lamharzi, N., Schally, A. V., and Koppan, M. (1998) Luteinizing hormone-releasing hormone (LH-RH) antagonist Cetrorelix inhibits growth of DU-145 human androgen-independent prostate carcinoma in nude mice and suppresses the levels and mRNA expression of IGF-II in tumors. *Regul. Pept.* **77,** 185–192.
81. Sica, G., Iacopino, F., Settesoldi, D., and Zelano, G. (1999) Effect of leuprorelin acetate on cell growth and prostate-specific antigen gene expression in human prostatic cancer cells. *Eur. Urol.* **35(Suppl 1),** 2–8.

82. Lamharzi, N., Schally, A. V., Koppan, M., and Groot, K. (1998) Growth hormone-releasing hormone antagonist MZ-5-156 inhibits growth of DU-145 human androgen-independent prostate carcinoma in nude mice and suppresses the levels and mRNA expression of insulin-like growth factor II in tumors. *Proc. Natl. Acad. Sci. USA* **95,** 8864–8868.
83. Diwan, M., Dawar, H., and Talwar, G.P. (1998) Induction of early and bioeffective antibody response in rodents with the luteinizing hormone-releasing hormone vaccine given as a single dose in biodegradable microspheres along with alum. *Prostate* **35,** 279–284.
84. Momma, T., Hamblin, M. R., and Hasan, T. (1997) Hormonal modulation of the accumulation of 5-aminolevulinic acid-induced protoporphyrin and phototoxicity in prostate cancer cells. *Int. J. Cancer* **72,** 1062–1069.
85. Momma, T., Hamblin, M. R., Wu, H. C., and Hasan, T. (1998) Photodynamic therapy of orthotopic prostate cancer with benzoporphyrin derivative: Local control and distant metastasis. *Cancer Res.* **58,** 5425-5431.
86. Romijn, J. C., Verkoelen, C. F., and Schroeder, F. H. (1988) Application of the MTT assay to human prostate cancer cell lines in vitro: Establishment of test conditions and assessment of hormone-stimulated growth and drug-induced cytostatic and cytotoxic effects. *Prostate* **12,** 99–110.
87. Horoszewicz, J. S., Leong, S. S., Kawinski, E., Karr, J. P., Rosenthal, H., Chu, T. M., et al. (1983) LNCaP model of human prostatic carcinoma. *Cancer Res.* **43,** 1809–1818.
88. Gleave, M., Hsieh, J.-T., Gao, C., von Eschenbach, A. C., and Chung, L. K. W. (1991) Acceleration of human prostate cancer growth in vivo by factors produced by prostate and bone fibroblasts. *Cancer Res.* **51,** 3753–3761.
89. Hoosein, N. M., Logothetis, C. J., and Chung, L. W. K. (1993) Differential effects of peptide hormones bombesin, vasoactive intestinal polypeptide and somatostatin analog RC-160 on the invasive capacity of human prostatic carcinoma cells. *J. Urol.* **149,** 1209–1213.
90. van Bokhoven, A., Varella-Garcia, M., Korch, K., and Miller, G. J. (2001) TSU-Pr1 and JCA-1 cells are derivatives of T24 bladder carcinoma cells and are not of prostatic origin. *Cancer Res.* **61,** 6340–6344.
91. Varella-Garcia, M., Boomer, T., and Miller, G. J. (2001) Karyotypic similarity identified by multiplex-FISH relates four prostate adenocarcinoma cell lines: PC-3, PPC-1, ALVA-31, and ALVA-41. *Genes Chrom. Cancer* **31,** 303–315.
92. Carroll, A. G., Voeller, H. J., Sugars, L., and Gelmann, E. P (1993) p53 oncogene mutations in three human prostate cancer cell lines. *Prostate* **23,** 123–134.
93. Isaacs, W. B., Carter, R. S., and Ewing, C. M. (1991) Wild-type p53 suppresses growth of human prostate cancer cells containing mutant p53 alleles. *Cancer Res.* **51,** 4716–4720.

# 3

# Growth of Prostatic Epithelial and Stromal Cells In Vitro

**Donna M. Peehl**

## 1. Introduction

Well-established techniques are now in place to culture several of the major types of cells in the prostate. Epithelial cells with characteristics of basal and/or secretory luminal cells can be grown in vitro, as can stromal cells with properties of fibroblasts and/or smooth muscle. In most cases, serum-free media are available for epithelial or stromal cell cultures. Methods have been developed to establish and investigate the properties of cocultures of prostatic epithelial and stromal cells. Use of these in vitro cell cultures has provided much of the information that guides current ideas about prevention and treatment of prostate cancer.

## 2. Materials

### 2.1. Collagen-Coated Dishes

The procedure for collagen-coated dishes is as follows: mix one part of cold, sterile collagen type I (Cohesion, Palo Alto, CA) with three parts of cold, sterile 0.013 *N* HCl. Aliquot into tissue culture dishes (0.2 mL per 35-mm dish, 0.3 mL per 60-mm dish, and 0.5 mL per 100-mm dish). Tilt and gently shake dishes until collagen solution is evenly distributed over bottom of each dish, then stack them in cupboards and allow them to dry for at least 3 d before use.

### 2.2. HEPES-Buffered Saline (HBS)

The procedure for obtaining HBS is as follows: 30 m*M* HEPES (238.3 g/20 L), 4 m*M* glucose (14.42 g/20 L), 3 m*M* KCl (4.48 g/20 L), 130 m*M* NaCl (151.94 g/20 L), 1 m*M* $Na_2HPO_4 \cdot 7H_2O$ (5.36 g/20 L), 0.0033 m*M* Phenol red·Na salt (0.02 g/20 L). All reagents can be purchased from Sigma-Aldrich

From: *Methods in Molecular Medicine, Vol. 81: Prostate Cancer Methods and Protocols*
Edited by: P. J. Russell, P. Jackson, and E. A. Kingsley © Humana Press Inc., Totowa, NJ

(St. Louis, MO). HEPES is then dissolved in ~19 L of $H_2O$. Bring the pH to 7.6 with 4 *N* NaOH. Add the rest of the components, dissolve, and bring the solution to a final volume of 20 L with $H_2O$ and store at –20°C for 1 yr, sterile, in 500-mL aliquots. Thawed HBS can be stored at 4°C for several months.

### 2.3. Trypsin/EDTA (T/E)

The procedure for T/E is as follows: dissolve 0.4 g of trypsin and then 0.4 g of EDTA·$Na_4$ salt in 180 mL of HBS. Bring to final volume of 200 mL with HBS and then store at –20°C, sterilized, in 5- or 10-mL aliquots. T/E should be thawed just before use and should not be frozen/thawed more than a few times.

### 2.4. Trypsin Inhibitor (TI)

The procedure for TI is as follows: dissolve 1 g of trypsin inhibitor in 900 mL of HBS. Bring to final volume of 1000 mL with HBS and store at 4°C, sterilized, in 50-mL aliquots for several months.

### 2.5. PFMR-4A Stock Solutions

**Stock 1A (50X)**

| Component | MW | Concentration in stock | Amount in stock (g/2 L) |
|---|---|---|---|
| L-arginine · HCl | 210.7 | $1 \times 10^{-1}$ *M* | 42.14 |
| Choline chloride | 139.6 | $5 \times 10^{-3}$ *M* | 1.40 |
| L-histidine · HCl · $H_2O$ | 209.6 | $1 \times 10^{-2}$ *M* | 4.19 |
| L-isoleucine | 131.2 | $3 \times 10^{-2}$ *M* | 7.87 |
| L-leucine | 131.2 | $1 \times 10^{-1}$ *M* | 26.24 |
| L-lysine · HCl · $H_2O$ | 182.7 | $2 \times 10^{-2}$ *M* | 7.31 |
| L-methionine | 149.2 | $3 \times 10^{-2}$ *M* | 8.95 |

Gentle warming (not too hot) while stirring will help components dissolve. After thawing, the solution must be warmed to 37°C to dissolve the precipitate. The solution can then be stored at –20°C for 1 yr in 400-mL aliquots.

**Stock 1B (50X)**

| Component | MW | Concentration in stock | Amount in stock (g/2 L) |
|---|---|---|---|
| L-phenylalanine | 165.2 | $3 \times 10^{-3}$ *M* | 0.99 |
| L-serine | 105.1 | $1 \times 10^{-2}$ *M* | 2.10 |
| L-threonine | 119.1 | $1 \times 10^{-1}$ *M* | 23.82 |
| L-tryptophan | 204.2 | $1 \times 10^{-3}$ *M* | 0.41 |
| L-valine | 117.2 | $1 \times 10^{-2}$ *M* | 2.34 |

After thawing, warm the solution to 37°C to dissolve the precipitate. The solution can then be stored at –20°C for 1 yr, in the dark, in 400-mL aliquots.

**Stock 1C (50X)**

| Component | MW | Concentration in stock | Amount in stock (g/2 L) |
|---|---|---|---|
| L-tyrosine | 181.2 | $3 \times 10^{-3}$ *M* | 1.09 |

Dissolve the solid in 100 mL of 4 *N* NaOH, dilute to 2 L with $H_2O$. The solution can be stored at –20°C for 1 yr in 400-mL aliquots.

**Stock 2 (100X)**

| Component | MW | Concentration in stock | Amount in stock (g/L) |
|---|---|---|---|
| Biotin | 244.3 | $3 \times 10^{-5}$ *M* | 0.007 |
| Ca · pantothenate | 238.3 | $1 \times 10^{-4}$ *M* | 0.024 |
| Niacinamide | 122.1 | $3 \times 10^{-5}$ *M* | 0.004 |
| Pyridoxine · HCl | 205.7 | $3 \times 10^{-5}$ *M* | 0.006 |
| Thiamine · HCl | 337.5 | $1 \times 10^{-4}$ *M* | 0.034 |
| KCl | 74.6 | $3.8 \times 10^{-1}$ *M* | 28.348 |

The solution can be stored at –20°C for 1 yr in 200-mL aliquots.

**Stock 3 (100X)**

| Component | MW | Concentration in stock | Amount in stock (g/L) |
|---|---|---|---|
| $Na_2HPO_4 \cdot 7H_2O$ | 268.1 | $8.1 \times 10^{-2}$ *M* | 21.72 |
| Folic acid | 441.4 | $3 \times 10^{-4}$ *M* | 0.13 |

Completely dissolve the $Na_2HPO_4 \cdot 7H_2O$ before adding the folic acid. Be sure that the folic acid dissolves completely. The solution can be stored at –20°C for 1 yr, in the dark, in 200-mL aliquots.

**Stock 4 (100X)**

| Component | MW | Concentration in stock | Amount in stock (g/500 L) |
|---|---|---|---|
| $FeSO_4 \cdot 7H_2O$ | 278.0 | $3 \times 10^{-4}$ *M* | 0.04 |
| $MgCl_2 \cdot 6H_2O$ | 203.3 | $5.2 \times 10^{-2}$ *M* | 5.29 |
| $MgSO_4 \cdot 7H_2O$ | 246.5 | $1.6 \times 10^{-2}$ *M* | 1.97 |
| $CaCl_2 \cdot 2H_2O$ | 147.0 | $9.2 \times 10^{-2}$ *M* | 6.76 |

Add 5 drops of concentrated HCl per 500 mL of Stock 4 to prevent precipitate of ferric hydroxides. The solution can be stored at room temperature for 1 yr in bottles tightly sealed with caps wrapped in parafilm, sterile, in 50-mL aliquots.

**Stock 5 (1000X)**

| Component | MW | Concentration in stock | Amount in stock (g/100 mL) |
|---|---|---|---|
| Phenol red · Na salt | 376.4 | $5.9 \times 10^{-3}$ *M* | 0.22 |

The solution can be stored at room temperature for 1 yr, sterilized, in 20-mL aliquots.

**Stock 6B (100X)**

| Component | MW | Concentration in stock | Amount in stock (g/L) |
|---|---|---|---|
| Sodium pyruvate | 110.0 | $2 \times 10^{-1}$ *M* | 22.0 |

The solution can be stored at –20°C for 1 yr in 200-mL aliquots.

**Stock 6C (100X)**

| Component | MW | Concentration in stock | Amount in stock (g/L) |
|---|---|---|---|
| Riboflavin | 376.4 | $1 \times 10^{-5}$ *M* | 0.004 |

Riboflavin is difficult to dissolve and requires extensive stirring. Cover with foil while stirring. The solution can be stored at –20°C for 1 yr, in the dark, in 200-mL aliquots.

**Stock 7 (100X)**

| Component | MW | Concentration in stock | Amount in stock (g/200 mL) |
|---|---|---|---|
| L-cystine | 240.3 | $1.5 \times 10^{-2}$ *M* | 0.72 |

Dissolve in ~180 mL of $H_2O$; while stirring, add concentrated HCl dropwise until the cystine has solubilized. Bring the solution to a final volume of 200 mL with $H_2O$. This solution should be made fresh.

**Stock 8 (100X)**

| Component | MW | Concentration in stock | Amount in stock (g/L) |
|---|---|---|---|
| L-asparagine | 150.1 | $2 \times 10^{-2}$ *M* | 3.00 |
| L-proline | 115.1 | $6 \times 10^{-2}$ *M* | 6.91 |
| Putrescine · 2HCl | 161.1 | $2 \times 10^{-4}$ *M* | 0.032 |
| Vitamin $B_{12}$ | 1355.4 | $1 \times 10^{-4}$ *M* | 0.136 |

The solution can be stored at –20°C for 1 yr, in the dark, in 200-mL aliquots.

**Stock 9 (100X)**

| Component | MW | Concentration in stock | Amount in stock (g/L) |
|---|---|---|---|
| L-aspartate | 133.1 | $2 \times 10^{-2}$ *M* | 2.66 |
| L-glutamate | 147.1 | $2 \times 10^{-2}$ *M* | 2.94 |
| L-alanine | 89.09 | $2 \times 10^{-2}$ *M* | 1.78 |
| Glycine | 75.1 | $2 \times 10^{-2}$ *M* | 1.50 |

Aspartate and glutamate are added to 900 mL of $H_2O$ containing 1 mL of Stock 5 (phenol red). While stirring, 4 *N* NaOH is added dropwise to maintain neutrality (pinkish orange) as the aspartate and glutamate dissolve. Alanine and glycine are then added and dissolved. Bring to a final volume of 1 L with $H_2O$. The solution can be stored at –20°C for 1 yr in 200-mL aliquots.

**Stock 10 (100X)**

| Component | MW | Concentration in stock | Amount in stock (g/L) |
|---|---|---|---|
| Hypoxanthine | 136.1 | $3 \times 10^{-3}$ *M* | 0.408 |
| 6,8-thioctic acid | 206.3 | $1 \times 10^{-4}$ *M* | 0.021 |
| Myo-inositol | 180.2 | $1 \times 10^{-1}$ *M* | 18.02 |
| Thymidine | 242.2 | $3 \times 10^{-3}$ *M* | 0.73 |
| $CuSO_4 \cdot 5H_2O$ | 249.7 | $1 \times 10^{-6}$ *M* | 0.00025 |

Hypoxanthine is dissolved in 100 mL of boiling $H_2O$ before adding to the stock. Thioctic acid is dissolved in a few drops of 1 *N* NaOH, diluted with 10 mL of $H_2O$, then added to the stock. $CuSO_4 \cdot 5H_2O$ is prepared by dissolving 0.025 g in 1 L of $H_2O$; 10 mL of this are added to the stock. The solution can be stored at –20°C for 1 yr, in the dark, in 200-mL aliquots.

**Stock 11 (1000X)**

| Component | MW | Concentration in stock | Amount in stock (g/100mL) |
|---|---|---|---|
| $ZnSO_4 \cdot 7H_2O$ | 287.5 | $5 \times 10^{-4}$ *M* | 0.014 |

The solution can be stored at room temperature for 1 yr, sterilized, in 10-mL aliquots.

### 2.6. Preparation of PFMR-4A (20 L)

Add to ~14 L of $H_2O$ in a carboy while stirring the following ingredients:

| Stock | Concentration | Amount (mL) |
|---|---|---|
| 1A | 50× | 400 |
| 1B | 50× | 400 |
| 1C | 50× | 400 |
| 2 | 100× | 200 |
| 3 | 100× | 200 |
| 5 | 1000× | 20 |
| 6B | 100× | 200 |
| 6C | 100× | 200 |
| 7 | 100× | 200 |
| 8 | 100× | 200 |
| 9 | 100× | 200 |
| 10 | 100× | 200 |

| Component | MW | Final concentration | Amount in stock (g/20 L) |
|---|---|---|---|
| Glucose | 180.2 | $7 \times 10^{-3}$ *M* | 25.23 |
| NaCl | 58.45 | $1 \times 10^{-1}$ *M* | 116.9 |
| $KH_2PO_4$ | 136.1 | $4.3 \times 10^{-4}$ *M* | 1.17 |
| L-glutamine | 146.1 | $2 \times 10^{-2}$ *M* | 58.44 |
| HEPES | 238.3 | $3 \times 10^{-2}$ *M* | 142.98 |

Bring pH to 7.4 with 4 *N* NaOH, then add:

| Component | MW | Final concentration | Amount in stock (g/20 L) |
|---|---|---|---|
| $NaHCO_3$ | 84.0 | $1.4 \times 10^{-2}$ *M* | 23.52 |

Bring to a final volume of 19,780 mL with $H_2O$. Mix well and filter sterilize through a 0.22-µm filter. The solution can be stored at –20°C for 1 yr, sterilized, in 494.5-mL aliquots. To finish the preparation, thaw, and then add 5 mL of sterile Stock 4 and 0.5 mL of sterile Stock 11 to each aliquot of 494.5 mL. Store at 4°C for up to 2 mo.

### 2.7. Cholera Toxin (CT)

The procedure for CT is as follows: add 1 mL of sterile $H_2O$ to a sterile vial containing 1 mg of CT (List Biological Laboratories, Inc., Campbell, CA) and swirl to dissolve. Then, transfer 1 mL of this 1 mg/mL solution to a sterile tube containing 9 mL of sterile $H_2O$; mix. Transfer 1-mL aliquots of this 100 µg/mL solution to sterile tubes and store at 4°C. CT should not be frozen.

### 2.8. Epidermal Growth Factor (EGF)

The procedure for EGF is as follows: add 1 mL of sterile $H_2O$ to a sterile vial containing 100 µg of EGF (Collaborative Biomedical Products, Bedford, MA). Swirl to dissolve, and transfer 100-µL aliquots of this 100 µg/mL solution to sterile tubes. EGF can be stored at –20°C until needed, then thaw and store at 4°C for 2 mo. EGF should not be refrozen.

### 2.9. Bovine Pituitary Extract (BPE)

BPE can be purchased from Hammond Cell/Tech (Alameda, CA) and should be stored at –70°C. To prepare for use in cell culture, thaw a bottle at 37°C and swirl to mix. Centrifuge the solution at 13,218*g* for 10 min to pellet any insoluble material. Repeat 2×. Pass the supernatant through a 0.45-µm filter. Finally, filter sterilize through a 0.22-µm filter. The extract is 14 mg/mL. BPE can be stored in 2-mL aliquots in sterile tubes at –20°C until needed, then thawed and stored at 4°C for 2 mo. BPE should not be refrozen.

### 2.10. Phosphoethanolamine (PEA)

Prepare a 0.1 *M* solution of PEA by dissolving 0.7 g of *o*-phosphorylethanolamine (Sigma-Aldrich) in ~45 mL of $H_2O$; bring the solution to a final volume of 50 mL, filter sterilize, and then store as 5-mL aliquots in sterile tubes at –20°C. PEA may be freeze/thawed.

### 2.11. Hydrocortisone (HC)

The procedure for preparing HC is as follows: prepare a 10 mg/mL solution by dissolving 100 mg of hydrocortisone (Sigma-Aldrich) in 10 mL of 100% ethanol. Transfer 1-mL aliquots into sterile tubes and store tightly sealed at room temperature.

### 2.12. Selenium (SE)

The procedure for SE is as follows: prepare a $3 \times 10^{-2}$ *M* solution by dissolving 0.039 g of selenious acid ($H_2SeO_3$) (Sigma-Aldrich) in 10 mL of $H_2O$. Filter sterilize, then transfer 0.1 mL of this solution into 9.9 mL of sterile $H_2O$; mix. Transfer 1-mL aliquots of this sterile $3 \times 10^{-4}$ *M* solution into sterile tubes and store at room temperature.

### 2.13. Gentamicin (GENT)

The procedure for preparing GENT is as follows: prepare a 40 mg/mL solution by dissolving 4 g of gentamicin sulfate (Sigma-Aldrich) in 100 mL of $H_2O$ and filter sterilize. Then, transfer 5-mL aliquots into sterile tubes and store at room temperature.

### 2.14. Retinoic Acid (RA)

The procedure for RA is as follows: prepare a 1 mg/mL ($3 \times 10^{-3}$ *M*) solution by dissolving 1 mg of all-*trans* retinoic acid (Sigma-Aldrich) in 1 mL of dimethylsulfoxide (DMSO). This solution is considered sterile. Store at –20°C, in the dark, as 25-µL aliquots in sterile amber tubes. (The solution may be frozen/thawed twice, but then it must be discarded.) Then, transfer 20 µL of a 1 mg/mL stock solution of all-*trans* retinoic acid to a tube containing 1.98 mL of DMSO; mix well. Then, transfer 100 µL of this 10 µg/mL solution to a tube containing 9.9 mL of DMSO and mix well. This solution is considered sterile and is 0.1 µg/mL ($3 \times 10^{-7}$ *M*). Store at –20°C, in the dark, as 25-µL aliquots in sterile amber tubes. Thaw fresh each day and discard any leftovers.

### 2.15. Insulin (IN)

The procedure for IN is as follows: add 25 mL of sterile $H_2O$ to a sterile vial containing 100 mg of insulin (Collaborative Biomedical Products), swirling to dissolve. Then, transfer 2-mL aliquots into sterile tubes and store at –20°C. After thawing an aliquot, store at 4°C for up to 2 mo (do not refreeze).

### 2.16. Vitamin E (VIT E)

The procedure for VIT E is as follows: transfer 100 µL of 100% α-tocopherol (Sigma-Aldrich) to a sterile tube containing 9.9 mL of DMSO. Tocopherol is very sticky, so try to get all of it rinsed off of the tip into the DMSO; then, vortex to sol-

ubilize. This solution is considered sterile and is $2.3 \times 10^{-2}$ *M*. Store at –20°C, in the dark, as 1-mL aliquots in sterile amber tubes. May be freeze/thawed.

### 2.17. MCDB 105

Prepare and store MCDB 105 medium according to manufacturer's instructions (Sigma-Aldrich).

### 2.18. Complete PFMR-4A

| Component (subheading) | Concentration of stock | Amount to add | Final concentration |
|---|---|---|---|
| PFMR-4A (**2.6**) | | 500 mL | |
| CT (**2.7**) | 100 µg/mL | 50 µL | 10 ng/mL |
| EGF (**2.8**) | 100 µg/mL | 50 µL | 10 ng/mL |
| BPE (**2.9**) | 14 mg/mL | 1.4 mL | 40 µg/mL |
| PEA (**2.10**) | 0.1 *M* | 500 µL | 0.1 m*M* |
| HC (**2.11**) | 10 mg/mL | 50 µL | 1 µg/mL |
| SE (**2.12**) | $3 \times 10^{-4}$ *M* | 50 µL | $3 \times 10^{-8}$ *M* |
| GENT (**2.13**) | 40 mg/mL | 1.25 mL | 100 µg/mL |
| RA (**2.14**) | 0.1 µg/mL | 50 µL | 0.01 ng/mL |
| IN (**2.15**) | 4 mg/mL | 500 µL | 4 µg/mL |
| VIT E (**2.16**) | $2.3 \times 10^{-2}$ *M* | 50 µL | $2.3 \times 10^{-6}$ *M* |

Mix together sterile components and store up to 2 wk at 4°C.

### 2.19. Complete MCDB 105

| Component (subheading) | Concentration of stock | Amount to add | Final concentration |
|---|---|---|---|
| MCDB 105 (**2.17**) | | 500 mL | |
| CT (**2.7**) | 100 µg/mL | 50 µL | 10 ng/mL |
| EGF (**2.8**) | 100 µg/mL | 50 µL | 10 ng/mL |
| BPE (**2.9**) | 14 mg/mL | 357 µL | 10 µg/mL |
| PEA (**2.10**) | 0.1 *M* | 500 µL | 0.1 m*M* |
| HC (**2.11**) | 10 mg/mL | 50 µL | 1 µg/mL |
| SE (**2.12**) | $3 \times 10^{-4}$ *M* | 50 µL | $3 \times 10^{-8}$ *M* |
| GENT (**2.13**) | 40 mg/mL | 1.25 mL | 100 µg/mL |
| RA (**2.14**) | 0.1 µg/mL | 50 µL | 0.01 ng/mL |
| IN (**2.15**) | 4 mg/mL | 500 µL | 4 µg/mL |
| VIT E (**2.16**) | $2.3 \times 10^{-2}$ *M* | 50 µL | $2.3 \times 10^{-6}$ *M* |

Mix together sterile components. MCDB 105 can be stored up to 2 wk at 4°C.

### 2. 20. MCDB 105 with 10% Fetal Bovine Serum (FBS) and GENT

The procedure is as follows: to 90 mL of MCDB 105 (*see* **Subheading 2.17.**), add 10 mL of FBS and 100 µg/mL of GENT (*see* **Subheading 2.13.**). Store at 4°C for up to 2 wk.

## 3. Methods

### 3.1. Primary Culture of Human Prostatic Epithelial Cells (see Note 1)

1. Collect a prostate tissue sample in a tube containing 5 mL of cold HBS (*see* **Subheading 2.2.**).
2. Store this tissue at 4°C for up to several hours if you are unable to process it immediately.
3. Transfer the tissue from the tube into a sterile dish (one piece per 60-mm dish).
4. Rinse tissue twice with HBS (*see* **Subheading 2.2.**) (5 mL per rinse).
5. Leave the tissue in the final HBS rinse and mince it into small pieces (~1 $mm^3$) using sterile scissors and tweezers.
6. With a broken-tip, stuffed pipet, transfer the pieces of tissue to a sterile 15-mL centrifuge tube. Pellet the pieces using a clinical centrifuge at full speed for 5 min.
7. Resuspend the tissue pieces in complete PFMR-4A (*see* **Subheading 2.18.**) containing 40 U/mL of Type 1 collagenase (Sigma-Aldrich; cat. no. C-0130), made fresh and filter sterilized.
8. Rock at 37°C overnight.
9. Pipet the digested tissue up and down vigorously with a 5-mL pipet to break up any remaining clumps.
10. Pellet the tissue using a clinical centrifuge at full speed for 5 min.
11. Rinse twice with HBS (*see* **Subheading 2.2.**), repeating **steps 9** and **10.**
12. Resuspend the pellet in 5 mL of complete PFMR-4A (*see* **Subheading 2.18.**) and transfer to one 60-mm, collagen-coated dish (*see* **Subheading 2.1.**). Incubate at 37°C in a humidified incubator containing 95% air/5% $CO_2$. Feed with complete PFMR-4A (*see* **Subheading 2.18.**) every 3–4 d.

### 3.2. Freezing Epithelial Cells (see Note 2)

1. Rinse cells once with HBS (*see* **Subheading 2.2**).
2. Add T/E (*see* **Subheading 2.3.**): 0.3 mL per 35-mm dish, 0.5 mL per 60-mm dish, and 1 mL per 100-mm dish.
3. Incubate at 37°C until the cells detach (1–5 min).
4. Resuspend the cells with TI (*see* **Subheading 2.4.**). Use 5 mL to suspend the cells and transfer them into a centrifuge tube, then another 5 mL to rinse the dish again.
5. Pellet the cells using a clinical centrifuge at full speed for 5 min.

6. Resuspend the cell pellet in Complete PFMR-4A (*see* **Subheading 2.18.**) plus 10% DMSO and 10% FBS at $10^4$ cells/mL. Transfer 1 mL aliquots into each cryotube. Seal tightly. When freezing multiple ampules of cells (>20), keep the cells on ice while aliquoting them into cryotubes.
7. Transfer the cryotubes to 4°C; do not place them in Styrofoam trays or any other container that would impede airflow. Store at 4°C for exactly 3 h.
8. Transfer the cryotubes to –70°C, overnight (again, be sure that air can freely circulate around cryotubes).
9. Transfer the cryotubes into a liquid nitrogen freezer for long-term storage.

### 3.3. Thawing Epithelial Cells (see Note 3)

1. Remove a cryotube from the liquid nitrogen freezer.
2. Place the cryotube in a 37°C water bath.
3. Agitate the cryotube to thaw quickly.
4. After making sure that the cryotube is tightly sealed, squirt the area around the lip with 95% ethanol. Use a Kimwipe to blot any excess ethanol from the depression in the cryotube cap, but do not touch the lip area.
5. Allow the area to dry thoroughly.
6. Transfer the contents of cryotube into a centrifuge tube containing 10 mL of HBS (*see* **Subheading 2.2.**). Pellet the cells using a clinical centrifuge at full speed for 5 min.
7. Resuspend the cell pellet in complete MCDB 105 (*see* **Subheading 2.19.**) and transfer the cells into a collagen-coated dish (*see* **Subheading 2.1.**). Incubate at 37°C in humidified incubator with 95% air/5% $CO_2$.
8. Feed the cells every 3–4 d with complete MCDB 105 (*see* **Subheading 2.19.**) and passage when ~50% confluent.

### 3.4. Passaging Epithelial Cells (see Note 4)

1. Follow **steps 1–5 of** Subheading 3.2.
2. Resuspend the cell pellet in Complete MCDB 105 (*see* **Subheading 2.19.**).
3. Transfer the cells to collagen-coated dishes (*see* **Subheading 2.1.**) at 200 cells per 60-mm dish (for clonal growth), or at densities ranging from $10^3$ to $10^4$ cells per 35-mm dish, $10^4$ to $10^5$ cells per 60-mm dish, or $10^5$ to $10^6$ cells per 100-mm dish.
4. Feed with complete MCDB 105 (*see* **Subheading 2.19.**) every 3–4 d until ~50% confluent. At this time, either passage or feed with Complete PFMR-4A (*see* **Subheading 2.18.**) every 3–4 d until the cells reach confluency.

### 3.5. Primary Culture of Human Prostatic Stromal Cells (see Note 5)

1. Follow **steps 1–11** of **Subheading 3.1.**
2. Resuspend the pellet in 5 mL of MCDB 105 (*see* **Subheading 2.17.**) with 10% FBS and 100 µg/mL GENT (*see* **Subheading 2.13.**). Transfer to one 60-mm tissue culture dish (not collagen-coated). Incubate.

3. Feed every 3–4 d after the cells attach until the stromal cells have grown out and are semiconfluent.

### 3.6. Freezing Stromal Cells (see Note 6)

1. Rinse the dish twice with HBS (*see* **Subheading 2.2.**).
2. Add T/E (*see* **Subheading 2.3.**), 0.3 mL per 35-mm dish, 0.5 mL per 60-mm dish, and 1 mL per 100-mm dish).
3. Incubate at 37°C until the cells detach (3–5 min).
4. Resuspend the cells with MCDB 105 (*see* **Subheading 2.17.**) containing 10% FBS and 100 µg/mL GENT (*see* **Subheading 2.13.**). Use 5 mL to resuspend the cells and transfer into a centrifuge tube then another 5 mL to rinse the dish.
5. Pellet the cells using a clinical centrifuge at full speed for 5 min.
6. Resuspend the cell pellet in MCDB 105 (*see* **Subheading 2.17.**) with 10% FBS and 100 µg/mL GENT (*see* **Subheading 2.13.**) and 10% DMSO at $5 \times 10^5$ cells per mL. Transfer 1-mL aliquots into each cryotube and seal tightly.
7. Follow **steps 7–9** of **Subheading 3.3.**

### 3.7. Thawing Stromal Cells (see Note 7)

1. Follow **steps 1–6** of **Subheading 3.3.**
2. Resuspend the cell pellet in MCDB 105 (*see* **Subheading 2.17.**) with 10% FBS and 100 µg/mL GENT (*see* **Subheading 2.13.**). Transfer the suspension into a tissue culture dish. Incubate at 37°C in a humidified incubator with 95% air/5% $CO_2$.
3. Feed the cells every 3–4 d with MCDB 105 (*see* **Subheading 2.17.**) and 10% FBS and 100 µg/mL GENT (*see* **Subheading 2.13.**). Passage when ~90% confluent.

### 3.8. Passaging Stromal Cells (see Note 8)

1. Follow **steps 1–5** of **Subheading 3.6.**
2. Resuspend the cells in MCDB 105 (*see* **Subheading 2.17.**) with 10% FBS and 100 µg/mL GENT (*see* **Subheading 2.13.**).
3. Transfer the cells to tissue culture dishes at the desired densities.
4. Feed with MCDB 105 (*see* **Subheading 2.17.**) with 10% FBS and 100 µg/mL GENT (*see* **Subheading 2.13.**) every 3 to 4 d until the desired confluency is reached.

## 4. Notes

1. A common tendency when establishing primary cell cultures is to think that the more tissue, the better. In fact, the opposite is true when establishing primary cultures of prostatic cells. The prostate is very heterogeneous, both at the tissue as well as the cellular level. Small tissue samples are obtained from radical or suprapubic prostatectomy specimens, from transurethral resections of the prostate, or from biopsies ***(1)***. Specimens are processed in such a way that histological assessment of the tissue of origin can be obtained from adjacent fixed or frozen sections.

   Typically, we dissect a small piece of tissue (~0.1 $mm^3$) from a radical prostatectomy specimen. The cut edges of the specimen are inked to mark the area, and

then the prostate is fixed, cut, and blocked ***(2)***. Histological assessment of tissue sections adjacent to the area removed for culture reveals whether the tissue of origin was normal, benign prostatic hyperplasia (BPH) or malignant.

Accurate histological assessment and histological purity of the tissue is essential because it is the main criterion for characterizing a primary culture as normal, BPH, or cancer. Until recently, few markers were available to distinguish cells from different origins in culture. Cytogenetic abnormalities were observed in primary cultures derived from adenocarcinomas ***(3)***, but no consistent abnormality was identified to use as a marker. Similarly, differences in growth rate and differential responses to growth factors between a culture derived from cancer versus another from a normal tissue was reported ***(4)***, but we have not observed any consistent differences of this type in the primary cultures that we have established from normal and malignant tissues.

Several recent developments, however, promise to yield new markers that can verify the origin of cells in culture as well as perhaps be used to separate subpopulations of cells from tissues for culture. Liu and co-workers ***(5)*** established the profile of expression of cluster of differentiation antigens by cell types in prostatic tissues, and identified particular cluster of differentiation antigens expressed differently by cancer versus normal cells. These investigators then used these cell surface molecules to sort live cells from tissues. This approach may permit the isolation of cancer cells from mixed cell populations and the direct establishment of these cells in culture. We recently identified a feature of primary cultures of cancer cells that may also definitely identify cancer cells in culture. In studies related to the role of vitamin D in prostate biology, we discovered that cancer cells have significantly less activity of the enzyme 1$\alpha$-hydroxylase than cells derived from normal tissues or BPH ***(6)***. Greater than 95% of the cancer-derived cultures had 10-fold or more less activity of this enzyme, clearly distinguishing the cultures of different origins.

Other markers are used to verify the epithelial nature of primary cultures and to evaluate their differentiated status. Typically, prostatic epithelial cultures express cytokeratins found in both basal and luminal epithelial cells in tissues (cytokeratins 5, 14, 8, and 18) ***(7–9)***. Whether this pattern of keratin expression is evidence of differentiation in culture is uncertain. Clearly, keratin expression is malleable and the culture environment can modulate keratin expression ***(10,11)***. Several of the most characteristic markers of secretory differentiation, such as expression of prostate-specific antigen and the androgen receptor, are generally not seen in monolayer cultures. Coculture with prostatic stromal cells, however, has been reported to induce expression of these secretory markers in prostatic epithelial cells ***(12)***.

2. Because primary cultures of prostatic epithelial cells are mortal, it is important to freeze a large number of aliquots from the initial culture to maintain the stock. We typically obtain about $10^6$ cells in the initial culture by about a week after initiation. By freezing $10^4$ cells per ampule, we establish a bank of 100 vials of cells. These are thawed as needed and serially passaged to expand cell number. We estimate that the cells have gone through about six population doublings in the initial culture. Attachment efficiency after thawing is about 30%, and doubling time during exponential

phase growth is about 24 h. Therefore, about $2 \times 10^5$ cells are obtained approx 1 wk after thawing one ampule of frozen cells from the bank. These cells will have gone through an additional six population doublings or so, leaving the opportunity for additional expansion until the lifespan limit of about 30 population doublings is reached.

Alternate freezing methods may be adequate, especially for those investigators who have access to automated cryogenic equipment.

3. It should be noted that cells would be extremely sparse immediately after thawing. As discussed in **Subheading 4.2.,** attachment efficiency after thawing is about 30%; therefore, the number of cells attached the day after thawing one ampule containing $10^4$ cells will be only $3 \times 10^3$ cells. This should not cause concern because the cells grow very robustly at low density. It should be noted that complete MCDB 105 (*see* **Subheading 2.19.**) is used to reestablish frozen and thawed cells in culture, whereas Complete PFMR-4A (*see* **Subheading 2.18.**) is used to establish primary cultures. We observed that complete MCDB 105 (*see* **Subheading 2.19.**) is superior for low-density growth (hence its use for clonal growth or for cultures >50% confluent), whereas complete PFMR-4A (*see* **Subheading 2.18.**) is superior for high-density growth (primary cultures or cultures >50% confluent).
4. Optimal passage or serial culture of prostatic epithelial cells occurs if the cells are processed when actively dividing and still relatively sparse (<50% confluent). Similarly, optimal proliferation in newly established serial cultures occurs if the cells are not inoculated at high densities. For example, if a confluent dish of cells (with $10^6$ cells per dish, for instance) is desired for a given experiment, it is better to inoculate the cells at a lower density ($10^4$ to $10^5$ cells per dish) and let them grow to confluency than to directly inoculate $10^6$ cells into the dish.

   As discussed in **Subheading 4.2.,** the cells become senescent after an average of 30 population doublings ***(13)***. Therefore, the cells can typically be passaged about five to six times before they cease proliferation. We typically use cells between population doublings 6 to 20 for most experimental purposes.

   Clonal growth assays are readily performed with prostatic epithelial cells in Complete MCDB 105 (*see* **Subheading 2.19.**) because this medium formulation supports the growth of very low density cells ***(14)***. Microtiter assays in 96-well plates also provide a means of evaluating growth regulation by a large number of experimental variables ***(15)***.
5. We do not perform any physical manipulations to separate epithelial from stromal cells after the tissue is digested. Instead, we rely on the selective growth of epithelial vs stromal cells in the media that we use to establish the respective cultures. When the digested tissue is inoculated into MCDB 105 (*see* **Subheading 2.17.**) with 10% FBS and GENT (*see* **Subheading 2.13.**) in standard tissue culture dishes, epithelial cells initially migrate out of the tissue fragments. However, over time, the epithelial cells degenerate and the cultures are replaced with stromal cells. It often takes several weeks to obtain a primary culture containing a fair number of stromal cells (usually present in clumps rather than uniformly distributed throughout the dish). Upon the first passage, any remnant epithelial cells are lost and the serial cultures are comprised solely of stromal cells.

The prostate is somewhat unique in that a large proportion of its stroma is composed of smooth muscle. The science of prostatic stromal cell culture has matured from simply growing fibroblast-like cells that were incompletely characterized to careful consideration and documentation of smooth muscle differentiation. A number of laboratories have described culture conditions that promote the development of the smooth muscle phenotype in prostatic stromal cells in vitro. We reported that transforming growth factor-β promoted the expression of smooth muscle markers in cultured human prostatic stromal cells ***(16)***. Other factors, such as basic fibroblast growth factor, epidermal growth factor, and platelet-derived growth factor, blocked the induction of the smooth muscle phenotype by transforming growth factor-β ***(17)***. Other investigators have reported that differentiation of cultured prostatic stromal cells is modulated by adrenergic receptor antagonists ***(18,19)***, estradiol, dexamethasone, and androgen ***(20)***. It will be interesting to identify the molecular pathways that regulate smooth muscle differentiation in prostatic stromal cells and compare that information to pathways delineated in smooth muscle cells from other tissues.

6. Standard protocols are used to freeze stromal cells. Alternate procedures, particularly those involving automated cryogenic equipment, may be successful. We have not determined the attachment efficiency of frozen and thawed stromal cells.
7. Standard protocols are used to thaw stromal cells.
8. Standard protocols are used to passage stromal cells. In contrast with epithelial cells, stromal cells passage well regardless of the density of the culture, as long as they are actively dividing and have not been maintained at confluency for extended periods. We typically feed a culture the day before passaging. We have not systematically evaluated the longevity of prostatic stromal cultures, but they typically can be passaged at least 20 times at 1:2 splits.

Growth assays with prostatic stromal cells are typically conducted in serum-containing media, although we and others ***(21,22)*** have reported limited proliferation in defined media. An overview of various culture methods for prostatic stromal cells, characterization of stromal cells in vitro, and types of experiments that have been performed with prostatic stromal cells is provided in a recent review article ***(23)***.

## References

1. Peehl, D. M., Wong, S. T., Terris, M. K., and Stamey, T. A. (1991) Culture of prostatic epithelial cells from ultrasound-guided needle biopsies. *Prostate* **19,** 141–147.
2. Schmid, H. P. and McNeal, J. E. (1992) An abbreviated standard procedure for accurate tumor volume estimation in prostate cancer. *Am. J. Surg. Pathol.* **16,** 184–191.
3. Brothman, A. R., Patel, A. M., Peehl, D. M., and Schellhammer, P. F. (1992) Analysis of prostatic tumor cultures using fluorescence in-situ hybridization (FISH). *Cancer Genet. Cytogenet.* **62,** 180–185.
4. Chopra, D. P., Grignon, D. J., Joiakim, A., Mathieu, P. A., Mohamed, A., Sakr, W. A., et al. (1996) Differential growth factor responses of epithelial cell cultures derived from normal human prostate, benign prostatic hyperplasia, and primary prostate carcinoma. *J. Cell Physiol.* **169,** 269–280.

5. Liu, A. Y., True, L. D., LaTray, L., Ellis, W. J., Vessella, R. L., Lange, P. H., et al. (1999) Analysis and sorting of prostate cancer cell types by flow cytometry. *Prostate* **40,** 192–199.
6. Hsu, J.-Y., Feldman, D., McNeal, J. E., and Peehl, D. M. (2001) Reduced 1a-hydroxylase activity in human prostate cancer cells correlates with decreased susceptibility to 25-hydroxyvitamin D3-induced growth inhibition. *Cancer Res.* **61,** 2852–2856.
7. Brawer, M. K., Bostwick, D. G., Peehl, D. M., and Stamey, T. A. (1986) Keratin protein in human prostatic tissue and cell culture. *Ann. NY Acad. Sci.* **455,** 729–731.
8. Cussenot, O., Berthon, P., Cochand-Priollet, B., Maitland, N. J., and Le Duc, A. (1994) Immunocytochemical comparison of cultured normal epithelial prostatic cells with prostatic tissue sections. *Exp. Cell Res.* **214,** 83–92.
9. Fry, P. M., Hudson, D. L., O'Hare, M. J., and Masters, J. R. (2000) Comparison of marker protein expression in benign prostatic hyperplasia in vivo and in vitro. *BJU Int.* **85,** 504–513.
10. Peehl, D. M., Wong, S. T., and Stamey, T. A. (1993) Vitamin A regulates proliferation and differentiation of human prostatic epithelial cells. *Prostate* **23,** 69–78.
11. Peehl, D. M., Leung, G. K., and Wong, S. T. (1994) Keratin expression: A measure of phenotypic modulation of human prostatic epithelial cells by growth inhibitory factors. *Cell Tissue Res.* **277,** 11–18.
12. Bayne, C. W., Donnelly, F., Chapman, K., Bollina, P., Buck, C., and Habib, F. (1998) A novel coculture model for benign prostatic hyperplasia expressing both isoforms of 5 alpha-reductase. *J. Clin. Endocrinol. Metab.* **83,** 206–213.
13. Sandhu, C., Peehl, D. M., and Slingerland, J. (2000) p16INK4A mediates cyclin dependent kinase 4 and 6 inhibition in senescent prostatic epithelial cells. *Cancer Res.* **60,** 2616–2622.
14. Wallen, E., Sellers, R. G., and Peehl, D. M. (2000) Brefeldin A induces p53-independent apoptosis in primary cultures of human prostatic cancer cells. *J. Urol.* **164,** 836–841.
15. Peehl, D. M., Erickson, E., Malspeis, L., Mayo, J., Camalier, R. F., Monks, A., et al. (1994) In vitro prostate cancer drug screen, in *Fundamental Approaches to the Diagnosis and Treatment of Prostate Cancer and BPH* (Imai, K., Shimazaki, J., and Karr, J. P., eds.), Academic Press, New York, pp. 57–71.
16. Peehl, D. M. and Sellers, R. G. (1997) Induction of smooth muscle cell phenotype in cultured human prostatic stromal cells. *Exp. Cell Res.* **232,** 208–215.
17. Peehl, D. M. and Sellers, R. G. (1998) Basic FGF, EGF, and PDGF modify TGF-beta-induction of smooth muscle cell phenotype in human prostatic stromal cells. *Prostate* **35,** 125–134.
18. Boesch, S. T., Corvin, S., Zhang, J., Rogatsch, H., Bartsch, G., and Klocker, H. (1999) Modulation of the differentiation status of cultured prostatic smooth muscle cells by an alpha1-adrenergic receptor antagonist. *Prostate* **39,** 226–233.
19. Smith, P., Rhodes, N. P., Ke, Y., and Foster, C. S. (1999) Influence of the alpha1-adrenergic antagonist, doxazosin, on noradrenaline-induced modulation of

cytoskeletal proteins in cultured hyperplastic prostatic stromal cells. *Prostate* **38,** 216–227.

20. Zhang, J., Hess, M. W., Thurnher, M., Hobisch, A., Radmayr, C., Cronauer, M. V., et al. (1997) Human prostatic smooth muscle cells in culture: estradiol enhances expression of smooth muscle cell-specific markers. *Prostate* **30,** 117–129.
21. Kassen, A., Sutkowski, D. M., Ahn, H., Sensibar, J. A., Kozlowski, J. M., and Lee, C. (1996) Stromal cells of the human prostate: initial isolation and characterization. *Prostate* **28,** 89–97.
22. Peehl, D. M., Sellers, R. G., and Wong, S. T. (1998) Defined medium for normal adult human prostatic stromal cells. *In Vitro Cell Dev. Biol. Anim.* **34,** 555–560.
23. Peehl, D. M. and Sellers, R. G. (2000) Cultured stromal cells: an in vitro model of prostatic mesenchymal biology. *Prostate* **45,** 115–123.

# 4

# Prostate Epithelial Stem Cell Isolation and Culture

**David L. Hudson and John R. W. Masters**

## 1. Introduction

Although epithelial stem cells are implicated in the etiology of both benign prostatic hyperplasia and cancer *(1,2)*, there has, until recently, been little information regarding their characteristics. Stem cells are well characterized in several other mammalian epithelial tissues, such as the lining of the gut *(3)* and the epidermis of the skin *(4–6)*. In both of these tissues, there is a small stem cell population that divides rarely to produce progeny that are either stem cells or transit amplifying cells. The latter are capable of rapid division but have a limited proliferative capacity and will ultimately produce fully differentiated, nonproliferative daughters.

Epithelial proliferation in the prostate is largely confined to the basal layer *(7,8)*, and this is where stem cells are believed to reside *(1,7)*. This population gives rise to an intermediate amplifying population that, in turn, differentiates into the secretory luminal compartment *(9–11)*. One of the main criteria for determining the presence of a stem cell compartment in a tissue is to show evidence for proliferative heterogeneity, that there are distinct sub-populations with differing capacities for cell division. There are three possibilities for the distribution of proliferative and nonproliferative populations in an epithelial tissue: all cells could have equal potential for cell division, only a subset of undifferentiated cells may divide, or, as in skin, there may be two main types of proliferative cells, the stem cell and the transit amplifying cell. The stem and transit amplifying cells may be distinguishable in vitro from colony morphology *(4,12)*, although the latter may have a wide distribution of proliferative capacity.

Recently, we described studies designed to explore proliferative heterogeneity in the prostate *(12)*. We showed the formation of two main types of colonies in culture that we postulated to represent the progeny of stem and transit ampli-

From: *Methods in Molecular Medicine, Vol. 81: Prostate Cancer Methods and Protocols*
Edited by: P. J. Russell, P. Jackson, and E. A. Kingsley © Humana Press Inc., Totowa, NJ

fying cells. Primary epithelial cells plated at clonal density on a 3T3 feeder layer (*see* **Note 1**) had a colony-forming efficiency of around 6% of plated cells. Colonies were defined as groups of cells containing 32 cells or more and were of two distinct morphological types, termed types I and II. Type I colonies, the majority of those formed, were irregular in shape and consisted of a mixture of cells with basal and differentiated phenotypes. They contained between 32 and 8500 cells with a cell density of less than 30 cells per linear mm. Approximately 1 in 10 colonies were larger than type I (at least 3 mm in diameter after 14 d in culture) and contained between 8000 and 40,000 small, undifferentiated cells. These type II colonies were round and had a high linear cell density of between 30 and 50 cells per mm. We hypothesized that type I colonies are the progeny of transit amplifying cells and type II colonies of stem cells.

Keratinocyte stem cells were isolated from human epidermis using cell surface expression of high levels of β1 integrins and rapid adhesion to extracellular matrix ***(4,5)***. The cells with the highest proliferative capacity adhered most rapidly to collagen. Adhesion of primary prostate cells to collagen I could also enrich for proliferative cells by rapid attachment, but we could not use this method to separate cells that produce type I and II colonies. This approach may prove useful in the future to further characterize cells by the use of alternative matrix molecules (*see* **Note 2**).

Recently, prostate epithelial cell culture was simplified by the development of a commercially available medium called PrEGM, one of the Clonetics™ optimized media from a range manufactured by BioWhittaker. This is provided as a base medium with frozen aliquots of nine separate additives, including bovine pituitary extract. Cell growth in PrEGM compares favorably with WAJC-404 ***(13)*** and produces similar colony-forming efficiencies, for primary cells, to that reported by Peehl and coworkers ***(14)*** with PFMR-4A ***(12)***. We believe that use of this medium is currently the best option for anyone venturing into prostate cell culture and, therefore, the procedures outlined in this chapter are based on this medium. One limitation for PrEGM, however, results from the manufacturer's reluctance to disclose the full recipe of the medium and the concentrations of the additives. This may be important for some studies. The techniques described for isolating and culturing single-cell epithelial suspensions are common to all methods of culture, however, and should be suitable for any other available media.

Although our work thus far has not produced definitive markers for isolating stem cells, studies of clonal cell growth of different epithelial populations will continue to provide valuable information about stem cells and their progeny. We have, therefore, detailed the methods used to identify proliferative heterogeneity in prostate epithelium and these may also be of use in studying the cell biology of prostate cancer.

This chapter will describe the production of a single-cell suspension from collagenase-digested prostate tissue and growth of these cells at clonal density with a 3T3 feeder layer (*see* **Note 3**) on collagen-coated dishes. The use of differential adhesion to enrich for the proliferative population will be described.

## 2. Materials

1. Collection medium: RPMI 1640 (Invitrogen Ltd., cat. no. 31870-025) with 20 m*M* HEPES (Sigma, cat. no. H4034) (*see* **Note 4**), 5% heat inactivated fetal calf serum (FCS), 1% penicillin (10,000 U/mL)/streptomycin (10,000 µg/mL; Invitrogen Ltd., cat. no. 15140-106), 1% Fungizone® (Amphotericin B, 250 µg/mL; Invitrogen Ltd., cat. no. 15290-034).
2. Collagenase solution: RPMI 1640, 5% FCS, Collagenase Type I (Sigma, cat. no. C9891) at 200 U/mL (*see* **Note 5**).
3. Sterile calcium and magnesium free phosphate-buffered saline (PBS; Invitrogen Ltd., cat. no. 14200-067).
4. Bovine serum albumin (BSA) fraction V (Sigma, cat. no. A9647).
5. 0.25% Trypsin (Invitrogen Ltd., cat. no. 25090-028) in versene (Invitrogen Ltd., cat. no. 15040-041; 0.02% EDTA solution in isotonically buffered saline).
6. Soybean trypsin inhibitor (Sigma, cat. no. T6522).
7. Serum-free DMEM (Imperial, cat. no. 7-430-14).
8. 3T3 growth medium: DMEM containing 10% FCS.
9. Prostate epithelial cell growth medium: PrEGM growth medium (Clonetics, cat. no. CC-3166) with BulletKit® (Cambrex) additives (*see* **Note 6**).
10. Vitrogen 100 (Nutacon, Leimuiden, The Netherlands) purified bovine dermal collagen diluted to 10 µg/mL in sterile PBS.
11. Mouse embryo Swiss-3T3 cells (American Type Culture Collection, Rockville, MD, cat. no. CCL-92), confluent T75 flasks (*see* **Note 7**).
12. Mitomycin C solution (Sigma, cat. no. M0503), prepared by dissolving mitomycin C powder in PBS to a concentration of 0.4 mg/mL and filter sterilizing; store as frozen aliquots at –20°C.
13. 1% Rhodanile blue stain (BDH [GURR]) (*see* **Note 8**).

## 3. Methods

### 3.1. Collagen Coating Tissue Culture Dishes

1. Dilute sterile Vitrogen 100 (a solution consisting mainly of bovine type I collagen) to a final concentration of 10 µg/mL in sterile PBS (*see* **Note 2** for the use of alternative extracellular matrix proteins).
2. Under sterile conditions, add 3 mL of collagen solution to each 60-mm tissue culture dish and incubate at 37°C for a minimum of 1 h or, alternatively, at 4°C overnight. Allow three replicate dishes per time point or condition if dishes are to be used for adhesion assays.
3. Remove coating solution from the dishes and wash three times with 5 mL of sterile PBS.

4. The dishes are now ready for the addition of 3T3 feeder cells for clonal growth studies (*see* **Subheading 3.2.**).
5. Dishes to be used for adhesion assays (*see* **Subheading 3.5.**) need to have nonspecific cell attachment blocked by incubating the dishes with 0.5 mg/mL heat denatured BSA (*see* **Note 9**) at 37°C for 1 h. Remove blocking solution and wash dishes three times with sterile PBS.
6. Add 2 mL of serum-free DMEM and incubate at 37°C for later use.

### 3.2. Preparation of 3T3 Feeder Layers

1. To a confluent flask of 3T3 cells (*see* **Note 7**), add mitomycin C to a final concentration of 4 µg/mL (a 1:100 dilution of a 0.4 mg/mL stock solution prepared by dissolving a 2-mg vial in 5 mL of PBS and filter sterilizing; store as frozen aliquots).
2. Incubate the cells with the mitomycin C for 2 h at 37°C.
3. Wash cell layers three times with PBS.
4. Add 2 mL of trypsin-versene solution and incubate cells at 37°C for 3 min.
5. Gently tap the flask to dislodge the cells from the plastic and check under the microscope.
6. Suspend the cells by adding sufficient 3T3 growth medium to make the total volume up to 10 mL and transfer the cell suspension to a universal.
7. Sediment the cells by centrifugation at 170*g* for 5 min.
8. Resuspend the cells in 10 mL of 3T3 growth medium.
9. Seed 3T3 cells into flasks or 6-cm dishes at one-third confluence (approx $1.5 \times 10^4$ cells/cm$^2$). Cells harvested from a confluent 75 cm$^2$ flask will be sufficient to seed $9 \times 25$ cm$^2$ flasks, or around $10 \times 6$ cm (22 cm$^2$) dishes.
10. Incubate the cells at 37°C overnight to attach and spread before adding the epithelial cells.

### 3.3. Prostate Tissue Preparation and Digestion

1. Tissue should be collected in a sterile container with collection medium as soon as possible after removal from the patient/donor.
2. In a laminar flow hood, wash the tissue pieces by rinsing three times with fresh collecting medium.
3. Transfer the tissue pieces to a 10-cm Petri dish and trim to remove all clotted blood and, in the case of TURP chips, heat-damaged tissue. Weigh the remaining tissue.
4. Mince the tissue finely, initially with scissors and a scalpel and then with two crossed scalpels until reduced to 1-mm$^3$ pieces.
5. Transfer the tissue pieces to a sterile 30-mL universal. Before digesting the tissue, it is necessary to remove traces of blood by washing. Add 20 mL of sterile PBS and resuspend the tissue. Allow the pieces to settle for 5 min then slowly aspirate the supernatant. Wash two more times or until the supernatant remains clear after the tissue has settled.
6. Resuspend the minced tissue in 7.5 mL of collagenase solution per gram of tissue, as determined at stage 3, and agitate gently on an orbital shaker for 18–20 h at 37°C.

7. At the end of the digestion period, pipet up and down gently with a 5-mL pipet to break up any large clumps and reduce the suspension to a cloudy broth (*see* **Note 10**).
8. Sediment the epithelial cells by centrifugation at 170*g* for 20 s. Using a transfer pipet, or 1-mL pipet, carefully transfer the loose pellet to a fresh universal, taking as little of the supernatant as possible. Resuspend the pellet in 10 mL of PBS and repeat the sedimentation step. Using gentle sedimentation, free stromal cells are left in the supernatant. The pellet now contains mainly epithelial cell organoids. Finally, give the cells one last wash in PBS, centrifuge at 170*g* for 10 min, and remove as much PBS as possible. The organoids can be plated directly for culture or digested into a single-cell suspension as below, for clonal growth studies.

### 3.4. Preparation of Single Epithelial Cell Suspension for Colony-Forming Assays

1. Prepare a feeder layer of mitomycin C-treated 3T3 cells (*see* **Subheading 3.2.**). This should ideally be done the day before plating the epithelial cells.
2. To a pellet of epithelial cell organoids (prepared as in **Subheading 3.3.**), add 2 mL of trypsin-versene and mix by pipetting up and down several times.
3. Seal the closed universal with parafilm and tape horizontally into the platform of an orbital shaker at 37°C.
4. Shake gently at 37°C for 20 min at sufficient speed to keep the suspension moving. After this time the acini will have been digested to a single-cell suspension.
5. Inhibit trypsin activity by adding 2 mL of 1 mg/mL soybean trypsin inhibitor and pellet the cells by centrifugation at 170*g* for 5 min.
6. Rinse twice by adding 10 mL of serum-free DMEM and sedimenting by centrifugation as above.
7. After the second wash resuspend the cell pellet in 5 mL of PrEGM and count the cells.
8. Remove the medium from the feeder cells and wash once with 3 mL of PrEGM to remove residual serum. Seed between $10^3$ and $10^4$ cells per T25 flask onto feeders and return to the incubator. Small colonies should become visible within 6 d, with type I and II colonies distinguishable at 14 d. At this point the cultures can either be fixed and stained (*see* **Note 11**) or colonies can be picked by ring cloning for further growth analysis. **Figure 1** shows the appearance of dishes fixed at 14 d demonstrating the morphology of the two main colony types, I and II.

### 3.5. Differential Adhesion Assays

1. Prepare a single-cell suspension as above and resuspend in serum-free DMEM at a density of 500 to 5000 cells per mL.
2. Add 2 mL of the cell suspension ($10^3$–$10^4$ cells per dish) to prewarmed, blocked matrix coated dishes (*see* **Subheading 3.1.**) and return dishes to the incubator. Set up three dishes for each cell density and time point.
3. After the required periods of time (5–60 min) remove the dishes from the incubator.

Fig. 1. Colony types formed in primary cultures of prostate epithelial cells. $10^3$ freshly isolated epithelial cells were plated onto a 6-cm dish with a feeder layer of irradiated 3T3 cells and grown for 14 d. The cells were fixed and stained. Two types of colony were formed: type I **(A,B)** are relatively small with a mixture of small proliferative and larger differentiated cells. These colonies are irregular in shape, have a cell density below 30 cells per linear millimeter, and contain from 32 to 8500 cells. Type II colonies **(C,D)** are large (at least 3 mm in diameter) and regular in shape. They consist mainly of small cells and have a high density of between 30 and 50 cells per millimeter. Type II colonies contain between 8000 and 40,000 cells by 14 d of culture. (Reproduced with permission of Lippincott Williams and Wilkins from Hudson et al. ***(12).***)

4. Gently pipet the medium over the dish surface to resuspend nonattached cells and remove from the dish. To determine the colony-forming ability of these less-adherent cells, transfer the medium to a sterile universal, otherwise discard.
5. Remove any remaining nonattached cells by rinsing the dish surface with fresh medium and add this, if required, to the cells removed at stage 4.
6. Add mitomycin C-treated 3T3 cells to each dish (as described in **Subheading 3.2.**) in 3 mL of PrEGM. As a control, one set of dishes should have been set up that did not have unattached cells removed.
7. If required, the unattached cells collected in stages 4 and 5 can be pelleted and added to feeder layer containing dishes to allow the colony-forming ability of the less-adherent cells to be studied.
8. All dishes should be returned to the incubator and grown for 14 d, changing the medium at 2– 3-d intervals.

9. The colony-forming ability of adherent cells can be assessed as described in **Note 12.**

## 4. Notes

1. Swiss 3T3 cells have been used for many years in feeder layers for various epithelial cells types and provide a supply of growth factors and extracellular matrix support, allowing clonal growth of epithelial cells from lower seeding densities than would otherwise be needed **(15)**.
2. Although we have extensively used collagen I for attachment assays, studies involving other epithelial cell types (i.e., **ref. 4**) have additionally used other extracellular matrix proteins, such as fibronectin, collagen IV, and Engelbreth-Holm-Swarm sarcoma laminin (25–100 µg/mL, all available from Sigma) and these may be useful for further examination of different epithelial cells.
3. To use 3T3 cells as a feeder layer, the cells are pretreated with mitomycin C, which binds to genomic DNA, inhibiting further cell division while allowing the cells to continue to produce growth factors and extracellular matrix proteins. The use of mitomycin C requires no specialist equipment and can be performed easily when cells are required. However, it is necessary to have cells growing at all times to ensure availability when clinical tissue is obtained.
4. Dissolve 0.48 g of tissue culture grade HEPES per 100 mL of collection medium in 10 mL of RPMI. Filter sterilize by passing through a 0.2-µm syringe filter and add to the rest of the RPMI.
5. For a 200 U/mL solution of collagenase, weigh out the required amount in a universal (the enzymatic units per mg are given with each batch). Add RPMI containing 5% FCS to dissolve the powder to a final concentration of 200 U/mL and filter sterilize through a 0.2-µm syringe filter. It is easier to weigh out an approximate amount and adjust the volume of RPMI to the correct concentration rather than to attempt to weigh a predetermined amount.
6. For maximal shelf life, this medium can be purchased with the epidermal growth factor, hydrocortisone, epinephrine, transferrin, insulin, retinoic acid, triiodothyronine, antibiotics, and bovine pituitary extract provided separately in frozen aliquots. Aliquots should be stored frozen and thawed at room temperature just before use. Complete medium should be stored at 4°C in the dark and only the required volume prewarmed to 37°C.
7. To maintain mouse 3T3 cells cultures until required, grow in DMEM medium with 10% FCS at 37°C with 5% $CO_2$. At weekly intervals, the cells can be split 1:10 by trypsinization and seeding into fresh flasks. If cells are required more rapidly, a split of 1:3 should produce confluent cultures within 3 d. Cells should be fed by changing the medium three times a week.
8. 1% Rhodanile blue stain ***(16)*** is a mixture of rhodamine (BDH [GURR], cat no. 341422X) and Nile blue (BDH [GURR], cat. no. 340594G) blue stains. To prepare, make up 2% solutions of each stain in distilled water and mix together equal volumes of each. Filter through Whatman paper prior to use. Freshly made stain will keep for several weeks and can be used several times if refiltered.

9. Heat denatured BSA prevents nonspecific attachment of cells to the tissue culture plastic, ensuring adhesion only via the extracellular matrix coating. Make a 10 mg/mL stock solution of BSA in PBS and filter sterilize through a syringe filter. Freeze at –20°C in 0.5 mL aliquots in sterile tubes. To heat denature BSA, thaw the required number of aliquots and heat to 80°C in a dry block for 3 min. Cool on ice and dilute 1:20 in PBS to 0.5 mg/mL. Each 0.5-mL aliquot will make 10 mL of blocking solution, sufficient for five dishes.
10. The epithelial component at this point contains macroscopic spheres of cells consisting of epithelial acini and small lengths of ducts.
11. To fix cultures, remove the growth medium and wash twice in PBS. Add 3 mL of 3.7% formaldehyde and incubate at room temperature for 10 min. Remove the formaldehyde and wash three times with distilled water. Stain by incubating dishes for 30 min in 1% rhodanile blue ***(16)***. Wash dishes in running water to remove excess stain and air-dry.
12. **Subheading 3.5.** allows the determination of the relative rate of attachment of colony-forming cells but not of the colony-forming ability of individual populations. To do this, allow the epithelial cells to attach as described but, instead of adding 3T3 cells at **Subheading 3.5.**, stage 6, harvest the cells by trypsinization, as described for 3T3 cells (*see* **Subheading 3.2.**), count by hemacytometer, and plate $10^3$ cells per T25 onto feeder cells (as described in **Subheading 3.4.**, stage 8). After 14 d, the cultures can be fixed and stained and colonies counted and scored for type.

## References

1. Bonkhoff, H. and Remberger, K. (1996) Differentiation pathways and histogenetic aspects of normal and abnormal prostatic growth: A stem cell model. *Prostate* **28,** 98–106.
2. Isaacs, J. T. and Coffey, D. S. (1989) Etiology and disease process of benign prostatic hyperplasia. *Prostate Suppl.* **2,** 33–50.
3. Potten, C. S. and Loeffler, M. (1990) Stem cells: Attributes, cycles, spirals, pitfalls and uncertainties. Lessons for and from the crypt. *Development* **110,** 1001–1020.
4. Jones, P. H. and Watt, F. M. (1993) Separation of human epidermal stem cells from transit amplifying cells on the basis of differences in integrin function and expression. *Cell* **73,** 713–724.
5. Jones, P. H., Harper, S., and Watt, F. M. (1995) Stem cell patterning and fate in human epidermis. *Cell* **80,** 83–93.
6. Li, A., Simmons, P. J. and Kaur, P. (1998) Identification and isolation of candidate human keratinocyte stem cells based on cell surface phenotype. *Proc. Natl. Acad. Sci. USA* **95,** 3902–3907.
7. Bonkhoff, H., Stein, U., and Remberger, K. (1994) The proliferative function of basal cells in the normal and hyperplastic human prostate. *Prostate* **24,** 114-118.
8. Hudson, D. L., Guy, A. T., Fry, P. M., O'Hare, M. J., Watt, F. M., and Masters, J. R. W. (2001) Epithelial differentiation pathways in the human prostate: identification of intermediate phenotypes by keratin expression. *J. Histochem. Cytochem.* **49,** 271–278.

9. Isaacs, J. T. (1987) Control of cell proliferation and cell death in the normal and neoplastic prostate: a stem cell model, in *Benign Prostate Hyperplasia, Vol II* (Rogers, C. H., Coffey, D. H., Cunha, G., Grayhack, J. T., Hinman, F., and Horton, R., eds.), National Institutes of Health, Bethesda, MD, pp. 85–94.
10. Xue, Y., Smedts, F., Debruyne, F. M. J., de la Rosette, J. J., and Schalken, J. A. (1998) Identification of intermediate cell types by keratin expression in the developing prostate. *Prostate* **34,** 292–301.
11. Bui, M. and Reiter, R. (1999) Stem cell genes in androgen-independent prostate cancer. *Cancer Metastasis Rev.* **17,** 391–399.
12. Hudson, D. L., O'Hare, M. J., Watt, F. M., and Masters, J. R. W. (2000) Proliferative heterogeneity in the human prostate: Evidence for epithelial stem cells. *Lab. Invest.* **80,** 1243–1250.
13. Fry, P. M., Hudson, D. L., O'Hare, M. J., and Masters, J. R. (2000) Comparison of marker protein expression in benign prostatic hyperplasia in vivo and in vitro. *BJU Int.* **85,** 504–513.
14. Peehl, D. M., Wong, S. T., and Stamey, T. A. (1988) Clonal growth characteristics of adult human prostatic epithelial cells. *In Vitro Cell Dev Biol.* **24,** 530–536.
15. Ham, R. G. (1974) Nutritional requirements of primary cultures. A neglected problem of modern biology. In Vitro **10,** 119–129.
16. Rheinwald, J. G. and Green, H. (1975) Serial cultivation of strains of human epidermal keratinocytes: the formation of keratinizing colonies from single cells. *Cell* **6,** 331–343.

# 5

# Generation of Immortal Human Prostate Cell Lines for the Study of Prostate Cancer

**Johng S. Rhim**

## 1. Introduction

Prostate cancer is the most common male cancer in the United States, as well as in the Western World, and the second leading cause of male cancer death in the United States ***(1)***. The recent progress made in identifying prostate cancer genes and understanding prostate cancer genetics is impressive. However, the basic mechanisms underlying prostate carcinogenesis remain poorly understood ***(2)***. A hurdle in understanding the molecular genetic changes in prostate cancer has been the difficulty in establishing premalignant lesions and primary prostate tumors as in vitro cell cultures. Primary epithelial cells grow for a finite lifespan and then senesce. Immortalization is defined by continuous growth of otherwise senescing cells and is believed to represent an early stage in tumor progression. To examine these early stages, we and others have developed in vitro models of prostate epithelial cell immortalization. To understand the many factors that are suspected to contribute to the development of this malignancy, there is a need for an in vitro human prostate epithelial (HPE) culture system. These models have been extremely important in identifying genetic and molecular changes involved in prostate cancer progression.

Until recently, in vitro cell culture models of human prostate carcinogenesis have not been widely available (*see* **Table 1**).

To date, only three readily available and well-studied long-term human prostate carcinoma cell lines exist (DU-145, PC-3, and LNCaP). All three were isolated from metastatic lesions, thus leaving a void in reagents representing long-term human cell lines derived from primary localized adenocarcinoma of the prostate. Nevertheless, their use has greatly contributed to our current

From: *Methods in Molecular Medicine, Vol. 81: Prostate Cancer Methods and Protocols*
Edited by: P. J. Russell, P. Jackson, and E. A. Kingsley © Humana Press Inc., Totowa, NJ

**Table 1**
**Immortalized Human Prostate Epithelial Cell Lines**

| Immortalizing agents | Immortalizing methods | References |
|---|---|---|
| SV40 (pRSV-T) | Strontium phosphate | ***7*** |
| SV40 large T (pMK16/SV40 Ori) | Lipofection | ***8*** |
| SV40 (SV40 Ori + neo) | Polybrene | ***5*** |
| SV40 (pRSV-T) | Lipofection | ***9*** |
| Ad12-SV40 | Infection | ***11*** |
| HPV-18 (pBR322) | Lipofection | ***18*** |
| HPV-18 (pSHPV-18m+neo) | Polybrene | ***6*** |
| HPV-16 E6-E7(LXSN 16 E6-E7) | Infection | ***20*** |
| | | ***21*** |
| Telomerase (LXSN-hTERT) | Infection | ***25*** |

SV40 Ori Origin = defective SV40 genome.

understanding of human prostate carcinogenesis and progression. As a result of a better understanding of the process of malignant transformation and the availability of recombinant DNA technology, new cell lines have been developed and characterized during the past few years. Serum-free media for growth and maintenance of primary normal and malignant prostate epithelial cells have been developed ***(3,4)***. The serum-free growth medium developed for human keratinocytes (K-SFM; Life Technologies, Inc., Gaithersburg, MD) was found to be very useful for growing and maintaining primary HPE cells and for the cultivation of long-term cultures of prostate HPE cells ***(5,6)***.

In this chapter, the various immortalizing agents and the current methods using the generation of HPE cell lines for the study of prostate cancer are reviewed.

## 2. Materials

### *2.1. Simian Papovaviris 40*

Immortalization of HPE cells in culture by simian papovavirus 40 (SV40) is a widely used experimental method to generate long-term cell lines for the study of malignant disease. Most SV40 immortalized human cells fail to form tumors when implanted into athymic nude mice. The first serum-free HPE cell line was established by using SV40 (*see* **Table 1**). Although Kaighn and coworkers ***(7)*** reported the transformation of neonatal prostate epithelial cells to immortality with SV40 early region (pRSV-T) genes in 1989, only recently has the transformation of adult HPE cells by the SV40 gene been achieved. In

1991, Cussenot and coworkers ***(8)*** described the establishment of a cell line after liposome-mediated transfection of normal adult HPE cells with the plasmid pMK16/SV40 Ori. Previous attempts to immortalize adult HPE cells have proven difficult ***(8)***. Strontium phosphate transfection has been successfully used to immortalize neonatal HPE cells using a plasmid containing the SV40 early region genes ***(7)*** but has failed when used on adult cells ***(8)***. Lee and coworkers ***(5)*** have succeeded in immortalizing adult HPE cells by polybrene-induced DNA transfection of plasmid (pRNS-1) containing an origin-defective SV40 genome together with a plasmid carrying the neomycin resistance gene. Establishment of immortalized HPE cell lines from prostatic carcinoma and benign prostatic hyperplasia using pRSV-T has recently been shown by lipofection transfection ***(9)***.

### 2.2. Adenovirus 12-Simian 40

Infection of adenovirus 12-simian 40 (AD12-SV40) into human epithelial cells has led to the establishment of a variety of transformed human cell lines from many types of epithelia ***(10)***. Webber and coworkers ***(11)*** have successfully established a HPE cell line from nonneoplastic adult human prostatic epithelium using Ad12-SV40. This is the only known Ad12-SV40-immortalized HPE cell line.

### 2.3. Human Papilloma Virus

Human papilloma virus (HPV) has been used to transform a variety of human epithelial cells in culture, including cervical breast cells ***(12,13)***. Generally, human epithelial cells immortalized by HPV are not tumorigenic. In an attempt to develop an in vitro model of carcinogenesis of the prostate, introduction of HPV DNA into HPE cells would be of special interest because of the immortalization potential of HPV and its possible link with prostate cancer etiology ***(14,15)***. It has been reported that HPV-immortalized HPE cells are more likely to retain growth and differential characteristics of normal prostate epithelial cells as shown in HPV immortalized human epithelial cells ***(16,17)***. This approach has resulted in the establishment of HPE cell lines of normal and malignant tissues ***(6,18)***.

### 2.4. HPV-16 E6-E7 Genes

The use of the amphotropic retroviruses to transduce HPV-16 E6-E7 genes into human cells has permitted the establishment of a wide variety of transformed human cell lines from many types of epithelia as well as from other cell lineages ***(19)***. The immortalized cell lines were nontumorigenic in nude mice and retained many of the differentiated characteristics of the primary cells; however, they invariably had chromosomal abnormalities. The generation of

immortal HPE cell lines derived from both normal and primary cancer specimens by HPV16 E6-E7 has been reported ***(20,21)***.

### 2.5. Telomerase

Telomerase is an enzyme responsible for replicating telomerase and is composed of an RNA subunit containing an integral catalytic subunit, human telomerase reverse transcriptase (hTERT). Telomerase is expressed low in most normal tissues but is known to become activated during tumorigenesis ***(22)***. Recent findings have implicated telomerase in the escape from cellular senescence. Transfection of hTERT into selective human cell types can itself induce immortalization ***(22–24)***. Interestingly, telomerase expression in human somatic cells does not induce changes associated with a transformed phenotype or an altered genetic phenotype. Recently, we have successfully established an immortalized HPE cell culture derived from a primary prostate tumor with telomerase ***(25)***.

## 3. Methods

### 3.1. Strontium Phosphate Transfection

1. The plasmid DNA is coprecipitated with strontium phosphate ***(26)***.
2. Experiments are conducted on neonatal HPE cells grown in 25 $cm^2$ flasks in P4-8F medium ***(7)***.
3. To prepare precipitates, solutions are warmed to room temperature. For a 25-$cm^2$ flask, 5 µg of DNA are transfected by consecutively mixing the DNA, 31 µL of 2 *M* $SrCl^2$, and sterile distilled $H^2O$ (total volume = 250 µL) in a sterile nonwettable plastic tube. This solution is added dropwise to 250 mL of 2× HEPES balanced salt solution, with mixing between drops to prevent high local concentrations of phosphate. Mixing is performed by adding the solution to the depression created in the 2× HEPES by a nitrogen gas stream. The precipitate increases in size, first forming small dust-like threads and then forming progressively larger networks. At the stage of fine dust, the precipitates are pipetted into the 25-$cm^2$ flasks.
4. After a 4-h treatment, the coprecipitate is removed, and the cells are shocked by the addition of 1.5 mL of 15% glycerol in medium for 30 s at room temperature.
5. The cell monolayer is washed three times with growth medium and refed.

### 3.2. Lipofectin Transfection

1. The liposome mixture is prepared by incubating 50 µg of lipofectin with 1 to 10 µg of plasmid DNA at room temperature for 15 min.
2. The liposome mixture is added to each 100-mm dish containing semiconfluent cells in 3 mL of fresh K-SFM
3. After incubation for 8 to 24 h, the lipofectin medium is removed, the cells are rinsed with phosphate-buffered saline (PBS), and 10 mL of fresh K-SFM are added per dish.

4. Untreated cells are included as a control.
5. Subcultures are prepared after the cells become confluent by inoculating $1 \times 10^6$ cells into 60-mm dishes.

### 3.3. Polybrene Transfection

1. Cells are split into $1 \times 10^6$ cells per dish.
2. The next day, the cells are washed with PBS.
3. Medium (2.5 mL) containing 10 µg/mL of polybrene (a total of 25 µg) are added to the cells.
4. DNA (1–10 µg) is further added into the polybrene-containing K-SFM.
5. The cells are incubated overnight in a 5% $CO_2$ incubator.
6. The cells are washed with PBS.
7. 30% DMSO (3–5 mL) in K-SFM are added to the cells for 4 min at room temperature.
8. After being shocked, the cells are washed with PBS, then fed with fresh K-SFM, and incubated before further subcultivation.

### 3.4. HPV16 E6-E7 Retrovirus Transduction

1. PA317 amphotropic packaging cell lines stably transfected with pLXSN 16 E6-E7 (HPV-16 E6 E7) ***(19)*** are grown to 70–80% confluence and are fed with fresh medium 24 h later. Filtered (0.22-µm) supernatants are collected after a further 24 h and stored in aliquots at –80°C. These supernatants are used as virus stocks.
2. One-day-old cultures (about 70–80% confluence, in 25-$cm^2$ flasks) are infected with 300 µL of virus stock in 3 mL of medium containing polybrene at a concentration of 5 µg/mL and incubated overnight.
3. The virus is then removed, and the medium is replaced with fresh K-SFM.
4. The selection medium, K-SFM with 200 µL/mL geneticin (G418), is added after 72 h.
5. Cultures are maintained in selective medium for 7 d.
6. The G418-selected transformed cells are then grown in fresh K-SFM and further expanded.
7. At this time, part of the culture is stored by cryopreservation and the other part is used for long-term propagation of the cells.

### 3.5. Telomerase Transduction

1. PA 317 packaging cells producing retrovirus-containing hTERT (pLXSN hTERT) ***(24)*** are grown to 70–80% confluence in 75-$cm^2$ flasks and are fed with 10 mL of fresh K-SFM medium. Supernatants are collected and 0.22 µm filtered after 24 h and stored in aliquots at –80°C. These aliquots are used as virus stocks.
2. One-day-old cultured cells (about 70–80% confluent in 25-$cm^2$ flasks) are infected with 300 µL of virus stock in 3 mL of fresh K-SFM containing polybrene at a concentration of 5 µg/mL and incubated overnight.
3. The virus is then removed, and the medium replaced.
4. The selection medium, K-SFM with 200 µg/mL G418, is added after 72 h.
5. Cultures are maintained in selective medium for 7 d.

6. The G418-selected transformed cells are then grown in fresh medium and further expanded.

## 4. Notes

1. Calcium phosphate transfection has been widely used to introduce cloned and genomic DNAs and RNAs into cultured cell lines and to infect animals. This technique gives transient expression and stable integration of cloned or genomic DNAs at high copy numbers by using a simple procedure and results in efficient expression of stable integrants. However, primary cultures of normal human epithelial cells are lysed by calcium phosphate precipitates and, at low concentrations, calcium ions in the presence of serum induce certain human epithelial cells to undergo squamous differentiation ***(27)***. In addition, calcium inhibits the growth of primary human prostate cells. The biological regulatory activity of $Ca^{2+}$ ions may also limit the use of calcium phosphate precipitates in other cell types.
2. Traditionally, DNA tumor viruses, such as SV40 and Ad12-SV40, have efficiently transformed rodent cells. Their ability in human cells is limited by the fact that viral infection results in a productive infection; thus, human cells transformed by SV40 continue to release virus ***(10)***. HPV infection of genital epithelium leads to neoplasia in vivo ***(28)***, but it has not been possible to propagate HPV infection of cells in vitro. To circumvent these problems, many investigators have introduced the DNA viral oncogenes into cells. To circumvent problems of inefficient delivery of genes into the cells and to avoid the use of differentiation-promoting agents, such as the effect of calcium on human epithelial cells, recombinant amphotropic retroviruses have been developed by using the LXSN vector and the PA 317 packaging cell line ***(29)***. Use of the replication deficient retroviral construct, LXSN 16 E6-E7 ***(19)***, containing the genes for HPV 16 E6 and E7 and a neomycin resistance gene, has efficiently permitted the establishment of a human prostate epithelial cell line. The retrovirus infection is a simple and highly efficient immortalization method.
3. As was discussed above, the number of immortalized human prostate cell lines for the study of prostate cancer has greatly increased. Using these model systems, investigators have identified genetic and molecular change that occur as a prostatic epithelial cells progressively changes from normal to immortal, then tumorigenic, and finally metastatic. Some of the changes that occur are directly related to the activities of the particular oncogene used for transformation. For example, p53 is constitutively overexpressed in SV40 transformed cells as a result of banding and stabilization of *p53* by large T antigen. Other changes may be intrinsic to prostate cells and possibly mimic changes that actually occur in the development of prostate cancer. When we created a tumorigenic subline of HPV-transformed HPE cells by treatment with *N*-nitrose-*N*-methylurea, we found a loss of chromosome 8p and 10p and a gain of chromosome 8q ***(30)***. Therefore, in vitro models of carcinogenesis may accurately reflect key processes involved in prostate cancer. However, these methods are not ideal because the immortalizing cells frequently contain viral oncogenic DNA and accompany major cytogenic alterations and growth deregulation. The immortalizing agents

(SV40 and HPV) may introduce many genetic and epigenetic artifacts into these cells, making it difficult to investigate specific alterations unique to tumors. Development of in vitro human cell models that mimic human prostate cancer progression would be ideal. SV40 and HPV infections do not appear to be related to prostate cancer development. Whether oncogenic HPVs are involved in the pathogenesis of prostate cancer has been a subject of great controversy. Conceptually, successful establishment of spontaneously immortalized human prostate cancer cell line derived from patients would be an ideal and major breakthrough in prostate cancer research. However, the generation of such cell lines has not been reported.

## References

1. Landis, S. H., Murray, H., Bolden, S., and Wingo, P. A. (1999) Cancer Statistics. *Ca. Cancer J. Clin.* **4,** 8–31.
2. Dong, F. T., Isaacs, W. B., and Isaacs, J. T. (1997) Molecular advances in prostate cancer. *Curr. Opin. Oncol.* **9,** 101–107.
3. Webber, M. M., Capronier-Rickenberg, D. M., and Donohue, R. E. (1984) Isolation and growth of adult human prostatic epithelium in serum-free, defined medium, in *Methods for Serum-Free Culture of Cells of the Endocrine System* (Banes, D. W., Sirbasku, D. A., and Sato, G., eds.), Alan R. Liss, Inc., New York, pp. 44–61.
4. Peehl, D. M. and Stamey, T. A. (1986) Serum-free growth of adult human prostatic epithelial cells. *In Vitro Cell Dev. Biol.* **22,** 82–90.
5. Lee, M. S., Garkovenko, E., Yun, J. S., Weijerman, P. C., Peehl, D. M., Chen, L. S., et al. (1994) Characterization of adult human prostatic epithelial cells immortalized by Polybrene-induced DNA transfection with a plasmid containing an origin-defective SV40 genome. *Int. J. Oncol.* **4,** 821–830.
6. Rhim, J. S., Webber, M. M., Bellow, D., Lee, M. S., Arnstein, P., Chen, L. S., et al. (1994) Stepwise immortalization and transformation of adult human prostate epithelial cells by a combination of HPV-18 and v-Ki-ras. *Proc. Natl. Acad. Sci. USA* **91,** 11874–11878.
7. Kaighn, M. E., Reddel, R. R., Lechner, J. F., Peehl, D. M., Camalier, R. F., Brash, D. E., et al. (1989) Transformation of human neonatal prostate epithelial cells by strontium phosphate transfection with a plasmid containing SV40 early region genes. *Cancer Res.* **49,** 3050–3056.
8. Cussenot, O., Berthon, P., Berger, R., Mowszowicz, I., Faille, A., Hojman, F., et al. (1991) Immortalization of human adult normal prostatic epithelial cells by liposomes containing large T-SV40 gene. *J. Urol.* **146,** 881–886.
9. Iype, P. T., Iype, E., Verma, M., and Kaighn, M. E. (1998) Establishment and characterization of immortalized human cell lines from prostate carcinoma and benign prostate hyperplasia. *Int. J. Oncol.* **12,** 257–263.
10. Rhim, J. S. (2000) Development of human cell lines from multiple organs, in *Toxicology For The Next Millennium* (Isfort, R.J. and Lederberg, J., eds.), New York Academy Of Sciences, New York, pp. 16–25.
11. Webber, M. M., Bello, D., Kleinman, H. K., Wantinger, D. D., Williams, D. E., and Rhim, J. S. (1996) Prostate specific antigen and androgen receptor induction and

characterization of an immortalized adult human prostate epithelial cell line. *Carcinogenesis* **17,** 1641–1646.
12. Woodworth, C. D., Doniger, J., and DiPaolo, J. A. (1989) Immortalization of human foreskin keratinocytes by various human papillomavirus DNAs corresponds to their association with cervical carcinoma. *J. Virol.* **63,** 159–164.
13. Band, V., Zajchowski, D., Kulesa, V., and Sager, R. (1990) Human papilloma virus DNAs immortalize normal human mammary epithelial cells and reduce their growth factor requirements. *Proc. Natl. Acad. Sci. USA* **87,** 463–467.
14. McNicol, P. J. and Dodd, J. G.(1990) Detection of human papillomavirus DNA in prostate gland tissue by using the polymerase chain reaction amplification assay. *J. Clin. Microbiol.* **28,** 409–412.
15. Anwar, K., Nakakuki, K., Shiraishi, T., Naiki, H., Yatani, R., and Inuzuka, M.(1992) Presence of ras oncogene mutations and human papillomavirus DNA in human prostate carcinomas. *Cancer Res.* **52,** 5991–5996.
16. Woodworth, C. D. Waggoner, S., Barnes, W., Stoler, M. H., and DiPaolo, J. A. (1990) Human cervical and foreskin epithelial cells immortalized by human papillomavirus DNAs exhibit dysplastic differentiation in vivo. *Cancer Res.* **50,** 3709–3715.
17. Yankaskas, J. R., Haizlip, J. E., Conrad, M., Koval, D., Lazarowski, E., Paradiso, A. M., et al. (1993) Papilloma virus immortalized tracheal epithelial cells retain a well-differentiated phenotype. *Am. J. Physiol.* **264,** C1219–C1230.
18. Weijerman, P. C., Konig, J. J., Wong, S. T., Niesters, H. G., and Peehl, D. M. (1994) Lipofection-mediated immortalization of human prostatic epithelial cells of normal and malignant origin using human papillomavirus type 18 DNA. *Cancer Res.* **54,** 5579–5583.
19. Galloway, D. A., Halbert, C. L., Demens, G. W., Foster, S. A., Blanton, R. A., Merrick, D., et al. (1996) Use of amphotropic retroviruses expressing human papillomavirus 16 E6 and E7 to determine the consequences of acute expression of the viral oncogenes and to establish immortalized human cell lines. *Radiat. Oncol. Invest.* **3,** 315–319.
20. Bright, R. K., Wocke, C. D., Emmert-Buck, M. R., Duray, P. H., Solomon, D., Fetsch, P., et al. (1997) Generation and genetic characterization of immortal human prostate epithelial cell lines derived from primary cancer specimens. *Cancer Res.* **57,** 995–1002.
21. Choo, C. K., Ling, M. T., Chan, K. W., Tsao, S. W., Zheng, Z., Zhang, D., et al. (1999) Immortalization of human prostate epithelial cells by HPV-16 E6 E7 open reading frames. *Prostate* **40,** 150–158.
22. Greider, C. W. (1999) Telomerase activation. One step on the road to cancer? *Trends Genet.* **15,** 109–112.
23. Kiyono, T., Foster, S. A., Koop, J. I., McDougall, J. K., Galloway, D. A., and Klingelhultz, A. J. (1998) Both Rb/p161INK4 an inactivation and telomerase activity are required to immortalize human epithelial cells. *Nature* **396,** 84–88.
24. Ratsch, S. B., Gao, Q., Srinivasan, S., Wazer, D. E., and Band, V. (2001) Multiple genetic changes are required for efficient immortalization of different subtypes of normal human mammary epithelial cells. *Radiat. Res*. **155,** 143–150.

25. Yasunaga, Y., Nakamura, K., Ewing, C. M., Isaacs, W. B., Hukku, B., and Rhim, J. S. (2001) A novel human cell culture model for the study of familiar prostate cancer. *Cancer Res.* **61,** 5969–5973.
26. Brash, D. E., Reddel, R. R., Quanrud, M., Yang, K., Farrell, M. P., and Harris, C. C. (1987) Strontium phosphate transfection of human cell in primary culture: Stable expression of the simian virus 40 large-T antigen gene in primary human bronchial epithelial cells. *Mol. Cell. Biol.* **7,** 2031–2034.
27. Praeger, F. C. and Gilchrest, B. A. (1986) Strontium stimulates human keratinocyte proliferation. *Clin. Res.* **34,** 775A.
28. Zur Hausen, H. (1991) Viruses in human cancers. *Science* **25,** 1167–1173.
29. Miller, A.D. (1992) Retroviral vectors. *Curr. Topics Microbiol. Immunol.* **158,** 1–24.
30. Rhim, J. S., Jin, S., Jung, M., Thraves, P., Kuettel, M. R., Webber, M. M., et al. (1997) Malignant transformation of human prostate epithelial cells by N-nitroso-N-methylurea. *Cancer Res.* **57,** 576–580.

# 6

# Spheroids of Prostate Tumor Cell Lines

**George Sgouros, Wei-Hong Yang, and Richard Enmon**

## 1. Introduction

Sutherland and coworkers developed and used the spheroid model in the 1970s for radiobiological studies ***(1–6)***. Spheroids are three-dimensional (spherical) clusters of tumor cells grown from one or several cell clones. The spheroid model contains many of the elements of a tumor xenograft including an extracellular matrix and cell–cell/cell–matrix interactions ***(7–10)***; a spatial geometry that can produce well-defined drug and nutrient concentration gradients ***(11,12)***; subpopulations of cells that are quiescent, hypoxic, necrotic, or near-necrotic ***(13)***; and the potential to monitor response over a protracted time-period after different treatment schedules ***(14)***. These similarities to a tumor xenograft are coupled with many of the experimental advantages of a monolayer culture including the ability to rigorously control experimental and treatment conditions, the ability to investigate response and study mechanisms, and also the ability to investigate a large number of agents and combinations rapidly and at low cost.

The limitations of this system include the absence of vasculature and of vascular-derived extracellular matrix, the absence of endogenous humoral agents (including cytokines and immune system components), and the absence of a framework for distant metastatic spread.

Compared with cell doubling times measured in monolayer culture, the rate and pattern of spheroid growth in vitro better matches that seen in tumors in vivo. Initial studies with spheroids demonstrated dose–response relationships that were in accord with tumors growing in vivo ***(15)***. Consistent with these observations, cells from spheroids are less sensitive to radiation than cells in monolayer culture ***(16–18)***. A number of different reasons for this have been postulated. In the case of radiation resistance, changes in cell, nuclear, and chromatin conformation

From: *Methods in Molecular Medicine, Vol. 81: Prostate Cancer Methods and Protocols*
Edited by: P. J. Russell, P. Jackson, and E. A. Kingsley © Humana Press Inc., Totowa, NJ

caused by multicellular contact may alter DNA conformation and thereby reduce the probability of DNA traversal (hit probability) by radiation and lead to decreased DNA damage in irradiated spheroids ***(19–22)***. Central hypoxia that is observed in spheroids, resulting in reduced induction of reactive oxygen species and associated free radical damage, also plays an important role depending upon the spheroid's diameter ***(23,24)***. Closely associated with the level of oxygenation, the presence of nonproliferating or quiescent (prolonged $G_0$-phase) cells is also likely to contribute to radioresistance because of increased repair of potentially lethal and sublethal damage ***(18,25–27)***.

The impact of intracellular contact on apoptosis induction may also contribute to resistance. Radiation induces cell cycle block or apoptosis via a collection of pathways that begin with the DNA damage sensors ***(28–31)***. These sensors activate signaling pathways that control progression through cell cycle checkpoints leading to cell cycle block and the opportunity for DNA damage repair or, alternatively, to apoptosis. Intercellular contact ***(32)*** and extracellular matrix communication ***(33)*** are known to inhibit apoptosis induction. These observations provide an additional possible mechanism for the reduced radiation sensitivity of cells in spheroids. These potential mechanisms for reduced sensitivity to radiation are also operative in the response to DNA-damaging agents.

Spheroids also show a greater resistance to almost all chemotherapeutic agents than cells in monolayer culture. These observations have been explained as arising either from reduced penetration or the reduced sensitivity of noncycling or hypoxic populations of cells found in spheroids ***(34–37)***. These observations have led to the concept of acquired multicellular drug resistance in which resistance arises as a result of the multicellular structure of tumors ***(38–40)***. Such resistance may occur in addition to the classic unicellular resistance mechanisms (e.g., P-glycoprotein, DNA repair enzyme amplification).

The various techniques for growing spheroids have been reviewed previously ***(41)***. Note that methods using suspension systems frequently require the initial use of microcarrier beads for attachment-dependent cells to thrive and are thus beyond the scope of this discussion (*see* **Note 1**). The focus of this chapter is on the growth of spheroids using the liquid overlay technique that was first described by Yuhas and coworkers ***(42)***. In addition, experimental design and methodological considerations in conducting studies with spheroids will be examined.

## 2. Materials

### 2.1. Liquid Overlay Technique

1. Bacteriological tissue culture dishes. The size and form of the dish is to be determined by application. Petri dishes are commonly used to aid in uniform spheroid inoculation and harvesting.

2. Bacto Agar (Difco, Detroit, MI).
3. Stock solution: prepare a solution of 2% (w/v) agar in dd$H_2O$; autoclave to dissolve the agar. Thereafter, follow standard sterile techniques and store at 4°C.

### *2.2. Spheroid Sectioning*

#### *2.2.1. Frozen Sectioning*

1. Tissue-Tek OCT Compound (Baxter, Deerfield, IL).
2. Tissue-Tek Cryomold 10 × 10 × 5 mm (Baxter, Deerfield, IL).

## 3. Methods

### *3.1. Liquid Overlay Technique*

The liquid overlay technique is one of the simplest approaches to growing spheroids. It involves providing conditions that promote cell–cell attachment over cell–stratum adhesion. This is most commonly accomplished by coating bacteriological Petri dishes with a thin layer of agar to prevent cells from adhering to the bottom of the dish. Cells are then grown in a static liquid medium over the agar base. Under such conditions small clusters of cells will form, and clusters of a common initial size may be collected for subsequent experimentation, growth monitoring, or characterization.

#### *3.1.1. Preparation of Agar-Coated Dishes*

If an autoclave is readily available, plates should be prepared fresh. Prepare a solution of 1% (w/v) agar in serum-free culture medium. Autoclave the solution to dissolve the agar and immediately prepare the plates. (Be aware that serum-containing media will form precipitates on autoclaving. Although innocuous, the precipitates will cloud the image on an inverted microscope.) Use enough agar solution to generously cover the base of the dish, remembering to leave sufficient room for overlay. For example, our laboratory uses a 5-mL base in each 100- × 20-mm dish. Allow the agar to cool before use.

Plates may also be prepared from a stock agar solution (*see* **Subheading 2.1.**). Microwave the agar briefly to liquefy it, then dilute by 50% with culture medium (i.e., 1% agar base) and prepare plates as described above. This method should only be used if ready access to an autoclave is a problem; repeated microwaving of the stock solution may compromise agar stability.

For both methods, plates may be prepared several days in advance; however, all care should be taken to maintain sterility. Additionally, the surface of the agar should not be allowed to dry completely as with bacterial cultures. Older agar surfaces should be prewetted before inoculation because the dry or tacky surface may allow significant cell adhesion.

#### 3.1.2. Cell Overlay

Single cells should be harvested by trypsinization from stock monolayer cultures at mid- or late-exponential growth. Between 0.6 and $2.5 \times 10^4$ cells/cm$^2$ of the agar surface in sufficient culture medium are required for spheroid formation: our laboratory uses between 0.5 and 2 million cells in 15 mL medium for each 100-mm agar dish (*see* **Note 3**).

#### 3.1.3. Spheroid Formation

Rotate the dish gently so as to evenly distribute the cells over the dish surface and place the dish in the incubator to afford a minimum of disturbance. After 5–10 d, spheroids of 100–200 µm in diameter will have formed, although the time required will vary considerably from cell line to cell line (*see* **Notes 1** and **4**). Under an inverted phase microscope that has been fitted with an ocular micrometer, spheroids of the same approximate diameter may be collected using an Eppendorf pipet (200-µL tip). To make it easier to collect spheroids using the pipet, first transfer the spheroids and medium to dish that is not agar coated. This makes it easier to pick up spheroids because the pipet tip can be held steady against the bottom surface of the dish. The selected spheroids may be placed in a separate dish for further experimentation.

### 3.2. Spheroid Experimentation and Manipulation

The typical spheroid experiment requires incubation of spheroids with a particular drug or medium formulation. The methods involved in washing spheroids after exposure to drugs, monitoring the effect of the drugs by measuring spheroid growth, and then assessing spheroid survival probability as a function of drug concentration are outlined below.

#### 3.2.1. Spheroid Drug Exposure

In a 60-mm dish, place 20–30 spheroids with a 4–7-mL incubation volume that includes the drug of interest at the appropriate concentration. If the incubation time is longer than 1 h, an agar-coated dish should be used to prevent spheroid adhesion to the dish surface.

#### 3.2.2. Spheroid Wash Procedure

After the appropriate incubation duration, remove the spheroids from the incubation dish and wash by sequentially transferring to three or more 35-mm dishes containing drug-free fresh medium. As before, transfer the spheroids using an Eppendorf pipet with a 200-µL tip. With each transfer collect the spheroids while including as little media as possible. Increase the number of dishes used if the volume of media included in picking up the spheroids is substantial.

### *3.2.3. Preparation of Agar-Coated Multi-Well Plates*

Microwave and autoclave the agar stock solution, as necessary. Place 5–6 drops of the agar solution in each well of a 24-well plate. It is important to keep the plate on a level surface and to place the same number of drops in each well. This will reduce the amount of microscope adjustment required when viewing the spheroids through a microscope for volume measurements. Allow the agar to cool before using.

### *3.2.4. Assessment of Spheroid Growth*

Place 1.5 mL of medium in each well of an agar-coated 24-well plate. Using an Eppendorf pipet, place a single spheroid in each well. With an inverted phase microscope fitted with an ocular micrometer, measure the maximum (= a) and minimum (= b) diameter of each spheroid in the well.

Use the following equation to estimate volume: $V = a \times b^2 \times \pi/6$.

Conduct the measurement 1 or 2 times per week. Although the spheroids are small, change the medium every week. As they grow, the medium in each well should be replaced two or three times per week depending on the size of the spheroids. Use a "pipet aid" pump with serological pipets to remove as much spent media as much as possible without disturbing the spheroids, then add new medium.

### *3.2.5. Spheroid Surviving Fraction*

The approaches to determining the clonogenic potential or surviving fraction for cells in monolayer culture do not generally apply to estimating the clonogenic potential of spheroids. An adaptation of the classic colony formation assay may, therefore, be used.

At the end of the growth-monitoring period, wells containing spheroids that have disaggregated or that appear to no longer be growing are identified and their contents (i.e., spheroids and/or individual cells) plated in another 24-well plate that has not been coated with agar. The plate is then incubated for 2 wk, and the number of wells that have established colonies are counted. The number of spheroids that formed colonies plus the number that continued to grow, divided by the total number monitored to the end of the experiment, gives the surviving fraction of spheroids obtained for that particular experiment.

An alternative, but related, approach to assessing dose-response is the spheroid control assay ***(43)***. This approach may be used when growth monitoring of the spheroids is not necessary.

Forty-eight hours after treatment, transfer spheroids individually to uncoated multi-well plates using a pipet. Place the plates in an incubator and monitor for

3 mo; replace the medium every week. Spheroids that lead to dense monolayer colonies during this period are scored as having survived.

### 3.3. Spheroid Sectioning

Immunohistochemistry or autoradiography of spheroids requires spheroid sectioning. The methodology for obtaining frozen and paraffin spheroid blocks for sectioning are described below. Sectioning is performed using a microtome or a cryomicrotome in the case of frozen blocks.

#### 3.3.1. Frozen Sectioning

Place 10–15 spheroids in 1% eosin for 10 min. This will stain the spheroids and make it easier to distinguish them during sectioning. Wash to remove any excess stain and use a pipet to collect the spheroids, ensuring that as little of the surrounding medium as possible is collected.

Place one drop of OCT on the center of a cryomold, and then put the spheroids on top of the OCT drop. Immediately place the cryomold on dry ice that has been placed in a container with pure ethanol. The dry ice-ethanol mixture must not spill to the top surface of the cryomold containing the OCT and the spheroids.

As soon as the OCT drop freezes, remove the cryomold from the dry ice-ethanol bath. Add more OCT to cover the spheroids and fill the remainder of the cryomold container. To avoid a fault line between the initial OCT drop and the additional OCT used to cover the spheroids, wait until the drop begins to thaw by looking at it through the clear OCT placed on top of it. Once it begins to clear again (i.e., it has thawed), quickly place the filled cryomold back onto the dry ice-ethanol bath. Again, ensure that no ethanol spills into the cryomold. After the OCT has frozen solid, the block may be removed from the cryomold and sectioned. Sections are typically cut at 5–10-µm thickness. Place sections on Superfrost/Plus microscope slides and follow the appropriate staining protocol.

#### 3.3.2. Paraffin Sectioning

Fix spheroids by immersion in 4% (w/v) paraformaldehyde. Leave them at 4°C for 4 h, then wash them twice in phosphate-buffered saline (PBS) for 10 min at 4°C. Transfer the spheroids into 70% ethanol and store them at 4°C until they are embedded in paraffin. (The spheroids may be stored in this way for up to 2 wk.)

Wash the spheroids twice in PBS for 10 min at 4°C. Place one drop of liquefied 1–2% agarose in PBS on a slide, and put the spheroids on top of the drop. Allow the drop to cool and solidify, then scrape it from the slide. Place the agarose in 4% paraformaldehyde for 1 h at 4°C, and then wash it twice in PBS for 30 min at 4°C before following a standard paraffin-embedding protocol.

## 4. Notes

1. Many tumor cell lines will spontaneously form spheroids when inoculated at high density in suspension cultures; however, prostatic lines will typically not form aggregates without the use of microcarrier beads under these conditions ***(44)***. When suspension cultures are desired, spheroids may be initiated using liquid-overlay techniques and then transferred to suspension vessels. Using this method, spheroids may be grown to a larger size than that attainable using liquid-overlay alone. This is presumably caused by increased nutrient/waste transport to/from the spheroid.
2. In general, the medium defined for growing cells in monolayer culture will apply to growing them as spheroids using the overlay culture technique. For certain cell lines, the addition of hormone or other growth factors may be necessary. There are no clear guidelines on what may be required; rather, hormones or growth factors that are known to increase proliferation in monolayer culture should be empirically investigated across a range of concentrations. For example, addition of 10 n*M* 17-β-estradiol is recommended for MCF-7 spheroid growth.
3. When performing the liquid-overlay technique, the number of cells seeded will depend on the cell line. For example, the MCF-7 breast cancer line requires $0.6–1.25 \times 10^4$ cells/cm$^2$, whereas the LNCaP prostate cancer line needs $1.25–2.5 \times 10^4$ cells/cm$^2$.
4. The time required for initial spheroid formation can be quite variable across different cell lines (e.g., MCF-7 needs 5–7 d, LNCaP needs 7–10 d).

## References

1. Sutherland, R. M., McCredie, J. A., and Inch, W. R. (1971) Growth of multicell spheroids in tissue culture as a model of nodular carcinomas. *J. Natl. Cancer Inst.* **46,** 113–120.
2. Sutherland, R. M., MacDonald, H. R., and Howell, R. L. (1977) Multicellular spheroids: A new model target for in vitro studies of immunity to solid tumor allografts. *J. Natl. Cancer Inst.* **58,** 1849–1853.
3. Franko, A. J. and Sutherland, R. M. (1978) Rate of death of hypoxic cells in multicell spheroids. *Radiat. Res.* **76,** 561–572.
4. Franko, A. J. and Sutherland, R. M. (1979) Oxygen diffusion distance and development of necrosis in multicell spheroids. *Radiat. Res.* **79,** 439–453.
5. Franko, A. J. and Sutherland, R. M. (1979) Radiation survival of cells from spheroids grown in different oxygen concentrations. *Radiat. Res.* **79,** 454–467.
6. Sutherland, R. M. (1988) Cell and environment interactions in tumor microregions: the multicell spheroid model. *Science* **240,** 177–184.
7. Nederman, T., Norling, B., Glimelius, B., Carlsson, J., and Brunk, U. (1984) Demonstration of an extracellular matrix in multicellular tumor spheroids. *Cancer Res.* **44,** 3090–3097.
8. Davies, C. D., Muller, H., Hagen, I., Garseth, M., and Hjelstuen, M. H. (1997) Comparison of extracellular matrix in human osteosarcomas and melanomas grow-

ing as xenografts, multicellular spheroids, and monolayer cultures. *Anticancer Res.* **17,** 4317–4326.
9. Ballangrud, A. M., Yang, W. H., Dnistrian, A., Lampen, N. M., and Sgouros, G. (1999) Growth and characterization of LNCaP prostate cancer cell spheroids. *Clin. Cancer Res.* **5,** 3171s–3176s.
10. Bates, R. C., Edwards, N. S., and Yates, J. D. (2000) Spheroids and cell survival. *Crit. Rev. Oncol. Hematol.* **36,** 61–74.
11. Nederman, T., Carlsson, J., and Malmqvist, M. (1981) Penetration of substances into tumor tissue—a methodological study on cellular spheroids. *In Vitro* **17,** 290–298.
12. Durand, R. E. (1981) Flow cytometry studies of intracellular adriamycin in multicell spheroids in vitro. *Cancer Res.* **41,** 3495–3498.
13. Gorlach, A. and Acker, H. (1994) $pO_2$- and pH-gradients in multicellular spheroids and their relationship to cellular metabolism and radiation sensitivity of malignant human tumor cells. *Biochim. Biophys. Acta* **1227,** 105–112.
14. Stuschke, M., Budach, V., Budach, W., Feldmann, H. J., and Sack, H. (1992) Radioresponsiveness, sublethal damage repair and stem cell rate in spheroids from three human tumor lines: comparison with xenograft data. *Int. J. Radiat. Oncol. Biol. Phys.* **24,** 119–126.
15. Santini, M. T., Rainaldi, G., and Indovina, P. L. (1999) Multicellular tumour spheroids in radiation biology. *Int. J. Radiat. Biol.* **75,** 787–799.
16. Dertinger, H. and Hulser, D. (1981) Increased radioresistance of cells in cultured multicell spheroids. I. Dependence on cellular interaction. *Radiat. Environ. Biophys.* **19,** 101–117.
17. Hinz, G. and Dertinger, H. (1983) Increased radioresistance of cells in cultured multicell spheroids. II. Kinetic and cytogenetic studies. *Radiat. Environ. Biophys.* **21,** 255–264.
18. Rodriguez, A., Alpen, E. L., Mendonca, M., and DeGuzman, R. J. (1988) Recovery from potentially lethal damage and recruitment time of noncycling clonogenic cells in 9L confluent monolayers and spheroids. *Radiat. Res.* **114,** 515–527.
19. Olive, P. L. and Durand, R. E. (1985) Effect of intercellular contact on DNA conformation, radiation-induced DNA damage, and mutation in Chinese hamster V79 cells. *Radiat. Res.* **101,** 94–101.
20. Gordon, D. J., Milner, A. E., Beaney, R. P., Grdina, D. J., and Vaughan, A. T. (1990) The increase in radioresistance of Chinese hamster cells cultured as spheroids is correlated to changes in nuclear morphology. *Radiat. Res.* **121,** 175–179.
21. Gordon, D. J., Milner, A. E., Beaney, R. P., Grdina, D. J., and Vaughan, A. T. (1990) Cellular radiosensitivity in V79 cells is linked to alterations in chromatin structure. *Int. J. Radiat. Oncol. Biol. Phys.* **19,** 1199–1201.
22. Frank, C., Weber, K. J., Fritz, P., and Flentje, M. (1993) Increased dose-rate effect in V79-multicellular aggregates (spheroids). Relation to initial DNA lesions and repair. *Radiother. Oncol.* **26,** 264–270.
23. Durand, R. E. (1983) Cellular oxygen utilization and radiation response of V-79 spheroids. *Adv. Exp. Med. Biol.* **159,** 419–434.

24. Gorlach, A. and Acker, H. (1994) The relationship of radiation sensitivity and microenvironment of human tumor cells in multicellular spheroid tissue culture. *Adv. Exp. Med. Biol.* **345,** 343–350.
25. Durand, R. E. (1984) Repair during multifraction exposures: spheroids versus monolayers. *Br. J. Cancer. Suppl.* **6,** 203–206.
26. Weichselbaum, R. R., Little, J. B., Tomkinson, K., Evans, S., and Yuhas, J. (1984) Repair of fractionated radiation in plateau phase cultures of human tumor cells and human multicellular tumor spheroids. *Radiother. Oncol.* **2,** 41–47.
27. Luk, C. K., Keng, P. C., and Sutherland, R. M. (1986) Radiation response of proliferating and quiescent subpopulations isolated from multicellular spheroids. *Br. J. Cancer* **54,** 25–32.
28. Smeets, M. F., Mooren, E. H., and Begg, A. C. (1994) The effect of radiation on G2 blocks, cyclin B expression and cdc2 expression in human squamous carcinoma cell lines with different radiosensitivities. *Radiother. Oncol.* **33,** 217–227.
29. Villa, R., Zaffaroni, N., Bearzatto, A., Costa, A., Sichirollo, A., and Silvestrini, R. (1996) Effect of ionizing radiation on cell-cycle progression and cyclin B1 expression in human melanoma cells. *Int. J. Cancer* **66,** 104–109.
30. Lakin, N. D. and Jackson, S. P. (1999) Regulation of p53 in response to DNA damage. *Oncogene* **18,** 7644–7655.
31. Pandita, T. K., Lieberman, H. B., Lim, D. S., Dhar, S., Zheng, W., Taya, Y., et al. (2000) Ionizing radiation activates the ATM kinase throughout the cell cycle. *Oncogene* **19,** 1386–1391.
32. Bates, R. C., Buret, A., van Helden, D. F., Horton, M. A., and Burns, G. F. (1994) Apoptosis induced by inhibition of intercellular contact. *J. Cell Biol.* **125,** 403–415.
33. Meredith, J. E. Jr., Fazeli, B., and Schwartz, M. A. (1993) The extracellular matrix as a cell survival factor. *Mol. Biol. Cell* **4,** 953–961.
34. Kwok, T. T. and Twentyman, P. R. (1985) The relationship between tumour geometry and the response of tumour cells to cytotoxic drugs—an in vitro study using EMT6 multicellular spheroids. *Int. J. Cancer* **35,** 675–682.
35. Kwok, T. T. and Twentyman, P. R. (1985) The response to cytotoxic drugs of EMT6 cells treated either as intact or disaggregated spheroids. *Br. J. Cancer* **51,** 211–218.
36. Durand, R. E. (1986) Chemosensitivity testing in V79 spheroids: Drug delivery and cellular microenvironment. *J. Natl. Cancer Inst.* **77,** 247–252.
37. Wartenberg, M., Hescheler, J., Acker, H., Diedershagen, H., and Sauer, H. (1998) Doxorubicin distribution in multicellular prostate cancer spheroids evaluated by confocal laser scanning microscopy and the "optical probe technique." *Cytometry* **31,** 137–145.
38. Kerbel, R. S., Rak, J., Kobayashi, H., Man, M. S., St Croix, B., and Graham, C. H. (1994) Multicellular resistance: A new paradigm to explain aspects of acquired drug resistance of solid tumors. *Cold Spring Harb. Symp. Quant. Biol.* **59,** 661–672.
39. Wartenberg, M., Frey, C., Diedershagen, H., Ritgen, J., Hescheler, J., and Sauer, H. (1998) Development of an intrinsic P-glycoprotein-mediated doxorubicin resistance in quiescent cell layers of large, multicellular prostate tumor spheroids. *Int. J. Cancer* **75,** 855–863.

40. Desoize, B. and Jardillier, J. (2000) Multicellular resistance: A paradigm for clinical resistance? *Crit. Rev. Oncol. Hematol.* **36,** 193–207.
41. O'Connor, K. C. (1999) Three-dimensional cultures of prostatic cells: Tissue models for the development of novel anti-cancer therapies. *Pharm. Res.* **16,** 486–493.
42. Yuhas, J. M., Li, A. P., Martinez, A. O., and Ladman, A. J. (1977) A simplified method for production and growth of multicellular tumor spheroids. *Cancer Res.* 37, 3639–3643.
43. Stuschke, M., Budach, V., Klaes, W., and Sack H. (1992) Radiosensitivity, repair capacity, and stem cell fraction in human soft tissue tumors: An in vitro study using multicellular spheroids and the colony assay. *Int. J. Radiat. Oncol. Biol. Phys.* **23,** 69–80.
44. Ingram, M., Techy, G. B., Saroufeem, R., Yazan, O., Narayan, K. S., Goodwin, T. J., et al. (1997) Three-dimensional growth patterns of various human tumor cell lines in simulated microgravity of a NASA bioreactor. *In Vitro Cell. Dev. Biol. Anim.* **33,** 459–466.

# 7

# Animal Models of Prostate Cancer

**Pamela J. Russell and Dale J. Voeks**

## 1. Introduction

Prostate cancer is now the most common malignancy and the second highest cause of cancer death of men in Western society. It has a reasonably slow doubling time, is initially androgen dependent (AD) or androgen sensitive (AS), produces prostate-specific antigen (PSA), and prostate specific membrane antigen (PSMA) and, with time, metastasizes to lymph nodes, bone, and other organs; it progresses to an androgen-independent (AI) state. Prostate cancer rarely arises spontaneously in animals, and human and animal prostates differ in their anatomy, cellular content, and in the development of spontaneous benign hyperplasia that commonly occurs in men as they age but rarely in other species. Existing prostate cancer models include rodent models, human cell lines (in the main derived from metastatic deposits), and gene transfer and transgenic models. Only the transgenic models provide the spectrum of disease as it occurs in men, with progression from prostate intraepithelial neoplasia (PIN) through AD to AI disease with metastases. Special systems have been devised to study the growth of prostate cancer cells in bone; these are described elsewhere in this book. The in vivo systems provide the appropriate cellular milieu allowing for epithelial cell–stromal cell interactions that are crucial to the behavior of prostate cancer cells. This chapter provides a critical appraisal of the models and some of their uses in studies of disease progression and for testing new therapeutic options.

## 2. The Normal Prostate Elements

### *2.1. Human Prostate*

The prostate differs among mammalian species by anatomy, biochemistry, and pathology. In the human, it comprises 70% glandular elements and 30% fibromuscular stroma and develops from the urogenital sinus by stimulation

From: *Methods in Molecular Medicine, Vol. 81: Prostate Cancer Methods and Protocols*
Edited by: P. J. Russell, P. Jackson, and E. A. Kingsley © Humana Press Inc., Totowa, NJ

with dihydroxytestosterone (DHT) ***(1)***. McNeal ***(2)*** has described four zones in the prostate, each in contact with a different area of the urethra. The peripheral zone contains 75% of the glandular content of the prostate and is the predominant site for adenocarcinomas; the transition zone contains <5% of the glandular content but is the predominant site of benign prostatic hyperplasia (BPH) ***(3)*** in which both glandular and stromal overproliferation may occur causing clinical symptoms related to pressure on the urethra ***(4)***.

### 2.2. Rodent Prostate

In the rodent, the prostate has anatomically distinct lobes with the dorsal or dorsolateral lobe being histologically and biochemically similar to the human prostate peripheral zone ***(5,6)***. The epithelial to stromal cell ratio in the mouse and rat prostate is ~5:1, but increased growth shifts the ratio towards the stromal component ***(7)***. This ratio is around 1:3 in the adult guinea pig ***(8)***.

Several studies describe spontaneous and induced hyperplasia ***(9)***, mostly of epithelial cells in the rat dorsal prostate, providing valuable models for study ***(10)***. In contrast, spontaneous BPH in the guinea pig occurs with age and, like humans, is generally characterized by stromal hyperplasia ***(8)***. Tumors of the rat prostate provide valuable models for study because of their dependence on androgen as a tumor promoter ***(10)***.

### 2.3. Prostate of Other Species

The canine is the only nonhuman species in which prostate cancer occurs frequently. Clinically aggressive disease with metastases arises spontaneously with age, and high-grade PIN, thought to be a potential precursor of prostate cancer, is often present in older dogs ***(11–13)***. The canine prostate is not lobular but rather is histologically homogenous consisting predominantly of epithelium with minimal stromal elements. Unlike the human prostate peripheral zone, there is no surrounding fibromuscular stroma ***(14)*** and whereas the canine prostate serves as a model for BPH ***(11–13)***, it contains diffuse epithelial proliferation but no stromal hyperplasia ***(13)***.

Primate prostates consist of cranial and caudal lobes with the cranial similar to the central zone of the human prostate and the caudal homologous to the transition and peripheral zones ***(15)***. Spontaneous and induced hyperplasia is predominantly found in the caudal zone, and sporadic cases of prostate cancer have also been documented ***(16)***. The human and chimpanzee prostates show particular anatomic and physiologic similarity; the chimpanzee prostate is histologically heterogeneous with ducts and acini surrounded by stroma, has poor lobal separation, uses DHT for growth and development, and produces many of the same proteins as the human prostate ***(17)***. The chimpanzee develops spontaneous BPH similar to human BPH in pathologic and clinical variables,

including prostate volume, PSA, histologic BPH, and urodynamics ***(15)***. The baboon also develops BPH; hormonal stimulation causes glandular and stromal hyperplasia in the caudal zone ***(18)***. Among the monkey species, the cynomolgus monkey prostate is the most similar to the human prostate. Unlike other monkey species, the cranial lobe is partly incorporated into the dorsal area of the caudal lobe, creating a transition zone, and considerable stroma is present ***(19)***.

## 3. Prostate Cancer in Rodents

Different models mimic various aspects of the clinical disease depending upon the site of origin in spontaneous and induced transplantable models, the strain of rat, and the protocol or carcinogen used. A recent workshop on animal models of prostate cancer ***(9)*** lists the characteristics and perceived strengths and limitations of rodent models of prostate cancer. Spontaneous prostate tumor models allow the natural course of multistep neoplasia to be followed without the need for chemical exposure. Carcinogens, especially in combination with testosterone, can induce prostate carcinomas in rats, but none are prostate-specific ***(20)***.

### *3.1. Spontaneous*

Spontaneous tumors include the Pollard rat tumors in Lobund-Wistar and Sprague-Dawley rats ***(21,22)*** and ACI/Seg rat prostate cancers in aging August × Copenhagen hybrids ***(23,24)***, but they tend to have low tumor incidence and long latency periods, as well as a lack of metastases. They have been described elsewhere in detail ***(9,25,26)***. The Dunning R-3327 rat prostatic adenocarcinoma model is the best known; it was derived by the passage of a spontaneous prostate tumor discovered at autopsy in a Copenhagen rat ***(27)***. Subcutaneously implanted tumors become palpable in ~60 d and histologically are well differentiated adenocarcinomas with both glandular and stromal elements. Multiple well-characterized sublines indicative of cancer progression have been developed ***(28)***, including AS lines (H subline) and AI tumors (A subline), which lack 5α-reductase and androgen receptors ***(29)*** and metastatic ***(30)*** sublines. Cell lines derived from the models are transfectable, transplantable, and produce reproducible metastases. A limitation of this model is the expression of nonprostatic proteins by the H subline ***(31)***. Nevertheless, the Dunning model has demonstrated utility by identifying genes important in the prostate, such as KAI-1, CD44, and β-thymosin ***(32)***.

The Shionogi mouse mammary carcinoma (SC-115) was established from a mammary adenocarcinoma but after passage in male DD/S mice was found to be AD. Serial passage has generated variant lines that include AI lines, as well as those sensitive to estrogens and glucocorticoids. These lines are useful for

studies of intermittent androgen therapy and for analysis of the mechanisms involved in the generation of androgen independence ***(25,33)***.

### 3.2. Induced

Prostate tumors have been induced by chronic administration of testosterone in Lobund-Wistar ***(34)*** and Noble rats ***(35,36)***, illustrating the critical role of androgens as promoters in the pathogenesis of prostate cancer. Chemical carcinogens have also been used to induce prostate cancers in Fischer F344 and Wistar ***(37)*** rats. The features of these models have been summarized elsewhere ***(9)***. Recently, studies of hormone-induced tumors in Noble rats indicated that insulin-like growth factor-1 (IGF-1) changed from paracrine production by stromal cells to an autocrine loop in prostate epithelial cells during cancer induction ***(38)***. The use of intraprostatic rather than iv administration of *N*-methyl-*N*-nitrosurea to Wistar rats increased the incidence and decreased the latency of prostate neoplasms and prevented the formation of tumors in other organs typically found after iv injection ***(39)***. Whereas induced prostate tumors show differences in their location in regions of the rat prostate-seminal vesicle complex ***(40)*** depending upon the agent used for induction and the strain of rats, they are particularly useful for studies of chemoprevention and dietary modulation and most develop a high incidence of invasive carcinomas, although bony metastases are rare. They do allow studies of the progression of disease. Cell lines have been derived from spontaneous ACI/Seg rat tumors, from Lobund-Wistar and from chemically induced Wistar rat tumors ***(9)***.

## 4. Xenografts

Xenografts provide the opportunity to study the expression of human genes within an in vivo context and within the particular organ environment of interest. They also allow an assessment of organ-preferred metastasis and the evaluation of important principles such as reciprocal stromal cell/epithelial interactions in association with altered hormonal status ***(41)***. Up until now, approx 25 xenograft models of human prostate cancer have been established and reported in the literature ***(42)***. The limitations of these models include a poor take rate from fresh operation material, relatively poor metastatic potential when implanted subcutaneously and potential species–species interactions that may influence tumor growth and progression ***(43)***. Recently *Alu*I/II *in situ* hybridization has been described as a rapid method for detecting malignant mouse cell contamination in human xenograft tissue from nude mice ***(44)***.

Apart from the growth of established human prostate cancer cell lines (described in Chapter 2) in immune-deficient mice, other xenograft lines, which may or may not grow in tissue culture, have also been established. Pretlow's group has been very active in attempting to grow primary prostate tumor

biopsies in nude or SCID mice but initially with only marginal success, despite the use of testosterone pellets and rapid transport from surgery to the laboratory ***(45)***. Others have found that small transplanted tumor pieces do not grow without α-DHT but that larger tumors grow after the removal of the α-DHT ***(46)***. The most used of Pretlow's xenograft lines is the CWR22 line, which is highly AD in vivo and relapses to an AI line, CWR22R, after androgen withdrawal ***(47)***, thus providing a useful model for studies of the progression of human prostate cancer. Studies in this model have suggested that IGF binding protein-5 (IGF-bp5) is upregulated in androgen receptor (AR)-positive xenografts and that IGF-bp5 may be a mediator of androgen-induced growth of CWR22 tumors ***(48)***. Microarray analysis of genes expressed in the AI, compared with AD, CWR22 xenografts has identified androgen-responsive genes whose expression decreases during androgen deprivation but which are subsequently reexpressed in the CWR22-R (AI) model at levels comparable with those in CWR22; these gene products include PSA, human kallikrein 2, the calcium-binding protein, S100P, and the FK-506-binding protein, FKBP51 ***(49)***. The results imply that evolution to AI is caused in part by reactivation of the androgen-response pathway in the absence of androgens but that this reactivation is probably incomplete. The AI xenograft, CSR222R, has been shown to highly express NKX3.1, a homeobox transcription factor that may have regulatory roles during prostate cancer progression ***(50)***. The CRW series of AI xenografts (CRW22, CWR22R, and SWR91) has also been extensively used as a model for drug activity evaluation because the sensitivities of the xenografts differ, mimicking the situation that occurs in patients ***(51)***. More recently, sc injection of peripheral blood from patients with metastatic prostate cancer has been used to establish xenografts in nude mice ***(52)***. Prostate cancer from 2 of 11 patients grew as metastases in the lungs of the nude mice.

PC-82 is one of several xenograft lines established in Rotterdam. PC-82 and PC-EW are AD prostate cancer xenograft lines ***(53,54)*** that are useful in studies of AR regulation ***(55)***. An AR-null model has been developed from the PC-82 line by growth in AR-null male nude mice lacking both AR and T-cell function ***(56)***. The results show that both the androgen-stimulated proliferation and the suppression of programmed cell death of PC-82 cells are initiated by the AR pathway directly within these cancer cells and do not involve initiation by AR-expressing stromal cells in a paracrine manner. A series of seven new prostate tumor xenografts were all diploid, except PC-374, and displayed heterogeneous expression of AR apart from PC-324 and PC-339, which were AR negative; this series covers a range of progression seen in patients and provides invaluable models for study ***(57)***. Honda and LuCaP xenografts are also both AS ***(58,59)***. A series of xenograft lines established in nude mice from prostate cancer metastases, DUKAP-1 and DUKAP-2 (AS), and DU9479 (AI), has

been used to confirm that alternative splicing of the fibroblast growth factor receptor 2 (FGF-R2), which has been shown to change from the FGF-R2 (IIIb) isoform (with high affinity for keratinocyte growth factor) to the FGF-R2 (IIIc) isoform (with a high affinity for basic and acidic fibroblast growth factors) with progression of prostate cancer in rats ***(60,61)***, also occurs in human prostate cancer ***(62)***. However, when therapy based on the use of basic fibroblast growth factor receptor-directed-toxin chimeras was used, it was necessary to alternatively target DU-145 tumor cells with a saporin immunotoxin to circumvent resistance ***(63)***.

The LuCaP23 xenograft series was established from different prostate metastases, two from lymph nodes (LuCaP 23.1 and 23.8) and one from a liver metastasis (LuCaP 23.12) ***(64)***. The xenografts show glandular differentiation, are AS, express PSA, and show decreased PSA expression after androgen withdrawal. The LuCaP 23.12 xenograft model has proved useful for studies of intermittent androgen therapy ***(65)***. Two populations of cells are represented in LuCaP xenografts; a neurone-specific enolase (NSE) positive population that is also positive for Bcl-2 emerges after castration, whereas the other population is NSE negative ***(66)***. Fluorescent *in situ* hybridization (FISH) analysis indicates differences in chromosomal rearrangements between LuCaP 23 and another xenografted line, RP22090, about which there is little information ***(67)***. The UCRU-PR-2 xenograft line, established from a patient with primary prostatic adenocarcinoma, is a small cell carcinoma of the prostate that is NSE positive and secretes pro-opiomelano-corticotropin-derived peptides ***(68,69)***. Cell lines have not been established in vitro from these lines. Xenografts propagated in SCID mice appear to grow more easily than those grown in nude mice. Six of eight explants from locally advanced or metastatic prostate cancer tissue were established ***(70)*** and were grown in a manner that recapitulates the clinical transition from AS to AI growth, accompanied by micrometastases. Four of these were PSA positive and two, LAPC-3 and LAPC-4, showed chromosomal abnormalities and expressed wild-type ARs. LAPC-3 is AI, whereas LAPC-4 is AS. The LAPC-4 xenograft has been propagated as a continuous cell line that retains its hormone-responsive characteristics, but the xenografted line can progress to AI when grown in female or castrated male mice. In this model, the AI sublines express higher levels of HER-2/neu than the AS cells. Forced overexpression of HER-2/neu in AD cells allowed ligand-independent growth. HER-2/neu activated the AR pathway in the absence of ligand and synergized with low levels of androgen to superactivate the pathway ***(71)***. As in human prostate cancer, prostate cancer xenografts secrete PSA, which is complexed with a murine protease inhibitor with high homology to murine alpha1-P1, and the percentage of free PSA is a characteristic of each xenograft line tested, in agreement with patient values at the time of tumor harvest ***(72)***.

Examination of 10 prostate cancer xenografts for deletions of PTEN, a tumor suppressor gene that appears to be frequently lost in prostate cancer, revealed a homozygous deletion in only 1 of 10 tumors; however, reduced or absent expression was seen in five tumors, and could be restored by treatment with 5-azadeoxycytidine, suggesting that hypermethylation was responsible ***(73)***.

Special methodology has been established for studying bony metastases by implanting prostate cancer cell lines in the femur of nude or SCID mice. These models are described in another chapter.

## 5. Transgenic and Reconstitution Models

The combination of advances in the hormonal control of reproduction, the harvest/manipulation and re-implantation of fertilized embryos, and recombinant DNA techniques led to the advent of transgenic technology nearly 20 years ago *(*reviewed in **refs.** ***74,75)***. The ability to introduce stably foreign genetic information into the mammalian cell line has been a landmark development in molecular biology, shifting emphasis back to the whole animal as an experimental model system. Transgenics offer a unique opportunity to study the effects of altered gene expression and ultimately carcinogenesis in the proper biologic milieu. The potential exists to create an animal model that faithfully represents the broad spectrum of human prostate cancer from early to late stages, allowing insight into key genetic events in tumor initiation and promotion and also serving as a tool to evaluate therapeutics. The majority of transgenic studies involve restricted transcription of various genes with oncogenic potential through the use of tissue-specific promoters. In prostate-directed transgenics (*see* **Table 1**), a number of promoter elements have been investigated ***(85)***.

Rat probasin is largely found in the dorsolateral region of the rodent prostate ***(86)***. Transcriptional activity is hormonally regulated and begins in the prostate at sexual maturity ***(87)***. Transgenic mice bearing the minimal rat probasin promoter region (–426 to +28) (PB) driving a chloramphenicol acetyltransferase reporter construct displayed highly restricted expression to the prostate with the most pronounced activity in the dorsolateral prostate ***(88)***. The androgen dependence of this promoter was found to require the region between –251 and –240 for androgen induction ***(89)***. In subsequent research, a large 11.5-kb fragment of the probasin promoter (LPB) containing upstream androgen and zinc regulatory regions was able to direct high levels of reporter expression specifically to prostate epithelial cells in transgenic mice ***(90)***. More recent studies have shown that the sequences necessary to target prostate-specific epithelial expression are contained within a small composite *PB* promoter, ARR2PB, and that high transgene expression can be regulated by both androgens and glucocorticoids ***(91)***.

**Table 1**
**Characteristics of Transgenic Mouse Models of Prostate Cancer**

| Model | Tissues involved | PIN–CaP progression | Metastasis (age of onset) | Androgen status | Reference |
|---|---|---|---|---|---|
| C3(1)-*TAg* | Prostate—ventral most affected<br>Urethra<br>Mammary gland<br>Salivary gland | 8–≥28 wk | No | Not determined | ***76*** |
| FG-*TAg* | Prostate<br>Adrenals<br>Adipose | 16–20 wk | Lymph<br>Adrenals<br>Kidney<br>Lung<br>Bone<br>Thymus<br>(20 wk) | AI | ***77*** |
| Cryptdin-2-*TAg* | Prostate—neuroendocrine cells | 8–≥12 wk | Lymph<br>Liver<br>Lung<br>Bone<br>(24 wk) | AI | ***78*** |
| LPB-*TAg** | Prostate—dorsolateral most affected | 10–≥22 wk | No | AD | ***79*** |
| Large PB-*TAg* | Prostate—PIN, PCa, NE,<br>in dorso-lateral, and ventral lobes | 2–12 mo | Lymph node<br>Liver<br>Lung | NE are AR negative | ***80*** |

| | | | | | |
|---|---|---|---|---|---|
| PB-*TAg* (TRAMP) | Prostate—dorsolateral most affected | 7–≥12 wk | Lymph<br>Lung<br>Kidney<br>Bone<br>Adrenals<br>(28 wk) | Variable | ***81*** |
| C3(1)-*Py-MT* | Prostate—ventral most affected<br>Lung<br>Vas deferens<br>Epididymus<br>Mammary gland<br>Salivary gland<br>Urethra | 11 wk (CaP) | No | Not determined | ***82*** |
| *PBECOR1* | Prostate—mild to severe hyperplasia, through low- to high-grade PIN to well-differentiated adenocarcinoma. | 4–24 mo | No | Not determined | ***83*** |
| *PSMA* or *PSM′* | Mice generated | Not determined | Not determined | Not determined | ***84*** |

*TAg,* SV40 large T and small t antigen; *TAg*,* SV40 large T antigen; *C3(1),* prostate steroid-binding protein promoter; *FG,* human fetal globin promoter; *LPB,* 11.5 kb probasin promoter; *PB,* 454 bp probasin promoter; *Py-MT,* polyomavirus middle T; PIN, prostatic intraepithelial neoplasia; CaP, prostate cancer.

When the *PB* promoter was used to drive expression of genes implicated in the induction of genomic instability (*ECO:RI* and c-*fox*), PBECO:R1 transgenic mice developed progressive prostate cancer ending with well-differentiated adenocarcinoma of the prostate, but c-*fos* was not associated with any pathology ***(83)***.

Recent interest has focused on PSA, a serine protease with nearly exclusive production by normal and, in most cases, neoplastic luminal prostatic epithelial cells (reviewed in **ref.** ***92)***. Its androgen-regulated promoter region has been isolated and characterized ***(93)***. Transgenic mice were generated bearing a reporter construct under the transcriptional control of the 632 bp proximal *PSA* promoter or the 6-kb PSA promoter containing an upstream enhancer region ***(94)***. Transgene expression was not detected with the 632 bp promoter. Mice bearing the 6-kb promoter demonstrated prostate-specific expression mirroring that seen in humans ***(94)***. In further research, transgenic mice harboring a 14-kb genomic sequence which encompassed the entire gene and adjacent flanking sequences had similar PSA expression patterns to those of humans ***(95,96)***.

Several transgenic models have generated hyperplasia in the prostate. The apoptosis suppressing proto-oncogene, *bcl-2,* under transcriptional control of the *C3(1)* promoter resulted in increased cell numbers in the prostatic stroma and epithelium ***(97)***, whereas CC3(1)-c-*myc* transgenic mice developed epithelial cell abnormalities similar to those seen in low-grade PIN ***(98)***. In related models, MMTV-int-2/*Fgf*-3 (fibroblast growth factor member) and MMTV-*kgf* (keratinocyte growth factor, which is upregulated in int-2-derived mammary tumors) caused prostate gland enlargement in transgenic mice ***(99,100)***. The *Cdc37* gene encodes a 50-kDa protein that targets intrinsically unstable oncoprotein kinases such as Cdk4, Raf-1, and src to the molecular chaperone Hsp90. Transgenic mice expressing Cdc37 in the prostate displayed a wide range of growth-related abnormalities, including prostatic epithelial cell hyperplasia and dysplasia ***(101)***. Transgenic mice overexpressing the prolactin gene also displayed dramatically enlarged prostates ***(102)***. Other transgenic models bearing MMTV-whey acidic protein (WAP) and metallothionein-transforming growth factor-α (TGF-α) developed hyperplasia of the coagulating gland epithelium ***(103,104)***.

Several of the current transgenic models of prostate cancer that display the most potential use tissue-specific regulatory regions to target expression of the SV40 large tumor antigen (*TAg*), which functions as an oncogene by binding to and interfering with the *p53* and *Rb* tumor suppressor genes ***(105)***. Losses of wild-type p53 and pRb function are considered to be critical events in prostate cancer progression ***(106)***. Separate models have been created employing the 5′ flanking region of the prostate steroid binding protein *C3(1)* gene ***(76)***, the

human fetal globin promoter ***(77)***, a region of the mouse *cryptdin-2* gene ***(78)***, the long *PB* promoter ***(79)***, or the minimal *PB* promoter ***(80)*** to drive the expression of *TAg*.

In the C3(1)-*TAg* model, male mice develop prostatic hyperplasia that progresses to adenocarcinoma in most animals by 7 mo of age in the ventral lobe and 11 mo of age in the dorsolateral lobe with occasional metastasis to lung ***(76,107)***. The mice display a progression from low- to high-grade PIN precursor lesions histologically resembling that found in humans ***(107)***. Female mice develop mammary adenocarcinoma in 100% of the animals by 6 mo of age ***(76)***. C3(1)-*TAg* transgenic mice often show H-*ras* mutations early in the development of prostate cancer ***(108)***. A mouse prostate cell line, Pr-14, has been established from these mice, and undergoes alterations in its differentiation dependent upon serum concentration when grown on Matrigel™ ***(109)***.

Transgenic mice from the fetal globin-*TAg* lines somewhat unexpectedly developed prostate tumors, brown adipose tumors, and adrenocortical tumors ***(77)***. In the line with prostate involvement, tumors originating from ventral and dorsal lobes showed mixed epithelial and neuroendocrine features and metastasized to lymph nodes and distant sites ***(110)***. Moreover, the gamma/*T-15* line containing the fetal globin promoter linked to SV40 *TAg* developed AI prostate carcinomas; studies using this line have suggested that prostatic transcription factors, GATA-2 and -3, are involved in the androgen regulation of the *PSA* gene ***(111)***.

The *cryptdin-2* gene was able to direct TAg expression to neuroendocrine cells in the prostate. Transgene expression begins between 7 and 8 wk of age, resulting in PIN within 1 wk ***(78)***. AI prostate cancer with local invasion develops rapidly with eventual metastasis to lymph nodes, liver, lung, and bone by 6 mo ***(78)***. This model demonstrates that prostate neuroendocrine cells are sensitive to transformation and resulting cancer is highly aggressive ***(78)***.

In the LPB model, a *TAg* deletion mutant (without expression of the small t antigen) was able to transform prostate epithelial cells of transgenic mice with an incidence of 100% by 10 wk of age ***(79)***. Progression typically proceeds through hyperplasia, low- and high-grade dysplasia, carcinoma *in situ*, adenocarcinoma, and local invasion in a manner similar to the human condition but without evidence of metastasis ***(79)***. The model also exhibits multifocality, reactive stromal proliferation, and AD growth of the primary tumor.

More recently, seven lines of transgenic mice with the large *PB* promoter linked to SV40 *TAg* that develop prostatic neoplasia have been described; one of these, 12T-10, developed low-grade PIN, high-grade PIN, microinvasion, invasive carcinoma, and poorly or undifferentiated carcinoma with neuroendocrine differentiation in sequential order ***(80)***. Metastases to lymph node, liver, and lung were common, often with neuroendocrine, AI status.

The PB-*TAg* transgenic adenocarcinoma mouse prostate (TRAMP) model appears to closely mimic the human disease. Mice show highly specific prostate expression of the transgene by 8 wk of age leading, to the development of adenocarcinoma in the dorsolateral region as early as 10–12 wk of age ***(81)***. Metastasis to the lymph nodes and lungs is present in 100% of mice by 28 wk of age ***(112)***. A longitudinal cohort analysis of prostate cancer progression in this line showed that primary tumors became palpable by 10–38 wk of age, with cancer death occurring between 24 and 39 wk of age ***(113)***. Castration studies demonstrated that prostate cancer is variable in AD as early as 12 wk of age ***(114)***. The TRAMP model reliably develops prostate adenocarcinoma that resembles the disease progression of human prostate cancer. TRAMP-BC cell lines were recently established from a TRAMP mouse that presented with hind leg paralysis and osteolytic and osteoblastic features of bony metastasis of the spine; when inoculated subcutaneously followed by primary tumor resection or via an intracardiac route, bony metastases occurred, providing a new model for this late-stage disease ***(115)***. The TRAMP model already is serving as a tool to investigate the basic science of prostate cancer initiation and progression, including the role of the IGF axis ***(116)***, transcription factors, EGF1 ***(117)***, cell spreading factors (RhoA) ***(118)***, and cell adhesion molecules (C-CAM) ***(119)***. Crossing of TRAMP mice with PB-*bcl*-2 transgenic mice decreased the latency to tumor formation, had no effect on metastasis, but reduced the incidence of AI prostate cancer, suggesting that *bcl*-2 can facilitate multistep prostate carcinogenesis in vivo ***(120)***. The TRAMP model also provides a tool to evaluate the efficacy of potential therapeutics, including hormone treatments ***(121)***, biological modifiers such as prostaglandins, which induce heat shock proteins ***(122)***, and immunotherapeutic strategies ***(123–125)***.

In a different model of prostate cancer, the role of signal transduction in prostatic epithelium transformation was investigated through the generation of transgenic mice bearing the polyomavirus middle T gene under transcriptional control of the C3(1) gene promoter ***(82)***. Androgen-responsive urogenital tissues expressing the transgene showed disrupted growth and development with the presence of hyperplasia, dysplasia, and invasive carcinoma ***(82)***. Expression of the transgene was detected in the ventral and dorsal prostate, epididymis, parotid gland, seminal vesicles, coagulating gland, and also in unexpected sites like the lung, where endogenous C3(1) is not detected in the rat ***(82)***.

PSMA, also known as folate hydrolase I, is a glutamate-preferring carboxypeptidase with at least two enzymatic activities, *N*-acetylated alpha-linked L-amino dipeptidase and a gamma-glutamyl carboxypeptidase (folate hydrolase) that is expressed in virtually 100% of prostate cancers and appears to be

upregulated as the cancer progresses. In the normal prostate however, the major form of PSMA mRNA is alternatively spliced to produce a truncated form of the protein, PSM′, which is missing the transmembrane domain and is localized in the cytosol ***(126)***. PSMA and PSM′ are not expressed in the prostate of any animals examined to date, but the mouse homolog, termed Holh1, is found in the mouse brain and kidney ***(127)***. Transgenic mice expressing PSMA or PSM′, together with *PSM* enhancer ***(128)*** in the prostate have been generated ***(84)*** and will be studied for the development of prostate cancer when placed on a low folate/methyl diet.

Thompson and co-workers ***(129)*** developed a transgenic gland model of prostate cancer mouse prostate reconstitution by using the ability of mesenchyme and epithelium from fetal urogenital sinus to form a mature prostate when grafted into the renal capsule of an adult mouse ***(130)***. Introduction of candidate genes into separate compartments allows for the study of stromal and epithelial interactions in carcinogenesis. After retroviral transfer of *ras* and *myc* to the dissociated urogenital sinus, the reconstituted prostate develops adenocarcinoma in a reproducible manner, whereas transfection with either *ras* or *myc* alone results in dysplasia or focal epithelial hyperplasia, respectively ***(129)***. Transfection of the urogenital epithelium with both *ras* and *myc* results in the development of carcinoma in 80% of animals after 8 wk when combined with the mesenchyme component. When urogenital mesenchyme is transfected with *ras* and *myc* and combined with the epithelium component, the reconstituted prostate develops dysplasia in 100% of animals ***(131)***. Numerous studies of prostate carcinogenesis have been performed in the mouse prostate reconstitution model, and resulting cell lines have been extensively used for basic and applied prostate cancer research ***(132,133)***.

## 6. Uses Of Preclinical Models of Prostate Cancer

The comparative utility of rodent models of prostate cancer was summarized in a recent workshop ***(9)***. Rat species that develop spontaneous prostate tumors are particularly useful for studies on mechanisms or enhancement of carcinogenesis and latency. In contrast, the biology of progression of prostate cancer can be studied in induced models that tend to become AI and show invasion and metastases. Experimental therapies for prostate cancer that metastasizes to the bone have used either Copenhagen rats, inoculated with R3327-MATLyLu (Dunning) prostate tumor cells with concomitant clamping of the inferior caval vein, which results in bony metastases ***(134)***, or the SCID models injected intrafemorally with prostate cancer cell lines ***(135)***. Biodistribution studies in the rat model have indicated preferential uptake of $^{186}$Rhenium-hydroxyethylidene diphosphonate ($^{186}$Re-HEDP) in bone tissue, particularly in areas of bone

formation and turnover, suggesting that such treatment has potential for treatment of prostate cancer that has disseminated to the skeleton. Problems of myelotoxicity would need to be carefully considered ***(134)***. Subsequent studies in Chacma baboons before clinical trials indicated that the radiation dose delivered to the bone marrow by $^{186}$Re-HEDP did not cause detrimental effects in baboons ***(136)***. Other researchers have used promoters from osteocalcin to drive expression of gene therapy in bony metastases ***(137)***.

### 6.1. Hormone Therapy

Because of their androgen-sensitivity, LNCaP cells and their sublines have been extensively used to study the effects of androgen ablation, including intermittent hormone therapy, both mainstays of treatment for patients with prostate cancer. However, such work is outside the scope of this chapter; the changes that occur in the AR are described in another chapter.

### 6.2. Novel Therapies

Metastatic human prostate cancer requires novel therapeutic strategies to overcome its low proliferative rate and its resistance to conventional chemotherapeutic agents. Some new approaches that have been tested in preclinical models of prostate cancer include interruption of angiogenesis, generation of apoptosis, the use of targeted toxins, targeted using antibodies or growth factors, and transcriptionally targeted gene therapy. Many other prospective treatments have also been used but are outside the scope of this review.

## 7. Concluding Remarks

Research into the development of models of prostate cancer representative of the heterogeneity of the disease in humans has yielded numerous breakthroughs in recent years. The combination of preneoplastic prostate models, early rodent models, human prostate cancer cell lines, xenografts with particular emphasis on distant site metastasis, and transgenics provides a great diversity of tools for the examination of prostate cancer and prostate cancer metastasis. Knowledge of the molecular mechanisms involved in the shift to invasive disease allows for the development of new treatment strategies. Existing models also serve to evaluate novel therapeutics in multiple stages of the disease encompassing AD and AI growth and the targeting of metastatic deposits.

## References

1. Brooks, J. D. (1998) Anatomy of the lower urinary tract and male genitalia, in *Campbell's Urology* (Walsh, P. C., ed.), W. B. Saunders, Philadelphia, pp. 89–128.
2. McNeal, J. E. (1981) The zonal anatomy of the prostate. *Prostate* **2,** 35–49.

3. Partin, A. W. and Coffey, D. S. (1998) The molecular biology, endocrinology, and physiology of the prostate and seminal vesicles, in *Campbell's Urology* (Walsh, P. C., ed.), W. B. Saunders, Philadelphia, pp. 1381–1428.
4. Shapiro, E., Becich, M. J., Hartanto, V., and Lepor, H. (1992) The relative proportion of stromal and epithelial hyperplasia is related to the development of symptomatic benign prostate hyperplasia. *J. Urol.* **147,** 1293–1297.
5. Price, D. (1963) Comparative aspects of development and structure in the prostate. *Monogr. Natl. Cancer Inst.* **12,** 2–25.
6. Zhau, C. Y., Tam, C. C., and Wong, Y. C. (1993) Morphogenesis and ductal development of the prostatic complex of the guinea pig. *J. Morphol.* **217,** 219–227.
7. Hayashi, N., Sugimura, Y., Kawamura, J., Donjacour, A. A., and Cunha, G. R. (1991) Morphological and functional heterogeneity in the rat prostatic gland. *Biol. Reprod.* **45,** 308–321.
8. Horsfall, D. J., Mayne, K., Ricciardelli, C., Rao, M., Skinner, J. M., Henderson, D. W., et al. (1994) Age-related changes in guinea pig prostatic stroma. *Lab. Invest.* **70,** 753–763.
9. Banerjee, P. P., Banerjee, S., Lai, J. M., Strandberg, J. D., Zirkin, B. R., and Brown, T. R. (1998) Age-dependent and lobe-specific spontaneous hyperplasia in the brown Norway rat. *Biol. Reprod.* **59,** 1163–1170.
10. Lucia, M. S., Bostwick, D. G., Bosland, M., Crockett, A. T., Knapp, D. W., Leav, I., et al. (1998) Workgroup 1: Rodent models of prostate cancer. *Prostate* **36,** 49–55.
11. Leav, I. and Ling, G. V. (1968) Adenocarcinoma of the canine prostate. *Cancer* **22,** 1329–1345.
12. Berry, S. J., Strandberg, J. D., Saunders, W. J., and Coffey, D. S. (1986) Development of canine benign prostatic hyperplasia with age. *Prostate* **9,** 363–373.
13. Waters, D. J. and Bostwick, D.G. (1997) Prostatic intraepithelial neoplasia occurs spontaneously in the canine prostate. *J. Urol.* **157,** 713–716.
14. McNeal, J. E. (1984) Anatomy of the prostate and morphogenesis of BPH, in *New Approaches to the Study of Benign Prostatic Hyperplasia* (Kimball, F. A., ed.), Alan R. Liss, New York, pp. 27–43.
15. Steiner, M. S., Couch, R. C., Raghow, S., and Stauffer, D. (1999) The chimpanzee as a model of human benign prostatic hyperplasia. *J. Urol.* **162,** 1454–1461.
16. Lewis, R. W. (1997) Benign prostatic hyperplasia in the nonhuman primate, in *New Approaches to the Study of Benign Prostatic Hyperplasia* (Kimball, F. A., ed.), Alan R. Liss, New York, pp. 235–255.
17. Lewis, R. W., Kim, J. C. S., Irani, D., and Roberts, J. A. (1981) The prostate of the nonhuman primate: normal anatomy and pathology. *Prostate* **2,** 51–70.
18. Karr, J. P., Kim, U., Resko, J. A., Schneider, S., Chai, L. S., Murphy, G. P. et al. (1984) Induction of benign prostatic hypertrophy in baboons. *Invest. Urol.* **23,** 276–289.
19. Kamischke, A., Behre, H. M., Weinbauer, G. F., and Nieschlag, E. (1997) The cynomolgus monkey prostate under physiological and hypogonadal conditions: an ultrasonographic study. *J. Urol.* **157,** 2340–2344.
20. Shirai, T., Takahashi, S., Cui, L., Futakuchi, M., Kato, K., Tamano, S., et al. (2000) Experimental prostate carcinogenesis—rodent models. *Mutat. Res.* **462,** 219–226.

21. Pollard, M. (1973) Spontaneous prostate adenocarcinomas in aged germfree Wistar rats. *J. Natl. Cancer Inst.* **51,** 1235–1241.
22. Pollard, M. and Luckert, P. (1985) Prostate cancer in a Sprague-Dawley rat. *Prostate* **6,** 389–393.
23. Shain, S. A., McCullough, B., and Segaloff, A. (1975) Spontaneous adenocarcinomas of the ventral prostate of aged AXC rats. *J. Natl. Cancer Inst.* **55,** 177–180.
24. Shain, S. A., Boesel, R. W., Kalter, S. S., and Heberling, R. L. (1981) A × C rat prostatic adenocarcinoma: Initial characterization of testosterone regulation of hormone receptors of cultured cancer cells and derived tumors. *J. Natl. Cancer Inst.* **66,** 565–574.
25. Gleave, M. E. and Hsieh, J.-T. (1997) Animal models in prostate cancer, in *Principles and Practice of Genitourinary Oncology* (Raghavan, D., Scher, H. I., Leibel, S. A. and Lange, P. H., eds.), Lippincott-Raven Publishers, Philadelphia, pp. 367–378.
26. Russell, P. J., Bennett, S., and Stricker, P. (1998) Growth factor involvement in progression of prostate cancer. *Clin. Chem.* **44,** 705–723.
27. Dunning, W. R. (1963) Prostate cancer in the rat. *Natl. Cancer Inst. Monogr.* **12,** 351–369.
28. Isaacs, J. T. (1987) Development and characteristics of the available animal models for the study of prostate cancer, in *Current Approaches to the Study of Prostate Cancer* (Coffey, D. S., Bruchovsky, N., Gardner, W. H., Resnick, M. I. and Karr, J. P., eds.), Alan R. Liss, New York, pp. 513–575.
29. Voigt, W., Feldman, M. and Dunning, W. F. (1975) 5α-Dihydrotestosterone-binding proteins and androgen sensitivity in prostatic cancer of Copenhagen rats. *Cancer Res.* **35,** 1840–1846.
30. Isaacs, J. T., Isaacs, W. B., Feitz, W. F. J., and Scheres, J. (1986) Establishment and characterization of seven Dunning rat prostatic cancer cell lines and their use in developing methods for predicting metastatic abilities of prostatic cancers. *Prostate* **9,** 261–281.
31. Goebel, H. W., Rausch, U., Steinhoff, M., Seitz, J., Bacher, M., et al. (1992) Arguments against the prostatic origin of the R-3327 Dunning H Tumor. *Virchows Arch. [B]* **62,** 9–18.
32. Bao, L., Loda, M., Janmey, P. A., Stewart, R., Anand-Apte, B., and Zetter, B. R. (1996) Thymosin beta 15: a novel regulator of tumor cell motility upregulated in metastatic prostate cancer. *Nat. Med.* **2,** 1322–1328.
33. Rennie, P. S., Bruchovsky, N., and Coldman, A. J. (1990) Loss of androgen-dependence is associated with an increase in tumorigenic stem cells and resistance to cell-death genes. *J. Steroid Biochem. Mol. Biol.* **37,** 843–847.
34. Pollard, M., Luckert, P. H., and Schmidt, M. A. (1982) Introduction of prostatic adenocarcinomas in Lobund-Wister rats by testosterone. *Prostate* **3,** 563–568.
35. Noble, R. L. and Hoover, L. (1975) The classification of transplantable tumors in Nb rats controlled by estrogen from dormancy to autonomy. *Cancer Res.* **35,** 2935–2941.
36. Noble, R. L. (1977) The development of prostatic adenocarcinoma in the Nb rat following prolonged sex hormone administration. *Cancer Res.* **37,** 1929–1933.

37. Shirai, T., Nakamura, A., Fukushima, S., Yamamoto, A., Tada, M., and Ito, N. (1990) Different carcinogenic responses in a variety of organs, including the prostate, of five different rat strains given 3,2′-dimethyl-4-aminobiphenyl. *Carcinogenesis* **11,** 793–797.
38. Wang, Y. Z. and Wong, Y. C. (1998) Sex hormone-induced prostatic carcinogenesis in the Noble rat: The role of insulin-like growth factor-I (IGF-I) and vascular endothelial growth factor (VEGF) in the development of prostate cancer. *Prostate* **35,** 165–177.
39. Schleicher, R. L., Fallon, M. T., Austin, G. E., Zheng, M., Zhang, M., Dillehay, D. L., et al. (1996) Intravenous vs intraprostatic administration of N-methyl-N-nitrosourea to induce prostate cancer in rats. *Prostate* **28,** 32–43.
40. Bosland, M. C., Chung, L. W. K., Greenberg, N. M., Ho, S-M., Isaacs, J. T., Lane, K., et al. (1996) Recent advances in the development of animal and cell culture models for prostate cancer research. A minireview. *Urol. Oncol.* **2,** 99–128.
41. Stearns, M. E., Ware, J. L., Agus, D. B., Chang, C. J., Fidler, I. J., Fife, R. S., et al. (1998) Workgroup 2: Human xenograft models of prostate cancer. *Prostate* **36,** 56–68.
42. van Weerden, W. M. and Romijn, J. C. (2000) Use of nude mouse xenograft models in prostate cancer research. *Prostate* **43,** 263–271.
43. Russell, P. J., Brown, J., Grimmond, S., Stapleton, P., Russell, P., Raghavan, D., et al. (1990) Tumour-induced host stromal-cell transformation: Induction of mouse spindle-cell fibrosarcoma not mediated by gene transfer. *Int. J. Cancer* **46,** 299–309.
44. Gao, J., Tombal, B., and Isaacs, J. T. (1999) Rapid in situ hybridization technique for detecting malignant mouse cell contamination in human xenograft tissue from nude mice and in vitro cultures from such xenografts. *Prostate* **39,** 67–70.
45. Pretlow, T. G., Wolman, S. R., Micale, M. A., Pelley, R. J., Kursh, E. D., Resnick, M. I., et al. (1993) Xenografts of primary human prostatic carcinoma. *J. Natl. Cancer Inst.* **85,** 394-398.
46. Baisch, H., Otto, U., and Fack, H. (1998) Growth of human prostate carcinomas with and without hormone alpha-dehydrotestosterone in nude mice. *Eur. Urol.* **34,** 505–511.
47. Nagabhushan, M., Miller, C. M., Pretlow, T. P., Giaconia, J. M., Edgehouse, N. L., Schwartz, S., Kung, et al. (1996) CWR22: the first human prostate cancer xenograft with strongly androgen-dependent and relapsed strains both in vivo and in soft agar. *Cancer Res.* **56,** 3042–3046.
48. Gregory, C. W., Kim, D., Ye, P., D'Ercole, A. J., Pretlow, T. G., Mohler, J. L., et al. (1999) Androgen-receptor up-regulates insulin-like growth factor binding protein-5 (IGFBP-5) expression in a human prostate cancer xenograft. *Endocrinology* **140,** 2372-2381.
49. Amler, L. C., Agus, D. B., LeDuc, C., Sapinoso, M. L., Fox, W. D., Kern, S., et al. (2000) Dysregulated expression of androgen-responsive and nonresponsive genes in the androgen-independent prostate cancer xenograft model CWR22-R1.*Cancer Res.* **60,** 6134–6141.
50. Korkmaz, K. S., Korkmaz, C. G., Ragnhildstveit, E., Kizildag, S., Pretlow, T. G., and Saatcioglu, F. (2000) Full-length cDNA sequence and genomic organization of

human NKX3A-alternative forms and regulation by both androgens and estrogens. *Gene* **260,** 25–36.
51. Chen, C. T., Gan, Y., Au, J. L., and Wientjes, M. G. (1998) Androgen-dependent and -independent human prostate xenograft tumors as models for drug activity evaluation. *Cancer Res.* **58,** 2777–2783.
52. Pretlow, T. G., Schwartz, S., Giaconia, J. M., Wright, A. L., Grimm, H. A., Edgehouse, N. L., et al. (2000) Prostate cancer and other xenografts from cells in peripheral blood of patients. *Cancer Res.* **60,** 4033–4036.
53. Hoehn, W., Schroeder, F. H., Riemann, J. F., Joesis, A. C., and Hermanek, P. (1980) Human prostatic adenocarcinoma: some characteristics of a serially transplantable line in nude mice (PC 82). *Prostate* **1,** 95-104.
54. van Weerden, W. M., van Kreuningen, A., Elissen, N. M., Vermeij, M., de Jong, F. H., van Steenbrugge, G. J., et al. (1993) Castration induced changes in morphology, androgen levels, and proliferative activity of human prostate cancer tissue grown in athymic nude mice. *Prostate* **23,** 149–163.
55. Ruizeveld de Winter, J. A., van Weerden, W. M., Faber, P. W., van Steenbrugge, G. J., Trapman, J., Brinkmann, A. O., et al. (1992) Regulation of androgen receptor expression in the human heterotransplantable prostate carcinoma PC-82. *Endocrinology* **131,** 3045–3050.
56. Gao, J. and Isaacs J. T. (1998) Development of an androgen receptor-null model for identifying the initiation site for androgen stimulation of proliferation and suppression of programmed (apoptotic) death of PC-82 human prostate cancer cells. *Cancer Res.* **58,** 3299–3306.
57. van Weerden, W. M., de Ridder, C. M., Verdaasdonk, C. L., Romijn, J. C., van der Kwast, T. H., Schroder, F. T., et al. (1996) Development of seven new human prostate tumor xenograft models and their histopathological characterization. *Am. J. Pathol.* **149,** 1055–1062.
58. Ito, Y. and Nakazato, Y. (1984) A new serially transplantable human prostatic cancer (Honda) in nude mice. *J. Urol.* **132,** 384–387.
59. Bladou, F., Vessella, R. L., Buhler, K. R., Ellis, W. J., True, L. D., and Lange, P. H. (1996) Cell proliferation and apoptosis during prostatic tumor xenograft involution and regrowth after castration. *Int. J. Cancer* **67,** 785–790.
60. Yan, G., Fukabori, Y., McBride, G., Nikolaropolous, S., and McKeehan, W. L. (1993) Exon switching and activation of stromal and embryonic fibroblast growth factor (FGF)-FGF receptor genes in prostate epithelial cells accompany stromal independence and malignancy. *Mol. Cell. Biol.* **13,** 4513–4522.
61. Carstens, R. P., McKeehan, W. L., and Garcia-Blanco, M. A. (1998) An intronic sequence element mediates both activation and repression of rat fibroblast growth factor receptor 2 pre-mRNA splicing. *Mol. Cell. Biol.* **18,** 2205–2217.
62. Carstens, R. P., Eaton, J. V., Krigman, H. R., Walther, P. J., and Garcia-Blanco, M. A. (1997) Alternative splicing of fibroblast growth factor receptor 2 (FGF-R2) in human prostate cancer. *Oncogene* **15,** 3059–3065.
63. Davol, P. A. and Frackelton, A. R., Jr. (1999) Targeting human prostatic carcinoma through basic fibroblast growth factor receptors in an animal model; characterizing and circumventing mechanisms of tumor resistance. *Prostate* **40,** 178–191.

64. Ellis, W. J., Vessella, R. L., Buhler, K. R., Bladou, F., True, L. D., Bigler, S. A., et al. (1996) Characterization of a novel androgen-sensitive, prostate-specific antigen-producing prostatic carcinoma xenograft: LuCaP 23. *Clin. Cancer Res.* **2,** 1039–1048.
65. Buhler, K. R., Santucci, R. A., Royai, R. A., Whitney, S. C., Vessella, R. L., Lange, P. H., et al. (2000) Intermittent androgen suppression in the LuCaP 23.12 prostate cancer xenograft model. *Prostate* **43,** 63–70.
66. Liu, A. Y., Corey, E., Bladou, F., Lange, P. H., and Vessella, R. L. (1996) Prostatic cell lineage markers: emergence of BCL2+ cells of human prostate cancer xenograft LuCaP 23 following castration. *Int. J. Cancer* **65,** 85–89.
67. Williams, B. J., Jones, E., Kozlowski, J. M., Vessella, R., and Brothman, A. R. (1997) Comparative genomic hybridization and molecular cytogenetic characterization of two prostate cancer xenografts. *Genes, Chromosomes Cancer* **18,** 299–304.
68. Pittman, S., Russell, P. J., Jelbart, M. E., and Raghavan, D. (1987) Flow cytometric and karyotypic analysis of a primary small cell carcinoma of the prostate: A xenografted cell line. *Cancer Genet. Cytogenet.* **26,** 165–169.
69. Jelbart, M., Russell, P. J., Fullerton, M., Russell, P., Funder, J., and Raghavan, D. (1988) Ectopic hormone production by a prostatic small cell carcinoma xenograft line. *Mol. Cell. Endocrinol.* **55,** 167–172.
70. Klein, K. A., Reiter, R. E., Redula, J., Moradi, H., Zhu, X. L., Brothman, A. R., et al. (1997) Progression of metastatic human prostate cancer to androgen independence in immunodeficient SCID mice. *Nat. Med.* **3,** 402–408.
71. Craft, N., Shostak, Y., Carey, M., and Sawyers, C. L. (1999) A mechanism for hormone-independent prostate cancer through modulation of androgen receptor signaling by the HER-2/neu tyrosine kinase. *Nat. Med.* **5,** 280–285.
72. Buhler, K. R., Corey, E., Stray, J. E., and Vessella, R. L. (1998) Study of free and complexed prostate-specific antigen in mice bearing human prostate cancer xenografts. *Prostate* **36,** 194–200.
73. Whang, Y. E., Wu, X., Suzuki, H., Reiter, R. E., Tran, C., Vessella, R. L., et al. (1998) Inactivation of the tumor suppressor PTEN/MMAC1 in advanced human prostate cancer through loss of expression. *Proc. Natl. Acad. Sci. USA*. **95,** 5246–5250.
74. Shuldiner, A. R. (1996) Transgenic animals. *Mol. Med.* **334,** 653–655.
75. Aharma, P. and Schreiber-Agus, N. (1999) Mouse models of prostate cancer. *Oncogene* **18,** 5349–5355.
76. Maroulakou, I. G., Anver, M., Garrett, L., and Green, J. E. (1994) Prostate and mammary adenocarcinoma in transgenic mice carrying a rat C3(1) simian virus 40 large tumor antigen fusion gene. *Proc. Natl. Acad. Sci. USA*. **91,** 11236–11240.
77. Perez-Stable, C., Altman, N. H., Brown, J., Harbison, M., Cray, C., and Roos, B. A. (1996) Prostate, adrenocortical, and brown adipose tumors in fetal globin/T antigen transgenic mice. *Lab. Invest.* **74,** 363–373.
78. Garabedian, E. M., Humphrey, P. A., and Gordon, J. I. (1998) A transgenic mouse model of metastatic prostate cancer originating from neuroendocrine cells. *Proc. Natl. Acad. Sci. USA* **95,** 15382–15387.

79. Kasper, S., Sheppard, P. C., Yan, Y., Pettigrew, N., Borowsky, A. D., Prins, G. S., et al. (1998) Development, progression, and androgen-dependence of prostate tumors in probasin-large T antigen transgenic mice: a model for prostate cancer. *Lab. Invest.* **78,** i–xv.
80. Greenberg, N. M., DeMayo, F., Finegold, M. J., Medina, D., Tilley, W. D., Aspinall, J. O., et al. (1995) Prostate cancer in a transgenic mouse. *Proc. Natl. Acad. Sci. USA.* **92,** 3439–3443.
81. Masumori, N., Thomas, T. Z., Chaurand, P., Case, T., Paul, M., Kasper, S A., et al. (2001) A probasin-large T antigen transgenic mouse line develops prostate adenocarcinoma and neuroendocrine carcinoma with metastatic potential. *Cancer Res.* **61,** 2239–2249.
82. Tehranian, A., Morris, D. W., Min, B. H., Bird, D. J., Cardiff, R. D., and Barry, P. A. (1996) Neoplastic transformation of prostatic and urogenital epithelium by polyoma virus middle T gene. *Am. J. Pathol.* **149,** 1177–1191.
83. Voelkel-Johnson, C., Voeks, D. J., Greenberg, N. M., Barrios, R., Maggouta, F., Kurtz, D. T., et al. (2000) Genomic instability-based transgenic models of prostate cancer. *Carcinogenesis* **21,** 1623–1627.
84. Bacich, D. J., Harsch, K. M., and Heston, W. D. (2000) The generation of mouse models for prostate carcinogenesis and development utilizing prostate-specific membrane antigen (PSMA), a unique folate hydrolase. Proc. Hormones and Cancer Conference, 2000, Port Douglas, Queensland, Australia, 3-7 November, A PSH-1.
85. Green, J. E., Greenberg, N. M., Ashendel, C. L., Barrett, J. C., Boone, C., Getzenberg, R. H., et al. (1998) Workgroup 3: Transgenic and reconstitution models of prostate cancer. *Prostate* **36,** 59–63.
86. Spence, A. M., Sheppard, P. C., Davie, J. R., Matuo, Y., Nishi, N., McKeehan, W. L., et al. (1989) Regulation of a bifunctional mRNA results in synthesis of secreted and nuclear probasin. *Proc. Natl. Acad. Sci. USA* **86,** 7843–7847.
87. Matusik, R. J., Kreis, C., McNichol, P., Sweetland, R., Mullin, C., Fleming, W. H., et al. (1986) Regulation of prostatic genes: role of androgens and zinc in gene expression. *Biochem. Cell. Biol.* **64,** 601–607.
88. Greenberg, N. M., DeMayo, F. J., Sheppard, P. C., Barrios, R., Lebovitz, R., Finegold, M., et al. (1994) The rat probasin gene promoter directs hormonally and developmentally regulated expression of a heterologous gene specifically to the prostate in transgenic mice. *Mol. Endocrinol.* **8,** 230–239.
89. Patrikainen, L., Shan, J., Porvari, K., and Vihko, P. (1999). Identification of the deoxyribonucleic acid-binding site of a regulatory protein involved in prostate-specific and androgen receptor-dependent gene expression. *Endocrinology* **140,** 2063–2070.
90. Yan, Y., Sheppard, P. C., Kasper, S., Lin, L., Hoare, S., Kapoor, A., et al. (1997) Large fragment of the probasin promoter targets high levels of transgene expression to the prostate of transgenic mice. *Prostate* **32,** 129–139.
91. Zhang, J., Thomas, T.Z., Kasper, S., and Matusik, R. J. (2000) A small composite probasin promoter confers high levels of prostate-specific gene expression through regulation by androgens and glucocorticoids in vitro and in vivo. *Endocrinology* **141,** 4698–4710.

92. Peehl, D. M. (1995) Prostate specific antigen role and function. *Cancer Suppl.* **75,** 2021–2026.
93. Lundwall, A. (1989) Characterization of the gene for prostate-specific antigen, a human glandular kallikrein. *Biochem. Biophys. Res. Commun.* **161,** 1151–1156.
94. Cleutjens, K. B., van der Korput, H. A., Ehren-van Eekelen, C. C., Sikes, R. A., Fasciana, C., Chung, L. W. K., et al. (1997) A 6-kb promoter fragment mimics in transgenic mice the prostate-specific and androgen-regulated expression of the endogenous prostate-specific antigen gene in humans. *Mol. Endocrinol.* **11,** 1256–1264.
95. Wei, C., Willis, R. A., Tilton, B. R., Looney, R. J., Lord, E. M., Barth, R. K., et al. (1997) Tissue-specific expression of the human prostate-specific antigen gene in transgenic mice: implications for tolerance and immunotherapy. *Proc. Natl. Acad. Sci. USA.* **94,** 6369–6374.
96. Willis, R. A., Wei, C., Turner, M. J., Callahan, B. P., Pugh, A. E., Barth, R. K., et al. (1998) A transgenic strategy for analyzing the regulatory regions of the human prostate-specific antigen gene: potential applications for the treatment of prostate cancer (review). *Int. J. Mol. Med.* **1,** 379–386.
97. Zhang, X., Chen, M. W., Ng, A., Ng, P. Y., Lee, C., Rubin, M., et al. (1997) Abnormal prostate development in C3(1)-bcl-2 transgenic mice. *Prostate* **32,** 16–26.
98. Zhang, X., Lee, C., Ng, P. Y., Rubin, M., Shabsigh, A., and Buttyan, R. (2000) Prostatic neoplasia in transgenic mice with prostate-directed overexpression of the c-myc oncoprotein. *Prostate* **43,** 278–285.
99. Tutrone, R. F. Jr., Ball, R. A., Ornitz, D. M., Leder, P., and Richie, J. P. (1993) Benign prostatic hyperplasia in a transgenic mouse: a new hormonally sensitive investigatory model. *J. Urol.* **149,** 633–639.
100. Kitsberg, D. I. and Leder, P. (1996) Keratinocyte growth factor induces mammary and prostatic hyperplasia and mammary adenocarcinoma in transgenic mice. *Oncogene* **13,** 2507–2515.
101. Stepanova, L., Yang, G., DeMayo, F., Wheeler, T. M., Finegold, M., Thompson, T. C., et al. (2000) Induction of human Cdc37 in prostate cancer correlates with the ability of targeted Cdc37 expression to promote prostatic hyperplasia. *Oncogene* **19,** 2186–2193.
102. Wennbo, H., Kindblom, J., Isaksson, O. G., and Tornell, J. (1997) Transgenic mice overexpressing the prolactin gene develop dramatic enlargement of the prostate gland. *Endocrinology* **138,** 4410–4415.
103. Hennighausen, L., McKnight, R., Burdon, T., Baik, M., Wall, R. J., and Smith, G. H. (1994) Whey acidic protein extrinsically expressed from the mouse mammary tumor virus long terminal repeat results in hyperplasia of the coagulation gland epithelium and impaired mammary development. *Cell Growth Differ.* **5,** 607–613.
104. Sandgren, E. P., Leutteke, N. C., Palmiter, R. D., Brinster, R. L., and Lee, D. C. (1990) Overexpression of TGF alpha in transgenic mice: Induction of epithelial hyperplasia, pancreatic metaplasia, and carcinoma of the breast. *Cell* **61,** 1121–1135.

105. Ludlow, J. W. (1993) Interactions between SV40 large-tumor antigen and the growth suppressor proteins pRB and p53. *FASEB J.* **7,** 866–871.
106. MacGrogan, D. and Bookstein, R. (1997) Tumour suppressor genes in prostate cancer. *Semin. Cancer Biol.* **8,** 11–19.
107. Shibata, M. A., Ward, J. M., Devor, D. E., Liu, M. L., and Green, J. E. (1996) Progression of prostatic intraepithelial neoplasia to invasive carcinoma in C3(1)/SV40 large T antigen transgenic mice: Histopathological and molecular biological alterations. *Cancer Res.* **56,** 4894–4903.
108. Yoshidome, K., Shibata, M. A., Maroulakou, I. G., Liu, M. L., Jorcyk, C. L., Gold, L. G., et al. (1998) Genetic alterations in the development of mammary and prostate cancer in the C3(1)Tag transgenic mouse model. *Int. J. Oncol.* **12,** 449–453.
109. Jorcyk, C. L., Liu, M. L., Shibata, M. A., Maroulakou, I. G., Komschlies, K, L., McPhaul, M. J., et al. (1998) Development and characterization of a mouse prostate adenocarcinoma cell line: ductal formation determined by extracellular matrix. *Prostate* **34,** 10–22.
110. Perez-Stable, C., Altman, N. H., Mehta, P. P., Deftos, L. J., and Roos, B. A. (1997) Prostate cancer progression, metastasis, and gene expression in transgenic mice. *Cancer Res.* **57,** 900–906.
111. Perez-Stable, C. M., Pozas, A., and Roos, B. A. (2000) A role for GATA transcription factors in the androgen regulation of the prostate-specific antigen gene enhancer. *Mol. Cell. Endocrinol.* **167,** 43–53.
112. Gingrich, J. R., Barrios, R. J., Morton, R. A., Boyce, B. F., DeMayo, F. J., Finegold, M. J., et al. (1996) Metastatic prostate cancer in a transgenic mouse. *Cancer Res.* **56,** 4096–4102.
113. Hsu, C. X., Ross, B. D., Chrisp, C. E., Derrow, S. Z., Charles, L. G., Pienta, K. J., et al. (1998) Longitudinal cohort analysis of lethal prostate cancer progression in transgenic mice. *J. Urol.* **160,** 1500–1505.
114. Gingrich, J. R., Barrios, R. J., Kattan, M. W., Nahm, H. S., Finegold, M. J., and Greenberg, N. M. (1997) Androgen-independent prostate cancer progression in the TRAMP model. *Cancer Res.* **57,** 4687–4691.
115. Foster, B. A. and Greenberg, N. M. (2001) New model of bone metastasis for prostate cancer: Cell lines derived from a bony metastasis in TRAMP. *Proc. Am. Assoc. Cancer Res.* **42,** A753.
116. Kaplan, P. J., Mohan, S., Cohen, P., Foster, B. A., and Greenberg, N. M. (1999) The insulin-like growth factor axis and prostate cancer: lessons from the transgenic adenocarcinoma of mouse prostate (TRAMP) model. *Cancer Res.* **59,** 2203–2209.
117. Abdulkadir, S. A., Qu, Z., Garabedian, E., Song, S. K., Peters, T. J., Svaren, J., et al. (2001) Impaired prostate tumorigenesis in Egr1-deficient mice. *Nat. Med.* **7,** 101–107.
118. Ghosh, P. M., Ghosh-Choudhury, N., Moyer, M. L., Mott, G. E., Thomas, C. A., Foster, B. A., et al. (1999) Role of RhoA activation in the growth and morphology of a murine prostate tumor cell line. *Oncogene* **18,** 4120–4130.

119. Pu, Y. S., Luo, W., Lu H. H., Greenberg, N. M., Lin, S. H., and Gingrich, J. R. (1999) Differential expression of C-CAM cell adhesion molecule in prostate carcinogenesis in a transgenic mouse model. *J. Urol.* **162,** 892–896.
120. Bruckheimer, E. M., Brisbay, S., Johnson, D. J., Gingrich, J. R., Greenberg, N., and McDonnell, T. J. (2000) Bcl-2 accelerates multistep prostate carcinogenesis in vivo. *Oncogene* **19,** 5251–5258.
121. Raghow, S., Kuliyev, E., Steakley, M., Greenberg, N., and Steiner, M. S. (2000) Efficacious chemoprevention of primary prostate cancer by flutamide in an autochtonous transgenic model. *Cancer Res.* **60,** 4093–4097.
122. Vanaja, D. K., Grossmann, M. E., Celis, E., and Young, C. Y. (2000) Tumor prevention and antitumor immunity with heat shock protein 70 induced by 15-deoxy-delta12,13-prostaglandin J2 in transgenic adenocarcinoma of mouse prostate cells. *Cancer Res.* **60,** 4714–4718.
123. Granziero, L., Krajewski, S., Farness, P., Yuan, L., Courtney, M. K., Jackson, M. R., et al. (1999) Adoptive immunotherapy prevents prostate cancer in a transgenic animal model. *Eur. J. Immunol.* **29,** 1127–1138.
124. Ciavarra, R, P, Somers, K. D., Brown, R. R., Glass, W. F., Consolvo, P. J., Wright, G. L., et al. (2000) Flt3-ligand induces transient tumor regression in an ectopic treatment model of major histocompatibility complex-negative prostate cancer. *Cancer Res.* **60,** 2081–2084.
125. Hurwitz, A. A., Foster, B. A., Kwon, E. D., Truong, T., Choi, E. M., Greenberg, N. M., et al. (2000) Combination immunotherapy of primary prostate cancer in a transgenic mouse model using CTLA-4 blockade. *Cancer Res.* **60,** 2444–2448.
126. Grauer, L. S., Lawler, K. D., Marignac, J. L., Kumar, A., Goel, A. S., and Wolfert, R. L. (1998) Identification, purification, and subcellular localization of prostate-specific membrane antigen PSM' protein in the LNCaP prostatic carcinoma cell line. *Cancer Res.* **58,** 4787–4789.
127. Bacich, D. J., Pinto, J. T., Gong, W. P., and Heston, W. D. (1991) Cloning, expression, genomic localization and enzymatic activities of the mouse homolog of prostate-specific membrane antigen/NAALADase/folate hydrolase. *Mamm. Genome* **12,** 117–123.
128. Watt, F., Brookes, D. E., Ho, T., Kingsley, E., Russell, P. J., Martorana, A., et al. (2001) A transcriptional enhancer of the prostate-specific membrane antigen gene. *Genomics* **73,** 243–254.
129. Thompson, T. C., Southgate, J., Kitchener, G., and Land, H. (1989) Multistage carcinogenesis induced by ras and myc oncogenes in a reconstituted organ. *Cell* **56,** 917–30.
130. Cuhna, G. R., Fujii, H., Neubauer, B. L., Shannon, J. M., Sawyer, L., and Reese, B. A. (1983) Epithelial-mesenchymal interactions in prostate development. I. Morphological observations of prostatic induction by urogenital sinus mesenchyme in epithelium of adult rodent urinary bladder. *J. Cell. Biol.* **96,** 1662–1670.
131. Royai, R., Lange, P. H., and Vessella, R. (1996) Preclinical models of prostate cancer. *Semin. Oncol.* **23,** 35–40.

132. Thompson, T. C., Kadmon, D., Timme, T. L., Merz, V. W., Egawa, S., Krebs. T., et al. (1991) Experimental oncogene induced prostate cancer. *Cancer Surveys,* **11,** 55–71.
133. Nasu, Y., Bangma, C. H., Hull, G. W., Lee, H. M., Wang, J., McCurdy, M. A., et al. (1999) Adenovirus-mediated interleukin-12 gene therapy for prostate cancer: suppression of orthotopic tumor growth and pre-established lung metastases in an orthotopic model. *Gene Ther.* **6,** 338–349.
134. Geldof, A. A., van den Tillaar, P. L., Newling, D. W., and Teule, G. J. (1997) Radionuclide therapy for prostate cancer lumbar metastasis prolongs symptom-free survival in a rat model. *Urology* **49,** 795–801.
135. Wu, T. T., Sikes, R. A., Ciu, Q., Thalmann, G. N., Kao, C., Murphy, C. F., et al. (1998) Establishing human prostate cancer cell xenografts in bone: induction of osteoblastic reaction by prostate-specific antigen-producing tumors in athymic and SCID/bg mice using LNCaP and lineage-derived metastatic sublines. *Int. J. Cancer* **77,** 887–894.
136. van Aswegen, A., Roodt, A., Marais, J., Botha, J. M., Naude, H., Lotter, M. G., et al. (1997) Radiation dose estimates of 186Re-hydroxyethylidene diphosphonate for palliation of metastatic osseous lesions: an animal model study. *Nucl. Med. Comm.* **18,** 582–588.
137. Chung, L.W. K., Kao, C., Sikes, R. A., and Zhau, H. E. (1997) Human prostate cancer progression models and therapeutic intervention. *Kinyokika Kiyo-Acta Urol. Jpn.* **43,** 815–820.

# 8

# Transgenic Mouse Models for Prostate Cancer

*Identification of an Androgen-Dependent Promoter and Creation and Characterization of the Long Probasin Promoter-Large T Antigen (LPB-*Tag*) Model*

**Susan Kasper, William Tu, Richard L. Roberts, and Scott B. Shappell**

## 1. Introduction

### *1.1. Mouse Models for Prostate Cancer*

An appropriate model to study the complex process of prostate tumorigenesis needs to reflect at least some aspects of the human disease presented in the clinic. The progression of prostate cancer includes the development of high-grade prostatic intraepithelial neoplasia (HGPIN, the precursor lesion for usual peripheral zone prostate cancer) ***(1)***, invasion, growth and potential dedifferentiation of organ confined tumor ***(2)***, extension outside of the prostate (either before or after local therapy), development of metastasis, and the progression from androgen-dependent (AD) to androgen-independent (AI) disease ***(3)***. Clinical observations have shown that androgen withdrawal has the greatest impact on the development and progression of prostate cancer. Therefore, androgen deprivation has been the gold standard in treating patients who have advanced prostate cancer ***(4,5)***. More than 80% of such patients show a favorable response, as evidenced by a decrease in serum prostate-specific antigen (PSA) levels and tumor regression, but tumor growth could resume despite continuous treatment ***(6)***. Although the progressive development of AI is poorly understood, the androgen receptor (AR) appears to be pivotal in the progression from AD to AI prostate cancer. Four possible mechanisms by which the AR may be actively involved in the development of AI include (1) mutations in the

From: *Methods in Molecular Medicine, Vol. 81: Prostate Cancer Methods and Protocols*
Edited by: P. J. Russell, P. Jackson, and E. A. Kingsley © Humana Press Inc., Totowa, NJ

AR ***(5,7–11)***; (2) AR amplification ***(12,13)***; (3) ligand-independent activation of AR through other signaling pathways ***(14–22)***; and (4) altered activity of AR coregulators (either co-activators or co-inhibitors) ***(22–24)***.

Thus, clinical data would dictate that an ideal mouse model for prostate cancer should include initial tumor growth restricted to the prostate, the development of precursor prostate intraepithelial neoplasia (PIN)-like lesions, progression to locally invasive tumor, dissemination of the disease (with metastasis to pelvic lymph nodes and bone), initial androgen-dependent (AD) growth and progression to AI growth. Our goal was to establish and characterize a transgenic mouse model that could be used to elucidate the key events both in the development of prostate cancer and in the progression and metastasis of prostate cancer. Several approaches to developing mouse models will be discussed, such as the creation and characterization of the Long Probasin Promoter-Large T antigen (LPB-*Tag*) mouse model (where the prostate-specific probasin, PB, promoter has been linked to the *Tag* gene) that illustrates the transgene overexpression model for prostate cancer.

### 1.2. Experimental Approaches

Establishing suitable model systems for prostate carcinoma has been hindered by several aspects. One has been the difficulty in establishing long-term cultures of prostate cancer cell lines from human prostate cancer tissue. In vivo propagation of human primary tumor cells has met with limited success using either commercially available or published cell lines. Several laboratories have developed xenograft models using human prostate tissue, Matrigel, and androgens to study the progression from AD to AI prostate cancer growth ***(25–28)***. A vertebral metastatic lesion has been developed to study metastasis ***(29)***. These systems exhibit some of the characteristics of clinical prostate carcinoma, including the expression of PSA, prostate-specific acid phosphatase ***(29),*** and AR, and could be used to investigate the more advanced stages of prostate cancer progression and metastasis. Limitations to all these systems include the possible development of additional genetic alterations with cell line progression and the inability to recapitulate epithelial–stromal interactions and other host factors. A further limitation in developing in vivo prostate carcinoma models has been that only a few species (e.g., rats and dogs) spontaneously develop prostate cancer, thereby limiting the number of animal models available for studying the entire process, leading to prostate cancer development. Numerous model systems, including canine and rat models, ex vivo reconstitution models, xenograft models, and cell line models have been reviewed elsewhere ***(30–33)***.

Transgenic techniques have permitted the development of unique mouse models that can be used to ascertain the mechanisms by which a specific gene influences the development of prostate cancer. The experimental approaches to

generate mouse models include (1) transgene overexpression; (2) knockout/knock-in technology; and (3) conditional expression systems.

### *1.2.1. Transgene Overexpression*

The most direct method to develop a mouse model for prostate cancer is to overexpress the potential cancer gene in the target tissue. The tools required to generate this model include a promoter that regulates transgene expression in a tissue-specific manner. Furthermore, overexpression of the transgene should result in a phenotype that resembles at least one of the clinical stages of prostate cancer, suggesting that it is involved in prostate cancer progression. Transgenic models have been generated using prostate-specific promoters, including those of androgen-regulated genes, such as PB and PSA, and other promoters that regulate transgene expression in the prostate in addition to other tissues (*see* **Table 1**).

The choice of the target gene includes (1) genes that have been implicated in human prostate cancer development; (2) genes related by sequence similarity to oncogenes or tumor suppressors; or (3) genes in signaling pathways that mediate signals involved in cell-cycle control, cell growth, or apoptosis. The phenotypic alterations associated with transgene expression observed thus far in various laboratories include epithelial hyperplasia with/without stromal hyperplasia [-426PB-T*ras* ***(34)***, -426PB-*fos* ***(35)***, C3(1)-*bcl-2* ***(36)***, MMTV-*kgf* ***(37)***, MMTV-*wap* ***(38)***, BK5-*IGF1* ***(39)***], invasive carcinoma superimposed on this background of atypical epithelial proliferation [-426PB-*Large T/small t antigens* (TRAMP) ***(40,41)***, LPB-*Tag* ***(42,43)***, -426PB-*fos* ***(35)***, C3(1)-*SV40 Large T/small t antigens* ***(36)***, C3(1)-*Polyoma middle T* ***(44)***, BK5-*IGF1* ***(39)***, cryptdin 2-*SV40* ***(45)***], and metastasis, including AI disease and neuroendocrine differentiation [-426PB-*Large T/small t antigens* (TRAMP) ***(40,41)***, C3(1)-*SV40 Large T/small t antigens* ***(36)***, cryptdin 2-*SV40* ***(45)***, fetal gamma globulin-*SV40 T antigen* ***(46)***, LPB- *Large T antigen* (Line 12T-10) ***(43)***, gp91-phox-*SV40 T antigen* ***(47)***] (*see* **Table 1**).

It is interesting to note that all of the more invasive tumor models have been generated using the *SV40 Large T* or *SV40 Large T/small t antigens* (*see* **Fig. 1**). The transformation domains of the *Large T antigen* interact with key tumor suppressor genes such as *p53* and members of the retinoblastoma family, such as *pRB*, *p107*, and *p103/pRB2*, as well as the co-activators p300 and CBP ***(48,49)***. The LPB-*Tag* mice demonstrate that the Large T antigen alone is sufficient to transform the prostatic epithelial cells. The small t antigen itself does not appear to cause transformation; however, it interacts with the A and catalytic C subunits of protein phosphatase 2A to decrease its activity, resulting in increased phosphorylation and activation of the mitogen-activated protein kinase family of kinases. The net effect is the amplification of the transforming

**Table 1**
**Approaches for Generating Transgenic Mouse Models for Prostate Cancer**

| Approach | System | Promoter-gene | Ref. |
|---|---|---|---|
| Over-expression | Prostate-specific promoter | -426PB-*CAT* | ***86*** |
| | | -426PB-*ras*T24 | ***34*** |
| | | -426PB-*large T/small t antigens* (TRAMP) | ***40,41*** |
| | | -426PB-*Eco*RI | |
| | | -426PB-*fos* | ***35*** |
| | | LPB-*CAT* | ***97*** |
| | | LPB-*large T antigen* (12T-7f) | ***42*** |
| | | LPB-*large T antigen* (12T-10) | ***43*** |
| | | $ARR_2$PB-CAT | ***89*** |
| | Promoter that targets prostate and other tissues | gp91-phox-*SV40 T antigen* | ***47*** |
| | | C3(1)-*SV40 T antigen* | ***36*** |
| | | C3(1)-*Polyoma middle T* | ***44*** |
| | | C3(1)-*bcl-2* | ***36*** |
| | | MMTV-*kgf* | ***37*** |
| | | MMTV-*wap* | ***38*** |
| | | Cryptdin-*SV40 T antigen* | ***45*** |
| | | BK5-*IGF1* | ***39*** |
| | | Fetal gamma globulin-*SV40 T antigen* | ***46*** |
| Knockout | Embryonic stem cells | *p53* | ***66*** |
| | | *PTEN+/–* | ***67*** |
| | | *PEN+/–/p27KIP1* | ***67*** |
| Knock-in | Embryonic stem cells | *p53* | ***68*** |
| Conditional expression | CRE-lox P system | ARR2PB-Cre | ***71*** |
| | Tet-on/Tet-off system | ND | ND |
| | Ecdysone | ND | ND |

*SV40 T antigen*, contains genes for both *large T antigen* and *small t antigen*. ND, not determined.

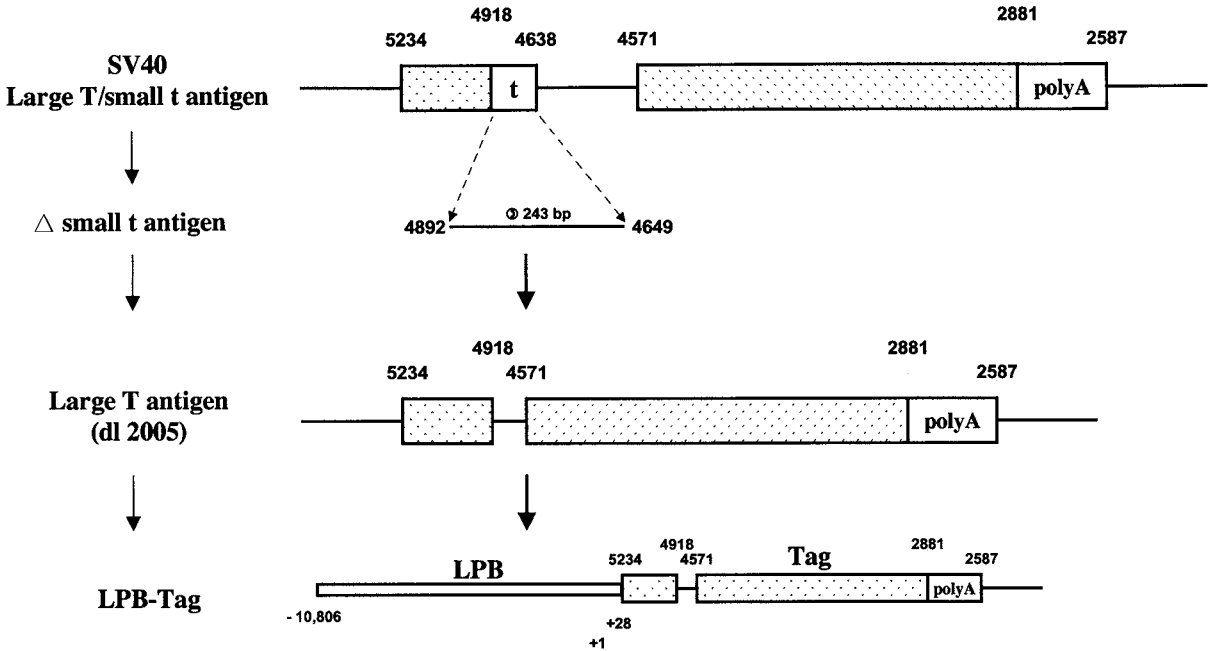


Fig. 1. Diagrammatic representation of the generation of the *Large T antigen* (dl 2005) construct. The *small t antigen* (243 bp) was excised, resulting in a *Simian Virus 40 (SV40) large T antigen* (*Tag*) gene deletion mutant (d1 2005), where the expression of the small t antigen has been removed ***(98).*** The numbers on top refer to those found in the SV40 genome ***(109).*** The 5′ flanking region of the rat probasin gene designated LPB (–10,834 to +28 bp) ***(97)*** was linked to the *Large T antigen* gene to create the LPB-*Tag* gene. This construct was subsequently used to generate the LPB-*Tag* mouse model for prostate cancer ***(42).***

activity of the Large T antigen, which results in mitogenesis (for review, *see* **ref. *50)***. Whether the SV40 model is relevant to the development and progression of human prostate cancer has been debated. The sequestering of p53 and the inactivation of pRB have been implicated in advanced stages of prostate cancer ***(51–54)***. SV40-like expression caused by potential exposure to SV40-contaminated vaccines in individuals born after 1963 has been associated with human mesogliomas, ependymomas, and osteosarcomas; however, the causal association between SV40 and these human tumors remains to be established (for review, *see* **ref. *55***).

The advantages of overexpressing a transgene is that the mechanisms of prostate cancer progression can be studied developmentally over time. However, the complex genetics of cancer suggests that the development of cancer will likely be the outcome of multiple or sequential changes and not just the overproduction of a single gene product. The secondary genetic alterations that accompany tumor progression in Large T overexpressing mice and whether they parallel similar changes in human prostate cancer development are still being elucidated ***(56,57)***. Thus, two different models (in which distinct gene products are overexpressed) can be crossbred to study the effects of two defined genetic changes on prostate cancer development.

### *1.2.2. Knockout/Knock-In Technology*

The only reported murine prostatic lesion to arise through a spontaneous mutation is the Tfm mouse, where a point mutation in the AR results in a frameshift mutation that inhibits the transactivation of the AR and prevents the development of the normal prostate ***(58–61)***. Spontaneous mutations resulting in a cancer phenotype do not apparently occur in the mouse. Therefore, to develop a mouse model of human cancer, an approach is necessary whereby the gene of interest can be inactivated either by a null mutation (knockout) or by subtly modifying the gene of interest and inserting it into the mouse genome (knock-in). Knockout (KO) mice are engineered by transfecting embryonic stem (ES) cells (derived, e.g., from 129/SV mice carrying the agouti phenotype) ***(62,63)*** with the gene-targeting construct, selecting transfectants and identifying clones where homologous recombination has occurred. The ES cells are subsequently microinjected into mouse blastocysts (often C57BL/6J, which have a nonagouti phenotype) and transferred into pseudopregnant females. The resulting chimeric offspring are identified by their agouti coat color. After at least six to eight crosses, germline transmission is indicated, in most cases, by a completely agouti coat color.

Knockout technology has allowed the generation of mouse strains with defined mutations in steroid hormone receptors and tumor suppressor genes to determine their potential importance in cancer development or other aspects of

prostate physiology. In estrogen receptor (ER) KO transgenic mice lacking a functional ERα, a mutation in the *ER* gene resulted in disruption of spermatogenesis and degeneration of the seminiferous tubules, although no obvious morphology changes in the prostate were observed ***(64)***. Recently, Risbridger and coworkers ***(65)*** reported that prostatic squamous metaplasia was induced both in *wt* mice and in BERKO mice (lacking a functional ERβ) treated with the synthetic estrogen diethylstilbestrol, whereas diethylstilbestrol treatment had no effect on the prostatic epithelium of ERKO mice, indicating an essential role for ERα in the induction of squamous metaplasia in prostatic epithelium.

Several tumor suppressor knockout models have produced mice with an increased susceptibility to developing prostate neoplasia. Prostatic morphology in *p53* null mice was altered by the appearance of large nucleated and multinucleated cells in addition to a suppression of apoptosis ***(66)***. The $PTEN^{-/-}$ mutation resulted in embryonic lethality, implying that the *PTEN* tumor suppressor gene was involved in embryonic development ***(67)***. The $PTEN^{+/-}$ heterozygotes developed hyperplasia/dysplasia, as seen by the increases in mitotic figures, cellularity, and complexity of the prostatic acini ***(67)***. However, *PTEN* haploinsufficiency alone did not result in overt prostate cancer. A second mutation, that is, the loss of *p27KIPI* expression, was required for the development of prostate carcinoma with complete penetrance by 3 mo of age ***(67)***, demonstrating the complexity of cancer genetics.

Recently, it has become possible to study the effects of human allelic variants in transgenic mice by replacing mouse genes with their human counterparts to determine their role in cancer susceptibility. A human homozygous p53 knock-in mouse strain was generated by replacing exons 4 to 9 of the endogenous mouse *p53* gene with the homologous human *p53* sequence ***(68)***. The human $p53^{+/+}$ gene permits normal biological function in the mouse and provides a model in which to study the effects of DNA damaging agents and pharmaceutical agents that may modulate the DNA-binding activity of human p53 in vivo ***(68)***.

The advantage of the KO system is that the expression of a gene can be selectively inactivated. If loss of expression of the gene in the homozygous mouse results in embryonic lethality, the heterozygous animal can often be used to study the role of the gene of interest in prostate cancer development. Indeed, the inactivation of tumor suppressor genes in a heterozygous mouse model closely resembles the presumed alterations in human prostate cancer, where inactivation of a tumor suppressor gene results in a predisposition to develop cancer. However, absence of a significant phenotype in a mouse model with such an alteration in a single gene certainly does not exclude a role for a similar alteration in human prostate cancer. In the latter, there may be many other genetic changes that are not recapitulated in the mouse model and under which circumstances the single gene alteration in question could be of functional significance.

The advantage of the knock-in system is that a mouse gene can be replaced by its human counterpart to study the effects of expressing the human protein in the mouse system. A disadvantage of these systems is that the time required to stably transfect and characterize the ES cells and generate the transgenic mice can take a significant period of time, up to several years.

### *1.2.3. Conditional Expression Systems*

The generation of a homozygous knockout transgenic mouse is labor intensive and may result in embryonic lethality, as seen by the pRB ***(69)*** and PTEN ***(67)*** mouse models. Several systems have been developed in which a promoter, regulated by enzymatic action or exogenous drugs, can allow for the conditional inactivation or activation of a transgene.

In the Cre-*lox*P system (DuPont-Merck Pharmaceutical Company), Cre-mediated DNA recombination occurs when the Cre enzyme recognizes a 32 bp *lox*P site and efficiently excises the gene located between two directly repeated *lox*P sites ***(70)***. Thus, the Cre enzyme can be targeted to the prostate in one mouse strain, and a selected gene thought to be involved in the prostate cancer process can be inserted between two directly repeated *lox*P sites and expressed in another mouse strain. When these two animals are crossbred, the gene of interest is sliced out, creating a mouse in which the gene is knocked out selectively in the prostate. For example, in the $ARR_2$PB-Cre mouse strain, the prostate specific probasin promoter $ARR_2$PB was linked to the *Cre* gene, with Cre expression thus targeted selectively to the prostate epithelium ***(71)***. The R26R mouse strain contains the ROSA26 conditional reporter, which is inserted between two directly repeated *lox*P sites. Crossbreeding the $ARR_2$-PB-*Cre* strain with the R26R strain resulted in the conditional expression of lacZ in the prostate when the ROSA26 reporter was floxed in a tissue-specific manner.

The advantage of the Cre-*lox*P system is that the ARR2PB-Cre mouse can be crossbred with any of multiple *lox*P models in which candidate tumor suppressor or cancer promoting genes can thus be selectively eliminated in the prostate to determine their involvement in prostate cancer development and progression. A potential problem is that cryptic *lox*P sites have been identified in yeast, and these may have eukaryotic counterparts, which could result in spurious Cre recombinase activity ***(72)***.

The Tet-Off/Tet-On systems (Clontech) ***(73–75)*** are based on the Tet repressor protein (TetR) and the Tet operator DNA sequence (*tetO*). In the Tet-Off system, the tetracycline-controlled transactivator (tTA) (composed of TetR and the VP16 activation domain) binds to the *tetO* sequence, inducing transcription of the transgene in the absence of the antibiotic Doxycycline. With the addition of Doxycycline, the antibiotic binds to tTA, preventing its binding to the *tetO* sequence and thereby inhibiting transcription. The oppo-

site occurs in the Tet-On system where addition of the antibiotic allows tTA to bind to the *tetO* sequence and transactivate transgene expression. Thus, transgene expression can be controlled by the exogenous addition or removal of antibiotic.

The ecdysone-inducible system (Invitrogen) ***(76,77)*** is based on three components, a plasmid expressing the ecdysone receptor (EcR) under a strong promoter, a plasmid expressing the retinoid X receptor (RXR) under the same promoter, and the relevant transgene subcloned into an expression vector, which has a minimal promoter containing several EcR binding sites. In the presence of ecdysone or muristerone A, EcR and RXR form heterodimers, bind to the EcR binding sites, and activate transgene expression. The inducible gene is controlled by the choice of promoter; for example, a prostate-specific promoter, such as the probasin $ARR_2PB$ or the PSA promoters, could be used to target the EcR, RXR, and relevant transgenes to the prostate.

The advantages of the inducible systems are that they can be regulated by the exogenous treatment with antibiotics or hormones and selectively modulate expression of genes of interest in a single organ, such as the prostate. A disadvantage of these systems is that detectable levels of transgene expression can occur if there are any leaks in the system. Furthermore, muristerone A and ponasterone A may have their own biological effects. For example, these inducers of ecdysone were found to potentiate the interleukin-3-dependent activation of the phosphoinositide 3-kinase (PI3K)/Akt pathway ***(78)***.

### *1.3. The LPB-*Tag *Mouse Model for Prostate Cancer*

The development of the LBP-*Tag* mouse model for prostate cancer used the transgene overexpression approach. The sequence of events, which resulted in the LPB-*Tag* mouse model included the identification and cloning of the PB gene, the identification and characterization of the PB androgen responsive region in vitro, development of the first-generation -426PB transgenics, generation of the LPB-*Tag* mouse model for prostate cancer using larger portions of the probasin promoter for higher levels of expression of a modified SV40 early region transgenes, characterization of prostate cancer progression in the LPB-*Tag* lines, 12T-7f, and 12T-10, and development of a more efficient third-generation $ARR_2PB$ promoter to target other genes to the prostate.

### *1.4. Characterization of the Promoter Region of a Prostate-Specific Gene*

#### *1.4.1. Isolation of RNA*

The mouse prostate consists of four pairs of symmetrically arranged lobes: the anterior (or coagulating gland), dorsal, lateral, and ventral prostatic lobes (*see* **Fig. 2**).

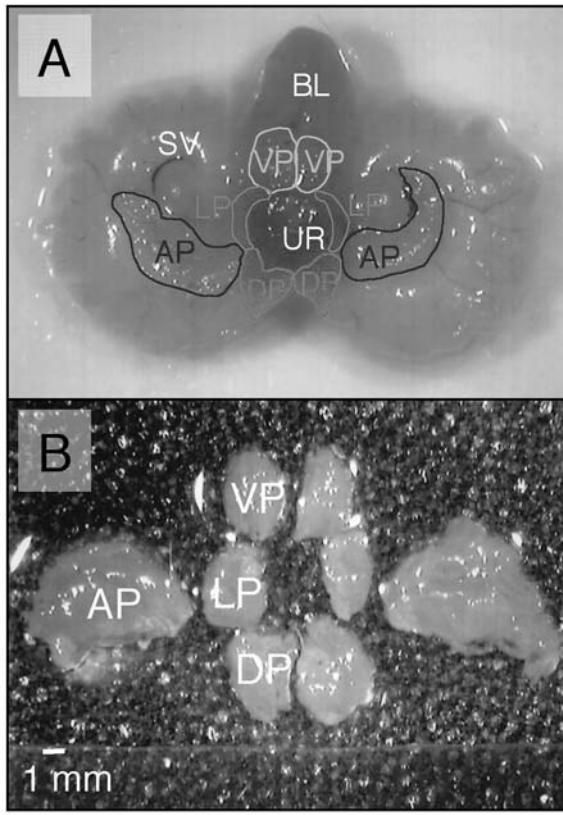


Fig. 2. Dissection of lobes of the mouse prostate. **(A)** Dorsal view of the mouse urogenital sinus with the urethra (UR ) central and pointing upwards and the bladder (BL) and seminal vesicles (SV) lying flat on the dissection surface. The mouse prostate consists of two anterior (AP), two dorsal (DP), two lateral (LP), and two ventral (VP) lobes symmetrically arranged around the urethra. **(B)** Dissection of the prostatic lobes, with an estimate of size (in mm).

In the wild-type or normal mouse prostate, the dorsal and lateral lobes are quite small and are often isolated together. Each lobe has a unique branching pattern and when gently teased apart, resembles a tree structure consisting of the distal, intermediate segment, and proximal regions ***(79)***. To isolate high-quality total RNA, it is necessary to dissect the prostatic tissue as quickly as possible. Furthermore, it is advantageous to separate the individual lobes because expression of the same gene may vary in the different lobes. The dorsolateral lobes are considered to be the most analogous to the peripheral zone of the human prostate from which the majority of clinically significant prostate cancers arise ***(80)***. Total RNA can be isolated from snap frozen tissue (immedi-

ately place in liquid nitrogen) or from tissues fixed in RNAlater™ (Ambion, Inc.), using a number of different RNA extraction kits, including the Rneasy™ kits by Qiagen Inc. (Valencia). An advantage of using RNAlater fixed tissue is that the entire prostate can be fixed overnight at 4°C and then dissected carefully at room temperature the next day. Furthermore, if dissection is not immediately possible, the fixed tissue can be blotted to remove excess RNAlater, stored at –80°C and dissected at a later date.

Probasin mRNA was originally identified in the dorsolateral lobes of the prostate ***(81–83)*** and was found to be androgen ***(81,84–86)*** and zinc ***(87)*** regulated. The probasin gene was subsequently cloned ***(84)*** and the 5′-flanking region of the probasin gene was analyzed in the transient transfection assays described below to determine whether it contained DNA elements that were regulated by androgens and which controlled prostate-specific expression.

### *1.4.2. Reporter Genes*

The ability of a promoter to regulate expression of a transgene and of agents, such as hormones, to modulate promoter activity are investigated in vitro using promoter segments coupled to a variety of reporter genes. Reporter systems are essential to determine the level of transcription induced by a promoter region in vitro analyses. There are numerous reporter genes available, and the choice of reporter gene is dependent upon several factors. These include the cell type used in the bioassay, the level of sensitivity required to see induction of reporter gene activity, and the reproducibility of the bioassay. The *CAT* gene was one of the first reporter genes available and CAT activity was measured by liquid chromatography. The current method of choice is determining *CAT* gene activity using the two-phase fluor diffusion assay ***(88),*** which generates an enzymatic slope that measures CAT activity over time. Cells cultured in 24-well plates provide sufficient protein to assay by this method.

Luciferase reporter genes (Promega) can serve as a transfection control for the CAT assay. The luciferase reporter system is more sensitive and will measure transcriptional activity at lower levels. It is also a high throughput assay and will determine rate of transcription in cells grown in a 96-well format. The assay is based on measuring the degree of luminescence generated by the firefly (*Photinus pyralis*) luciferase gene as it catalyses the oxidation of the luciferin substrate. The *Renilla* (*Renilla reniformis*) luciferase gene is often used as a secondary control reporter gene or transfection control ***(89)*** that is measured at the same time in the dual-luciferase reporter assay system (Promega). Because this is a very sensitive reporter, background luminescence levels may be higher.

The beta galactosidase reporter gene is also commonly used. However in certain cell types (e.g., prostate cell lines), background staining is a considera-

tion when calculating the induction of reporter gene activity ***(90)***. A series of fluorescent reporter genes have been developed whereby the gene product is determined at a specific wavelength (Clontech). The jellyfish (*Aequoria victoria*) green fluorescent protein has been used extensively, and the simplicity of the assay is very appealing. The transfected cells are place under a blue light (488 nm/507 nm) and the cells expressing the transgene are instantly observed. The assay can also be quantitative because the cells can be harvested, lysed, and the fluorescence determined ***(91)***.

### *1.4.3. Transient Transfection Assays and Characterization of the Androgen-Responsive Probasin Promoter*

Several human prostate cell lines are available to analyze reporter gene activity in vitro. The human LNCaP prostate cell line is androgen receptor positive and produces PSA. Although the LNCaP AR has a point mutation in the steroid-binding domain (codon 868, Thr to Ala), it is still functional and LNCaP cell growth can be modulated by androgens ***(92)***. The human prostate cancer PC-3 and DU-145 cells lines do not contain a functional AR. Therefore, an expression vector containing the AR is cotransfected with the test and transfection control plasmids in the transient transfection assay when studying potential AR-modulated promoters. Derivatives from these cell lines, as well as new cell lines [for example, TSU ***(93)***, Hpr-1], are currently being developed and will hopefully provide cells potentially more representative at specific stages of malignant prostate epithelial cell development.

The probasin promoter was extensively characterized in the LNCaP and PC-3 cell lines using either the CAT or the luciferase reporter systems. In transient transfection studies, two distinct androgen receptor binding sites, ARE-1 (located at position -236 to -223) and ARE-2 (at position -140 to -117), were required for maximal androgen induction of CAT gene expression in the PC-3 human prostate cell line ***(85)***. Neither binding site alone could induce *CAT* gene expression in response to androgen treatment ***(94)***, androgen-specific transcriptional activation could not be reconstituted by linking two or three copies of either ARE-1 or ARE-2 alone ***(95)***, and a point mutation in either site resulted in a loss of AR binding and *CAT* gene expression ***(94)***. Because neither ARE alone could induce transcription, they did not function independently as DNA response elements. Therefore, the DNA elements were renamed androgen receptor binding site-1 and -2 (ARBS-1, ARBS-2) and the region encompassing both elements (-244 to -96) was named the androgen-responsive region (ARR). These constructs were also tested in numerous nonprostatic cell lines and were found to be prostate-cell specific ***(89,96)***. The next step was to determine whether the PB promoter could target transgenes to the mouse prostate in vivo.

### *1.4.5. Identification and Characterization of a Prostate-Specific Promoter*

In developing a mouse model for prostate cancer, the relevant transgene should ideally be targeted to the prostate in a tissue-specific manner. The analysis of the 5′-flanking region of the gene in vitro is essential in characterizing the regulation of gene expression; however, it is still necessary to generate a transgenic animal model to determine whether the promoter contains tissue-specific DNA elements. For example, the -426 PB ***(86)*** and -11,500 to +28 bp LPB ***(97)*** promoters were linked to the *CAT* gene and targeted to the mouse prostate to determine whether *CAT* gene expression would occur in the prostate alone. Although the LPB promoter induced higher levels of *CAT* gene expression, the smaller -426 bp fragment was sufficient for prostate-specific expression. Transgene expression was also cell-specific, occurring only in the epithelial cells ***(97)***. Furthermore, *CAT* gene expression rose in parallel with androgen production during prostate growth and maturation, indicating that it was developmentally regulated. *CAT* gene expression dropped to basal levels after castration, and expression could be restored to precastration levels with exogenous androgen treatment ***(86,97)***. In conclusion, the PB promoter was prostate-specific, epithelial cell-specific, and regulation of PB-*CAT* gene expression was androgen-dependent.

## ***1.5. Generation of LPB*-Tag *Transgenic Mice***

The LPB construct was chosen because it resulted in the higher levels of transgene expression than shorter portions of the probasin promoter. Determining which transgene to target to the prostate was based on several parameters. Previous oncogenes expressed in the prostate, such as T*ras*, *fos*, *bcl-2*, *kgf*, and *wap*, primarily induced epithelial hyperplasia with/without stromal hyperplasia. The Large T antigen was chosen to develop the LPB-*Tag* mouse model because it blocks the function of both Rb and p53, resulting in a potentially more aggressive cancer phenotype ***(48)***. In this model, the specific *SV40 Large T antigen* gene contained a deletion mutation (d1 2005) that removes the expression of the small t antigen ***(98)*** (*see* **Fig. 1**). The 5′-flanking region of the rat probasin gene was designated LPB (–11,500 to +28 bp) ***(97),*** and this promoter region was linked to the *Tag* gene and microinjected into the male pronucleus of a fertilized oocyte. Appropriate references for all of these procedures have been described previously ***(99)***.

The LPB-*Tag* founders were identified by the polymerase chain reaction (PCR)-based screening assay using isolated tail DNA ***(97),*** and the mouse lines were maintained in the same strain as that of the founders (CD-1). The primers used to identify the LPB-*Tag* transgene were the PB forward primer 5′-TAGCATCTTGTTCTTAGTCTT-3′ and the *Tag* reverse primer 5′-CTCCTTTCAAGACCTAGAAGGTCCA-3′. Exon 7 of the endogenous mouse casein gene

served as an internal control for the PCR (forward primer 5′-GATGT-GCTCCAGGCTAAAGTT-3′, reverse primer 5′-AGAAACGGAATGTTGTG-GAGT-3′) ***(86)***.

### *1.6. Characterization of the LPB-*Tag *Transgenic Mouse Model of Prostate Carcinoma*

#### *1.6.1. Phenotypic Changes Induced by Transgene Expression*

Essential for identifying transgene-induced phenotypic changes in prostate morphology is an understanding of normal mouse prostate histology (*see* **Fig. 3**). The normal mouse prostate has similarities and distinct differences compared to the human prostate. Although the mouse prostate consists of four individual lobes, the basic architecture of each lobe is similar. Ducts and glands are surrounded by a thin rim of stroma, immediately surrounded by periprostatic fat, without the prominent stroma encasing benign glands and a prostatic capsule as in the human prostate (*see* **Fig. 3**). The familiar anatomic and functionally significant zones of the human prostate (i.e., transition zone, peripheral zone, central zone, and anterior fibromuscular stroma) are not appreciated in the mouse prostate. The thin stroma is composed of one to three layers of spindled cells, with contractile or smooth muscle differentiation, in a collagen rich matrix (*see* **Fig. 3**). Nerves and ganglia are evident in periprostatic fat. The anterior prostate has a more complex tufting and even cribriform epithelial lining compared to a more simple columnar lining in other lobes.

In all prostatic lobes, the branching ducts and glands have two cell layers, similar to benign human prostate glands. Basal epithelial cells are not conspicuous by light microscopy, but similar to the human, are identifiable by immunostaining for high molecular weight cytokeratins ***(100)***. It is postulated that the basal cells may represent progenitor or precursor cells for differentiated secretory cells, with a subset representing the stem cells of the prostate. However, it still needs to be determined whether the undifferentiated cords of epithelial cells in the prostatic bud or the basal cells are the prostatic stem cells ***(100)***. Basal cells give rise to the luminal epithelial and neuroendocrine cell lineages ***(100,101)***. Luminal epithelial cells can also dedifferentiate into a neuroendocrine phenotype under the right conditions, for example, LNCaP cells acquire neuroendocrine morphology in response to treatment with agents that activate protein kinase A ***(102,103)***. The epithelial cells lining the distal and intermediate segments are tall columnar epithelial cells. Those in the distal segment appear to have the highest mitotic index, whereas the epithelial cells in the intermediate segments are mitotically quiescent but produce secretory proteins. In contrast, the epithelial cells in the proximal ducts are low columnar or cuboidal in shape and undergo apoptosis at a higher rate ***(79)***. Secretory cells in

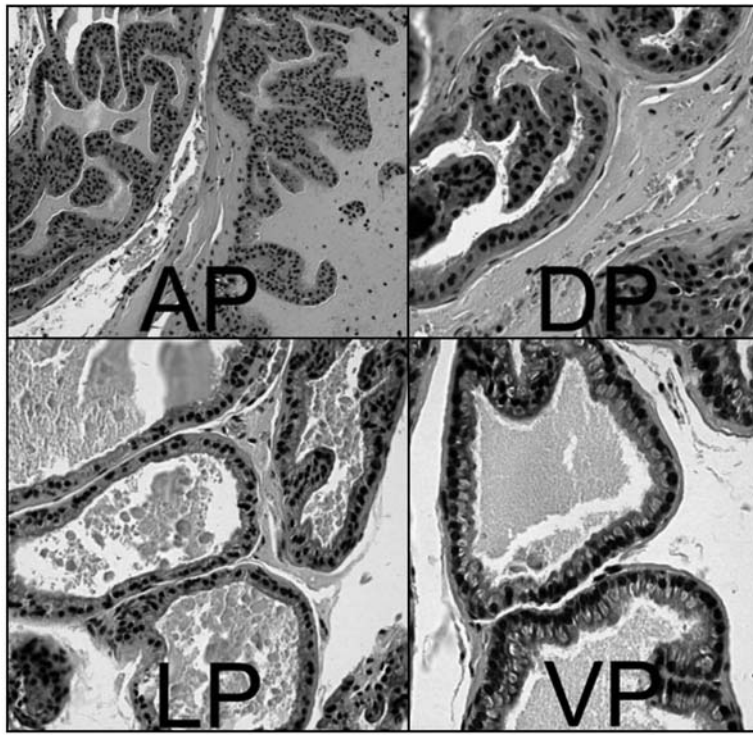


Fig. 3. Histology of normal (wild-type) mouse prostate lobes. AP, anterior prostate: compared with other lobes, the epithelium lining glands in the AP shows a more complex architecture, with tufting and cribriforming. Secretory cells have generally eosinophilic cytoplasm and round uniform nuclei. Prominent luminal secretions are typically evident. Ducts and glands of dorsal prostate (DP), lateral prostate (LP), and ventral prostate (VP) have a more simple columnar epithelial lining, with generally eosinophilic cytoplasm in the DP and more clear cytoplasm in LP and VP. Note the extremely thin rim of stroma surrounding the glands, e.g., in LP and VP images, immediately surrounded by peri-prostatic adipose tissue.

the anterior and dorsal prostate tend to have a more eosinophilic granular cytoplasm in routine sections, whereas those of the lateral and ventral prostate have a clearer or vacuolated cytoplasm. The relationship of this apparent zonal distribution of proliferation and apoptosis to human prostate remains to be demonstrated. The neuroendocrine cells in the normal gland, identifiable by immunostaining for neuropeptides, such as chromogranin, are sparsely interspersed throughout the epithelial cells, reaching the lumen with a thin small apical surface ***(101)***. This basic architecture changes little with age, although there may be a thickening of the stromal layer as the mice age.

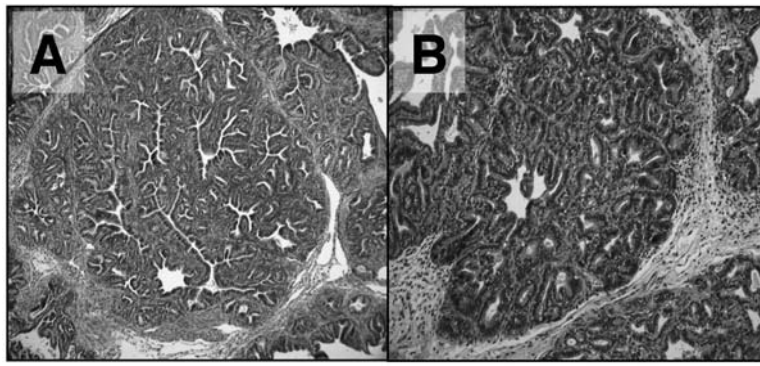


Fig. 4. Marked atypical epithelial proliferation with accompanying hypercellular stroma in LPB-*Tag* mouse prostate. (**A**) Dorsolateral prostate from 19-wk-old 12T-5 mouse showing symmetric lobular expansion of branching ducts of markedly atypical epithelial cells, with associated hypercellular stroma. Although clearly demonstrating an increase in glandular spaces compared to wild-type mice, the symmetric and uniform development of this lesion has led us to regard this an *in situ* neoplastic process. However, foci of possible microinvasion are often noted (e.g., bottom left). (**B**) Dorsolateral prostate from 22-wk-old 12T-7s mouse showing extension of atypical glands into periprostatic fat, bottom left.

Several LPB-*Tag* lines were initially identified and maintained, demonstrating different rates of neoplastic prostate growth ***(42,43)***. Initially, transformation is multifocal with clusters of cells containing elongated, hyperchromatic nuclei interspersed among the normal epithelial cells exhibiting typically round, basally located nuclei. By 8 to 9 wk of age, 100% of the cells are transformed and express the LPB-*Tag* transgene (as seen by immunohistochemistry) ***(42)***. Tumor growth progresses to a lesion considered homologous to human low-grade prostatic intraepithelial neoplasia (LGPIN) with epithelial stratification and mild nuclear atypia and high-grade prostatic intraepithelial neoplasia (HGPIN) with marked nuclear atypia (*see* **Fig. 4, Fig. 5C**). Most of the faster growing lines show prominent epithelial proliferation, with generally symmetric and diffuse lobular expansion by atypical epithelial cells, accompanied by a hypercellular stroma, in the anterior and dorsolateral prostate (*see* **Fig. 4**). Small peripheral acini appear to connect up to more central larger duct profiles, maintaining a lobular arrangement and sharing similar nuclear atypia. Although similar lesions in other models have been regarded as well-differentiated adenocarinoma ***(40,41,104)***, the relative uniformity of these lesions has led us to consider these as precursor lesions, especially as against this background, architecturally distinct foci of unequivocal stromal and periprostatic fat invasion are seen. The rapid growth rate of the prostate in most LPB-*Tag* lines

(e.g., 12T-5, 12T-7s, and 12T-7f) precludes maintaining these mice much beyond 5 mo, and invasion and metastases are seen only rarely. In the ventral prostate of these faster growing lines and in all lobes of the 12T-10 line, epithelial proliferation with prominent nuclear atypia occurs within normal duct and gland profiles, morphologically more analogous to human HGPIN (*see* **Fig. 5**).

In the LPB-*Tag* line 12T-10, the HGPIN progresses to foci of apparent microinvasion, with extension of single tumor cells and small nests and occasional gland formation into the surrounding stroma. Progressively larger invasive carcinoma foci show cytologic and architectural features typical of human neuroendocrine carcinoma. In summary, the histopathology of 12T-10 transgenic mouse prostates showed LGPIN with rapid progression to HGPIN by 2 mo of age, development of microinvasion over 4 to 7 mo, and invasive carcinoma with histological features of glandular or neuroendocrine (NE) differentiation by 11 mo ***(43)***. Up to 88% mice aged ≥9 mo developed metastatic tumors, as confirmed by histology and/or *Tag* immunohistochemistry, with metastasis to regional lymph nodes, liver, and lung being most common and with metastases showing NE differentiation. The NE differentiation was confirmed by immunostaining and ultrastructural analysis ***(43)***. Development of large invasive foci and metastatic tumors with NE differentiation was paralleled by reduced immunostaining for AR, suggesting development of androgen insensitive tumor (*see* **Fig. 5**).

### *1.6.2. Magnetic Resonance Imaging to Follow Neoplastic Prostate Growth and Regression*

Magnetic resonance imaging (MRI) is a noninvasive method that has been used by multiple laboratories in an effort to follow a neoplastic growth in an individual animal. Whether current instrument resolutions can allow for detection of unequivocal invasive foci against a more uniform background of HGPIN and or stromal growth remains to be established. Prostate growth can be monitored by measuring changes in organ volume from week to week (Masumori, M., Kasper, S., and Matusik, R. J., unpublished data). Furthermore, this technique can also be used to determine the rate of prostate regression in response to castration or chemical hormonal ablation and determine the time to AI prostate cancer, as potentially evidenced by prostate regrowth. Careful correlation will be required to demonstrate whether intact animal imaging correlates with specific pathologic changes. Potential advantages of MRI are that the entire process of prostate cancer development, including the development of AI growth, may be determined in the individual animal. These studies depend on the availability of an MRI machine for small animals. Future higher resolution images and more specific contrasting agents will decrease background and generate sharper images for analysis.

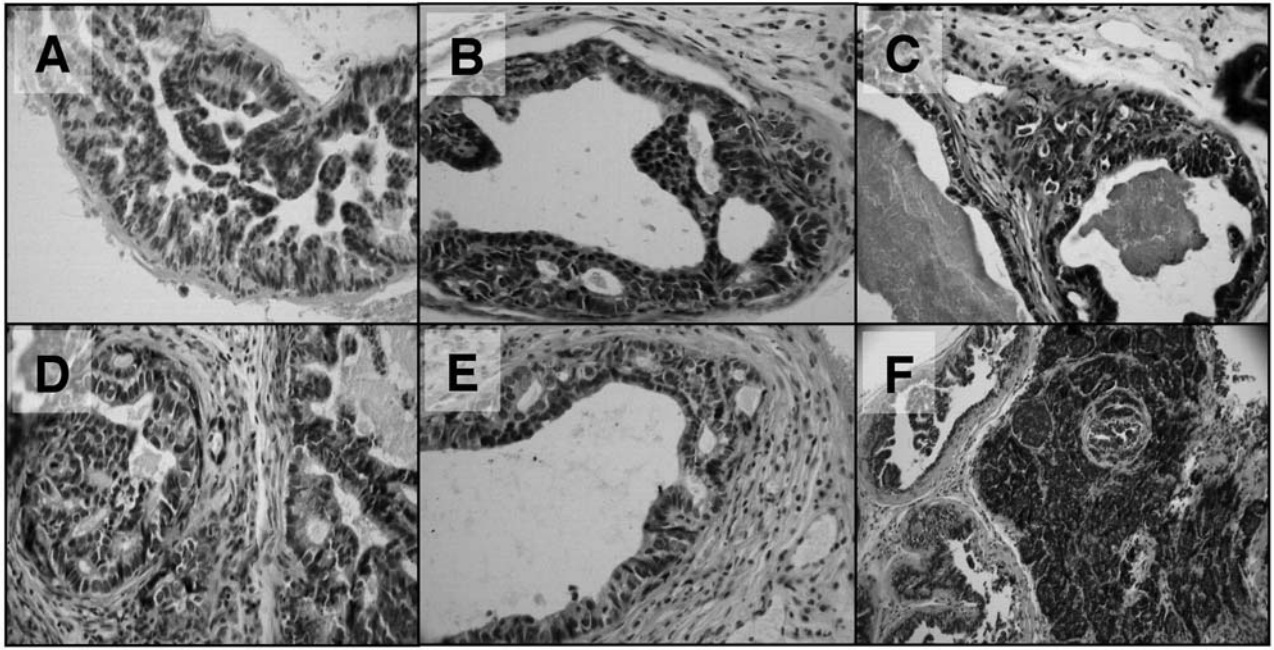


Fig. 5. Histologic progression of prostate carcinoma in LPB-*Tag* Line 12T-10 mouse. (**A**) HGPIN, with proliferation of atypical epithelium within preexisting duct/gland profiles, without accompanying stromal hypercellularity. There is nuclear stratification, enlargement, and hyperchromasia. **(B, C, D)** Microinvasive carcinoma in background of HGPIN, with extension of single cells, nests of cells, and even distinct glands (adenocarcinoma, bottom left) into stroma; (**E**) invasive adenocarcinoma, with malignant glands invading into a thickened stroma and possible reactive peri-prostatic connective tissue; (**F**) extensively invasive undifferentiated carcinoma. Sheets of malignant cells show cytologic features of neuroendocrine carcinoma, with scant cytoplasm, nuclear hyperchromasia, nuclear molding, and occasional rosette formation. Adjacent and entrapped HGPIN gland profiles are evident. Tumor metastases in these mice are composed of identical neuroendocrine carcinoma.

### *1.6.3. Allograft Model*

Allograft models can be used to analyze and characterize the metastatic potential of a primary tumor. For example, a 3-$mm^3$ block of 12T-10 VP invasive primary tumor with NE differentiation was implanted subcutaneously in the back of an 8-wk-old athymic male mouse, tumor growth was monitored, and the mouse was sacrificed after 18 wk ***(43)***. Extensive liver metastases and lung micrometastases were present, with similar NE carcinoma differentiation. Hence, the pattern of metastases is similar to that of the prostate carcinoma developing in intact 12T-10 mice, both of which are similar to that reported for human prostate carcinoma with extensive NE differentiation or small cell carcinoma ***(43)***. Whereas metastatic tumor develops over 11–12 mo in intact mice, high volume metastases are present within 3–4 mo in the allograft model. Tumor growth and metastases are unaffected by castration, indicating the hormone refractoriness of this end stage 12T-10 carcinoma. The tumor has been maintained by further *sc* passages, with similar histologic features, cytogenetic alterations, and metastatic behavior ***(43)***. Hence, the allograft model represents an attractive model for studying mechanisms of growth and metastasis of advanced androgen insensitive carcinoma.

### *1.6.4. Mass Spectrometry to Fingerprint Metastatic Lesions*

Microarray and proteomic analyses are useful tools for identifying changes in gene and protein expression during tumor progression. We have used matrix-assisted laser desorption/ionization time-of-flight (MALDI- TOF) mass spectrometry (MS) to generate and compare protein patterns from different mouse tissues and to compare protein profiles of benign prostate, prostate tumor, and metastatic prostate tumor. The accuracy of MALDI MS is ± 1 to 2 Daltons for proteins up to 30,000 Daltons, with accuracy decreasing slightly as mass increases. The instrumental accuracy can distinguish between two amino acids differing by one mass unit (such as asparagine and aspartic acid) in a given peptide sequence. In addition, it can distinguish proteins in the low parts per million for peptides and proteins ≥5000 Daltons. The mass size (m/z) can serve as a fingerprint to identify a given protein. Even postsecondary modifications, such as phosphorylation, methylation, and acetylation, add a distinct mass to a protein. Glycosylation and the number of glycosylation sites can also be determined, as seen by the spermine binding protein ***(105)***.

We have used MALDI MS to fingerprint proteins from metastatic lesions and compare them with the protein profiles generated from primary tumors ***(43)***. Protein profiles generated by MALDI-TOF-MS of the ventral lobe of a 12T-10 transgenic mouse as well as from NE allografts and liver metastasis showed identical protein profiles, supporting further that the origin of the liver metastases was the prostate and suggesting such technology may be useful in

identifying proteins overexpressed with development of advanced invasive and metastatic AI tumor ***(43)***.

### 1.7. Next-Generation PB Promoter

The basic requirements in designing a promoter include a fragment of DNA, which can be easily subcloned and which targets high level of specific transgene activity to the prostate. The LPB promoter targets high levels of specific transgene activity to the luminal epithelial cells of the prostate. However, the size of the LPB fragment is large enough to make routine subcloning difficult and to make it inaccessible for any gene therapy vectors because most viral constructs cannot accommodate DNA fragments of that length. Thus, the promoter region has been extensively characterized and the resulting newly designed $ARR_2PB$ promoter was developed for multiple applications, including analysis of androgen receptor function, creating new transgenic animal models of prostate cancer, and developing gene therapy vectors to treat prostate cancer. The composite $ARR_2PB$ (<500 bp) promoter conferred high levels of transgene activity both in cell culture and in transgenic animal models ***(71,106)***. Therefore, this small promoter region was as effective as the large LPB DNA fragment and transgene expression was still prostate epithelial cell specific, with an additional characteristic in that transgene expression could now be regulated by glucocorticoids as well as by androgens ***(106)***. These studies have demonstrated that the $ARR_2PB$ promoter has many desirable features as a potent and a tissue-specific promoter for targeting prostate cells. In addition, the small size of $ARR_2PB$ allows for ease of subcloning into any vector system, including viral vectors for gene therapy ***(107)***.

The $ARR_2PB$-Cre mouse model (PB-Cre4) was developed by Wu and coworkers ***(71)*** by linking the $ARR_2PB$ promoter to the Cre site-specific DNA recombinase gene. Cre gene expression was detected in all lobes of the mouse prostate, and Cre-mediated activation of LacZ activity in PB-Cre4/R26R double transgenic mice demonstrated that Cre was expressed postnatally and in a prostatic epithelium-specific manner. The PB-Cre4 mice were also crossbred with floxed *RXRα* allelic mice, achieving selective elimination of *RXRα* in the prostate. Thus, the PB-Cre4 mouse model will be particularly useful because these mice can be crossbred with any floxed model to analyze the loss of expression of a potential tumour suppressor, oncogene, growth factor, or cell cycle protein that may regulate normal prostate development or promote the development of prostate cancer.

### 1.8. Conclusion and Significance

The mouse models available today have provided us the tools to begin addressing the mechanisms by which prostate cancer develops and becomes a clinically significant disease. There are several prostate-specific promoters

available (probasin, PSA) that can be used to target a transgene to the prostate. Conditional expression technology provides the potential for controlling transgene expression during normal prostate and prostate tumor development, and analytical techniques such as MALDI-MS and microarrays provide high throughput, sensitive assays to facilitate analysis of prostate samples. The discovery of new genes involved in prostate tumorigenesis will provide additional mouse models to study the complex genetics of tumorigenesis. Although the development of transgenics has focused on oncogenes, tumor suppressors, and growth factors more often found in the prostatic epithelial cells, stromal factors could also play an important role because normal prostate development occurs through the close interaction between the stromal/mesenchymal and epithelial compartments. No transgenic mouse models are available to overexpress stromal proteins and determine their role in prostate cancer. Therefore, cloning genes to stromal mesenchymal factors could provide novel targets for generating transgenic models for prostate cancer, as well as stromal-specific promoters to specifically target transgenes to the prostatic stroma. Genes involved in prostate tumorigenesis could potentially serve as biological markers to reliably predict prostate cancer stage or the rate at which prostate cancer progresses into clinically significant disease and provide potential targets for novel therapies.

## 2. Materials

### 2.1. Two-Phase Fluor Diffusion Assay to Determine CAT Gene Activity

1. Lysis buffer: 100 m*M* Tris-HCl, pH 7.8, containing 0.1% Triton X-100.
2. Reaction mix: 2 µL [$^3$H]-Acetyl CoA (Amersham TRK-688), 50 µL 5 m*M* Chloramphenicol (dissolved in $H_2O$), 7.5 µL 1 *M* Tris-HCl, pH 7.8, 15.5 µL dd$H_2O$.
3. [$^3$H]-Acetyl CoA (Amersham TRK-688).
4. ScintiLene (cat. no. SX2-4, Fisher Scientific, Pittsburgh, PA).

### 2.2. Preparation of Tail DNA

Digestion buffer (100 mL): 5 mL 1 *M* Tris-HCl, pH 8.0, 20 mL 0.5 *M* EDTA, 2 mL 5.0 *M* NaCl, 10 mL 10% SDS, 63 mL sterile $H_2O$.

### 2.3. Primer Sequences

1. –240Pbf primer: 5′-TAGCATCTTGTTCTTAGTCTT-3′.
2. *Tag*-r primer: 5′-CTCCTTTCAAGACCTAGAAGGTCCA-3′.
3. *mbc*-f primer: 5′-GATGTGCTCCAGGCTAAAGTT-3′.
4. *mbc*-r primer: 5′-AGAAACGGAATGTTGTGGAGT-3′.

### 2.4. PCR for Genotyping

1. PCR mix (50 µL total volume): 5.0 µL 10X reaction buffer (supplied by Perkin Elmer); 3.0 µL 25 m*M* $MgCl_2$ (Perkin Elmer); 0.5 µL 10 m*M* dNTPs (Perkin

Elmer); 0.5 µL –240Pbf primer (Integrated DNA Technologies); 0.5 µL *Tag*-r primer (Integrated DNA Technologies); 0.35 µL of mbc-f primer (Integrated DNA Technologies); 0.35 µL of mbc-r primer (Integrated DNA Technologies); 0.2 µL of Taq Polymerase (1 U; Perkin Elmer); 38.6 µL of nuclease-free $H_2O$ (Promega); 1.0 µL of DNA.

### 2.5. Immunohistochemistry

#### 2.5.1. Buffers

1. 0.01 *M* citrate buffer, pH 6.0 (600 mL total volume): 10.8 mL of 0.1 *M* anhydrous citric acid (1.921 g/100 mL); 49.2 mL 0.1 *M* tri-sodium citric acid (14.705 g/500 mL); 540.0 mL $H_2O$.
2. 10X phosphate-buffered saline (PBS); pH 7.4 (2 L total volume): 160.0 g NaCl; 4.0 g KCl; 28.8 g $Na_2PO_4$; 4.8 g $KH_2PO_4$. Dissolve in ~1500 mL Milli-Q $H_2O$, adjust the pH to 7.4 with HCl, and bring to a volume of 2 L.
3. Blocking buffer 1% digoxigenin (DIG) blocking reagent (Roche) in Tris NaCl, pH 7.5: combine 12.1 g of Tris and 8.8 g of NaCl in 950 mL of Milli-Q $H_2O$ and adjust the pH to 7.5 with HCl; add 1 g of DIG blocking reagent to 100 mL of this solution. Alternatively, combine 50 mL of 1 *M* Tris-HCI pH 7.5, 15 mL of 5 *M* NaCl, and 435 mL of $H_2O$. To this, add 5 g of Blocking Reagent (Roche) and stir until the powder dissolves.

#### 2.5.2. Antibodies

**Table 2** summarizes the antigens, the primary and secondary antibodies, and the antigen retrieval methods used to characterize the LPB prostate tumors. The PAP system with secondary antibodies was purchased from Sternberger Monoclonals Inc.

#### 2.5.3. Reagents

1. Peroxidase Blocking Reagent (Dako).
2. Rabbit PAP, a peroxidase-antiperoxidase complex containing horseradish peroxidase and immunospecific pure rabbit antiperoxidase (Sternberger Monoclonals Inc.).
3. DAB solution. It is important to wear gloves for this procedure! Combine one drop of DAB per 1 mL of DAB substrate [Dako Liquid DAB Substrate-Chromogen System (K3466)].

## 3. Methods

### 3.1. Two-Phase Fluor Diffusion Assay to Determine CAT Gene Activity

Harvest the transfected cells (LNCaP, PC-3, etc.) and lyse by freeze thawing in 300 µL of lysis buffer. Samples can be stored at –70°C at this time if the assay is to be performed at a later date. For the CAT assay, calculate the protein concentration in the samples. If CAT activity is anticipated to be low,

**Table 2**
**Summary of the Antigens, Primary and Secondary Antibodies and the Antigen Retrieval Protocols Used in Characterizing the LPB-*Tag* Mouse Model for Prostate Cancer**

| Antigen | Company | Primary antibody (4°C O/N) | Negative control | Second (1:300, 2 h RT) | PAP (1:500, 1 h RT) | Antigen retrieval |
|---|---|---|---|---|---|---|
| Tag | Oncogene | 1:100 | Mouse IgG | #501 | #405 | 1 *M* urea |
| AR (N-20) | Santa Cruz | 1:100 | Blocking peptide (N-20)P, 5X | #503 | #401 | 1 *M* urea |
| Cytokeratin | Dako | 1:1000 | Rabbit IgG | #503 | #401 | Proteinase K (Dako) |
| CGA (SP-1) | Diasorin | 1:1000 | Rabbit IgG | #503 | #401 | 0.01 *M* citrate |
| Serotonin | Sigma | 1:5000 | Rabbit IgG | #503 | #401 | 0.01 *M* citrate |
| α-Actin | Sigma | 1:1500 | Mouse IgG | #501 | #405 | 1 *M* urea |
| DLP | G. Cunha | 1:1000 | Rabbit IgG | #503 | #401 | 1 *M* urea |
| Probasin R23 | R. J. Matusik | 1:1000 or 1:2000 | Rabbit IgG | #503 | #401 | 1 *M* urea |

use 200 µg of protein in a final volume of 200-µL lysis buffer per reaction. Aliquot the samples into small glass vials (borosilicate scintillation vials, Kimble). Do not use plastic vials. Heat the samples at 65°C for 10 min to inactivate endogenous deacetylase activity, and then let them cool to room temperature for 10 min.

In a glass vial, make up enough reaction mix for all the samples tested. Therefore, make up one or two extra reactions to account for pipet variability. Add 75 µL of the reaction mix (at room temperature) to each tube. Set up a maximum of 48 reactions. If the assay is very large, the length of time required to count the same sample between two runs is too long. Because this is an enzymatic reaction, the counts should be taken on the linear portion of the curve.

Layer on 3 mL of ScintiLene, taking care not to mix the phases. ScintiLene is the only scintillation cocktail that works. Anything similar to this will not work—they have all been tested!

Cycle in the scintillation counter through at least five cycles to get a good linear regression line. Calculate the slope of the line using a linear regression program. Because the slope is determined in cpm/min/200 µg of protein, it is converted into dpm/min/mg (cpm/mg protein divided by the percent efficiency of the counter).

### 3.2. Identification of *LPB*-Tag Transgenic Animals

The animals were tagged using numbered ear tags and a crimp tool from National Band and Tag Co. (Newport, KY), and tail DNA was prepared as follows.

At 3 wk of age, clip a less than 0.5-cm fragment of tail, placing it in an appropriately numbered microfuge tube. Place the tube on dry ice if you want to store it or on wet ice if it will be processed that day. (Note: you can add the sample directly to the digestion mixture if desired.) It is very important to clean the scissors and forceps after taking each sample to remove any traces of blood, which could contaminate the PCR. Repeat the process until all animals are tagged. Tail DNA should be prepared immediately. Samples can be stored at –70°C if necessary.

### 3.3. Preparation of Tail DNA

Add 600 µL of digestion buffer and 25 µL of Proteinase K (10 mg/mL) to each tube. Incubate overnight at 55°C with shaking. Spin the microfuge tubes for 15 min at full speed, and then transfer 500 µL of each supernatant into a microfuge tube containing 1 mL of room temperature absolute ethanol. Invert gently and hook out the DNA with a glass microcapillary tube (Kimax-51 no. 34505). Transfer the DNA into a tube containing 1000 µL of sterile water and allow it to dissolve overnight.

### 3.4. PCR for Genotyping

The PCR mix (*see* **Subheading 2.4.**) is cycled as follows using a Perkin Elmer Gene Amp PCR System 9600, MicroAmp reaction tubes (cat. no. N801-0580, Applied Biosystems) and caps (cat. no. N801-0535, Applied Biosystems).

| | |
|---|---|
| Step 1 | 95°C for 2 min |
| Step 2 | 50°C for 45 s |
| Step 3 | 72°C for 45 s |
| Step 4 | 95°C for 1 min |
| Step 5 | Return to Step 2 and cycle 29 times |
| Step 6 | 50°C for 1 min |
| Step 7 | 72°C for 7 min |
| Step 8 | 4°C for continuation |
| Step 9 | End |

Add loading buffer to the samples, and separate them on a 1.5% agarose gel containing ethidium bromide. The Tag PCR product should be 430 bp in size and the Casein PCR product 540 bp.

### 3.5. Generic Immunohistochemical Protocol

#### 3.5.1. Day 1

Select the tissues to be sectioned, cut in 5- to 6-µm sections, and mount two sections per precleaned Superfrost plus slide (cat. no. 48311-703, VWR Scientific). Process the appropriate positive or negative control tissues in the same manner. Deparaffinize, rehydrate, and prepare the sections by antigen retrieval for ≥3 min in: 2X 100% xylene, 2X 100% ethanol, 1X 70% ethanol, and 1X 50% ethanol. Rinse the slides briefly in Milli-Q $H_2O$.

For citrate antigen retrieval, place the slides in a rack and submerge them in 600 mL of 0.01 *M* citrate in a 1-L beaker. Cover the beaker with a sheet of plastic cling film. Pierce the sheet to make air holes. Microwave (Sharp Carosel II, model R3A93, 60 Hz) the slides at 100% power for 8 min, then at 30% power for 22 min. Allow the slides to sit in the beaker/buffer at room temperature for 1 h.

Wash the slides twice in PBS (5 min/wash), and then wipe away the excess buffer. Encircle the sections with wax using a PAP pen (Electron Microscope Sciences), then incubate them in Dako Peroxidase Blocking Reagent for 5 min. Wash the slides twice in PBS (5 min/wash), and then place them into blocking buffer which has been chilled to 4°C and incubate at room temperature for 30 min. Wipe off the excess buffer, place the slides in a precooled slide box and add 100 µL of the negative control solution onto one section and 100 µL of the antibody solution onto the adjacent section, making sure that each solution

stays within the circle drawn with the PAP pen. Place the cover on the slide box and incubate the slides overnight at 4°C.

### 3.5.2. Day 2

Carefully blot the solutions off each slide, taking care that they do not mix, and place the slides in a slide holder. Wash the slides in PBS for 3×, 5 min each. During this time, prepare a 1:300 dilution of the secondary antibody in PBS. Wipe the excess buffer off the slides and place them in the slide box. Add 100 µL of secondary antibody to each section. Replace the slide box cover and incubate for 2 h at room temperature. Blot off the secondary antibody and wash the slides in PBS for 3×, 5 min each. Prepare a solution of rabbit PAP diluted 1:500 in PBS and add 100 µL to each section. Incubate for 1 h at room temperature, and then blot the PAP solution off and wash the slides in PBS for 3×, 5 min each. Place the slides in a slide rack and immerse them in 50 m*M* Tris-HCI, pH 7.4. Make up the DAB solution, ensuring that gloves are worn during the process. Add one drop of DAB for each mL of the DAB substrate. Remove one slide from the Tris-HCl solution, blot off the excess buffer, wipe the back of the slide with a Chemwipe, and place the slide onto the stage of a microscope. Add 100 µL of DAB solution to each section and monitor the sections for color development. Stop the reaction by blotting off the excess DAB solution and immediately placing the slide into a slide rack sitting in milliQ $H_2O$. Take care to keep the background staining at a minimum by assessing the reactions in which the primary antibody was omitted. Repeat this process for each slide.

Counterstain with hematoxylin as follows:

- Filter the hematoxylin before use.
- Place the slides in metal slide rack.
- Dip the slides 2X in Harris hematoxylin.
- Dip the slides 2X in tap water, pour off the water, then rinse in running tap water for 1 min.
- Dip the slides 10X in $NH_3$.
- Rinse the slides in running tap water for >1 min.
- Dip the slides 45X in 95% ethanol.
- Place the slides in 100% ethanol for 3 min, with one change of 100% ethanol.
- Place the sides in xylene to clear for 3 min, with two changes of xylene.
- Leave the slides in the last xylene clearing step until they are mounted.

Take each slide out of the xylene with forceps, blot off the excess xylene, wipe the back of the slide with a Chemwipe, and mount using two to three drops of Cytoseal 60 (cat. no. 8310-4, Stephens Scientific). Avoid air bubbles, but do not press too hard on the tissue. Blot off any excess Cytoseal 60. Store the slides in a cardboard folder.

### 3.6. Automated Immunohistochemical Protocol

The staining is performed on the Ventana automated immunostainer following the manufacturer's protocol. The antibody is a rabbit anti-mouse cytokeratin 5 antibody distributed by Covance. Antigen retrieval utilizes Trilogy buffer (Cell Marque) and the slides are microwaved for 1 min at 100% power, 25 min in a steamer (any model where the slides are exposed to steam only), and 15 min at room temperature. The antibody is used at a 1:500 dilution (in primary antibody diluent; cat no. 251-018, Ventana Medical Systems, Inc) and the slides are mounted as described above (*see* **Subheading 3.5.**).

### 3.7. Mass Spectrometry for Fingerprinting Metastatic Lesions

Tissue samples (from normal prostate or prostate tumor) are blotted by pressing the tissue onto a carbon-embedded polyethylene membrane for 5 min, transferring proteins through noncovalent interactions onto the membrane (for general reference, *see* **ref.** ***108)***. The blotted area is washed with water to remove residual tissue fragments, salts, and excess blood and then air-dried. A matrix composed of 20 mg/mL sinapinic acid (Sigma) in acetonitrile/0.1% trifluoroacetic acid in $H_2O$ (1:1, v/v) is deposited onto the blotted areas and allowed to dry. Mass spectrometry analyses are performed using a DE-STR MALDI time-of-flight mass spectrometer (Applied Biosystems). The instrument is operated in the linear mode under optimized delayed extraction conditions. An internal mass calibration is performed on each spectrum using the mass values of the previously measured singly and doubly charged ions of the $\alpha$ and $\beta$ chains of hemoglobin, the singly charged molecular ions of bovine insulin (molecular weight, 5733.6; Sigma) and horse heart cytochrome *c* (molecular weight, 12360.1; Sigma) (for example, *see* **ref.** ***43)***.

## Acknowledgments

The authors wish to thank Dr. Robert J. Matusik for his enthusiasm in discussing all topics related to prostate research and for his tireless pursuits in studying the mechanisms of prostate cancer development. This work was supported by the Frances Williams Preston Laboratories of the T. J. Martell Foundation and the Mouse Models for Human Cancer Consortium (NCI U01-CA84239).

## References

1. Bostwick, D. G. (1996) Prospective origins of prostate carcinoma. Prostatic intraepithelial neoplasia and atypical adenomatous hyperplasia (review). *Cancer* **78,** 330–336.
2. Greene, D. R., Wheeler, T. M., Egawa, S., Dunn, J. K., and Scardino, P. T. (1991) A comparison of the morphological features of cancer arising in the transition zone and in the peripheral zone of the prostate. *J. Urol.* **146,** 1069–1076.

3. Wilding, G. (1992) The importance of steroid hormones in prostate cancer. *Cancer Surv.* **14,** 113–130.
4. Brewster, S. F. and Simons, J. W. (1994) Gene therapy in urological oncology: principles, strategies and potential. *Eur. Urol.* **25,** 177–182.
5. Taplin, M. E., Bubley, G. J., Shuster, T. D., Frantz, M. E., Spooner, A. E., Ogata, G. K., et al. (1995) Mutation of the androgen-receptor gene in metastatic androgen-independent prostate cancer (see comments). *N. Engl. J. Med.* **332,** 1393–1398.
6. Kelly, W. K. and Scher, H. I. (1993) Prostate specific antigen decline after antiandrogen withdrawal: the flutamide withdrawal syndrome. *J. Urol.* **149,** 607–609.
7. Bentel, J. M. and Tilley, W. D. (1996) Androgen receptors in prostate cancer. *J. Endocrinol.* **151,** 1–11.
8. Reid, P., Kantoff, P., and Oh, W. (1999) Antiandrogens in prostate cancer. *Invest. New Drugs* **17,** 271–284.
9. Buchanan, G., Yang, M., Harris, J. M., Nahm, H. S., Han, G., Moore, N., et al. (2001) Mutations at the boundary of the hinge and ligand binding domain of the androgen receptor confer increased transactivation function. *Mol. Endocrinol.* **15,** 46–56.
10. Giovannucci, E., Stampfer, M. J., Krithivas, K., Brown, M., Dahl, D., Brufsky, A., et al. (1997) The CAG repeat within the androgen receptor gene and its relationship to prostate cancer. *Proc. Natl. Acad. Sci. USA* **94,** 3320–3323.
11. Irvine, R. A., Yu, M. C., Ross, R. K., and Coetzee, G. A. (1995) The CAG and GGC microsatellites of the androgen receptor gene are in linkage disequilibrium in men with prostate cancer. *Cancer Res.* **55,** 1937–1940.
12. Koivisto, P., Kononen, J., Palmberg, C., Tammela, T., Hyytinen, E., Isola, J., et al. (1997) Androgen receptor gene amplification: A possible molecular mechanism for androgen deprivation therapy failure in prostate cancer. *Cancer Res.* **57,** 314–319.
13. Miyoshi, Y., Uemura, H., Fujinami, K., Mikata, K., Harada, M., Kitamura, H., et al. (2001) Fluorescence in situ hybridization evaluation of c-myc and androgen receptor gene amplification and chromosomal anomalies in prostate cancer in Japanese patients. *Prostate* **43,** 225–232.
14. Gregory, C. W., Hamil, K. G., Kim, D., Hall, S. H., Pretlow, T. G., Mohler, J. L., et al. (1998) Androgen receptor expression in androgen-independent prostate cancer is associated with increased expression of androgen-regulated genes. *Cancer Res.* **58,** 5718–5724.
15. Chen S-y, Wang, J., Yu G, Liu, W., and Pearce, D. (1997) Androgen and glucocorticoid receptor heterodimer formation. A possible mechanism for mutual inhibition of transcriptional activity. *J. Biol. Chem.* **272,** 14087–14092.
16. Ruijter, E., Van De Kaa, C., Miller, G., Ruiter, D., Debruyne, F., and Schalken, J.(1999) Molecular genetics and epidemiology of prostate carcinoma. *Endocr. Rev.* **20,** 22–45.
17. Craft, N., Shostak, Y., Carey, M., and Sawyers, C. (1999) A mechanism for hormone-independent prostate cancer through modulation of androgen receptor signaling by the HER-2/neu tyrosine kinase. *Nat. Med.* **5,** 280–285.
18. Yeh, S., Lin, H. K., Kang, H. Y., Thin, T. H., Lin, M. F., and Chang, C. (1999) From HER2/Neu signal cascade to androgen receptor and its coactivators: A novel

pathway by induction of androgen target genes through MAP kinase in prostate cancer cells. *Proc. Natl. Acad. Sci. USA.* **96,** 5458-5463.
19. Wen, Y., Hu, M. C., Makino, K., Spohn, B., Bartholomeusz, G., Yan, D. H., et al. (2000) HER-2/neu promotes androgen-independent survival and growth of prostate cancer cells through the Akt pathway. *Cancer Res.* **60,** 6841–6845.
20. Rajah, R., Valentinis, B., and Cohen, P. (1997) Insulin-like growth factor (IGF)-binding protein-3 induces apoptosis and mediates the effects of transforming growth factor- beta1 on programmed cell death through a p53- and IGF-independent mechanism. *J. Biol. Chem.* **272,** 12181–12188.
21. Hayes S. A., Zarnegar, M., Sharma, M., Yang, F., Peehl, D. M., ten Dijke P., et al. (2001) SMAD3 represses androgen receptor-mediated transcription. *Cancer Res.* **61,** 2112–2118.
22. Kang, H. Y., Lin, H. K., Hu, Y. C., Yeh, S., Huang, K. E., and Chang, C. (2001) From transforming growth factor-beta signaling to androgen action: Identification of Smad3 as an androgen receptor coregulator in prostate cancer cells. *Proc. Natl. Acad. Sci. USA.* **98,** 3018–3023.
23. Fujimoto, N., Yeh, S., Kang, H. Y., Inui, S., Chang, H. C., Mizokami, A., et al. (1999) Cloning and characterization of androgen receptor coactivator, ARA55, in human prostate. *J. Biol. Chem.* **274,** 8316–8321.
24. Kang, H. Y., Yeh, S., Fujimoto, N., and Chang, C. (1999) Cloning and characterization of human prostate coactivator ARA54, a novel protein that associates with the androgen receptor. *J. Biol. Chem.* **274,** 8570–8576.
25. de Pinieux, G., Legrier, M. E., Poirson-Bichat, F., Courty, Y., Bras-Goncalves, R., Dutrillaux, A. M., et al. (2001) Clinical and experimental progression of a new model of human prostate cancer and therapeutic approach. *Am. J. Pathol.* **159,** 753–764.
26. Gregory, C. W., Kim, D., Ye, P., D'Ercole, A. J., Pretlow, T. G., Mohler, J. L., et al. (1999) Androgen receptor up-regulates insulin-like growth factor binding protein-5 (IGFBP-5) expression in a human prostate cancer xenograft. *Endocrinology* **140,** 2372–2381.
27. Nickerson, T., Chang, F., Lorimer, D., Smeekens, S. P., Sawyers, C. L., and Pollak, M. (2001) In vivo progression of lapc-9 and lncap prostate cancer models to androgen independence is associated with increased expression of insulin-like growth factor i (igf-i) and igf-i receptor (igf-ir). *Cancer Res.* **61,** 6276–6280.
28. Zhau, H. E., Li, C. L., and Chung, L. W. (2000) Establishment of human prostate carcinoma skeletal metastasis models. *Cancer* **88,** 2995–3001.
29. Korenchuk, S., Lehr, J. E., MClean, L., Lee, Y. G., Whitney, S., Vessella, R., et al. (2001) VCaP, a cell-based model system of human prostate cancer. *In Vivo* **15,** 163–168.
30. Navone, N. M., Logothetis, C. J., von Eschenbach, A. C., and Troncoso, P. (1998) Model systems of prostate cancer: uses and limitations. *Cancer Metastasis Rev.* **17,** 361–371.
31. van Weerden, W. M. and Romijn, J.C. (2000) Use of nude mouse xenograft models in prostate cancer research. *Prostate* **43,** 263–271.

32. Bostwick, D. G., Ramnani, D., and Qian, J. (2000) Prostatic intraepithelial neoplasia: Animal models 2000. *Prostate* **43,** 286–294.
33. Waters, D. J., Bostwick, D. G., and Murphy, G. P. (1998) Conference summary: First International Workshop on Animal models of Prostate Cancer. *Prostate* **36,** 47–48.
34. Barrios, R., Lebovitz, R. M., Wiseman, A. L., Weisoly, D. L., Matusik, R. J., DeMayo, F., et al. (1996) RasT24 driven by a probasin promoter induces prostatic hyperplasia in transgenic mice. *Transgenics* **2,** 23–28.
35. Voelkel-Johnson, C., Voeks, D. J., Greenberg, N. M., Barrios, R., Maggouta, F., Kurtz, D. T., et al.(2000) Genomic instability-based transgenic models of prostate cancer. *Carcinogenesis* **21,** 1623–1627.
36. Shibata, M. A., Maroulakou, I. G., Jorcyk, C. L., Gold, L. G., Ward, J. M., and Green, J. E. (1996) p53-independent apoptosis during mammary tumor progression in C3(1)/SV40 large T antigen transgenic mice: Auppression of apoptosis during the transition from preneoplasia to carcinoma. *Cancer Res.* **56,** 2998–3003.
37. Kitsberg, D. I. and Leder, P. (1996) Keratinocyte growth factor induces mammary and prostatic hyperplasia and mammary adenocarcinoma in transgenic mice. *Oncogene* **13,** 2507–2515.
38. Hennighausen, L., McKnight, R., Burdon, T., Baik, M., Wall, R. J., and Smith, G. H. (1994) Whey acidic protein extrinsically expressed from the mouse mammary tumor virus long terminal repeat results in hyperplasia of the coagulation gland epithelium and impaired mammary development. *Cell Growth Differ.* **5,** 607–613.
39. DiGiovanni, J., Kiguchi, K., Frijhoff, A., Wilker, E., Bol, D. K., Beltran, L., et al. (2000) Deregulated expression of insulin-like growth factor 1 in prostate epithelium leads to neoplasia in transgenic mice. *Proc. Natl. Acad. Sci. USA* **97,** 3455–3460.
40. Greenberg, N. M., DeMayo, F. J., Finegold, M. J., Medina, D., Tilley, W. D., Aspinall, J. O., et al. (1995) Prostate cancer in a transgenic mouse. *Proc. Natl. Acad. Sci. USA.* **92,** 3439–3443.
41. Gingrich, J. R., Barrios, R. J., Morton, R. A., Boyce, B. F., DeMayo, F. J., Finegold, M. J., et al. (1996) Metastatic prostate cancer in a transgenic mouse. *Cancer Res.* **56,** 4096–4102.
42. Kasper, S., Sheppard, P. C., Yan, Y., Pettigrew, N., Borowsky, A. D., Prins, G. S., et al. (1998) Development, progression and androgen-dependence of prostate tumors in transgenic: A model for prostate cancer. *Lab. Invest.* **78,** 319–334.
43. Masumori, N., Thomas, T. Z., Case, T., Paul, M., Kasper, S., Chaurand, P., et al. (2001) A probasin-large T antigen transgenic mouse line develops prostate adeno and neuroendocrine carcinoma with metastatic potential. *Cancer Res.* **61,** 2239–2249.
44. Tehranian, A., Morris, D. W., Min, B. H., Bird, D. J., Cardiff, R. D., and Barry, P. A. (1996) Neoplastic transformation of prostatic and urogenital epithelium by the polyoma virus middle T gene. *Am. J. Pathol.* **149,** 1177–1191.
45. Garabedian, E. M., Humphrey, P. A., and Gordon, J. I. (1998) A transgenic mouse model of metastatic prostate cancer originating from neuroendocrine cells. *Proc. Natl. Acad. Sci. USA.* **95,** 15382–15387.

46. Perez-Stable, C., Altman, N. H., Brown, J., Harbison, M., Cray, C., and Roos, B. A. (1996) Prostate, adrenocortical, and brown adispose tumors in fetal globin T antigen transgenic mice. *Lab. Invest.* **74,** 363–373.
47. Skalnik, D. G., Dorfman, D. M., Williams, D. A., and Orkin, S. H. (1991) Restriction of neuroblastoma to the prostate gland in transgenic mice. *Mol. Cell. Biochem.* **11,** 4518–4527.
48. Pipas, J. M. and Levine, A. J. (2001) Role of T antigen interactions with p53 in tumorigenesis. *Semin. Cancer Biol.* **11,** 23–30.
49. Ali, S. H. and Decaprio, J. A. (2001) Cellular transformation by SV40 large T antigen: Interaction with host proteins. *Semin. Cancer Biol.* **11,** 15–23.
50. Rundell, K. and Parakati, R. (2001) The role of the SV40 ST antigen in cell growth promotion and transformation. *Semin. Cancer Biol.* **11,** 5–13.
51. Myers, R. B., Oelschlager, D., Srivastava, S., and Grizzle, W. E. (1994) Accumulation of the p53 protein occurs more frequently in metastatic than in localized prostatic adenocarcinomas. *Prostate* **25,** 243–248.
52. Bookstein, R., Rio, P., Madreperla, S. A., Hong, F., Allred, C., Grizzle, W. E., et al. (1990) Promoter deletion and loss of retinoblastoma gene expression in human prostate carcinoma. *Proc. Natl. Acad. Sci. USA.* **87,** 7762–7766.
53. Bookstein, R., Shew, J. Y., Chen, P. L., Scully, P., and Lee, W. H. (1990) Suppression of tumorigenicity of human prostate carcinoma cells by replacing a mutated RB gene. *Science* **247,** 712–715.
54. Bookstein, R., MacGrogan, D., Hilsenbeck, S. G., Sharkey, F., and Allred, D. C. (1993) p53 is mutated in a subset of advanced-stage prostate cancers. *Cancer Res.* **53,** 3369–3373.
55. Jasani, B., Cristaudo, A., Emri, S. A., Gazdar, A. F., Gibbs, A., Krynska, B., et al. (2001) Association of SV40 with human tumours. *Semin. Cancer Biol.* **11,** 49–61.
56. Shibata, M. A., Ward, J. M., Devor, D. E., Liu, M. L., and Green, J. E. (1996) Progression of prostatic intraepithelial neoplasia to invasive carcinoma in C3(1)/SV40 large T antigen transgenic mice: Histopathological and molecular biological alterations. *Cancer Res.* **56,** 4894–4903.
57. Huss, W. J., Hanrahan, C. F., Barrios, R. J., Simons, J. W., and Greenberg, N. M. (2001) Angiogenesis and prostate cancer: identification of a molecular progression switch. *Cancer Res.* **61,** 2736–2743.
58. Charest, N. J., Zhou, Z. X., Lubahn, D. B., Olsen, K. L., Wilson, E. M., and French, F. S. (1991) A frameshift mutation destabilizes androgen receptor messenger RNA in the Tfm mouse. *Mol. Endocrinol.* **5,** 573–581.
59. He, W. W., Kumar, M. V., and Tindall, D. J.(1991) A frame-shift mutation in the androgen receptor gene causes complete androgen insensitivity in the testicular-feminized mouse. *Nucleic Acids Res.* **19,** 2373–2378.
60. Cunha, G. R. and Lung, B. (1978) The possible influence of temporal factors in androgenic responsiveness of urogenital tissue recombinants from wild-type and androgen-insensitive (Tfm) mice. *J. Exp. Zool.* **205,** 181–193.
61. Cunha, G. R. and Chung, L. W. (1981) Stromal-epithelial interactions—I. Induction of prostatic phenotype in urothelium of testicular feminized (Tfm/y) mice. *J. Steroid Biochem.* **14,** 1317–1324.

62. Zheng, B., Mills, A. A., and Bradley, A. (1999) A system for rapid generation of coat color-tagged knockouts and defined chromosomal rearrangements in mice. *Nucleic Acids Res.* **27,** 2354–2360.
63. Hertzog, P. J. and Kola, I. (2001) Overview. Gene knockouts. *Methods Mol. Biol.* **158,** 1–10.
64. Eddy, E. M., Washburn, T. F., Bunch, D. O., Goulding, E. H., Gladen, B. C., Lubahn, D. B., et al. (1996) Targeted disruption of the estrogen receptor gene in male mice causes alteration of spermatogenesis and infertility. *Endocrinology* **137,** 4796–4805.
65. Risbridger, G. P., Wang, H., Frydenberg, M., and Cunha, G. (2001) The metaplastic effects of estrogen on mouse prostate epithelium: Proliferation of cells with basal cell phenotype. *Endocrinology* **142,** 2443–2450.
66. Colombel, M., Radvanyi, F., Blanche, M., Abbou, C., Buttyan, R., Donehower, L. A., et al. (1995) Androgen suppressed apoptosis is modified in p53 deficient mice. *Oncogene* **10,** 1269–1274.
67. Di Cristofano, A., De Acetis, M., Koff, A., Cordon-Cardo, C., and Pandolfi, P. P. (1998) Pten and p27KIP1 cooperate in prostate cancer tumor suppression in the mouse. *Nat. Genet.* **27,** 134–135.
68. Luo, J. L., Yang, Q., Tong, W. M., Hergenhahn, M., Wang, Z. Q., and Hollstein, M. (2001) Knock-in mice with a chimeric human/murine p53 gene develop normally and show wild-type p53 responses to DNA damaging agents: a new biomedical research tool. *Oncogene* **20,** 320–328.
69. Wang, Y., Hayward, S. W., Donjacour, A. A., Young, P., Jacks, T., Sage, J., et al.(2000) Sex hormone-induced carcinogenesis in Rb-deficient prostate tissue. *Cancer Res.* **60,** 6008–6017.
70. Sauer, B. (1998) Inducible gene targeting in mice using the Cre/lox system. *Methods* **14,** 381–392.
71. Wu, X., Wu, J., Huang, J., Powell, W. C., Zhang, J., Matusik, R. J., et al. (2001) Generation of a prostate epithelial cell-specific Cre transgenic mouse model for tissue-specific gene ablation. *Mech. Dev.* **101,** 61–69.
72. Sauer, B. (1992) Identification of cryptic lox sites in the yeast genome by selection for Cre-mediated chromosome translocations that confer multiple drug resistance. *J. Mol. Biol.* **223,** 911–928.
73. Lottmann, H., Vanselow, J., Hessabi, B., and Walther, R. (2001) The Tet-On system in transgenic mice: Inhibition of the mouse pdx-1 gene activity by antisense RNA expression in pancreatic beta-cells. *J. Mol. Med.* **79,** 321–328.
74. Zhu, Z., Ma, B., Homer, R. J., Zheng, T., and Elias, J. A. (2001) Use of the tetracycline-controlled transcriptional silencer (tTS) to eliminate transgene leak in inducible overexpression transgenic mice. *J. Biol. Chem.* **276,** 25222–25229.
75. Freundlieb, S., Schirra-Muller, C., and Bujard, H. (1999) A tetracycline controlled activation/repression system with increased potential for gene transfer into mammalian cells. *J. Gene Med.* **1,** 4–12.
76. Wakita, K., McCormick, F., and Tetsu, O. (2001) Method for screening ecdysone-inducible stable cell lines. *Biotechniques* **31,** 414–418.

77. Saez, E., Nelson, M. C., Eshelman, B., Banayo, E., Koder, A., Cho, G. J., et al. (2000) Identification of ligands and coligands for the ecdysone-regulated gene switch. *Proc. Natl. Acad. Sci. USA* **97,** 14512–14517.
78. Constantino, S., Santos, R., Gisselbrecht, S., and Gouilleux, F. (2001) The ecdysone inducible gene expression system: unexpected effects of muristerone A and ponasterone A on cytokine signaling in mammalian cells. *Eur. Cytokine. Netw.* **12,** 365–367.
79. Lee, C., Sensibar, J. A., Dudek, S. M., Hiipakka, R. A., and Liao, S. T. (1990) Prostatic ductal system in rats: regional variation in morphological and functional activities. *Biol. Reprod.* **43,** 1079–1086.
80. Price, D. (1963) Comparative aspects of development and structure in the prostate, in *Biology of the Prostate and Related Tissues* (Vollmer, E. P. and Kauffmann, G., eds.) US Government Printing Office, Washington, D.C., pp. 1–28.
81. Spence, A. M., Sheppard, P. C., Davie, J. R., Matuo, Y., Nishi, N., McKeehan, W. L., et al. (1989) Regulation of a bifunctional mRNA results in synthesis of secreted and nuclear probasin. *Proc. Natl. Acad. Sci. USA.* **86,** 7843–7847.
82. Spence, A. M., Sheppard, P. C., Davie, J. R., Matuo, Y., Nishi, N., McKeehan, W. L., et al. (1989) Regulation of a bifunctional mRNA results in synthesis of secreted and nuclear probasin. *Proc. Natl. Acad. Sci. USA* **86,** 7843–7847.
83. Matuo, Y., Nishi, N., Muguruma, Y., Yoshitake, Y., Kurata, N., and Wada, F. (1985) Localization of prostatic basic protein ("probasin") in the rat prostates by use of monoclonal antibody. *Biochem. Biophys. Res. Commun.* **130,** 293–300.
84. Dodd, J. G., Sheppard, P. C., and Matusik, R. J. (1983) Characterization and cloning of rat dorsal prostate mRNAs. Androgen regulation of two closely related abundant mRNAs. *J. Biol. Chem.* **258,** 10731–10737.
85. Rennie, P. S., Bruchovsky, N., Leco, K. J., Sheppard, P. C., McQueen, S. A., Cheng, H., et al. (1993) Characterization of two cis-acting elements involved in the androgen regulation of the probasin gene. *Mol. Endocrinol.* **7,** 23–36.
86. Greenberg, N. M., DeMayo, F. J., Sheppard, P. C., Barrios, R., Lebovitz, M., Finegold, M., et al. (1994) The rat probasin gene promoter directs hormonally and developmentally regulated expression of a heterologous gene specifically to the prostate in transgenic mice. *Mol. Endocrinol.* **8,** 230–239.
87. Matusik, R. J., Kreis, C., McNicol, P., Sweetland, R., Mullin, C., Fleming, W. H., et al. (1986) Regulation of prostatic genes: role of androgens and zinc in gene expression. *Biochem. Cell Biol.* **64,** 601–607.
88. Nachtigal, M. W., Nickel, B. E., Klassen, M. E., Zhang, W., Eberhardt, N. L., and Cattini, P. A. (1989) Human chorionic somatommammotropin and growth hormone gene expression in rat pituitary tumour cells is dependent on proximal promoter sequences. *Nucleic Acids Res.* **17,** 4327–4337.
89. Zhang, J., Thomas, T. Z., Kasper, S., and Matusik, R. J. (2000) A small composite probasin promoter confers high levels of prostate-specific gene expression through regulation by androgens and glucocorticoids in vitro and in vivo. *Endocrinology* **141,** 4698–4710.

90. Cleutjens, K. B., van der Korput, H. A., Ehren-van Eekelen, C. C., Sikes, R. A., Fasciana, C., Chung, L. W., et al. (1997) A 6-kb promoter fragment mimics in transgenic mice the prostate- specific and androgen-regulated expression of the endogenous prostate- specific antigen gene in humans. *Mol. Endocrinol.* **11,** 1256–1265.
91. Daelemans, D., De Clercq, E., and Vandamme, A. (2001) A quantitative GFP-based bioassay for the detection of HIV-1 Tat transactivation inhibitors. *J. Virol. Methods* **96,** 183–188.
92. Veldscholte, J., Berrevoets, C. A., Ris-Stalpers, C., Kuiper, G. G., Jenster, G., Trapman, J., et al. (1992) The androgen receptor in LNCaP cells contains a mutation in the ligand binding domain which affects steroid binding characteristics and response to antiandrogens. *J. Steroid Biochem. Mol. Biol.* **41,** 665–669.
93. Liu, N., Gao, F., Han, Z., Xu, X., Underhill, C. B., and Zhang, L. (2001) Hyaluronan synthase 3 overexpression promotes the growth of TSU prostate cancer cells. *Cancer Res.* **61,** 5207–5214.
94. Kasper, S., Rennie, P. S., Bruchovsky, N., Sheppard, P. C., Cheng, H., Lin, L., et al. (1994) Cooperative binding of androgen receptors to two DNA sequences is required for androgen induction of the probasin gene. *J. Biol. Chem.* **269,** 31763–31769.
95. Kasper, S., Rennie, P. S., Bruchovsky, N., Lin, L., Cheng, H., Snoek, R., et al. (1999) Selective activation of the probasin androgen responsive region by steroid hormones. *J. Mol. Endocrinol.* **22,** 313–325.
96. Brookes, D. E., Zandvliet, D., Watt, F., Russell, P. J., and Molloy, P. L. (1998) Relative activity and specificity of promoters from prostate-expressed genes. *Prostate* **35,** 18–26.
97. Yan, Y., Sheppard, P. C., Kasper, S., Lin, L., Hoare, S., Kapoor, A., et al. (1997) A large fragment of the probasin promoter targets high levels of transgene expression to the prostate of transgenic mice. *Prostate* **32,** 129–139.
98. Sleigh, M. J., Topp, W. C., Hanich, R., and Sambrook, J. F. (1978) Mutants of SV40 with an altered small t protein are reduced in their ability to transform cells. *Cell* **14,** 79–88.
99. Hogan, B., Beddington, R., Costantini, F., and Lacy, E. (eds.) (2001) *Manipulating the Mouse Embryo, A Laboratory Manual, 2nd edition*. Cold Springs Harbor Press.
100. Hayward, S. W., Brody, J. R., and Cunha, G. R. (1996) An edgewise look at basal epithelial cells: three-dimensional views of the rat prostate, mammary gland and salivary gland. *Differentiation* **60,** 219–227.
101. Bonkhoff, H. and Remberger, K. (1998) Morphogenetic concepts of normal and abnormal growth in the human prostate. *Virchows Arch.* **433,** 195–202.
102. Cox, M. E., Deeble, P. D., Bissonette, E. A., and Parsons, S. J. (2000) Activated 3′,5′-cyclic AMP-dependent protein kinase is sufficient to induce neuroendocrine-like differentiation of the LNCaP prostate tumor cell line. *J. Biol. Chem.* **275,** 13812–13818.

103. Zelivianski, S., Verni, M., Moore, C., Kondrikov, D., Taylor, R., and Lin, M. F. (2001) Multipathways for transdifferentiation of human prostate cancer cells into neuroendocrine-like phenotype. *Biochim. Biophys. Acta* **1539,** 28–43.
104. Gingrich, J. R., Barrios, R. J., Foster, B. A., and Greenberg, M. N. (1999) Pathologic progression of autochthonous prostate cancer in the TRAMP model. *Prostate Cancer Prostatic Dis.* **6,** 1–6.
105. Chaurand, P., DaGue, B. B., Ma, S., Kasper, S., and Caprioli, R. M. (2001) Strain-based sequence variations and structure analysis of murine prostate specific spermine binding protein using mass spectrometry. *Biochemistry* **40,** 9725–9733.
106. Zhang Z. F., Thomas, T. Z., Kasper, S., and Matusik, R. J. (2000) A small composite probasin promoter confers high levels of prostate-specific gene expression through regulation by androgens and glucocorticoid in vitro and in vivo. *Endocrinology* **141,** 4698–4710.
107. Andriani, F., Nan, B., Yu, J., Li, X., Weigel, N. L., McPhaul, et al. (2001) Use of the probasin promoter arr(2)pb to express bax in androgen receptor-positive prostate cancer cells. *J. Natl. Cancer Inst.* **93,** 1314–1324.
108. Chaurand, P., Stoeckli, M., and Caprioli, R. M. (1999) Direct profiling of proteins in biological tissue sections by MALDI mass spectrometry. *Anal. Chem.* **71,** 5263–5270.
109. Hamer, D.H. and Walling, M. (1982) Regulation in vivo of a cloned mammalian gene: cadmium induces the transcription of a mouse metallothionein gene in SV40 vectors. *J. Mol. Appl. Genet.* **1,** 273–288.

# 9

# In Vivo Models of Human Prostate Cancer Bone Metastasis

**Julie M. Brown**

## 1. Introduction

According to the American Cancer Society, adenocarcinoma of the prostate is the most common newly-diagnosed cancer in men and was the second-leading cause of cancer-related death in men more than 60 yr of age in the year 2000 ***(1)***. Much of the morbidity and mortality associated with prostate cancer is the result of its progression to distant metastasis, particularly to bone: more than 70% of patients present at autopsy with bone metastases ***(2,3)***. These lesions are usually osteoblastic with a strong lytic component, such that normal bone is resorbed and replaced with woven bone ***(4)***, which is disorganized and has reduced bone mineral density ***(5)***. Resulting fractures, compressions, and pain compromise the quality and quantity of life of the patient and represent a grave problem for clinicians. Bone metastases are classically difficult to treat and monitor effectively ***(6)***, although recent advances in the analgesic use of radionuclides and bisphosphonates offer new strategies to combat bone pain ***(7,8)***.

To gain an understanding of the processes involved in prostate cancer bone metastasis and therefore to design and implement better therapeutic strategies, there is a need to study these processes in a suitable in vivo system. Although the use of spontaneous and induced models and transgenic mouse models have been useful tools in the study of prostate cancer, human prostate cancer xenografts provide the opportunity to study the organ-specific expression of human genes within an in vivo context. Attempts have been made to produce xenografts in a range of animals, including chick embryos ***(9)***, but rodents have remained a popular choice because they are economical and easy to use. Specific methods have been developed to study bony metastases from human prostate cancers in exper-

From: *Methods in Molecular Medicine, Vol. 81: Prostate Cancer Methods and Protocols*
Edited by: P. J. Russell, P. Jackson, and E. A. Kingsley © Humana Press Inc., Totowa, NJ

imental animal models. In this chapter, three methodologies for the study of the metastasis to bone of prostate cancer are presented: the direct injection of human prostate cancer cells into bone of mice that are immunocompromised; methods to produce spontaneous bone metastases of human prostate cancer cells in mice; and methods used to engraft human bone into mice for the study of species-specific trafficking and bone metastasis. The advantages, limitations, and suitability of each model are discussed as a guide to help investigators choose the most appropriate model to test their hypotheses.

No model yet exists that can successfully reproduce the whole metastatic process and all of the environmental interactions that occur in the human disease. However, available models have utility in the study of different aspects of human prostate cancer bone metastasis. It is therefore critical to formulate carefully the questions one wishes to ask and then to select judiciously the model(s) with which to answer them. Other aspects of the human disease progression that remain understudied include the role of the immune system in prostate cancer bone metastasis. The development of new models that also facilitate study of this aspect will bring us a step closer to a fuller understanding of the disease process in humans.

## 2. Materials

The following materials are required for the methodologies described below:

1. Six to eight-week-old male athymic mice, severe combined immunodeficient (SCID) mice, or nonobese diabetic SCID (NOD-SCID) mice, plus sterilized cages, food, and water.
2. Anesthetic reagents, sterilized surgical instruments for mouse surgery and bone dissociation, suture and wound clips, 18–30-gauge syringe needles, heat lamp, shaver, cotton swabs and alcohol swabs, Matrigel (for LNCaP injection into nonosseous tissues), all used for implantation of cells into the mice.
3. Cultured prostate cancer cell lines, including LNCaP, PC-3 and DU-145 cells.
4. Tissue culture reagents, such as RPMI medium or T-medium, trypsin, and Hank's buffered saline solution or phosphate-buffered saline and assorted tissue culture plasticware.
5. Trypan blue, a hemocytometer and a light microscope for quantitation of viable cells.
6. Serum prostate-specific antigen (PSA) kits and calipers to monitor tumor growth.

## 3. Methods

### 3.1. Intraosseous Injection

Several studies have emerged in recent years wherein prostate cancer cells derived from human cell lines or from patient samples have been introduced directly into the bone marrow cavity of immunocompromised mice.

Injection of prostate cancer cells into the tibia is based on a method developed in a study of the metastasis to bone of human osteosarcoma in athymic mice ***(10)***.

1. Prepare prostate cancer cell suspensions from trypsinized confluent cultures or from mechanically-dissociated tumors that have been serially passaged in mice.
2. Load a 1-mL syringe with cells at $2 \times 10^7$ mL in Hank's buffered saline solution (HBSS) without a needle to avoid shearing. Attach a 26-gauge needle and expel the air.
3. Holding the recipient mouse with its ankle joint immobilized and its knee flexed, insert the needle through the skin directly into the proximal epiphysis of the tibia using a gentle unforced drilling motion. The needle tip should be inserted 3 to 5 mm into the marrow space. Then, inject approx $2 \times 10^5$ cells in 20 µL of HBSS.
4. Release the pressure and withdraw the needle using the same drilling motion.
5. Monitor the mice by palpation and serum PSA, where appropriate, to gauge tumor growth. As controls for the procedure, mice are injected with the vehicle alone. As a control for age-related changes in the bone, mice of the same age are sacrificed alongside mice in the test groups.
6. Endpoint tumors can be visualized by autoradiography and characterized by immunohistochemistry and histomorphometry ***(11)***.

For expected results and alternative bone injection sites with technique limitations, please *see* **Notes 1** and **2** ***(12–18)***.

### *3.2. Spontaneous Metastasis of Human Xenografted Prostate Cancer to Bone*

Among the features of a desirable human xenograft model of prostate cancer in rodents is the ability of the introduced cancer cells to home specifically to bone. This allows the study of metastatic processes that could not be examined using the models described in the previous section. Several investigators have performed studies on the propensity of prostate cancer cells to colonize bone selectively using cell lines and xenografts that metastasize spontaneously to bone after injection into the circulation or following orthotopic implantation.

#### *3.2.1. Subcutaneous Implantation Method*

Metastasis from the subcutis is rare, but an LAPC xenograft line ***(19)***, LAPC-4, derived from sc implantation of diced clinical material with Matrigel, spread to peripheral blood, bone marrow, and spleen in 50% of implanted mice, although no bone metastases were detected.

#### *3.2.2. Intravenous and Intracardiac Injection Methods*

Prostate cancer cells have been detected in the peripheral blood and bone marrow ***(20–24)***, leading to the hypothesis that prostate cancer cells dissemi-

nate at least in part through hematogenous spread. Models in which prostate cancer cells are introduced directly into the circulation may therefore have utility in the understanding of the metastatic process.

Intravenous injection of prostate cancer cells into the lateral tail vein of the mouse using a 26-gauge needle, or smaller, is a common procedure.

1. Anesthetize the mice and clean the tail with alcohol. The tail can be heated gently using a lamp to promote vasodilation.
2. With the bevel facing up, a 26- or 27-gauge needle is inserted into one of the lateral tail veins in the distal third of the tail and 1 to $10 \times 10^6$ prostate cancer cells in 100 to 200 µL of HBSS is gently injected ***(17,25–27)***. After withdrawing the needle, apply pressure to promote clot formation.

Limitations to the technique (*see* **Note 3**) and refinements, such as occlusion (*see* **Note 4**) are discussed below.

#### Intracardiac Injection

An extension of the principle of injecting cells into the venous circulation is to inject the cells directly into the heart ventricles, or intracardiac injection.

1. Place mice in a supine position after they have been anesthetized with methoxyflurane and make an upper midline vertical incision. Retract the liver to permit visualization of the heart.
2. Inject $5 \times 10^5$ prostate cancer cells (LNCaP, PC-3M sublines, or C4-2) in 50 µL of phosphate-buffered saline (PBS) into the base of the left ventricle through the diaphragm using a 30-gauge needle. Close the wound with wound clips.

For comparisons between metastasis after these two injection methods and technique limitations, please *see* **Notes 5** and **6** ***(33)***, respectively.

### *3.2.3. Surgical Orthotopic Implantation Method*

Direct implantation into the primary organ may provide the most clinically appropriate model of prostate cancer bone metastasis in mice. The following method of surgical orthotopic implantation (SOI) for prostate cancer cells was developed almost 10 yr ago ***(34)*** and has been adapted by several investigators to develop cell lines for the study of metastasis.

1. Anesthetize mice with methoxyflurane and place in a supine position. Swab the abdomen with alcohol and make a lower midline abdominal incision to expose the bladder and male accessory sex glands. Move these aside using a cotton swab on the posterior surface of the bladder and seminal vesicles, and retract them anteriorly and inferiorly.
2. Prepare cultured prostate cancer cells for injection by trypsinization and resuspension in HBSS. Only use populations with more than 90% viability (Trypan blue exclusion).

3. Draw up cells into a 1-mL syringe and, using a 30-gauge needle, inject 20 µL ($1.25 \times 10^5 - 5 \times 10^6$ cells) into the base of either dorsal prostatic lobe near the junction with the seminal vesicle. Close the abdominal incision using several wound clips.

For limitations and adaptations to this technique, *see* **Notes 7** and **8.** Several cell lines have been passaged through mice using this technique and now exhibit marked propensities to metastasize to specific organs (*see* **Note 9**) ***(35–38)***.

### *3.3. Engrafted Mouse Models of Metastasizing Human Prostate Cancer*

In the last 10 yr, some exciting work has been conducted using immunocompromised mice that have been engrafted with normal human tissues as target sites for cancer metastasis. These studies began with the examination of metastasis of non-Hodgkin's lymphoma in SCID mice that had been engrafted with fetal human thymus, spleen, and liver ***(39)***. In another study, it was shown that human melanomas will invade engrafted human skin, stimulate angiogenesis, and metastasize to the lungs, whereas those tumor cells introduced into mouse skin grew diffusely ***(40)***. Implantation of fetal human bone marrow into SCID mice (the SCID-hu model) was initiated by Namikawa and coworkers ***(41),*** who found that human myeloid leukemias preferentially grew in engrafted human bone, maintaining their phenotype and ability to propagate in successive passages through the mice. This group also demonstrated that human small-cell lung carcinoma cells metastasize preferentially to human lung and bone marrow grafts without compromising the homologous mouse organs ***(42)***. Another study examined the homing to engrafted bone of prostate cancer using fetal tissues for implantation using a method similar to that described below ***(25)***.

1. Anesthetize and shave the flanks of 6-wk-old male SCID mice; swab with alcohol. Make an incision through the skin to expose the underlying muscle.
2. Fragments (8 $mm^3$) of lung and intestine tissues from 16–22-wk-old fetuses are implanted through the incisions. Fetal femurs and humeri of the same gestation period are split longitudinally and again transversely to produce four half-cylinders of bone. These are implanted subcutaneously into another incision in the mouse flank and positioned such that the exposed marrow surface of the bone is against underlying muscle.
3. Introduce LNCaP, PC-3, and DU-145 prostate cancer cells by tail vein injection ($1 \times 10^6$ cells in 200 µL of HBSS) or by direct injection onto the exposed marrow surface of the engrafted bone ($1 \times 10^4$ PC-3 or DU-145 cells, and $5 \times 10^4$ LNCaP cells in 20 µL of HBSS) using a 27-gauge needle.

Using this procedure, 26% of mice injected with PC-3 cells developed tumors in the human bone after injection into the circulation via the lateral tail vein, whereas injection with LNCaP and DU-145 cells produced no evidence of metastasis in the engrafted tissues. All three cell lines produced metastases in the mouse lung to varying extents. Six weeks after direct injection into the human bone, 75–100% of the injection sites produced tumors (osteoblastic/mixed, LNCaP; osteolytic, DU-145 and PC-3).

A previous study showed that adult human bone fragments did not engender a blood supply and required exogenous cytokines to prevent deterioration ***(43)***. However, two groups ***(27,44)*** have successfully engrafted adult human bone in mice to study the trafficking to bone of prostate cancer using methods similar to that described below.

1. Mince trabecular bone obtained from the rib of consented patients undergoing surgery for lung cancer into pieces approx 125 mm3 in size and keep in RPMI medium for less than 1 h.
2. Implant through a small skin incision into the left flank of anesthetized 3- to 4-wk-old male NOD-SCID mice. These animals have reduced natural killer cell activity, absence of complement activity, and defects in macrophage function in addition to the impairment of B- and T-cell development found in SCID mice.
3. After 3–4 wk, anesthetize the mice and carefully inject with $1 \times 10^7$ LNCaP or $5 \times 10^6$ PC-3 cells in 200 µL of sterile PBS supplemented with 0.1% bovine serum albumin via the lateral tail vein. Administer the injectate over 15 s, as higher numbers of injected cells or rapid injection results in 75% mouse mortality within 10 min of injection as the result of pulmonary embolism.
4. As controls for homing to a cut site, inject mice with cells via the lateral vein after a skin incision without bone implantation. To control for species specificity, mouse bone is implanted into the right lower flank of some of the mice. To control for tissue specificity, implant human adult lung fragments of 8 $mm^3$. Implant all mice in the test groups with human adult bone and in addition, either human adult lung fragments, or mouse bone implants.
5. Measure bone tumor size using calipers and extract tumors after sacrifice for analysis by histology, histochemistry, and immunohistochemistry to prove that they are derived from human prostate cancer and to characterize the osteogenic response. Because NOD-SCID mice have little or no serum immunoglobulin levels, mouse monoclonal antibodies can be used in immunohistochemical analyses ***(27)***.

In reported procedures, implanted tissues were shown to be adequately vascularized with human endothelial cells, and they were differentiated and of normal architectural appearance 16 wk after implantation. Prostate cancer cells did not colonize the control incisions. Some metastasis to implanted mouse bone

and native mouse bone was observed for the PC-3 line (5% and 15%, respectively) but none was seen with LNCaP injection. No metastasis to human lung was observed but low incidence of metastasis to mouse lung was seen (10%, LNCaP; 25%, PC-3). Additional metastases to lymph nodes (LNCaP and PC-3) and adrenal glands and liver (PC-3 only) were also shown. However, all metastases to mouse tissues were small (lung colonies were 1 $mm^3$), whereas after 8 wk, those in the bone were 228.45 ± 50.2 $mm^3$ (PC-3 cells) and 116.72 ± 35.4 $mm^3$ (LNCaP cells). The tumors in bone displayed expected morphologies: they were poorly differentiated and were osteoblastic and PSA-positive (LNCaP) or osteolytic and PSA-negative (PC-3) ***(27)***. Refinements to this method have been used by others (*see* **Note 10**).

## 4. Notes

1. Using this method, LNCaP cells produce mixed/ osteoblastic lesions within 4 mo, whereas PC-3 cells produce osteolytic lesions that result in total bone destruction at the injection site within 4 wk. A set of xenograft lines, the LuCaP series, derived from samples from radical prostatectomies, resections, and tissue acquisition necropsies (where tissue samples were obtained shortly after patient death) produce a robust osteoblastic response in the tibia. All of these lines with the exception of PC-3 produce serum PSA within 4–12 wk. A limitation to the use of the LuCaP series is that thus far, none can grow in vitro and therefore they cannot be fully characterized ***(12*** and personal communication). There is no evidence to suggest that spontaneous metastasis to other bones or nonosseous tissues occurs with this method or that there is extrusion of the cells upon withdrawal of the needle ***(10)***. This injection model has been used successfully to study the effects of prostate cancer treatment modalities, including bisphosphonates ***(13–15)*** and osteoprotegerin ***(16),*** on the establishment and development of bone metastases of prostate cancer.
2. Alternative bones may be used for injection. When the aforementioned cell lines and xenografts were injected into the lumbar vertebrae of SCID and athymic mice by a similar procedure using a 30-gauge needle, the resulting lesions were visible by radiography, but were small and studies were not continued ***(11)***. Intrafemoral injection is performed ***(17)*** by exposing the distal femur after anesthesia of athymic and SCID mice by making an incision in the right knee, followed by splitting the patellar tendon and muscle longitudinally. A scalpel blade is used to drill a hole in the cortex, through which 50 µL of cells ($5 \times 10^5$–$1 \times 10^6$ cells suspended in PBS or culture medium) are injected. The hole is sealed with bone wax after removing the needle, the patellar tendon is repositioned, and the incision sutured. Alternatively, 1 to $5 \times 10^5$ LNCaP or PC-3 cells suspended in PBS can be injected directly through the patella and into the intrafemoral marrow cavity using a 27-gauge needle ***(18)***. This is a more complex procedure than intratibial injection and requires meticulous surgical techniques. However, the tumors produced in this comparatively large marrow space

may allow for a more protracted examination of the effects of bone metastasis-directed therapies.

For other bones the following procedures may be used. For intra-iliac injection ***(17)***, a 27-gauge needle attached to a tuberculosis syringe is inserted dorsally through the skin, 5 mm lateral to the spine and 5 mm below the iliac crest. The needle is gently rotated and guided into the bone until the cortex is penetrated, then $1 \times 10^6$ cells are injected in 50 µL of T-medium plus 10% fetal bovine serum. A higher take rate is seen in SCID/bg mice than in athymic mice, with a shorter latency period to tumor development. Site-specific effects are observed, with no tumors produced using the pericranial administration route ***(17)***. The differences seen between the trabecular bones (iliac crest and distal femur) and the intramembranous bones (pericranium) may reflect the structure of the bone at these sites: trabecular bones have a high component of bone marrow, exhibit endochondral bone formation, and have a high rate of bone remodeling, whereas the intramembranous bones of the cranium do not.

3. This technique failed to produce bone metastases in some studies after the injection of LNCaP, C4-2, or PC-3 cells ***(17,26)***. However, in studies in which human bone was engrafted, successful colonization of the human ***(25,27)*** and mouse ***(27)*** bone was shown following tail vein injection (*see* **Subheading 3.3.** above).
4. The lumbar vertebrae are the most common sites of prostate cancer bone metastasis ***(28)***. It is thought that prostate cancer cells might traffic to these sites under increased abdominal pressure via the periprostatic venous vessels to Batson's plexus, the vertebral venous plexus ***(29–31)***. In one method, the inferior vena cava was occluded to promote lumbar vertebral metastasis after intravenous injection of prostate cancer cells. Bone metastasis was detected in 19% of occluded mice and not at all in control injected mice, whereas pulmonary metastases decreased from 88% in control mice to 32% in occluded mice ***(32)***.
5. Where intravenous and intracardiac injection methods have been compared side by side, the intracardiac method produced more metastases overall and to bone in particular ***(17,26)***. One study also showed that SCID/bg mice provided a more favorable environment for the establishment of spontaneous metastases to the bone than did athymic mice, with metastases arising in the paraspinal soft tissue and spine, limbs and mandible after intracardiac injection of C4-2 and PC-3 cells, respectively.
6. The intracardiac injection technique, although producing moderate levels of bone metastases, has several drawbacks; it is labor intensive, it requires a high level of skill, and can lead to the compromise, by disseminating prostate cancer cells, of other nonosseous organs, including lungs, kidneys, and spleen ***(33)***.
7. In the original study ***(34)***, LNCaP and PC-3M cells were injected and were shown to form tumors in the orthotopic site, but metastases to nonosseous sites were rare, and not detected at all in bones.
8. An adaptation of the SOI technique was used in more recent studies: PC-3 cells that had been transfected with green fluorescent protein were passaged in vivo through continual transplant in subcutaneous sites, then the tumors were

extracted and minced into fragments of approx 1 $mm^3$. After exposure of the prostate using the method described above, the prostatic capsule was opened, and two tumor fragments were inserted. This was closed with 8-0 surgical suture and the abdominal incision closed using 6-0 surgical suture. This approach produced spontaneous and extensive bone metastases in 60% of the animals examined, as well as metastases to a range of nonosseous organs, including the lung, liver, and brain ***(45)***.

9. Another study ***(26)*** demonstrated metastasis to lymph nodes after injection with PC-3M cells. These were serially passaged in vivo, with metastatic tissue being implanted again into the orthotopic site after expansion in culture. After several passages, the subline PC-3M-LN4 was developed, which produces distal bone metastases (60% in the mandible, 20% in the femur) after intracardiac injection. A range of LNCaP sublines was similarly derived where LNCaP cells were co-injected subcutaneously with bone fibroblasts and resulting tumors were serially passaged in vivo by several rounds of SOI or subcutaneous injection and in vitro expansion. The LNCaP subline C4-2 produces tumors at the orthotopic site in 100% of injected mice and metastasizes to bone, resulting in paraplegia in 10–50% of injected mice ***(35)***. Another cell line from the same laboratory, ARCaP (androgen-repressed prostate cancer), metastasized to bone from the orthotopic site (16% of injected animals) but not from the subcutis ***(36)***. Two other lines, MDA PCa 2a and 2b, were derived from a single bone metastasis ***(37)***. Although an osteoblastic reaction was found after direct injection of MDA PCa 2b into the intrafemoral marrow cavity ***(38),*** these cell lines have not thus far been shown to metastasize spontaneously back to bone after orthotopic or subcutaneous (with Matrigel) injection of 2 to $5 \times 10^6$ cells.
10. An alternative study used fragments of adult human bone derived from patients undergoing total arthroplasty ***(44)*** and implanted these into the thigh muscle of irradiated SCID mice that were injected 2 mo later near the implantation site with PC-3 or LAPC-4 prostate cancer cells. Osteolytic reactions were observed at the engrafted bone sites. However, because the cells were injected close to the implantation site, no process of distant metastasis was studied.

## 5. Summary

### *5.1. Intraosseous Injection*

Intrabone injection models, although valuable in the examination of bone metastases in vivo, do not provide a method for the study of the process of metastasis. By the direct introduction of prostate cancer cells to the metastatic site, the progression of prostate cancer from organ-confined disease to bone metastases via extravasation, migration, trafficking, and intravasation of the cells cannot be studied. However, such models provide elegant, clinically relevant models of prostate cancer disease in bone that can be used in the study of the interactions between prostate cancer and the bone micro-

environment and in the evaluation of therapies directed against the development of bone metastases.

### 5.2. Spontaneous Metastasis of Human Xenografted Prostate Cancer to Bone

The use of spontaneously metastasizing human prostate cancer models has many advantages. In addition to the study of the interactions with bone, as with the models described in the previous section, the process of metastasis to distant sites can be examined, clinical situations can be duplicated because primary tumors can be removed and occult metastases treated, and organ-specific gene/protein expression can be determined. A drawback is that the intravenous, intracardiac, or intraprostatic injection of cells can be labor intensive and can produce metastases in nonosseous sites that can overtake the animal before bony metastases are apparent. However, these models provide clinically relevant tools for the study of the mechanisms of metastasis and for the study of therapies that are directed toward metastatic cells trafficking to the bone or situated and established in the secondary site.

### 5.3. Engrafted Mouse Models of Metastasizing Human Prostate Cancer

The use of human bone xenografts as targets for prostate cancer metastasis is a further step towards understanding the complexity of the disease processes that occur during the interactions of human prostate cancer cells with human bone. However, there are questions regarding the suitability of engrafting bone from patients with lung cancer or arthritis that may already be undergoing pathologic processes, which could confound interpretation of the data. The use of adult long bone fragments that are not diseased, such as from nonunion fractures after accidental damage or orthopedic procedures, may be more suitable. As reported, the procedure also requires the injection of large numbers of cells to produce metastases *(27)*.

Implantation of fetal bone also demonstrated tissue- and species-specific homing of human prostate cancer cells to human bone and required the injection of only 1 to $5 \times 10^4$ cells. However, there are disadvantages to its use. Fetal bone differs from adult bone in several respects: The cycling rates of hematopoietic precursors and osteoprogenitors differ *(46)*, as do their responses to hematopoietic factors *(47)* and ability to differentiate *(48)*. Fetal bone at the gestational stage of 16–22 wk has been largely formed by intramembranous ossification. Some endochondral ossification occurs, resulting in the replacement of the cartilage template by woven bone. However, in adults, woven bone has been replaced with mature lamellar bone. Taking all of

these factors into consideration, the use of fetal bone from stage 16–22 wk for these metastasis studies may not model accurately the processes involved in adult bone colonized by prostate cancer.

## References


1. Greenlee, R. T., Murray, T., Bolden, S., and Wingo, P. A. (2000) Cancer statistics, 2000. CA Cancer J. Clin. **50,** 7–33.
2. Franks, L. M. (1956) The spread of prostate cancer. *J. Pathol. Bacteriol.* **72,** 603–611.
3. Zetter, B. R. (1990) The cellular basis of site-specific tumor metastasis. *N. Eng. J. Med.* **332,** 605–612.
4. Goltzman, D. (2001) Mechanisms of the development of osteoblastic metastases. *Cancer* **80,** 1581–1587.
5. Baron, R. (1999) Anatomy and ultrastructure of bone, in *Primer on the Metabolic Bone Diseases and Disorders of Mineral Metabolism,* 4th ed. (Favus, M. J., ed.), Lippincott, Williams and Wilkins, Philadelphia, pp. 3–10.
6. Coleman, R. E. (1998) Monitoring of bone metastases. *Eur. J. Cancer* **34,** 252–259.
7. Hamdy, N. A. and Papapoulos, S. E. (2001) The palliative management of skeletal metastases in prostate cancer: Use of bone-seeking radionuclides and bisphosphonates. *Semin. Nucl. Med.* **31,** 62–68.
8. Carlin, B. I. and Andriole, G. L. (2000) The natural history, skeletal complications, and management of bone metastases in patients with prostate carcinoma. *Cancer* **88,** 2989–2994.
9. Kobayashi, T., Koshida, K., Endo, Y., Imao, T., Ichibayashi, T., Sasaki, T., and Namiki, M. A chick embryo model for metastatic human prostate cancer. *Eur. Urol.* **34,** 154–160.
10. Berlin, O., Samid, D., Donthineni-Rao, R., Akeson, W., Amiel, D., and Woods, V. L. Jr. (1993) Development of a novel spontaneous metastasis model of human osteosarcoma transplanted orthotopically into bone of athymic mice. *Cancer Res.* **53,** 4890–4895.
11. Corey, E., Quinn, J. E., Bladou, F., Brown, L. G., Roudier, M., Brown, J. M., et al. (2002) Establishment and characterization of an osseous prostate cancer model: Direct intratibial injection of human prostate cancer cells. *Prostate* **52,** 20–33.
12. Ellis, W. J., Vessella, R. L., Buhler, K. R., Bladou, F., True, L. D., Bigler, S., et al. (1996) Characterisation of a novel androgen-sensitive, prostate-specific antigen-producing prostatic carcinoma xenograft: LuCaP 23. *Clin. Cancer Res.* **2,** 1039–1048.
13. Clarke, N. W., McClure, J., and George, N. J. (1992) Disodium pamidronate identifies differential osteoclastic bone resorption in metastatic prostate cancer. *Br. J. Urol.* **69,** 64–70.
14. Stearns, M. E. and Wang, M. (2001) Alendronate blocks metalloproteinase secretion and bone collagen I release by PC-3 ML cells in SCID mice. *Clin. Exp. Metastasis* **16,** 693–702.

15. Stearns, M. and Wang, M. (1996) Effects of alendronate and taxol on PC-3 ML cell bone metastases in SCID mice. *Invasion Metastasis* **16,** 116–131.
16. Zhang, J., Dai, J., Qi, Y., Lin, D. L., Smith, P., Strayhorn, C., et al. (2001) Osteoprotegerin inhibits prostate cancer-induced osteoclastogenesis and prevents prostate tumor growth in the bone. *J. Clin. Invest.* **107,** 1235–1244.
17. Wu, T. T., Sikes, R. A., Cui, Q., Thalmann, G. N., Kao, C., Murphy, C. F., et al. (1998) Establishing human prostate cancer cell xenografts in bone: Induction of osteoblastic reaction by prostate-specific antigen-producing tumors in athymic and SCID/bg mice using LNCaP and lineage-derived metastatic sublines. *Int. J. Cancer* **77,** 887–894.
18. Soos, G., Jones, R. F., Haas, G. P., and Wang, C. Y. (1997) Comparative intraosseal growth of human prostate cancer cell lines LNCaP and PC-3 in the nude mouse. *Anticancer Res.* **17,** 4253–4258.
19. Klein, K. A., Reiter, R. E., Redula, J., Moradi, H., Zhu, X. L., Brothman, A. R., et al. (1997) Progression of metastatic human prostate cancer to androgen independence in immunodeficient SCID mice. *Nat. Med.* **3,** 402–408.
20. Corey, E., Arfman, E. W., Liu, A. Y., and Vessella, R. L. (1997) Improved reverse transcriptase-polymerase chain reaction protocol with exogenous internal competitive control for prostate-specific antigen mRNA in blood and bone marrow. *Clin. Chem.* **43,** 443–452.
21. Melchior, S. W., Corey, E., Ellis, W. J., Ross, A. A., Layton, T. J., Oswin, M. M., et al. (1997) Early tumor cell dissemination in patients with clinically localized carcinoma of the prostate. *Clin. Cancer Res.* **3,** 249–256.
22. Ellis, W. J., Vessella, R. L., Corey, E., Arfman, E. W., Oswin, M. M., Melchior, S. W.. et al. (1998) The value of a reverse transcriptase polymerase chain reaction assay in preoperative staging and follow-up of patients with prostate cancer. *J. Urol.* **159,** 1134–1138.
23. Corey, E., Arfman, E. W., Oswin, M. M., Melchior, S. W., Tindall, D. J., Young, C. Y., et al. (1997) Detection of circulating prostate cells by reverse transcriptase-polymerase chain reaction of human glandular kallikrein (hK2) and prostate-specific antigen (PSA) messages. *Urology* **50,** 184–188.
24. Gelmini, S., Tricarico, C., Vona, G., Livi, L., Melina, A. D., Serni, S., et al. (2001) Real-time quantitative reverse transcriptase-polymerase chain reaction (RT-PCR) for the measurement of prostate-specific antigen mRNA in the peripheral blood of patients with prostate carcinoma using the taqman detection system. *Clin. Chem. Lab. Med.* **39,** 385–391.
25. Nemeth, J. A., Harb, J. F., Barroso, U. Jr, He, Z., Grignon, D. J., and Cher, M. L. (1999) Severe combined immunodeficient-hu model of human prostate cancer metastasis to human bone. *Cancer Res.* **59,** 1987–1993.
26. Pettaway, C. A., Pathak, S., Greene, G., Ramirez, E., Wilson, M. R., Killion, J. J., et al. (1996) Selection of highly metastatic variants of different human prostatic carcinomas using orthotopic implantation in nude mice. *Clin. Cancer Res.* **2,** 1627–1636.

27. Yonou, H., Yokose, T., Kamijo, T., Kanomata, N., Hasebe, T., Nagai, K., et al. (2001) Establishment of a novel species- and tissue-specific metastasis model of human prostate cancer in humanized non-obese diabetic/severe combined immunodeficient mice engrafted with human adult lung and bone. *Cancer Res.* **61,** 2177–2182.
28. Galasko, C. (1981) The anatomy and pathways of skeletal metastases, in *Bone Metastasis* (Weiss, L. and Gilbert, H. A., eds.), G.K. Hall Medical Publishers, Boston, pp. 49–63.
29. Batson, O. V. (1940) Function of vertebral veins and their role in the spread of metastases. *Ann. Surg.* **112,** 138–149.
30. Batson, O. V. (1942) The role of the vertebral veins in metastatic processes. *Ann. Intern. Med.* **16,** 38–45.
31. Nishijima, Y., Uchida, K., Koiso, K., and Nemoto, R. (1992) Clinical significance of the vertebral vein in prostate cancer metastasis, in *Prostate Cancer and Bone Metastasis* (Karr, J. P. and Yamanaka, H., eds.), Plenum Press, New York, pp. 93–100.
32. Shevrin, D. H., Kukreja, S. C., Ghosh, L., and Lad, T. E. (1988) Development of skeletal metastasis by human prostate cancer in athymic nude mice. *Clin. Exp. Metastasis* **6,** 401–409.
33. Rabbani, S. A., Harakidas, P., Bowlin, T., and Attardo, G. (1998) Effect of nucleoside analogue BCH-4556 on prostate cancer growth and metastases in vitro and in vivo. *Cancer Res.* **58,** 3461–3465.
34. Stephenson, R. A., Dinney, C., Gohji, K., Ordonez, N. G., Killion, J., and Fidler, I. J. (1992) Metastatic model for human prostate cancer using orthotopic implantation in nude mice. *J. Natl. Cancer Inst.* **84,** 951–957.
35. Thalmann, G. N., Anezinis, P. E., Chang, S. M., Zhau, H. E., Kim, E. E., Hopwood, V. L., et al. (1994) Androgen-independent cancer progression and bone metastasis in the LNCaP model of human prostate cancer. *Cancer Res.* **54,** 2577–2581.
36. Zhau, H., Chang, S. M., Chen, B. Q., Wang, Y., Zhang, H., Kao, C., et al. (1996) Androgen-repressed phenotype in human prostate cancer. *Proc. Natl. Acad. Sci. USA.* **93,** 15152–15157.
37. Navone, N. M., Olive, M., Ozen, M., Davis, R., Troncoso, P., Tu, S. M., et al. (1997) Establishment of two human prostate cancer cell lines derived from a single bone metastasis. *Clin. Cancer Res.* **3,** 2493–2500.
38. Yang, J., Logothetis, CJ., Peleg, S., Sikes, C. R., Raymond, A. K., Jamal, N., et al. (2001) Prostate cancer cells induce osteoblast differentiation through a Cbfa1-dependent pathway. *Cancer Res.* **61,** 5652–5659.
39. Waller, E. K., Kamel, O. W., Cleary, M. L., Majumdar, A. S., Schick, M. R., Lieberman, M., and Weissman, I. L. (1991) Growth of primary T-cell non-Hodgkin's lymphomata in SCID-hu mice: Requirement for a human lymphoid microenvironment. *Blood* **78,** 2650–2665.
40. Juhasz, I., Albelda, S. M., Elder, D. E., Murphy, G. F., Adachi, K., Herlyn, D., et al. (1993) Growth and invasion of human melanomas in human skin grafted to immunodeficient mice. *Am. J. Pathol.* **143,** 528–537.

41. Namikawa, R., Ueda, R., and Kyoizumi, S. (1993) Growth of human myeloid leukemias in the human marrow environment of SCID-hu mice. *Blood* **82,** 2526-2536.
42. Shtivelman, E. and Namikawa, R. (1995) Species-specific metastasis of human tumor cells in the severe combined immunodeficiency mouse engrafted with human tissue. *Proc. Natl. Acad. Sci. USA*. **92,** 4661–4665.
43. Heike, Y., Ohira, T., Takahashi, M., and Nagahiro, S. (1995) Long-term human hematopoiesis in SCID-hu mice bearing transplanted fragments of adult bone and bone marrow cells. *Blood* **86,** 524–530.
44. Tsingotjidou, A. S., Zotalis, G., Jackson, K. R., Sawyers, C., Puzas, J. E., Hicks, D. G., et al. (2001) Development of an animal model for prostate cancer cell metastasis to adult human bone. *Anticancer Res.* **21,** 971–978.
45. Yang, M., Jiang, P., Sun, F. X., Hasegawa, S., Baranov, E., Chishima, T., et al. (1999) A fluorescent orthotopic bone metastasis model of human prostate cancer. *Cancer Res.* **59,** 781–786.
46. Christensen, R. D. (1987) Circulating pluripotent hematopoietic progenitor cells in neonates. *J. Pediatr.* **110,** 623–625.
47. Emerson, S. G., Thomas, S., Ferrara, J. L., and Greenstein, J. L. (1989) Developmental regulation of erythropoiesis by hematopoietic growth factors: analysis on populations of BFU-E from bone marrow, peripheral blood, and fetal liver. *Blood* **74,** 49–55.
48. Ikuta, K., Kina, T., MacNeil, I., Uchida, N., Peault, B., Chien, Y. H., et al. (1990) A developmental switch in thymic lymphocyte maturation potential occurs at the level of hematopoietic stem cells. *Cell* **62,** 863–874.

# 10

# Effects of Fixation on Tissues

**Elin Mortensen and Julie M. Brown**

## 1. Introduction

### *1.1. Background*

The primary aim of tissue fixation is to preserve tissue in the long term, ideally without causing alterations in morphology or biochemical integrity. Optimal fixation should therefore inhibit autolysis while preserving enzyme activity and antigen reactivity. However, some of these requirements are mutually exclusive. For example, to stop autolysis, proteolytic enzymes must be inhibited ***(1)***. At present, it is not possible to find a fixation technique that fulfils all of these criteria.

The two most common fixation methodologies are alcohol- and aldehyde-based fixation. Alcohol-based fixatives, used in various concentrations and with different additives, have been shown to give good morphological detail, and tissues fixed in alcohol can be used for immunohistochemistry and molecular biology studies. However, they fix slowly and therefore are not feasible for larger specimens. They also are relatively expensive. Formaldehyde is the most commonly used fixative for routine histopathology and will be the focus of this chapter; whereas for electron microscopy, glutaraldehyde is usually preferred. Formaldehyde is the preferred fixative for a range of applications because it is inexpensive, easily accessible, stable, and can be used with almost any tissue (reviewed in **ref.** ***2)***. Furthermore, formaldehyde does not overfix, where tissues could harden unpredictably and variably within a specimen, nor does it cause distortions of cellular detail caused by shrinkage. Formaldehyde is also sometimes used in a modified form, such as Bouin's fixative, or with zinc or mercury added. However, there are limitations to the use of formaldehyde-fixed tissues, which will be discussed in **Subheadings 1.4.** and **1.6.3.**

From: *Methods in Molecular Medicine, Vol. 81: Prostate Cancer Methods and Protocols*
Edited by: P. J. Russell, P. Jackson, and E. A. Kingsley © Humana Press Inc., Totowa, NJ

### 1.1.1. History

Formaldehyde, discovered by Burtlow in 1859, is a simple molecule with a molecular weight of 30 and is a gas that readily dissolves in water, with a saturation point at about 40%. Formaldehyde solution had an initial application as an antiseptic agent to treat or prevent wound infections (reviewed in **ref. *2)***. Its use as a fixative developed from a fortuitous observation made during this study by the investigator Ferdinand Blum when he noted that the skin of his fingers had hardened after coming into contact with the solution ***(2)***. Testing a mouse preserved in formaldehyde showed that the tissues were as hardened as with alcohol fixation and, when tested for histopathological fixation using various staining techniques of that time, the fixed tissues were found to stain well and to be superior to tissues fixed in alcohol in that comparatively marginal shrinkage and distortion of the tissue was observed.

### 1.1.2. Nomenclature

The nomenclature associated with formaldehyde can be inconsistent. It is variously known as formic aldehyde, formol, formaldehyde, and formalin, the latter being the commercially available solution that contains 37 to 38% formaldehyde by gas weight ***(3)***. For practical purposes, formaldehyde is commonly used as a 4% solution, or as a 10-fold dilution producing 10% formalin (1.3 *M*) for tissue fixation in histopathology laboratories.

### 1.1.4. Contamination

Commercially, formaldehyde is easily synthesized from methanol, but even if stored in a concentrated solution, several reactions can occur that will contaminate the stock. Formaldehyde can undergo spontaneous condensation reactions with itself that can be inhibited by the addition of alcohols, such as 10% methanol. This is not known to have deleterious effects on the fixation process. Another reaction that can occur is the oxidization of formaldehyde to formic acid: Formaldehyde may contain small quantities of formic acid produced as a result of the manufacturing process or as the result of storage because formaldehyde readily oxidizes to formic acid in the presence of atmospheric oxygen ***(4)***. No changes in nuclear size were observed when specimens of rat liver were fixed in formaldehyde to which formic acid had been added, which suggests that formic acid does not cause large-scale cytomorphometric changes (reviewed in **ref. *2)***. However, formic acid can cause difficulties with the fixation of blood-rich tissue specimens because acid formaldehyde hematin, also called formalin pigment, can precipitate in the tissue when the pH is below 6.0 (reviewed in **ref. *2)***. This is also a problem with acetic alcoholic formalin fixatives (*see* Telleysniczky's solution,

**Subheading 1.5.**). To avoid this, most laboratories use phosphate-buffered formalin to maintain the desired pH.

## *1.2. Properties*

### *1.2.1. Mechanism of Fixation*

Formaldehyde has a low molecular weight and will therefore easily diffuse into the tissue. Early studies (reviewed in **ref. *2)*** showed that it has a relatively constant rate of penetration into tissue over a fivefold concentration range (8–40%), but it is a very slow fixative.

When formaldehyde is dissolved in water, it hydrates rapidly to form methylene glycol (reviewed in **ref. *2)***, which constitutes most of the solution, leaving a small fraction of carbonyl formaldehyde. The immersion of tissues in this solution results in the rapid penetration of the tissues by an excess of methylene glycol and a relatively small quantity of carbonyl formaldehyde. The equilibrium of the aqueous reaction favors hydration to methylene glycol; more carbonyl formaldehyde is only produced by dissociation of methylene glycol when the small fraction of carbonyl formaldehyde in solution is removed by forming covalent bonds with the immersed tissues (reviewed in **ref. *2)***. This latter reaction is slow, which gives some indication why formaldehyde can penetrate tissues rapidly (as methylene glycol) but fixes them slowly (as carbonyl formaldehyde).

However, there are still many unanswered questions about the molecular mechanism of tissue fixation. Chemical studies indicate that formaldehyde is electrophilic and reacts easily with biological macromolecules ***(5)***, including proteins and nucleic acids, by forming crosslinks with the most reactive functional groups, such as primary amines and thiols, followed by their linking to less reactive sites such as primary amides. Clearly, intra- and intermolecular associations such as these could potentially alter the tissue and cellular phenotype and histological appearance. Furthermore, because formaldehyde mainly crosslinks with proteins, glycoproteins, polysaccharides, and nucleic acids, many of the other molecules present in the cells and tissues could be lost unless they are mechanically enclosed in the fixed tissue. This may occur with some high molecular polysaccharides and mucosubstances, such as glycogen. Most lipids are lost because they are dissolved during alcohol and xylene dehydration. Low-molecular weight substances and electrolytes disappear almost totally under fixation and dehydration and are flushed out with the water ***(1)***.

### *1.2.2. Length and Temperature of Fixation*

Other important considerations in the fixation process are the length of time to which the tissue must be exposed to formaldehyde and at which temperature.

Some investigators advocate increased temperatures whereas others recommend chilling to slow down autolysis during fixation. The kinetics of formaldehyde fixation were examined by fixing sections of rat kidney in radiolabeled formaldehyde at 25 or 37°C for up to 48 h ***(2)***. The sections were 16 µm thick so that penetration of the fixative would not influence the kinetics of the reaction. After a thorough washing, the radioactivity of the sections was measured by liquid scintillation counting. Fixation with formaldehyde reached equilibrium after exposure for 24 h at 25°C or 18 h at 37°C, suggesting that fixation of tissues with formaldehyde occurs faster at 37°C than at room temperature.

Tissue penetration is a function of the square root of exposure time; therefore, solid specimens that are considerably thicker than those tested in the study above may take longer to become completely fixed. Formaldehyde in a 4% solution is known to require 24 h to achieve a 20-mm penetration into tissues (reviewed in **ref. *2***). This is a problem because the prolonged fixation of large tissues may delay diagnosis and may result in autolysis of the unfixed part of tissues while in the process of fixation at ambient temperatures. Fixation, then, is a compromise between time-progressive formaldehyde damage of protein antigens and autolytic degradation. Therefore, any method that accelerates fixation would limit autolysis and time spent immersed in formaldehyde and thereby better preserve antigen and DNA.

### *1.3. Methods for Accelerating Fixation*

#### *1.3.1. Microwave Fixation*

Fixation of large specimens, such as the prostate, can cause incomplete fixation in the center with good fixation at the periphery or manifest as a mixture of incompletely and completely fixed tissue. Cutting the surgical specimen accelerates fixation, but the anatomical orientation is easily lost.

An alternative method for accelerated fixation is to use microwave treatment. The increase in temperature during microwave treatment will increase the speed of the dehydration process from methylene glycol to formaldehyde ***(6)***. Investigators should be cautious, however, because formaldehyde vapors present a working hazard because of their carcinogenic properties. A study has shown that by injecting formaldehyde into the surgically removed prostate at multiple sites (≥50) and thereafter performing microwave treatment not only gives a better morphology but also better antigen preservation compared with microwave treatment alone or conventional fixation.

#### *1.3.2. Agitation During Fixation*

The specimen can be agitated during the fixation process using a rotating plate or shaker. This movement of the tissue in the formaldehyde has been

shown significantly to accelerate fixation (personal communication, Professor Christer Busch, University Hospital of Northern Norway).

### *1.3.3. Effect of Atmospheric Pressures During Fixation*

Another approach has been to fix tissues in formaldehyde solutions at altered atmospheric pressure. The rate of chemical reactions varies directly with atmospheric pressure; therefore, a decrease in pressure will be expected to slow down the process, whereas an increase in pressure would be anticipated to accelerate fixation ***(2)***.

## *1.4. Analysis of Formaldehyde-Fixed Tissues*

### *1.4.1. Effects on Cells and Tissues*

A major concern in the use of formaldehyde or, indeed, any fixative, is the amount of distortion produced in the tissues. The distortion could be caused by either the shrinkage or swelling of cells or extracellular tissue. Physiological saline solution has an osmolarity around 250 to 300 mOsm, whereas an unbuffered solution of formalin without methanol exerts an osmotic pressure of 1300 mOsm. (reviewed in **ref. *2)***. Therefore, cells that are exposed to formaldehyde will initially swell, but the fixation properties of formaldehyde will soon inhibit this process and the more concentrated the solution, the faster the swelling will cease ***(1)***. In general, however, tissues shrink slightly but not significantly when fixed in formaldehyde (reviewed in **ref. *2)***. Fixation may not be the main cause of any observed distortions of tissue structure: Subsequent processing procedures, including dehydration and paraffin embedding, could potentially distort cells and tissues more than the original fixative.

The usefulness of tissues for measurement of nuclear morphometry, DNA flow cytometry, or investigation of mitotic activity may be compromised by the choice of fixative. To confirm this, cytomorphology in histological sections after fixation in various fixatives was examined ***(7)***. Five-millimeter slices of guinea pig liver were fixed in a range of fixatives, including acetone, 4% formaldehyde, Bouin's solution, and ethanol. Of the parameters tested, which included fixative acidity, under- and overstretching of the paraffin sections, and air-drying, the acidity of the different solutions was most likely to be the cause of differences in nuclear area. The nuclear area was found to be approx 25% lower when the tissue was fixed in 4% formaldehyde, pH < 3, when compared with pH 5 to 9.

### *1.4.2. Immunohistochemistry*

The use of immunohistochemistry to determine antigen expression in a neoplasm is steadily increasing. However, alteration of tissues after fixation, such

as crosslinking of proteins, can cause antigen masking *(8),* and paraffin processing can alter protein conformation. This masking can be reversed to some degree by exposing tissues to high temperatures *(2,8,9)*. The controlled proteolysis of tissue sections can also be beneficial for demasking, and a wide range of proteolytic enzymes are commercially available, such as trypsin and proteinase K. The development of demasking techniques has extended the applicability of immunohistochemistry *(10–12)*. However, antigen retrieval techniques must be used with care to avoid digestion of tissue or overstaining (background staining). Most laboratories have their own modified method of antigen retrieval adapted to suit their fixation technique and antigen of interest. Although antigen retrieval techniques can be used to improve immunohistochemical detection of antigens, the initial fixation scheme used on the tissues still remains central to optimize immunohistochemistry as a diagnostic tool.

As addressed in **Subheading 1.2.2.**, the length of exposure time of tissues to formaldehyde is important in fixation. To mimic the clinical setting, Leong and Gilham *(13)* used sections of prostate and other tissues and fixed their sections in 4% formaldehyde for 6 h up to 30 d. In histopathology laboratories, tissue specimens are usually fixed for 1 d but sometimes over a weekend period. After 3 d, some of the antigen staining was reduced, and after 7 d, further reduction, or even loss, of staining was noted. Vimentin, desmin, and neurofilaments were most sensitive to formalin exposure, and after 1 d of exposure to formalin, no staining was achieved without any antigen retrieval technique. Cytokeratins also needed antigen retrieval and still only stained weakly. Lymphocyte antigens (except lymphocyte common antigen LCA) were lost after a 3-d exposure to formaldehyde. Only a few antigens, including prostate specific antigen, were still immunoreactive after 14 d. All tissues were from autopsy cases.

Another study used fresh prostate specimens to study the effects of fixation time on immunostaining *(8)*. Prostatectomy specimens were sliced; one piece was snap-frozen and the other pieces were placed in formaldehyde. At exposure times of up to 36 h, a slice was removed from the fixative and processed for histology and immunostaining. Results were compared with staining intensity in frozen sections that were designated 100%. The results showed no changes in p53 staining intensity after 36 h of fixation in formalin. Cytokeratin staining was 10% reduced after 10 h but was stable until 24 h, after which a steady decline to 25% occurred by 36 h. E-cadherin was stable until 12 h, with a steep decline thereafter; by 24 h, it was reduced by 50% and by 36 h the section exhibited no detectable staining, despite the application of antigen retrieval techniques.

As described previously, microwave irradiation can accelerate fixation (*see* **Subheading 1.3.1.**). Therefore, it is possible that immunohistochemistry may

be more effective on these specimens because a reduction in exposure time to the fixative may result in less antigen masking. In one study ***(6)***, prostates that were fixed in formaldehyde by standard methodology had suboptimal staining for E-cadherin in 84% of the specimens examined, which showed mainly as a rim at the periphery of the gland. The number of cases with homogenous immunostaining throughout the entire tissue section increased to 93% when specimens were fixed by formaldehyde injection at multiple sites and thereafter subjected to microwave treatment, confirming that the best result was achieved by the combination of formalin injections and microwave treatment.

Even for small tissue specimens, microwave treatment can be beneficial ***(14)***. A study compared tissues from various organs fixed by microwave irradiation for 5–8 s in dilute aldehyde mixture (2% formaldehyde and 0.05% glutaraldehyde) with routine formaldehyde fixation. The microwave treatment did not affect morphology adversely, and immunostaining for epithelial membrane antigen, LCA, S-100 protein, and chromogranin were similar for formalin fixation alone compared with microwave fixation. However, antigen retrieval was not necessary in the group treated with microwaves. Rather, it caused tissue digestion. This shows that even for small tissue specimens (such as core biopsies) that will fix fast, microwave treatment can be beneficial.

Fixation by microwave and immersion of tissues in saline solution without any fixatives added has been shown to give good staining results on immunohistochemistry (personal communication, Professor Anthony Leong, University of Newcastle, Newcastle, Australia), but the long-term stability of these tissues has not been studied.

Data suggest that for effective use of immunohistochemistry as a diagnostic tool, biopsy specimens should be exposed to formaldehyde long enough to ensure proper fixation before further processing in dehydrating agents. To avoid loss of antigen reactivity, tissue sections should not be exposed to formaldehyde for longer than 24 h. If exposed to formaldehyde for longer durations, for whatever reason, this must be taken into consideration when interpreting the results. This is particularly important in larger studies when material from several laboratories using different fixation schemes is compared.

### *1.5. Other Fixatives*

A strong glutaraldehyde-based fixative has recently been used for prostate tissues ***(15)***. It has the apparent advantage over formaldehyde that the molecule contains two aldehyde groups, which results in faster fixation as the result of a better ability to make crosslinks. Furthermore, it has been shown to have other superior qualities to formaldehyde in the area of morphological preservation. The buffered glutaraldehyde fixative, Solufix (Tissue Technologies, Australia), has been shown to preserve the prostatic secretory granules that are found in

normal prostate cells but not in cancer. This has been suggested to be of diagnostic value ***(16)***. This fixative could, however, cause crosslinks that will mask antigens and give poor immunostaining; therefore, specific antigen retrieval protocols are required to handle tissues that have been fixed in this manner. In a short communication, various antigen retrieval techniques were used on 20 needle biopsies and 5 transurethral resections all fixed in glutaraldehyde ***(17)***. The results showed that all antibodies (high molecular weight cytokeratin, antibodies to prostate-specific antigen, LCA, S-100 protein, vimentin, chromogranin A, and broad-spectrum cytokeratins AE1/AE3 and CAM 5.2) showed good staining with the optimal retrieval scheme.

A study performed to assess staining intensities of various antibodies in tissues fixed in standard preparations of neutral buffered formalin, acid formalin, zinc formalin, alcoholic formalin, ethanol, methanol, and Bouin's fixative ***(18)*** showed that none of these fixatives was adequate for all antigens. Neutral-buffered formalin (NBF) was the fixative that generally gave the poorest results. Ethanol and methanol gave optimal results for p53 and broad-spectrum keratins, whereas aldehydes such as unbuffered zinc formalin were best for demonstrating transforming growth factor-α and p185 (Her2/neu) staining. It must be noted that no antigen retrieval techniques were used in this study and that the reduced sensitivity observed with formalin-fixed tissues could be reversed by antigen retrieval techniques.

Although alcohol-based fixation can give better morphology, it penetrates tissues slower than formaldehyde and therefore is best for small specimens (<5 mm thick), such as core biopsies ***(19)***. Also, commercially available antibodies have been primed for use on formaldehyde-fixed tissue, and new protocols might be needed for tissues fixed in alcohol-based fixatives. Therefore, investigators need to compare the performance of their antibodies of interest on ethanol-fixed tissue with that on tissues fixed using other fixatives before settling on a single method of fixation.

Acetic alcoholic formalin (Telleysniczky's solution) ***(20)*** gives good morphology and fixes rapidly. It can be used with most commercially available immunohistochemical kits. Disadvantages include its cost and the fact that it causes destruction of cytoplasmic organelles, which makes the tissue unsuitable for electron microscopy.

### *1.6. Analysis of Nucleic Acids Extracted from Formaldehyde-Fixed Tissue*

Archived paraffin-embedded tissues provide a valuable resource for diagnostic and investigative studies using new technologies and have made it possible for pathologists and scientists to study the molecular biology of cancers and diseases with known outcome.

### *1.6.1. Extraction of DNA from Formaldehyde-Fixed Tissue*

During fixation in formaldehyde, DNA is crosslinked to its associated histones and other proteins, which confers rigidity on the molecule and makes it susceptible to mechanical shearing and degradation. This can be minimized by making thick tissue sections, by careful handling of DNA-containing solutions, and by extracting greater quantities of DNA from a large specimen to counterbalance losses caused by shearing. Some protocols for DNA extraction from fresh tissues have been successfully adapted to archival material in paraffin blocks in some instances. For example, high molecular weight genomic DNA from paraffin-embedded tissue was analyzed for gene rearrangements by digesting the DNA with restriction enzymes followed by Southern blotting ***(21,22),*** and gene amplification was examined in paraffin-embedded tumor specimens using dot-blot hybridization of genomic DNA ***(23,24)***. Despite this, degradation of DNA isolated from paraffin-embedded tissues can result in loss of sensitivity of molecular biology techniques ***(25)***. DNA degradation can be inhibited by microwave fixation ***(6),*** possibly through the inactivation of endogenous DNase activity by immediate fixation. Using microwave fixation, DNA of much larger size can be obtained from paraffin-embedded material, expanding the possibilities for molecular analysis of the DNA. Low molecular weight partially degraded DNA can be analyzed using the polymerase chain reaction (PCR) with careful design and selection of primers ***(26,27),*** as used in many recent studies using paraffin-embedded tissues. Characterization of the amplified DNA can be performed using standard methodologies such as cloning and sequencing.

### *1.6.2. Extraction of RNA from Formaldehyde-Fixed Tissue*

RNA is susceptible to degradation by RNases; therefore, specific precautions are required to eliminate them from tissues. The conditions under which tissues are processed for pathological analysis are neither sterile nor RNase-free; however, these processes can also inactivate RNases. Therefore, any RNA that remains intact after tissue fixation stays relatively stable once embedded in paraffin. RNA can be extracted from paraffin-embedded tissues using RNase-free protocols, including guanidinium-isothiocyanate procedures that were designed for use with fresh tissues ***(28–30)***. Quantitation of messenger RNA derived from paraffin-embedded tissues by dot-blot hybridization or by reverse-transcription PCR (RT-PCR) has been successful and has had applications in determining infection with RNA viruses ***(28–34)***.

### *1.6.3. Limitations of Formaldehyde-Fixed Tissue for Molecular Biology*

Because molecular biology can be performed on formaldehyde-fixed, paraffin-embedded tissue, it opens up possibilities of using archival material.

H&E-stained tissues can be useful for pinpointing areas of interest to be microdissected.

However, there are a number of technical limitations for using paraffin-embedded sections for molecular studies. Given the extreme sensitivity of the PCR technique, the most obvious is the risk of contamination from the routine histology laboratory during initial paraffin embedding or sectioning, which could result in a false-positive result. On the other hand, false-negative results may occur because of degradation of DNA/RNA and the reagents used during the fixation/sectioning process could inhibit DNA polymerase.

A study to determine the suitability of fixatives for analysis by DNA hybridization ***(35)*** used six lymph nodes with lymphomas and one with reactive hyperplasia that were aliquotted into various fixatives. DNA extracted after fixation with formaldehyde, glutaraldehyde, or Michel's medium, and phosphate-buffered saline was of low yield and poor purity. Methanol acetic acid caused DNA degradation. In contrast, ethanol fixation yielded large amounts of high molecular weight DNA that was adequate for hybridization. This study showed that ethanol fixation provides a good alternative to frozen material and can be used for hybridization studies when frozen material cannot be obtained. Similarly, the authors of another large study ***(19)*** concluded that ethanol preserves DNA and RNA well. They also suggested preservation methods for future uses, such as using low-melt embedding compounds that reduce RNA hydrolysis compared with paraffin embedding at high temperatures. Another suggestion was to use reversible protein crosslinking agents that inhibit movement of biomolecules by inhibiting RNase and proteinase activity. DNA, mRNA, and proteins can be retrieved after reversal of crosslinking. This method could be useful for specialized techniques, such as layered expression scanning, in which individual proteins and their in vivo binding partners are captured and measured.

### 1.7. Fixation Procedures Recommended for Prostate Tissue

Various fixation procedures can be used for the prostate gland and any biological tissue, depending upon the type of investigation to be performed. For research purposes, fixation techniques can be optimized to yield good results for specific purposes, such as immunohistochemistry and molecular biology. However, most human specimens used for research purposes have been processed in a diagnostic pathology department using routine fixation and embedding methods. It is therefore crucial that these laboratories use the optimal method for good morphology, immunohistochemistry, and molecular biology but also keep in mind the future use of the material for research purposes. Despite the increased work and time spent in preparation, optimization of the primary fixation will facilitate further diagnostic investigation and research.

### *1.7.1. Fixation of Prostate Core Biopsies*

For diagnostic purposes, usually six to twelve core biopsies are taken from the prostate gland and submitted to the laboratory floating free in separate formaldehyde-filled containers. The biopsy pieces are placed in a tissue cassette. Core biopsies from prostate gland are usually thin and will therefore be fixed rapidly. It is critical to ensure that the cores are fixed properly, which usually means for at least 6 h, before further processing and to avoid exposure to formaldehyde for longer than 24 h. A recent study ***(36)*** found that carefully stretching the biopsy in the tissue cassette before fixation increased the amount of tissue available for diagnosis by 26% because curved biopsies, in which not all tissue is at the same level at cutting, were avoided.

### *1.7.2. Fixation of Whole Prostates After Radical Prostatectomies*

It has become increasingly important to sample unfixed tissues from radical prostatectomies for research purposes. Therefore, methods for harvesting fresh tissue have been developed ***(37)***. In our laboratory (Dept. of Pathology, University Hospital of Northern Norway), whole prostates are transported on ice to the pathology laboratory immediately after surgical extraction. Under aseptic conditions, the tissue is palpated and cut transversely into the firm area representing the tumor. The cut section is frozen immediately by immersion in liquid nitrogen/isopentane and stored in a –70°C freezer. A section from normal prostate is cut out and processed in an identical manner. From both normal and tumor-bearing areas, a small piece of tissue ($1 \times 2 \times 2$ mm) is kept in fixative for electron microscopy. The incision in the remaining prostate is sutured by metallic clips to restore normal anatomy and to avoid tissue distortion during formaldehyde fixation. We insert a spiral stent into the urethra and immediately immerse the whole prostate in formaldehyde, ensuring at least a 10-fold excess of formaldehyde by volume when compared with the size of the prostate. The prostate is then agitated overnight by rotating on a rotating board. The fixed prostates are then weighed and measured in three planes. They are inked ventrally, dorsally, on the left side and the right side using four different colors of ink before cutting. The seminal vesicles are cut off the prostate gland, sliced halfway through longitudinally, and folded out like a butterfly. Both halves of each side are embedded. The apex is cut off and sliced in thin sagittal sections. The remaining prostate gland is then sliced in 5-mm transverse sections, and each slice is embedded without further cutting (*see* **Fig. 1**).

In this way, the entire prostate is embedded and a good overview of the tumor area is obtained. As described earlier in this chapter (*see* **Subheading 1.3.1.**), microwave treatment in combination with formalin injection at multiple sites yielded good fixation, gave better immunohistochemical staining, and

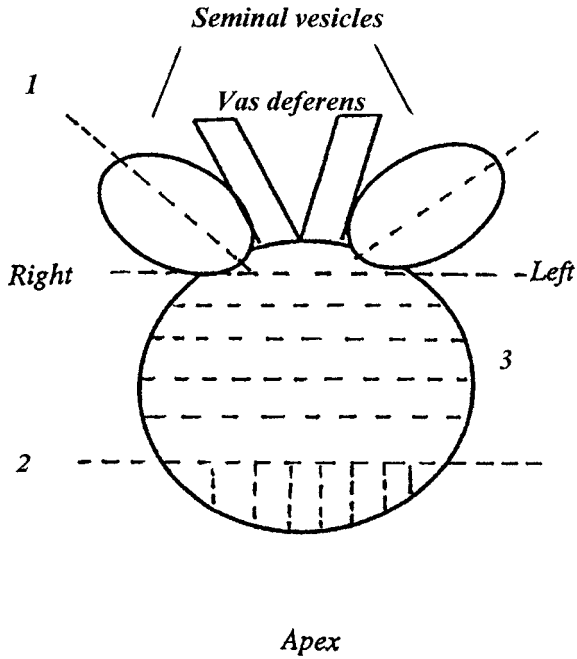


Fig. 1. Schematic representation of the prostate gland with seminal vesicles (SV) and vas deferens (VD) attached. After the SV and VD are cut off the prostate, the SV are sliced halfway through *(1)* before embedding. The apex of the prostate is then cut off *(2)* and cut in sagittal sections, as indicated by the dotted lines. The remaining prostate tissue *(3)* is cut into 5-mm transverse sections, as indicated.

DNA of larger sizes can be obtained. This method is, however, more laborious, and heated formalin vapors can cause a work hazard. Therefore, it may not be optimal in a busy routine laboratory practice.

### *1.7.3. Fixation of Prostate Cancer Bone Metastases*

The harvesting and analysis of prostate cancer bone metastasis samples is critical to understanding the pathophysiology of the disease and its response to treatment. There are several methods for handling normal bone samples that can be applied to dealing with bone metastases. Frozen sections, plastic (methacrylate) embedding, or decalcification followed by paraffin embedding are all established methods that have specific applications. For example, decalcification and paraffin embedding simplifies handling of the tissue but can be a slow process, particularly if EDTA decalcification is used, and can result in a loss of antigenicity. Frozen sections can preserve certain antigens that may be altered or lost through the use of fixatives and/or the decalcification procedure,

but the tissues must be processed immediately. Alternatively, plastic embedding is extremely useful for techniques, such as histomorphometry, because morphological details are preserved, but incomplete penetration of the sample with the plastic can result in poor sections. With the development of resins that can be removed after sectioning and improved antigen retrieval methods, plastic-embedded bone may be able to be used for DNA and mRNA analysis ***(38,39)*** as well as for immunohistochemistry ***(40)***. Therefore, the first point to be established when obtaining bone samples is the purpose of the study. Then, if the tissue is to be decalcified and examined for protein expression or activity, the stability of the protein/antigen to be examined must be established.

If the bone is to be decalcified or embedded in plastic, it must first be fixed in 10% NBF at 4°C for 24 to 48 h. Then, the sample must be thoroughly rinsed with several changes of water. It is important to ensure that the sample is adequately decalcified before embedding: if calcium is still present, the bone will not section well and may produce artifactual staining. Likewise, overdecalcification is a common cause of loss of specimen morphology, resulting in poor histological detail and the possibility of swelling or fragmentation, as well as reduction in hematoxylin staining.

Several decalcification methods are available, including commercial preparations that can decalcify bone rapidly. However, the most widely used method involves the use of 10% formic acid. Treatment of bone samples with 10% formic acid for more than 24 h can result in DNA hydrolysis, although limiting exposure to more dilute acid for a shorter time can preserve the DNA for analyses ***(41)***. The sample must be rotated while immersed in formic acid to ensure even decalcification. After 24 h, a sample of the formic acid is tested by adding an equal volume of saturated ammonium oxalate. A white precipitate or cloudiness in the mixture indicates that the formic acid is saturated with calcium, and decalcification is incomplete. It is then necessary to change the formic acid in the sample and retest after another 24 h. This is repeated until the test does not produce a precipitate. In this case, decalcification is complete and the sample can be processed for paraffin embedding.

Other acids, such as nitric and hydrochloric acids, can be used with cortical bone because they will rapidly remove calcium, although they are not suited to delicate tissues, such as bone marrow, beause they can damage cellular morphology and ultrastructure. EDTA (5–10%) is a less harsh method than formic acid, but it penetrates tissues poorly, takes longer to remove calcium, must be changed frequently, and can be expensive over time. However, intact DNA can be retrieved from EDTA-treated samples, and *in situ* hybridization and comparative genomic hybridization studies have been successfully completed on tissues decalcified in this manner ***(42)***. Unfortunately, chemical tests such as the ammonium oxalate procedure cannot be used with EDTA because the calcium-

EDTA complex is soluble. The best way to test for adequate decalcification in these cases is to perform autoradiography, where a clear film will show the absence of calcium, or to use a flexibility test. However, the latter test requires experience to gauge the optimal point in the decalcification process.

There are variations on plastic-embedding procedures, depending upon the polymers used and their ratios. The following procedure is based on one that was established to facilitate the rapid embedding of bone marrow biopsies (*see* **ref. *43***, adaptations by Dr. M. Roudier, University of Washington, personal communication). After fixation of samples in ice-cold NBF, the samples are dehydrated in ethanol (70% changed daily for 3 d; 95% for 1 d; then 100% changed daily for 3 d). Over at least 2 d, the samples are penetrated with infiltration medium (methylmethacrylate, benzoyl peroxide, plastoid N, and methyl benzoate) before being embedded in modified infiltration medium (methylmethacrylate, benzoyl peroxide, plastoid N, and *N,N*-dimethylaniline) under inert gas. After polymerization, the medium will contract; therefore, more medium can be added and allowed again to polymerize. At this point, sections can be made using tungsten carbide blades and processed accordingly.

## 2. Conclusion

Tissues extracted from patients must be handled rapidly and carefully. It is critical to design the studies for which the tissue will be used before selection of a fixation method because some analytical techniques are sensitive to specific fixatives. We have focused on the use of formaldehyde in this chapter because it is by far the most commonly used fixative for histopathology worldwide. It has obvious advantages such as its low cost, availability, applicability to routine practice, retention of cellular and tissue morphology for microscopic analysis, and its low interference with analytical techniques, such as immunohistochemistry. However, there are limitations to its use, which have been described in this chapter. Its crosslinking ability can mask some antigens, making retrieval necessary in some cases; it presents some working hazards because the fumes may be carcinogenic; it has a slow fixation rate; and it is not optimal for molecular biology studies. Some of these disadvantages can be minimized by using methods to accelerate fixation and enzyme or heat pretreatment to retrieve antigens. Formaldehyde fixation can be further optimized by careful monitoring of pH, fixation time and temperature, atmospheric pressure, and by the judicious use of agitation and microwave irradiation. Standardization of these parameters will make it easier to compare and analyze results between different laboratories.

Formaldehyde fixation may be superseded by the development of new technologies that produce high-quality histological detail, provide ease-of-use in a clinical setting, permit recovery of mRNA and protein of sufficient quality for

molecular profiling studies and immunohistochemistry, and maintain tissue specimen stability in the long term. Although many factors must be considered when developing and evaluating a new or improved clinical methodology, continued improvements in tissue processing methodologies will be important in determining the molecular biology of various diseased human cell types.

## References


1. Asplund, M. and Brunk, U. (1975) Osmotiska forhallen under aldehydfixering. *Laboratoriet* **9,** 1–11.
2. Fox, C. H., Johnson, F. B., Whiting, J., and Roller P. P. (1985) Formaldehyde fixation. *J. Histochem. Cytochem.* **33,** 845–853.
3. Bancroft, J. D. and Stevans, A. (1999) *Theory & Practice of Histological Techniques* 4th ed, Churchill Livingstone, New York.
4. Walker, J. F. (1964) Formaldehyde, in *American Chemical Society Monograph Series,* 3rd ed., Reinhold, New York.
5. Feldman, M. Y. (1973) Reactions of nucleic acids and nucleoproteins with formaldehyde. *Prog. Nucleic Acid Res. Mol. Biol.* **13,** 1–49.
6. Ruijter, E. T., Miller, G., Aalders, T. W., Van De Kaa, C. A., Schalken, J. A., Debruyne, F. M., et al. (1997) Rapid microwave-stimulated fixation of entire prostatectomy specimens *J. Pathol.* **183,** 369–375.
7. Baak, J. P. A. (1991) *Manual of Quantitative Pathology in Cancer Diagnosis and Prognosis,* Springer-Verlag, Berlin and Heidelberg.
8. Taylor, C. R., Shi, S. R., and Cote, R. J. (1996) Antigen retrieval for immunohistochemistry. Status and need for greater standardization. *Appl. Immunohistochem.* **4,** 144–166.
9. Shi, S.-R., Imam A., Young, L., Cote, R. J., and Taylor C. R. (1995) Antigen retrieval immunohistochemistry under influence of pH using monoclonal antibodies *J. Histochem. Cytochem.* **43,** 193–201.
10. Shi, S.-R., Cote, R. J., and Taylor C. R. (1997) Antigen retrieval immunohistochemistry: Past, present and the future. *J. Histochem. Cytochem.* **45,** 327–343.
11. Shi, S.-R. Cote, R. J., Young, L. L., and Taylor, C. R. (1997) Antigen retrieval immunohistochemistry: Practice and development. *J. Histotechnology* **20,** 145–154.
12. Pileri, S. A. Roncandor, G., Ceccarelli, C., Piccioli, M., Briskomatis, A., Sabbatini, E., et al. (1997) Antigen retrieval techniques in immunohistochemistry: Comparison of different methods. *J. Pathol.* **183,** 116–123.
13. Leong, A. S. Y. and Gilham, P. N. (1989) The effects of progressive formaldehyde fixation on the preservation of tissue antigens. *Pathology* **21,** 266–268.
14. Login, G. R., Schnitt, S. J., and Dovrak, A. M. (1987) Rapid microwave fixation of human tissues for light microscopic immunoperoxidase identification of diagnostically useful antigens. *Lab. Invest.* **57,** 585–591.
15. Cohen, R. J., McNeal, J. E., Meehan, K., and Wilce, M. (2000) Luminal contents of benign and malignant prostatic glands: Correspondence to altered secretory mechanisms. *Hum. Pathol.* **32,** 94–101.

16. Cohen, R. J. and Beales, M. (2000) Prostate secretory granules in normal and neoplastic prostate glands: A diagnostic aid to needle biopsy. *Hum. Pathol.* **31,** 1515–1519.
17. Cohen, R. J., Fischer, G., and McNeal, J. E. (2001) Immunostains after gluteraldehyde-based tissue fixation. *Hum. Pathol.* **32,** 242–243.
18. Arnold, M. M., Srivastava, S., Fredenburgh, J., Stockard, C. R., Myers, R. B., and Grizzle, W. E. (1996) Effects of fixation and tissue processing on immunohistochemical demonstration of specific antigens. *Biotech. Histochem.* **71,** 224–230.
19. Gillespie, J. W., Best, C. J. M., Bichel, V. E., Cole, K. A., Greenhut, S. F., Hewitt, S. M., et al. (2002) Evaluation of non-formalin tissue fixation for molecular profiling studies. *Am. J. Pathol.* **160,** 449–457.
20. Russell, P. and Farnsworth, A. (1997) Examination of the ovarian specimen, in *Surgical Pathology of the Ovaries* (Russell, P. and Farnsworth, A., eds.), Churchill Livingstone, Edinburgh, pp. 25–37.
21. Goelz, S. E., Hamilton, S. R., and Vogelstein, B. (1985) Purification of DNA from formaldehyde fixed and paraffin embedded human tissue. *Biochem. Biophys. Res. Commun.* **130,** 118–126.
22. Dubeau L., Chandler, L. A, Gralow, J. R., Nichols, P. W., and Jones, P. A. (1986) Southern blot analysis of DNA extracted from formalin-fixed, paraffin-embedded pathology specimens. *Cancer Res.* **46,** 2964–2969.
23. Wong, A. J., Ruppert, J. M., Eggelston, J., Hamilton, S. R., Baylin, S. B., and Vogelstein, B. (1986) Gene amplification of c-myc and N-myc in small cell carcinoma of the lung. *Science* **233,** 461–464.
24. Tsuda, H., Shimosato, Y., Upton, M. P., Yokota, J., Tereda, M., Okira, M., et al. (1988) Retrospective study on amplification of N-myc and c-myc genes in pediatric solid tumors and its association with prognosis and tumor differentiation. *Lab. Invest.* **59,** 321–327.
25. Mies, C., Houldsworth, J., and Changanti, R. S. K. (1991) Extraction of DNA from paraffin blocks for Southern blot analysis. *Am. J. Surg. Pathol.* **15,** 169–174.
26. Park, J. S., Leake, J. F., Sharma, B. K., Toki, T., Kessis, T. O., Ambros, R. A., et al. (1991) Variability in beta-globin and HPV DNA amplification by PCR from fixed tissues. *Mod. Pathol.* **4,** 667–670.
27. Honma, M., Ohara, Y., Murayama, H., Saho, K., and Ivasali, Y. (1993) Effects of fixation and varying target length on the sensitivity of polymerase chain reaction for detection of human T-cell leukemia virus type I proviral DNA in formalin-fixed tissue sections. *J. Clin. Microbiol.* **31,** 1799–1803.
28. Stanta, G. and Schneider, C. (1991) RNA extracted from paraffin-embedded human tissue is amenable to analysis of PCR amplification. *Biotechniques* **11,** 304–408.
29. Woodall, C. J., Watt, N. J., and Clements, G. B. (1993) Simple technique for detecting RNA viruses by PCR in single sections of wax embedded tissue. *J. Clin. Pathol.* **46,** 276–277.
30. Hilton, D. A., Variend, S., and Pringle, J. H. (1993) Demonstration of coxackie virus RNA in formalin-fixed tissue sections from childhood myocarditis cases by in situ hybridization and the polymerase chain reaction. *J. Pathol.* **170,** 45–51.

31. Akyol, G., Dash, S., Shieh, Y. S., Malter, J. S., and Gerber, M. A. (1992) Detection of hepatitis C virus RNA sequences by polymerase chain reaction in fixed live tissue. *Mod. Pathol.* **5,** 501–504.
32. Jackson, D. P., Quirke, P., Lewis, F., Boylston, A.W., Sloan, J. M., Robertson, D., and Taylor, J. R. (1989) Detection of measles virus RNA in paraffin-embedded tissue (letter). *Lancet* **1,** 1391.
33. Redline, R. W., Genest, D., and Tycko B. (1991) Detection of enteroviral infection in paraffin-embedded tissue by the RNA polymerase chain reaction technique. *Am. J. Clin. Pathol.* **96,** 568–571.
34. Navas, S., Castillo, I., and Carreno, V. (1993) Detection of plus and minus HCV RNA in normal liver of anti-HCV-positive patients (Letter). *Lancet* **341,** 904–905.
35. Bramwell, N. H. and Burns B. F. (1988) The effect of fixative type and fixation time on the quantity and quality of extractable DNA for hybridization studies on lymphoid tissue. *Exp. Hematol.* **16,** 730–732.
36. Rogatch, H., Moser, P., Volgger, H., Horninger, W., Bartsch, G., Mikuz, G., et al. (2000) Diagnostic effect of an improved pre-embedding method of prostate needle biopsy specimen. *Hum. Pathol.* **31,** 1102–1107.
37. Egevad, L., Engstrom, K., and Busch, C. (1998) A new method for handling radical prostatectomies enabling fresh tissue harvesting, whole mount sections, and landmarks for alignment of sections. *J. Urol. Pathol.* **9,** 17–26.
38. Church, R. J., Hand, N. M., Rex, M., and Scotting, P. J. (1997) Non-isotopic in situ hybridisation to detect Sox gene mRNA in plastic-embedded tissue. *Histochem. J.* **29,** 625–629.
39. Warren, K. C., Coyne, K. J., Waite, J. H., and Cary, S. C. (1998) Use of methacrylate de-embedding protocols for in situ hybridisation on semithin plastic sections with multiple detection strategies. *J. Histochem. Cytochem.* **46,** 149–155.
40. McCluggage, W. G., Roddy, S., Whiteside, C., Burton, J., McBride, H., Maxwell, P., et al. (1995) Immunohistochemical staining of plastic embedded bone marrow trephine biopsy specimens after microwave heating. *J. Clin. Pathol.* **48,** 840–844.
41. Brown, R. S., Edwards, J., Bartlett, J. W., Jones, C., and Dogan, A. (2002) Routine acid decalcification of bone marrow samples can preserve DNA for FISH and CGH studies in metastatic prostate cancer. *J. Histochem. Cytochem.* **5,** 113–116.
42. Alers, J. C., Krijtenburg, P.-J., Vissers, K. J., and van Dekken, H. (1999) Effect of bone decalcification procedures on DNA in situ hybridisation and comparative genomic hybridisation: EDTA is highly preferable to a routinely used acid decalcifier. *J. Histochem. Cytochem.* **47,** 703–709.
43. Lebeau, A., Muthmann, H., Sendelhofert, A., Diebold, J., and Lohrs, U. (1995) Histochemistry and immunohistochemistry on bone marrow biopsies. A rapid procedure for methyl methacrylate embedding. *Pathol. Res. Practice* **191,** 121–129.

# 11

# Background, Methods, and Protocols for the Histopathological Diagnosis of Prostate Carcinoma

**Warick Delprado**

## 1. Introduction

The histopathological diagnosis of malignancy has traditionally been said to be the gold standard by which all other methods of investigation and diagnosis are defined and assessed. Although this is still largely true, the other chapters in this book attest to the fact that it may not be true for much longer, or at least it may become less golden. More interestingly, it is probably already not true in the diagnosis of premalignant conditions. This is significant clinically because, as in all cancers, the earlier the diagnosis of prostate cancer, the better the chance of cure. However, histopathological diagnosis is still the most powerful tool in use today in patient management and, as such, it is appropriate to review the histopathological diagnosis of carcinoma, its methods, and protocols to define the arena in which other techniques are used and useful.

There is a range of specimens that can be obtained from the prostate for histopathological diagnosis. Although they all tend to be processed initially in the same manner, their interpretation varies, and the range of information obtained is different for the different specimen types. In all cases, prognostic histopathological information must be presented in such a way as to be useful to the clinician managing the patient, to the patient in his understanding of his condition, and to other medical and scientific workers interested in and involved in the understanding of prostate cancer.

Histopathological methods and protocols should be considered from two aspects, (1) the technical aspects of specimen handling and processing and (2) the diagnostic aspects of specimen interpretation.

From: *Methods in Molecular Medicine, Vol. 81: Prostate Cancer Methods and Protocols*
Edited by: P. J. Russell, P. Jackson, and E. A. Kingsley © Humana Press Inc., Totowa, NJ

## 2. Technical Aspects of Specimen Handling and Processing

### 2.1. Specimen Types

Specimens can be obtained at four different types of procedures. Transurethral resection of prostate (TURP) results in multiple chips of prostatic tissue with a wide range of sizes and a wide range of specimen volumes and weights. This procedure is usually performed in patients with lower urinary tract symptoms, such as hesitancy, dribbling, and frequency (prostatitism).

Suprapubic prostatectomy is performed less commonly than TURP and involves the resection of the prostate in one or several large nodules. It is usually performed in patients with prostatitism.

Transrectal ultrasound guided needle biopsy (TRUS or core biopsy) is performed in patients being investigated for possible carcinoma of the prostate. Biopsies are taken from areas of hypoechogenicity in the prostate, as well as randomly and from palpable areas of prostate gland irregularity or firmness. It results in cores of tissue approx 1–1.5 mm in diameter and that vary in length from just a few millimeters to up to 20–25 mm. Biopsies are usually taken from the posterior region of the upper (base), middle, and lower (apex) regions of the prostate, on the right and left. There is usually therefore a minimum of six biopsies, but as clinicians go in search of smaller and smaller tumors and take more and more biopsies anteriorly and laterally, there can be as many as 12 different cores for examination.

Radical prostatectomy involves the removal of the whole prostate after the diagnosis of carcinoma has been established from one of the previous specimen types. It involves the removal of the whole of the prostate with attached seminal vesicles and distant vas deferens, usually with preservation of adjacent nerves. Information obtained from this specimen is critical in defining patient prognosis and planning treatment.

Special biopsies for research and ancillary investigations can be taken from surgical specimens. These research core biopsies are usually larger than diagnostic core biopsies and are taken in a directed manner from areas of apparent or suspected carcinoma from fresh tissue after surgical removal.

### 2.2. Fixatives and Stains

Tissue can be received fresh or fixed. Fresh tissue is important when one plans to use samples for other investigations or molecular studies. Fixed tissue is required for routine histopathology. Fixation is usually in 10% formalin, although special fixatives can be used. Sections are routinely stained with H&E stains to give the traditional pink and blue appearance. Special stains used in the diagnosis of carcinoma are mainly of the immunoperoxidase type. Electron microscopy has little use in prostate cancer diagnosis.

## 2.3. Methods

### 2.3.1. Histological Processing and Examination

Macroscopic specimens need to be examined, cut, and sliced to select areas for processing on glass slides for microscopic histopathological examination. Macroscopic specimens must be fixed and processed in a similar manner. All specimens should be fixed in 10% formalin. Formalin penetrates tissue at a rate of approx 1 mm/h, so small specimens (core biopsies and TURP chips) require only short fixation times of a few hours, although larger specimens (suprapubic prostatectomy and radical prostatectomy) require several hours fixation, usually overnight. In the same manner, processing through alcohols and wax embedding can be performed more quickly in smaller specimens compared to larger specimens.

TURP specimens should be weighed. Specimens consist of multiple chips of tissue ranging from only a few grams in weight up to 60–80 g, although average specimens weigh between 10 and 30 g. Although it is theoretically possible to examine all pieces, in practice this would be too much tissue. It has been shown that examination of 12 g of randomly selected chips will detect 90% of all tumors and miss no high-grade tumors ***(1)***.

Suprapubic prostatectomy specimens should be weighed and sliced at 2–3-mm intervals. Any areas of obvious tumor or yellow discoloration should be sectioned and examined histologically. Otherwise, random blocks should be taken, one for every 10 g of tissue.

TRUS core biopsies need to be entirely processed and fully examined. They often contain very small areas of carcinoma; therefore, the cores need to be cut and examined at several different levels through the diameter of the core of tissue. Several authors have proposed special handling techniques ***(2)***. The cores will usually be labeled by the clinician as to the location in the prostate from where they were taken. This labeling needs to be maintained during the processing so as to allow reporting of the location of the tumor. The cores are sometimes very thin, less than 1 mm, and have to be carefully orientated, embedded, and cut. One way of ensuring that all the tissue is sectioned is to paint the cores with blue ink. This allows the tissue to be better visualized in the paraffin block (*see* **Note 1**).

Radical prostatectomy specimens should be weighed and measured. The prostate should be painted with ink, either blue or green, to define the surgical resection margins. Because important staging information is obtained from examination of the specimen, multiple sections from the prostate must be cut and processed. The region of the upper part of the prostate near the bladder is termed the base. The region at the lower end of the prostate near the urethra is termed the apex. All of the apex and base surgical margins must be examined, as well as the central portion of the prostate and the seminal vesicles.

Research biopsies can be taken from the radical prostatectomy specimen after it has been removed from the patient but before fixation. The biopsies can be taken from the region of palpable abnormality or the region corresponding to the area of tumor as detected by the needle biopsies. After the biopsy is taken, the cavity created should be painted with ink (usually green) to define the margins of the cavity and to separate these margins from the true surgical resection margins.

### 2.3.2. Histological Reporting of Specimens

Certain details need to be recorded in the reporting of all histological specimens for the purpose of conveying to the clinician as much prognostic information as possible ***(3–5)***. Aspects of this will be detailed later, but a list is appropriate at this point.

TURP chip reports should include presence of carcinoma, type of carcinoma, percent of chips involved, Gleason score, perineural invasion, or vascular invasion.

Suprapubic prostatectomy reports should include presence of carcinoma, type of carcinoma, estimated percent of total tissue involved, perineural invasion, and vascular invasion.

TRUS biopsy reports should include presence of carcinoma, type of carcinoma, number of cores involved, percent of each core involved, percent of total tissue involved, Gleason score, perineural invasion, vascular invasion, and any evidence of capsular penetration / extraprostatic extension.

Radical prostatectomy reports should include presence of carcinoma, type of carcinoma, location of carcinoma within prostate, volume or percent of prostate involved by carcinoma, presence of capsular penetration and extraprostatic extension, state of surgical resection margins, including presence and extent of positive margins, Gleason score, seminal vesicle involvement, and lymph node involvement. Reports should include an addended graphical report showing a diagram of the prostate and the location of the carcinoma, as well as capsule penetration and margin involvement locations.

### 2.3.3. Use of Special Stains

Routine special stains (for mucus, collagen, iron, etc.) have little use in reporting of most carcinomas of the prostate. Mucus stains can be used to demonstrate pools of mucus in colloidal type carcinomas but actually add little to the interpretation. However, immunoperoxidase stains are particularly useful in the diagnosis of carcinoma, particularly in TURP and core biopsy specimens.

Immunoperoxidase stains for high molecular weight cytokeratin, particularly 34βE12 ***(6)***, are extremely useful in demonstrating the presence of basal cells. Basal cells are absent in invasive carcinoma; therefore, demonstration of

the presence of basal cells in a small group of atypical glands in a needle biopsy indicates that the glands are benign (*see* **Note 2**). However, partial loss of basal cells does occur in some benign conditions, so presence or absence of basal cells cannot be used on its own as an unequivocal criterion for malignancy. Other immunoperoxidase stains for chromogranin and synaptophysin are occasionally useful in demonstrating neuroendocrine differentiation in poorly differentiated tumors with small cell carcinoma features that require additional chemotherapy.

### *2.3.4. Use of Special Fixatives*

Most histopathological specimens are fixed in 10% formalin. Electron microscopic specimens are the major exception, being fixed in glutaraldehyde. Recently there have been some articles that suggest that fixation of prostatic core biopsies in a glutaraldehyde-based fixative (under the name of Solufix) would assist in the diagnosis of carcinoma ***(7,8)***. It is claimed that normal prostate glands from tissue fixed in Solufix have a pronounced red coloration of the cytoplasm of the cells. It is claimed that this red coloration is lost in carcinoma. Studies with this fixative are too few to allow complete comment on its usefulness. However, a personal unpublished series of 20 cases fixed in Solufix was interesting. The series consisted of tissues with a range of diagnoses, including benign, atrophic, preneoplasia (PIN), carcinoma, and postradiotherapy (brachytherapy). Although the benign glands did indeed stain red, carcinoma cases showed a range of degrees of loss of coloration. More importantly, some benign conditions, such as atrophic glands and postbrachytherapy glands, also showed a loss of coloration. Because these are often the major differential diagnoses of small atypical glands in core biopsies, the usefulness of the fixative is reduced. Use of the fixative also required modification of the normal immunoperoxidase staining protocol because the antigen was masked in normal stains. However, the fixative was effective in demonstrating the presence of basal cells in benign glands. Overall, this is a potentially exciting but as yet unproven adjunct to diagnosis of carcinoma.

## 3. Diagnostic Aspects of Specimen Interpretation

Histopathological diagnosis of malignancy is a descriptive art based on pattern recognition in a clinical context. The diagnosis of any malignancy must be performed in a sequential manner. It is the aggregation of a large amount of information that allows diagnosis and understanding of a malignancy. (This volume is a testimony to this fact.) In histopathological diagnosis, this requires an approach that commences with an assessment of and information about the patient, then assessment of the tumor mass macroscopically, then of the struc-

ture of the tumor microscopically, and finally of the cells that make up the tumor (*see* **Note 4**). Terms used to describe the identified patterns have been standardized and allow communication of information about the tumor. However, primary in the diagnosis of any tumor is first an understanding of normal and the range of normal.

## 3.1. Definitions of Malignancy

### 3.1.1. Tumor Terminology Definitions

A tumor refers properly simply to a swelling. It has come to be used in general terminology as synonymous with a neoplasm. Neoplasms have been defined as uncontrolled growths of tissues or cells, beyond the normal function of the cells and that persist after the cessation of the stimulation that evoked the change ***(9)***. Neoplasms are often named from the tissue of origin, with the addition of *-oma* (for example: adenoma, osteoma), with qualifiers relating to architecture (papilloma) ***(9)***. Carcinoma refers to malignant epithelial tumors. Sarcoma refers to malignant stromal derived tumors. Prostatic carcinomas derived from glands in the prostate are termed adenocarcinomas.

### 3.1.2. Cellular Terminology Definitions

Neoplastic appearance and behavior can be assessed by starting at the gross appearance and behavior of the cells and following the same type of sequential approach. Therefore, starting with the big picture, metastasis refers to the ability of the tumor to spread from its origin, usually via lymphatic or vascular pathways. Prostatic adenocarcinoma, like most carcinomas, tends to metastasize first to lymph nodes. Infiltration refers to the ability of the tumor to spread into surrounding tissue, such as bladder. Differentiation indicates the degree to which the tumor replicates the tissue of origin. Therefore, well-differentiated tumors have architectures similar to normal tissue (such as prostate glands in a well-differentiated adenocarcinoma), whereas poorly differentiated tumors show loss of the normal architectural patterns. Finally, at the individual cell level, we can talk about the relationship of the nucleus to the cytoplasm (nuclear/cytoplasmic ratio), the size of the nucleus, and the nuclear features. These nuclear features are known as the degree of anaplasia (pleomorphism, irregularity, hyperchromasia, chromatin clumping). The nucleolus is also assessed as to size and shape.

## 3.2. Normal (Benign) Prostatic Architecture and Morphology

The prostate consists of zones referred to as peripheral or posterior, central, and transitional. Normal prostatic tissue ***(10)*** consists of fibromuscular stroma containing benign peripheral glands and ducts that drain into the prostatic ure-

thra. The stroma consists of smooth muscle and fibrous stromal cells. The epithelium of the glands and ducts has two cell layers. There is an outer basal or myoepithelial cell layer and an inner luminal or secretary cell layer. The most common types of carcinoma arise from the lumenal cells, and generally the presence of myoepithelial cells indicates a benign gland. Both the lumenal and myoepithelial cells stain positive for cytokeratin immunoperoxidase stains. Specifically, the lumenal cells are negative, and the myoepithelial cells are positive for high molecular weight cytokeratins, such as 34βE12 (*see* **Note 2**).

Many benign conditions can mimic adenocarcinoma by having some but not all features of malignancy. This is particularly true of atrophy, hyperplasia, and posttreatment (especially radiation) appearances. Some of these conditions are essentially normal in elderly patients (for example, benign hyperplasia).

## *3.3. Prostatic Carcinoma*

### *3.3.1. Classification of Prostatic Carcinoma*

Any classification of tumors of a particular organ includes the main tumor types plus variants that are rare ***(11,12)***. The classification of malignancies of the prostate can be summarized as follows:

- Epithelial (carcinomas)
  - Adenocarcinoma (conventional/small acinar)
  - Prostatic duct carcinoma
  - Rare types (mucinous, signet ring, adenosquamous, squamous, basaloid and adenocystic, transitional cell, small cell, sarcomatoid, lymphoepithelial, undifferentiated)
- Mesenchymal
- Mixed epithelial/mesenchymal
- Other (e.g., lymphoma) and secondary tumors
- Preneoplastic (precursor) conditions (carcinoma *in situ*)

## *3.4. Morphology of Adenocarcinoma* (see *Note 3)*

### *3.4.1. Macroscopic*

Assessment of a biopsy or surgical specimen begins with an analysis of the macroscopic appearances—does the specimen appear normal, and if not why not? There are few macroscopic clues of malignancy in needle biopsy specimens. TURP specimens containing areas of carcinoma will generally appear more yellow macroscopically. Radical prostatectomy specimens (and to a lesser extent suprapubic prostatectomy specimens) that contain carcinoma will show areas of loss of the normal tissue pattern, firmness to palpation, and accentuated yellow or white coloration. Advanced carcinomas will have distorted, irregular margins.

### 3.4.2. Microscopic

Microscopic assessment of malignancy begins with a low power assessment (*see* **Note 3**), followed by increasingly higher magnification reviews. Low magnification power assessment draws the attention of the observer to areas of abnormality and raises the possibility of malignancy. High magnification assessment confirms the diagnosis of malignancy and the tumor type. In addition to these major features of malignancy, there are other, minor, features that are useful in diagnosing malignancy. These are features of prostatic adenocarcinoma that are not unique to malignancy but are more common in malignant glands compared with benign glands and that add additional information to the process of diagnosing carcinoma.

### 3.4.3. Low-Magnification Appearances

Architectural abnormalities are recognized at low power and are characterized by loss of the normal pattern of glands and stroma. This is usually characterized by increased numbers of glands in a disorganized pattern. This disorganization can be either abnormal nodules of glands or an infiltrative pattern, with separation of the normal lobules and glands by abnormal glands. There will usually be a higher density of glands in carcinoma. In high-grade carcinomas, the pattern of glands will be lost and replaced by cribriform masses or solid masses and sheets of cells or even individual infiltrating cells. Areas of necrosis in glands are also a feature of high grade malignancy. Intravascular and perineural invasion seen at low-to-medium magnification is also strongly indicative of carcinoma.

### 3.4.4. Medium Magnification Appearances

Medium power assessment allows abnormal gland features and shapes to be recognized. Instead of the usual round smooth-shaped glands of benign tissue, carcinoma glands are often angular and irregular, variable in size and shape, and branched or fused (back-to-back glands with no intervening stroma). Glands usually appear darker or more basophilic at this magnification because of nuclear and cytoplasmic changes. Minor diagnostic features are seen in the lumen of the glands (*see* **Fig. 1**).

The absence of basal cells can often be seen at this power, and this can be confirmed by immunoperoxidase studies for 34βE12 and assessment at high power (*see* **Note 2**).

### 3.4.5. High-Magnification Appearances

Individual cellular changes are recognized at higher power. There is a change in the nuclear/cytoplasmic ratio, with larger nuclei taking up a bigger

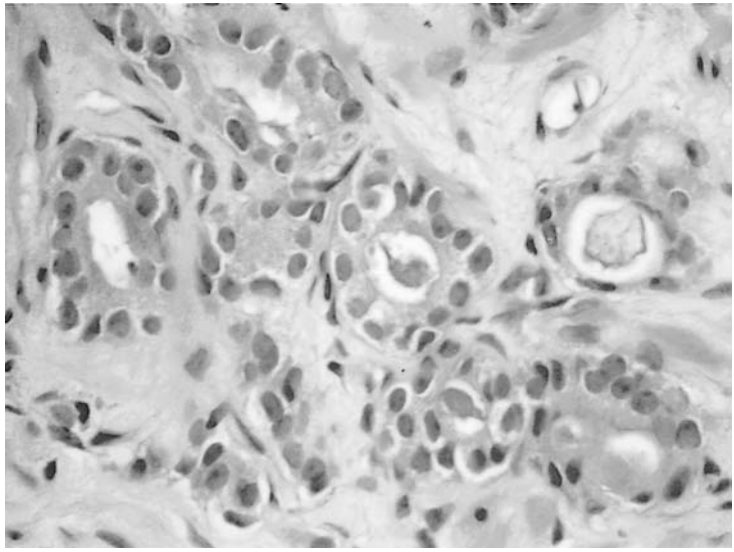

Fig. 1. Prostatic carcinoma characterized by infiltrating glands that are irregular (H&E, ×20).

proportion of the volume of the cell. The cytoplasm will generally lose the slight eosinophilia and appear clear or amphophilic. There is loss of the normal cytoplasmic secretary snouts. The nuclear membrane (chromatinic ring) will be irregular, and there will be changes in the nuclear chromatin from smudging to irregular clumping. One of the most important diagnostic features in prostatic adenocarcinoma cells is the presence of large nucleoli. They are large, eosinophilic, and often irregular in shape. Mitotic figures can be seen at high power. These are very rare in benign tissue.

### *3.4.6. Minor Diagnostic Features of Prostate Adenocarcinoma*

As well as the traditional (so-called major) features of malignancy (as outlined in **Subheading 3.1.2.**) discussed above, there are features of tumors that are not actually features of malignancy, but are more common in malignancy and add additional weight to the diagnosis.

- Necrosis, particularly in the center of large cellular masses and cribriform groups of glands (comedonecrosis) is a feature of high-grade malignancy.
- Perineural infiltration, where carcinoma completely surrounds a nerve by infiltrating in the perineural space (as opposed to simply indenting or distorting a nerve), is common in prostate carcinoma, and in some parts of the prostate is suggestive of prostatic capsular penetration and extraprostatic spread.

- Collagenosis refers to small balls or aggregates of collagen within the lumen of glands and between cells. It rarely, if ever, occurs in benign prostates and as such is very suggestive of carcinoma.
- Lumenal basophilic (blue) mucus in a loose pattern in the lumen is more common in carcinoma.
- Lumenal eosinophilic (pink) secretions seen in carcinoma are often dense and granular.
- Lumenal crystalloids are long thin eosinophilic structures seen in a range of prostate conditions, but more commonly in carcinoma.

### 3.4.7. Grade

The grade of a carcinoma refers to the degree of deviation from normal behavior of the tumor, or the likely malignant potential. Low-grade tumors have low malignant potential and tend to be organ confined at presentation, whereas high-grade tumors tend to be anaplastic, poorly differentiated, and behave very aggressively with rapid local infiltration and metastatic potential. There are a number of grading systems used in prostatic carcinoma. The most widely used system is Gleason grading.

The Gleason grading system is a relatively simple system masked in complexity and mysticism. It is based on architectural pattern alone (*see* **Note 4**) ***(11,12)***. Basically, a grade of 1 to 5 is applied to the pattern of the glandular architecture. Low-grade, well-differentiated tumors are grade 1, with increasing numbers to very poorly differentiated, high-grade tumors being grade 5 (*see* below). As prostatic adenocarcinoma usually has a range of appearances, there will be a dominant or primary pattern, and less common or secondary and tertiary patterns. Traditionally, the number of the dominant grade and the secondary grades are added together to give the Gleason Score, which is written as a sum out of 10. For example, if the most pronounced pattern is grade 3, with a secondary pattern of grade 4, then the Gleason Score is 7 (3 + 4 = 7). Recent studies, however, have resulted in a slight modification to this system ***(13)***. It has been shown that even a small amount of high-grade tumor results in a poorer prognosis ***(14)***. Therefore, the presence of even small areas of high-grade tumor should be included in the score. For example, if the primary and secondary grades are 3 and 2, but there are some areas of grade 4 carcinoma present, the Gleason Score is 7 (3 + 4 = 7) and not 5 (3 + 2 = 5).

Gleason grade 1 carcinoma is characterized by a localized area of carcinoma in a circumscribed, rounded mass or nodule with a smooth margin. The glands are small, single, and regular with little separation between each gland. Gleason grade 2 carcinoma is characterized by a localized, rounded area of carcinoma with single, separate, round glands in a loose, slightly separated

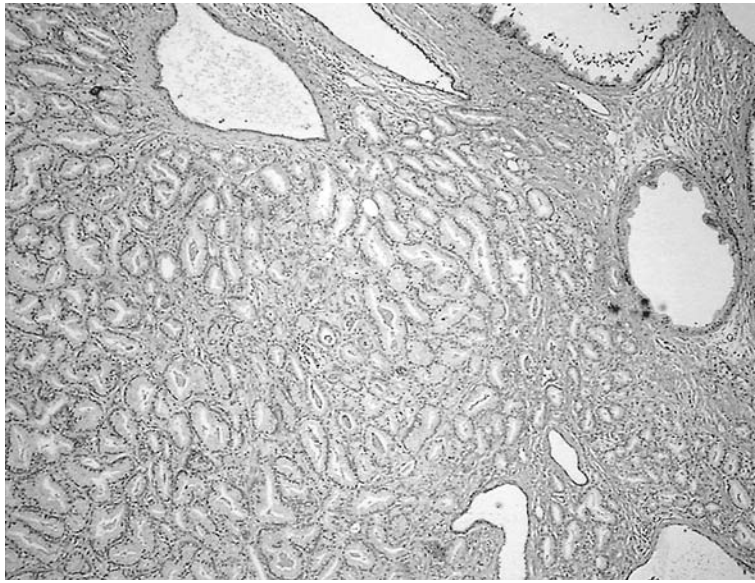

Fig. 2. Prostatic carcinoma, Gleason grade 2 (H&E, ×4).

arrangement. The glands are separated from each other by no more than the diameter of the glands. The margin of the nodule may be slightly irregular, with minor infiltration at the edges (*see* **Fig. 2**).

Gleason grade 3 carcinoma is characterized by infiltrative growth pattern between pre-existing benign glands. Glands are single and separated in an irregular manner. They are relatively uniform but are usually variable and irregular in outline (*see* **Fig. 3**).

There are subcategories recognized histologically, but these are not included in the final score numbering. Subcategory 3A has small glands, sometimes with loss of the lumen to form a solid small nest. Subcategory 3B has small, circumscribed papillary and cribriform areas. Gleason grade 4 carcinoma is characterized by an infiltrative growth pattern of fused or back-to-back glands that are very irregular in outline and distribution (*see* **Fig. 4**).

There are often large irregular cribriform areas. Subcategory 4B is composed of large clear or pale cells (hypernephroid) often in solid, nodular areas that appear more circumscribed. Gleason grade 5 carcinoma is characterized by large, irregular cribriform or solid areas with central necrosis (**Fig. 5A**) or infiltrating undifferentiated single cells with no gland formation (**Fig. 5B**).

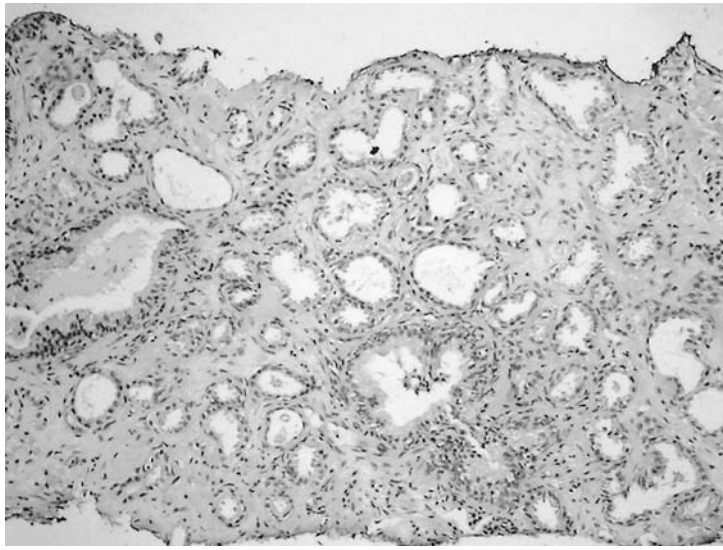

Fig. 3. Prostatic carcinoma, Gleason grade 3 (H&E, ×10).

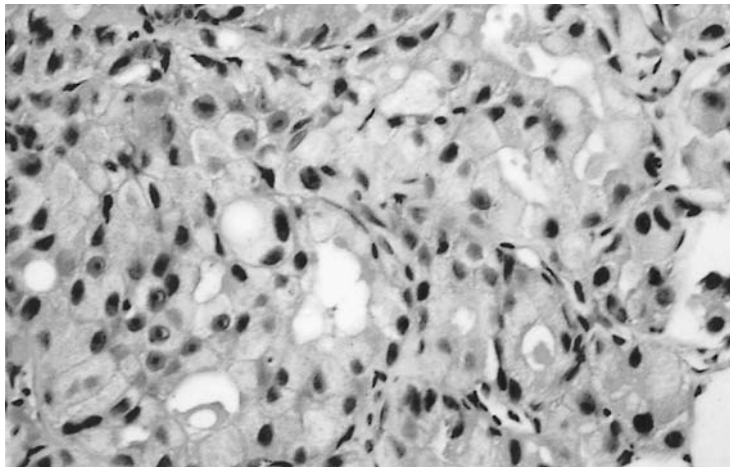

Fig. 4. Prostatic carcinoma, Gleason grade 4 (H&E, ×20).

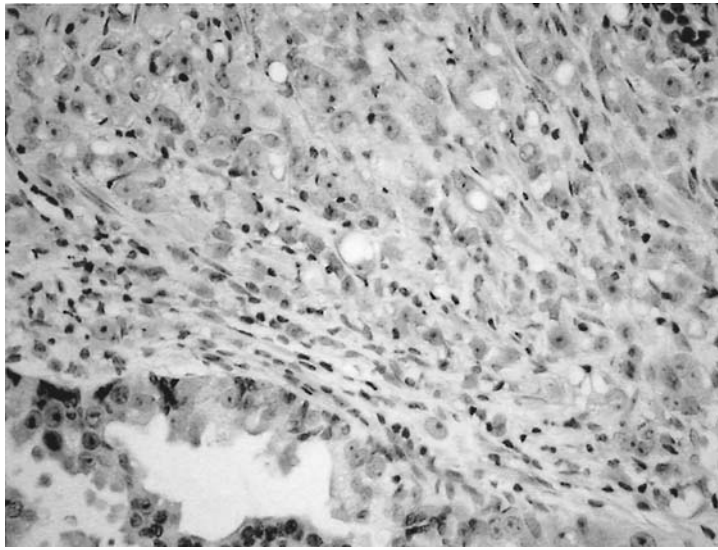

Fig. 5. Prostatic carcinoma, Gleason grade 5 (H&E, ×20).

### *3.4.8. Large-Duct/Ductal Carcinoma*

Large-duct carcinoma of the prostate is a specific subtype of prostate carcinoma that needs to be mentioned at this stage so as it can be recognized as an entity but also because of confusion with prostatic preneoplastic conditions. It is probably part of the spectrum of intraduct carcinoma (*see* **Subheading 3.5.3.**). It occurs mainly in the central portion of the prostate and may bulge or extent into the prostatic urethra. It is characterized by large glandular spaces having a papillary or endometrioid pattern. Many of the papillae have true fibrovascular cores. It may extend into the peripheral part of the prostate and is often associated with areas of small acinar carcinoma. Initially described as having a better prognosis, this is probably not true.

## *3.5. Preneoplastic Conditions*

The definition and even existence of prostatic adenocarcinoma precursors or preneoplastic conditions has been hotly debated for many years. It is now generally accepted that there is at least one identifiable condition that is a precursor of malignancy, with strong debate on a possible second ***(11,12,15–17)***.

### *3.5.1. Prostatic Intraepithelial Neoplasia (PIN)*

PIN is characterized by the proliferation or expansion of large glandular spaces lined by cytologically malignant cells. It occurs in pre-existent large

glands and ducts and is seen primarily in the peripheral or posterior part of the prostate. It is believed to be the precursor of small acinar carcinoma of higher-grade type. The pre-existent glands are expanded and lined by cytologically atypical cells, which appear cytologically malignant. It is divided into low grade and high grade and has a range of architectural patterns. The low-grade type is not proven to be clinically significant and is not reported. The high-grade type is characterized by malignant cells lining a pre-existent gland with either a tufted, micropapillary, cribriform, or flat architecture. It is usually associated with areas of invasive small acinar carcinoma. There is persistence of the basal cells, as seen on 34βE12 staining, at least in part.

#### *3.5.2. Adenosis*

Adenosis or atypical adenomatous hyperplasia is much more controversial, and its role as a precursor lesion is not confirmed. It is characterized by the proliferation of small acinar glands lined by cells lacking cytological features of malignancy. It has been proposed that this is the precursor lesion of low-grade prostate adenocarcinoma. There is persistence of basal cells on 34ßE12 stains, at least focally or partially.

#### *3.5.3. Intraduct Carcinoma*

Although not strictly a precursor lesion, the entity of intraduct carcinoma needs to be mentioned at this point. This entity is characterized by large cribriform and papillary areas with features of PIN. It is usually present, however, in larger areas and extends from the peripheral to central zones. It is proposed that this represents a particular type of growth of carcinoma that is associated with poor prognosis ***(18–20)***. There is persistence of basal cells on 34βE12 staining.

### *3.6. Pseudoneoplastic Conditions*

Many benign conditions have features that are easily mistaken for carcinoma and should always be considered and excluded before a diagnosis of carcinoma is made ***(11)***.

#### *3.6.1. Prostatic Hyperplasia (Benign Myoadenomatous Hyperplasia)*

Hyperplasia of glands, stroma, and muscle is very common in the prostate, particularly in middle-aged to elderly males. It is characterized by nodular areas of proliferation of glands, muscle, and stroma. Glands can show papillary and cribriform areas but lack cytological features of malignancy.

#### *3.6.2. Basal Cell Hyperplasia*

Proliferation of the basal cells can result in multilayering that is suggestive of PIN or carcinoma. There is absence of cytological features of malignancy.

Stains for 34βE12 (*see* **Note 2**) are strongly positive and help in not making a diagnosis of malignancy. Rare types of basal cell neoplasia can occur.

### *3.6.3. Atrophy*

Atrophy may be either simple or disorganized and called postatrophic hyperplasia. The presence of irregular, small, disorganized glands can easily be mistaken for carcinoma. There is, however, an absence of cytological features of malignancy and persistence of basal cells on 34βE12 staining (*see* **Note 2**).

## 4. Notes

1. Paint TRUS biopsies to visualize in paraffin block and ensure all tissue is cut in a single plane.
2. Immunoperoxidase for high molecular weight cytokeratin demonstrating basal cells should be performed in all cases with atypical glands suspicious for malignancy.
3. Do not go straight to high-power microscopy to diagnose malignancy. All cells look higher grade on high power.
4. If in doubt when diagnosing malignancy anywhere in the body, follow the below sequence for further investigation:
   - Ask for clinical history (PSA, past history, family history)
   - Take more blocks
   - Cut deeper levels on the available blocks
   - Do special stains (mucus)
   - Do immunoperoxidase stains
   - Would flow cytometry be useful (e.g., lymphoma)?
   - Would immunofluorescence be useful (not relevant in prostate)?
   - Would electron microscopy be useful (to define cell differentiation)?
   - Diagnostic feature clues
     - Major
     - Minor
     - Special stains/ipx
   - Gleason grading of carcinoma is summarized as follows:
     - (1) circumscribed areas of small, regular glands;
     - (2) relatively circumscribed areas of small, regular, slightly separated glands;
     - (3) infiltrative growth of single, irregular glands;
     - (4) infiltrative growth of fused/back-to-back glands;
     - (5) infiltrative growth of single, undifferentiated cells or large masses with necrosis.

## References

1. Murphy, W. M., Dean P. J., Brasfield, J. A., and Tatum, L. (1986) Incidental carcinoma of the prostate. How much sampling is adequate? *Am. J. Surg. Pathol.* **10,** 170–174.
2. Rogatsch, H., Moser, P., Volgger, H., Horninger, W., Bartsch, G., Mikuz, G., et al. (2000) Diagnostic effect of an improved preembedding method of prostate needle biopsy specimens. *Hum. Pathol.* **31,** 1102–1107.

3. Bostwick D. G. and Montironi, R. (1997) Evaluating radical prostatectomy specimens: Therapeutic and prognostic importance. *Virchows Arch.* **430,** 1–16.
4. Epstein, J. I., Partin, A. W., Sauvageot, J., and Walsh, P. C. (1996) Prediction of progression following radical prostatectomy. A multivariate analysis of 721 men with long-term follow-up. *Am. J. Surg. Pathol.* **20,** 286–292.
5. Lerner, S. E., Blute, M. L., Bergstralh, E. J., Bostwick, D. G., Eickholt, J. T., and Zincke, H. (1996) Analysis of risk factors for progression in patients with pathologically confined prostate cancers after radical retropubic prostatectomy. *J. Urol.* **156,** 137–143.
6. Iczkowski, K. A., Cheng L., Crawford, B. G., and Bostwick, D. G. (1999) Steam heat with an EDTA buffer and protease digestion optimizes immunohistochemical expression of basal cell-specific antikeratin 34-Beta-E12 to discriminate cancer in prostatic epithelium. *Mod. Pathol.* **12,** 1–4.
7. Cohen, R. J., McNeal, J. E., Edgar, S. G., Robertson, T., and Dawkins, H. J. S. (1998) Characterisation of cytoplasmic secretary granules in prostatic epithelium and their transformation induced loss in dysplasia and adenocarcinoma. *Hum Path.* **29,** 1488–1494.
8. Cohen, R. J., McNeal, J. E., Redmond, S. L., Meehan, K., Thomas, R., Wolce, M., et al. (2000) Lumenal contents of benign and malignant prostate glands: correspondence to altered secretary mechanisms. *Hum. Path.* **31,** 94–100.
9. Cotran, R. S., Kumar, V., and Collins, T. (1999) Neoplasia, in *Robbins Pathologic Basis of Disease*, 6th ed, (Cotran, R. S., Kumar, V. and Collins, T., eds.), WB Saunders Company, Philadelphia, pp. 260–271.
10. McNeal, J. E. (1992). Prostate, in *Histology for Pathologists* (Sternberg, S. S., ed.), Raven Press, New York, pp. 749–763.
11. Bostwick, D. G. (1997) Neoplasms of the prostate, in *Urologic Surgical Pathology* (Bostwick, D. G. and Eble, J. N., eds.), Mosby, St. Louis, pp. 343–421.
12. Young, R. H., Srigley, J. R., Amin, M. B., Ulbright, T. M., and Cubilla, A. L. (2000) Tumours of the prostate gland, seminal vesicles, male urethra and penis, in *Atlas of Tumor Pathology*, Third Series, Fascicle 28, Armed Forces Institute of Pathology (AFIP), Washington.
13. Yang, X. J., Lecksell, K., Potter, S. R., and Epstein, J. I. (1999) Significance of small foci of Gleason score 7 or greater prostate cancer on needle biopsy. *Urology* **54,** 528–532.
14. Pan, C., Potter, S.R., Partin, A. W., and Epstein, J. I. (2000) The prognostic significance of tertiary Gleason patterns of higher grade in radical prostatectomy specimens: a proposal to modify the Gleason grading system. *Am. J. Surg. Pathol.* **24,** 563–569.
15. McNeal, J. E. and Bostwick, D. G. (1986) Intraduct dysplasia: A premalignant lesion of the prostate. *Hum. Pathol.* **17,** 64–71.
16. Weinstein, M. H. and Epstein, J. I. (1993) Significance of high grade PIN on needle biopsy. *Hum. Pathol.* **24,** 624–629.
17. Kappel, T. J., Kuskowski, M., Willmott, L., and Cherwitz, D. L. (1995) Prostatic intraepithelial neoplasia and atypical adenomatous hyperplasia (adenosis). *J. Surg. Pathol.* **1,** 77–85.

18. McNeal, J. E. and Yemoto, C. E. M. (1996) Spread of adenocarcinoma within prostatic ducts and acini. *Am. J. Surg. Pathol.* **20,** 802–814.
19. Wilcox, G., Soh, S., Charkaborty, S., Scardino, P. T., and Wheeler, T. M. (1998) Patterns of high grade prostatic intraepithelial neoplasia associated with clinically aggressive prostate cancer. *Hum. Pathol.* **29,** 1119–1123.
20. Cohen, R. J., McNeal, J. E., and Baillie, T. (2000) Patterns of differentiation in intraduct carcinoma of the prostate: Significance for cancer progression. *Prostate* **43,** 11–19.

# 12

# Realizing the Potential of Ejaculate/Seminal Fluid in Detecting and Predicting Natural History

**R. A. Gardiner, Michelle Burger, Judith A. Clements, and Martin F. Lavin**

## 1. Introduction

### *1.1. Current Practice*

The widespread acceptance of prostate-specific antigen (PSA) testing by clinicians as evidence of prostatic pathology and recognition that elevated levels in serum often precede overt disease has permitted a much earlier identification of patients with prostatic epithelial changes, particularly cancer. Prostate cancer patients thus identified are very often asymptomatic with clinically benign prostates on digital rectal examination.

Transrectal ultrasound (TRUS) examination of the prostate had been refined over a number of years but, by itself, remains unreliable as a method for diagnosing prostate cancer. However, a useful role for TRUS in diagnosis evolved after the popular acceptance of PSA testing because it enabled spatial positioning of spring-loaded biopsy needles and provided a more objective approach to obtaining tissue core samples than was previously possible.

### *1.2. Limitations of PSA/TRUS Biopsy Approach*

TRUS-guided biopsies of the prostate provide tissue cores that are examined using standard histological techniques. Unfortunately, a significant proportion of malignancies are missed with this method of diagnosis and, recently, a minimum of eight biopsies has been advocated (with further biopsies for larger glands), as opposed to the empirically derived sextant cores recommended in the past ***(1–3)***.

Over the past 15 yr, information provided from TRUS biopsies has been scrutinized to try to provide prognostic information that is arguably even more

From: *Methods in Molecular Medicine, Vol. 81: Prostate Cancer Methods and Protocols*
Edited by: P. J. Russell, P. Jackson, and E. A. Kingsley © Humana Press Inc., Totowa, NJ

important than the diagnosis of cancer itself. Despite exhaustive analyses, which are ongoing ***(4)***, this approach remains less than perfect in terms of predictability. Furthermore, even with a low PSA trigger of <4 μg/L as an indication for biopsy, tumor burden remains considerable. A recently proposed PSA cutoff of 3 μg/L would certainly help to diagnose the condition earlier but inevitably would increase the number of TRUS biopsies performed on men without cancer as a consequence—despite taking into account free/total PSA ratios in sera and transition zone measurements ***(5–8)***.

Thus, although current methods of diagnosis enable earlier detection, most patients at diagnosis continue to have considerable tumor volume. Furthermore, the adaptations alluded to above appear unlikely to be able to provide the quantum leap necessary for providing a high diagnostic sensitivity and specificity at the same time as detecting the tumor considerably earlier and providing improved prognostic information for the treating clinician and the patient.

### 1.3. Rationale

Because the PSA/TRUS-driven approach to diagnosis that dominates clinical detection of prostate cancer is invasive, expensive, and imprecise, we have been examining ejaculate as an alternative approach over the past few years. Our operating hypothesis is that the exocrine effluent of the prostate, expelled with vigorous prostatic smooth muscle contraction during ejaculation, reflects cellular perturbations accurately and is consequently the most relevant biological material to examine in early diagnosis. In our studies, we have examined both the epithelial cellular and the supernatant components as separate entities.

This chapter describes methods developed to analyze genes and proteins in ejaculate as a means for determining early detection of prostate cancer and for prognosticating, so that available treatments may be tailored more effectively and appropriately for individual patients.

### 1.4. Cytology

The initial observation, which alerted us to the likely diagnostic value of seminal fluid, was cytological ***(9)***. Confirmed by others, we have demonstrated unequivocally the potential of the cellular component of ejaculate for diagnosing and characterizing prostatic cancer ***(9–11)***.

Cytologically, using morphological, architectural, and phenotypic criteria, atypical or frankly malignant cells were identified in specimens from approximately two-thirds of prostate cancer patients ***(9,10)*** (*see* **Fig. 1**).

Significantly, abnormal cytological findings were evident up to 2 yr before detection of cancer by repeated TRUS-guided biopsies. Furthermore, many of the patients with false-positive results have subsequently had positive biopsies that demonstrated histological evidence of cancer.

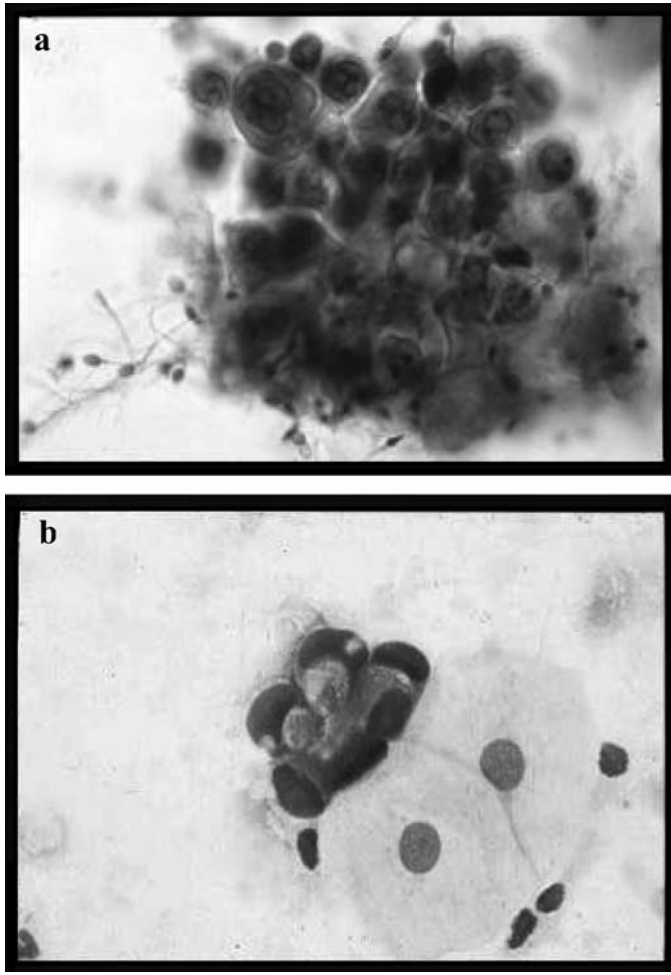


Fig. 1. Low-powered photomicrographs illustrating prostatic cancer cells in ejaculate. **(A)** Note the rounded, hyperchromatic nuclei and relatively scanty cytoplasm of the aggregated cells. Sperm are evident in the section. **(B)** Microacinar formation, a characteristic of prostate cancer, is evident. (Figure reproduced with permission from Gardiner et al., *Br. J. Urol.* **78,** 414–418.)

### *1.5. Confirmation of Prostatic RNA in Ejaculate and Urethral Washings*

It was then confirmed that adequate numbers of prostatic cells are present in seminal fluid and urethral washings (voided urine immediately after ejaculation) using adaptations of standard molecular techniques ***(12)***. In this study, 94% of 80 ejaculate and 90% of 52 urethral washings specimens from 67

patients who subsequently underwent TRUS-guided biopsies were positive for PSA reverse-transcription polymerase chain reaction (RT-PCR). No differences in PSA positivity were observed for men who had been vasectomized, indicating little or no contribution to the PSA-positive cells from the testes. All urine specimens from five men, who had radical prostatectomies, and 10 women were negative for PSA RT-PCR, illustrating the prostate-specificity of this approach ***(12)***.

### 1.6. Sensitivity of RT-PCR Analysis

After demonstrating unequivocally that adequate numbers of prostatic cells were present in the large majority of ejaculate and urethral washings from middle-aged and elderly men suspected of harboring prostate cancer, the next step was to establish the sensitivity of our modified approach. This was determined by the addition (spiking) of human prostate tumor LNCaP cells to female urine and performing RT-PCR for PSA. As few as 10 LNCaP cells were detected by PSA RT-PCR in these urine samples ***(12)***.

Although these findings substantiated the hypothesis that prostatic cells are present in both ejaculate and postejaculate urethral washings in adequate numbers for discriminating analyses by RT-PCR and that this method is sufficiently sensitive for examination of this body fluid, differentiation of malignant cells is not possible using PSA RT-PCR. Consequently, the next phase of the research has been focused on identifying discriminating molecular markers to establish a predictive profile to permit accurate prediction of the natural history of individual patients' tumors.

### 1.7. Gene-Based Diagnostic Approaches

Although a considerable number of molecular changes have been reported in prostate cancer, these changes have all been studied in tissues; therefore, their utility in the context of a diagnostic profile in ejaculate is unknown. Many of these will not be suited to this purpose because of a low abundance of altered expression of individual genes, even in tumor-rich tissue specimens, or they are not expressed in the tumor cells *per se*. In other words, potentially useful genes must be significantly upregulated (or downregulated) by the majority of prostatic epithelial cells, or of clonal groups within the tumor, to be expected to be represented in the population of prostate cancer cells retrieved from ejaculate. Consequently, careful selection is essential in choosing appropriate candidates for detailed evaluation.

The introduction and availability of real-time PCR, which enables detection of quantitative differences in gene products, has considerably increased the diagnostic potential of PCR. Thus, relative differences in expression are pertinent. The use of quantitative PCR lessens the reliance on the relatively uncom-

mon occurrence of tumor-specific epithelial changes with malignancy. As a consequence, a number of putative markers {such as PTI1 ***(13)***, insulin growth factors 1 and 2 [IGF-1 and IGF-2] ***(14,15)***, bone morphogenetic protein 6 [BMP-6] ***(16–19)***, and somatostatin receptor-1 [SSTR1] ***(20)***}, previously discounted after qualitative RT-PCR evaluation in our laboratory, warrant revisiting with quantitative PCR analyses to examine possible differential expression between benign and malignant specimens. Further potential candidates being considered for screening studies are included in the **Notes** section.

### 1.8. Microarray Profiling

In addition to critically evaluating potential candidates cited in the scientific literature, it is most desirable to identify additional genes useful for the detection and characterization of prostate cancer so that the best profile may be collated using as few markers as is necessary. Until recently, differential display PCR was the commonest method used for detecting differences in gene expression but, since the advent of microarray approaches, the role for differential display has become limited. We have used cDNA microarray profiling and real-time RT-PCR to identify genes that are potential candidates for use in prostate cancer detection and treatment. Using this approach, we have identified two genes, δ-catenin and prostate-specific membrane antigen (PSMA; PSMA also having been reported previously by others), which are overexpressed in prostate cancer compared with specimens from men with benign prostatic hyperplasia (BPH) ***(21)***.

### 1.9. Supernatant Analyses

In addition, studies on ejaculate supernatant have been performed examining the proposal that changes in the ratio of free/total PSA in ejaculate may reflect the presence of malignancy, as it does in serum, and that the magnitude of these changes reflects tumor burden in the prostate, a parameter which can not be appreciated by identifying molecular changes. Thus, alterations in supernatant at the protein level promise to complement molecular aberrations in maximizing clinical information provided.

The function of PSA in seminal fluid is considered to be to process substrates, such as the seminal vesical-derived proteins, seminogelin I and II, and fibronectin, thus aiding in the rapid dissolution of the seminal coagulum ***(22, 23)***. In ejaculate, the proportion of PSA bound to the inhibitor, α-1 antichymotrypsin ($\alpha_1$ACT), is the reverse to that in serum in which greater than 80% is bound. Indeed, almost all PSA in seminal fluid is in the free state (or smaller forms), presumably reflecting its prime site of activity, with the small amount of complexed PSA bound primarily to protein C inhibitor and, to a lesser degree, to $\alpha_2$-macroglobulin ***(24,25)***. Of interest, $\alpha_1$ACT, which is produced

predominantly by the liver but also by prostatic cells ***(26,27),*** is present together with high levels of PSA in prostatic fluid, but PSA-ACT complexes are thought not to occur, possibly caused by the presence of inhibitors ***(28,29)***.

The findings from our preliminary work indicated that, although free/total PSA ratios in ejaculate supernatant did not demonstrate a conclusive difference between patient groups ***(29),*** this relationship warrants further investigation (*see* **Notes 1–5**). As further protein markers are identified, in particular kallikrein/PSA-related gene products, these will be studied.

### 1.10. Other Approaches

Recently, Wang and coworkers ***(30)*** reported their findings from a pilot study using expressed prostatic fluid obtained from anaesthetized patients in which telomerase activity was determined using the telomeric repeat amplification as previously described ***(31)***. They found telomerase activity in 25 of 30 prostate cancer patients, but no activity was detectable in specimens from eight of nine patients who did not have clinical evidence of prostate cancer ***(30)***. Examining cell-enriched samples of ejaculate, Suh and coworkers ***(32)*** were unable to detect telomerase-positive cells using the telomeric repeat amplification assay from any prostate cancer patients, although this assay was positive for all nine samples spiked with LNCaP cells ***(32)***.

Using magnetic resonance spectroscopy, Lynch and Nicholson ***(33)*** examined prostatic fluid obtained by prostatic massage from anesthetized patients (10 men with BPH, 4 with prostate cancer, and 12 controls). They found a significant difference for the citrate to spermine ratio in specimens from patients with prostate cancer who had higher levels of spermine. Eleven patients with established aplasia also produced ejaculate specimens. No difference was seen between samples obtained by expression or ejaculation ***(33)***.

### 1.11. Conclusion

Our current thrust is directed to extending molecular studies to develop a discriminating profile of upregulated (or downregulated) genes identified in the scientific literature and from our microarray studies to use on an enriched population of prostatic epithelial cells from cell pellets. We foreshadow that a discriminating profile of molecular markers will provide diagnostic and prognostic information currently not available. Protein analyses of the supernatant component of ejaculate, particularly of the gene products of the PSA/kallikrein family, promise to indicate changes correlating with prostatic tumor burden. Thus, the molecular and protein supernatant contributions to diagnosis are expected to be complementary rather than competitive. Consequently, it is anticipated that the use of ejaculate will become routine in detect-

ing prostate cancer and in prognosis so that treatment approaches may be optimized for individual patients.

## 2. Materials

### *2.1. Sample Collection and RNA Extraction*

1. Human ejaculate/seminal fluid (*see* **Note 1**).
2. Urethral washings from voided urine immediately after ejaculation.
3. Percoll gradient column (1.08 g/mL).
4. HPV-transformed cell line (used as control for microarray) (*see* **Note 2**).

### *2.2. Cell Enrichment*

Simply applying established methods for detecting molecular changes in seminal fluid samples fails to take into account inapparent complexities, even in specimens from vasectomized males; this has also been recognized by others ***(32)***. To maximize the availability of prostatic epithelial cells present in the samples, they must first be separated from sperm, sperm precursors, inflammatory, and urothelial cells

A Percoll gradient column (1.08 g/mL) is used to separate mononuclear cells (particularly urothelial cells) from sperm and other constituents of ejaculate.

1. Load 1 mL of resuspended cell pellet over 2 mL of Percoll/medium solution and centrifuge for 30 min at 300*g* and 4°C.
2. Remove isolated mononuclear cells at the interface between the two layers using a curved glass pipet and store in medium containing 10% glycerol at –70°C.

Given the association of PSMA (prostate specific membrane antigen) and tumors ***(34–37)***, we plan to further enrich prostate cancer cells using a PSMA antibody by the use of a modified magnetic bead/PSMA antibody approach subsequent to the use of a Percoll gradient (Dynal™ Pty Ltd).

### *2.3. Microarray/Real-Time PCR*

Altered gene expression as detected molecularly may be from prostatic epithelial or stromal cells, including cells from the supporting vasculature. Therefore, *in situ* hybridization or immunohistochemical studies on tissue sections are a prerequisite before proceeding to consider these gene products as candidate markers for the examination of disaggregated cells in ejaculate.

## 3. Methods

### *3.1. Sample Collection*

1. Ejaculate is directed into 20 mL of Hank's balanced salt solution with the urethral washings voided into a sterile microurine container. Because seminal fluid is rich in

enzymic activity, obtaining fresh specimens is of paramount importance. Specimens must be processed within 2 h of collection.
2. Separate the cellular and supernatant components by centrifugation at 700*g* and 4°C for 10 min in 50-mL Falcon® tubes, then store at –80°C. If urine samples do not appear to have a pellet, then 250 µL of the lowermost urine is used.

### 3.2. Confirmation of Prostatic Cellular RNA in Seminal Fluid and Urethral Washings

Reproducible methods for extracting and isolating RNA and confirming that it is of prostatic origin have been developed as follows.

#### 3.2.1. RNA Extraction of Fresh Samples

1. For every 0.1 g of pellet or 150 µL of urine, reference prostate tissue samples or cell lines, add 1 mL of TRI reagent, vortex, and aliquot 1-mL samples into 1.5-mL microcentrifuge tubes for separate processing until the final resuspension. RNA is extracted according to the manufacturer's protocol. Perform all procedures on ice.
2. Precipitate at –20°C for ≥1 h.
3. Wash the final pellet twice in ice-cooled 75% ethanol, dry at 60°C, and resuspend.

#### 3.2.2. cDNA Synthesis

1. Eight microliters (of 32 µL) total RNA from ejaculate or urine specimens or 2 µL of tissue or cell line RNA is incubated with 1 µL of random hexamers (250 ng/µL; Pharmacia), with sterile water added to a final volume of 10 µL at 70°C for 10 min and then placed on ice.
2. Add a 10-µL aliquot of cDNA synthesis master mix (2X First Strand Buffer, Gibco; 0.02 *M* dithiothreitol (DTT), Gibco; and 1 mL of dNTP mix [dATP, dTTP, dCTP, dGTP]) and incubate for 10 min at 25°C followed by 2 min at 42°C.
3. Add 160 U of Superscript II reverse transcriptase (Gibco) for an additional incubation at 42°C for 75 min, followed by a 15 min 70°C heat inactivation.
4. Then, place the cDNA synthesis reaction on ice, centrifuge at 12,000*g* and store at –80°C. Use a negative control (RNA replaced with resuspension solution) to detect any DNA contamination.

#### 3.2.3. $\beta_2$-Microglobulin PCR

The quality of extracted RNA is verified by PCR amplification of the above cDNA for the transcript of a ubiquitously expressed gene, $\beta_2$-microglobulin.

1. The reaction conditions are 1.2 µ*M* of each primer (exon 2 sense, genomic nucleotides 1401–1422: 5′-TGAATTGCTATGTGTCTGGGT-3′ and exon 3 antisense, genomic nucleotides 2241 to 2262: 5′-CCTCCATGATGCTGCTTACAT-3′), 2 m*M* $MgCl_2$ , 200 µ*M* of each dNTP, 0.5 U AmpliTaq (Perkin Elmer), 1X PCR buffer II (Perkin Elmer), and 0.5 µL of the above cDNA samples in a 25-µL total

reaction volume. Thermal cycling conditions are 94°C (2 min), 40 cycles of 94°C (45 s), 54°C (90 s), and 72°C (35 s), followed by final extension at 74°C (10 min).
2. Electrophorese PCR products on a 1.5 % agarose gel in 0.04 *M* Tris/0.02 *M* acetic acid/0.001 *M* EDTA (TAE) with 0.5 mg/mL ethidium bromide. The expected size of the $\beta_2$-microglobulin PCR product is 248 bp.

### *3.2.4. PSA PCR*

1. Set up 0.8 µ*M* of each primer (5′ untranslated region sense, cDNA nucleotides 20 to 37: 5′-GCACCCGGAGAGCTGTGT-3′ and exon 2/3 overlap, antisense, cDNA nucleotides 1475–1482/3111–1123: 5′-GATCACGCTTTTGTTCCTGAT-3′) with 1 U AmpliTaq (Perkin-Elmer) and 1.0 µL of the above cDNAs in a 20-µL reaction. Incubate the tubes at 94°C for 2 min, followed by 37 cycles at the above conditions (*see* **Subheading 3.2.3.**), except for an annealing temperature of 55°C. The expected size of this PCR product is 250 bp.

### *3.2.5. DNA Sequencing*

To confirm the specific amplification of the PSA transcript, DNA sequencing is performed on PSA PCR products from three different samples (prostate tissue, ejaculate collected in Hank's, and urine) obtained from three different non-vasectomized subjects. Excise the PCR bands from the 1.5% agarose gel (*see* **Subheading 3.2.3.**), purify on Qiagen gel spin-clean columns, and sequence using the recommended protocol for the ABI nucleotide fluorescence sequencer. The 5′UT PSA PCR forward primer is used as the sequencing primer.

## *3.3. Microarray Profiling*

1. Examine the outermost edges of the collected samples for molecular analysis by histology and confirm whether the sample has BPH or malignancy (together with its Gleason score).
2. Homogenize tissue fragments using a Polytron PK® homogenizer, in 1 mL TRI of reagent per 50 mg of tissue and subsequently extract RNA using the recommended protocol.
3. Resuspend total RNA is resuspended in 10 m*M* DTT with 40 U Rnase-OUT to a final concentration of 1 µg/µL and store at –70°C.

### *3.3.1. Identification of Overexpressed Genes Using Filter Arrays*

1. Hybridize ATLAS™ Cancer 2.0 Arrays (1176 human genes, Clontech) and Genefilters™ (3408 Human genes, Research Genetics) with total RNA labeled with [$\alpha$-$^{33}$P]dATP by reverse transcription. Incubate 3 µL of total RNA/primer mix (2–5 µg of total RNA and 1X CDS primer mix, Clontech) at 70°C for 2 min and chill on ice.
2. Incubate the RNA/primer mix at 37°C for 2 min.

3. Add the mix to a 10-µL reverse transcription reaction (1X First Strand Buffer, Gibco-BRL; 1X dNTP mix (for dATP), Clontech; 3.5 µL [$\alpha$-$^{33}$P]dATP (3000 Ci/mmol, 10 Ci/mL); 5 m*M* DTT, and 200 U Superscript II™, Gibco-BRL) and incubate at 37°C for 90 min.
4. Add termination mix (Clontech).
5. Make up the probes to 50 µL with sterile TE buffer (50 m*M* Tris-HCL (pH 7.0); 10 m*M* EDTA) and purify using ProbeQuant™ spin columns (Promega).
6. Collect the eluent and heat at 100°C for 3 min.
7. Rinse the filters with dd$H_2O$ and prehybridize with 0.5 mg of sheared salmon testes DNA in 5 mL ExpressHyb solution (Clontech) per sample at 42°C for 60 min in a Hybaid oven.
8. Mix the 50-µL probe with 5 µL of 10X denaturing solution (1 *M* NaOH, 10 m*M* EDTA) and incubate at 68°C for 20 min. Add 5 µL of Cot 1 DNA 1 (1 µg/µL) and 60 µL 2X neutralizing solution (1 *M* $NaH_2PO_4$, pH 7) and incubate the probe at 68°C for another 10 min.
9. Add the probe to the prehybridized filter and allow to hybridize at 42°C overnight. Wash the hybridized filters twice for 30 min at 50°C in 2X SSC buffer (0.15 *M* sodium chloride and 15 n*M* Tri-sodium citrate): 1% SDS and twice for 30 min at 50°C in 0.1X SSC, 0.5% SDS.
10. Then, expose the moist filters on Phosphoimager cassettes overnight. Arrays are visualized and quantified using the Phosphoimager software Imagequant, and further analysis is performed with EXCEL. Select genes that are consistently overexpressed in all prostate cancer samples, threefold or higher than the nontumor control, for further analysis.

### *3.3.2. Identification of Overexpressed Genes with Glass Slide Arrays*

1. Label 30 µg of prostate tissue (tumor or BPH) total RNA, isolated as described above (*see* **Subheading 3.2.1.**), with Cyt5 dUTP (Amersham) by reverse transcription using primer $p(DT)_{15}$ (Roche) and Superscript II (Gibco-BRL).
2. Add termination mix (1.25 m*M* EDTA, 0.1 *M* NaOH) and incubate at 65°C for 10 min.
3. Add neutralization solution (0.1 *M* HCL, 0.1 *M* Tris, pH 8.0) and purify the labeled cDNA using a QIAquick™ PCR purification kit (Qiagen).
4. Use 30 µg of a transformed normal cell line, PZ-HPV-7 (ATCC), as an internal reference and label with Cy3 dUTP (Amersham) and purify as described. Add the reference cDNA to the Cy5-labeled cDNA and hybridize overnight at 42°C in 50% deionized formamide (AmrescoO), 4X SCC, and 0.25% SDS onto a Human V6 custom microarray prepared at the Queensland Institute of Medical Research.
5. Wash the slides once in 0.2X SSC; 0.05% SDS at room temperature, twice in 0.2X SSC at room temperature; and scan with a GMS 418 Array Scanner (Genetic Microsystems). The data are analyzed with Imagene™ (Biodiscovery, Inc) and GeneSpring™ (GeneWorks) software packages. Select genes that are consistently overexpressed in all prostate cancer specimens, threefold or higher than the BPH sample, for further analysis.

### *3.3.3. Real-Time PCR*

Genes identified on the arrays and candidate genes are screened against larger numbers of prostate adenocarcinoma and BPH samples. Primers for these genes have been designed using Taqman (PE Biosystems) guidelines and optimized using Amplitaq Gold.

1. Check cDNA prepared from 1 µg of original RNA stocks using standard protocols by PCR using Amplitaq Gold™ (94°C 10 min hot start; 94°C for 30 s, 58°C for 30 s, and 72°C for 30 s for 35 cycles) with primers for the housekeeping gene $\beta_2$-microglobulin.
2. After optimization, real-time PCR is performed in 15-µL reactions (cDNA; 0.6 µ*M* each primer; 1X SYBR Green® Master Mix (PE Biosystems) using the Rototgene real-time PCR machine (Corbett, Sydney Australia). The amplification protocol includes a 94°C for 10-min hotstart, 94°C for 5-s denaturing step, 58°C for 5-s annealing step, and 72°C for 10-s extension step for 35 cycles.
3. Analyze each marker against a standard curve determined by expression of the housekeeping gene $\beta_2$-microglobulin in the normal prostate epithelial HPV-18-transformed cell line, PZ-HPV-7, and standardize individual samples for differences in concentrations. Perform further statistical analysis using EXCEL and examine the ratios of gene expression/105 copies of $\beta_2$-microglobulin in samples of prostate cancer and BPH tissues.

## 4. Notes

1. It is our clinical experience that prostatic fluid is much more efficiently obtained by ejaculation than by prostatic massage. Others have also reported difficulty in expressing prostatic fluid from prostate cancer patients, even when anaesthetized ***(33)***. Ejaculation is physiological, easily repeated, and not hampered by the subjective and unpleasant exercise of digital compression. Because historically prostatic massage has resulted in poor yields of cells for cytological studies ***(38)***, we have not used this approach to collection.

   In addition to the ejaculate sample, urethral washings from voided urine immediately after ejaculation are collected because voided urine displaces residual seminal fluid remaining in the urethra. Furthermore, cells in this component are more likely to be from mitotically active acini furthest from the urethra, so that they may prove to be more important diagnostically than ejaculate alone. If so, this would be fortuitous because some men consider the provision of an ejaculate specimen unacceptable but are more than happy to provide urethral washings immediately after ejaculation.

   Initially, we explored the possibility of collecting specimens in a condom and having these placed immediately into home freezers (*see* **Fig. 2**).

   However, difficulties were encountered with RNA extraction and thawing; therefore, this strategy has been discarded. To date, specimens have been obtained from 392 men, of whom 240 underwent TRUS-guided biopsies subsequently. A

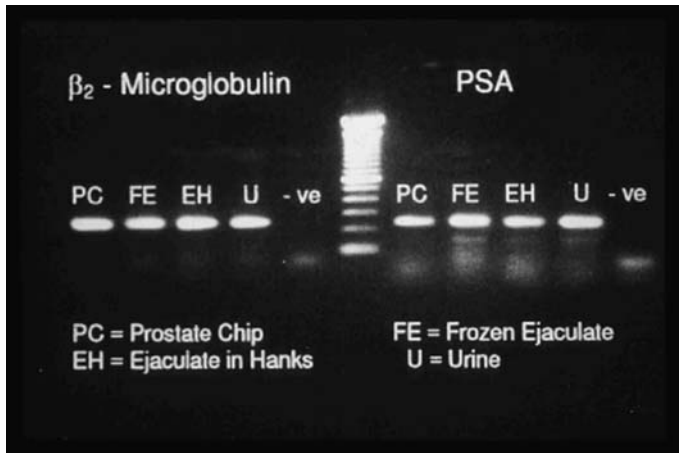


Fig. 2. Photograph demonstrating positive bands for $\beta_2$ microglobulin and PSA for tumor, ejaculate in Hank's solution, urethral washings, and frozen ejaculate.

total of 124 were diagnosed as having prostate cancer, and 41 men (<30 yr) without a family history of prostatic cancer have served as controls. It is our experience that the large majority of men proceeding to TRUS biopsies are able to provide specimens for these analyses.

2. It is difficult to obtain normal prostatic tissue as a reference. Berry and coworkers ***(39)*** reported that, from autopsy specimens, the first pathological signs of BPH are evident in prostates from men between 31 and 40 yr. In the absence of significant pelvic pathology, the only justification for operative removal of a normal prostate in men <25 yr is from donors at the time of organ harvesting for transplantation, after special consent has been arranged. For that reason, an HPV-transformed cell line is used as a routine when normal prostatic tissue is required. However, because the diagnostic reference clinically is BPH, it is arguably more appropriate to use BPH tissue for comparison in these studies.
3. In addition to members of the kallikrein gene family (detailed in another chapter of this volume), other prostate markers have been reported. PSMA gene expression has been detected in both benign tissue and prostate cancer. Unlike PSA, which is downregulated in prostate cancer, PSMA is upregulated in malignant prostatic cells ***(40)***. Other potential genes, such as those for the TURP-27 antigen, present in ductal epithelial cells of normal, benign, and malignant prostate cells ***(41)***; PR92 antigen, elevated in serum from patients with aggressive prostate and breast cancers ***(42)***; and the gene called PB39 and its splice variant, upregulated at the RNA level within prostate cancer cells, have been flagged as being sufficiently and abundantly overexpressed to be used in discriminating analyses ***(43)***. Certain gene families are of particular interest, with the cell-adhesion family of genes containing several markers potentially relevant. Expression of aberrant integrin $\alpha 6\beta 1$ with invasive prostate cancer cells ***(44)*** promises to be useful.

Some other observed molecular changes, reflecting different perturbations in function by prostate cancer cells, provide even further possible markers for consideration. These include upregulation at the RNA level of vascular endothelial growth factor, in particular isoform 189 ***(45,46)***, which is highly relevant in terms of neovascularization. Peroxisome proliferator-activated receptor α (a member of the nuclear receptor superfamily of ligand-activated transcription factors) is absent or only weakly expressed in benign prostatic epithelial cells. However, a recent study reported that expression was directly related to increasing Gleason score, with 61% Gleason 8 to 10 and 30% of Gleason 7 cells expressing peroxisome proliferator-activated receptor αcompared with <20% of tumors with low Gleason scores ***(47)***. ELAC2, a candidate prostate cancer susceptibility gene recently described and that maps to chromosome 17p, also warrants consideration ***(48)***.

DD3/PCA3 is a recently identified prostate-specific gene, expressed at low levels in normal prostate but highly expressed in tumor tissues. Using real-time RT-PCR, deKok et al. reported that DD3/PCA3, which is not translated, had a mean increase in expression of 54-fold in 24 tumor tissues compared with 10 healthy prostatic and five BPH tissues ***(49)***.

Recent studies have implicated the endothelin axis and in particular endothelin-1 (ET-1) in prostate cancer progression. This axis consists of three endothelin peptides (ET-1, ET-2, and ET-3) and two endothelin receptors ($ET_A$ and $ET_B$). ET-1 is produced by endothelial cells and normal prostatic epithelium with very high concentrations in normal ejaculate. ET-1 is overexpressed by CaP cells ***(50)***. In prostate cancer, the predominant endothelin receptor subtype shifts from $ET_B$ in normal prostate to $ET_A$. Through the $ET_A$ receptor, ET-1 stimulates the growth of CaP cells and acts synergistically with other growth factors ***(50,51)***.

Thus, these genes or their products are all very likely candidates as potential diagnostic and/or prognostic indicators in ejaculate, either in a molecular profile on shed cells or as secreted proteins. However, before they can be considered as useful discriminators, they need to be scrutinized with respect to their relative abundance in prostate cancer tissues and ranked in terms of their potential to complement other members of the profile.

4. The findings from our preliminary work indicated that, although free/total PSA ratios in ejaculate supernatant did not demonstrate a conclusive difference between patient groups, this relationship warrants further investigation.

   As detailed in our manuscript ***(29)***, antibodies from different companies were used in assaying for free and total PSA components. Furthermore, female serum was used as the diluent because the assays were performed in a commercial laboratory using assayers calibrated for establishing free/total PSA ratios in male serum. Consequently, we are revisiting this relationship using antibodies from the same manufacturer together with an assay specifically designed for use in seminal fluid, this being undertaken in collaboration with Drs. Wang, Rittenhouse, and Mikolajozk (Hybritech Corporation). We also recognize that evaluating changes in this relationship sequentially over a period of time may have a more pertinent role in the early diagnosis of prostate cancer ***(29)***.

5. A variety of spectroscopic techniques is available to provide information about the components of tissues ***(52–56)***.

   Magnetic resonance spectroscopy has been the form of spectroscopic analysis evaluated most extensively in prostate cancer. However, its main limitations are that it does not generate clearly resolved signals from molecules >10,000 Daltons, thus limiting analysis of many proteins, and volumes of at least 500 µL are required for analysis ***(33)***. Lynch and Nicholson examined prostatic fluid obtained by prostatic massage from anaesthetized patients (10 men with BPH, 4 with prostate cancer and 12 controls. They encountered difficulty expressing sufficient prostatic fluid from prostate cancer patients but found a significant difference for the citrate to spermine ratio in specimens from patients with prostate cancer who had higher levels of spermine ***(33)***.

   It has been known for a long time that citrate is highly abundant in the normal human prostate, residing mostly in the luminal spaces ***(57,58)***. In both primary and in secondary malignant prostate tissues citrate levels are significantly lower than in BPH and normal prostate in which citrate levels are extremely high ***(59,60)***. Furthermore, it is thought that the reduction in citrate precedes the morphological change to a malignant phenotype being present in premalignant cells ***(58,61)***.

   Lower levels of citrate in cancerous tissue have been attributed to a reduction of citrate secretion ***(57,62,63)***. In addition, it is proposed that normal prostate glandular epithelial cells are citrate producing: a high zinc accumulation prevents citrate oxidation in these cells. These cells contain a zinc transport mechanism responsible for intracellular accumulation of zinc. With neoplastic change, the prostate cell loses its ability to accumulate zinc, attributed to loss of a zinc transporter in the cell membrane. The inability to accumulate zinc leads to a reduction in intracellular zinc, which in turn results in removal of the zinc inhibition of citrate oxidation.

   The changes with malignancy studied spectroscopically relate predominantly to citrate alone or in relation to choline (and/or creatine) and, with few exceptions in vitro, involve solid tissue specimens ***(33,58,64)***. In contrast to the decrease in citrate, choline levels are generally increased in malignant areas ***(58,65)***. However, both spermine and zinc levels have been reported to be reduced in prostatitis, a not infrequent accompaniment of prostate cancer ***(66)***. We are planning to examine seminal fluid spectroscopically to build on the work of Lynch and Nicholson ***(33)***, who examined changes in prostatic fluid in disease using magnetic resonance spectroscopy, particularly in relation to changes in citrate, spermine, and choline.

## References

1. Presti, J. C. Jr, Chang, J. J., Bhargava, V., and Shinohara, K. (2000) The optimal systematic prostate biopsy scheme should include 8 rather than 6 biopsies: Results of a prospective clinical trial. *J. Urol.* **163,** 163–166.
2. Brossner, C., Bayer, G., Madersbacher, S., Kuber, W., Klingler, C., and Pycha, A. (2000) Twelve prostate biopsies detect significant cancer volumes (>0.5 mL). *BJU Int.* **85,** 705–707.

3. Naughton, C. K., Miller, D. C., Mager, D. E., Ornstein, D. K., and Catalona, W. J. (2000) A prospective randomized trial of 6 versus 12 prostate biopsy cores: Impact on cancer detection. *J. Urol.* **164,** 388–392.
4. Partin, A. W., Kattan, M. W., Subong, E. N., Walsh, P. C., Wojno, K. J., Oesterling, J. E., Scardino, P. T. and Pearson, J. D. (1997) Combination of prostate-specific antigen, clinical stage, and Gleason score to predict pathological stage of localized prostate cancer. A multi-institutional update. *JAMA* **277,** 1445–1451.
5. Catalona, W. J., Partin, A. W., Slawin, K. M., Brawer, M. K., Flanigan, R. C., Patel, A., et al. (1998) Percentage of free prostate-specific antigen to enhance differentiation of prostate cancer from benign prostatic disease: A prospective multicenter clinical trial. *JAMA* **279,** 1542–1547.
6. Djavan, B., Zlotta, A. R., Byttebier, G., Shariat, S., Omar, M., Schulman, C. C., and Marberger, M. (1998) Prostate specific antigen density of the transition zone for early detection of prostate cancer. *J. Urol.* **160,** 411–419.
7. Djavan, B., Zlotta, A., Kratzik, C., Remzi, M., Seitz, C., Schulman, C. C., and Marberger, M. (1999) PSA, PSA density, density of transition zone, free/total PSA ratio & PSA velocity for early detection of prostate cancer in men with serum PSA 2.5 to 4.0 ng/ml. *Urology* **54,** 517–522.
8. Djavan, B., Zlotta, A. R., Remzi, M., Ghawidel, K., Bursa, B., Hruby, S., et al. (1999) Total & transition zone prostate volume and age: how do they affect the utility of PSA-based diagnostic parameters for early prostate cancer detection? *Urology* **54,** 846–852.
9. Gardiner, R. A., Samaratunga, M. L. T. H., Gwynne, R. A., Clague, A., Seymour, G. J. S., and Lavin, M. F. (1996) Abnormal prostatic cells in ejaculates from men with prostatic cancer—a preliminary report. *Br. J. Urol.* **78,** 414–418.
10. Gardiner, R. A., Samaratunga, M. L. T. H., Rohde, P., Clements, J. A., Hyland, V., and Lavin, M. F. (1997) Re: malignant cytological washings from radical prostatectomy specimens: A possible mechanism for local recurrence of prostate cancer following surgical treatment of organ confined disease (letter). *J. Urol.* **158,** 889.
11. Barren, R. J. III, Holmes, E. H., Boynton, A. L., Gregorakis, A., Abdel-Aziz, A., Cobb, O. E., et al. (1998) Method for identifying prostate cells in semen using flow cytometry. *Prostate* **36,** 181–188.
12. Clements, J. A., Rohde, P., Allen, V., Hyland, V. J., Samaratunga, M. L. T. H., Tilley, W. D., et al. (1999) Molecular detection of prostate cells in ejaculate and urethral washings in men with suspected prostate cancer. *J. Urol.* **61,** 1337–1343.
13. Shen, R., Su, Z. Z., Olsson, C. A., and Fisher, P. B. (1995) Identification of the human prostatic carcinoma oncogene PTI-1 by rapid expression cloning and differential RNA display. *Proc. Natl. Acad. Sci. USA* **92,** 6778–6782.
14. Li, S. L., Goko, H., Xu, Z. D., Kimura, G., Sun, Y., Kawachi, M. H., et al. (1998) Insulin like growth factor 1 in human prostate, breast, bladder & paraganglioma tumors. *Cell Tissue Res.* **291,** 469–479.
15. Mantzoros, C. S., Tzonou, A., Signorello, L. B., Stampfer, M., Trichopoulos, D., and Adami, H. O. (1997) Insulin like growth factor 1 in relation to CaP and BPH. *Br. J. Cancer* **76,** 1115–1118.

16. Bentley, H., Hambdy, F. C., Hart, K. A., Seid, J. M., Williams, J. L., Johnstone, D., and Russell, R. G. (1992) Expression of bone morphognenetic proteins in human prostatic adenocarcinoma and benign prostatic hyperplasia. *Br. J. Cancer* **66,** 1159–1163.
17. Harris, S. E., Harris, M. A, Mahy, P., Wozney, J., Feng, J. Q., and Mundy, G. R. (1994) Expression of bone morphogenetic protein messenger RNAs by normal rat and human prostate and prostate cancer cells. *Prostate* **24,** 204–211.
18. Hambdy, F. C., Autzen, P., Robinson, M. C., Home, C. H., Neal, D. E., and Robson, C. N. (1997) Immunolocalization and messenger RNA expression of bone morphogenetic protein-6 in human benign and malignant prostatic tissue. *Cancer Res.* **57,** 4427–4431.
19. Barnes, J., Anthony, C. T., Wall, N., and Steiner, M. S. (1995) Bone morphogenetic protein-6 expression in normal and malignant prostate. *World J. Urol.* **13,** 337–343.
20. Sinisi, A. A., Bellastella, A., Prezioso, D., Nicchio, M. R., Lotti, T., Salvatore, M., et al. (1997) Different expression patterns of somatostatin receptor subtypes in cultured epithelial cells from human normal prostate and prostate cancer. *J. Clin. Endocrinol. Metab.* **82,** 2566–2569.
21. Burger, M..J., Mould, M., Samaratunga, H.M., Clements, J., Lavin, M.F., and Gardiner, R.A. (2002) Expression analysis of δ-catenin and prostate specific membrane antigen; their potential as diagnostic markers for Prostate Cancer. *Int. J. Cancer* **100,** 228–237.
22. Rittenhouse, H. G., Finlay, J. A., Mikolajczyk, S. D., and Partin A. W. (1998) Human kallikrein 2 (hK2) and prostate-specific antigen (PSA): Two closely related, but distinct, kallikreins in the prostate. *Crit. Rev. Clin. Lab. Sci.* **35,** 275–368.
23. Lilja, H., Oldbring, J., Rannevik, G., and Laurell, C.-B. (1987) Seminal vesicle-secreted proteins and their reactions during gelation and liquefaction of human semen. *J. Clin. Invest.* **80,** 281–285.
24. Christensson, A. and Lilja, H. (1994) Complex formation between protein C inhibitor and prostate specific antigen in vitro and in human semen. *Eur. J. Biochem.* **220,** 45–53.
25. Otto, A., Bar, J., and Birkenmeier, G. (1998) Prostate-specific antigen forms complexes with human-$\alpha_2$-macroglobulin and binds to the -$\alpha_2$-macroglobulin receptor-related protein. *J. Urol.* **159,** 297–303.
26. Permanetter, W. and Meister, P. (1984) Distribution of lysozyme (muraminidase) and (1-antichymotrypsin in normal and neoplastic epithelial tissues: a survey. *Acta Histochem.* **74,** 173–179.
27. Bjork, T., Hulkko, S., Bjartell, A., di Sant'gnese, A., Abrahamsson, P.-A., and Lilja H. (1994) $\alpha_1$-antichymotrypsin production in PSA-producing cells is common in prostate cancer but rare in benign prostatic hyperplasia. *Urology* **43,** 427–433.
28. Qian, Y., Sensibar, J. A., Zelner, D. J., Schaeffer, A. J., Finlay, J. A., Rittenhouse, H. G., and Lee, C. (1997) Two-dimensional gel electrophoresis detects prostate-specific antigen-$\alpha_1$-antichymotrypsin complex in serum but not prostatic fluid. *Clin. Chem.* **43,** 352–359.

29. Clements, J. A., Merritt, T., Devoss, K., Swanson, C., Hamlyn, L., Scells, B., et al. (2000) Inactive free:total prostate specific antigen ratios in ejaculate from men with suspected and known prostate cancer, compared with young control men. *BJU Int.* **86,** 453–458.
30. Wang, Z., Ramin, S. A., Tsai, C., Lui, P., Herbert, P. J., Kyeyune-Nyombi, E., et al. (2001) Detection of telomerase activity in prostatic fluid specimens. *Urol. Oncol.* **6,** 4–9.
31. Kim, N. W., Piatyszek, M. A., Prowse, K. R., Harley, C. B., West, M. D., Ho, P. L., et al. (1994) Specific association of human telomerase activity with immortal cells and cancer. *Science* **266,** 2011–2015.
32. Suh, C. I., Shanafelt, T., May, D. J., Shroyer, K. R., Bobak, J. B., Crawford, E. D., et al. (2000) Comparison of telomerase and GSTP1 promoter methylation in ejaculate, potential screening for prostate cancer. *Mol. Cell Probes* **14,** 211–217.
33. Lynch, M. J. and Nicholson, J. K. (1997) Proton MRS of human prostatic fluid: Correlations between citrate, spermine and myo-inositol levels and change with disease. *Prostate* **3,** 248–255.
34. Liu, H., Moy, P., Kim, S., Xia, Y., Rajasekaran, A., Navarro, V., et al. (1997) Monoclonal antibodies to the extracellular domain of prostate-specific membrane antigen also react with tumor vascular endothelium. *Cancer Res.* **57,** 3629–3634.
35. Chang, S. S., Reuter, V. E., Heston, W. D., Bander, N. H., Grauer, L. S., and Gaudin, P. B. (1999) Five different anti-prostate-specific membrane antigen (PSMA) antibodies confirm PSMA expression in tumor-associated neovasculature. *Cancer Res.* **59,** 3192–3198.
36. Silver, D. A., Pellicer, I., Fair, W. R., Heston, W. D., and Cordon-Cardo, C. (1997) Prostate-specific membrane antigen expression in normal and malignant human tissues. *Clin. Cancer Res.* **3,** 81–85.
37. Jassim, A. and Festenstein, H. (1987) Immunological and morphological characterisation of nucleated cells other than sperm in semen of oligospermic donors. *J. Reprod. Immunol.* **11,** 77–89.
38. Sharifi, R., Rhee, H., Shaw, M., Nagubadi, S., Ray, V., and Guinan ,P. (1983) Evaluation of cytologic techniques for diagnosis of prostatic cancer. *Urology* **21,** 417–420.
39. Berry, S. J., Coffey, D. S., Walsh, P. C., and Ewing, L. L. The development of human benign prostatic hyperplasia with age. *J. Urol.* **132,** 474–479.
40. Israeli, R. S., Powell, C. T., Fair, W. R., and Heston, W. D. (1993) Molecular cloning of a complementary DNA encoding a prostate-specific membrane antigen. *Cancer Res.* **227,** 227–230.
41. Wright, G. L. Jr, Beckett, M. L., Lipford, G. B., Haley, C. L., and Schellhammer, P. F. (1991) A novel prostate carcinoma-associated glycoprotein complex (PAC) recognized by monoclonal antibody TURP-27. *Int. J. Cancer* **47,** 717–725.
42. Kim, Y. D., Robinson, D. Y., and Tomita, J. T. (1888) Monoclonal antibody PR92 with restricted specificity for tumor-associated antigen of prostate and breast carcinoma. *Cancer Res.* **48,** 4543–4548.

43. Emmert-Buck, M. R., Strausberg, R. L., Krizman, D. B., Bonaldo, M. F., Bonner, R. F., Bostwick, D. G., et al. (2000) Molecular profiling of clinical tissue specimens: feasibility and applications. *Am. J. Pathol.* **156,** 1109–1115.
44. Foster, C. S., Bostwick, D. G., Bonkoff, H., Damber, J.-E., van der Kwast, T., Montironi, R., and Sakr, W. A. (2000) Cellular and molecular pathology of prostate cancer precursors: WHO Consensus Conference June 8-9 2000.*Scand. J. Urol. Nephrol.* **34,** 18–43.
45. Liu, X. H., Kirschenbaum, A., Yao, S., Stearns, M. E., Holland, J. F., Claffey, K., and Levine, A. C. (1999) Upregulation of vascular endothelial growth factor by cobalt chloride-simulated hypoxia is mediated by persistent induction of cyclooxygenase-2 in a metastatic human prostate cancer cell line. *Clin. Exp. Metastasis* **17,** 687–694.
46. Chen, H. J., Treweeke, A. T., Ke, Y. Q., West, D. C., and Toh, C. H. (2000) Angiogenically active vascular endothelial growth factor is over-expressed in malignant human and rat prostate carcinoma cells. *Br. J. Cancer* **82,** 1694–1701.
47. Collett, G. P., Betts, A. M., Johnson, M. I., Pulimood, A. B., Cook, S., Neal, D. E., et al. (2000) Peroxisome proliferator-activated receptor alpha is an androgen-responsive gene and is highly expressed in prostatic adenocarcinoma. *Clin. Cancer Res.* **6,** 3241–3248.
48. Tavtigian, S. V., Simard, J., Teng, D. H., Abtin, V., Baumgard, M., Beck, A., et al. (2001) A candidate prostate cancer susceptibility gene at chromosome 17p. *Nat. Genet.* **27,** 172–180.
49. de Kok, J.B., Verhaegh, G.W., Roelofs, R.W., Hessels, D., Kiemeney, B.A., Aalders, T.W., et al. (2002) DD3 (PCA3), a very sensitive and specific marker to detect prostate cancer. *Cancer Res* **62,** 2695–2698.
50. Nelson, J.B., Chan-Tack, K., Hedican, S.P., Magnuson, S.R., Opgenorth, T.J., Bova, G.S., Simons, J. W. (1996) Endothelin-1 production and decreased endothelin B receptor expression in advanced prostate cancer. *Cancer Res* **56,** 663–668.
51. Gohji, K., Kitazawa, S., Tamada, H., Katsuoka, Y., and Nakajima, M. (2001) Expression of endothelin receptor A associated with prostate cancer progression. *J. Urol.* **165,** 1033–1036.
52. Holgersson, J., Pimlott, W., Samuelsson, B. E., and Breimer, M. E. (1989) Electron ionization mass spectrometry for sequence analysis of glycosphingolipid mixtures by fractional evaporation in the ion source. Mass spectrometric evidence for an eleven-sugar glycolipid. *Rapid Commun. Mass Spectrom.* **3,** 400–404.
53. Costello, C. E. and Vath, J. E. (1990) Tandem mass spectrometry of glycolipids. *Meth. Enzymol.* **193,** 738–768.
54. Dell, A. (1990) Preparation and desorption mass spectometry of permethyl and peracetyl derivatives of oligosaccharides. Meth. Enzymol. **193,** 647–660.
55. Favretto, D., Seraglia, R., Traldi, P., Curcuruto, O., and Hamdan, M. (1994) Electrospray vs. matrix-assisted laser desorption/ionization I. Some examples in the protein field. *Organic Mass Spectrom.* **29,** 526–532.
56. Perreult, H. and Costello, C. E. (1994) Liquid secondary ionization, tandem and matrix-assisted laser desorption/ionization time-of-flight mass spectrometric char-

acterization of glycosphingolipid derivatives. *Organic Mass Spectrom.* **29,** 720–735.
57. Costello, L. C. and Franklin, L. B. (1991) Concepts of citrate production secretion by the prostate. 1. Metabolic relationships. *Prostate* **18,** 25–46.
58. Costello, L. C., Franklin, R. B., and Narayan, P. (1999) Review article: citrate in the diagnosis of prostate cancer. *Prostate* **38,** 237–245.
59. Cooper, J. F. and Imheld, H. (1959) The role of citric acid in the physiology of the prostate; a preliminary report. *J. Urol.* **81,** 157–163.
60. Marberger, H., Marberger, E., Mann, T., and Lutwak-Mann, C. (1962) Citric acid in human prostatic secretion and metastasizing cancer of the prostate gland. *Br. Med. J.* **1,** 835–836.
61. Cooper, J. E. and Farid, I. (1964) The role of citric acid in the physiology of the prostate. Lactic/citrate ratios in benign and malignant prostatic homogenates as an index of prostatic malignancy. *J. Urol.* **92,** 533–536.
62. Scheibler, M. R., Miyamoto, K. K., White, M., Maygarden, S. J., and Mohler, J. L. (1993) In vivo high resolution 1H spectroscopy of the human prostate: Benign prostatic hyperplasia, normal peripheral zone and adenocarcinoma. *Magn. Reson. Med.* **29,** 285–291.
63. Cornel, E. B., Smits, G. A. H. J., Oosterhof, G. O. N., Karthaus, H. F. M., Debruyne, F. M. J., Schalken, J. A., and Heerschap, A. (1993) Characterization of human prostate cancer, benign prostatic hyperplasia and normal prostate by in-vitro $^{1}$H and $^{3}$P magnetic resonance spectroscopy. *J. Urol.* **150,** 2019–2024.
64. Kavanagh, J. P (1985) Sodium, potassium, calcium, magnesium, zinc, citrate and chloride content of human prostatic and seminal fluid. *J. Reprod. Fertil.* **75,** 35–41.
65. Heerschap, A., Jager, G. J., van der Graaf, M., Barentz, J. O., De La Rosette, J. J., Oosterhof, G. O. N., et al. (1997) In vivo proton spectroscopy reveals altered metabolite content in malignant prostate tissue. *Anticancer Res.* **17,** 1455–1460.
66. Anderson, R. U. and Fair, W. R. (1976) Physical and chemical determinations of prostatic secretion in benign hyperplasia, prostatitis and adenocarcinoma. *Invest. Urol.* **14,** 133–140.

# 13

# Bisulfite Methylation Analysis of Tumor Suppressor Genes in Prostate Cancer from Fresh and Archival Tissue Samples

**Susan J. Clark, Douglas S. Millar, and Peter Molloy**

## 1. Introduction

It is now well established that, in addition to genetic changes that may include germ line and somatic DNA alterations, cancers can also arise as a result of a series of epigenetic DNA mutations ***(1)***. In mammals, DNA is methylated at cytosine residues in the 5′ position of CpG dinucleotides. The genomic methylation pattern is established in the early embryo before implantation and is then stably maintained throughout differentiation ***(2)***. However, in cancer the methylation pattern of the cell is altered, with repeated DNA regions often undergoing hypomethylation and CpG island promoter regions undergoing hypermethylation ***(3)***. Hypomethylation of DNA is thought to be involved in the expression of previously dormant proto-ongogenes, and hypermethylation of the promoter regions is associated with gene silencing. Hypermethylation of tumor suppressor genes and other CpG island genes, such as *p15*, *p16*, estrogen receptor, E-cadherin, *VHL*, *HIC-1*, and retinoblastoma and corresponding transcriptional silencing have been demonstrated in many different forms of cancer ***(1)***. However, each cancer appears to have a specific subset of genes that are susceptible to methylation ***(4)***. Therefore, detection of the methylation of these genes could provide a useful diagnostic tool to identify the cancer cell and monitor the cancer during therapy.

The technique of bisulfite genomic sequencing provides a positive method for the identification of methylated cytosines in genomic DNA ***(5)***. The method has been widely adopted for the study of methylation in a wide range of processes, such as cancer research, genomic imprinting, early development, and X-inactivation ***(6,7)***. The technique involves the treatment of DNA with

From: *Methods in Molecular Medicine, Vol. 81: Prostate Cancer Methods and Protocols*
Edited by: P. J. Russell, P. Jackson, and E. A. Kingsley © Humana Press Inc., Totowa, NJ

sodium bisulfite, resulting in deamination of unmethylated cytosine residues to uracil without deamination of the methylated derivative 5′-methylcytosine. Subsequent polymerase chain reaction (PCR) amplification results in the previously unmethylated cytosine residues being amplified from uracil as thymine and the methylated cytosines being amplified as cytosine ***(5,8–11)***. The extent of the methylation state can be quickly assessed either by the use of restriction enzymes or by direct PCR sequencing ***(12)***.

Although some common genetic alterations have been identified during prostate cancer progression ***(13–15)*** and potential susceptibility genes for prostate cancer identified, the molecular and epigenetic events leading to prostate cancer development are at present ill-defined ***(16)***. To study common epigenetic mutations in prostate cancer, we modified the bisulfite method to analyze the methylation state of DNA from paraffin-embedded tissue. DNA extracted from archival sources, such as paraffin, is generally of poor quality and yield and can be in a highly degraded state before the bisulfite reaction. Therefore, the high degradation rate associated with the bisulfite reaction coupled with poor quality DNA can result in inconsistent amplification. To address this problem, we developed a simple extraction protocol optimized on paraffin block and slide tissue samples to produce reliable bisulfite PCR amplification of a wide range of tumor suppressor and oncogenic markers. Bisulfite PCR primers were designed to determine the methylation status of the *p15*, *p16*, E-cadherin, retinoblastoma, estrogen receptor, *HIC-1*, *KAI-1*, *VHL*, Glutathione-S-transferase P1, *Bcl-2*, and endothelin-B genes. All of these genes have been reported to be abnormally expressed and/or methylated to some extent in prostate cancer.

In this chapter, the basic protocols for the methylation analysis of common tumor suppressor genes from paraffin-embedded tissue/slide and prostate tissue culture cells are given.

## 2. Materials

All solutions should be prepared using high-quality distilled (such as MilliQ; Millipore, Bedford, MA) or deionized water.

1. Lysis buffer: 7 *M* guanidinium hydrochloride, 5 m*M* EDTA, 100 m*M* Tris/HCl, pH 6.4, 1% Triton X-100, 50 µg/mL Proteinase K (Sigma), 100 µg/mL yeast tRNA.
2. Phenol:chloroform (1:1) mix.
3. DNA buffer: 10 m*M* Tris, pH 8.0, 0.1 m*M* EDTA.
4. 10 m*M* hydroquinone is made from a 1 in 10 dilution of a 100 m*M* hydroquinone stock (0.55 g in 50 mL, freshly prepared).
5. 2 *M* sodium metabisulfite (BDH): (dissolve 7.6 g in 20 mL of $H_2O$ and adjust to pH 5.0 with 10 *M* NaOH). The solution of bisulfite is achieved by gently inverting the reagent/$H_2O$ mixture, with minimum mixing and aeration, and may require pH adjustment before all is dissolved.

6. Desalting column: Promega Wizard DNA Clean-Up System.
7. PCR buffer: 67 m*M* Tris/HCl, 16.6 m*M* ammonium sulfate, 1.7 mg/mL bovine serum albumin, and 10 m*M* β-mercaptoethanol in DNA buffer.
8. Taq polymerase: AmpliTaq DNA Polymerase (Perkin-Elmer).
9. TAE buffer (1X): 40 m*M* Tris acetate, 1 m*M* EDTA, pH 8.0.
10. 2X SSC buffer: 0.3 *M* NaCl, 0.03 *M* $Na_3$ citrate.
11. T4 polynucleotide kinase buffer: 70 m*M* Tris-HCl, pH 7.6, 10 m*M* $MgCl_2$, 5 m*M* dithiothreitol.
12. Hybridization buffer: 1 m*M* EDTA, pH 8.0, 0.5 *M* sodium phosphate, pH 7.2, 7% SDS.
13. SAM buffer: 50 m*M* NaCl, 10 m*M* Tris-HCl, pH 8.0, 10 m*M* EDTA, 1 m*M* dithiothreitol, 270 μ*M* *S*-adenosylmethionine.
14. TTL buffer: 6 *M* LiCl, 300 m*M* Tris-HCl, pH 8.0, 0.3% Tween 20.
15. NaOH/Triton solution (0.15 *M* NaOH/ 0.075% Triton X-100): Dissolve 0.3 g of NaOH in 50 mL of Milli-Q water with 37.5 μL Triton X-100.
16. TT buffer: 10 m*M* Tris-HCl, pH 8.0, 0.1% Tween 20.
17. Magnetic beads: Dynabeads M-280 Streptavidin magnetic beads (10 mg/mL) (Dynal AS, Oslo, Norway).
18. A or C Master Mix (Applied Biosystems): 0.5 μL 10X MOPS; 0.5 μL 10X $Mn^{2+}$/isocitrate buffer; 2 μL M13-21 dye primer (JOE dye for A or FAM dye for C) and 1 μL α-thio-d/ddN mixture.
19. G or T Master Mix (Applied Biosystems): 1.5 μL 10X MOPS; 1.5 μL 10X $Mn^{2+}$/isocitrate buffer; 4 μL M13-21 dye primer (TAMRA dye for G or ROX dye for T) and 3 μL α-thio-d/ddN mixture.
20. Loading buffer: 5 μL of recrystallized deionized formamide, 1 μL 50 m*M* $Na_2$ EDTA, pH 8.0, 30 mg/mL blue dextran.

## 3. Methods

### *3.1. DNA Extraction from Fresh Tumor Samples and Cell Lines*

1. Fresh prostate tissue (4 mm thick) is frozen in liquid $N_2$ and stored at –70°C or in liquid $N_2$.
2. Histology of an adjacent tissue slice is used to identify a region of cancer.
3. A 5-mm diameter punch (similar to a cork borer) is used to remove tissue from the frozen slice.
4. The tissue punch is ground under liquid $N_2$ with a mortar and pestle.
5. Add 400 μL of lysis buffer to the ground tissue, transfer the mixture to a 1.5-mL tube, and incubate for 16 h at 55°C.
6. For cell lines, pellet $1 \times 10^7$ cells, add 400 μL of lysis buffer, and incubate for 16 h at 55°C.
7. Vortex the samples and centrifuge at top speed for 2 min to pellet the cell debris.
8. Remove the supernatant into a clean tube and dilute with 200 μL of $H_2O$ to reduce the salt concentration.
9. Extract the supernatant twice with 400 μL of phenol:chloroform mix and collect the upper aqueous phase.

10. Add 900 µL of ice-cold ethanol to the aqueous phase and leave for 1 h or more at 20°C.
11. Centrifuge the solution at top speed for 10 min at 4°C, then remove the supernatant and resuspend the pellet in 20 to 50 µL of DNA buffer.

### 3.2. DNA Extraction from Paraffin Block Samples

1. Trim the excess wax from the cored tissue (5-mm punches) from both a grossly cancerous region and matched normal tissue from the same paraffin block.
2. Place the core in a 1.5-mL tube and add 400 µL of lysis buffer.
3. Thoroughly homogenize the samples with disposable 1.5-mL pestles and incubate in 1.5-mL tubes for 48 h at 55°C.
4. After incubation, subject the samples to five freeze/thaw cycles of dry ice for 5 min followed by 95°C for 5 min.
5. Vortex the samples and centrifuge at top speed for 2 min to pellet the cell debris.
6. Remove the supernatant into a clean tube and dilute with 200 µL of $H_2O$ to reduce the salt concentration.
7. Extract the supernatant twice with 400 µL of phenol:chloroform mix.
8. Add 900 µL of ice-cold ethanol and leave for 1 h or more at –20°C.
9. Centrifuge the solution at top speed for 10 min at 4°C, then remove the supernatant and resuspend the pellet in 15 µL of DNA buffer.

### 3.3. DNA Extraction from Slide Samples

1. Scrape into clean 1.5-mL tubes approx 2- × 1-cm sections of the cell monolayer from a slide.
2. Add 400 µL of lysis buffer.
3. Thoroughly homogenize the samples with disposable 1.5-mL pestles and incubate for 48 h at 55°C.
4. After incubation, subject the samples to five freeze/thaw cycles of dry ice for 5 min followed by 95°C for 5 min.
5. Vortex the samples and centrifuge at top speed for 2 min to pellet the cell debris.
6. Remove the supernatant into clean tubes and dilute with 200 µL of $H_2O$ to reduce the salt concentration.
7. Extract the supernatant twice with 400 µL of phenol:chloroform mix.
8. Add 900 µL of ice-cold ethanol and leave for 1 h or more at –20°C.
9. Centrifuge the solution at top speed for 10 min at 4°C, then remove the supernatant and resuspend the pellet in 15 µL of DNA buffer.

### 3.4. Bisulfite Conversion Protocol

1. Digest genomic DNA from cell line material with an appropriate restriction enzyme in an 18 µL volume (*see* **Note 1**).
2. Do not digest DNA isolated from formaldehyde-fixed slides or paraffin-embedded material (*see* **Note 2**). Instead, add 10 µg of tRNA to the DNA to a final volume of 18 µL (*see* **Note 3**).

3. Denature the DNA (18 µL) in a final volume of 20 µL by adding 2 µL of freshly prepared 3 *M* NaOH to a final concentration of 0.3 *M* and incubate for 15 min at 37°C (*see* **Note 4**).
4. Prepare fresh solutions of 10 m*M* hydroquinone and 2 *M* sodium metabisulfite, pH 5.0 (*see* **Note 5**).
5. Add 208 µL of metabisulfite and 12 µL of 10 m*M* hydroquinone to the denatured DNA to a final volume of 240 µL.
6. Overlay with 100 µL of mineral oil and incubate in the dark at 55°C for 4 to 16 h. Small DNA amounts (100 pg) require as little as 4 h incubation, and large DNA amounts (1–2 µg) require 16 h (*see* **Note 6**).
7. Recover the bisulfite-treated DNA from under the oil layer by snap freezing the reaction and removing the unfrozen oil.
8. Remove free bisulfite by passing the sample through a desalting column (e.g., Promega Wizard column) and elute in 50 µL of Milli-Q $H_2O$.
9. Add 5.5 µL of freshly prepared 3 *M* NaOH to a final concentration of 0.3 *M* and incubate the sample at 37°C for 15 min.
10. Neutralize the solution by the addition of 33.3 µL of 5 *M* ammonium acetate, pH 7.0, and add 300 µL of ethanol. Add an extra 10 µg of tRNA at this stage (*see* **Note 7**).
11. Leave at –20°C for 1 to 2 h.
12. Centrifuge the solution at top speed for 10 min at 4°C, remove the ethanol, dry, and resuspend the sample in 10 to 50 µL of DNA buffer and store at –20°C (*see* **Note 8**).

### 3.5. PCR Amplification and Primers

1. The strand-specific nested primers used for amplification of bisulfite-treated DNA are indicated in **Table 1**.
2. Add 2 µL of bisulfite-treated genomic DNA, 200 µ*M* of each of the four dNTPs, 6 ng/µL of each of the outer primers, 1 to 2 m*M* $MgCl_2$, 2 U of Taq polymerase, and PCR buffer to a final volume of 50 µL.
3. Add 20 µL of mineral oil.
4. Incubate at 94°C/2 min × one cycle; 94°C /1 min, 50 to 60°C/2 min, 72°C/3 min × five cycles; 94°°C /0.5 min, 50 to 60°C/2 min, 72°C/1.5 min × 25 cycles; and 72°C/6 min × one cycle (*see* **Note 9**).
5. Remove 2 µL of DNA from the first round amplification reaction and add to a reaction mix containing 200 µ*M* of each of the four dNTPs, 6 ng/µL of each of the inner primers, 1 to 2 m*M* $MgCl_2$, 2 U of Taq polymerase, and PCR buffer to a final volume of 50 µL.
6. Add 20 µL of mineral oil.
7. Incubate at 94°C /2 min × one cycle; 94°C/1 min, 50 to 60°C/2 min, 72°C/3 min × five cycles; 94°C /0.5 min, 50 to 60°°C/2 min, 72°C/1.5 min × 25 cycles; and 72°C/6 min × one cycle.

**Table 1**
**Bisulfite Gene Primers**

| Gene | Genebank accession no. | Primer | Sequence |
|---|---|---|---|
| p16 | U12818 | p16-4 (8–33) | GAGGAGGGGTTGGTTGGTTATTAGAG (F) |
| | | p16-5 (31–336) | TACCTAATTCCAATTCCCCTACAAAC (R) |
| | | p16-6 (250–273) | CTACAAACCCTCTACCCACCTAAA (R) |
| GSTP1 | M24485 | GST-9 (967–993) | TTTGTTGTTTGTTTATTTTTTAGGTTT (F) |
| | | GST-10 (1307–1332) | AACCTAATACTACCAATTAACCCCAT (R) |
| | | GST-11 (999–1027) | GGGATTTGGGAAAGAGGGAAAGGTTTTTT (F) |
| | | GST-12 (1281–1306) | ACTAAAAACTCTAAAAACCCCATCCC (R) |
| HIC-1 | L41919 | HIC-1 (1291–1319) | TTTTTTGTGGTTTGGATTTGTTTAAGAAG (F) |
| | | HIC-2 (1452–1477) | TTGTTTTTTTAGAAGTTGGAGGAGGT (F) |
| | | HIC-3 (1760–1786) | ATCTCCTCACTACTACTCTTATAATCA (R) |
| | | HIC-4 (1907–1935) | CAACTACTCAAAACTAAAAAAACCCTTAC (R) |
| Estrogen receptor | X62462 | EST 1 (3012–3036) | GATTTTTTATATTAAAGTATTTGGG (F) |
| | | EST 2 (3039–3063) | GGTTTTATTGTATTAGATTTAAGGG (F) |
| | | EST 3 (3281–3308) | CTATTAAATAAAAAAAAACCCCCCAAAC (R) |
| E-cadherin | L34545 | ECAD 1 (791–820) | ATTTAGTGGAATTAGAATAGTGTAGGTTTT (F) |
| | | ECAD 2 (831–868) | TAGATTTTAGTTTTTTTAGGTTAGAGGG (F) |
| | | ECAD 3 (1139–1165) | CTACAACTCCAAAAACCCATAACTAAC (R) |

| | | | |
|---|---|---|---|
| KAI-1 | U67266 | KAI 3 (527–549) | GGGTTTTAGTTTTAGTTGGGTT (F) |
| | | KAI 4 (527–549) | GTTTTTTTAAAGGGTTAGGGGG (F) |
| | | KAI 5 (527–549) | AAAACTAAAACTAACTTTACCTATAATTATC (R) |
| | | KAI 6 (527–549) | CTAAAAATTCAAAACTAATAACTAAAACTCC (R) |
| BCL-2 | X51898.1 | Bcl 1 (831–957) | TATTTATAAGGTTAGAAAGGGTTTAGG (F) |
| | | Bcl 2 (1010–1036) | GTTTTAGTAGGTTTGAGTAGAAGGTTT (F) |
| | | Bcl 3 (1316–1343) | CTCTACACAACCCAACCAATTTCCTATA (R) |
| | | Bcl 4 (1347–1373) | AAACTATAATACCTATCCTCTTACTTC (R) |
| VHL | AF010238.1 | VHL-1 (476–504) | GGAAATATAGTAAAGAGTTGGTTTAGTTT (F) |
| | | VHL-2 (519–546) | TAGTTTAAGGTGTTGGAGGATTTTTTTG (F) |
| | | VHL-3 (1316–1343) | ACCTCCATCTCCTCCTCAACACCCAAT (R) |
| Endothelin-B receptor | D13162.1 | Endo-1 (1241–1266) | TTTTGGAGTAGGTAGTAGTATGTAGT (F) |
| | | Endo-2 (1290–1313) | GTTTTGGTTGTGTTGGTTTTTGTT (F) |
| | | Endo-3 (1612–1637) | AATAATTCTCAAAAATATAAAATTCC (R) |
| | | Endo-4 (1681–1709) | ATACAACAAATCTCCCAAAACCAACATAA (R) |
| p15 | S75756 | p 15 1 (59–92) | GTTTTTTGGTTTAGTTGAAAAGGGAATTTTTTGT (F) |
| | | p 15 2 (87–117) | TTTTGTGGGTTGGTTTTTTATTTTGTTAGAG (F) |
| | | p 15 4 (564–533) | ACTTCCAAAAACTATCCCACCTTCTCCACTAA (R) |
| | | p 15 5 (356–333) | CCTTCCTAAAAAACCTAAACTCAA (R) |
| Retinoblastoma | L11910 | Rb 15 (1662–1695) | ACCCCAGCCTAAAAAAAATAATTCTAAATAAAA (F) |
| | | Rb 16 (1714–1743) | AATACCTCCTAAAAAACCCCTAAACCCAC (F) |
| | | Rb 17 (1926–1948) | TTTTAAGGTTTTTTGAGAAAAAT (R) |
| | | Rb 18 (1949–1978) | GATTTTTTTGGATTTTGGTTATAAAAATAA (R) |

### 3.6. Testing PCR Bias

For a quantitative measurement of methylation in a sample containing both methylated and unmethylated DNA, it is important to determine the PCR bias for each primer pair to ensure equal amplification of both methylated and unmethylated DNA molecules *(17)* (*see* **Note 10**).

1. Digest 4 µg of unmethylated genomic DNA (e.g., isolated from blood or placenta) with a restriction enzyme and ethanol precipitate by standard methodology.
2. Resuspend the digested DNA in 180 µL of SAM buffer.
3. Divide the DNA into two equal aliquots: to one aliquot add 4 U of *Sss*I methylase (methylated aliquot) and retain the other as the unmethylated aliquot.
4. Incubate both aliquots at 37°C for 2 h.
5. Mix in various ratios to create samples containing 100, 90, 75, 50, 25, 10, and 0% methylated DNA in a volume of 18 µL.
6. Treat samples with bisulfite as described above (*see* **Subheading 3.4.**).
7. Use these DNA mixes to test amplification conditions for each primer set.
8. Bias is determined by methylation restriction analysis (*see* **Subheading 3.7.**).

### 3.7. Methylation Restriction Analysis

1. Digest PCR products with the following restriction enzymes to determine methylation and conversion.
2. *Bst*UI digestion can be used to determine methylation (*see* **Note 11**). *Taq*I digestion can be used to determine methylation and conversion (*see* **Note 12**). *Hpa*II digestion can be used to determine conversion (*see* **Note 13**).
3. The bisulfite reaction is not always 100% efficient, and unconverted DNA can sometimes be amplified (*see* **Note 14**). This can cause problems with quantification of methylation. It is therefore important to test for nonconversion either by restriction cutting or by hybridization with probes to converted or unconverted DNA (*see* **Subheading 3.8.**).

### 3.8. Hybridization for Converted/Unconverted DNA

PCR products can be tested for conversion efficiency by hybridization with an internal oligonucleotide specific for unconverted DNA (*see* **Note 15**). This can be done by Southern transfer of the PCR product or by dot blot.

1. For Southern transfer, prepare a 2% agarose gel (a mix of 1% agarose and 1% Nusieve agarose) in 1X TAE buffer.
2. Load 10 µL of each PCR onto the gel and electrophorese.
3. Transfer the gel onto a Hybond-N+ membrane as follows:
4. Fill a tray with 0.4 *M* NaOH. Make a platform with a glass plate and cover it with a wick from two sheets of Whatman 3MM filter paper, saturated with blotting buffer.
5. Cut the edges off the gel and place it face down on the wick, avoiding air bubbles beneath.
6. Wet a sheet of Hybond-N+ membrane with water and then with 0.4 *M* NaOH and place it on top of the gel. Avoid bubbles beneath the membrane.

7. Place three sheets of 3MM Whatman paper wet with blotting buffer on top of the membrane. Surround the gel with cling film to prevent the blotting buffer being absorbed directly into the paper towels above.
8. Place a stack of absorbent paper towels on top of the Whatman paper. Place a glass plate on top of the paper towels and put a weight on top. Allow the transfer to proceed for 16 h.
9. Carefully remove the paper towels and Whatman paper. Before removing the membrane from the gel, mark the membrane with pencil to allow later identification of tracks.
10. Briefly and carefully rinse the membrane with 2X SSC, and wrap it in Whatman paper until required.
11. Label oligo probes with $\gamma[^{32}P]$ -ATP by adding 1 µL of Oligo (100 ng/uL), 1 µL of 10X T4 kinase buffer, 5 µL of 10X T4 kinase buffer, 5 µL of water, 2 µL of $\gamma[^{32}P]$ -ATP (20 uCi), and 1 µL of T4 polynucleotide kinase.
12. Incubate at 37°C for 1 h.
13. At the end of the reaction, add the probe directly to 10 mL of hybridization buffer.
14. Prehybridize the membrane in 10 mL of hybridization solution at 45°C for at least 30 min.
15. Discard the prehybridization solution and hybridize the membrane at 45°C with 10 mL of hybridization solution containing the radiolabeled Oligo for at least 4 h.
16. After hybridization, wash the membrane in 50 mL of prewarmed 2X SSC/0.1% SDS at 45°C for 15 min. Repeat twice.
17. Check the membrane for residual radioactivity, and then wash the membrane with 0.1X SSC/0.1% SDS at 45°C for another 15 min.
18. Wrap the membrane in a plastic bag and expose it to a Phosphorimager.

## 3.9. Direct Sequencing PCR Product

### 3.9.1. Biotinylated/M13 PCR Amplification and Bead Purification

1. For automated direct sequence and Genescan analysis, reamplify PCR products from the first round PCR using Biotinylated/M13 tailed primer pairs (*see* **Notes 16** and **17**).
2. From the first round amplification, add 5 µL of DNA to a reaction mix containing 200 µ*M* of each of the four dNTPs, 12 pmol of the biotinylated primer, and 40 pmol of the M13-tailed inner primers, 3 m*M* $MgCl_2$, and 3 U of AmpliTaq DNA polymerase (Perkin Elmer) and PCR buffer to a final volume of 100 µL.
3. Add 20 µL of mineral oil.
4. Incubate at 94°C/2 min × one cycle; 94°C/1 min, 50–60°C/2 min, 72°C/3 min × five cycles; 94°C/0.5 min, 50–60°C/2 min, 72°C/1.5 min × 25 cycles; and 72°C/6 min × one cycle.
5. For magnetic bead purification of the biotinylated PCR products, take a 15-µL aliquot of magnetic beads and wash them with 200 µL of TTL buffer.
6. Apply a Dynal magnet particle concentrator (Dynal MPC).
7. Resuspend the beads in 20 µL of TTL buffer with gentle pipetting.

8. Transfer the beads to 45 µL of the PCR containing 200–400 ng of DNA and incubate at 43°C for 12–15 min.
9. Apply the magnet again and discard the supernatant.
10. Resuspend the beads in 200 µL of freshly prepared NaOH/Triton solution.
11. Incubate at room temperature for 4 min to denature the DNA.
12. Apply the magnet, discard the supernatant, and rinse the beads with 200 µL of TT Buffer (*see* **Note 18**).
13. Resuspend the bead pellet in 7.2 µL of MilliQ water and store at 4°C until used for sequencing (*see* **Note 19**).

### 3.9.2. Direct PCR Sequencing Reactions

1. Perform direct PCR sequencing reactions using a PRISM Sequenase Dye Primer Sequencing Kit (PE/ABI) on an automated DNA Sequencer (ABI) ***(1)***.
2. Set up four tubes for each base reaction.
3. Anneal 1 µL of bead-bound template with 4 µL of A or C master mix or 3 µL of bead-bound template with 10 µL of G or T master mix.
4. Incubate at 65°C for 2 min, then at room temperature for 15 min (*see* **Note 20**).
5. Place tubes on ice and add 2 µL of Sequenase/pyrophosphatase enzyme to the A or C reactions and 4 µL to the G or T reactions.
6. Incubate at 37°C for 15 min.
7. Place on ice and pool the four individual reactions in 200 µL of TT buffer.
8. Apply a magnet, remove the supernatant, and wash the beads with 200 µL of TT buffer.
9. Resuspend the bead-bound reactions in 4 µL of loading buffer and heat at 100°C for 2 min, then place on ice.
10. Load onto a 6% polyacrylamide urea gel using an automated DNA sequencer (*see* **Note 21**).

### 3.9.3. Quantitative Genescan Analysis

1. For quantitation by Genescan, use the FAM M13(-21) Dye Primer (blue) for both C and T sequencing reactions ***(1)***.
2. Perform sequencing reactions as described for the C reaction above (*see* **Subheading 3.9.2.**).
3. Terminate the reaction with 100 µL of TT buffer.
4. Apply the magnet, remove the supernatant, and wash the beads with 100 µL TT buffer.
5. Add 0.8 µL of Applied Biosystems GENE-SCAN-350 TAMRA Size Standard (yellow) and 3.7 µL of loading buffer to each C and T reaction.
6. Load C and T reactions on separate lanes on the sequencing gel.
7. Preprocess the sequence gel file into GENESCAN format using a modified version of GENESCAN 672 analysis software (UNLOCK 1.0).
8. Use GENESCAN Analysis Version 1.2.0 to analyze the results.
9. Calculate the percent methylation using peak height of the C vs peak height of the C plus peak height of the T for each position (*see* **Note 22**).

## 4. Results and Discussion

### 4.1. Methylation Analysis of Multiple Genes from Prostate Cell Lines and Fresh Tumor Samples

DNA was extracted from five widely used prostate cancer cell lines, LNCaP, DU-145, PC-3, and its two metastatic cell line derivatives, PC-3M and PC-3MM. The DNA was bisulfite treated and amplified using the different gene sets (*see* **Table 1**). To assay for methylation, the PCR products were digested with *BstU*I (*see* **Fig. 1**). **Table 2** summarizes the results of digestion. PC-3 and its derivatives were hypermethylated in *GSTP1*, *ER*, *p16*, *E-cad*, *HIC*I and the endothelin B receptor gene. All cell lines were unmethylated for *Rb* and *p15*. The results confirmed that many genes are susceptible to hypermethylation in long-term cell culture.

### 4.2. Optimization of the Bisulfite-Mediated PCR from Archival Samples

We optimized the extraction procedure for the isolation of DNA from archival sources to enable quantitative methylation analysis. Overnight incubation of paraffin block material (matched normal and cancer samples) in small volumes of Lysis Buffer (200 µL) is insufficient to allow the release of cellular DNA (*see* **Fig. 2A**) because none of the 18 samples gave positive methylation PCR signals. Doubling the volume of extraction buffer to 400 µL significantly increased the DNA yield because 8/18 (44%) of the samples gave the correct bisulfite-derived amplification product (*see* **Fig. 2B**). Increasing the time of incubation in the lysis buffer from 16 to 48 h resulted in a further increase in the efficiency of amplification to 12/18 (67%) (*see* **Fig. 2C**). We found that repeated cycles of freezing and boiling had a considerable effect on the quantity and quality of the DNA extract obtained from paraffin block tissue samples (*see* **Fig. 3**).

The inclusion of the cycle freeze/boiling coupled with a 48-h incubation in 400 µL of lysis buffer resulted in a strong amplification product in 18/18 (100%) samples (*see* **Fig. 4D**) and, therefore, this combination was used for all subsequent extraction procedures.

We used this protocol to amplify different genes from varying locations to test the robustness of the method. **Figure 4** shows methylation-based PCR amplification of the estrogen receptor, p15, p16, and retinoblastoma gene performed on the same paraffin DNA extracts. In each case all 18 extracts (nine cancer and nine matched normal) amplified consistently for each of the respective genes, demonstrating the consistency of the extraction procedure when applied to target genes of different chromosomal locations.

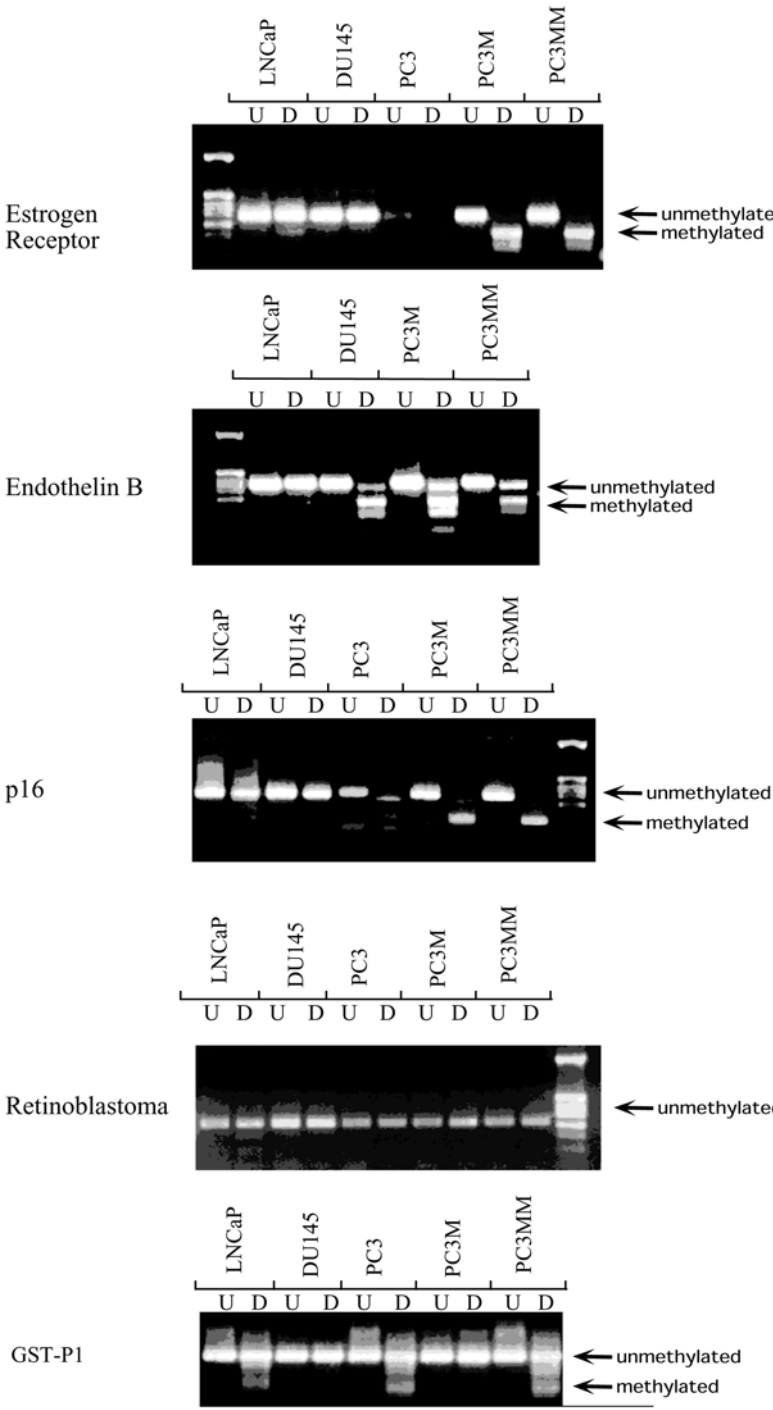
LNCaP
DU145
PC3
PC3M
PC3MM
U D U D U D U D U D
Estrogen Receptor
unmethylated
methylated
LNCaP
DU145
PC3M
PC3MM
U D U D U D U D
Endothelin B
unmethylated
methylated
LNCaP
DU145
PC3
PC3M
PC3MM
U D U D U D U D U D
p16
unmethylated
methylated
LNCaP
DU145
PC3
PC3M
PC3MM
U D U D U D U D U D
Retinoblastoma
unmethylated
LNCaP
DU145
PC3
PC3M
PC3MM
U D U D U D U D U D
GST-P1
unmethylated
methylated

Fig. 1. Methylation analysis of bisulfite-amplified DNA from prostate cell lines. Five different prostate cancer-associated genes (estrogen receptor, endothelin B, *p16*, retinoblastoma, and *GSTP1*) were tested for methylation in the prostate cell lines LNCaP, DU-145, PC-3, PC-3M, and PC-3MM. The PCR products amplified from bisulfite-treated DNA isolated from the cell lines were either undigested (U) or digested (D) with *Bst*UI. Any undigested PCR product indicates unmethylated CpG sites in the DNA and digested PCR product represents methylated CpG sites in the DNA.

**Table 2**
**Methylation Status of Prostate Cancer Cell Lines**

| | GSTP | ER | p15 | p16 | E-cad | VHL | Rb | HIC | Endo | KAI | Bcl-2 |
|---|---|---|---|---|---|---|---|---|---|---|---|
| LNCaP | +++ | + | – | + | – | + | + | ++ | – | – | – |
| Du145 | – | – | – | – | – | – | – | ++++ | ++ | + | – |
| PC3 | +++ | – | – | ++ | – | – | – | ++ | ++ | – | – |
| PC3M | – | ++++ | – | ++++ | + | – | – | +++ | +++ | ++ | – |
| PC3MM | +++ | ++++ | – | ++++ | + | – | – | +++ | ++ | + | ++ |

Level of methylation indication by *Bst*UI digestion –: no methylation, +: low < 25% methylation, ++: medium 25–50% methylation, +++: 50–75% high methylation, ++++: complete 75–100% methylation.

Material obtained from archival histopathology slides is also a possible source of DNA to study methylation. The optimized extraction procedure that was described for paraffin tissue (*see* **Subheading 3.2.**) was also applied to small quantities of tissue scrapped from microscope slides from patients with prostate cancer. Four individual slides consisting of prostatic chip material and needle biopsy samples were included. Methylation-based PCR amplifications were performed using three different gene sets on each extract to assess the consistency of amplification obtained from each sample type. All three amplifications yielded positive PCR signals from each slide (*see* **Fig. 5**); therefore, the isolation method can be used successfully for the methylation analysis from each source of tissue.

### *4.3. Methylation Analysis in Prostate Cancer*

DNA was extracted from 11 paraffin blocks derived from patients undergoing radical prostatectomy (Gleason scores ranging from 4–8). After extraction, the DNA was bisulfite-treated and subjected to PCR using the different primer gene sets (*see* **Table 1**). Control digests using the enzyme *Hpa*II were con-

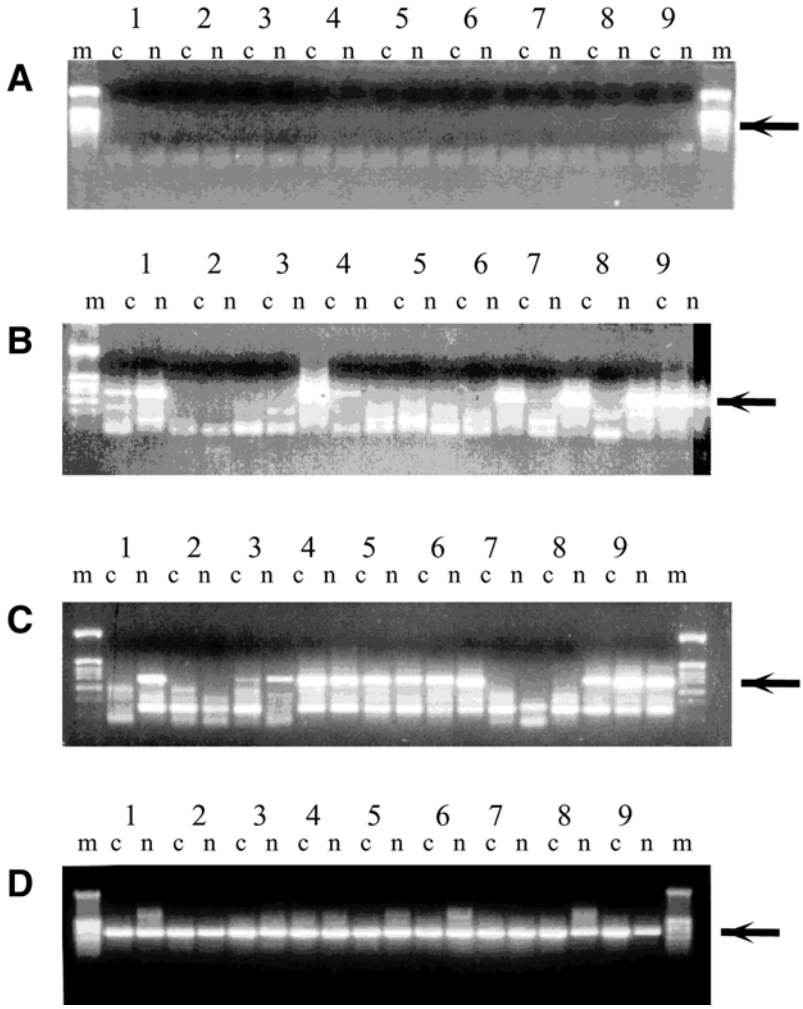


Fig. 2. DNA extraction method from paraffin-embedded tissue affects bisulfite-mediated PCR amplification. DNA was extracted from nine cancer (c) and matched normal (n) paraffin-embedded tissues by **(A)** 16-h incubation in 200 µL of lysis buffer, **(B)** 16-h incubation in 400 µL of lysis buffer, **(C)** 48-h incubation in 400 µL of lysis buffer, **(D)** 48-h incubation in 400 µL of lysis buffer followed by five cycles of freeze/boil (*see* **Subheading 3.2.**). The extracted DNA was bisulfite treated and amplified with GSTP1 primers. Lanes 1 through 9 show the tissue sample and the arrow indicates the PCR amplicon, (m) is the pBR322 *Hinf*I size markers. The poor integrity of the DNA resulted in either no amplication (A) or amplification of multiple bands (B,C).

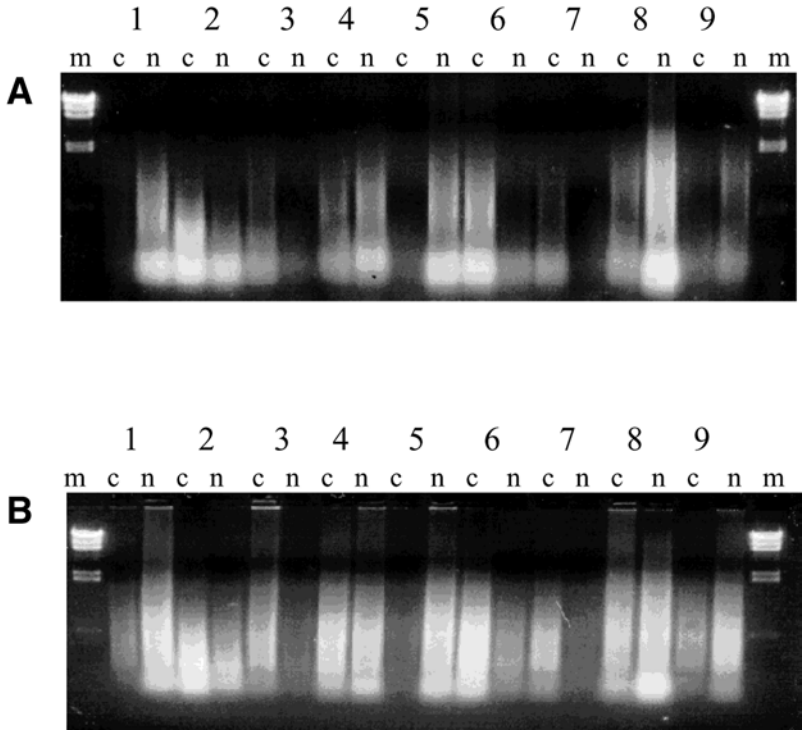


Fig. 3. The effect of freeze/boil cycles on DNA quality from paraffin-embedded prostate tissue. DNA was extracted from nine cancer (c) and matched normal (n) tissues in 400 µL of lysis buffer, either **(A)** without freeze/boil steps or **(B)** with five cycles of freeze/boil steps (*see* **Subheading 3.2.**). (m) is the pBR322 *Hinf*I size markers.

ducted to ensure that the PCR fragments analyzed contained fully converted molecules (*see* **Fig. 6**).

Southern blot hybridization with converted and unconverted probes was also used to test for complete bisulfite reaction in the amplified products (not shown). This is important as lack of conversion of bisulfite-treated DNA in this technique can lead to false-positive signals after restriction digestion (*see* **Note 23**). The methylation state of the products that did not hybridize with unconverted probe was analyzed by digestion with the restriction enzymes *Bst*UI and *Taq*I (*see* **Fig. 6**). **Table 3** shows a summary of the methylation analysis of the PCR fragments after restriction enzyme digestion. Unlike the cancer cell line samples, only one gene, *GSTP1*, was consistently methylated in 91% (10/11) primary prostate cancers. No methylation was seen either in the two normal prostate samples (Norm A and B) or in the matched normal tissue. Only limited methylation

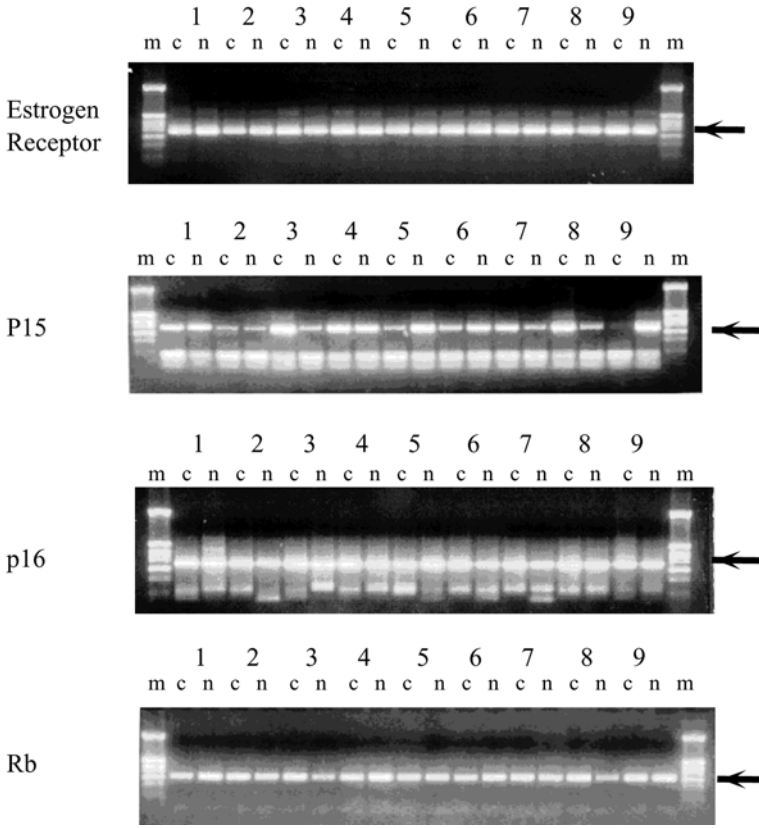


Fig. 4. Amplification of bisulfite-treated DNA from paraffin-embedded prostate cancer samples. Examples of PCR amplification from DNA extracted from nine cancer (c) and matched normal (n) tissues. The DNA was bisulfite treated and amplified with a variety of primer sets, including estrogen receptor, p15, p16, and Rb. Lanes 1 through 9 show the tissue sample and the arrow indicates the PCR amplicon, (m) is the pBR322 *Hinf*I size markers.

was seen in other genes in the cancer samples. Interestingly, endothelin- B Receptor was found to be methylated in one of the normal prostate tissues (Norm A), as well as in a number of the matched normal samples.

To confirm that the results of the restriction digests, some of the samples were subjected to bisulfite genomic sequencing and quantitation by Genescan analysis (*see* **Fig. 7**).

The results of the genomic sequencing reactions were very similar if not identical to those seen with the restriction digests. Bisulfite genomic sequencing also revealed that the methylation pattern present in the prostate cancer

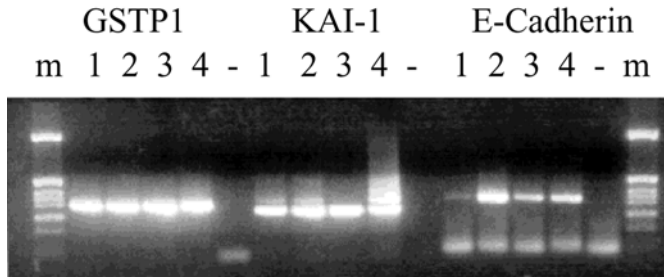


Fig. 5. Amplification of bisulfite-treated DNA from slides. Four individual slides consisting of prostatic chip (1, 2) and needle biopsy (3, 4) samples were used to isolate DNA for bisulfite treatment and amplification. Examples are shown of amplification with the GSTP1, Kai-1, and E-cadherin primer sets. (-) indicates the no DNA control and (m) is the pBR322 *Hinf*I size markers.

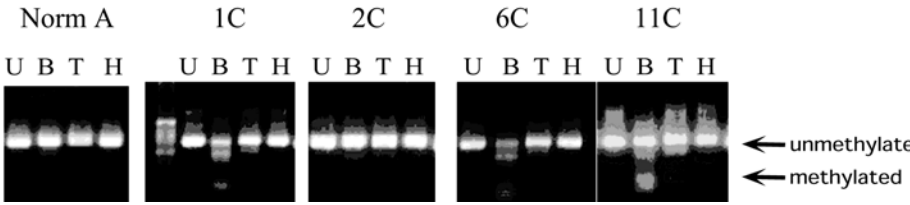


Fig. 6. Methylation analysis of bisulfite-amplified DNA from prostate tissue. Examples are shown of the PCR product amplified using GSTP1 primers from four prostate tissue samples: one normal (Norm A) and four cancer samples (1C, 2C, 6C, and 11C). The products were either undigested (D) or digested with *Bst*UI (B), *Taq*I (T), and *Hpa*II (H). The arrows indicate either the methylated or unmethylated DNA.

samples was not confined to specific sites or areas in the promoter region but encompassed the entire promoter region amplified.

From these studies, it is clear that hypermethylation of a number of genes is fairly common event in prostate cancer cell line material, with 6/11 (54%) of the genes assayed showing methylation in at least three of the cell lines analyzed. However, in the primary prostate cancer tissues hypermethylation of multiple genes was quite a rare event with only 1/11 (9%) of the same genes showing consistent methylation in the cancer samples. These results demonstrate that genes in cell culture can contain completely altered epigenetic phenotype. Of the 11 genes tested, *GSTP1* was found to be the most commonly methylated in prostate cancer tissue, with over 90% of primary cancers demonstrating aberrant hypermethylation.

**Table 3**
**Methylation Status in Prostate Cancer**

| | Gleason | GST | ER | p15 | p16 | E-cad | VHL | Rb | HIC | Endo | KAI | Bcl-2 |
|---|---|---|---|---|---|---|---|---|---|---|---|---|
| Norm. A | | – | – | – | – | – | – | – | – | + | – | – |
| Norm. B | | – | – | – | – | – | – | – | – | – | – | – |
| 1N | | – | – | – | – | – | – | – | – | – | – | – |
| 1C | 3+3 | +++ | – | – | – | – | – | – | ++ | – | – | – |
| 2N | | – | – | B | ++ | – | – | – | – | + | – | – |
| 2C | 3+3 | – | – | – | – | – | – | – | – | + | – | – |
| 3N | | – | – | – | – | – | – | – | – | + | – | – |
| 3C | 3+3 (Hor.) | ++ | ++ | – | – | – | – | – | – | – | – | – |
| 4N | | – | – | – | – | – | – | – | – | – | – | – |
| 4C | 3+3 | ++ | – | – | – | – | – | – | ++ | – | – | – |
| 5N | | – | – | – | – | – | – | – | – | + | – | – |
| 5C | 3+5 | ++++ | – | – | – | – | – | – | + | – | ++ | – |
| 6N | | – | – | – | – | – | – | – | – | + | – | – |
| 6C | 2+2 | ++ | – | – | – | – | – | – | – | ++ | – | – |
| 7N | | – | – | – | – | – | – | – | – | ++ | – | – |
| 7C | 3+3 (Hor.) | ++ | – | – | – | – | – | – | ++ | – | – | – |
| 8N | | – | – | – | – | – | – | – | – | – | – | – |
| 8C | 2+2 | ++ | – | – | – | – | – | – | – | – | – | – |
| 9N | | – | – | – | – | – | – | – | – | ++ | – | – |
| 9C | 3+3 | ++++ | – | – | – | – | ++ | – | + | ++ | – | – |
| 10N | | – | – | – | – | – | – | – | – | – | – | – |
| 10C | 2+3 | +++ | ++ | – | – | – | – | – | – | ++ | – | – |
| 11N | | – | – | – | – | – | – | – | – | ++ | – | – |
| 11C | 2+3 | +++ | – | – | – | – | – | – | – | – | – | – |

Level of methylation indication by *Bst*UI digestion –: no methylation, +: low < 25% methylation, ++: medium 25–50% methylation, +++: 50–75% high methylation, ++++: complete 75–100% methylation.

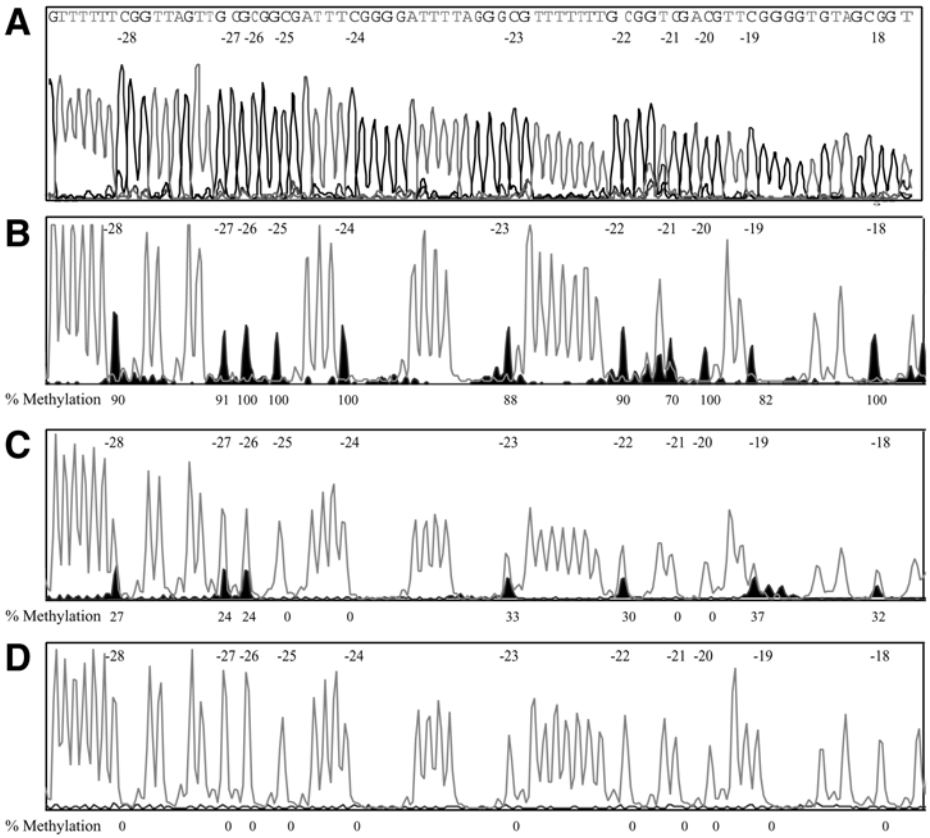


Fig. 7. Sequence and Genescan analysis of the GSTP1 amplified product. **(A)** Direct PCR sequence analysis of the PCR product amplified from bisulfite-treated LNCaP cells. Genescan C and T quantitative methylation analysis of the PCR products amplified from bisulfite-treated **(B)** LNCaP cells, **(C)** paraffin-embedded prostate cancer sample (1C), and **(D)** paraffin-embedded prostate matched normal sample (1N). CpG sites are shown in the top of the panels and are numbered relative to the start of transcription. The percent methylation below each site is shown and is calculated by percentage of the peak height of the C track vs the peak height of the C + T tracks.

## 5. Notes

1. Bisulfite reaction: Digest DNA before bisulfite treatment with a restriction enzyme that does not cut within the target sequence. This serves to reduce the size of the fragments so that the DNA can fully denature.
2. Do not digest DNA isolated from formaldehyde-fixed slide or paraffin-embedded material because it is already quite degraded and denatured by the boiling steps.

3. tRNA is added to the tube as a carrier to avoid the small quantity of DNA sticking to the 1.5-mL Eppendorf tube.
4. To ensure complete denaturation, it is important to prepare the 3 *M* sodium hydroxide just before use.
5. It is important to prepare both the hydroquinone and the sodium metabisulfite just before use and to keep them in the dark because both are susceptible to oxidation. Store the stock bottles in a dry and dark place and do not use after 6 mo.
6. Do not incubate small DNA amounts (100 pg) isolated from paraffin tissue with bisulfite for longer than 4–6 h because DNA degradation can substantially reduce the DNA yield.
7. The extra tRNA is added to aid in precipitation of small quantities of DNA.
8. Because of the limiting quantities of DNA isolated from paraffin/slides, resuspend the bisulfite-treated DNA in only 10 µL of DNA buffer.
9. Each set of primers needs to be optimized for magnesium and temperature conditions.
10. Bias in PCR occurs because the methylated DNA is C or G rich in comparison with the unmethylated DNA, which is T or A rich after bisulfite conversion. This is particularly noticeable in the amplification of CpG island that contains DNA. In fact, the melting temperatures of the strands can be quite different, leading to the selective amplification of one strand vs the other.
11. Methylation restriction digestion: *Bst*U1 (CGCG) will digest if the sequence is methylated; *Bs*tU1 (TGTG) will fail to digest if the sequence is unmethylated.
12. *Taq*1 (TCGA) will digest if methylated and converted (from CCGA); *Taq*1 (TTGA) will fail to digest if unmethylated.
13. *Hpa*II (CCGG) will only cut if unconverted.
14. Sometimes unconverted DNA can be amplified preferentially because of the PCR bias (*see* **Note 10**). However, preferential amplification of unconverted DNA is more of problem when using methylation-specific primers. In contrast to the primers described in **Table 1** that do not contain CpG sites, methylation-specific primers primers contain a number of CpG sites and therefore often promote amplification of unconverted DNA.
15. The hybridization oligo should be 15–20 bases in length and should contain a high ratio of C residues. Try to avoid CpG sites. Make two oligos: (1) a conversion probe that contains the C residues converted to T residues and (2) unconverted probe that contains the original sequence.
16. Direct PCR sequencing: The forward primers were biotinylated at the 5′ end during synthesis using biotin amidite from Applied Biosystems (PE/ABI) according to manufacturer's directions.
17. The reverse primers were tagged at the 5′ end with the sequence for the M13 (-21) universal primer.
18. It is important to remove all traces of NaOH/Triton rinse and TT Buffer washes as any remaining liquid may affect the sequencing reaction.
19. All washes and resuspensions were done with gentle pumping with a pipet, and the nonbiotinylated strand was not used.

20. Incubation at 65°C for 15 min ensures complete primer annealing.
21. Gel preparation, electrophoresis and sequencing data collection are described in the ABIDNA Sequencer User Manual (PE/ABI).
22. Using this calculation, the degree of methylation greater that 25% can be reliably estimated. Less than 25% methylation is difficult to estimate if there is a large background or noise in the sequence profile.
23. The bisulfite conversion reaction is not 100% efficient and therefore some molecules that amplify may be partially unconverted. It is often necessary to perform multiple bisulfite reactions and multiple PCR reactions and test each set with *Hpa*II digestion to ensure that only the PCR reactions that are fully converted are used for methylation analysis.

## References

1. Baylin, S. B., Herman, J. G., Graff, J. R., Vertino, P. M., and Issa, J. P. (1998) Alterations in DNA methylation: A fundamental aspect of neoplasia, in *Advances in Cancer Research* (Vandewoude, G. F. and Klein, G., eds.), Academic Press, San Diego, pp. 141–196.
2. Warnecke, P. M., Mann, J. R., Frommer, M., and Clark, S. J. (1998) Bisulfite sequencing in preimplantation embryos: DNA methylation profile of the upstream region of the mouse imprinted H19 gene. *Genomics* **51,** 182–190.
3. Jones, P. A. and Laird, P. W. (1999) Cancer epigenetics comes of age. *Nat. Genet.* **21,** 163–167.
4. Melki, J. R., Vincent, P. C., and Clark, S. J. (1999) Cancer-specific region of hypermethylation identified within the HIC1 putative tumour suppressor gene in acute myeloid leukaemia. *Leukemia* **13,** 877–883.
5. Clark, S. J., Harrison, J., Paul, C. L., and Frommer, M. (1994) High sensitivity mapping of methylated cytosines. *Nucl. Acids Res.* **22,** 2990–2997.
6. Stirzaker, C., Millar, D. S., Paul, C. L., Warnecke, P. M., Harrison, J., Vincent, P. C., et al. (1997). Extensive DNA methylation spanning the Rb promoter in retinoblastoma tumors. *Cancer Res.* **57,** 2229–2237.
7. Warnecke, P. M. and Clark, S. C. (1999) DNA methylation profile of the mouse skeletal a-actin promoter during development and differentiation. *Mol. Cell. Biol.* **19,** 164–172.
8. Clark, S. J. and Frommer, M. (1995) Deamination with NaHSO3 in DNA methylation studies, in *DNA And Nucleoprotein Structure In Vivo* (Saluz, H. P. and Wiebauer, K., eds.), Springer-Verlag, R. G. Landes Company, Austin, pp. 123–132.
9. Clark, S. J. and Frommer, M. (1997) Bisulphite genomic sequencing of methylated cytosines, in *Laboratory Methods for the Detection of Mutations and Polymorphisms in DNA* (Taylor, G., ed.), CRC Press, New York, pp. 151–162.
10. Clark, S. J., Harrison, J., and Frommer, M. (1995) CpNpG methylation in mammalian cells. *Nat. Genet.* **10,** 20–27.
11. Clark, S. J., Harrison, J., and Molloy, P. L. (1997) Sp1 binding is inhibited by (m)Cp(m)CpG methylation. *Gene* **195,** 67–71.

12. Paul, C. L. and Clark, S. J. (1996) Cytosine methylation: Quantitation by automated genomic sequencing and GENESCAN analysis. *BioTechniques* **21,** 126–133.
13. Isaacs, W. B., Bova, S. G., Morton, R. A., Bussemakers, M. J. G., Brooks, J. D., and Ewing, C. M. (1995) The molecular biology of prostate cancer progression. *Cancer Surv.* **23,** 19–31.
14. Isaacs, J. T. (1997) Molecular markers for prostate cancer metastasis: Developing diagnostic methods for predicting the aggressiveness of prostate cancer. *Am. J. Pathol.* **150,** 1511–1521.
15. Konishi, N., Cho, M., Yamamoto, K., and Hiasa, Y. (1997) Genetic changes in prostate cancer. *Pathol. Int.* **47,** 735–747.
16. Rennie, P. S. and Nelson, C. C. (1998) Epigenetic mechanisms for progression of prostate cancer. *Cancer Metast. Rev.* **17,** 401–409.
17. Warnecke, P. M., Stirzaker, C., Melki, J. R., Millar, D. S., Paul, C. L., and Clark, S. J. (1997) Detection and measurement of PCR bias in quantitative methylation analysis of bisulphite-treated DNA. *Nucleic Acids Res.* **25,** 4422–4426.

# 14

# Production and Characterization of Antipeptide Kallikrein 4 Antibodies

*Use of Computer Modeling to Design Peptides Specific to Kallikrein 4*

**Tracey J. Harvey, Ying Dong, Loan Bui, Russell Jarrott, Terry Walsh, and Judith A. Clements**

## 1. Introduction

To date, prostate-specific antigen (PSA) has proven to be the most useful tumor marker for prostate cancer ***(1–3)***. However, the PSA test does not discriminate well between men with benign disease and early prostate cancer, and it does not discriminate between aggressive and slow-growing cancers ***(4,5)***. Although a useful additional discriminator ***(5),*** the advent of free/total PSA assays has not significantly improved this outcome. Thus, an inability to make an early diagnosis has led to the increased burden of metastatic disease, and many patients are overtreated because clinically aggressive disease cannot be distinguished from clinically insignificant disease.

PSA, a serine protease, is encoded by the *KLK3* gene, which is a member of the human kallikrein (*KLK*) gene family ***(6)***. Another kallikrein that is found at high levels in the prostate is the hK2 enzyme, which is a product of the *KLK2* gene ***(7)***. At the immunohistochemical level, hK2 staining is more intense in poorly differentiated tumors than lower grade tumors or hyperplastic glands; in contrast, PSA staining becomes more heterogeneous and less intense in poorly differentiated disease ***(8,9)***. Serum hK2 levels, along with free/total PSA, are suggested to enhance the biochemical detection of prostate cancer ***(10–13)*** and have been proposed to even predict disease that is organ confined ***(14,15)***. These findings have led to the suggestion that hK2, or the combination of PSA and hK2 assays, might help provide better discrimination between

From: *Methods in Molecular Medicine, Vol. 81: Prostate Cancer Methods and Protocols*
Edited by: P. J. Russell, P. Jackson, and E. A. Kingsley © Humana Press Inc., Totowa, NJ

benign and malignant prostatic disease and/or an improved prognostic indicator of disease progression.

Until recently, the *KLK* family consisted of just three members: *KLK1*, which encodes tissue kallikrein, and the *KLK2* and *KLK3* genes ***(16–18)***. However, with the identification of several new genes, the expanded family now contains 15 members ***(19,20)***, several of which are highly expressed in the prostate ***(19,21–26)***. Our premise is that these other newly discovered prostatic kallikreins may also be useful biomarkers for prostate cancer. One of these genes is the *KLK4* gene, which was independently cloned and characterized by four different groups ***(21–23,27)***. To provide a tool to assess the usefulness of hK4 as an additional biomarker for this disease, we took the approach of raising antipeptide antibodies to hK4 because recombinant hK4 enzyme was not initially available.

Previous studies have successfully used molecular modeling to determine antigenic epitopes and subsequently produce peptides and antipeptide antisera specific for hK2 ***(28–30)***. The difficulty with this approach is the high homology observed between PSA and hK2 (77% at the protein level) and the need to scrutinize proposed immunogens to ensure sufficient specificity. This is less of a problem when designing such peptides for hK4 because it is less similar in sequence to PSA and hK2 and, indeed, the larger *KLK* family overall (25–45%) ***(18,19)***. Thus, we have used a similar approach and modeled the predicted protein sequence of hK4 against that of PSA to determine sequences in loop regions on the outer surface of the molecule that were likely to be antigenic. The regions of highest dys-homology against hK1, hK2, and PSA were then chosen for peptide synthesis. At the time of the development of these peptides, the eleven most recent members of the human *KLK* family were not yet identified. However, given the low degree of homology between these newer genes and hK4 (25–45%), this was not considered a problem and, indeed, retrospective analysis of these regions confirms their specificity.

The studies outlined below describe the molecular modeling of hK4, choice of peptide immunogens, and the characterization of the subsequent antibodies raised using an indirect ELISA, immunohistochemistry, and Western blot analysis.

## 2. Materials

### *2.1. Tissue Samples and Cell Culture Media*

Prostate tissue samples were obtained at surgery from men with prostate cancer who underwent radical prostatectomy at the Royal Brisbane Hospital, Brisbane, Australia. Tissues were formalin fixed and paraffin embedded before use for immunohistochemistry. Informed consent was obtained. These studies were approved by the Institutional Ethics Committees of the Royal Brisbane Hospital and Queensland University of Technology.

Cell lines were obtained from American Type Culture Collection and maintained using Dulbecco's Modified Eagles Medium (DMEM) containing phenol red, supplemented with 10% inactivated fetal bovine serum (FBS), 50 U/mL penicillin, and 50 µg/mL streptomycin.

### 2.2. Enzyme-Linked Immunosorbent Assay (ELISA) Reagents

1. ELISA Blocking solution 1: 10% (w/v) skim milk powder, 10% sucrose, diluted in phosphate-buffered saline, pH 7.4 (phosphate-buffered saline [PBS]: 2 m*M* KCl, 150 m*M* NaCl, 20 m*M* $Na_2HPO_4$, 2 m*M* $KH_2PO_4$), with 0.05% (v/v) Tween-20 (PBST).
2. ELISA Blocking solution 2: 0.1% gelatin, diluted in PBS.

### 2.3. Recombinant Protein Purification Reagents

1. His affinity resin: TALON Metal Affinity resin (Clontech) was used. This resin is designed specifically for the purification of protein fused to a 6X histidine tag. Before use, the resin should be washed three times with 1 mL of 1X extraction buffer per 100 µL of resin.
2. Extraction buffer (pH 7.0): 50 m*M* sodium phosphate buffer, 300 m*M* NaCl.
3. Complete protease inhibitor cocktail (Roche Diagnostics): contains a mixture of several protease inhibitors with broad inhibitory specificity for serine, cysteine, and metallo-proteases. For addition to samples, one tablet is resuspended in 1 mL of PBS to give a 50X stock solution, which is then diluted to 1X in the samples.

### 2.4. Western Blot Analysis Solutions

#### 2.4.1. Separation of the Proteins by Sodium Dodecyl Sulphate (SDS) Polyacrylamide Gel Electrophoresis

1. 40% acrylamide/bisacrylamide 29:1 stock solution (Bio-Rad). Store at 4°C in the dark for 12 mo.
2. Ammonium persulfate stored as a 10% (w/v) solution in dd$H_2O$ at 4°C for a few months; *N*,*N*,*N*′,*N*′-Tetramethylethylendiamine (TEMED) stored at 4°C.
3. Resolving gel: 10% (from stock acrylamide/bisacrylamide 29:1), 25% (v/v) 1.5 *M* Tris-HCl (pH 8.8), 0.1% SDS, double-distilled (dd) $H_2O$ to the final volume of the gel. 0.1% ammonium persulfate, 0.06% (v/v) TEMED.
4. Stacking gel: 4% (from stock acrylamide/bisacrylamide 29:1), 1.7% (v/v) 0.5 *M* Tris-HCl (pH 6.8), 0.1% SDS, dd$H_2O$ to the final volume of the gel; ammonium persulfate 0.1%; TEMED 0.06% (v/v).
5. Tris-glycine electrophoresis buffer (running buffer): 25 m*M* Tris, 250 m*M* glycine, 0.1% (w/v) SDS (pH 8.3). It can be made as a 5X stock solution and stored indefinitely at room temperature.
6. 2X sample buffer: 0.1 *M* Tris (pH 6.8), 4% SDS, 20% glycerol, dd$H_2O$ to the final volume, 0.2% (w/v) bromophenol blue, and stored at –20°C. Add 200 m*M* dithiothreitol or 0.05% (v/v) β-mercaptoethanol fresh if required for reducing gels.

#### 2.4.2. Transfer

1. 40X bicarbonate transfer buffer: 200 m*M* NaHCO, 120 m*M* $Na_2CO_3$, pH to 9.9. To prepare 1X transfer buffer (5 m*M* $NaHCO_3$, 3 m*M* $Na_2CO_3$, 20% methanol, pH 9.9), dilute one part of the 40X stock with 31 parts of ddH2O, then add 8 parts of methanol to make it 20% (v/v). To avoid precipitation, do not add methanol directly to the 40X stock. Prechill the transfer buffer at –20°C for 1 h before use.
2. Ponceau-S-red: commercially available from Sigma.

#### 2.4.3. Antibody Hybridization Buffer

1. Tris-buffered saline (TBS): 100 m*M* Tris base (pH 7.5), 150 m*M* NaCl (10X TBS stock solution can be made for convenience). Add 0.5 mL Tween-20 per liter of buffer to make up 1X TBS-T20 (TBST).

#### 2.4.4. Other Reagents

1. Five percent (w/v) nonfat skim milk powder in TBST. Store at 4°C for 1 wk.
2. Affinity purified anti-hK4 peptide rabbit antibodies. Aliquots stored at –80°C.
3. Horseradish peroxidase goat anti-rabbit IgG.
4. Chemiluminescence reagent: SuperSignal West Femto (PIERCE, Rockford, IL). The kit consists of luminol/enhancer solution (50 mL) and stable peroxide solution (50 mL). It is stable for several months at 4°C.

### 2.5. Immunohistochemistry

1. Deparaffinization, rehydration, and antigen retrieval: xylene, absolute ethanol, 90–70% ethanol, $H_2O$, TBS, 5% (w/v) urea in 0.1 *M* Tris buffer (pH 9.5).
2. Inhibition of endogenous peroxidase and blocking nonspecific binding: 3% (v/v) hydrogen peroxide ($H_2O_2$), 18% (v/v) methanol in TBS, 5% (w/v) nonfat skim milk powder in TBS.
3. Immunostaining: anti-K4 peptide antibodies, Envision peroxidase polymer (DAKO).
4. Detection of peroxidase activity: 0.05% (w/v) 3,3′-diaminobenzidine in PBS 0.02% (v/v) $H_2O_2$.
5. Counterstaining: Mayer Haematoxylin.

## 3. Methods

### 3.1. Computer Modeling

Modeling of the hK4 protein was performed using the Swiss-Model program at the ExPASy Molecular Biology Server website (http://www.expasy.ch). The resulting Pdb files were then visualized using the Swiss-Pdb Viewer v3.6b3 software. The protein model for PSA was superimposed with the hK4 model to determine which outer-loop regions were markedly different within each protein. A surface epitope, near the C-terminal end of the protein, was distinctly different in sequence from the same region within the PSA protein model. Subsequently, it

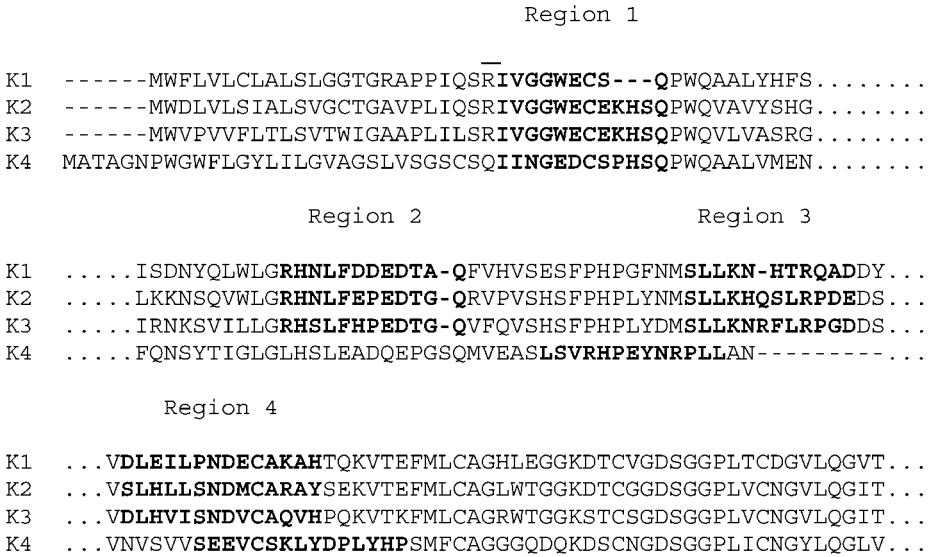


Fig. 1. Multiple sequence alignment of several regions of hK1-hK4.The antigenic surface epitopes for hK1-K3 in the same region as the loops selected for hK4 (by computer modeling) are shown in bold. The first peptide, designated N-terminal, is found within region 1; the second peptide, mid-region, was selected from within region 2/3; the third peptide, C-terminal, is shown within region 4. Arrow represents the cleavage site for activation of hK4 enzyme to its mature form.

was shown to be significantly different from all other kallikrein protein sequences available at the time (region 4 in **Fig. 1**). A second epitope, within the mid-region of the protein (region 2/3 in **Fig. 1**), was also found by molecular modeling to be distinct from PSA as well as from other members of the family by alignment of the protein sequence. A peptide was also synthesized using the N-terminal mature protein sequence (region 1 in **Fig. 1**), even though this region is relatively conserved within the kallikrein family, because we wished to have antibodies directed against the N-terminal region as well as a mid-region and the C-terminal (*see also* **Note 1**).

### 3.2. Antibody Production

The peptides described above were synthesized commercially (Chiron Technologies Pty Ltd, Victoria, Australia). Antibody production was also contracted commercially (Chiron). Briefly, these peptides were coupled to a carrier protein, diphtheria toxoid, using maleimidocaproyl-N-hydroxysuccinimide as the linker. Two rabbits were then immunized against a mixture of the three peptide-carrier protein conjugate, which was emulsified by mixing with 2 vol of com-

**Table 1**
**Indirect ELISA**

| | Antibody | | | | | |
|---|---|---|---|---|---|---|
| Peptide | N-term | Mid-region | C-term | hK1 (PAb) | hK2 (MAb) | hK3 (PAb) |
| N-term | ++++ | – | – | + | – | + |
| Loop 4 | + | ++++ | – | + | – | + |
| Loop 6 | +++ | +++ | ++++ | + | – | + |

In this assay, the crossreactivity between the hK4 peptides and their respective antibodies was initially determined (left column). It was observed that the N-terminal and mid-region antibodies crossreacted with one of the other peptides, whereas the C-terminal antibody was very specific for its cognate peptide. Subsequent studies to examine the crossreactivity of the hK4 peptides with other antibodies demonstrated that all three peptides crossreact with polyclonal antibodies against hK1 and hK3. This may simply reflect the polyclonal nature of these antibodies and not necessarily a lack of specificity. However, no interaction was seen between the hK4 peptides and a monoclonal antibody raised against hK2. Further studies will need to be performed with other monoclonal antibodies against other kallikreins. Absorbance reading (450 nm) scale: (–) is background, (+) is ≤1.000, (++) is 1.001–2.000, (+++) is 2.001–3.000, (++++) is 3.001–4.000.

plete Freund's Adjuvant. A second immunization was given 2 wk later using incomplete Freund's Adjuvant. The animals were then bled via vein puncture at 35 and 49 d after the first immunization. Affinity-purified antibodies were obtained for each of the three peptides using Sepharose 6B columns coupled with the peptides. Biotinylated peptides were also synthesized for subsequent use in an indirect ELISA to determine the avidity of the antibodies (*see* **Subheading 3.4.1.**).

### 3.3. Antibody Characterization

Three different methods—an ELISA, transient expression of recombinant hK4 followed by Western blot analysis, and immunohistochemistry—were used to characterize the hK4 peptide antibodies. The methods used for these approaches are detailed below and the results of these experiments shown in **Tables 1** and **2** and **Figs. 2** and **3** (*see also* **Note 2**).

### 3.4. hK4 ELISA

#### 3.4.1. Indirect ELISA to Determine Avidity and Crossreactivity Between hK4 Peptides and Antibodies (**Table 1**)

1. The streptavidin-coated microtiter plates were incubated with 400 µL of Blocking solution 1 for 2 h at room temperature and then the wells were washed with PBST.
2. Biotinylated peptide (200 µL) was added and left overnight at 4°C to coat the plate. The following day, the plates were washed with PBST and 200 µL of the appropri-

**Table 2**
**Competition ELISA**

| | Antibody | | |
|---|---|---|---|
| | N-term | Mid-region | C-term |
| **Protein** | | | |
| hK1 | ++ | ++ | ++++ |
| hK2 | + | ++ | ++++ |
| hK3 | +/++ | ++ | ++++ |
| **Peptide** | | | |
| hK4 std | ++ | ++ | ++++ |

Crossreactivity of the hK4 antibodies with other kallikreins. This assay tests the ability of the hK1-3 proteins to inhibit the binding of the hK4 antibodies to their corresponding peptide. In this type of ELISA, a decrease in absorbence is indicative of a crossreaction. The N-terminal antibody crossreacts to some degree with hK2 and hK3 but not with hK1, whereas the Mid-region and C-terminal antibodies do not crossreact with any of the three proteins and are specific for hK4. The same scale as described in **Table 1** was used for the absorbence readings at 450 nm.

ate antibody was added, that is, anti-N-terminal (1:500), anti-mid-region (1:500) and anti-C-terminal (1:1500) **(Table 1)**. Antibodies against other family members, such as K1, K2, and PSA, were tested for crossreactivity with the peptides by substituting the peptide-specific antibodies with one of the following: polyclonal anti-K1 (1:100, Calbiochem), monoclonal anti-K2 (1:1000, a gift from Hybritech Corp., San Diego, CA), or polyclonal anti-PSA (1:1000, Dako) **(Table 1** and **Note 2)**. These antibodies were also incubated with the plate-bound peptides for either 2 h at room temperature or overnight at 4°C depending on the avidity of the antibody. All antibodies and antigens were diluted using PBST.

3. Wells were washed again with PBST and 200 µL of substrate, 2,5-tetramethylbenzidine, which was added for 10 min. The colorimetric reaction was then stopped by the addition of 100 µL of 1 *M* HCl.
4. An absorbance reading was then obtained for each well using an ELISA plate reader at a wavelength of 450 nm and a correction wavelength of 650 nm.

### *3.4.2. Competition ELISA to Determine the Crossreactivity Between the hK1-3 Proteins and the hK4 Antibodies (**Table 2**)*

For these studies, the same protocol as above was used except that the primary incubation of peptide-specific antibodies with their cognate plate-bound peptides (**step 2** in **Subheading 3.4.1.**, above) was performed after the peptide-

specific antibodies had been preincubated, separately, for 2 h at room temperature with each of the following proteins: purified hK1 (a gift from Dr D. Proud, Division of Clinical Immunology, Johns Hopkins University School of Medicine, Baltimore, MD), recombinant hK2 (a gift from Hybritech Corp., San Diego, CA) and purified hK3 (Genzyme Diagnostics, CA) **(Table 2)**. In each case, 1 vol of the protein was mixed with 1 vol of the antibody, which had been appropriately diluted, such that the final dilution of antibody was identical to that used in **step 2**, **Subheading 3.4.1.** Two hundred microliters of this mix was then added to the well and left overnight at 4°C. This replaces the primary antibody step detailed above in **step 2**.

## 3.5. Production of Recombinant hK4 Protein

### 3.5.1. Transient Transfection of Mammalian Cell Line, COS7

1. COS7 cells were seeded into 80-$cm_2$ tissue culture flasks to result in a 70–80% confluent monolayer 2 d later. Cells were washed with DMEM containing 1% FBS and then 1 mL of this medium was added to the flask.
2. Plasmid DNA (7.5 µg), hK4 cDNA in the vector pcDNA3.1His (Clontech), was diluted in 75 µL of serum-free OPTI-MEM medium (Life Technologies) in a polystyrene tube for each transfection. In a separate tube, 60 µL of Lipofectamine were added to 500 µL of OPTI-MEM for each transfection. The Lipofectamine mix was added dropwise to the diluted DNA and incubated for 15 min at room temperature.
3. The liposome/DNA solution was then added to 10 mL of DMEM + 5% FBS on the cells in a dropwise manner, and the flask incubated overnight at 37°C in 5% $CO_2$.
4. The following day, the medium was replaced with 20 mL of DMEM + 5% FBS and the cells incubated for 2–3 d at 37°C. One 80-$cm^2$ flask of cells was then harvested on d 2 and d 3 after transfection. The tissue culture fluid was clarified by centrifugation at 750*g* for 5 min at 4°C and stored at –20°C. Cells were harvested by scraping them from the flask and resuspending in 5 mL of PBS. The cells were pelleted also by centrifugation at 750*g* for 5 min at 4°C. The supernatant was removed and the pellet stored at –20°C.

### 3.5.2. Purification of Recombinant K4 Protein Using the His Tag

1. The cell pellets were thawed and resuspended in 1 mL of $H_2O$, vortexed for 1 min, left on ice for 15 min, and centrifuged at 18,000*g* for 5 min at 4°C. The supernatant was transferred to a new tube and 100 µL of the washed His affinity resin (*see* **Materials**) and 20 µL of protease inhibitors were added. Similarly, 100 µL of washed His affinity resin and 100 µL of protease inhibitors were added to 5 mL of the original tissue culture fluid (*see* **Note 3**).
2. These samples were rotated for 1 h at 4°C. The resin was pelleted by centrifugation at 9000*g* for 2 min at 4°C. The supernatant was removed and the resin washed twice with 1 mL of 1X extraction buffer (pH 7.0) containing 20 µL of protease inhibitors. The samples were stored at 4°C before the addition of electrophoresis sample buffer (*see* **Note 4**).

### 3.6. Western Blot Analysis

1. Equal amounts of electrophoresis sample buffer were added to 10–20 µL of the His-resin purified samples (described in **Subheading 3.5.2.**). The samples were boiled for 5 min and centrifuged briefly at 18,000*g*. The samples were electrophoresed through a 10% SDS-polyacrylamide gel.
2. The proteins were transferred to a Protran membrane (Schleicher and Schuell, Dassel, Germany), in 1X bicarbonate buffer containing 20% (v/v) methanol using a wet transfer apparatus (Bio-Rad) at 200 mA for 2 h (*see* **Note 5**).
3. The membrane was blocked with 5% skim milk in TBS + 0.05% Tween-20 overnight at 4°C to reduce nonspecific binding.
4. The membrane was incubated with an affinity-purified anti-hK4 peptide antibody (1/500 dilution) for 2 h at room temperature. The blot was washed three times for 5 min with TBS/Tween-20, and then incubated for 1 h with a horseradish peroxidase (HRP) goat anti-rabbit IgG (1/2000 dilution) at room temperature.
5. Finally, the blot was incubated with chemiluminescent substrate as described by the manufacturer, then exposed to X-ray film for visualization. These results are shown in **Fig. 2**.

### 3.7. Immunohistochemistry

1. Deparaffinization, rehydration, and antigen retrieval: Formalin-fixed paraffin blocks from prostate cancer tissues were sectioned (4 µm), deparaffinized in xylene, and rehydrated through descending graded alcohols to TBS. Then the antigen was retrieved by microwave heat treatment in 5% urea in 0.1 *M* Tris buffer (pH 9.5) for 5 min (*see* **Note 6**).
2. Inhibition of endogenous peroxidase and blocking of nonspecific binding: After $H_2O_2$ treatment (3% $H_2O_2$ and 18% methanol in TBS for 10 min), the sections were incubated for 2 h with the affinity-purified anti-hK4 peptide antibody (1/250 dilution) at room temperature. The EnVision$^{+TM}$ peroxidase (anti-rabbit) polymer (DAKO) was then added according to the manufacturer's instructions.
3. Peroxidase activity was detected using 3,3′-diaminobenzidine as the chromogen and with $H_2O_2$ as the substrate.
4. The sections were counterstained with Mayer haematoxylin for 5 min and the slides mounted with a coverslip. The results are shown in **Fig. 3**.
5. Negative controls are usually performed by using normal rabbit serum at the same dilution as the primary antibody or primary antibody preabsorbed with hK4 peptides instead of the primary antibody.

## 4. Notes

1. In general, when designing such peptides as immunogens, a length of at least 9 to 12 amino acids should be selected. This will ensure that optimal amounts of peptides are produced while still providing an appropriate epitope sequence for antibody binding. Efficient conjugation to immunogens for the immunization of animals is best achieved with limited numbers of cysteines within the peptide

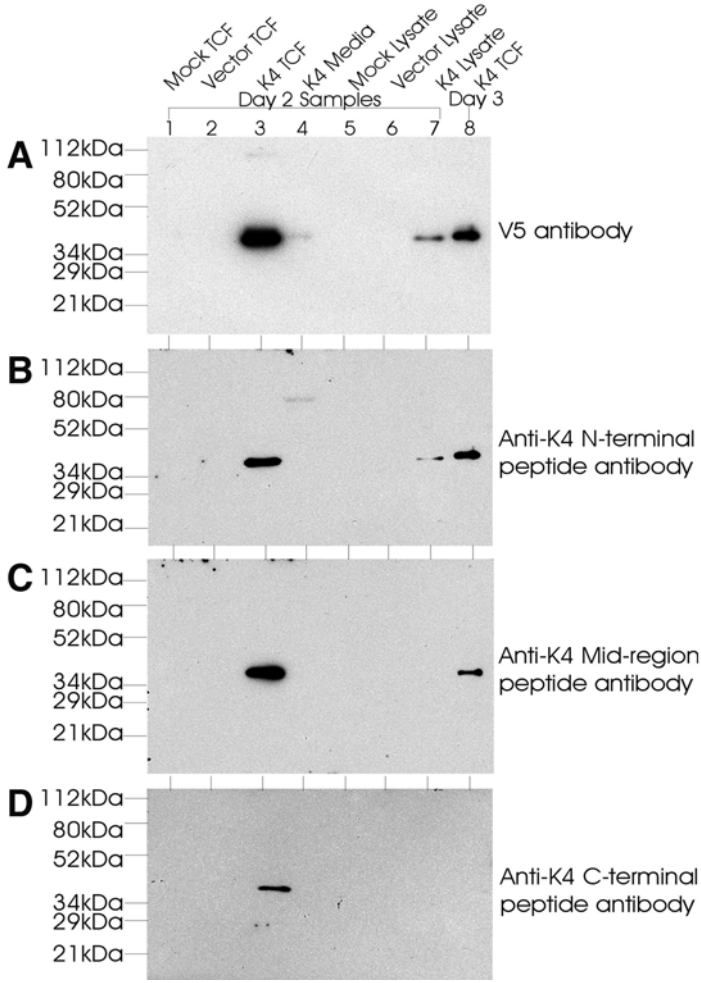


Fig. 2. Western blot analysis with V5 antibody **(A)** and affinity purified antipeptide hK4 antibodies (**B**: anti-hK4 N-terminal peptide Ab; **C:** anti-hK4 mid-region peptide Ab; **D:** anti-hK4 C-terminal peptide Ab) of samples from mock-, vector only, and *KLK4*-transfected COS-7 cells at Day 2 (lanes 1–7) or Day 3 (lane 8). Tissue culture fluid (lanes 1–3, 8) and cell lysate (lanes 5–7) were collected and hK4 protein purified using His resin. For comparison, a tissue culture fluid sample was taken before the addition of the His resin (lane 4). The size of the protein molecular weight markers is shown at the left. A hK4 protein of $M_r$ 40,000 was detected by all three antibodies within cells transfected with the *KLK4* cDNA. These results were verified further using a V5 antibody (Invitrogen), as the construct used for transfection contains a V5 epitope just upstream of the *KLK4* gene insert. Thus, the hK4 antipeptide antibodies can detect recombinant hK4 and presumably native hK4.

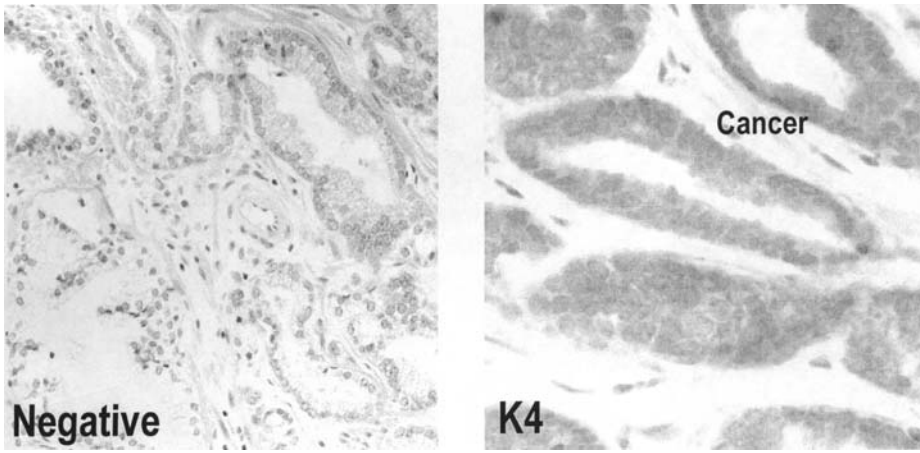


Fig. 3. Immunohistochemistry using the pooled N-terminal and mid-region hK4 antipeptide antibodies (1:250) on a prostate cancer tissue section showing positive immunostaining in the epithelial-derived malignant cells (right panel). The left panel shows the negative control obtained when the primary antibody was replaced with PBS. A similar pattern was obtained (that is, no staining was observed) when the anti-hK4 primary antibodies were preabsorbed with the peptide immunogens. Moreover, the same pattern of positive immunostaining seen in the right hand panel was observed when the primary anti-hK4 antibodies were preabsorbed with PSA (hK3) or hK2 proteins, indicating that there was no crossreactivity with these similar kallikreins and that the antipeptide antibodies are specific for hK4.

sequence. This precaution will restrict the covalent attachment sites of the peptide to the immunogen, maximizing the potential for a more uniform population of derived antibodies. Additionally, the lower the number of cysteines, the less is the chance of unproductive oligomers and covalent conformers produced by disulfide formation. Furthermore, for the production of sufficient amounts of antisera, larger animals such as rabbits or sheep should be used.

2. From the results in the ELISA experiments, it is clear that the choice of antibodies for crossreactivity studies is very important. For example, if a polyclonal antibody is used in the assay and found to crossreact with the peptide of interest, it does not necessarily mean that the peptide is as nonspecific, as it appears as the polyclonal antiserum itself may not be entirely specific. The use of monoclonal antibodies, if available, is much more desirable and will give a more accurate representation of the peptide's specificity. Nevertheless, given the high homology within certain regions of the kallikreins, even monoclonal antibodies can crossreact with other family members.
3. When purifying recombinant proteins using polyhistidine-affinity resin, samples should be kept on ice or at 4°C throughout the entire procedure to minimize the

level of degradation of the protein. If the protein you are working with is rather unstable, it is also very important to include a mixture of different protease inhibitors in each step to further reduce the degradation of the protein. If the protein is still being degraded it is important to try different protease inhibitors as individual proteins are effected to variable degrees by different proteases.

4. The extraction buffer (pH 7.0) used in the recombinant protein purification process preserves the native structure and surface charge characteristics of a wide range of soluble proteins during the harvest from an expression host. However, some proteins are not stable or do not adsorb at pH 7.0; therefore, changing the pH of the extraction buffer may be of benefit. However, increasing the pH allows amino acids other than histidine to bind to the resin and thereby increases the nonspecific binding. Denaturing buffers (e.g., containing guanidine-HCl) enhance the protein solubility and thus may be helpful if the protein of interest has been expressed in an insoluble form.
5. The 1X carbonate buffer used for electroblotting should be made up fresh and chilled every time. The methanol should be added just prior to setting up the transfer for best results.
6. For antigen retrieval, before immunohistochemistry, both the temperature and the time at this temperature ($2 \times 5$ min boiling), as well as the pH of the antigen retrieval buffer are important for correct staining. 0.1 *M* sodium citrate buffer (pH 6.0) is often used instead of the 5% urea in 0.1 *M* Tris buffer (pH 9.5) as antigen retrieval solution. Different buffer and pH combinations should be tried for optimum specific staining and limited nonspecific background.

## References

1. Polascik, T. J., Oesterling, J. E., and Partin, A. W. (2000) Prostate specific antigen: A decade of discovery—what we have learned and where we are going. *J. Urol.* **163,** 1259–1260.
2. Carducci, M. A., DeWeese, T. L., and Nelson, J. B. (1999) Prostate-specific antigen and other markers of therapeutic response. *Urol. Clin. North. Am.* **26,** 291–302.
3. Brawer, M. K., Benson, M. C., Bostwick, D. G., Djavan, B., Lilja, H., Semjonow, A., et al. (1999) Prostate-specific antigen and other serum markers: Current concepts from the World Health Organization Second International Consultation on Prostate Cancer. *Semin. Urol. Oncol.* **17,** 206–221.
4. Frydenburg, M., Stricker, P. D., and Kaye, K. W. (1997) Prostate cancer diagnosis and management. *Lancet* **349,** 1681–1687.
5. Beduschi, M. C. and Oesterling, J. E. (1998) Percent free PSA: the next frontier in PSA testing. *Urology* **51 (5A suppl),** 98–109.
6. Riegman, P. H., Vlietstra, R. J., van der Korput, J. A., Romijn, J. C., and Trapman J. (1989) Characterization of the prostate-specific antigen gene: A novel human kallikrein-like gene. *Biochem. Biophys. Res. Commun.* **159,** 95–102.
7. Rittenhouse, H. G., Finlay, J. A., Mikolajczyk, S. D., and Partin, A. W. (1998) Human kallikrein 2 (hK2) and prostate specific antigen (PSA): two closely related but distinct kallikreins in the prostate. *Crit. Rev. Clin. Lab. Sci.* **35,** 275–368.

8. Tremblay, R. R, Deperthes, D., Tetu, B., and Dube, J. Y. R. (1997) Immunohistochemical study suggesting a complementary role of kallikreins hK2 and hK3 (prostate-specific antigen) in the functional analysis of human prostate tumors. *Am. J. Pathol.* **150,** 455–459.
9. Darson, M. F., Pacelli, A., Roche, P., Rittenhouse, H. G., Wolfert, R. L., Young, et al. (1997) Human glandular kallikrein 2 (hK2) expression in prostatic intraepithelial neoplasia and adenocarcinoma: A novel prostate cancer marker. *Urology* **49,** 857–862.
10. Young, C. Y., Seay, T., Hogen, K., Charlesworth, M. C., Roche, P. C., Klee, G. G., and Tindall, D. J. (1996) Prostate-specific human kallikrein (hK2) as a novel marker for prostate cancer. *Prostate* **(Suppl 7),**17–24.
11. Kwiatkowski, M. K., Recker, F., Piironen, T., Pettersson, K., Otto, T., Wernli, M., and Tscholl, R. (1998) In prostatism patients the ratio of human glandular kallikrein to free PSA improves the discrimination between prostate cancer and benign hyperplasia within the diagnostic "gray zone" of total PSA 4 to 10 ng/mL. *Urology* **52,** 360–365.
12. Magklara, A., Scorilas, A., Catalona, W. J., and Diamandis, E. P. (1999) The combination of human glandular kallikrein and free prostate-specific antigen (PSA) enhances discrimination between prostate cancer and benign prostatic hyperplasia in patients with moderately increased total PSA. *Clin. Chem.* **45,** 1960–1966.
13. Nam, R. K., Diamandis, E. P., Toi, A., Trachtenberg, J., Magklara, A., Scorilas, A., et al. (2000) Serum human glandular kallikrein-2 protease levels predict the presence of prostate cancer among men with elevated prostate-specific antigen. *J. Clin. Oncol.* **18,** 1036–1042.
14. Haese, A., Becker, C., Noldus, J., Graefen, M., Huland, E., Huland, H., and Lilja, H. (2000) Human glandular kallikrein 2: A potential serum marker for predicting the organ confined versus non-organ confined growth of prostate cancer. *J. Urol.* **163,** 1491–1497.
15. Recker, F., Kwiatkowski, M. K., Piironen, T., Pettersson, K., Huber, A., Lummen, G., and Tscholl, R. (2000) Human glandular kallikrein as a tool to improve discrimination of poorly differentiated and non-organ-confined prostate cancer compared with prostate-specific antigen. *Urology* **55,** 481–485.
16. Riegman, P. H., Vlietstra, R. J, Suurmeijer, L., Cleutjens, C. B., and Trapman, J. (1992) Characterization of the human kallikrein locus. *Genomics* **14,** 6–11.
17. Evans, B. A., Yun, Z. X., Close, J. A., Tregear, G. W., Kitamura, N., Nakanishi, S., et al. (1988) Structure and chromosomal localization of the human renal kallikrein gene. *Biochemistry* **27,** 3124–3129.
18. Schedlich, L. J., Bennetts, B. H., and Morris, B. J. (1987) Primary structure of a human glandular kallikrein gene. *DNA* **6,** 429–437.
19. Harvey, T. J., Hooper, J. D., Myers, S. A., Stephenson, S. A., Ashworth, L. K., and Clements, J. A. (2000) Tissue-specific expression patterns and fine mapping of the human kallikrein (*KLK*) locus on proximal 19q13.4. *J. Biol. Chem.* **275,** 37397–37406.
20. Yousef, G. M., Chang, A., Scorilas, A., and Diamandis, E. P. (2000) Genomic organization of the human kallikrein gene family on chromosome 19q13.3-q13.4. *Biochem. Biophys. Res. Commun.* **276,** 125–133.

21. Stephenson, S. A., Verity, K., Ashworth, L. K., and Clements, J. A. (1999) Localization of a new prostate-specific antigen-related serine protease gene, *KLK4*, is evidence for an expanded human kallikrein gene family cluster on chromosome 19q13.3-13.4. *J. Biol. Chem.* **274,** 23210–23214.
22. Yousef, G. M., Obiezu, C. V., Luo, L. Y., Black, M. H. and Diamandis EP. (1999) Prostase/KLK-L1 is a new member of the human kallikrein gene family, is expressed in prostate and breast tissues, and is hormonally regulated. *Cancer Res.* **59,** 4252–4256.
23. Nelson, P. S., Gan, L., Ferguson, C., Moss, P., Gelinas, R., Hood, L., and Wang, K. (1999) Molecular cloning and characterization of prostase, an androgen-regulated serine protease with prostate-restricted expression. *Proc. Natl. Acad. Sci. USA* **96,** 3114–3119.
24. Mitsui, S., Yamada, T., Okui, A., Kominami, K., Uemara, H., and Yamaguchi, N. (2000) A novel isoform of a kallikrein-like protease, TLSP/hippostatin, (PRSS20), expressed in the human brain and prostate. *Biochem. Biophys. Res. Commun.* **272,** 205–211.
25. Yousef, G. M., Scorilas, A., Magklara, A., Soosaipilli, A., and Diamandis, E. P. (2000) Molecular cloning of the human kallikrein 15 gene (*KLK15*): Upregulation in prostate cancer. *J. Biol. Chem.* **276,** 53–61.
26. Hooper, J. D., Bui, L. T., Rae, F. K., Harvey T. J., Myers, S. A., Ashworth, L. K., and Clements, J. A. (2001) Identification and characterisation of *KLK14*, a novel kallikrein serine protease gene located on human chromosome 19q13.4 and expressed in prostate and skeletal muscle. *Genomics* **73,** 117–122.
27. Hu, J. C., Szhang, C., Sun, X., Yang, Y., Cao, X., Ryu, O., and Simmer, J. P. (2000) Characterisation of the mouse and human PRSS17 genes, their relationship to other serine proteases and the expression of PRSS17 in developing mouse incisors. *Gene* **251,** 1–8.
28. Bridon, D. P. and Dowell, B. L. (1995) Structural comparison of prostate-specific antigen and human glandular kallikrein using molecular modelling. *Urology* **45,** 801–806.
29. Piironen, T., Villoutreix, B. O., Becker, C., Hollingsworth, K., Vihinen, M., Bridon, D., et al. (1998) Determination and analysis of antigenic epitopes of prostate specific antigen (PSA) and human glandular kallikrein 2 (hK2) using synthetic peptides and computer modeling. *Protein Sci.* **7,** 259–269.
30. Michel, S., Deleage, G., Charrier, J. P., Passagot, J., Battail-Poirot, N., Sibai, G., et al. (1999) Anti-free prostate-specific antigen monoclonal antibody epitopes defined by mimotopes and molecular modeling. *Clin. Chem.* **45,** 638–650.

# 15

# The Androgen Receptor CAG Repeat and Prostate Cancer Risk

**Peter E. Clark, Ryan A. Irvine, and Gerhard A. Coetzee**

## 1. Introduction

The androgen receptor (AR) gene comprises eight exons located at chromosome Xq11-12 and encodes an mRNA transcript of approx 11 kb ***(1–5)***. Situated within exon 1 of the AR gene is a polymorphic CAG trinucleotide repeat, which encodes a polyglutamine (poly-Q) tract of variable length in the N-terminal domain of the AR protein. The normal size range of this poly-Q tract is between 6 and 39 repeats ***(6,7)***. The gene is considered a good candidate to play a role in the etiology of prostate cancer because of this variation and the well-documented importance of AR signaling in prostate development and tumor growth. Although earlier family studies failed to link prostate cancer to the AR locus, the CAG repeat variations of this locus have been considered to play a modifying role in prostate cancer risk (as apposed to causing it). The AR on the X chromosome is, furthermore, thought to contribute to the increased brother/brother vs father/son risk associations observed in several studies ***(8–10)***. More recently, however, linkage to the AR locus (LOD score 3.06, $p$ = 0.00053) was observed in 254 families if, and only if, Gleason score, age of onset, male-to-male transmission, and/or number of affected first-degree family members were included as covariates ***(10)***.

### *1.1. The Evolution of the AR CAG Repeat*

Over the course of primate evolution, the AR CAG microsatellite has progressively expanded ***(11,12)***. For example, it has been shown that the mean uninterrupted CAG repeat size in Old World marmoset, macaque, and drill monkeys is 3, 7, and 8, respectively ***(11)***. Furthermore, several other human microsatellite repeats are longer than in the equivalent genes in primates, sug-

From: *Methods in Molecular Medicine, Vol. 81: Prostate Cancer Methods and Protocols*
Edited by: P. J. Russell, P. Jackson, and E. A. Kingsley © Humana Press Inc., Totowa, NJ

gesting a selection bias towards expansion of these microsatellite repeats over the course of human evolution ***(13)***. Any such mutational bias and resulting directional expansion of the microsatellite repeats would, of course, be expected to be evolutionarily tolerated only so long as these changes did not result in a significant decrease in reproductive fitness, such as a functional disruption of the protein.

### 1.2. The AR CAG Repeat and Kennedy's Disease

Abnormal expansion of the CAG microsatellite to 40 repeats or more results in a rare, X-linked, neurodegenerative disorder in adults called spinal and bulbar muscular atrophy (SBMA), also known as Kennedy's disease ***(14,15)***. The hallmark of the disease is progressive muscle atrophy secondary to progressive loss of motor neurons in both the brain stem and spinal cord. In addition, men frequently develop symptoms consistent with partial androgen insensitivity, including gynecomastia and testicular atrophy, which are indicative of aberrant AR function ***(16,17)***. In support of this, in vitro transient cotransfection experiments have demonstrated that the mutant AR encoded for in SBMA has reduced transactivation activity when compared with wild-type AR while maintaining normal androgen-binding affinities ***(18,19)***. Numerous studies have subsequently demonstrated an inverse relationship between CAG repeat length and AR transactivation activity over a wide range of CAG repeat sizes that encompass the entire range of normal AR alleles ***(20–23)***. Thus, the abnormal AR poly Q tract expansion seen in men with SBMA results in a loss of AR transactivation competency, which manifests itself as partial androgen insensitivity. Androgen receptors with the smaller poly Q tract in normal men can then, in effect, be viewed as having a gain of function through an increase in transactivation activity, and as a consequence result in an apparent increase in androgen sensitivity.

### 1.3. The AR CAG Repeat and Prostate Cancer Risk

In 1992, Edwards and coworkers ***(6)*** reported on the allelic frequency distribution of AR based on the CAG repeat size in different US racial-ethnic populations as part of a larger survey of genetic variation in a series of different trimeric and tetrameric tandem repeats. This study found that among African Americans, who are at a higher risk for developing prostate cancer, the frequency of AR alleles with less than 22 CAG repeats was 65%, as compared with 53% in Caucasians, who are at intermediate risk, and 34% in Asian Americans, who are at lower risk. Because of the apparent correlation between the overall racial-ethnic population risk for developing prostate cancer and the frequency for this arbitrarily defined short CAG allele, we ***(24)*** postulated that the number of men with short CAG AR alleles should be enriched in a population

**Table 1**
**Summary of Studies Evaluating the Role of the AR CAG in Prostate Cancer Risk, Progression, and Age at Onset**

| Study | Subjects | Risk | Stage/grade | Age at Onset |
|---|---|---|---|---|
| Irvine et al. ***(25)*** | US Caucasian | Yes (with GGC) | NA | NA |
| Hardy et al. ***(43)*** | US Caucasian | NA | No | Yes |
| Ingles et al. ***(26)*** | US Caucasian | Yes | Yes | NA |
| Giovannucci et al. ***(7)*** | US Caucasian | Yes | Yes | No |
| Stanford et al. ***(27)*** | US Caucasian | Yes | No | Yes |
| Hakimi et al. ***(28)*** | US Caucasian | Yes | Yes | No |
| Ekman et al. ***(29)*** | Swedes | Yes | NA | NA |
| Correa-Cerro et al. ***(33)*** | French/German | No | No | No |
| Edwards et al. ***(34)*** | British | No | No | NA |
| Bratt et al. ***(35)*** | Swedes | No | Yes | Yes |
| Lange et al. ***(36)*** | US Caucasian | No | No | No |
| Hsing et al. ***(30)*** | Shanghai Chinese | Yes | No | NA |
| Nam et al. ***(31)*** | Canadian | No | Yes | NA |

NA = not applicable or not addressed.

of prostate cancer patients when compared with a control population. We further hypothesized that because a shorter CAG AR allele encodes for a more transcriptionally active receptor, this could promote tumorigenesis by enhancing prostatic epithelial cell turnover.

In 1995, we tested this hypothesis directly in a small case/control study examining 68 prostate cancer patients and 123 control subjects ***(25)***. As in the study by Edwards and coworkers ***(6)***, there was a high prevalence of short CAG AR alleles among the African-American controls. There was, in addition, a modest, though not significant, enrichment of short CAG AR alleles in the Caucasian prostate cancer population. These supportive results were later confirmed and further extended in an expanded follow-up study using the same prostate cancer patients but a larger control population ***(26)***. A significantly higher prevalence of short CAG AR alleles was noted among prostate cancer patients. This was especially true for patients with advanced disease, defined as tumors that progressed outside of the prostatic capsule.

Numerous studies have subsequently been published evaluating the role of the AR CAG microsatellite polymorphism and the risk of developing prostate cancer (summarized in **Table 1**). The largest such study, by Giovannucci and coworkers ***(7)*** used a population selected from the Physicians Health Study. Five hundred and eighty seven prostate cancer cases and 588 controls were

selected from this large cohort of 22,071 US, predominantly Caucasian (95%), male physicians, 40–84 yr old. The large sample size of this study allowed the authors to stratify the case patients by tumor grade and stage. They observed a highly significant inverse correlation between CAG repeat length and the risk of developing prostate cancer when the CAG repeat size was analyzed as a continuous variable. As with our results, short CAG AR alleles correlated with an increased risk of developing advanced disease, defined as a high-stage or high-grade tumor; however, this correlation did not exist for low-stage/-grade disease. Thus, a man with an AR CAG repeat length of 19 was 2.5 times more likely to develop high grade/stage prostate cancer than an individual with a CAG repeat size of 25, but no more likely to develop low grade/stage disease.

In 1997, Stanford and coworkers ***(27)*** published a different study analyzing CAG repeat length and prostate cancer risk in 301 Caucasian prostate cancer cases and 277 matched controls. This study noted only a small increase in CAG alleles less than 22 repeats in size in the cancer patients when compared with the controls. Nevertheless, when the CAG repeat size was examined as a continuous variable, they observed an overall age-adjusted relative odds of developing prostate cancer of 0.97. In contrast to both our study and that of Giovannucci et al., there was no apparent distinction between the risk of developing localized vs advanced disease among the men in this study.

Another study by Hakimi and coworker ***(28)*** in Caucasian men measured the CAG repeat length among 59 prostate cancer patients and 370 controls. Six of the 59 cases (10%) had a short CAG AR allele, that is, less than 18 repeats, whereas only 11 of 370 controls (3%) had a short CAG allele ($p = 0.02$). Furthermore, 5 of 6 (83%) patients with short CAG AR alleles had advanced disease, defined as prostate cancer involving the lymph nodes.

More recently, other studies ***(29,30)*** found that CAG alleles were significantly shorter among Swedish and Shanghai Chinese prostate cancer patients compared to controls. Nam and coworkers ***(31)*** found an increased risk associated with shorter CAG repeats only among patients at low risk for recurrence and not for patients at high risk of recurrence. In another recent study, Platz and coworkers ***(32)*** used multivariable, pooled logistic regression to adjust for potential dietary and lifestyle factors in a sample of African-Americans, Asians, and Caucasians and concluded that the AR CAG repeat difference remained a significant factor in explaining the excess risk of prostate cancer among African-American men. In contrast to the numerous above-mentioned studies, no significant correlations between CAG repeat length and prostate cancer risk were found among French or German men ***(33),*** British Caucasians ***(34),*** nor among a different cohort of Swedish men ***(35)***. Also, Lange and coworkers ***(36)*** found no correlation between any prostate cancer parameter and AR CAG repeat length among US Caucasians.

The reasons for the disparate results are not clear but might be related to the heterogeneous nature of the disease itself or caused by unknown covariates or confounders not being taken into account. For example, it is possible that there are other, as yet unidentified, functional genetic changes (like the GGN repeat or single nucleotide polymorphisms) near the CAG microsatellite with which it is in partial linkage disequilibrium. Because such putative variations were not controlled for in the studies referred to above, they could influence the results between studies. Furthermore, prostate cancer patients present with everything from clinically insignificant disease, such as a small focus of Gleason score 2 disease, which is biologically indolent and unlikely to impact on a patient's health, to high-risk aggressive disease, such as a Gleason score 10 tumor, which has spread beyond the prostate and is likely to be fatal. The relative proportions of high- vs low-risk disease and localized vs advanced disease most likely vary across studies and could account for at least part of the differences between them. Furthermore, differences may also exist in how the control populations were defined and how it was determined that the controls did not have prostate cancer. For example, was the absence of prostate cancer only self-reported by the participant, was PSA and digital rectal examination screening performed, or was the information solely obtained from medical records or tumor registries? The studies also vary with respect to their racial and socioeconomic distribution. For example, many do not contain a significant number of African American subjects whereas one of the largest is limited to health professionals. Further methodological differences may include how the short vs long CAG repeat length was defined in different studies or whether this was treated as a continuous variable. Not all of these studies may have adequately controlled for known or suspected dietary or hormonal risk factors for prostate cancer, such as high fructose intake, high calcium intake, low tomato consumption, cigarette smoking, low physical activity, or high serum androgen levels, all factors known to influence prostate cancer risk. With the number of potential confounding variables, it is perhaps not surprising that these studies have often reached disparate conclusions. A final answer, then, awaits the difficult task of resolving all of these many challenging issues.

Although the epidemiologic studies, discussed above, explore the apparent correlation between AR CAG repeat variation and prostate cancer risk, they do not address the molecular mechanisms that underlie changes in AR transactivation activity caused by CAG repeat variation. For example, protein partners that interact with the poly-Q stretch are largely unknown at present. Methods addressing such mechanistic studies are currently being developed in many laboratories and should aid in the interpretation of the association results. Such development is necessary to ultimately evaluate the utility of prior knowledge of a man's AR CAG repeat in risk assessments.

### 1.4. Cell Culture Studies

Several investigators have demonstrated that although ARs with larger CAG repeats have normal ligand binding affinities, they have lower transactivation activity in in vitro transient cotransfection studies *(18–23)*. For example, Chamberlain and coworkers in 1994 *(19)* showed that an AR construct with 49 CAG repeats had approximately 17% less transactivation activity on the MMTV promoter than an AR construct with 25 CAG repeats. Similarly, in 1995 Kazemi-Esfarjani and coworkers *(20)* observed a 30–40% decrease in transactivation, again on the MMTV promoter, when the CAG repeat size increased from 12 to 40 residues. Another study, however, found blunted AR transactivation activity with either expansion or contraction of the CAG microsatellite from 20 repeats *(37)*. Although the protein expression levels of AR have been found to be stable across CAG repeat sizes from 9 to 42, at least two studies have found that AR constructs with larger repeats (50–52) are unstable and undergo degradation (possibly in a ligand-dependent fashion) producing degradation products of approximately 70 to 74 kDa *(22,38)*.

The moderate poly-Q size effect in vitro in AR transactivation activity observed in most studies is thought to be mediated, at least in part, through altered functional interactions with the AR coactivator complex. For example, in transient cotransfection experiments, the relative decrease in AR transactivation activity with increasing CAG size is larger in p160 coactivator mediated enhancement of AR activity than in AR activity measured alone *(22)*. This effect is most likely secondary to steric hindrance of the interaction of p160 with the AR caused by the increased CAG size. However, the possibility that direct effects mediated via other cofactors, be they cell, promoter, and/or AR-specific, cannot be completely excluded. A candidate for such a cofactor is the RAS related G-protein, also known as Ran or AR-associated protein 24, which has been shown to bind to the poly-Q stretch of the N terminal domain of AR and appears to coactivate the AR in a poly-Q size-dependent manner *(39)*. Given this protein's well-described role in the nuclear transport of proteins, it is possible that Ran less efficiently transports AR with a larger CAG repeat into the nucleus, which may explain the observed poly-Q dependent variation in coactivation *(40)*. Clearly, more studies are needed to clarify this hypothesis.

## 2. Materials

### 2.1. Polymerase Chain Reaction (PCR) Materials

The materials used for the PCR reactions can be obtained in kit form from any one of many commercial suppliers. The storage and usage conditions are as recommended by the particular supplier. For example, any of many temperature-stable polymerases might be used. The materials for the polyacrylamide

gel electrophoresis are standard and commercially available from many suppliers (note the toxic nature [inhalation and skin exposure] of unpolymerized acrylamide powder and solutions). The [α-$^{32}$P]dCTP used in the PCR reactions is radioactive and appropriate exposure protection needs to be taken including Plexiglas shields and the use of safety eyeglasses.

### 2.2. Cell Culture Transfection Materials

Cell culture plasticware and media are generic and available from many suppliers. The medium is prepared, stored, and used as recommended by them. DNA transfection materials and luciferase detection kits are stored and used as recommended by the particular supplier.

## 3. Methods

### 3.1. Determination of the AR CAG Repeat Number

Two methods are commonly employed to measure CAG repeat number from genomic DNA of men. The first is manual ***(25)*** and the second semi-automated ***(7)***. A point to remember is that the AR is located on the X chromosome, so that each man has only one allele and thus one size of the CAG repeat. Furthermore, the polymerase amplification of the DNA fragment that contains the CAG repeat results in so-called stutter bands caused by slippage of the enzyme during the DNA polymerization. Obviously, size measurements must consider the same band product across samples.

#### 3.1.1. Manual Method

The exon 1 CAG repeat of the AR is amplified from about 10 ng of genomic DNA in two rounds of PCR using *Taq* DNA polymerase and nested primers ***(41)***. The outside or first round PCR primers are 5′-GTGCGCGAAGTGATCCAGAA-3′ and 5′-TCTGGGACG-CAACCTCTCTC-3′. The inside or second round PCR primers are 5′-AGAGGCC-GCGAGCGCAGCACCTC-3′ and 5′-GCTGTGAAGGTTGCTGTTCCTCAT-3′. The first round of PCR consists of 17 cycles of the following steps: 94°C for 1 min; 55°C for 1 min; and 72°C for 1.5 min. The second round, performed with 1 μL of the first-round reaction and 2 μCi of [α-$^{32}$P]dCTP, consists of 28 cycles of the following steps: 94°C for 1 min; 66°C for 1 min; and 72°C for 1.5 min. Second round PCR products are then separated on 5% denaturing polyacrylamide gels that are subsequently exposed to X-OMAT film. The number of CAG repeats is determined by comparing the size of the predominant PCR product (i.e., the middle radiographic band, **Fig. 1**) to a series of previously sequenced CAG size standards. All unknown samples from a particular autoradiogram are then ranked accord-

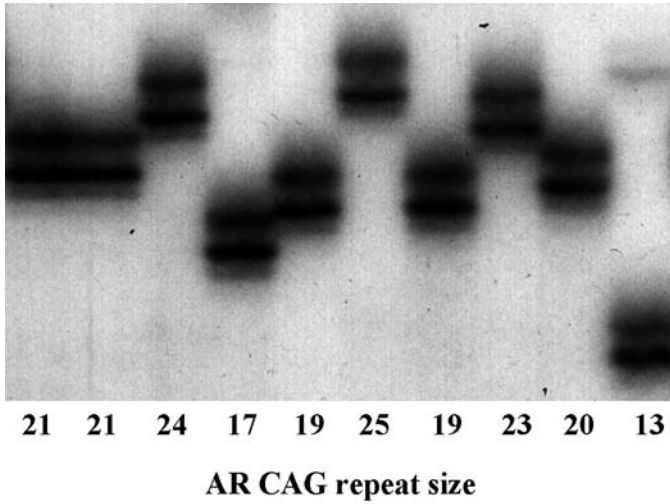


Fig. 1. Autoradiogram of CAG-amplified products resolved on Urea/PAGE.

ing to relative size and run a second time to confirm or modify the original CAG size determination.

#### *3.1.2. Semi-Automated Method*

The exon 1 CAG repeat of the AR is amplified using fluorescent labeled primers 5′-TCC-AGAATCTGTTCCAGAGCGTGC-3′ and 5′-GCTGTGAAG-GTTGCTGTTCCTCAT-3′. Products are resolved and sized utilizing a denaturing polyacrylamide gel and an automated fluorescence detection system (Genescan; Applied Biosystems).

### *3.2. Measurement of AR Transactivation Activity Using Transient Cotransfection Assays*

These methods are adapted from those of Buchanan and coworkers ***(42)***.

Prostate cancer cells (PC-3, DU-145 or LNCaP) are plated into 96-well culture plates at a density of 15,000 cells/well. The next day, the cells are transfected with plasmids and Lipofectamine2000 Reagent. The latter are prepared using two tubes as follows (per well):

1. Mix 25 µL of medium with 100 ng of reporter gene plasmid (Luciferase under control of an androgen response element-containing promoter) and 2.5 ng of receptor plasmid (AR expression plasmid) in one tube.
2. Mix 25 µL of medium and 0.4 µL of Lipofectamine2000 in another tube. Tubes 1 and 2 are combined, mixed, and incubated at room temperature 20–30 min (transfection solution). Culture medium is removed from the wells, replaced with 50 µL

of the transfection solution, and incubated for 3–5 h. The transfection solution is then replaced with 200 µL of culture medium and incubated for 36–48 h. Luciferase activity is then measured in cell lysates using Promega's luciferase reporter kit.

Normally, experiments are constructed using quadruplicate wells/experimental points. The total amount of DNA being transfected per well in a particular experiment is balanced across all experimental points by using equivalent molar amounts of all promoter elements (using empty vectors so that limited general transcription factors are the same across all experimental conditions) as well as equivalent DNA mass (using the promoter-less plasmid pCAT basic [Promega] as filler DNA).

## Acknowledgments

The work of the authors reported herein was supported from grants of the NIH (R55CA/OD73821 and R01CA84890) and Department of Defense (DAMD170010102).

## References

1. Lubahn, D. B., Joseph, D. R., Sullivan, P. M., Willard, H. F., French, F. S., and Wilson, E. M. (1988) Cloning of human androgen receptor complementary DNA and localization to the X chromosome. *Science* **240,** 327–330.
2. Lubahn, D. B., Brown, T. R., Simental, J. A., Higgs, H. N., Migeon, C. J., Wilson, E. M., et al. (1989) Sequence of the intron/exon junctions of the coding region of the human androgen receptor gene and identification of a point mutation in a family with complete androgen insensitivity. *Proc. Natl. Acad. Sci. USA* **86,** 9534–9538.
3. Chang, C. S., Kokontis, J., and Liao, S. T. (1988) Structural analysis of complementary DNA and amino acid sequences of human and rat androgen receptors. *Proc. Natl. Acad. Sci. USA* **85,** 7211–7215.
4. Tilley, W. D., Marcelli, M., Wilson, J. D., and McPhaul, M. J. (1989) Characterization and expression of a cDNA encoding the human androgen receptor. *Proc. Natl. Acad. Sci. USA* **86,** 327–331.
5. Brown, C. J., Goss, S. J., Lubahn, D. B., Joseph, D. R., Wilson, E. M., French, F. S., et al. (1989) Androgen receptor locus on the human X chromosome: Regional localization to Xq11-12 and description of a DNA polymorphism. *Am. J. Hum. Genet.* **44,** 264–269.
6. Edwards, A., Hammond, H. A., Jin, L., Caskey, T., and Chakraborty, R. (1992) Genetic variation at five trimeric and tetrameric tandem repeat loci in four human population groups. *Genomics* **12,** 241–253.
7. Giovannucci, E., Stampfer, M. J., Krithivas, K., Brown, M., Dahl, D., Brufsky, A., et al. (1997) The CAG repeat within the androgen receptor gene and its relationship to prostate cancer. *Proc. Natl. Acad. Sci. USA* **94,** 3320–3323.
8. Monroe, K. R., Yu, M. C., Kolonel, L. N., Coetzee, G. C., Wilkens, L. R., Ross, R. K., and Henderson, B. E. (1995) Evidence of X-linked or recessive genetic component to prostate cancer risk. *Nat. Med.* **1,** 827–829.

9. Narod, S. A., Dupont, A., Cusan, L., Diamond, P., Gomez, J.-L., Suburu, R., and Labrie F. (1995) The impact of family history on early detection of prostate cancer. *Nat. Med.* **1,** 99–101.
10. Goddard, K. A. B., Witte, J. S., Suarez, B. K., Catalona, W. J., and Olson, J. M. (2001) Model-free linkage analysis with covariates confirms linkage of prostate cancer to chromosomes 1 and 4. *Am. J. Hum. Genet.* **68,** 1197–1206.
11. Rubinsztein, D. C., Leggo, J., Coetzee, G. A., Irvine, R. A., Buckley, M., and Ferguson-Smith, M. A. (1995) Sequence variation and size ranges of CAG repeats in the Machado-Joseph disease, spinocerebellar ataxia type 1 and androgen receptor genes. *Hum. Mol. Genet.* **4,** 1585–1590.
12. Choong, C. S., Kemppainen, J. A., and Wilson, E. M. (1998) Evolution of the primate androgen receptor: a structural basis for disease. *J. Mol. Evol.* **47,** 334–342.
13. Rubinsztein, R. C., Amos, W., Leggo, J., Goodburn, S., Jain, S., Li, S.-H., eet al. (1995) Microsatellite evolution—evidence for directionality and variation in rate between species. *Nat. Genet.* **10,** 337–343.
14. La Spada, A. R., Wilson, E. M., Lubahn, D. B., Harding, A. E., and Fischbeck, K. H. (1991) Androgen receptor gene mutations in X-linked spinal and bulbar muscular atrophy. *Nature* **352,** 77–79.
15. La Spada, A. R., Roling, D. B., Harding, A. E., Warner, C. L., Spiegel, R., Hausmanowa-Petrusewicz, I., et al. (1992) Meiotic stability and genotype-phenotype correlation of the trinucleotide repeat in X-linked spinal and bulbar muscular atrophy. *Nat. Genet.* **2,** 301–304.
16. Arbizu, T., Santamaria, J., Gomez, J. M., Quilez, A., and Serra, J. P.A. (1983) Family with adult spinal and bulbar muscular atrophy X-linked inheritance and associated with testicular failure. *J. Neurol. Sci.* **59,** 371–382.
17. Nagashima, T., Seko, K., Hirose, K., Mannen, T., Yoshimura, S., Arima, R., et al. (1988) Familial bulbo-spinal muscular atrophy associated with testicular atrophy and sensory neuropathy: autopsy case report of two brothers. *J. Neurol. Sci.* **87,** 141–152.
18. Mhatre, A. N., Trifiro, M. A., Kaufman, M., Kazemi-Esfarjani, P., Figlewicz, D., Rouleau, G., and Pinsky, L. (1993) Reduced transcriptional regulatory competence of the androgen receptor in X-linked spinal and bulbar muscular atrophy. *Nat. Genet.* **5,** 184–188.
19. Chamberlain, N. L., Driver, E. D., and Miesfeld, R. L. (1994) The length and location of CAG trinucleotide repeats in the androgen receptor N-terminal domain affect transactivation function. *Nucl. Acids Res.* **22,** 3181–3186.
20. Kazemi-Esfarjani, P., Trifiro, M. A., and Pinsky, L. (1995) Evidence for a repressive function of the long polyglutamine tract in the human androgen receptor: possible pathogenetic relevance for the (CAG)n-expanded neuronopathies. *Hum. Mol. Genet.* **4,** 523–527.
21. Tut, T. G., Ghadessy, F. J., Trifiro, M. A., Pinsky, L., and Yong, E. L. (1997) Long polyglutamine tracts in the androgen receptor are associated with reduced transactivation, impaired sperm production, and male infertility. *J. Clin. Endocrinol. Metab.* **82,** 3777–3782.

22. Irvine, R. A., Ma, H., Yu, M. C., Ross, R. K., Stallcup, M. R., and Coetzee, G. A. (2000) Inhibition of p160-mediated coactivation with increasing androgen receptor polyglutamine length. *Hum. Mol. Genet.* **9,** 267–274.
23. Beilin, J., Ball, E. M., Favaloro, J. M., and Zajac, J. D. (2000) Effect of the androgen receptor CAG repeat polymorphism on transcriptional activity: specificity in prostate and non-prostate cell lines. *J. Mol. Endocrinol.* **25,** 85–96.
24. Coetzee, G. A. and Ross, R. K. (1994) Prostate cancer and the androgen receptor. *J. Natl. Cancer Inst.* **86,** 872–873.
25. Irvine, R. A., Yu, M. C., Ross, R. K., and Coetzee, G. A. (1995) The CAG and GGC microsatellites of the androgen receptor gene are in linkage disequilibrium in men with prostate cancer. *Cancer Res.* **55,** 1937–1940.
26. Ingles, S. A., Ross, R. K., Yu, M. C., Irvine, R. A., La Pera, G., Haile, R. W., and Coetzee, G. A. (1997) Association of prostate cancer risk with genetic polymorphisms in vitamin D receptor and androgen receptor. *J. Natl. Cancer Inst.* **89,** 166–170.
27. Stanford, J. L., Just, J. J., Gibbs, M., Wicklund, K. G., Neal, C. L., Blumenstein, B. A., and Ostrander, E. A. (1997) Polymorphic repeats in the androgen receptor gene: molecular markers of prostate cancer risk. *Cancer Res.* **57,** 1194–1198.
28. Hakimi, J. M., Schoenberg, M. P., Rondinelli, R. H., Piantadosi, S., and Barrack, E. R. (1997) Androgen receptor variants with short glutamine or glycine repeats may identify unique subpopulations of men with prostate cancer. *Clin. Cancer Res.* **3,** 1599–1608.
29. Ekman, P., Gronberg, H., Matsuyama, H., Kivineva, M., Bergerheim, U. S., and Li, C. (1999) Links between genetic and environmental factors and prostate cancer risk. *Prostate* **39,** 262–268.
30. Hsing, A. W., Gao, Y. T., Wu, G., Wang, X., Deng, J., Chen, Y. L., et al. (2000) Polymorphic CAG and GGN repeat lengths in the androgen receptor gene and prostate cancer risk: a population-based case-control study in China. *Cancer Res.* **60,** 5111–5116.
31. Nam, R. K., Elhaji, Y., Krahn, M. D., Hakimi, J., Ho, M., Chu, W., et al. (2000) Significance of the CAG repeat polymorphism of the androgen receptor gene in prostate cancer progression. *J. Urol.* **164,** 567–572.
32. Platz, E. A., Rimm, E. B., Willett, W. C., Kantoff, P. W., and Giovannucci, E. (2000) Racial variation in prostate cancer incidence and in hormonal system markers among male health professionals. *J. Natl. Cancer Inst.* **92,** 2009–2017.
33. Correa-Cerro, L., Wohr, G., Haussler, J., Berthon, P.,Drelon, E., Mangin, P., et al. (1999) (CAG)nCAA and GGN repeats in the human androgen receptor gene are not associated with prostate cancer in a French-German population. *Eur. J. Hum. Genet.* **7,** 357–362.
34. Edwards, S. M., Badzioch, M. D., Minter, R., Hamoudi, R., Collins, N., Ardern-Jones, A., et al. (1999) Androgen receptor polymorphisms: association with prostate cancer risk, relapse and overall survival. *Int. J. Cancer* **84,** 458–465.
35. Bratt, O., Borg, A., Kristoffersson, U., Lundgren, R., Zhang, Q. X., and Olsson, H. (1999) CAG repeat length in the androgen receptor gene is related to age at diag-

nosis of prostate cancer and response to endocrine therapy, but not to prostate cancer risk. *Br. J. Cancer* **81,** 672–676.
36. Lange, E. M., Chen, H., Brierley, K., Livermore, H., Wojno, K. J., Langefeld, C. D., et al. (2000) The polymorphic exon 1 androgen receptor CAG repeat in men with a potential inherited predisposition to prostate cancer. *Cancer Epidemiol. Biomarkers Prev.* **9,** 439–442.
37. Gao, T., Marcelli, M., and McPhaul, M. J. (1996) Transcriptional activation and transient expression of the human androgen receptor. *J. Steroid Biochem. Mol. Biol.* **59,** 9–20.
38. Butler, R., Leigh, P. N., McPhaul, M. J., and Gallo, J. M. (1998) Truncated forms of the androgen receptor are associated with polyglutamine expansion in X-linked spinal and bulbar muscular atrophy. *Hum. Mol. Genet.* **7,** 121–127.
39. Hsiao, P. W, Lin, D. L., Nakao, R., and Chang, C. (1999) The linkage of Kennedy's neuron disease to ARA24, the first identified androgen receptor polyglutamine region-associated coactivator. *J. Biol. Chem.* **274,** 20229–20234.
40. Rush, M. G., Drivas, G., and D'Eustachio, P. (1996) The small nuclear GTPase Ran: how much does it run? *BioEssays* **18,** 103–112.
41. Tsai, Y. C., Simoneau, A. R., Spruck, C. H. III, Nichols, P. W., Steven, K., Buckley, J. D., and Jones, P. A. (1995) Mosaicism in human epithelium: Macroscopic monoclonal patches cover the urothelium. J. Urol. **153,** 1697–1700.
42. Buchanan, G., Yang, M., Harris, J. M., Nahm, H. S., Han, G., Moore, N., et al. (2001) Mutations at the boundary of the hinge and ligand binding domain of the androgen receptor increased transactivation function. *Mol. Endrocrinol.* **15,** 46–56.
43. Hardy, D. O., Scher, H. I., Bogenreider, T., Sabbatini, P., Zhang, Z. F., Nanus, D. M., and Catterall, J. F. (1996) Androgen receptor CAG repeat lengths in prostate cancer: correlation with age of onset. *J. Clin. Endocrinol. Metab.* **81,** 4400–4405.

# 16

# Studies on Androgen Receptor Mutations and Amplification in Human Prostate Cancer

**Zoran Culig, Alfred Hobisch, Martin Erdel, Georg Bartsch, and Helmut Klocker**

## 1. Introduction

Prostate cancer is a heterogenous neoplasm that is palliatively treated with androgen ablation therapy. Endocrine therapy aims to block the androgen receptor (AR), which has a central role in the transmission of extracellular signals and is therefore responsible for regulating proliferation and secretion. AR is expressed in all stages of prostate cancer and, therefore, the regulation of its expression and function are of great interest ***(1,2)***. AR point mutation was first described in the prostate cancer cell line LNCaP ***(3)***. This mutation leads to an enhanced activation of the AR by various steroidal and nonsteroidal AR antagonists. The presence of AR mutations was analyzed in the tissues of prostate cancer patients, and the protocols described in this chapter are designed to allow detection and functional analysis of these mutations (for review, *see* **ref. *4***). This chapter describes methods for analysis of AR structure in tissue samples; RNA isolation, synthesis of cDNA, polymerase chain reaction (PCR) amplification, and sequencing, as well as those needed for analysis of function of mutated receptors; and transient transfection, ligand-binding assay, and reporter gene assay.

Amplification of the AR gene is detected in about one-third of the patients who fail endocrine therapy ***(5,6)***. These findings indicate that the AR has an important role during the progression of prostate cancer. We have established an in vitro model that has allowed us to monitor the changes similar to those that occur in prostate cancer patients ***(7)***. In these long-term androgen-ablated cells, proliferation is regulated by androgen in a hypersensitive manner, and AR expression and activation increase during propagation in vitro. However,

From: *Methods in Molecular Medicine, Vol. 81: Prostate Cancer Methods and Protocols*
Edited by: P. J. Russell, P. Jackson, and E. A. Kingsley © Humana Press Inc., Totowa, NJ

AR amplification was not observed in the newly generated cell line. Comparative genomic hybridization, which was used to detect gene amplification in that study, is also described in this chapter.

## 2. Materials

### 2.1. Isolation of Total RNA

1. Guanidine thiocyanate (GTC) buffer: 4 *M* guanidine thiocyanate (Merck), 0.5% sodium-N-lauroyl-sarcosine (Boehringer), 25 m*M* sodium citrate, pH 7.0 (Sigma), 1 drop/100 mL of silicone-antifoaming agent (Merck). 0.1 *M* mercapthoethanol (Sigma), and 20 µg/mL glycogen (Boehringer) should be added immediately before use. GTC buffer should be stored at +4°C and protected from light.

### 2.2. cDNA Synthesis

1. Random hexanucleotide primers (Boehringer).
2. Avian myeloblastosis virus (AMV) reverse transcriptase (Promega).
3. Ribonuclease inhibitor (Promega). This reagent should be stored at –20°C.
4. AMV buffer: 50 m*M* Tris HCl, pH 8.3.

### 2.3. PCR Amplification

1. Taq polymerase (Promega) stored at –20°C.
2. dNTPs, sense, and antisense oligonucleotides should be stored at –20°C.

### 2.4. Purification of PCR Fragments

1. QIAquick Gel Extraction Kit (Quiagen).

### 2.5. Sequencing

1. Automated DNA sequencer (Applied Biosystems).
2. Sequencing buffer, dNTPs, dye-labeled dideoxyterminators.
3. Taq DNA polymerase, sequencing grade.
4. Sephadex-50 spin columns (Pharmacia).

### 2.6. Liposome-Mediated Transfection

1. Lipofectamine (Life Technologies).
2. Unlabeled methyltrienolone (R1881) (New England Nuclear), dissolved in absolute ethanol, and added to cell culture medium to a concentration of 0.001 to 1 n*M*.
3. Estradiol (Sigma), dissolved in absolute ethanol, and added to cell culture medium to a concentration of 1–100 n*M*.
4. Progesterone (Sigma), dissolved in absolute ethanol, and added to cell culture medium to a concentration of 1–100 n*M*. Dihydrotestosterone (Sigma), dissolved in absolute ethanol, and added to cell culture medium to a concentration of 0.1–10 n*M*.
5. Hydroxyflutamide (Schering Plough), dissolved in DMSO, and added to cell culture medium to a concentration of 0.1–10 µ*M*.

6. Bicalutamide (Astra Zeneca), dissolved in DMSO, and added to cell culture medium to a concentration of 0.1–10 μ*M*.
7. Epidermal growth factor (Life Technologies), dissolved in phosphate-buffered saline (PBS), and added to cell culture medium to a concentration of 10–50 ng/mL.
8. Insulin-like growth factor (Boehringer Mannheim), dissolved in PBS, and added to cell culture medium to a concentration of 10–50 ng/mL.

### 2.7. Ligand-Binding Assay

1. Synthetic androgen methyltrienolone (R1881), $^{3}$H-labeled and unlabeled.
2. Scintillation liquid, Opti Phase (Pharmacia).

### 2.8. Chloramphenicol Acetyltransferase Assay

1. 5X Reporter lysis buffer (Promega) diluted 1:4.
2. CAM solution: 1.3 mg/mL chlormaphenicol in 0.3 *M* Tris-HCl, pH 7.0.
3. Acetyl-Co-A solution: 10 μg/mL acetyl-CoA in 50 mM sodium-acetate, pH 5.0, under $N_2$.
4. Mix per probe (CAT mix): 20 μL CAM solution, 0.5 μL acetyl-CoA (cold), 0.125 μL acetyl-Co-A ($^{3}$H labeled).

### 2.9. Comparative Genomic Hybridization

1. Software (Perceptive Scientific International).
2. Biotin- and digoxigenin-labeled dUTPs (Boehringer).
3. Leitz Aristoplan epifluorescence microscope (Leica) equipped with a cooled integrating black and white charge-coupled device Image Point camera (Photometrics).
4. Triple band-pass filter set (Chroma Technology).
5. Polyvar 2 microscope (Reichert) equipped with a video camera (Hamamatsu Photonics).
6. DNA Polymerase I (Roche).
7. Dnase I (Roche).

## 3. Methods

### 3.1. Isolation of RNA from Tissue Samples (see Note 1)

Small pieces of tissue are removed at radical prostatectomy, classified as cancerous or normal by a pathologist, snap frozen, and stored at –80°C until use. AR analysis could also be performed in fine-needle aspirates, which were expelled from the needle into PBS solution. The pellet should be collected by centrifugation at 1500*g* for 2 min at 0°C.

Total RNA is isolated from samples by guanidine thiocyanate-acid phenol extraction. The samples are placed in tubes and lysed in 0.6 mL of GTC buffer on ultrasound disintegration. This step is followed by the addition of 0.6 mL of acid phenol, 0.06 mL of sodium acetate, and 0.15 mL of chloroform. The samples should be vigorously vortexed and centrifuged at 12,000*g* for 15 min at 4°C.

The two phases should be clearly visible. The upper phase, which contains RNA, should be removed very carefully with a pipet and precipitated overnight with 1 vol of isopropanol at –20°C. The next day, RNA is recovered by centrifugation at 12,000*g* for 30 min at 4°C. The pellet should be washed twice with 75% ethanol, dried by vacuum centrifugation, and dissolved in 10 to 20 µL of water.

### 3.2. cDNA Synthesis (see Note 2)

Total RNA is boiled for 2 min in a waterbath and cooled on ice. For cDNA synthesis, 0.4–0.5 µg of RNA should be taken. The cDNA mix contains 200 p*M* of random hexanucleotide primers, 10 U of AMV reverse transcriptase, and 50 U of ribonuclease inhibitor in a total volume of 40 µL of AMV buffer. For cDNA synthesis, four cycles are performed in a thermocycler instrument as follows: 10 min at 20°C, 10 min at 25°C, and 30 min at 42°C.

### 3.3. PCR Amplification (see Note 3)

cDNA fragments of the AR are amplified and isolated by PCR. One to three µL of cDNA is mixed with a solution which contains 10 m*M* Tris HCl, 50 m*M* KCl, 1.5 m*M* $MgCl_2$, 1% gelatine, 0.1% Triton X-100, 25 p*M* of each primer, 200 µ*M* of dNTPs, and 1.25 U of Taq DNA polymerase. Amplification of AR fragments from the N-terminal region requires addition of 2–5% of DMSO because of a high content of guanine and cytosine. The solution should be overlaid with 30 µL of mineral oil. AR amplification is performed in the thermocycler according to the following program: cycle 1, denaturation for 2 min at 95°C; cycles 1–30, strand separation for 30 s at 94°C followed by 15 s at 96°C, annealing for 1 min at 55°C, and DNA synthesis for 2 min at 73°C. The extension phase takes 3 min for short fragments and 10 min for longer N-terminal fragments. PCR is terminated by cooling down to 0°C. One-tenth of each sample is electrophoresed on a 2% agarose gel in TAE buffer and visualized by ethidium bromide staining.

### 3.4. Purification of PCR Samples (see Note 4)

The fragments are purified by preparative electrophoresis in low-melting agarose gels and can be obtained by two repeated cycles of freezing and thawing. After electrophoresis, the fragment bands should be cut out and snap frozen in liquid nitrogen. This step is followed by centrifugation for at 12,000*g* for 10 min at room temperature. The fragments may then used for the second PCR amplification. For each fragment, four PCR amplifications in a total volume of 100 µL are performed. The purification of fragments before sequencing is performed by following the QIAquick Gel Extraction Kit Protocol using a microcentrifuge. The PCR solution is mixed with 1/10 vol 3 *M* sodium acetate,

pH 5.1, and 2 vol of 100% ethanol. Precipitation is acomplished at –20°C overnight or at –80°C (2 × 30 min) with thawing and mixing in-between and 10,000g centrifugation at 4°C for 30 min in a tabletop microcentrifuge. The pellet is washed once with 75% ethanol. After vacuum drying in the Speedvac, the pellet is redissolved in 100 µL of buffer or water. Oil should then be removed. Afterwards, five volumes of Buffer PB (supplied with the kit) are added to 1 vol of the PCR reaction and mixed. A QIAquick spin column is placed in a 2-mL collection tube. To bind the DNA, the sample is applied to the QIAquick column and centrifuged for 3 min at 1200*g*. The flow-through is then discarded, and the column placed back in the same tube. Then, 750 µL of Buffer PE (supplied with the kit) is added to the QIAquick column, which is then centrifuged for 60 s at 10,000*g*. Again, the flow through is discarded at that time and the column is centrifuged for an additional 1 min at maximum speed. After this step, the column should be put in a clean 1.5-mL microfuge tube. Elution of the DNA is achieved by the addition of 50 µL of Buffer EB (supplied with the kit) or water directly onto the center of the QIAquick membrane. The column should be left for 10 min and then centrifuged for 3 min at 1200*g*.

### 3.5. Sequencing (see Note 5)

An automated sequencer and dye terminator kit are used for direct sequencing of the AR cDNA fragments by the dideoxynucleotide chain termination method with fluorescent labels. For the sequencing reaction, 30–90 ng of DNA of a PCR product is required. The DNA sequencing reaction is performed in a total volume of 20 µL with 100 ng of cDNA fragment, 10 pmol of a primer, and 9 µL of a premix containing sequencing buffer, dNTPs, dye-labeled dideoxyterminators, and sequencing-grade Taq DNA polymerase. The sample should be overlaid with 30 µL of mineral oil. The sequencing reaction is performed in a thermocycle according to the following program: cycle 1, 1 min at 96°C; cycles 1–25, 40 s at 96°C, 1 min at 55°C, and 4 min at 60°C. The products are subsequently purified using Sephadex-50 spin columns and precipitated by adding 0.1 vol of 3 *M* sodium acetate and 1.2 vol of isopropanol. After centrifugation, the pellets are washed with 75% ethanol and dried by vacuum centrifugation. The samples should be dissolved in 4 µL of formamide and 1 µL of 50 mmol EDTA, denaturated by heating to 92°C for 2 min, cooled on ice, and loaded onto the sequencing gel.

### 3.6. Liposome-Mediated Transfection (see Note 6)

To study functional consequences of an AR mutation, androgen-responsive reporter and AR cDNA should be transfected into COS or CV-1 monkey kidney cells, in which high transfection efficiency can be achieved, or AR-negative

prostate cancer cells, DU-145, and PC-3. Lipofection is a method that yields reproducible results and does not damage the cells. Various reagents are available for liposome-mediated transfection. The procedure with Lipofectamine, which is a liposome formation of a polycationic lipid and a neutral lipid in membrane-filtered water, will be described in this chapter. The cells should be seeded into plates the day before transfection. Transfections can be performed in 6-, 12-, 24-, 48-, and 96-well plates. For 6-well plates, 150,000 cells/well are used. Transfection with Lipofectamine must be performed under serum-free conditions. Before beginning the experiments, transfection conditions are optimized for each cell line using a reporter plasmid with a constituitively active promoter. Under experimental conditions, the ratio of reporter gene: AR cDNA should be 10:1.

First, the DNA-Lipofectamine complex should be prepared. For this purpose, 150 µL of serum-free medium should be put in a polystyrol tube and the appropriate volume of Lipofectamine (determined during optimization) added. A second tube should be used for dilution of plasmid DNA in the same amount of serum-free medium. The two solutions should be combined, mixed gently, and incubated at room temperature for 30 min. During this incubation, the cells should be washed with PBS. After incubation, the appropriate amount of serum-free medium needed for the transfection (for one well of a 6-well plate, 1 mL of serum-free medium is used) is added to the DNA/Lipofectamine mixture and transferred onto the cells. Complete medium (1 mL/well, 6-well plate) is added 6 to 8 h after transfection. Steroid and peptide hormones and steroid hormone antagonists are added 18 to 24 h after transfection, over the range of concentrations listed above (*see* **Subheading 2.6.**). At that time, the medium is replaced. The cells should be incubated with these compounds for 24–30 h.

### 3.7. Ligand-Binding Assay

Transfected cells grow for 48 h in flasks and, after that period, the ligand-binding assay is performed. The assay medium (AM) contains 3% charcoal-stripped fetal calf serum, supplemented with 10 m*M* HEPES to prevent a change in pH. To prepare hot binding solution (HBS), radiolabeled $^{3}$H-R1881 is added. Nonspecific binding solution contains HBS and a 200-fold molar excess of nonlabeled androgen; this concentration is required to displace the radiolabeled androgen. The assay is performed in duplicate in 1.5-mL Eppendorf tubes. The binding assay is performed under five different conditions: (1) 12.5 µL HBS and 187.5 µL AM; (2) 25 µL HBS and 175 µL AM; (3) 50 µL HBS and 150 µL AM; (4) 100 µL HBS and 100 µL AM; and (5) 200 µL AM. After preparation of these solutions, 1 mL of cell suspension ($5 \times 10^6$ cells in AM) is added. The samples should be protected from light. They are mixed and incubated at RT for 90 min. After incubation, the pellets are recovered by centrifugation and washed twice with 500 µL of ice-cold medium. Finally, the pel-

lets are lysed, vortexed in 1 mL of scintillation liquid, and the radioactivity determined in a β-scintillation counter.

### 3.8. CAT Assay

Cells are transfected and incubated with hormones as described above (*see* **Subheading 3.6.**). After incubation of transfected cells with supplements, the medium should be completely removed. The cells are lysed with the Reporter lysis buffer (400 µL/well, 6-well plate, shaking) for about 30 min. Fifty microliters of the lysate are taken into 4-mL polypropylene vials and 50 µL of lysis buffer is added along with 20 µL of CAT mix. The samples are overlaid with 750 µL of scintillation liquid. The incubation period is 2 h at 55°C in a water bath. Extraction is achieved by vigorous mixing of each sample for 1 min and centrifugation at 1500*g* for 3 min. The reaction is stopped by placing the samples at 4°C for 1 h. Radioactivity is measured in a β-counter. One blank sample and one total activity sample should be included as controls.

### 3.9. Comparative Genomic Hybridization

To study amplification of the AR in prostate cancer cell lines, comparative genomic hybridization is performed. Test DNA is isolated from cultured cells by standard methods. Test and normal reference DNAs are labeled with biotin-16-dUTP and digoxigenin-11-dUTP, respectively, following nick translation protocols ***(8)***. Briefly, the reaction is conducted at 15°C for 60–90 min with 1 µg of template DNA in a 50-µL volume containing labeled and unlabeled nucleotide mixture, DNA polymerase I, and DNase I. Reaction time and the amounts of the enzymes were adjusted so that the probe size distribution after labeling was a 500–2000-bp smear in a nondenaturing agarose gel. Two-hundred nanograms of each of the labeled DNAs are combined together with unlabeled Cot-1 DNA, denatured, and hybridized for 2 d at 37°C to good-quality normal male metaphase spreads (generated in the cytogenetic laboratory of the Department of Biology, University of Innsbruck). Biotin- and digoxigenin-labeled probes are visualized with fluorescein isothiocyanate and tetrarhodamine isothiocyanate, respectively. Chromosomes were identified on the basis of inverted grey level 4,6-diamino-2-phenolidol banding. The results were evaluated using a digital image analysis system. Three single-color images are recorded and processed by the MacProbe 3.3 software on an epifluorescence microscope, which is equipped with a cooled integrating black and white charge-coupled device camera and a triple band-pass filter set in combination with single band-pass excitation filters to sequentially excite 4,6-diamino-2-phenolidol, fluorescein isothiocyanate and tetrarhodamine isothiocyanate without any registration shift between images. Green to red (tumor cell line to normal) fluorescence intensity ratios along the length of all chromosomes in

the metaphase spreads are calculated. This allows an objective assignment of DNA sequence copy number changes of the tumor cell lines to chromosomal regions. After normalization of absolute fluorescence intensities within each metaphase to an average of 1.0, the results are plotted as green to red ratio profiles for each human chromosome from pter to qter.

## 4. Notes

1. The protocol described is optimized for small amounts of tissue, such as those obtained at fine-needle biopsy.
2. If more than 0.5 μg of RNA is used for cDNA synthesis, the synthesis and following amplifications of PCR fragments are less efficient.
3. Addition of DMSO is very important for successful amplification of AR fragments from the N-terminal region, which have a high GC content.
4. If spectrophotometric analysis indicates that there are inpurities in the DNA, they should not be used for sequencing.
5. The sequencing plates should be thoroughly cleaned before loading samples. This step is sometimes time-consuming but should be performed with great care. Also, there should be no air bubbles after gel casting.
6. In DU-145 prostate cancer cells, it is difficult to achieve a very high (e.g., 100-fold) increase in reporter gene activity after transfection of an androgen-responsive reporter and AR cDNA. However, the results are, in most cases, reproducible. Before the cells are seeded on plates for transfection, they should grow for 24 h on 175-$cm^2$ flasks. If the cells are confluent, the induction of reporter gene activity is very low. For transfection, polystyrol cell culture ware has to be used to prevent binding of the DNA.

## References

1. Hobisch, A., Culig, Z., Radmayr, C., Bartsch, G., Klocker, H., and Hittmair, A. (1995) Distant metastases from prostatic carcinoma express androgen receptor protein. *Cancer Res.* **55,** 3068–3072.
2. Hobisch, A., Culig, Z., Radmayr, C., Bartsch, G., Klocker, H., and Hittmair, A. (1996) Androgen receptor status of lymph node metastases from prostate cancer. *Prostate* **28,** 129–135.
3. Veldscholte, J., Ris-Stalpers, C., Kuiper, G. G. J. M., Jenster, G., Berrevoets, C., Claassen, E., et al. (1990) A mutation in the ligand binding domain of the androgen receptor of human LNCaP cells affects steroid binding characteristics and response to anti-androgens. *Biochem. Biophys. Res. Commun.* **17,** 534–540.
4. Buchanan, G., Greenberg, N. M., Scher, H.I., Harris, J. M., Marschall, V. R., and Tilley, W.D. (2001) Collocation of androgen receptor gene mutations in human prostate cancer. *Clin. Cancer Res.* **7,** 1273–1281.
5. Visakorpi, T., Hyytinen, E., Koivisto, P., Tanner, M., Keinanen, R., Palmberg, C., et al. (1995) In vivo amplification of the androgen receptor gene and progression of human prostate cancer. *Nat. Genet.* **9,** 401–406.

6. Cher, M. I., Bova, G. S., Moore, D. H., Small, E. J., Carroll, P. R., Pin, S. S., et al. (1996) Genetic alterations in untreated metastases and androgen-independent prostate cancer detected by comparative genomic hybridization and allelotyping. *Cancer Res.* **56,** 3091–3102.
7. Culig, Z., Hoffmann, J., Erdel, M., Eder, I. E., Hobisch, A., Hittmair, A., et al. (1999) Switch from antagonist to agonist of the androgen receptor blocker bicalutamide is associated with prostate tumour progression in a new model system. *Br. J. Cancer* **81,** 242–251.
8. Langer, P. R., Waldrop, A. A., and Ward, D. C. (1981) Enzymatic synthesis of biotin-labeled polynucleotides: novel nucleic acid affinity probes. *Proc. Natl. Acad. Sci. USA* **78,** 6633–6637.

# 17

# Proteomics in the Analysis of Prostate Cancer

**Soren Naaby-Hansen, Kohji Nagano, Piers Gaffney, John R. W. Masters, and Rainer Cramer**

## 1. Introduction

High-throughput DNA analysis has generated a wealth of information on predicted gene products and resulted in databases containing the complete genome sequences from several organisms. However, a comprehensive functional interpretation of this huge amount of nucleic acid sequence data remains. Therefore, the major challenges of the postgenomic era are the understanding of gene function as well as the regulatory perturbations induced by disease.

Transcriptomics allows a global, quantitative analysis of gene expression by measuring the mRNAs transcribed by the genome at a given time. An integrated view of the gene activation patterns at different cellular states can thus be achieved by comparative transcriptomic analysis. However, protein isoforms generated by posttranscriptional mRNA splicing or by posttranslational modifications of proteins cannot be predicted from a nucleic acid sequence or from mRNA transcript levels. Temporal differences between gene transcription and translation, as well as differential stability and turnover rates of mRNAs and proteins, may also participate in the observed lack of correlation between mRNA transcript levels and protein expression levels ***(1)***.

To achieve a correct annotation of gene functions, transcriptional profiling must therefore be complemented by other approaches that allow the expression and activity levels of the gene products, e.g., the proteins, to be profiled. Proteomics is the large-scale study of proteins aimed to identify and characterize all proteins expressed by an organism or in a tissue. This can lead to elucidation of the complex patterns of regulatory networks, which leads to activation of the genes and determines activation, interactions, and compartmentalization of their products. Proteomics originates from the term proteome, a linguistic

From: *Methods in Molecular Medicine, Vol. 81: Prostate Cancer Methods and Protocols*
Edited by: P. J. Russell, P. Jackson, and E. A. Kingsley © Humana Press Inc., Totowa, NJ

analogue to genome, defined as the entire protein complement expressed by a genome or by a cell or tissue type ***(2)***.

Proteomics dates back to the late 1970s, when a small number of laboratories started to build databases of protein expression profiles, using the newly developed technique of two-dimensional gel electrophoresis (2-DE). The key steps in classical proteomics are the separation of proteins in a sample by 2-DE and their subsequent quantitation and identification. However, a protein's expression level may not reflect its functional state, and protein profiling provides no data regarding a protein's subcellular site of action or its interaction partners. This is why the focus of modern proteomics has broadened considerably to include these basic aspects of cell biology. Blackstock and Weir recently suggested distinguishing two related but distinct forms of proteomics, namely expression proteomics and cell-map proteomics ***(3)***. Expression proteomics relies on 2-DE to generate quantitative maps of protein expression levels, akin to EST maps, whereas cell-map proteomics generates physical maps of the functional cellular machines, e.g., the protein complexes, by their systematic isolation, identification, characterization, and localization. Protein interaction studies may use BIAcore™ technology, two-hybrid screening ***(4)***, or phage display ***(5)*** methods, whereas multi-protein complexes can be isolated by affinity purification utilizing gene-tagging, fusion proteins, antibodies, peptides, DNA, RNA, or small targeting molecules ***(6)***.

By focusing on the functional products of the genome, proteomics provides an indispensable complementary to genomics. Proteins are ultimately responsible for all processes that take place within a cell, and the mechanism of action of the vast majority of drugs are mediated through proteins. Only 2% of diseases are believed to be monogenic ***(7)***, hence, the major challenge now is to understand how the regulatory networks of proteins are related and lead to the other 98% of diseases ***(8)***. Proteomics holds great promise in the field of cancer biology, including the identification of marker proteins, dissection of signaling pathways affected by proto-oncogenes, and drug-target identification and validation.

In this chapter, we will focus on a few examples of how the powerful combination of 2-DE (for a technical review, *see* **ref. *9***), bioinformatics, and mass spectrometric (MS) analysis can be applied in the study of prostate cancer.

### *1.1. Protein Expression Analysis*

Protein expression level comparison (differential display of expression) is the classical example of how 2-DE-based proteomics can be used in the study of global changes induced by cancer. Usually, extracts of normal and tumor cells (biological fluids or tissue biopsies) are separated by 2-DE, visualized, and subjected to quantitative computer comparison. Differentially expressed proteins are subsequently cored from the gels and identified by MS analysis

and database searches. Using such an approach, Celis and colleagues have identified a novel biomarker, psoriasin, from the urine of patients with squamous cell carcinoma of the bladder, which may be valuable for noninvasive follow-up of patients suffering these tumors ***(10)***. However, routine broad pH-range 2-DE analysis of complex mixtures, such as total cell or tissue extracts, is biased toward long-lived abundant proteins ***(11)***. Low-abundance proteins (which could be the functionally most interesting) tend to be masked by housekeeping proteins, which are present in several orders of magnitude higher concentrations, and they are often undetectable because of limited sensitivity and spot overlap. Differentially expressed cytoskeletal proteins will consequently dominate a comparison of morphologically distinct cell lines. Sample handling, separation, and detection methods must therefore be modified, to ensure biological relevance of expression proteomic analysis of cell lines.

Sample prefractionation techniques (sequential extraction, subcellular fractionation, or prefractionation based on different physiochemical properties) aim to reduce the diversity and complexity of protein mixtures, thus increasing the number and concentration of distinct subsets of proteins that can be resolved in a series of complementary narrow pH range 2-D gels.

This approach increases the number of features that can be separated and should be combined with sensitive, MS-compatible detection methods, such as silver staining, metal chelate staining, or fluorescence dye staining/labeling, for optimal analysis of cell lines grown in monolayers.

Fluorescent dyes offer a broader dynamic and linear quantitative range of detection than silver staining (for review, *see* **ref. *12***). Proteins can be covalently derivatized with fluorophores prior to separation or subjected to post-electrophoretic staining with fluorescence dyes.

**Figure 1A** demonstrates prelabeling of free cysteine residues in unreduced extracts of cultured prostate cells. Tx-100 extracts of a tumor cell line derived from primary adenocarcinoma of the prostate and of a cell line generated from autologous benign prostate epithelium ***(13)*** were labeled with 15 m*M* of an iodoacetamide derivate of Cy3 for 30 min at 30°C. Unreacted fluorophore was removed from the sample by centricon centrifugation (5000-Da cutoff). The proteins were subsequently dialyzed against $H_2O$ overnight, speed vacuum concentrated, and dissolved in reducing 2-DE lysis buffer before being separated by 2-DE. This method can be used to monitor changes in cysteine availability (due to alterations in protein activity, oxidation, association/dissociation, or conformation), in response to changing experimental conditions or differences in cellular homeostasis.

Difference gel electrophoresis (DIGE), in which two or three samples labeled with different fluorescence probes can be run in a single 2-DE gel, offers the opportunity of direct comparison of different samples, thus avoiding gel to gel variations inherent to comparative gel analysis ***(14)***.

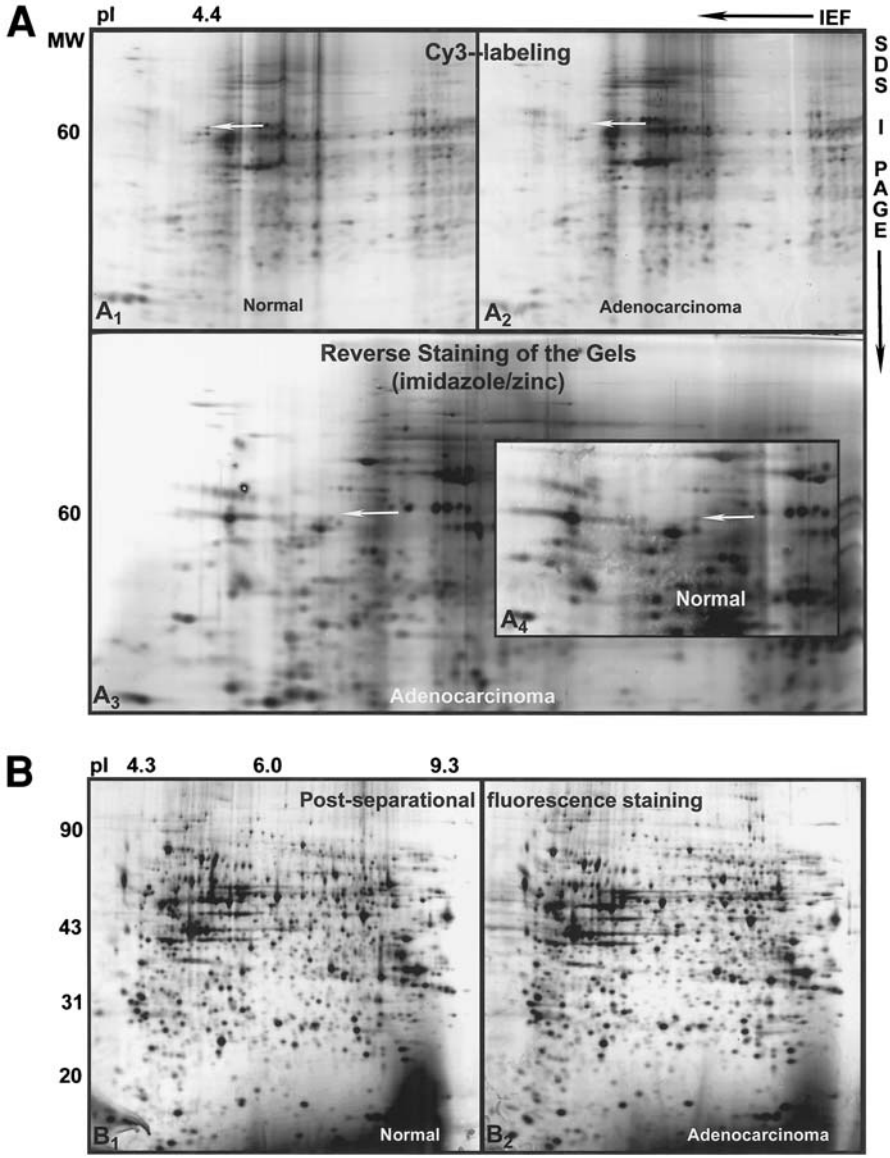


Fig. 1. Comparison of protein expression levels in immortalized human prostate epithelial cell lines derived from the same patient ***(13).*** **(A)** Comparison of proteins levels after Cy3-labeling of free cysteine residues ($A_1$ and $A_2$). Proteins were separated by carrier ampholyte based IEF/PAGE. The gels were stained with zinc ***(9)*** after visualization of fluorescence labeling by laser scanning ($A_3$ and $A_4$). Horizontal arrow shows protein labeled in normal but not in cancer cells. **(B)** Comparison of the same two cell lines by postseparational fluorescence staining. Proteins were separated by immobilized pH gradient-based 2-DE, using nonlinear broad pH range strips (pH 3–10). Differences in the expression levels of several proteins can be observed.

The currently available commercial dyes for DIGE were first reported by Minden and colleagues ***(14)*** and are built around the relatively photobleaching resistant Cy3 and Cy5 dye cores. In our hands the original one-spot preparative procedures proved extremely unreliable, but pure samples of both dyes could be obtained with some modification of the conditions and, at each stage, separation from byproducts of the desired intermediates. The fluorophores of the Cy3 and Cy5 cores are very similar but differ in the length of their central $(CH)_3$ and $(CH)_5$ polymethine chains, respectively. This difference in size is compensated for by replacing a methyl in the Cy5 derivative with a propyl in the Cy3. Thus, these matched dyes are nearly the same size and proteins labeled with either have near identical electrophoretic mobilities.

Because most of the proteins that are likely to be of interest in cancer biology have low cellular abundances, one would prefer to label all accessible reactive residues to maximize sensitivity. Saturation labeling of lysine, with an average occurrence of 5.8% among protein sequences, at first appears a reasonable choice and the dyes of Minden and colleagues ***(14)*** are *N*-hydroxysuccinimide esters, which readily react with primary amines. However, such a large degree of labeling interferes with the physical properties of tagged proteins, as well as tryptic digestion, so that in practice minimal labeling in which just one in six proteins is crosslinked to a single dye molecule is necessary. Apart from the loss in sensitivity, this has an additional disadvantage in that the detectable-labeled protein spot does not necessarily exactly coincide with the prevalent unlabeled protein. Consequently, a post-DIGE stain is still required to visualize the bulk of the protein prior to coring and MS analysis.

Saturation labeling of cystine residues, at an occurrence of only 1.8%, might be expected to circumvent the difficulties inherent in saturation lysine labeling for DIGE. To this end, we have synthesized propyl-Cy3 and methyl-Cy5 dyes in which the carboxylate moieties of the original lysine-reactive dyes have been replaced with a primary amine that may be readily converted to cystine-reactive iodoacetamides or more selective maleimides. Initial experiments show much promise with the expected gains in sensitivity. Additionally, cystine-reactive dyes target significantly different protein populations from lysine labeling, and the populations sampled can be further selected depending on whether or not a reducing agent is included in the labeling protocol. However, saturation labeling amplifies small differences between Cy3- and Cy5-derivatized proteins so that a significant number, if still the minority, of paired spots do not exactly overlap, complicating the analysis.

Several dyes are available for noncovalent fluorescence staining of proteins after electrophoretic separation ***(12)***. **Figure 1B** demonstrates a classic expression level comparison between total cell extracts from the same two cell lines which were used in **Fig. 1A.** The proteins were visualized by postseparational

staining with an analogue of SYPRO dyes, which is intercalated into sodium dodecyl sulphate-micelles ***(15)***. This type of staining offers detection sensitivity competitive with silver staining and is compatible with downstream MS analysis. However, because some proteins may be detected by one procedure but not the other and vice versa, the most complete 2-D map is generally achieved by computer-assisted assembly of images obtained from several staining and labeling techniques.

As mentioned earlier, difference gel electrophoresis offers the opportunity of direct comparison of different samples, thus avoiding gel-to-gel variations inherent to comparative gel analysis. However, as both carrier ampholyte-based isoelectric focusing gels and immobilized pH gradient gels (IPG strips) have practical thresholds for protein loads, above which loss of buffering capacity leads to spot fusion and co-migration, the sensitivity of the DIGE technique becomes inferior to the one-sample one-gel approach.

Nongel separation techniques, such as multi-dimensional liquid chromatography and the isotope-coded affinity tag method ***(16)***, are currently being optimized for large-scale proteomic application to circumvent the problems associated with gel electrophoresis. These techniques further increase the compatibility of the sample for MS analysis, resulting in less discrimination of proteins, which are difficult to analyze on/from gels. Isotope labeling also enables quantification via mass spectrometry and can therefore be used for the identification of differentially expressed proteins.

### 1.2. Cell Surface Labeling

The most desirable cancer markers are present in easy accessible biological fluids and are expressed on the surface of the transformed cells. Several methods are available for more or less specific labeling of cell surface components.

Vectorial surface labeling can be achieved by chemical incorporation of radioisotopes (such as $^{125}I$ or $^{3}H$) in the core of the protein or its carbohydrate or lipid side chain(s) ***(17,18)***. A less hazardous and thus more desirable approach than performing vectorial radiolabeling is to derivatize surface proteins with fluorophores, biotin, or even better with compounds possessing properties for both peptide quantification and affinity purification, such as isotope-coded affinity tagging ***(16)***. The latter method, which involves a deuterated biotin derivative, has been successfully combined with whole cell trypsination, avidin-bead precipitation of the tagged peptides and MS analysis. This approach has enabled identification of novel surface proteins, which presumably are specific for prostate cancer cells (Ruedi Aebersold, at AACR 91st Annual Meeting 2000, San Francisco, CA).

Proteins expressed on the surface of prostate cancer cells can similarly be labeled with the water-soluble, cell-impermeable biotin analog, sulfo-NHS-

LC-biotin. Biotinylated proteins can then be visualized by blotting with enzyme-conjugated avidin (*see* **Fig. 2B**) or concentrated for further analysis via affinity-purification. The number of surface exposed proteins that could be labeled with biotin comprised less than 10% of the number of silver stained proteins (*see* **Fig. 2**). However, such an interpretation must be taken with caution, as only approx 60–70% of proteins stain with silver ***(19)*** and hydrophobic proteins are under-represented in 2-D gels ***(20)***. The latter situation tends to be aggravated when IPG strips are used for first-dimensional separation. Interpretation of the protein patterns is further complicated by the negative charge of the sulfo-group in sulfo-NHS-LC-biotin. Multiple forms of a protein migrating at distinct horizontal positions can both be generated by posttranslational modifications (i.e., glycosylation or phosphorylation) and by biotin labeling. If a protein possesses multiple lysine groups assessable for biotinylation, labeling will produce charge-trains, where each form represent the protein with a different number of sulfo-biotin molecules attached (arrowheads in **Fig. 2B**).

Nevertheless, by careful analysis and critical interpretations, 2-DE-based proteomics can be successfully used to identify putative prostate cancer surface markers and to study their regulation (Naaby-Hansen et al., in preparation).

### *1.3. Metabolic Labeling*

The effect of biological stimuli and/or drug action on the synthesis of proteins and their posttranslational modifications can be studied by metabolic radiolabeling strategies, using isotope-labeled precursors (e.g., amino acid, monosaccharide, or lipid) or [$^{32/33}$P]orthophosphate. In combination with 2-DE and quantitative computer analysis, such approaches may reveal important differences between the patterns of co-ordinate regulation in normal and cancer cells, and provides a method for drug mode-of-action studies.

The effect of long-term interferon gamma (INF-γ) stimulation of prostate cancer cells was studied (*see* **Fig. 3**). Metabolic labeling with [35S]-methionine/cysteine for various time periods in the presence or absence of INF-γ was used to monitor protein synthesis. INF-γ stimulation of the adenocarcinoma cells resulted in changes in both the rate of protein synthesis and posttranslational modifications of newly synthesized proteins. The synthesis of a protein with molecular weight of 61 kDa and pI of 4.2 was increased by long-term stimulation with INF-γ. The protein spot was cored from a fluorescence stained semi-preparative 2-D gel and identified as calreticulin by MS analysis (*see* below).

Calreticulin is the major $Ca^{2+}$ binding/storage protein in the endoplasmic reticulum (ER) of a variety of nonmuscle cell types, and like the closely related ER chaperone calnexin, CRT, is a lectin that interacts specifically with partially trimmed, monoglucosylated, N-linked oligosaccharides via its P-domain ***(21)***.

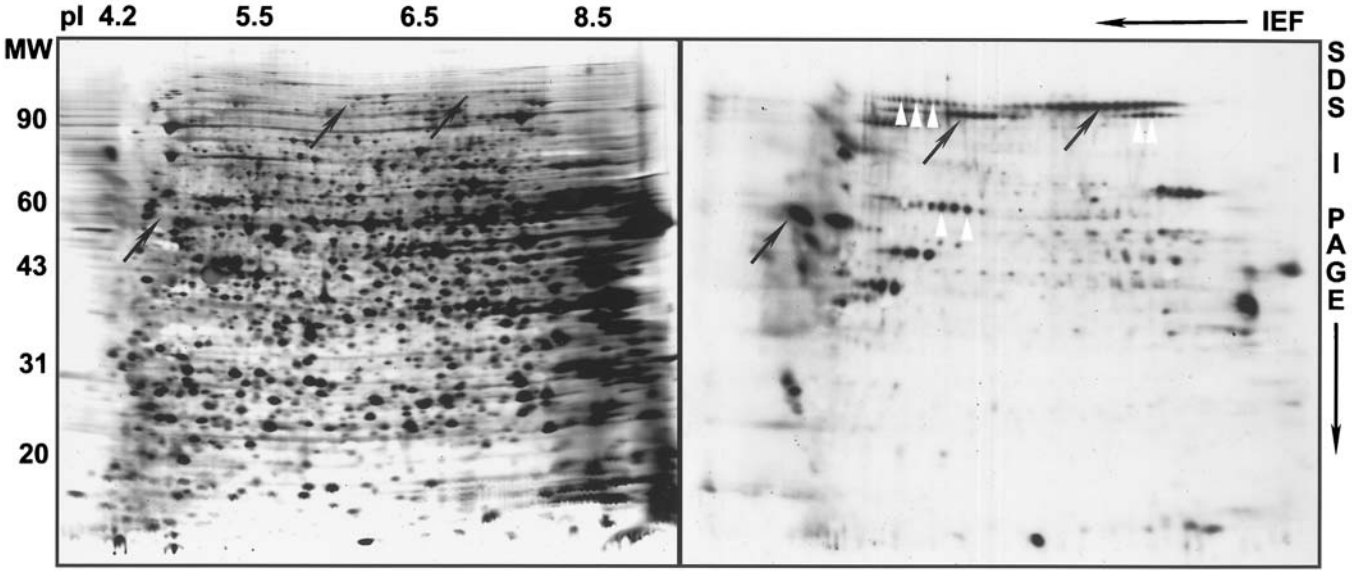


Fig. 2. Biotin labeling of surface exposed proteins. Left: proteins visualized by silverstaining. Right: biotinylated proteins visualized by affinity blotting with HRP-avidin. Oblique arrows indicate strongly labeled proteins that are difficult/impossible to identify on silver stained gels. White arrowheads indicate charge-trains (*see* text for details).

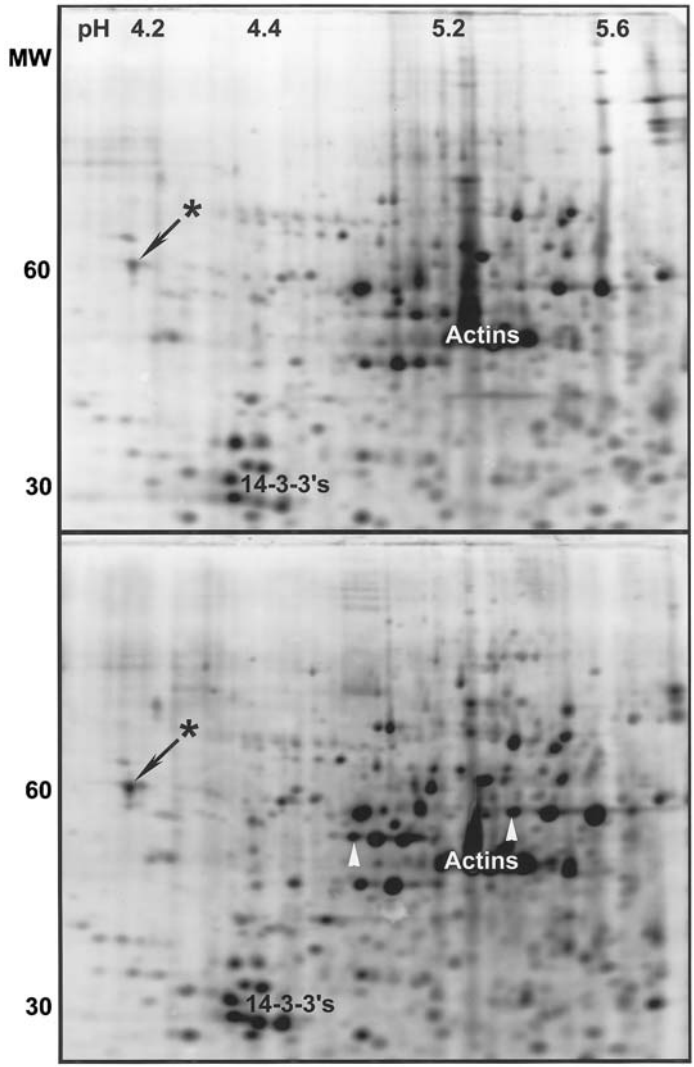


Fig. 3. Analysis of INF-γ induced protein synthesis. Proteins were visualized by autoradiography after biosynthetic labeling with [$^{35}$S]-methionine/cysteine for 18 h, in absence of stimuli (top) or during continuous stimulation with INF-γ (500 U/mL). The positions of actins and 14-3-3 proteins are indicated, note the increase in synthesis of 14-3-3 forms in response to INF-γ. The protein indicated by an arrow and a star was identified on a silver-stained gel, excised, and subjected to mass spectrometry analysis (*see* below). White arrow heads indicate acidic isoforms of proteins generated by INF-γ-induced phosphorylation. The unaltered protein forms migrate at the right end of the charge-trains.

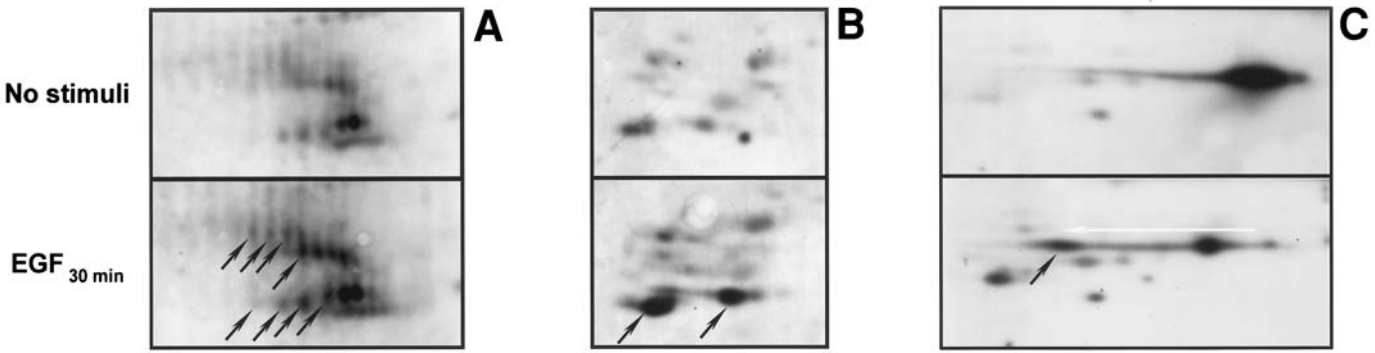


Fig. 4. Analysis of phosphosignaling in response to EGF stimulation. **(A)** EGF-induced phosphorylation demonstrated by metabolic labeling with [$^{33}$P]-orthophosphate. Note increase in radiolabeling of acidic isoforms (oblique arrows). **(B)** Phosphorylation of threonine residues demonstrated by immunoblotting with monoclonal antibody to phospho-threonine. Note increase in immunostaining. **(C)** Phospho-induced changes in the electrophoretic migration of ERK1. ERK1 was identified by immunoblotting. Note the shift toward the acidic end of the gel in response to EGF induced phosphorylation (arrows).

The upregulation of a chaperone involved in ER processing of newly synthesized proteins is hardly surprising because INF-γ stimulation resulted in a general increase in protein synthesis (compare **Fig. 3A,B**).

### *1.4. Analysis of Cell Signaling Pathways*

The high resolution of 2-DE based proteomic analysis offers unique opportunities for dissection of the signaling pathways in prostate epithelium and for studies of their perturbations by cancer, drug action, and by changes in growth conditions. Epidermal growth factor induced changes of the phospho-protein pools can thus be visualized by [$^{32/33}$P]orthophosphate labeling (*see* **Fig. 4A**), by blotting with monoclonal antibodies (MAbs) to specific phospho-residues (*see* **Fig. 4B**) or by the changes in migration patterns that are induced by phosphatase treatment of the samples. Phosphorylation results in a more acidic migration pattern, which can easily be demonstrated by immunoblotting (*see* **Fig. 4C**).

### *1.5. Protein Identification by Mass Spectrometry*

Although 2-DE separates proteins with high resolution, it is practically impossible to identify proteins from 2-DE gel spots just by their position on the gel. Protein modification and degradation can lead to substantial gel spot shifts in both dimensions. Another practical limitation is the physical size of gels and gel spots. On a standard 2-DE gel less than 12,000 spots can theoretically be resolved (gel size of 180 mm × 200 mm and an average spot size of 2 mm diameter). However, there are about 30,000 predicted human genes, plus two to four times as many splice variants. Including their posttranslational modifications and degradation products, it becomes quite obvious that subsequent analyses have to be conducted to identify 2-DE separated human proteins. The technique widely recognized to be best for this task is mass spectrometry ***(6,11,22,23)***.

Mass spectrometric analysis can be extremely accurate, sensitive and fast. In time-of-flight (TOF) MS, the primary analysis time is less than 1 ms for even large macromolecules (>100,000 kDa). High analytical sensitivity has been demonstrated on zeptomole ($10^{-21}$ *M*) amounts of sample ***(24,25),*** although for 2-DE gel spot analysis realistic sensitivity limits are around the low femtomole level ***(26)***. It has recently been reported that MS sensitivity exceeds the analytical sensitivity of silver staining ***(27)***. Equally important to sensitivity is its mass measurement accuracy ***(11,28)*** of usually 5–200 ppm for low mass (<5 kDa) analysis, leading to an extremely high confidence in protein identification by techniques such as peptide mass mapping (PMM) using peptide mass fingerprints from MS experiments ***(6,11)*** and peptide sequencing using peptide fragmentation mass spectra from tandem mass spectrometry (MS/MS) experiments ***(6,11)***.

In proteomics, MS analysis is dominated by two ionization techniques: matrix-assisted laser desorption/ionization (MALDI) MS ***(29)*** and electrospray ionization (ESI) MS ***(30,31)***. Because of their distinct sample desorption/ionization mechanisms, these two ionization techniques are usually interfaced to rather different sample introduction systems and mass analyzers. For high-throughput protein identification from 2-DE gel spots, PMM by MALDI TOF MS is unchallenged because of its speed and simplicity. However, higher confidence in protein identification can be achieved by using MS/MS to obtain sequence information by peptide ion fragmentation. The fragmentation method usually used is low-energy collision-induced dissociation and, coupled with ESI, this method has been most widely established for MS/MS peptide sequencing.

The vast majority of identification strategies by MS are based on the analysis of proteolytic peptides because the direct analysis of proteins by MS is generally unfavorable because of severe limitation in several key areas, such as detection, resolution, and fragmentation. Protein heterogeneity caused by modifications and degradation further complicates identification by direct protein analysis. MS analysis of proteolytic products, on the other hand, can be undertaken with higher MS performance but without significantly losing information necessary for high confidence identification.

The strategy used to identify the 2-DE gel spot, which is marked by a star in **Fig. 3**, comprises tryptic in-gel digestion and PMM. For PMM, a MALDI TOF mass spectrum of the tryptic peptide mixture was acquired (*see* **Fig. 5A**).

From this spectrum, a peptide ion mass list was compiled and submitted to a database search program (MS-Fit, ProteinProspector, UCSF, http://prospector.ucsf.edu) searching the SWISS-PROT protein database. The in-gel digestion protocol can be found in the appendix, and the search parameters can be obtained in **Fig. 5B.** In this case, the masses of 16 peptides of the human protein calreticulin (SWISS-PROT accession number P27797) match peptide ion masses measured by MALDI TOF MS. These peptides cover 40% of the amino acid sequence. Although 197 entries have been selected by the search shown in **Fig. 5B**, only matches for human calreticulin and its homologs in other species have more than 20% sequence coverage. Together with the number of matching peptide ion masses, protein identification can be achieved with an extremely high confidence. In addition, information obtained from the gel such as approximate values for molecular weight and pI of the protein can dramatically increase the accuracy of the search. In the presented case, limiting the molecular weight range in accordance with a gel molecular weight measurement accuracy of ±25% results in the selection of the five calreticulin entries only.

In our institute, more than 90% of all identifications of the main protein in a 2-DE gel spot are obtained with PPM by MALDI TOF MS. The remaining identi-

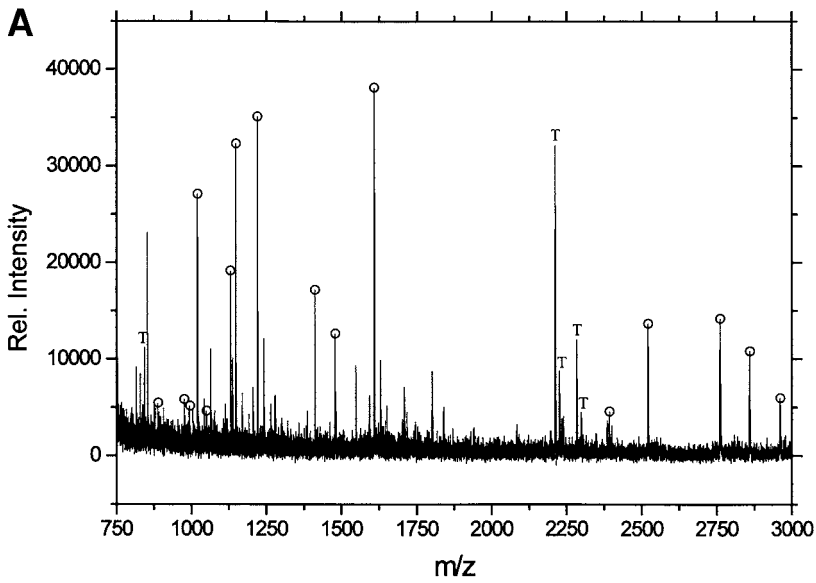


Fig. 5. Protein identification by peptide mass mapping of the gel spot sample marked by star in **Fig. 3.** **(A)** MALDI MS tryptic peptide mass fingerprint from the in-gel digest. **(B)** (*see* next page) Database search results using the 55 monoisotopic masses of the most intense unknown isotope-resolved ion signals in **(A).** Tryptic peptide ion signals matching peptide masses of human calreticulin (SWISS-PROT accession number P27797) are marked with a circle. Trypsin autolysis product ion signals are marked with a T. The spectrum is internally calibrated using the two protonated trypsin autolysis products at the monoisotopic mass of m/z 842.5100 and 2211.1046. The search engine MS-FIT (ProteinProspector, UCSF, http://prospector.ucsf.edu) was used for database searching.

fications are achieved by ESI MS/MS using collision-induced dissociation and a directly coupled nano-high-performance liquid chromatography system to the ion source for on-line sample purification and concentration. Usually, 0.5 µL of the tryptic in-gel digest mixture is used for MALDI TOF MS leaving 4.5 µL for further analysis such as ESI MS/MS. The routine sensitivity for protein identification lies in the low femtomole range of sample loaded on a 2-DE gel.

### *1.6. Summary*

Currently, 2-DE is the only well-established technique that can deliver fast, qualitative, and quantitative analysis of complex protein distributions in combination with parallel protein purification. However, 2-DE is not only applicable to study steady-state expression level differences but should be used in studies of dynamic cellular events to gain full potential of the technique. The use of

B

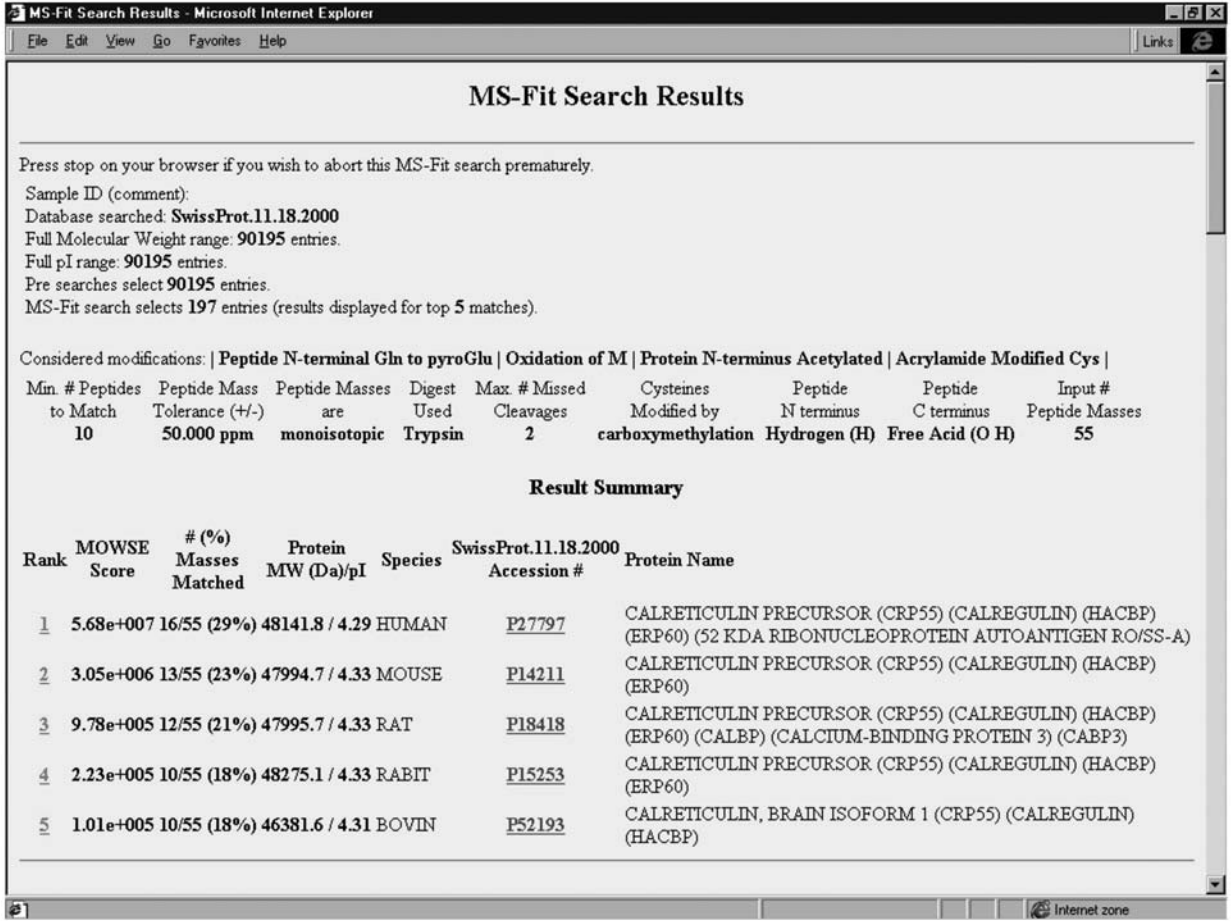


# MS-Fit Search Results

Press stop on your browser if you wish to abort this MS-Fit search prematurely.

Sample ID (comment):
Database searched: **SwissProt.11.18.2000**
Full Molecular Weight range: **90195** entries.
Full pI range: **90195** entries.
Pre searches select **90195** entries.
MS-Fit search selects **197** entries (results displayed for top **5** matches).

Considered modifications: | **Peptide N-terminal Gln to pyroGlu** | **Oxidation of M** | **Protein N-terminus Acetylated** | **Acrylamide Modified Cys** |

| Min. # Peptides to Match | Peptide Mass Tolerance (+/-) | Peptide Masses are | Digest Used | Max. # Missed Cleavages | Cysteines Modified by | Peptide N terminus | Peptide C terminus | Input # Peptide Masses |
|---|---|---|---|---|---|---|---|---|
| **10** | **50.000 ppm** | **monoisotopic** | **Trypsin** | **2** | **carboxymethylation** | **Hydrogen (H)** | **Free Acid (O H)** | **55** |

## Result Summary

| Rank | MOWSE Score | # (%) Masses Matched | Protein MW (Da)/pI | Species | SwissProt.11.18.2000 Accession # | Protein Name |
|---|---|---|---|---|---|---|
| 1 | **5.68e+007** | **16/55 (29%)** | **48141.8 / 4.29** | HUMAN | P27797 | CALRETICULIN PRECURSOR (CRP55) (CALREGULIN) (HACBP) (ERP60) (52 KDA RIBONUCLEOPROTEIN AUTOANTIGEN RO/SS-A) |
| 2 | **3.05e+006** | **13/55 (23%)** | **47994.7 / 4.33** | MOUSE | P14211 | CALRETICULIN PRECURSOR (CRP55) (CALREGULIN) (HACBP) (ERP60) |
| 3 | **9.78e+005** | **12/55 (21%)** | **47995.7 / 4.33** | RAT | P18418 | CALRETICULIN PRECURSOR (CRP55) (CALREGULIN) (HACBP) (ERP60) (CALBP) (CALCIUM-BINDING PROTEIN 3) (CABP3) |
| 4 | **2.23e+005** | **10/55 (18%)** | **48275.1 / 4.33** | RABIT | P15253 | CALRETICULIN PRECURSOR (CRP55) (CALREGULIN) (HACBP) (ERP60) |
| 5 | **1.01e+005** | **10/55 (18%)** | **46381.6 / 4.31** | BOVIN | P52193 | CALRETICULIN, BRAIN ISOFORM 1 (CRP55) (CALREGULIN) (HACBP) |

Fig. 5. *(Continued)*

2-DE in combination with specific labeling techniques and subcellular fractionation enables detailed studies of spatiotemporal cellular changes such as signal transduction pathways and translocation processes as well as their perturbations by disease and drug treatment.

In proteomics, particularly in global proteome mapping, mass spectrometry is so far the only technique, which is sensitive, accurate, and fast enough to cope with the future challenges for large-scale protein identification. In addition, MS can also provide structural information for further characterization of proteins and their modifications, such as phosphorylation and glycosylation.

Bioinformatic integration of data from such versatile, conditional studies combined with data obtained by cell-map proteomics and by transcriptomic analysis will hopefully lead to a more comprehensive understanding of prostate cancer, and to new approaches in diagnosis, prevention, and treatment of the disease.

## 2. Materials

### *2.1. Metabolic Labeling Protocols*

1. Labeling medium: 90% methionine/cysteine-free DMEM, 10% DMEM with 0.2 mCi/mL Promix (Amersham).
2. Lysis buffer: 8 *M* urea, 2 *M* thiourea, 4% CHAPS, 65 m*M* dithiothreitol (DTT), protease inhibitors (use fx. Cocktail tablets from Boehringer Mannheim) and phosphatase inhibitors (1 μ*M* okadaic acid, Fenvalerate, and bpVphen).

### *2.2. Phosphorylation Labeling*

Sodium phosphate-free DMEM, fatty acid free bovine serum albumin, $^{33}$P-orthophosphate, recombinant growth factor (EGF), phosphate-buffered saline (PBS), and fetal calf serum.

## 3. Methods

All procedures should be optimized according to cell line/tissue and experimental design.

You may benefit from extensive piloting with one-dimensional gels, especially in time-course studies and pulse-chase experiments.

### *3.1. Metabolic Labeling Protocols*

#### *3.1.1. Long-Term Biosynthetic Labeling of Methionine- and Cysteine-Containing Proteins*

The protocol used for biosynthetic labeling of proteins is essentially identical to the classical long-term $^{35}$S-labeling procedure, published by numerous authors, including Patterson and Garrels ***(32)***.

1. Remove culture medium by aspiration and wash cells twice in methionine/cysteine-free DMEM. Leave cells in this medium for 15 min at 37°C in 5% $CO_2$ incubator.
2. Aspirate the medium and incubate cells in labeling medium for 18 h with or without cytokines. Use 4 mL of medium per 10-cm dish and 7.5 mL per 15-cm dish.
3. Remove the medium and wash the cells twice with plain PBS. Remove the washing medium thoroughly by aspiration.
4. Add lysis buffer (a minimum of 400 µL for a 10-cm dish and 600 µL for a 15-cm dish) and harvest cells by scraping (you may perform this and the following steps cold—on ice).
5. Pass the mixture through a 25-gauge needle several times and then centrifuge at 20,000*g* for 10 min to pellet nuclei and nonsolubilized material.
6. Remove an aliquot for determination of protein concentration (e.g., by the Bradford method) and snap-freeze the sample.

#### *3.1.2. Phosphorylation Labeling (see **Note 1**)*

1. Synchronize cells by serum starvation overnight (if possible). Use the same confluency throughout experimental series because this influences signaling in most cell types grown in monolayers.
2. Wash cells twice in sodium phosphate-free DMEM plus 0.1% fetal calf serum and incubate for 30 min in this buffer.
3. Initiate labeling by adding $^{33}$P-orthophosphate (100 µCi/mL) to the sodium phosphate-free medium for 1–6 h (optimize according to cell line and experimental design).
4. Stimulate (or sham stimulate) cells with growth factor (optimal concentration should be experimentally determined for each cell line) for variable periods at 37°C (start, e.g., with 5, 10, 20, 30, and 60 min).
5. Remove medium by aspiration.
6. Lyse cells on ice as above (*see* **Subheading 3.1.1.**). Leave the sample on ice and perform quick Bradford analysis.
7. Phosphoproteins should be separated immediately after determination of protein concentration (to avoid loss of labile sites). We find separation by carrier ampholyte IEF to be superior to immobilized pH gradients for this type of analysis.

### *3.2. Cell Surface Biotinylation of Cultured Cells Grown in Monolayer*

This procedure has been modified from Naaby-Hansen et al. ***(18)***.

1. Remove medium by aspiration and wash cells twice with chilled PBS.
2. Add fresh solution of sulfo-HNS-LC-biotin (1.7 m*M* [1 mg/mL] in PBS).
3. Remove solution carefully after 5 min.
4. Quench reaction by adding 50 m*M* $NH_4Cl$ in PBS. Incubate for 10 min at 4°C.
5. Remove solution and wash cells three times with PBS.
6. Lyse cells as described above (*see* **Subheading 3.1.1.**).

## 3.3. Protein Identification by Mass Spectrometry

### 3.3.1. In-Gel Digestion (see **Notes 2–6**)

1. Prepare the following solutions: 25 m*M* ammonium bicarbonate (ABC)/50% acetonitrile (ACN) in water; 10 m*M* DTT/25 m*M* ABC in water; 50 m*M* iodoacetic acid/25 m*M* ABC in water; 25 m*M* ABC in water; and 50% ACN/5% trifluoroacetic acid (TFA).
2. Excise gel pieces. Choose a piece size that represents a good compromise between maximal protein recovery and minimal interference of gel-associated contaminants.
3. Wash the gel pieces twice with 25 m*M* ABC/50% ACN for 5 min. Use a volume sufficient to cover the gel pieces. After each wash, remove the supernatant and discard the gel-loading pipet tips.
4. Dry the gel pieces in a speed vacuum drier.
5. Rehydrate the gel pieces with 20 µL of a 10 m*M* DTT/25 m*M* ABC solution.
6. Incubate the sample at 50°C for 45 min.
7. Remove the supernatant.
8. Add 20 µL of a 50 m*M* iodoacetic acid/25 m*M* ABC solution.
9. Incubate the sample in the dark at room temperature for 1 h.
10. Remove the supernatant.
11. Wash the gel pieces twice with 25 m*M* ABC/50% ACN as in **step 3.**
12. Dry the gel pieces in a speed vacuum drier.
13. Prepare a 25 m*M* ABC solution containing modified trypsin with a trypsin concentration of 10 ng/µL.
14. Rehydrate the gel pieces with 3 to 6 µL of the trypsin containing 25 m*M* ABC solution. For 2-DE gel spots with a diameter of 2 mm, a total amount of 30 ng of modified trypsin usually ensures a moderate detection of trypsin autolysis products, which can then be used for internal mass calibration. Total trypsin amounts may vary depending on the protein amount.
15. Add 15 µL of 25 m*M* ABC solution to immerse the gel piece sufficiently.
16. Incubate the sample at 37°C overnight.
17. Add 20 µL of 50% ACN/5% TFA.
18. Extract and store the supernatant in a SlickSeal tube. Undertake an additional extraction of the digest mixture with 20 µL of 50% ACN/5% TFA and add the second extraction to the first (*see* **Note 6**).
19. Concentrate the recovered digest mixture by drying in a speed vacuum drier.
20. Resuspend the dried digest mixture in 5 µL of $H_2O$.
21. Store samples at 4°C for subsequent mass spectrometric analysis.

### 3.3.2. MALDI Sample Preparation and Analysis (see **Notes 7** and **8**)

1. Prepare a saturated aqueous 2,5-dihydroxybenzoic acid (DHB) solution.
2. Spot 0.5 µL of the peptide digest mixture on the MALDI target plate.
3. Add 1 µL from the supernatant of the DHB solution to the sample droplet.
4. Dry the sample droplet with a warm stream of air.
5. Carry out MALDI analysis.

## 4. Notes

1. Radioisotope incorporation can be determined following TCA precipitation of the sample as described by Link and Bizios ***(33)*** and absolute quantitation of 2D gel protein spots following biosynthetic radiolabeling can be performed as described by Gygi and Aebersold ***(34)***.
2. The purer the materials you use, the smaller the sample contamination will be. This can prevent potential problems for the mass spectrometric analysis.
3. A clean environment and careful sample handling is mandatory to avoid sample contamination, particularly by keratins from skin and hair.
4. Bigger gel pieces should be cut into smaller pieces to increase the surface-to-volume ratio for a higher protein accessibility.
5. **Step 3** (*see* **Subheading 3.3.1.**) destains Coomassie-stained gel pieces. Any other staining techniques might require further destaining steps. However, this protocol can also be used for silver-stained gel pieces, if superficial silver-staining has been performed using a protocol published by Shevchenko and colleagues ***(35)***.
6. **Steps 18–20** (*see* **Subheading 3.3.1.**) can be omitted to avoid any sample loss caused by peptide adhesion to the tube walls during these steps, particularly the drying step.
7. After the preparation of the saturated DHB solution, it is advisable to produce a clear supernatant for further usage. The solution should therefore be microcentrifuged, and undissolved DHB, mainly found on the surface, should be removed. Sample crystallization is very important in MALDI MS. Sometimes the sample might not crystallize completely, and a thin gel-like sample film is obtained. In these cases, diluting the initial peptide digest mixture with water often improves crystallization and the MALDI process. Another important issue seems to be the purity of DHB. Commercially available DHB varies dramatically in its effective use as MALDI matrix. Recrystallization of DHB can improve its quality. DHB as well as other matrices can also be bought as a ready-to-use matrix solution (Hewlett Packard, Böblingen, Germany). One alternative is α-cyano-hydroxycinnamic acid. This matrix compound is probably used in many more MS laboratories because of its ease of use. However, DHB is substantially more tolerant to contaminants and better suited for labile analyte molecules because of its cooler ionization character. This can ultimately result in higher sensitivity, because additional sample cleaning and preparation steps such ZipTip™ clean-ups can be omitted. Although the MALDI sample preparation with DHB is the simplest, even for relatively contaminated samples, the MALDI data acquisition is complicated as a result of the necessity to find a sweetspot for analyte ion production. Samples with DHB as matrix typically crystallize with bigger, often needle-like crystals forming a rim and a more amorphous crystalline area inside. Best MALDI MS results can usually be obtained from the rim area and big crystals. Spectra obtained from the inside area are generally inferior with lower analyte ion signal and a higher degree of cation adduct formation. It seems that DHB as matrix provides an on-target inherent sample purification because of its crystallization.
8. Because of the variety of MALDI mass spectrometers and possible parameter settings, the analysis step is not discussed.

## 5. Database Search Programs

http://prospector.ucsf.edu
http://prowl.rockefeller.edu/cgi-bin/ProFound
http://www.matrixscience.com

At these sites, further links to database search engines and mass spectrometry sites can be found.

## References

1. Gygi, S. P., Rochon, Y., Franza, B. R., and Aebersold, R. (1999) Correlation between protein and mRNA abundance in yeast. *Mol. Cell. Biol.* **19,** 1720–1730.
2. Wasinger, V. C., Cordwell, S. J., Cerpa-Poljak, A., Yan, J. X., Gooley, A. A., Wilkins, M. R., et al. (1995) Progress with gene-product mapping of the Mollicutes: Mycoplasma genitalium. *Electrophoresis* **16,** 1090–1094.
3. Blackstock, W. P. and Weir, M. P. (1999) Proteomics: Quantitative and physical mapping of cellular proteins. *TIBTECH* **17,** 121–127.
4. Uetz, P., Giot, L., Cagney, G., Mansfield, T. A., Judson, R. S., Knight, J. R., et al. (2000) A comprehensive analysis of protein-protein interactions in Saccharomyces cerevisiae. *Nature* **403,** 623–627.
5. Zozulya, S., Lioubin, M., Hill, R. J., Abram, C., and Gishizky, M. L. (1999) Mapping signal transduction pathways by phage display. *Nat. Biotech.* **17,** 1193–1198.
6. Pandey, A. and Mann, M. (2000) Proteomics to study genes and genomes. *Nature* **405,** 837–846.
7. Strohman, R. (1994) Epigenesis: the missing beat in biotechnology? *Biotechnology* **12,** 156–164.
8. Wang, J. H. and Hewick, R. M. (1999) Proteomics in drug discovery. *Drug Discovery Today* **4,** 129–133.
9. Link, T. L. (ed.) (1999) *2-D Proteome Analysis Protocol.* Humana, Totowa, NJ.
10. Ostergaard, M., Wolf, H., Orntoft, T. F., and Celis, J. E. (1999) Psoriasin (S100A7): A putative urinary marker for the follow-up of patients with bladder squamous cell carcinomas. *Electrophoresis* **20,** 349–354.
11. Naaby-Hansen, S., Waterfield, M. D., and Cramer, R. (2001) Proteomics—Postgenomic cartography to understand cell function. *Trends Pharmacol. Sci.* **22,** 376–384.
12. Patton, W. F. (2000) A thousand points of light: The application of fluorescence detection technologies to two-dimensional gel electrophoresis and proteomics. *Electrophoresis* **21,** 1123–1144.
13. Bright, R. K., Vocke, C. D., Emmert-Buck, M. R., Duray, P. H., Solomon, D., Fetsch, P., et al. (1997) Generation and genetic characterization of immortal human prostate epithelial cell lines derived from primary cancer specimens. *Cancer Res.* **57,** 995–1002.
14. Unlu, M., Morgan, M. E., and Minden, J. S. (1997) Difference gel electrophoresis: A single gel method for detecting changes in protein extracts. *Electrophoresis* **18,** 2071–2077.

15. Page, M. J., Amess, B., Townsend, R. R., Parekh, R., Herath, A., Brusten, L., et al. (1999) Proteomic definition of normal human luminal and myoepithelial breast cells purified from reduction mammoplasties. *Proc. Natl. Acad. Sci. USA* **96,** 12589–12594.
16. Gygi, S. P., Rist, B., Gerber, S. A., Turacek, F., Gelb, M. H., and Aebersold, R. (1999) Quantitative analysis of complex protein mixtures using isotope-coded affinity tags. *Nat. Biotech.* **17,** 994–999.
17. Naaby-Hansen, S., Flickinger, C. J., and Herr, J. C. (1997) Two-dimensional gel electrophoretic analysis of vectorially labeled surface proteins of human spermatozoa. *Biol. Reprod.* **56,** 771–787.
18. Naaby-Hansen, S. (1990) Electrophoretic map of acidic and neutral human spermatozoal proteins. *J. Reprod. Immunol.* **17,** 167–185.
19. Patton, W. F., Pluskal, M. G., Skea, W. M., Buecker, J. L., Lopez, M. F., Zimmermann, R., et al. (1990) Development of a dedicated two-dimensional gel electrophoresis system that provides optimal pattern reproducibility and polypeptide resolution. *Biotechniques* **8,** 518–527.
20. Chevallet, M., Santoni, V., Poinas, A., Rouquie, D., Fuchs, A., Kieffer, S., et al. (1998) New zwitterionic detergents improve the analysis of membrane proteins by 2-D electrophoresis. *Electrophoresis* **19,** 1901–1909.
21. Krause, K.-H. and Michalak, M. (1997) Calreticulin. *Cell* **88,** 439–443.
22. Jungblut, P. and Thiede, B. (1997) Protein identification from 2-DE gels by MALDI mass spectrometry. *Mass Spectrom. Rev.* **16,** 145–162.
23. Yates, J. R. III. (1998) Mass spectrometry and the age of the proteome. J. Mass Spectrom. **33,** 1–19.
24. Guetens, G., Van Cauwenberghe, K., De Boeck, G., Maes, R., Tjaden, U. R., van der Greef, J., et al. (2000) Nanotechnology in bio/clinical analysis. *J. Chromatogr. B, Biomed. Sci. Appl.* **739,** 139–150.
25. Belov, M. E., Gorshkov, M. V., Udseth, H. R., Gordon, A. A., and Smith, R. D. (2000) Zeptomole-sensitivity electrospray ionization-fourier transform ion cyclotron resonance mass spectrometry of proteins. *Anal. Chem.* **72,** 2271–2279.
26. Wilm, M., Shevchenko, A., Houthaeve, T., Breit, S., Schweigerer, L., Fotsis, T., and Mann, M. (1996) Femtomole sequencing of proteins from polyacrylamide gels by nano-electrospray mass spectrometry. *Nature* **379,** 466–469.
27. Eckerskorn, C., Strupat, K., Schleuder, D., Hochstrasser, D., Sanchez, J.-C., Lottspeich, F., and Hillenkamp, F. (1997) Analysis of proteins by direct-scanning infrared-MALDI mass spectrometry after 2D-PAGE separation and electroblotting. *Anal. Chem.* **69,** 2888–2892.
28. Clauser, K., Baker, P., and Burlingame, A. L. (1999) Role of accurate mass measurement (±10 ppm) in protein identification strategies employing MS or MS/MS and database searching. *Anal. Chem.* **71,** 2871–2882.
29. Gross, J. and Strupat, K. (1998) Matrix-assisted laser desorption/ionisation-mass spectrometry applied to biological macromolecules. *Trends Anal. Chem.* **17,** 470–484.
30. Kebarle, P. (2000) A brief overview of the present status of the mechanisms involved in electrospray mass spectrometry. *J. Mass Spectrom.* **35,** 804–817.

31. Cole, R.B. (2000) Some tenets pertaining to electrospray ionization mass spectrometry. *J. Mass Spectrom.* **35,** 763–772.
32. Patterson, S. D. and Garrels, J. I. (1994) Two-dimensional gel analysis of post-translational modifications, in *Cell Biology, A Laboratory Handbook* (Celis, J., ed.), Academic Press Inc., San Diego, CA, pp. 249–257.
33. Link, A. J. and Bizios, N. (1999) Measuring the radioactivity of 2-D protein extracts, in *2-D Proteome Analysis Protocols* (Link, A. J., ed.) Humana, Totowa, NJ, pp. 105–108.
34. Gygi, S. P. and Aebersold R. (1999) Absolute quantitation of 2-D protein spots, in *2-D Proteome Analysis Protocols* (Link, A. J., ed.) Humana, Totowa, NJ, pp. 417–422.
35. Shevchenko, A., Wilm, M., Vorm, O., and Mann, M. (1996) Mass spectrometric sequencing of proteins from silver-stained polyacrylamide gels. *Anal. Chem.* **68,** 850–858.

# 18

# Application of Gene Microarrays in the Study of Prostate Cancer

**Colleen C. Nelson, Douglas Hoffart, Martin E. Gleave, and Paul S. Rennie**

## 1. Potential Clinical Applications of Gene Arrays

Gene macro- and microarrays have become an increasingly popular tool to investigate gene expression patterns by simultaneously analyzing the expression of thousands of genes in a single experiment. Through careful array design and appropriate analytical tools, one can relate gene expression patterns across large series of data to determine clusters of genes that are co-ordinately regulated as well as correlate patterns to particular disease states or experimental conditions. This approach has been applied to derive relationships between clinical parameters of certain cancers with gene profiles, which potentially may be used as prognostication tools or for identification of therapeutic targets. Although still in its infancy as a clinical laboratory tool, there are several recent reports that illustrate the power of gene microarrays for differential cancer diagnosis. For example, analysis of mRNA from diffuse large B-cell lymphomas using gene microarrays with approx 18,000 cDNA clones revealed two distinct gene expression patterns that were indicative of newly uncovered cancer subtypes and that were predictive of disease survival *(1)*. Similarly, there is some preliminary evidence from gene microarray analyses to suggest that gene expression patterns in human breast cancers form two distinctive clusters that correlate with cell proliferation rates and activation of the interferon signal transduction pathway *(2),* although no direct clinical or pathological connections were noted.

To date, there are no reports where gene array analyses of prostate cancers have resolved into distinctive clusters or patterns with prognostic implications. However, several individual genes have been shown to be differentially expressed in comparisons of prostate cancer cell lines with other tissues and

From: *Methods in Molecular Medicine, Vol. 81: Prostate Cancer Methods and Protocols*
Edited by: P. J. Russell, P. Jackson, and E. A. Kingsley © Humana Press Inc., Totowa, NJ

cell lines *(3,4)* and in androgen-responsive vs androgen-independent clones *(5,6)*. As a baseline to subsequent gene analyses of androgen-mediated response of prostate cancers, one group has attempted to define the prostate transcriptome, which they found to consist of ~16,000 distinct transcripts *(7)*. With the human genome complete, a great deal of effort will now be made to create cDNA or oligonucleotide equivalent microarrays that are a complete representation of the entire genome, which is currently estimated to comprise ~35,000 unique genes *(8*; International Human Genome Consortium, 2001).

Equipped with gene microarrays containing comprehensive gene sets, one can now determine the spectra of genes that are expressed or repressed in the prostate during development, growth, aging, and during tumor formation and progression. These gene profiles will allow for insight into temporal patterns of gene expression with respect to normal prostate function and during various stages of prostate cancer, including dysplasia, tumor progression, metastasis, and ultimately hormone independence. Thus, the application of microarrays to the study of cancer will provide an unprecedented level of comprehensive information of the molecular changes that underpin phenotypic changes in the dynamics of progression from early lesions to invasive cancer and metastasis.

To the academic researcher, gene microarrays offer the opportunity to identify clusters of co-ordinately regulated genes associated with specific biological pathways and physiological stimuli. Genes associated with, rather than causative of, cellular cascades of gene expression can be determined experimentally by gene knockout or knockin strategies where the effect on the transcriptome is determined after a gene of interest is overexpressed or blocked. Furthermore, the ordering of cellular information will allow the identification of communication networks within the cell and illuminate potential factors that control cellular responses. Those genes that regulate cascades of downstream genes associated with a poor prognostication have the potential to be ideal therapeutic targets.

Using experimental model systems, it is possible to determine the function of individual genes and to target genes at critical control points for therapeutic intervention either by direct targeting of the gene expression through antisense technologies or by using small molecule inhibitors specifically aimed at a particular pathway. Gene expression profiles can also be used to stage tumors accurately and to serve as molecular prognosticators and treatment response indicators. It is likely that research and clinical applications of gene microarrays will revolutionize how cancer and almost all other diseases are diagnosed and treated.

## 2. Fundamental Aspects of Gene Arrays

In essence, a gene array is simply an orderly arrangement of unique DNA molecules (cDNA or oligonucleotides) affixed to an insoluble matrix, such as

nylon or glass. In the manner of a reverse Northern dot blot, the array is used as a template for hybridization of a suitably radioactive or fluorescent-labeled probe derived from mRNA from a specific tissue or cell type. However, in most cases, the amount of hybridization measured is an estimate of the relative amount of gene transcription, not the absolute amount. Hence, the type of data obtained is described in terms of the level of expression of a specific gene in one sample vs another. Information, such as absolute number of transcripts in a given cell, can be estimated by inclusion of a standard curve incorporated into the array in which unique genes from a distant species (e.g., *Arabidopsis*) are spotted on the array and the corresponding RNAs in known concentrations are spiked into the labeling reaction. Characterized, alternatively spliced transcripts can be monitored by careful array design of isolated gene exons.

Although the basic theme is the same, there are a variety of different types of gene array formats. Low-density or macroarrays are presently the most readily available commercially (e.g., ClonTech Atlas™ Arrays, Genome Solutions, Research Genetics, and Incyte Genomics) and usually contain from a few hundred to a few thousand genes spotted onto a nylon or similar membrane. Hybridizations to macroarrays are generally performed with radiolabeled probes and the spot diameters may range from 400 to 2000 microns. By comparison, microarrays (or high-density arrays) may contain 30,000 or more individual cDNAs or expressed sequence tags with spots 100–250 microns in size, which are affixed to a more rigid matrix, such as a specially treated glass slide and which are normally hybridized with a fluorescent-labeled probe. The higher density can be achieved on glass because there is not an appreciable wicking effect that occurs on nylon membranes. Derivations of microarrays include the Affymetrix oligonucleotide arrays, which are manufactured using a combinatorial chemistry method where a related series of short oligonucleotides (25 base oligomers) are synthesized on a solid surface. Although they are one of the highest density arrays currently available, their widespread usage is hampered by their high cost and by restricted versatility and handling options. Similarly, another cutting-edge microarray technology is the Nanogen microelectronic arrays or chips, which use an electric field to immobilize genes and to regulate the hybridization reaction.

Because the primary goal of this chapter is to provide practical guidelines for the preparation and use of gene arrays by most investigators working in prostate cancer research, the focus is on the more generally used macroarrays and cDNA-based microarrays. The topics that are covered in detail in subsequent sections are as follows: (1) sample selection; (2) preparation and labeling of cDNA probes; (3) printing of gene arrays; (4) validation and normalization procedures; and (5) data and bioinformatic analyses.

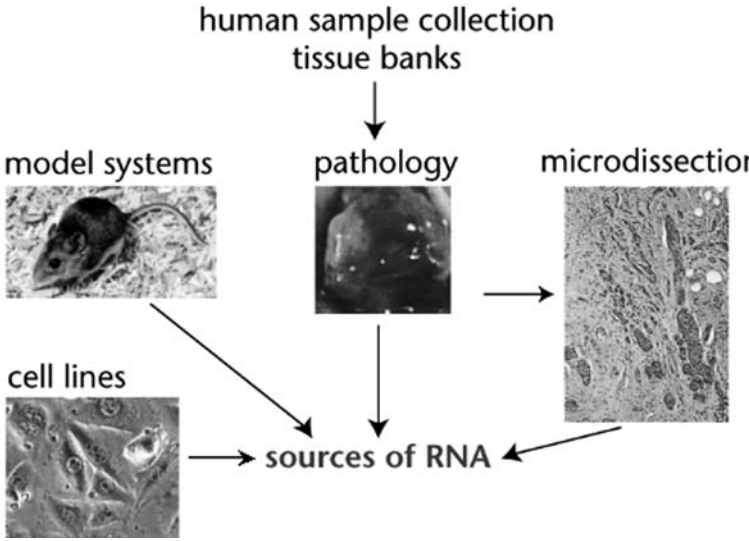


Fig. 1. Tissue sources for hybridization probes. The primary types of cell and tissue sources for isolation of RNA used in gene array experiments are illustrated.

## 3. Sample Selection for Gene Array Analysis

The sources of biological material for examination of gene expression patterns differ in their complexity and appropriateness for scientific inquiry. Complexity ranges from clonal/homogeneous cell lines and tumor models, through to human biopsy tissue, which display both interperson variation and variation in composition of cell types (e.g., stromal and epithelial compartments) (*see* **Fig. 1**). In the most reductionist or minimalist type of experiments, cell lines, such as PC-3 or LNCaP human prostate cancer cells, can be used for comparing the impact of a single treatment (e.g., ± androgen replacement) or perturbation on gene expression patterns. The mRNA population is relatively homogeneous and can be used to determine effects of a hormone, chemical, or the expression of a transfected, exogenous gene. Similarly, cell lines can be used to determine the temporal or concentration effects initiated by an experimental agent. However, although cell lines are effective tools for examining or dissecting the specific impact of a given treatment on gene expression, they often do not accurately portray what occurs in vivo after similar treatments or manipulations. Because of the growth-advantage conditions in which cell lines are cultured (i.e., bathed in serum and growth factors), there are often signal transduction pathways and cell cycle pathways that are

artificially turned on at full bore. In vivo, the same pathways are normally regulated by the limited availability of growth factors and oxygen as well as by contact inhibition of adjoining cells. Therefore, many questions regarding complex disease processes, such as prostate tumor progression, must be addressed initially in tumor model systems in vivo to provide a more accurate and realistic evaluation of the tumor transcriptome and its response to specific treatments.

Although in vivo tumor models like the LNCaP-nude mouse system are more realistic representations of prostate cancers in the human population and at the same time limit the extent of inter-person variation seen in human biopsies, they do possess the biological and genetic complexity inherent in having multiple cell types within a single sample. Gene expression analysis is collected simultaneously for stromal and endothelial cell types as well as for the malignant epithelium. This makes the analysis more complicated. To determine the cell type of origin of an altered message, one can perform *in situ* hybridization or immunohistochemistry on matching tissue sections. Alternatively, this issue can be addressed before examination of the gene profile by visual or laser capture microdissection of malignant epithelial cells from host endothelium and stromal cell populations. This approach may allow for examination of the malignant cells but is not typically used to isolate host stromal and endothelial cells. The yield of intact RNA is often limiting from dissected tissue, so that techniques for linear amplification of mRNA will need to be improved to aid in the miniaturization of sample size. For these reasons, microdissection is generally impractical for this type of experiment and the cell heterogeneity factor may best be corrected at the analytical stage.

In the process of prostate tumor progression, it is important to appreciate that nonmalignant cells within the tumor also respond and contribute to changes in the microenvironment. Hence, molecular changes in stromal and endothelial components of a tumor can be critical to overall tumor growth and metastasis. Accordingly, one must take into consideration gene expression changes in the nonmalignant cells, which reside in the tumor to factor in all influences on its molecular phenotype. As discussed above, this requires some form of accurate pathological assessment and/or tissue microdissection. If this technology is not readily available, then subsequent identification of the cell type(s) responsible for a particular change in gene expression can sometimes be accomplished by performing *in situ* hybridizations; or if the appropriate antibodies are available, immunohistochemistry. These types of analyses are greatly aided by the use of tumor/tissue arrays in which hundreds of tumor core sections are arrayed on a single microscope slide and simultaneously analyzed.

## 4. Preparation and Labeling of cDNA Probes

### 4.1. Isolation of RNA

To create the complex probes for array hybridization, it is important to be able to isolate high-quality, intact RNA from the cellular source. Some labeling techniques can be performed with total RNA, whereas other methods may require the isolation of poly-A RNA. RNA isolation from laboratory cell lines is a straightforward and easily controlled procedure, whereas isolation of RNA from tissues requires extra consideration. Tissues must be processed rapidly, which is a major complication in clinical samples, especially those obtained from patients in which the samples must be first evaluated pathologically. A further problem is that clinical samples are often placed in fixatives that are incompatible with the isolation of intact RNA. Although new fixation compounds and procedures are being developed which circumvent this problem, they are not being rapidly incorporated into routine practice in pathology laboratories because of uncertainties as to the quality of histologic preparations obtained using these new fixatives, as well as the absence of any apparent value to the pathologist over the traditional pathological assessment of tissues.

Cell cultures and tissue samples are typically processed by rapid exposure to extraction solutions coupled with immediate tissue homogenization. For this purpose, a number of kits and solutions are commercially available. These include phenolic reagents such as Trizol, which rapidly extracts RNA into the aqueous phase and simultaneously denatures RNAses. An assortment of other kits is also available for RNA extraction using a variety of solid phase separation chemistries. Typically 10–20 μg of total RNA or 0.1 to 1 μg of mRNA is needed for a labeling reaction.

### 4.2. Radioactive Probes

Once total RNA is extracted, one can directly create labeled cDNA copies of polyadenylated RNA using a polyoligonucleotide-dT (poly-dT) primer and the enzyme reverse transcriptase. The poly-dT primer is often anchored with a 5′G, C, or A to minimize the length of poly A repeat copied within the labeled probe. For hybridizations with macroarrays spotted on nylon membranes, radioactive labeling is optimized by incorporation of a $^{33}$P- rather than a $^{32}$P-labeled nucleotide. The use of $^{33}$P-labeling has the benefit of high sensitivity without the bloom problems associated with higher energy emitters such as $^{32}$P.

### 4.3. Fluorescent Probes

Preparing probes for glass microarrays typically involves creating a fluorescent-labeled probe. One of the best reasons for using fluorescence is that both

experimental and control samples can be hybridized on the same array because the two samples can be labeled with fluorescent tags having different emission wavelengths (e.g., red dye vs green dye). This can also be accomplished by incorporation of a fluorescent-nucleotide analog, typically Cy-3 (green) or Cy-5 (red) dUTP using reverse transcriptase with a poly-dT primer (*see* **Fig. 2**). In principle, if there is more expression of a given gene in one sample over the other, then that dye signal will be stronger, essentially providing an intra-array competition where inter-array differences are normalized. Fluorescence is generally detected using confocal scanners with multiple lasers for creating the correct excitation wavelengths and charge-coupled devices or photomultiplier tubes for detection.

Unfortunately, because of the bulky side chain of the fluorescent nucleotides, fluorescent labeling is a far less efficient process compared to using radiolabeled nucleotides. Also, extra attention in experimental design is needed because different fluorescently labeled nucleotides are not incorporated equally (Cy-3 is about 5 times as efficient as Cy-5). To get around these problems, direct linkage methods are being developed for covalently labeling purified mRNA. This process is greatly enhanced by isolation of mRNA before labeling, which is often limiting in many samples. A compromise method that is being investigated is the incorporation of a small, modified nucleotide by reverse transcriptase (e.g., amino allyl dUTP) followed by specific coupling of a monofunctional reactive cyanine dye to the modified nucleotide. Other improvements in labeling efficiency are needed and will presumably be forthcoming in the near future. Protocols currently in practice to deal with problems in labeling efficiencies are described in later sections dealing with validation and normalization procedures.

## 5. Printing of Gene Arrays

### *5.1. Bacterial Clones on Nylon Arrays*

Gene expression arrays can be created in a number of formats from a variety of biological sources, ranging from bacterial colonies to polymerase chain reaction (PCR) products of cDNA clones, to gene specific oligonucleotides. Direct spotting of bacterial clones onto nylon membranes is the crudest format. Bacterial clone-generated arrays are inexpensive to create and densities of ~4000 clones on an 8- × 12-cm membrane can easily be achieved with reasonably good resolution. After alkaline lysis, colonies can be probed with $^{33}$P-labeled cDNA and analyzed on a PhosphorImager. Differences in bacterial colony growth must be taken into consideration. This is most easily dealt with by stripping the membrane and then rehybridizing with a primer universal to the plasmid vector. The intensity of the plasmid hybridization is subsequently

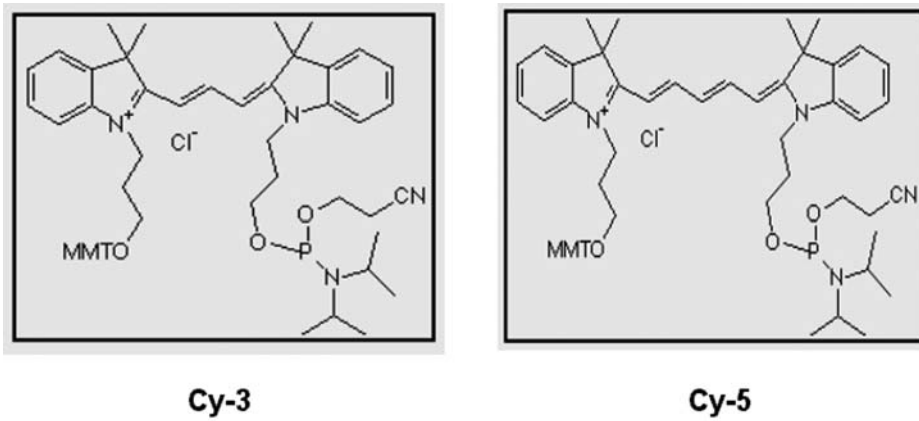


Fig. 2. Fluorescent dyes used for labeling cDNA probes. Probes used for hybridization experiments with glass microarrays generally use Cy-3 (excitation, 550 nm; emission, 570 nm) and Cy-5 (excitation, 649 nm; emission, 670 nm) fluorescent-labeled nucleotides.

used to normalize gene-specific intensities. This format is the least expensive and most rapid form for array data generation; however, the noise to signal ratio may be significant and interfere with interpretation of the results.

### 5.2. PCR Products on Nylon Arrays

The signal to noise ratio is dramatically improved by printing PCR products onto nylon membranes, where densities of ~10,000 genes may be printed on an 8- × 12-cm membrane. Membranes are probed as described above with $^{33}$P-labeled cDNA and can be normalized by reprobing with a similarly labeled universal PCR primer. Analysis is best performed using a PhosphorImager in which a minimum of 50-micron resolution can be achieved. Limitations in analysis may result due to the maximum resolution of the phosphor screen or the instrument (50 microns), which defines the practical limits on gene density. Therefore, typically gene spot diameters must be in the range of 400 microns or greater to be accurately quantitated. The advantage to this format is that nucleic acid binding and hybridization to nylon membranes is a straightforward application that is routinely used in most molecular biology research laboratories. Also, there has been a dramatic increase in the availability of PhosphorImagers for quantitative analysis, which allows for up to 5 orders of magnitude of dynamic range in signal intensity. Additionally, membranes can be stripped and reprobed multiple times for determining the gene profiles in a number of different samples. Overall, nylon membranes are a very reliable array format that can be used in most laboratory settings. A drawback to using nylon membrane arrays is that the semi-solid support nature of the material can warp during hybridization and washing, causing distortion of the array, which leads to difficulty in analysis.

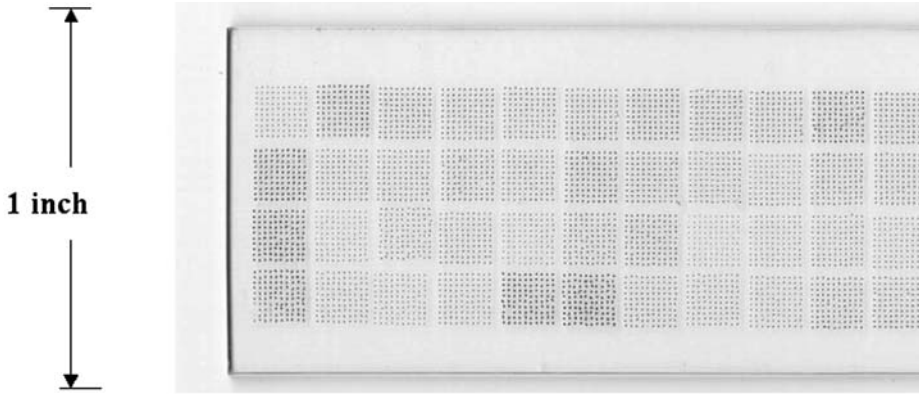


Fig. 3. High-density spotting onto glass. An illustrative example of high-density spotting by printing 6400 spots onto a glass microscope slide using ink rather than DNA.

### *5.3. PCR Products on Glass Arrays*

To achieve higher density gene arrays (on the order of ~30,000 genes), PCR products or oligonucleotides can be printed onto specially treated glass slides (*see* **Fig. 3**). The types of glass slides used have a variety of attachment chemistries, ranging from polylysine to more complex proprietary chemistries. Slide chemistries differ in their attachment efficiencies, stability, and background levels after hybridization. A fusion of technologies is evident with nylon-coated glass slides, which combine the advantage of the strong nucleic acid attachment properties of nylon with a solid, miniaturized glass support that is less prone to warping and can be used for detection of nonradioactive, fluorescent probes using a microarray fluorescence reader.

PCR products must be purified, validated, and concentrated prior to printing. To perform these procedures in a high-throughput manner requires the use of liquid handling robotics and equipment for handling 96- and 384-well microtiter plates. PCR production and clean-up adds significantly to the array cost. Alternatively, "longmers" or oligonucleotides <70 bases are being synthesized in 96-well plates in sets that represent greater than 10,000 selected genes. These oligonucleotides have a large up-front cost but are then ready for printing virtually thousands of arrays. Commitment to undertake this sort of array production is only cost efficient if a very large number of arrays are needed over a relatively continuous time frame.

## 6. Validation and Normalization Procedures

### *6.1. Preparation of a Standard Curve*

In printing custom arrays, it is very important to build in appropriate controls and normalization tools. For instance, additional spotting of *Arabidopsis* genes

on an array, coupled with hybridizations using samples spiked with the corresponding cDNA in defined concentrations, allows for construction of a standard curve for mRNA intensity. This standard curve is used to optimize the image acquisition during multiple readings of glass microarrays with alterations to such parameters as laser intensity, fluorescent sensitivity and gain, in order to maximize the dynamic range of detection. These adjustments are critical to make the most of the results obtained from the hybridization experiment. The use of a standard curve also gives a tool to estimate absolute mRNA abundance, which can be used as a normalization tool for creating a relational data base of gene expression results. To monitor hybridization efficiency across the area of the slide, other genes and spiked probe pairs can be used and monitored for the relative uniformity of hybridization. Some custom-made slides rely on one data point for a single gene representation, whereas it is preferred to have duplicate spots for each gene present on the slide. In the data analysis, duplicate points should not vary in intensity greater than 10%. This helps factor out any anomalies in the hybridization experiment.

### 6.2. Selection of Standards

One of the most consistent findings from gene array experiments is that there is no such thing as a housekeeping gene that remains constant under all circumstances. Accordingly, several new methods are being applied and field tested to resolve the inherent problem of normalization between samples. There is no common consensus, and different groups have adopted different protocols for normalization. A procedure that is gaining increasing popularity is the use of a pooled reference set of RNA samples. The ideal reference sample would have reasonable representation of every gene spotted on the array. To achieve this from biological sources, a practice has been adopted to pool RNA from a number (usually >10) of different cell lines grown in culture. This large pool of RNA is then used as an internal standard to correct for differences in labeling and hybridization efficiencies. The RNA pool is expected to remain constant and reproducible over a reasonable period of time. As a bonus, this type of standard can also be used to illuminate all spots and therefore correct for inconsistencies in printing of arrays. The main difficulty with this method of standardization is in its reproduction and the relative quantitation. If all spots are created by a single set of PCR primers, another alternative for standardization is to hybridize with a universal primer set. This provides unbiased information to quantitate the molar amount of target spotted, the spot morphology as well as a tool to aid in estimation of the number of mRNA molecules hybridized to the spot. Yet another approach is to use overall intensity between samples as a normalization tool, on the assumption that overall mRNA levels should be

equivalent between samples. However, this assumption becomes less valid with a decrease in gene representation.

### *6.3. Fluorescent Dye Corrections*

It is well recognized that bias in labeling with different fluorescent dyes is significant due to substantial differences in incorporation and detection efficiencies. To correct for this, the industry standard for acceptable gene microarray procedure is that experiments must include reverse labeling and that data obtained must be nearly equivalent. For example, this means that a sample must be first labeled with Cy-3 and the reference labeled with Cy-5 in one experiment, and then in a parallel experiment, the dye labeling must be reversed such that the sample is labeled with Cy-5 and the reference with Cy-3. Data sets that are not reproducible through this procedure must be treated as invalid in further analyses. Clearly, to improve the quality and validity of array data currently being generated, advancements in fluorescent chemistries and detection are needed to help overcome the biases that are associated with the use of Cy-3 and Cy-5.

## 7. Hybridization Procedures

### *7.1. Hybridizations with Macroarrays*

The generation of high-quality and reproducible gene expression data from arrays is very dependent on the hybridization and washing procedures employed. The even distribution of the hybridization and washing solutions are critically important for achieving good specific probe-gene interaction with the least amount of nonspecific background. With nylon or equivalent macroarrays (*see* **Fig. 4**), the procedures are essentially identical to those already used in most research labs for Southern blotting. This traditionally involves placing the membrane in a sealed bag or container with the labeled cDNA probes in hybridization solution, which is then agitated in a salt- and temperature-controlled environment to adjust for the optimal stringency. Because gene arrays are usually compared in paired samples, particular care must be given to ensure that the hybridization conditions are identical for both arrays.

### *7.2. Hybridizations with Glass Microarrays*

Hybridization with gene microarrays on glass slides or comparable rigid matrices is performed similarly to nylon macroarrays, except that extra consideration is given to evaporation and to handling the small volumes of hybridization solutions (<75 μL) compared with the 2–10 mL of hybridization solution used for nylon membranes. The options for microarrays range from simple adaptations of common laboratory equipment and make-do solutions, to complete custom-made flow cells or automated microfluidics stations. Simple

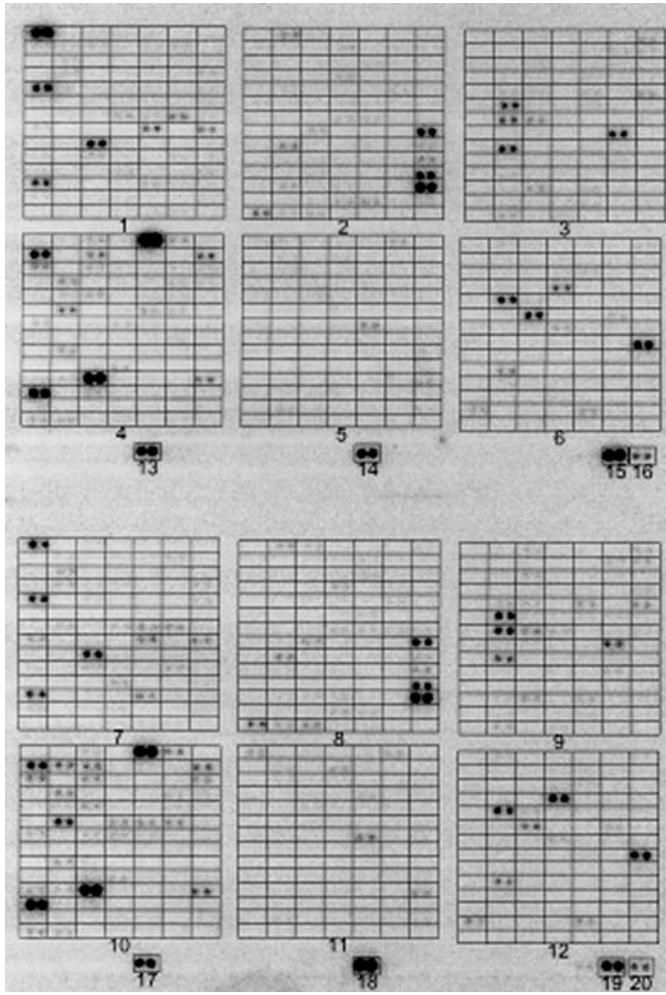


Fig. 4. Hybridization experiment with a nylon macroarray. An illustrative example of hybridization with radioactively-labeled cDNA to a ClonTech Atlas™ human cancer nylon expression array with double-spotted DNA of 588 genes known to have cancer-related functions.

adaptations include enclosing array slides in 50-mL screw cap tubes and placing them inside an incubator or waterbath for temperature regulation. Evaporation is controlled by covering the hybridization solution with a coverslip or sandwiching microarray slides face to face. Inexpensive chambers and small hybridization cassettes are also available to control humidity during hybridization. At the high end, automated microfluidics stations are available that can process up to 25 slides simultaneously, control temperature through a plate

beneath the slides, and more tightly regulate conditions during hybridization as well as perform uniform washings. The main advantages of such stations are in the consistency of treatments with which the slides are processed as well as the higher capacity that can be accommodated, both of which may be critical for the creation of large relational data bases. Actual hybridization solutions and conditions will vary depending on the nature of the material spotted and the slide chemistry. A variety of websites have been compiled by microarray users that are an excellent source of technical tips for arraying (*see* **Table 1**).

## 8. Data and Bioinformatic Analyses

With the increased biological interest in all things genomic, caused in large part by the recent completion of the initial sequencing phase of the Human Genome Project, the field of bioinformatics has witnessed an explosive growth as a vital tool in the management and exploration of genomic data within and across many species.

### *8.1. Scope of Bioinformatics in Microarrays*

With respect to macro/microarray experiments, the bioinformatic requirements do not start with the glass slide (or nylon membrane) nor even the resultant image file, but must cover the entire microarray life cycle right from the initial design and manufacture of the target(s) and probe(s), through the hybridization process, slide or membrane spotting and image creation and data analysis (*see* **Table 1**, i). Information linking the entire process is necessary to monitor and ensure acceptable quality control measures, historical tracking of genomic data (i.e., the genealogy of each spot), as well as provide valid and reproducible analytical results; any weak or missing link in this chain of informational flow will ultimately result in unreliable, and therefore scientifically useless data and wasted resources. Unfortunately, most existing software, both free and commercial, has focused exclusively on postmicroarray production, namely image analysis, as the entire goal of bioinformatics. The equally important task of historical spot tracking can sometimes be covered by the addition of a Laboratory Information Management System in which all laboratory entities are recorded in some form of database (typically relational) for later query, retrieval, and analysis.

### *8.2. Toward a Universal Microarray Data Standard*

With the rapidly expanding field of microarray technology, several ad hoc groups have coalesced to try and define methodological approaches to capture and manage the data generated from such high-throughput techniques. Of these, the Microarray Gene Expression Database group, MGED (*see* **Table 1**, ii), has gained international acceptance with their proposed Minimum Information About a Microarray Experiment, MIAME (*see* **Table 1**, iii). As the title

**Table 1**
**Selection of Bioinformatic Software Tools Platforms for Microarray Experiments[a]**

| Web address | Description |
|---|---|
| *Websites referenced in chapter* | |
| (i) http://www.cs.washington.edu/homes/jbuhler/research/array | Jeremy Buhler's site outlining the steps involved in a typical comparative microarray experiment |
| (ii) http://www.mged.org | MGED home site |
| (iii) http://www.mged.org/Annotations-wg/index.html | MIAME home site |
| (iv) http://www.xml.org/ | XML home site |
| (v) http://maggie.cbr.nrc.ca/~gordonp/xml/ | Paul Gordon's review site of XML for biology |
| (vi) http://beamish.lbl.gov/ | Paul Spellman's site for draft of MIAME proposal |
| (vii) http://www.nhgri.nih.gov/DIR/LCG/15K/HTML/img_analysis.html#anchor318897 | NHGRI site for image analysis |
| (viii) http://rana.lbl.gov/EisenSoftware.htm | Michael Eisen's site with Cluster, Treeview and ScanAlyze programs |
| *General gene expression and microarray links* | |
| http://www.gene-chips.com/ | General website on all aspects of microarray technology, maintained and updated regularly by Leming Shi of BASF Corp |
| http://industry.ebi.ac.uk/~alan/MicroArray/ | Useful site with bioinformatic links to microarray information, maintained by Alan Robinson of the European Bioinformatics Institute (EBI) |
| http://www.bioinformatik.de/cgi-bin/browse/Catalog/Microarray_Technology/ | Another useful collection of links to bioinformatics sites |
| http://www.nbif.org/links/browse.php | A collection of links to many bioinformatics and genomics sites by National Biotechnology Information Facility (NBIF) |
| http://www.bsi.vt.edu/ralscher/gridit/ | A list of microarray technology links maintained by Virginia Tech and the Forest Biotechnology Group at North Carolina State University |
| http://www.biologie.ens.fr/en/genetiqu/puces/microarraysframe.html | Collection of microarray links maintained by the École normale supérieure (ENS) in Paris |
| http://linkage.rockefeller.edu/wli/microarray/ | A collection of papers focusing on microarray technology maintained by Wentian Li at Rockefeller University |
| http://www.hgmp.mrc.ac.uk/GenomeWeb/nuc-genexp.html | A collection of gene Expression and microarrays links maintained by Human Genome Mapping Project Resource Centre (UK) |

| | |
|---|---|
| http://www.sciencemag.org/feature/plus/sfg/resources/res_rschctr.html#bio | A collection of links to bioinformatic and genome centers maintained by Science Magazine |
| http://genome-www4.Stanford.EDU/MicroArray/SMD/resources.html | A collection of microarray resources maintained by the Stanford Microarray Group |
| *Free software* | |
| http://www.microarrays.org/AMADFaq.html | AMAD (Another MicroArray Database)—a free, web-driven database system written entirely in PERL and JavaScript, and intended for use with microarray generated data. The system was written by Mike Eisen, Max Diehn, Paul Spellman, and Joseph DeRisi and is an evolving project |
| http://www.ncgr.org/research/genex/ | GeneX—a free, collaborative Internet database and toolset for gene expression data developed by the National Center for Genome Resources (NCGR) and the Computational Genomics Group at the University of California, Irvine |
| http://rana.lbl.gov/EisenSoftware.htm | Michael Eisen software (Cluster, Treeview, ScanAlyze)—a set of free programs, with source code, used for image quantification and data visualization of gene expression data |
| http://tagc.univ-mrs.fr | TAGC (Technologies Avancées pour la Génome et le Clinique) ELOGE—a software suite to assist gene expression profiling, being developed jointly by TAGC and their commercial side IPSOGEN (for nonacademic use) |
| *Commercial software* | |
| http://www.spotfire.com | SpotFire Array Explorer™—is a data analysis package focusing on clustering and profile analysis |
| http://www.rii.com | Rosetta Inpharmatics, Rosetta Resolver™—is a software/hardware combination of analysis software, database, and server for working with microarray gene expression data |
| http://www.applied-maths.com/home.html | Applied Maths, GeneMaths™ —is a software package designed for analysis of high-density microarrays and gene chips |
| http://www.sigenetics.com | Silicon Genetics GeneSpring™—is a software program for gene expression data visualization and manipulation |
| http://www.lionbioscience.com/htm/c_1/index_c_1.htm | LION biosciences AG—is a collection of software aimed at the analysis, visualization and storage of microarray gene expression data, as well as more general genomic investigations |
| http://www.biodiscovery.com/products/ImaGene/imagene.html | Biodiscovery Imagene™—is an image analysis and visualization program for microarray gene expression data |

[a]Note: this listing should not be construed as an endorsement; it is simply meant as a selective (i.e., nonexhaustive) list of available microarray software vendors, tools, products and services for researchers considering microarray experimentation. Also, it should be noted that, like all software, the existing microarray analysis software, both academic and commercial, encompass a broad range in quality, from crash-prone to robust, from incorrect to accurate results, and from user-hostile to user-friendly. Words are no replacement for experience.

suggests, this proposal attempts to specify the minimum information that must be reported about a microarray-based gene expression monitoring experiment to ensure the interpretability, as well as potential verification of the results by third parties. According to the MIAME draft, the minimum information about a published microarray-based gene expression experiment should include descriptions of the following:

- Experimental design: the set of the hybridization experiments as a whole;
- Array design: each array used and each element (spot) on the array;
- Samples: samples used, the extract preparation and labeling;
- Hybridizations: procedures and parameters;
- Measurements: images, quantitation, specifications;
- Controls: types, values, specifications.

By reviewing these proposed requirements, researchers can get a better understanding of the essential information that should be tracked for any of their own microarray experiments. Fortunately, instead of starting from scratch on the development of novel, customized microarray software, many existing solutions, both free-for-academia and commercial, are available as an increasing number of academic researchers as well as commercial vendors of microarray software have incorporated these specifications into their respective products (along with specialized, competitive enhancements) to provide at least some level of compatibility and standardization between gene expression. It should be noted, however, that few, if any, of the software products currently available handle 100% of a particular microarray-creation laboratory's requirements, so some amount of software customization and creation of specialized tools is typical in most cases.

### 8.3. Challenges to Bioinformatics

As mentioned previously, current microarray technologies can accurately deposit DNA samples as spots with diameters typically less than 200 microns onto glass slides using custom-built or commercially available spotting robots. This level of reproducible accuracy allows the laboratory scientist to easily, and routinely spot tens of thousands of genes of interest onto a single, standard-size microscopic glass slide. With this many-fold increase in the number of gene expression levels available for parallel comparisons across thousands of genes, there is a corresponding increase (typically many orders of magnitude) in the overall throughput of genomic data.

From a bioinformatic point of view, this dataset represents many challenges. Even a relatively small set of DNA placed on a microarray slide will generate an enormous amount of genomic and computational data. Information must be tracked and stored not only for the genomic data (i.e., the genes) present on the slides, but also for a myriad of other relevant properties of the

microarray, including the steps before and after the creation of the microarray slide (e.g., protocols used, array spotting hardware and configuration settings used, image analysis, experimental results, etc). Many of these considerations have been anticipated and incorporated into the MIAME proposal (and therefore, supported by vendors and academia), but most laboratories will find some degree of specialized requirements in their microarray data creation, storage, and analysis needs that are unique to their particular environment. With the selection of the appropriate software and hardware platform, this customization process should be easy and relatively simple; therefore, it is prudent to produce a list of requirements as detailed as possible before investing in any particular microarray platform and to test as many demonstration versions of potential software packages (and hardware platforms) as possible.

### *8.4. A Common Microarray Description Language*

Recognizing that the proliferation of different hardware and software combinations in the microarray field may be jeopardizing the development of suitable standards for communication between various microarray data formats, there are currently attempts to provide a common, standardized protocol, or language, to address this, based on a more multi-purpose, existing international standard, eXtensible Markup Language, XML (*see* **Table 1**, iv). Although there are a number of competing alternatives (*see* **Table 1**, v), one implementation of a microarray-based XML dialect that appears to have the majority of support from the international microarray community is the MicroArray Markup Language (MAML), originally drafted by MGED and currently managed by Paul Spellman at Stanford (*see* **Table 1**, vi). MAML was designed as a consensus-based standard for exchanging and storing data from microarray experiments. The language provides a framework for describing experiments done on all types of DNA arrays and a format to represent microarray data in a flexible way, which allows the representation of both raw and processed data. The specification is also compatible with the MIAME definitions.

### *8.5. Image Analysis in Microarray Research*

Assuming there is a suitable laboratory information management system available to handle the necessary DNA spot tracking (genealogy), the next most important bioinformatic component for microarray production is image analysis. Almost all bioinformatic analyses currently discussed in the literature are focused on image analysis, which at a basic level is simply the extraction of DNA probe intensities from a graphic file (e.g., files with a .TIFF, .BMP, .JPG, or .GIF extension) that is output from slide-scanning hardware.

A branch of the National Institutes of Health, the National Human Genome Research Institute, NHGRI (*see* **Table 1**, vii), established in 1989 to head the

Human Genome Project for the (NIH) has a useful website that discusses some of the main steps in microarray image analysis as well as providing free analysis software (Macintosh only) to perform these steps.

Once an image file has been created from the scan of a microarray slide, a software program must correctly identify the exact locations of the spots on a graphic representation of the slide and assign spot intensities. However, before the assignment of accurate spot intensities or comparisons of these spot intensities can be made, two steps must be performed to allow valid evaluations: background removal and data normalization. Background removal is needed to pull the non-specific noise out of the signal detected for a particular spot. A typical example might be where the intensity values for a control and experimental spot are 8 and 12, respectively, which implies, initially, that there is a 50% increase in the experiment condition. However, if a background noise level of 4 is subtracted from both signal intensities, it becomes apparent from the now corrected values of 4 (control) and 8 (experiment), that we are actually seeing a 100% increase in signal intensity. A complicating factor in background removal is in the exact determination of where on the microarray to use for the background value. Possible solutions, available in most software packages in the field, include use of local background around individual spots on the array, or use of the lowest signal intensities on the array as background. The latter method may more accurately reflect non-specific background as it represents nonspecific binding of targets to probe.

Normalization is the process of standardizing across multiple microarrays to allow valid comparisons and has been discussed earlier in the section on Validation and Normalization Procedures (*see* **Subheading 1.6.**). Normalization is almost always required, at least to some extent, since a number of complicating factors can influence signal intensities that are not related to gene expression levels. These include different labeling reaction efficiencies, different hybridization efficiencies, and unequal starting amounts of cDNAs or RNA. Several methods of normalizing gene expression data have been discussed throughout the literature. As indicated earlier, so-called housekeeping genes, i.e., genes that were thought to remain unaffected by the hybridization process, were originally used, but have been shown to be problematic in that they have been found to vary over a series of experiments ***(9)***. The next refinement to normalization was to use a more global approach to the problem. By assuming that the overall level of gene expression remains constant or unaffected by the experimental conditions and that changes are equally distributed between expression level increases and decreases, one can sum all the intensities for control and experimental spots and equilibrate them to create a normalized set of data. These assumptions have also been shown to be invalid in some cases,

so another tool has recently been introduced, namely the use of exogenous RNA as a form of normalization.

### *8.6. Data Analysis and Visualization Techniques in Microarray Research*

Once the background noise has been removed from the gene expression intensity data and the complete set of experiments has been normalized, the resultant dataset can be output, typically as a text file for input to more sophisticated data visualization tools. Such tools have become necessary because of the sheer quantity of the generated data that is beyond the ability of manual inspection.

Several tiers of data visualization tools can be found in the various academic and commercial offerings in the microarray arena. At the most basic level, most packages provide some form of ratio histogram plot capability. Ratio histogram plots are aimed at simple binary experiments, involving a control and one experimental condition (*see* **Fig. 5**). The plot then displays the genes ranked in order of magnitude from greatest induction to greatest reduction, thus highlighting the genes that show the greatest fold (±) changes.

If a researcher is interested in studying more that a single experimental condition, for example, investigating a time-series or multi-treatment experiment, then the analyses becomes far more computationally intensive, as does the visualization method. By far the most common technique currently employed in most software tools is some form of clustering analysis. Clustering algorithms attempt to present similar genes, based on some user-specified, mathematically derived similarity criteria or metric, in a visual fashion as groups (clusters) of related patterns (usually color-coded), which can lead the researcher to identification of "related" gene subsets for further investigation.

The inherent assumption underlying clustering is that by finding genes that behave similarly across the experimental conditions, you will identify genes of related structure or function. Unlike a gene expression ratio histogram, where the focus is strictly on the changing genes, clustering methodologies incorporate the entire dataset. Current software implementations of clustering algorithms include an ever-increasing array of techniques and terminologies including k-means, self-organizing maps ***(10),*** hierarchical clustering ***(11),*** neural net clustering, and Bayesian ***(12–16)***; all of which aim at grouping the genes into meaningful clusters.

Correspondingly, the variety of similarity metrics available, even in the free software community (*see* **Table 1**, viii) are exhaustive (e.g., centered and uncentered correlation, centered and uncentered absolute correlation, Spearman rank correlation, and Kendall's tau). Theoretically, it is assumed that these different similarity metrics should return comparable results at an overall level, with

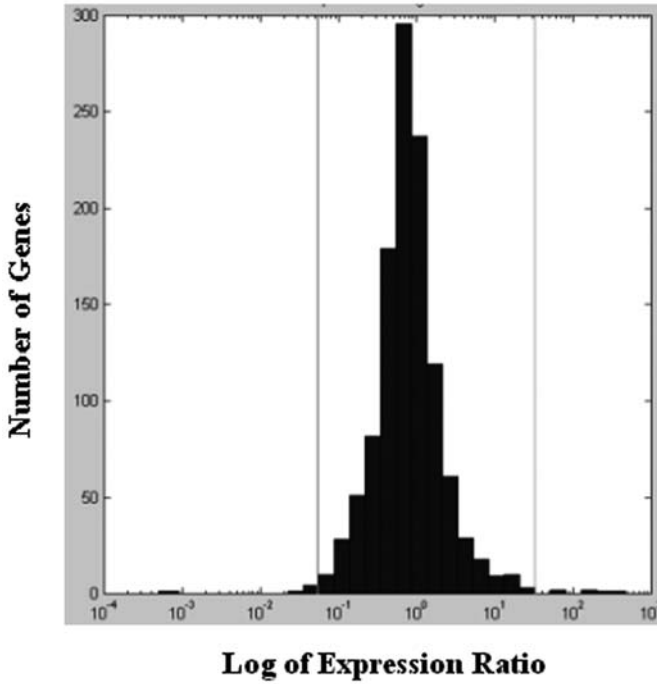


Fig. 5. Ratio histogram. Typical example of a gene expression ratio histogram for a control vs experimental study, with values in log scale to better highlight fold changes.

minor differences, like total number of clusters found, so that the user can safely pick any metric without fundamentally changing the overall clustering results.

### *8.7. On the Horizon in Microarray Bioinformatics*

Future directions in clustering techniques, indeed, in the bioinformatics field in general, will undoubtedly be in the successful combining of expression data with other experimental and clinical data, to be able to link genomic data with such seemingly unrelated measures as biochemical, behavioral and other clinical observations, to provide better diagnostic and treatment modalities.

## 9. Conclusions and Significance

Gene arrays provide a powerful new tool that takes advantage of the growing knowledge of the genomes of humans and other organisms. Complementary to obtaining complete nucleotide sequences for every gene in an entire genome, the application of gene microarrays will be fundamental to simultaneously discovering the functional relationships of these genes in the context of defined

physiological conditions. In particular, this technology platform will rapidly advance our understanding of gene functions that are critical to various cellular pathways that participate in the development and progression of prostate and other cancers. Through this understanding, new diagnostic/prognostic markers and therapeutic targets will be illuminated, tested, and validated. Furthermore, it is envisioned that in the future, gene microarray analysis of a prostate cancer patient's tumor will guide the selection of a treatment specifically tailored for that individual's unique gene expression profile. For example, one can imagine that custom synthesis of specific antisense oligonucleotides designed for selectively knocking out the function of a few critical cell survival genes when coupled with androgen withdrawal or chemotherapy will enhance eradication of prostate tumors. Alternatively, the overall gene expression profile may indicate that the cancer is essentially indolent and that the best treatment is watchful waiting. Clearly, gene microarrays will revolutionize how we treat this disease.

## References

1. Alizadeh, A. A., Eisen, M. B., Davis, R. E., Ma, C., Lossos, I. S., Rosenwald, A., et al. (2000) Distinct types of diffuse large B-cell lymphoma identified by gene expression profiling. Nature **403,** 503–511.
2. Perou, C. M., Jeffrey, S. S., van de Rijn, M., Rees, C. A., Eisen, M. B., Ross, D. T., et al. (1999) Distinctive gene expression patterns in human mammary epithelial cells and breast cancers. *Proc. Natl. Acad. Sci. USA* **96,** 9212–9217.
3. Porkka, K. P. and Visakorpi, T. (2001) Detection of differentially expressed genes in prostate cancer by combining suppression subtractive hybridization and cDNA library array. *J. Pathol.* **193,** 73–79.
4. Carlisle, A. J., Prabhu, V. V., Elkahloun, A., Hudson, J., Trent, J. M., Linehan, W. M., et al. (2000) Development of a prostate cDNA microarray and statistical gene expression analysis package. *Mol. Carcinog.* **28,** 12–22.
5. Bubendorf, L., Kolmer, M., Kononen, J., Koivisto, P., Mousses, S., Chen, Y., et al. (1999) Hormone therapy failure in human prostate cancer: analysis by complementary DNA and tissue microarrays. *J. Natl. Cancer Inst.* **91,** 1758–1764.
6. Amler, L. C., Agus, D. B., LeDuc, C., Sapinoso, M. L., Fox, W. D., Kern, S., et al. (2000) Dysregulated expression of androgen-responsive and nonresponsive genes in the androgen-independent prostate cancer xenograft model CWR22-R1. *Cancer Res.* **60,** 6134–6141.
7. Nelson, P. S., Han, D., Rochon, Y., Corthals, G. L., Lin, B., Monson, A., et al. (2000) Comprehensive analyses of prostate gene expression: Convergence of expressed sequence tag databases, transcript profiling and proteomics. *Electrophoresis* **21,** 1823–1831.
8. Venter, J.C., Adams, M. D., Myers, E. W., Li, P. W., Mural, R. J., Sutton, G. G., et al. (2001) The sequence of the human genome. *Science* **291,** 1304–1351.
9. Suzuki, T., Higgins, P. J., Crawford, D. R., Suzuki, T., Higgins, P. J., and Crawford, D. R. (2000) Control selection for RNA quantitation. *Biotechniques* **29,** 332–337.

10. Toronen, P., Kolehmainen, M., Wong, G., and Castren, E. (1999) Analysis of gene expression data using self-organizing maps. *FEBS Lett.* **451,** 142–146.
11. Eisen, M. B., Spellman, P. T., Brown, P. O., and Botstein, D. (1998) Cluster analysis and display of genome-wide expression patterns. *Proc. Natl. Acad. Sci. USA* **95,** 14863–14868.
12. Alon, U., Barkai, N., Notterman, D. A., Gish, K., Ybarra, S., Mack, D., and Levine, A. J. (1999) Broad patterns of gene expression revealed by clustering analysis of tumor and normal colon tissues probed by oligonucleotide arrays. *Proc. Natl. Acad. Sci. USA* **96,** 6745–6750.
13. Ben-Dor, A., Shamir, R., and Yakhini, Z. (1999) Clustering gene expression patterns. *J. Comput. Biol.* **6,** 281–297.
14. Hilsenbeck, S. G., Friedrichs, W. E., Schiff, R., O'Connell, P., Hansen, R. K., Osborne, C. K., and Fuqua, S. A. (1999) Statistical analysis of array expression data as applied to the problem of tamoxifen resistance. *J. Natl. Cancer Inst.* **91,** 453–459.
15. Wittes, J. and Friedman, H. P. (1999) Searching for evidence of altered gene expression: a comment on statistical analysis of microarray data. *J. Natl. Cancer Inst.* **91,** 400–401.
16. Ross, D. T., Scherf, U., Eisen, M. B., Perou, C. M., Rees, C., Spellman, P., et al. (2000) Systematic variation in gene expression patterns in human cancer cell lines. *Nat. Genet.* **24,** 227–235.

# 19

# Enhancer Trap Method Using a Green Fluorescent Protein Reporter Plasmid for Cloning Tissue-Specific Enhancers Active in Prostate Cells

**Fujiko Watt and Peter Molloy**

## 1. Introduction

Understanding the development and function of the prostate requires elucidation of the mechanisms through which genes are specifically activated in the prostate and the means by which they are regulated. Studies of development in many systems has led to a model showing that control of gene expression is exerted through three types of sequence region. The area immediately upstream or overlapping with the start site of transcription, the promoter, is important in defining the point(s) where transcription starts and, through the binding of specific transcription factors, may be involved in basal levels of transcription, responses to hormones or other regulatory factors, or in the tissue specificity of the gene's expression. Enhancers are sequence regions separate from the promoter that act to increase the level of transcription from a promoter. They may be located upstream or downstream of a gene or within an intron, and characteristically their action is independent of their orientation and position relative to the promoter and is relatively independent of distance. In many cases, enhancers confer strongly tissue-specific expression, and they may exhibit significant selectivity in the promoters they activate. A third class of regulatory sequence is the locus control region (LCR). LCRs control the activation of sets of genes and are typically located at a significant distance from them (e.g., 50 kb). Their role is believed to be in the opening up of regions or domains of chromatin.

In the postgenome era, genomic sequence of many genes has become available. From available databases, protein-coding regions can be predicted, and

From: *Methods in Molecular Medicine, Vol. 81: Prostate Cancer Methods and Protocols*
Edited by: P. J. Russell, P. Jackson, and E. A. Kingsley © Humana Press Inc., Totowa, NJ

the promoter region can be defined by determining the transcription start site of a gene. However, *cis*-regulatory elements that act over a distance cannot be determined by such methods. Identification of such regions is important for understanding mechanisms governing specific control of genes and for practical application in controlled expression of therapeutic genes in targeted tissue for gene therapy. Conventional methods of searching for enhancers have been systematic walking or deletion through large segments 5′ of the gene, although enhancers can lie in the 3′ flanking region as well as within introns of a gene. An alternative approach has been to identify in vivo DNase hypersensitive sites in and around active genes as potential control regions.

The method described here allows one to quickly screen 50–100-kb DNA directly and clone DNA fragments containing enhancer activity without walking from the promoter region. Related approaches have been used previously for the isolation of regulatory sequences including protein secretion signal sequences ***(1–3)***. The method involves making a DNA library of random partially overlapping restriction fragments covering the gene. These fragments are cloned into a vector containing the green fluorescent protein (GFP) reporter gene under the control of a basal promoter. The library is then screened for enhancer-containing DNA fragments by transfection of plasmids into tissue culture cells and identifying those that provide higher GFP reporter protein expression than the promoter only plasmid. Application of the method for identification of the prostate-specific membrane antigen gene enhancer by cloning fragments upstream of the PSM 1-kb proximal promoter ***(4)*** using the vector pPSMentrap is described (*see* **Fig. 1**). However, the method can be applied for the cloning of other developmental or tissue-specific enhancer regions by replacing the PSM promoter. We have also prepared a vector with a minimal promoter based on the adenovirus major late promoter that contains only sequences encompassing the TATA box and initiation region of transcription.

Once positive clones have been isolated, they can be readily mapped and positioned relative to the parent cosmid using standard restriction digestion. Flanking primers can be used to sequence in from the ends of the clones and so align with genomic sequence information. The enhancer trap vector is also designed with flanking restriction sites to enable convenient recloning to allow further evaluation of enhancer activity ***(5)***.

## 2. Materials

### 2.1. Bacterial Culture

1. Competent cells with high transformation efficiency: DH5-α ElectroMAX™ (Life Technologies Inc., Gaithersburg, MD).
2. Electroporator: Bio-Rad *E. Coli* Pulser Apparatus or Life Technologies Cell Porator®.
3. LB agar plates.

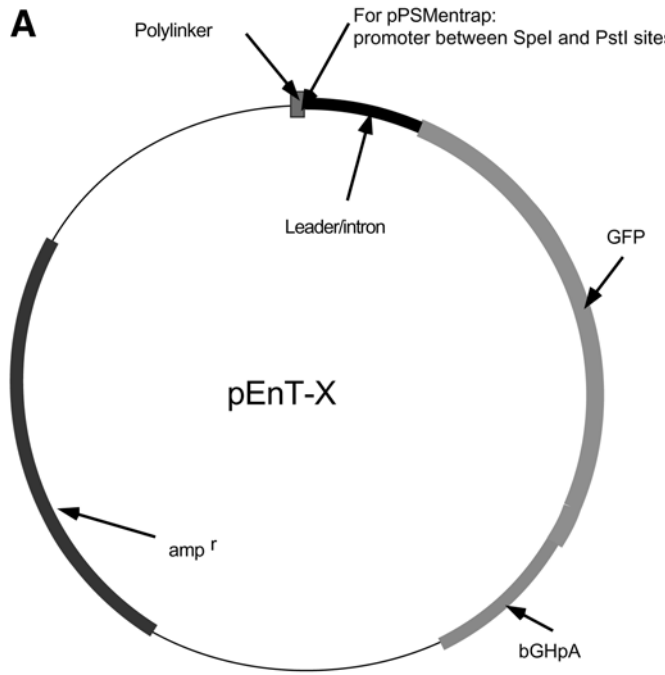


Fig. 1. Enhancer trap vectors. **(A)** The promoterless vector pEnT-X is shown. It comprises a polylinker sequence (*see* **B** on next page) into which a promoter of choice may be cloned before library preparation, leader and intron sequences derived from the pCI plasmid (Promega), the GFP coding sequences and bovine growth hormone polyadenylation signal. In the pPSMentrap vector, the 1.1-kb promoter region is cloned between the polylinker *Spe*I site and the *Pst*I site present in the leader region upstream of the splice site ***(5).*** *(Figure continues.)*

4. Phosphate buffer: 1 L is prepared by dissolving 23.13 g of $KH_2PO_4$ (0.17 *M*) and 125.4 g $K_2HPO_4$ (0.72 *M*) and autoclaving.
5. Terrific broth for liquid culture: combine in 900 mL and autoclave 12 g of Tryptone (Bacto), 24 g of yeast extract (Difco), and 4 mL of glycerol. After autoclaving, add 100 mL of phosphate buffer.
6. SOC medium: in 950 mL of deionized water, dissolve 20 g of Tryptone (Bacto), 5 g of yeast extract (Difco), and 0.5 g NaCl. Add 10 mL of 250 m*M* KCl, adjust the pH to 7.0 with 5 *N* NaOH, and adjust the final volume to 1 L. After autoclaving add 20 mL of 0.22-µm filter sterilized 1 *M* glucose and 5 mL of sterile 2 *M* $MgCl_2$.
7. Ampicillin (50 mg/mL) or other suitable antibiotics.
8. Matrix templates (7 rows by 7 columns).
9. 96-Well microtiter plates.

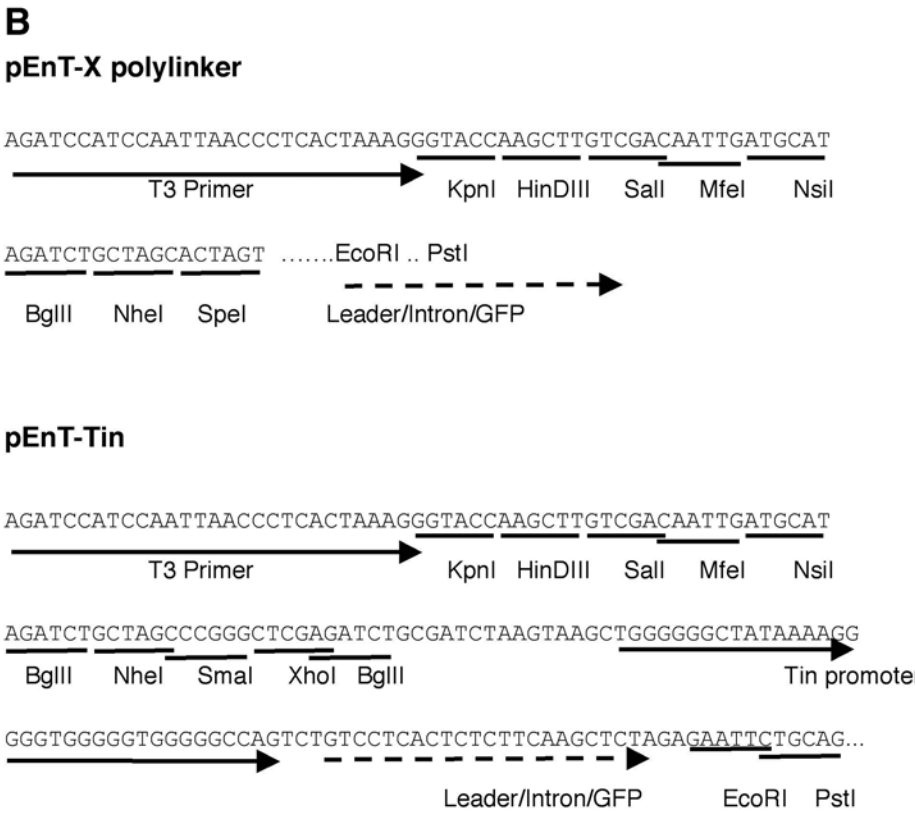


Fig. 1. *(Continued)* **(B)** Sequences of polylinker and promoter regions of the promoterless enhancer trap vector, pEnT-X, and vector with minimal promoter, pEnT-Tin. Restriction sites and the positions of the T3 sequencing primer site and Tin promoter are shown.

### 2.2. DNA and DNA Preparation and Manipulations

1. Cosmid DNA, in this case bacteriophage cosmid P1-683 containing the 5′ half and upstream flanking regions of the prostate specific membrane antigen gene (FOLH1). DNA should be column-purified (e.g., Qiagen column).
2. Enhancer trap vector, here pPSMentrap (*see* **Fig. 1**).
3. QIAGEN Plasmid Mini Kit for small scale purification of plasmid DNA.
4. UltraClean™ DNA Purification Kit (Mo Bio Laboratories Ltd) or GeneClean II (Q.Biogene).
5. Restriction enzymes and 10X buffers, including *Mfe*I and *Tsp509*I (New England Biolabs).
6. Calf intestinal phosphatase (Roche, cat. no. 108 138).
7. CIP buffer: 50 m*M* Tris-HCl, 100 m*M* NaCl, 1 m*M* dithiothreitol, pH 7.9.

8. T4 DNA ligase, 10X ligase buffer (New England Biolabs).
9. 3 *M* sodium acetate, pH 6.0.
10. Ethanol.
11. Agarose and low melting temperature agarose
12. TAE buffer: 40 m*M* Tris-acetate, 1 m*M* EDTA, pH 7.5
13. Crystal Violet.
14. TE: 10 m*M* Tris-HCl, pH 8.0, 0.1 m*M* EDTA.
15. High DNA Mass Ladder (Life Technologies, cat. no. 10496-016).

### 2.3. Tissue Culture

1. Cell line in which the gene of interest is expressed, that is, LNCaP (American Type Culture Collection).
2. T-Medium for LNCaP and other prostate lines ***(6)***. A 500-mL batch of medium is prepared from the following: 400 mL of D-MEM, low glucose (GIBCO, cat no. 430-1600EA), 100 mL of Kaighn's modification of F-12 medium (F-12K; GIBCO, cat no. 211227-014), and fetal bovine serum, charcoal/dextran treated (Hyclone, cat. no. A-1120), added to 5%, plus 1 mL of each of the following additives:
   a. Insulin (Sigma, cat no. I1882): a 10 mg/mL stock solution is made by the addition of 10 mL of acidified water (0.1 mL of glacial acetic acid) to 100 mg of insulin. This is stable for 1 yr at 2–8°C. Before use, dilute a 250-µL aliquot to 1 mL with 0.1% BSA/PBS to give a 500X solution (2.5 mg/mL). Alternatively, add 68 U (680 µL) per 500 mL of medium of human insulin (Humulin; 100 U/mL, Lilly) to a final concentration of 5 µg/mL.
   b. Tri-iodothyronine (T3; Sigma, cat. no. T6397 or T5516): a 20 µg/mL stock solution is prepared by dissolving 1 mg of T3 in 1 mL of 1 *N* NaOH and diluting to 50 mL with sterile water. Store frozen as aliquots. Before use, dilute to 1 µg/mL in 0.1% bovine serum albumin (BSA)/phosphate-buffered saline (PBS), and then add 68.25 µL to 10 mL in 0.1% BSA/PBS for 6.825 ng/mL solution to a final concentration of 13.65 pg/mL.
   c. Transferrin (Sigma, cat. no. T0519 or T5391): a 2.5 mg/mL stock solution is prepared in 0.1% BSA/PBS and stored frozen as 1-mL aliquots. This is stable for 30 d at 2–8°C. Final concentration should be 5 µg/mL.
   d. Biotin (Sigma, cat. no. B4639): prepare a 0.122 mg/mL stock solution by dissolving 1.22 mg in 10 mL of 0.1%BSA/PBS + four drops of 1 *N* NaOH. Final concentration should be 244 ng/mL.
   e. Adenine (Sigma, cat. no. A3259): dissolve at 12.5 mg/mL in 0.1% BSA/PBS. Final concentration should be 25 µg/mL.

### 2.4. Transfections

1. Polystyrene tubes, 15 mL.
2. DOTAP transfection agent (Boehringer Mannheim).
3. 20 m*M* HEPES buffer, pH 7.4, filter sterilized.
4. UV fluorescence microscope with 488 nm filter for visualization of GFP.
5. Six-well tissue culture plates or 35-mm tissue culture dishes.

## 3. Methods

### 3.1. Preparation of the Vector (see Notes 1–6)

1. 2 Plasmid pPSMEnTrap (2 μg) is digested with 30 U of *MfeI* in 50 μL of NEB Buffer 4 buffer for 3 h at 37°C.
2. Sodium acetate (3 *M*, 5 μL) is added, followed by 120 μL of ethanol; the suspension is mixed and held at –20°C for 30–60 min.
3. After centrifugation in a microfuge at 15,000*g* for 10 min at 4°C, the supernatant is removed, and the pellet air-dried and resuspended in 40 μL of CIP buffer.
4. Calf intestinal phosphatase (1 U) is added and the mixture incubated at 37°C for 1 h.
5. EDTA (250 m*M*, 1 μL) and 40 μL of phenol:chloroform (1:1) are added, and the mix vortexed vigorously for 30 s and centrifuged at 15,000*g* for 2 min at room temperature.
6. The supernatant is removed to a fresh tube and extracted twice with 500 μL of diethyl ether. After addition of the diethyl ether, the mixture is shaken vigorously for about 20 s, centrifuged at 13,000*g* for 20 s at room temperature, and the ether removed with a drawn-out Pasteur pipet.
7. The sample is loaded onto a 1% low melting point agarose gel and electrophoresed at 10 V/cm till the fast blue dye reaches the end of the gel.
8. The vector band is visualized by staining with crystal violet; the gel is soaked for 15 min in 0.25% crystal violet solution in 0.5X TAE buffer. After rinsing, the band is visualized on a light box.
9. The band is excised with minimal excess agarose and transferred to a preweighed tube.
10. The excised band is weighed, then dissolved in 3 vol of Mo Bio Ultra Salt solution, with thorough mixing.
11. The solution is incubated at 55°C for at least 5 min to completely melt the gel.
12. Mo Bio Ultra Bind resin (7 μL) is added, and the solution is incubated for 5 min at room temperature, mixing several times.
13. The suspension is centrifuged in a microfuge at 15,000*g* for 5 s at room temperature, and the supernatant discarded.
14. The pellet is resuspended in 1 mL of Mo Bio Ultra Wash, then again centrifuged at 15,000*g* for 5 s at room temperature, and the supernatant is discarded.
15. The supernatant is removed and the pellet again centrifuged at 15,000*g* for 5 s at room temperature. All traces of the Ultra Wash solution are removed by aspirating with a drawn-out Pasteur pipet.
16. TE (15 μL) is added, and the pellet is resuspended by pipetting up and down.
17. The solution is incubated at room temperature for 5 min and then centrifuged at 15,000*g* for 1 min at room temperature.
18. The DNA-containing supernatant is removed to a fresh tube, with care being taken to avoid any transference of the resin.

### 3.2. Preparation of Insert Fragments by Partial Digestion (see Notes 1–6)

1. Cosmid P1-683 DNA, 20 µg, is cut in a 200-µL reaction in NEB buffer 1 at 65°C with 10 U of *Tsp590*I.
2. At 5-min intervals, 40-µL aliquots of the reaction are removed and their digestion stopped by the addition of 2.5 µL of 250 m*M* EDTA.
3. The DNA is pooled and ethanol precipitated by the addition of 10 µL of 3 *M* sodium acetate and 450 µL of ethanol.
4. After 1 h at –20°C, the DNA is recovered by centrifugation at 15,000*g* for 20 min at 4°C.
5. After removal of the supernatant and air-drying, the DNA pellet is resuspended in 40 µL of TE.
6. Half of the digested DNA is electrophoresed slowly on a 1% agarose gel in TAE buffer alongside a DNA marker ladder.
7. The gel is stained for 15 min with 10 µg/mL ethidium bromide in TAE buffer and rinsed for 15 min in TAE buffer.
8. DNA is visualized with long wavelength (395 nm) UV light and the region of the gel migrating between 1 and 2 kb is excised and transferred to a weighed tube.
9. DNA is recovered using the Ultra Clean system (*see* **Subheading 3.1.**, **steps 10–18**).

### 3.3. Preparation of the Library (see Notes 7–13)

The approach to preparation and screening of the library is based on that used by Tashiro and colleagues ***(1,2)***.

1. Combine approx 50 ng of prepared vector with 50–100 ng of insert fragments, 1.5 µL of 10X T4 ligase buffer, 0.75 µL of 10 m*M* ATP, and 0.2 U of T4 DNA ligase in a 15-µL reaction.
2. Incubate at 4°C for at least 6 h.
3. Add 3 µg of tRNA, 1 µL of 3 *M* sodium acetate, and 40 µL of ethanol.
4. Hold at –20°C for at least 1 h, centrifuge at 15,000*g* for 10 min at 4°C and remove the supernatant.
5. Rinse the pellet with 50 µL of 70% ethanol and allow it to air-dry.
6. Resuspend the pellet in 10 µL of TE.
7. Aliquots (3.3 µL) of the ligation mix are mixed with 40 µL of competent cells and electoporated according to the electroporator manufacturer's instructions.
8. After culture at 37°C in SOC medium for 1 h, the transformation mixes are plated out in a series of dilutions on L Broth plates containing 100 µg/mL ampicillin and grown overnight at 37°C.
9. Up to 20 separate colonies are picked and assessed by standard miniprep methods to confirm the presence of inserts of the expected size, before large-scale library screening is undertaken. At least 75% of the plasmids should contain the inserts.

10. Colonies are picked onto LB agar plus ampicillin plates in 7 × 7 grids and also inoculated into 200 µL of L Broth plus 200 µg/mL ampicillin in microtiter trays.
11. Trays are sealed with air-permeable sealing tape and incubated at 37°C with shaking overnight.
12. For each grid set of 49 colonies, 60 µL of each culture is combined to give a total of 2940 µL to be processed for DNA isolation.
13. DNA is isolated from each pool using a Qiagen miniprep kit and following the manufacturer's protocols.
14. DNA is resuspended in 40 µL of TE by gentle pipetting.
15. DNA levels are quantified carefully by linearizing an aliquot of the plasmid preparation with *Not*I and electrophoresing on a 1% agarose gel in TAE buffer alongside mass standard DNA markers.

### 3.4. First Screening of fhe Library (see Notes 7–13)

1. On the day before transfection, LNCaP cells are plated at 30% confluency into 35 mm dishes and cultured overnight in T-medium.
2. For each DNA pool, 2.5 µg of DNA are adjusted to 25 µL with HEPES buffer in a 15-mL polystyrene tube.
3. Samples of control DNAs (2.5 µg), pPSMentrap (background control), and pCI-GFP (positive control) are also prepared as described in **step 2**.
4. A mix of DOTAP (15 µL per sample) and HEPES buffer (35 µL per sample) is prepared in a separate 15-mL polystyrene tube.
5. DOTAP mix (50 µL) is added to each of the DNA samples and contents mixed by flicking the tubes.
6. Mixes are let stand for 15 min at room temperature.
7. In the meantime, medium is removed from dishes of LNCaP cells and replaced with 1 mL of T-medium containing 5% charcoal-stripped FCS.
8. After a 15-min incubation, 1 mL of complete T-medium is added to each DNA/DOTAP mix and the solution transferred to a dish of cells (giving a total of 2 mL of medium per dish).
9. Dishes are incubated without changing the medium and examined at 24, 48, and 72 h for GFP expression under a fluorescence microscope.
10. Positive pools are identified by the greater number and intensity of fluorescing cells in comparison with the promoter alone transfection (*see* **Fig. 2**).

### 3.5. Second and Final Transfection Screenings of Library (see Notes 12 and 13)

1. Positive pools of colonies are re-inoculated as 7 × 7 matrices in microtiter plates and grown as described (*see* **Subheading 3.3.**).
2. For each matrix, 150 µL of cultures from each row are pooled (1050 mL) for DNA preparation, and likewise for each of the seven columns. Thus, each individual clone is represented in two DNA preparations (one row and one column).
3. DNA from each pool is prepared and quantified as described (*see* **Subheading 3.3.**).
4. The pools are transfected into LNCaP cells as described (*see* **Subheading 3.4.**).

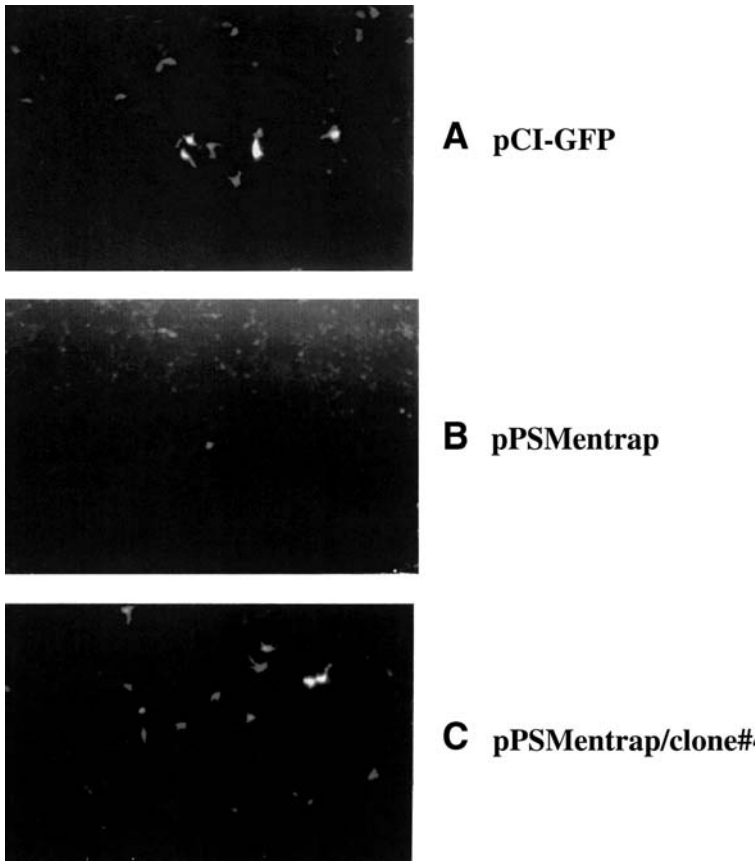


Fig. 2. Fluorescence microscopy of transfected cells. Cells were visualized 72 h after transfection. **(A)** Cells transfected with the positive control pCI-GFP; **(B)** cells transfected with the empty pPSMentrap vector; **(C)** cells transfected with pPSMentrap containing cloned insert #4.

5. Potential positive individual clones are identified from the rows and columns of pooled DNAs that gave positive signals (e.g., Row 2, Column 5).
6. Candidate individual clones are then regrown as 1-mL cultures, DNA is isolated, and transfection performed, as described previously (*see* **Subheadings 3.3.** and **3.4.**).

Once purified, inserts in clones can be studied by a variety of means ***(5)***. Restriction analysis and sequence data allow definition and localization of the enhancer region. The enhancer trap clones can be used directly for transfections into other cell types to examine specificity of action or the enhancer with or without promoter can be recloned into other vectors (e.g., luciferase-expressing) to allow more quantitative studies of enhancer function.

## 4. Notes

1. Cloning of *Tsp509*I ((AATT) partial restriction products into *Mfe*I-cut (G(AATTC) pPSMentrap is described. *Sau3A*I partial digestion products may be cloned into the *Bgl*II site in the polylinker and a variety of six-base cutter enzyme fragments into other polylinker sites.
2. Before library construction, the vector preparation should be evaluated by transforming (1) vector alone, (2) vector alone, religated, and (3) vector ligated with a suitable restriction fragment, e.g., a 1–2-kb *EcoR*I fragment. At least a fivefold increase in colony numbers should be seen with an insert fragment, and there should be no increase in colony numbers after religation of the phosphatase-treated vector alone.
3. For cloning of enhancers from other genes, trap vectors incorporating the gene's promoter may be prepared by replacement of the PSM 1 kb promoter region. The vector pTINentrap (*see* **Fig. 1**) with a minimal promoter that contains only sequences encompassing the TATA box and initiation region of transcription can be used for cloning enhancers from any gene. However, it needs to be recognized that some enhancers will not activate transcription from heterologous promoters and may not be identified by this approach.
4. Partial digestion using enzymes with 4-base recognition sequences provides for an optimal random cloning of all regions of the cosmid. Because the frequency of sites will vary across the sequence it is important to pool digests from different time points. Regions with more cutting sites will be present at higher levels in less digested DNA and regions with less frequent cut sites will be better represented at later digestion times.
5. Most enhancer regions are contained within 1 kb, so selecting a size range of 1 to 2 kb for cloning makes it likely that some inserts will contain the entire enhancer region. If enhancer sequences are spread over a larger distance, shorter regions may still provide partial activity and be detected.
6. Pilot studies of partial restriction enzyme digestion conditions should be conducted prior to preparative-scale digestions.
7. Although a higher ratio of insert fragments to vector may increase the yield of colonies, it will also increase the proportion of plasmids with double inserts—confounding mapping and localization of the inserts.
8. After taking aliquots of cultures for DNA preparation, remaining cultures can be stored by addition of an equal volume of 30% glycerol in LB broth, snap-freezing with liquid nitrogen or in an ethanol/dry ice bath before transferring to a –70°C freezer.
9. Screening of individual colonies should demonstrate that they contain inserts of appropriate size. More colonies can be surveyed by pooling a number (up to five or six) similar-sized colonies in each culture tube. A series of insert bands should be detected. Because enhancer fragments are often unstable, deletion products could appear and it may be hard to eliminate them. In such cases, one can still proceed with the screening, but culture growth should be kept to a minimum. Screening can still be successful as long as a significant fraction of intact insert remains.

10. For PSM enhancer screening, media depleted in steroids (charcoal/dextran-treated fetal bovine serum) was used because expression of the endogenous *PSM* gene is repressed by androgen. For other genes, appropriate culture conditions that provide optimal expression of the endogenous gene should be chosen. Similarly transfection reagents and conditions should be those that have been optimized for the cell line being used.
11. When identifying candidate positive DNA pools, both the range of fluorescence intensity and number of fluorescing cells should be compared with the promoter-alone control as well as the positive, GFP-expressing control. With pools of 49 clones, even a small number of brightly fluorescing cells can be indicative of a positive clone.
12. It is better to conduct second and third screenings within minimum time, e.g., 1 to 2 wk. This minimizes the loss of viability of bacterial cultures. The frequency of strongly fluorescing clones should increase on the second and third screenings.
13. Although we describe detection of positive clones by microscopic visualization, other approaches are possible. If background expression from the promoter alone Trap vector is sufficiently low, detection of GFP expression in a suitable fluorescent plate reader is possible. Also, use of a fluorescently activated cell sorter should allow detection and isolation of transfected cells showing enhanced GFP expression. Plasmid DNA can be recovered from harvested cells and retransformed into bacteria to isolate candidate clones.

## References

1. Tashiro, K., Tada, H., Heilker, R., Shirozu, M., Nakano, T., and Honjo, T. (1993) Signal Sequence Trap: A cloning strategy for secreted proteins and Type I membrane proteins. *Science* **261,** 600–603.
2. Tashiro, K., Nakano, T., and Honjo, T. (1996) Signal sequence trap, in *Methods in Molecular Biology*, *Vol 69: cDNA Library Protocols* (Cowell, I. G. and Austin, C. A., eds.) Humana, Totowa, NJ, pp. 203–219.
3. Hill, D. P. and Wurst, W. (1993) Gene and enhancer trapping: Mutagenic strategies for developmental studies. *Curr. Topics Devel. Biol.* **28,** 181–206.
4. O'Keefe, D. S., Su, S. L., Bacich, D. J., Horiguchi, Y., Luo, Y., Powell, C. T., et al. (1998) Mapping, genomic organization and promoter analysis of the human prostate-specific membrane antigen gene. *Biochim. Biophys. Acta* **1443,** 113–127.
5. Watt, F., Martorana, A., Brookes, D. E., Ho, T., Kingsley, E., O'Keefe, D. S., et al. (2001) A Tissue-specific enhancer of the prostate-specific membrane antigen gene, FOLH1. *Genomics* **73,** 243–254.
6. Thalmann, G. N., Sikes, R. A., Chang, S-M., Johnston, D. A., von Eschenbach, A. C., and Chung, L. W. K. (1996) Suramin-induced decrease in prostate-specific antigen expression with no effect on tumor growth in the LNCaP model of human prostate cancer. *J. Natl. Cancer Inst.* **88,** 794–801.

# 20

# Targeted Alpha Therapy of Prostate Cancer

**Barry J. Allen, Yong Li, Syed M. A. Rizvi, and Pamela J. Russell**

## 1. Introduction

Prostate cancer (PC) is now the second most common cause of death from cancer in men after lung cancer ***(1)***. Brachytherapy, prostatectomy, or external beam radiation can effect a cure, with a life expectancy of at least 10 yr at diagnosis ***(2)***. Survival depends on the disease being organ confined, specimen confined, or margin positive, with failure rates of 12, 30, and 60%, respectively. Despite aggressive therapy, a significant percentage of men will die of disseminated disease ***(3)***. Moreover, radical therapy can have distressing side effects. ranging from surgical mortality, incontinence, impotence, bowel damage, and stricture ***(4)***.

Currently, there are no means to inhibit the development of metastases that eventually cause the death of the patient. PC grows slowly, and early dissemination of cancer cells may occur before the disease becomes clinically apparent. Because it is hard to identify those early-stage PCs that will become metastatic, many patients receive unnecessary radical therapy, often causing an unacceptably poor quality of life ***(3)***. Cytotoxic chemotherapy is poorly tolerated by patients with PC, and systemic therapy of metastatic disease is limited to androgen deprivation, in which objective tumor regression is seen in only 2–3% of patients. Almost inevitably, an androgen-independent disease will appear, with median time to progression of 12–18 mo and median survival of only 1 yr ***(5)***. Endocrine therapy is palliative, improving the quality of life but not extending life. Bone-seeking radiopharmaceuticals, such as Strontium-89 ($^{89}$Sr) and Samarium-153 ($^{153}$Sm), that exchange with the calcium component of hydroxyapatite and concentrate in osteoblastic lesions provide palliation in 75–80% of hormone-refractory patients ***(6)***. A new therapy is urgently needed to kill cancer cells in transit or at the preangiogenic stage. We

From: *Methods in Molecular Medicine, Vol. 81: Prostate Cancer Methods and Protocols*
Edited by: P. J. Russell, P. Jackson, and E. A. Kingsley © Humana Press Inc., Totowa, NJ

propose that alpha-emitting radioisotopes that are targeted to PC cells have the potential to control such subclinical disease and so inhibit the development of metastatic PC.

### 1.1. Alpha Radiation

#### 1.1.1. Properties

Alpha-emitting radionuclides ***(7)*** emit alpha particles with energies up to an order of magnitude greater than most betas rays. However, their ranges are two orders of magnitude less because alpha particles have a linear energy transfer (LET) around 100 times greater than that for beta rays. This results in a high relative biological effectiveness (RBE). Accordingly, a greater fraction of the total energy is deposited in cells with alphas and a few nuclear hits can kill a cell ***(8)***. Thus, 100-fold enhancement in radiation dose ***(9,10)*** could be delivered to the nucleus of a cancer cell if a smart carrier were employed to take the alpha-radionuclide to that cancer cell.

Studies using Astatine-211 ($^{211}$At) and Bismuth-212 ($^{212}$Bi) ***(11,12)*** have provided encouraging results. Being a lanthanide, Terbium-149 $^{149}$Tb) could be a preferred alpha source ***(7),*** but the 15% alpha branching ratio means that only one in six decays will be effective. Astatine-211 is a pseudo-halide and can label carriers directly, as in methylene blue. However, stability with larger molecules is inadequate and chelation with monoclonal antibodies (MAbs) is preferred. Cytotoxicity and microdosimetry of $^{211}$At-chimeric MAbs against human glioma and melanoma cells showed that cell killing required an average of only one to two alpha particle hits to the cell nucleus ***(13)***. Bismuth-213 can be produced from an Actinium-225 ($^{225}$Ac) generator, and this approach to targeted alpha therapy (TAT) was pioneered by the Memorial Sloan Kettering group ***(14)***.

The evidence for TAT has been previously reviewed ***(15)*** and in more recent studies, the Sydney group has produced alpha conjugates (ACs) for melanoma ***(16,17)***, leukaemia ***(18),*** colorectal ***(19),*** breast ***(20,21),*** and prostate ***(22,23)*** cancers. In addition, our group has been successful in producing the alpha-emitting $^{149}$149Tb (EC, $\beta^+$, $\alpha$, $t_{1/2}$ = 4.1 h) using the isotope separator facility ISOLDE at CERN, Geneva, Switzerland, by the on-line mass separation of the spallation reaction products of 1 GeV pulsed proton beam onto a Ta target ***(24)***. A positron emitter, $^{152}$Tb, as an analogue to $^{149}$Tb, was produced at the National Tandem Accelerator, Australia National University (ANU) at Canberra, Australia, using the $^{nat}$Nd($^{12}$C,xn) reaction ***(25–27)***. Comparative properties of alpha-emitting radioisotopes are given in **Table 1**.

**Table 1**
**Alpha-Emitting Radioisotopes**

| Radio-isotope | Reference | Energy (MeV) | Half-life | Percent alpha decay | Chelator required | Application |
|---|---|---|---|---|---|---|
| Tb149 | ***7*** | 4 | 4 h | 15 | y | MAb |
| At211 | ***39*** | 5.98, 7.45 | 7.21 h | 41.8, 58.2 | n<br>y | MTB<br>MAb |
| Bi212 | ***33*** | 8.79 | 60 min | 100 | y | MAb |
| Bi213 | ***14,20,21*** | 8.35 | 46 min | 98 | y | MAb, PAI2 |
| Ac225 | ***83,84*** | 5.8, 6.3, 6.8, 8.35 | 10 d | 400 | y | MAb |

MTB, methylene blue; PAI2, plasminogen activator inhibitor; MAb, monoclonal antibody.

### *1.2. Production of Radioisotopes*

#### *1.2.1. Astatine-211*

Astatine-211 was first produced in 1940 at the new Berkeley cyclotron ***(28)*** by the $^{209}Bi(\alpha,2n)^{211}At$, still the major route of production. Yields of 41 MBq/μAh (1.1 mCi/μAh) have been reported ***(29)***, allowing production runs of 2000 MBq (54 mCi) with an internal target. Care must be taken to minimize production of the 8.3 d $^{210}At$, which then decays to the 138-d alpha emitter, Polonium-210 ($^{210}Po$). Avoidance of this undesirable source of radiation can be achieved by limiting the alpha-bombarding energy to a maximum value of 28 MeV. As there is no stable or long-lived analogue of astatine to serve as a carrier, all chemical work must be performed at the tracer level. For example, the concentration of $^{211}At$ in 1 mL of a solution with 15 MBq activity (400 μCi) is only $10^{-9}$ *M* or 0.02 ppb.

Weinreich ***(30)*** has reviewed successful therapeutic strategies that use $^{211}At$; these include intravascular therapy, radioimmunotherapy, and metabolic trapping of astinated metabolites to inhibit the growth of various cancers in in vivo models. As of 1990, only one patient had been treated using $^{211}At$ ***(31)***, for incurable recurrent carcinoma of the tongue. Complete tumor remission was observed in the region supplied by the lingual artery, with no observed side effects or adverse reactions. However, a clinical trial of TAT of cystic glioma is current at Duke University ***(32)***.

#### *1.2.2. Terbium-149*

Unlike $^{211}At$, $^{149}Tb$ has the advantage that there are many radiolanthanides with similar properties, and the long-lived isotope $^{152}Tb$ (17.5 h) has identical

chemical properties. The beta-emitting radioisotope $^{153}$Sm (commercially available) and $^{152}$Tb can be used as benchmarks to develop techniques. Terbium-152 is also a strong positron emitter, allowing pharmacokinetic studies. Terbium-149 was produced for experimental use using a 12 MV tandem accelerator *(27),* and together with the ISOLDE group at CERN, Geneva, in quantities sufficient for clinical use *(27)*. In addition, $^{152}$Tb is used to produce positron emission tomography images with a phantom. Terbium-149 has advantages from the dosimetry and safety aspect. Only $^{149}$Tb has a gamma ray emission comparable to Technicium-99m ($^{99m}$Tc) (140 keV) for which the collimators of gamma cameras are optimized in nuclear medicine.

Saturated yields of up to 70 μCi of $^{149}$Tb using the Praseodymium-141 reaction at 70 MeV [$^{141}$Pr($^{12}$C, 4n)$^{149}$Tb] on a 10 MV tandem accelerator and 240 μCi can be obtained with the Neodymium-142 reaction to produce Dysprosium-149, which beta decays to Tb-149 [$^{142}$Nd(12C, 5n)$^{149}$Dy->$^{149}$Tb at 90-100 MeV *(27)*. If a natural Nd target is used, then $^{152}$Tb is produced abundantly. This decays by positron emission with energies up to 2.8 MeV. However, this isotope cannot be separated from $^{149}$Tb without a mass spectrometer, causing competition for receptor sites with $^{149}$Tb-AC. These activities are ample for in vitro experiments and should allow many in vivo studies; they have allowed the initial separation and purification of products and synthesis of the $^{152}$Tb-AC.

Production of 0.5 GBq (15 mCi) of $^{149}$Tb has been achieved at the ISOLDE facility at the CERN spallation source, being sufficient for patient treatments. Two microamp of 1 GeV protons from the synchrocyclotron bombarded a tantalum foil 122 g cm$^{-2}$. Reaction products were ionized and accelerated from the source by means of a 60 kV potential. The 149 mass component was separated in a magnetic field and deposited for 75 min on an aluminium foil.

### *1.2.3. Actinium-225*

Actinium-225 can be produced by proton, neutron, and deuteron reactions or by spallation. A high yield is obtained with 20 to 30 MeV deuterons on a Radium-226 ($^{226}$Ra) target by the reaction $^{226}$Ra(d,3n)$^{225}$Ac. Actinium-226 is also produced by the (d,2n) reaction, but its short half-life of 29 h allows purification of the Actinium fraction to yield nearly pure $^{225}$Ac. The fission cross section from the deuteron reaction is small and contamination by fission products is not expected to be a problem. Other reactions that need to be examined are protons on Thorium-232 ($^{232}$Th) to yield Protactinium-229 ($^{229}$Pa), which decays by alpha emission to $^{225}$Ac [$^{232}$Th(p,4n)$^{229}$Pa(α)$^{225}$Ac] and $^{226}$Ra(n,2n) $^{225}$Ac. Our group produced the first accelerator spallation production of the Ac-Bi generator at the CERN GeV spallation source at Geneva, and $^{225}$Ac was shipped to Sydney, where $^{213}$Bi was eluted, opening up the possibility of developing another supply channel for this generator.

### *1.2.4. Generators*

The US Department of Energy at Oak Ridge, Tennessee, separates Thorium-229 ($^{229}$Th) from waste products of the Cold War $^{233}$Th enrichment program for nuclear submarine reactor fuel, but the quantity available is limited and may not be sufficient for extensive, future clinical applications. TAT has progressed slowly because of, *inter alia*, the difficulty in obtaining adequate activities and a regular supply of the alpha emitter at the appropriate research laboratory. The supply problem can now be overcome by using a generator where a long-lived parent isotope decays to the short-lived alpha-emitting daughter, which can then be used for alpha therapy. The $^{224}$Ra:$^{212}$Pb/$^{212}$Bi generator (Argonne National Laboratory, Chicago) used by Horak and colleagues ***(33)*** suffered from two problems: (1) the long-lived parent $^{224}$Ra can cause disposal problems; (2) the generator is contaminated with $^{212}$Pb, a beta emitter, and $^{212}$Bi (obtained by decay of $^{212}$Pb) itself emits betas. These beta emissions reduce the therapeutic ratio for TAT because the betas may cause collateral damage to critical healthy cells without increasing cytotoxicity for isolated or preangiogenic cells.

A second generator that does not suffer from disposal problems arising from long-lived radioisotopes is the $^{225}$Ac (10 d): $^{213}$Bi (46 min) generator. Bismuth-213 is suitable for TAT because of its characteristic nuclear, physical, and chemical properties. It has a half-life of 45.6 m and emits a 1.96 MeV beta to decay to $^{213}$Po, which instantly decays with the emission of an 8.35 MeV alpha. A gamma ray at 440 keV is emitted at 27% fractional abundance.

The USDOE now supplies Ac:Bi generators as Ac-nitrate in 0.1 *M* nitric acid, with activity $6 \times 10^4$ Ci/g, at more than 10 mCi/mL concentration. Purity is >98% $^{225}$Ac with <2% $^{225}$Ra. The Ac is supplied in a glass screw cap bottle in a nonreturnable container, with activity up to 20 to 30 mCi. The alpha particle-emitting radionuclide, $^{213}$Bi, can be produced from such a $^{225}$Ac/$^{213}$Bi generator column, being eluted with 250 μL of freshly prepared 0.15 *M* distilled and stabilized hydriodic acid followed by washing with 250 μL water. Two hours are allowed for $^{213}$Bi to grow back in the generator for the next elution. The availability of the Ac:Bi generator, either from the United States or accelerator-produced, opens up a new technology that makes possible targeted alpha therapy for clinical trials around the world. McDevitt and colleagues ***(34)*** have studied and developed this generator concept in detail.

## *1.3. Targeting*

TAT requires that the radioisotope be carried specifically to cancer cells while avoiding normal tissues. This can theoretically be achieved by radiolabeling molecules, such as ligands, antibodies, or inhibitors, that bind to target

molecules expressed in high concentration on the surface of tumor cells. We describe here the use of two targeting agents, the MAb J591, against the external domain of the prostate-specific membrane antigen (PSMA), and PAI-2, a natural protein inhibitor of urokinase plasminogen activator (uPA), that binds to uPA bound to the surface receptor uPAR on prostate cancer cells. Each targeting molecule requires a bifunctional chelator that reacts both with the carrier molecule and the radioisotope.

### 1.3.1. Monoclonal Antibody, J591

PSMA is 750-amino acid, type 2 transmembrane glycoprotein expressed on the surface of prostate epithelial cells, first identified on the prostate cell line, LNCaP, by the MAb 7E11C5, that binds to an internal epitope of the antigen. Indium-111 ($^{111}$In)-labeled 7E11C5 antibody has been successfully used for in vivo imaging of occult prostate cancer lesions using the ProstaScint™ scan (Cytogen, Princeton, NJ) ***(35)***. Two forms of PSMA exist: a truncated form (PSM′) found intracellularly in normal prostate epithelial cells and the transmembrane form expressed at higher levels in PC ***(36)***. Because of its enzyme activities ***(37),*** PSMA is now known as folate hydrolase 1 (FOLH1). Expression is seen in most PCs and metastatic lesions ***(38–41),*** is present in PC in the absence of androgen ***(38),*** and is elevated during androgen-deprivation therapy ***(39)***. Weak expression occurs in brain, salivary gland, and small intestine ***(36,38,42,43)***. J591, one of several MAbs ***(44)*** against PSMA, was prepared from BALB/c mice immunized with LNCaP cells ***(41)***; it detects two distinct extracellular epitopes of PSMA (PSMAext1 and PSMAext2), can bind viable PSMA-expressing cells, and reveals the presence of PSMA in the neovasculature of various malignant neoplasms, but not in normal vasculature ***(40,41)***. PSMA peptides also have been used in immunotherapeutic Phase I and II clinical trials for prostate cancer ***(45,46)***. Thus, J591 MAb is a promising antibody for targeting treatment to metastatic prostate cancer.

### 1.3.2. PAI-2

The plasminogen activator system is important in tumor growth and metastasis ***(47–49)***. Both in vitro and in vivo, uPA is mitogenic, mediates pericellular proteolysis promoting tumor cell invasion, and enhances angiogenesis. Bound to its specific cell surface receptor, uPA converts inactive plasminogen into the active serine protease, plasmin, that cleaves extracellular matrix components including laminin, fibronectin, and collagen ***(50,51)***. uPA activity is regulated by plasminogen activator inhibitors type 1 and 2 (PAI-1 and PAI-2) ***(49,52)***. Clinical studies have demonstrated that high levels of uPA ***(53,54),*** PAI-1

***(55,56),*** and receptors for uPA, uPAR ***(57–59)*** are associated with poor prognosis in some human cancers whereas high levels of PAI-2 are associated with a favorable prognosis in cancer patients ***(60–62)***. Others have shown the opposite or no effect.

PAI-2 is a serine protease inhibitor that forms SDS-stable 1:1 complexes with uPA ***(52)***. Cell surface-bound uPA is thought to be accessible to PAI-2 that can inhibit cancer cell invasion and metastasis ***(52,63)***. Pharmacokinetic and biodistribution studies of human recombinant Iodine-125 ($^{125}$I)-labeled PAI-2 in control and test nude mice bearing human colon cancer (uPA-positive HCT 116 cell line) xenografts ***(63)*** have shown that $^{125}$I-PAI-2 localizes in 0.5 cm$^3$ tumor xenografts and clears more quickly from major organs than from tumors. Using $^{213}$Bi-PAI-2 conjugates, our group has successfully targeted breast cancer in vitro ***(20,21)*** and in vivo ***(20)***. Low-dose $^{213}$Bi-PAI-2 therapy prevented breast cancer metastasis whereas the tolerance dose in nude mice was found to be 6 mCi/kg for iv injection). Li and colleagues ***(23)*** have also shown that PAI-2 binds to PC-3 human PC cells in vitro and in vivo, providing a potential target for TAT.

### *1.3.3. Chelation*

Bismuth-213 can be chelated to MAbs and proteins using linking agents such as diethylenetriaminepentacetic acid (DTPA), 1,4,7,10-tetraazacyclododecane-*N*,*N*′,*N*″,*N*‴-tetracetic acid (DOTA), and 1,4,8,11-tetraazacyclotetradecane—*N*,*N*′,*N*″,*N*‴-tetracetic acid ***(13,33,64,65)***.

Because of their short life times, stability requirements for the ACs are not as limiting as those for the long-lived beta immunoconjugates, and long preparation times are not useful. Hence, derivatives of DTPA are currently most often used.

The radiolabel required for TAT must be attached to the delivery molecule by use of a bifunctional chelate. The methods we used for preparation and attachment of the chelates to J591 and PAI-2 are described here.

## 2. Materials

### *2.1. Antibodies*

For our studies, $IgG_1$ J591 MAb was provided by BZL Biologics. An isotype control MAb, anti-MOPC (A2), was provided by the Department of Microbiology, University of New South Wales. Rabbit anti-mouse IgG conjugated to horseradish peroxidase was purchased from Dakopatts (Glostrup, Denmark); goat anti-mouse fluorescein isothiocyanate conjugated MAb from Silenus (Sydney, NSW, Australia), and anti-Ki67 mouse MAb (clone MIB1) from Immunotech SA (France).

## 3. Methods

### 3.1. Conjugation of Bifunctional Chelate to Antibodies

1. The labeling procedure for antibodies was that used by Rizvi and colleagues ***(16)***.
2. Prepare and sterilize buffers: 0.5 *M* sodium acetate, pH 5.5, for purification of conjugate and for instant thin-layer chromatography (ITLC) and phosphate-buffered saline (PBS), pH 7.0, for purification of the labeled conjugate.
3. Prepare the chelator, cyclic anhydride of diethylenetriaminepentacetic acid (DTPA; Aldrich Chemical Company) in a concentration of 1 mg/mL in chloroform and purified under a stream of nitrogen.
4. Mix chelator:antibody (test or control) at a molar ratio of 20 (cDTPA):1(J591 [$IgG_1$] and incubate on ice for 45 min.
5. Measure the conjugated MAb by using the Bio-Rad DC Protein Assay Reagent Kit on a Bio-Rad Model 550 Plate Reader, and purify on a PD10 column (Pharmacia Biotech) according to the manufacturer's instructions, using 0.5 *M* sodium acetate at pH 5.5 as the eluting buffer.
6. After a 20-min incubation, the labeled antibody is again purified on another PD-10 column using PBS at pH 7.0 as the eluting buffer.
7. The conjugates so obtained are then tested for radiolabeling efficiency by ITLC using Gelman paper (strip size $1 \times 9$ cm) and 0.5 *M* sodium acetate, pH 5.5, as the solvent. Cut the strip into sections and assess using a gamma counter to give the percentage of activity at the origin; which is the labeling efficiency.

### 3.2. Conjugation of Bifunctional Chelate to PAI-2

1. cDTPA is conjugated to PAI-2 and bovine serum albumin according to the method described by Ranson and colleagues ***(21)***.
2. The concentration of cDTPA-labeled PAI-2 is assessed by the BIORAD DC Protein Assay Reagent Kit.
3. The binding activity of cDTPA-labeled PAI-2 is examined for its ability to form complexes after a 30-min incubation with equimolar amounts of active human uPA at room temperature ***(63)*** and by activity assays as described ***(21)***.
4. The uPA/conjugated PAI-2 complexes are detected by SDS-PAGE (12% nonreducing gel) (*see* **Fig. 1**). Standard curves are constructed using uPA.
5. Typical labeling results are shown for PAI-2 (*see* **Fig. 2**), where labeled MAb is found at the origin and free $^{213}Bi$ at the solvent front. A labeling efficiency of 92% was obtained for alpha-J591 and 75–90% for alpha-PAI-2.

### 3.3. In Vitro Studies

To determine the effects of TAT, a series of in vitro tests need to be performed. These include determining the antigen status of the cell lines to be targeted (by immunohistochemistry and flow cytometry), stability of the ACs, whether the labeling of the carrier molecule interferes with its ability to bind to its target, whether killing of cells is affected by incubation with specific, but not with nonspecific ACs, and methodology to determine the mechanism

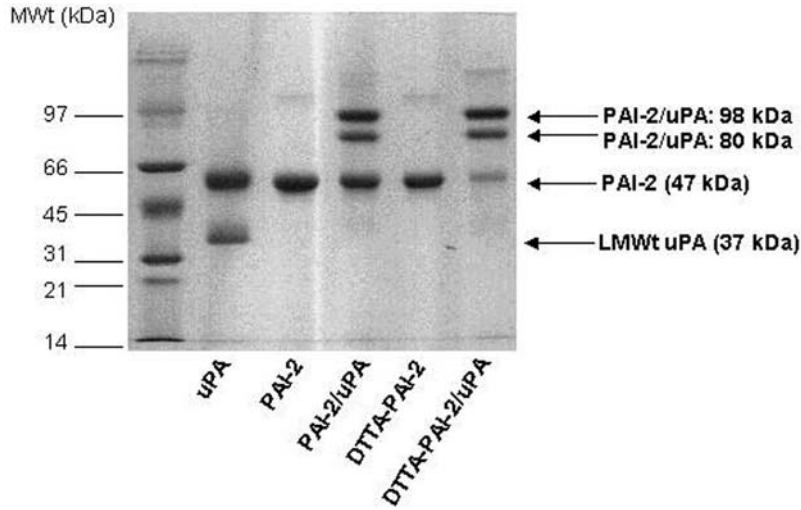


Fig. 1. Coomassie-stained 12% SDS-polyacrylamide gel electrophoresis (PAGE) showing complex formation between high and low molecular weight tc-uPA and PAI-2 or cDTPA-PAI-2. Complexes were formed by incubating either labeled or unlabeled PAI-2 with equimolar amounts of tc-uPA for 1.5 h at 37°C. The reaction was terminated by adding 5X nonreducing SDS-PAGE sample buffer (20% v/v) to the reaction mix. LMWt corresponds to low molecular weight uPA that retains enzymatic activity of native uPA.

of cell killing. Several methods to provide answers to these questions are outlined below, together with some experimental data that have been obtained when these methods were used with the J591 MAb or with PAI-2 as targeting moieties.

### *3.3.1. Cell Lines*

The LNCaP-LN-3 (designated LN-3) human PC cell line (obtained from C. Pettaway, MD Anderson Hospital, Houston, TX ***(66)*** was used for targeting with the J591 antibody. It is an androgen-sensitive, highly metastatic line, established from LNCaP cells ***(67)*** that retains expression of prostate-specific antigen ***(68),*** PSMA ***(38),*** and a mutated androgen receptor ***(69)***. Androgen-independent human PC-3 cells were used for targeting of PAI-2. LN-3 cells and PC-3 cells were maintained under standard conditions with 10% (v/v) heated-inactivated fetal bovine serum in a humidified atmosphere of 5% $CO_2$ at 37°C. The cultures were fed twice weekly, and passaged when preconfluent using 0.05% trypsin/0.02% EDTA (Life Technologies, Inc., Grand Island, NY). Cells were mycoplasma free.

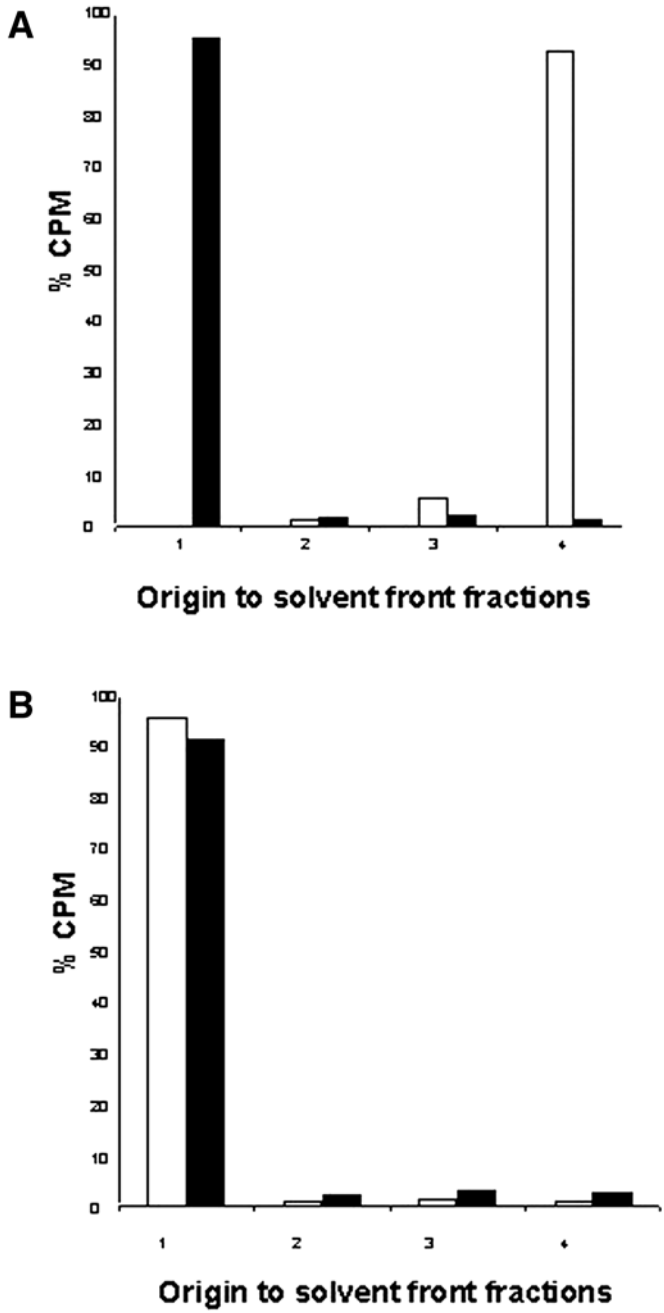


Fig. 2. Analysis of $^{213}$Bi-PAI-2 (α-PAI-2). **(A)** Aliquots (10 mL) of freshly eluted alpha-PAI-2 (filled bars) or $^{213}$Bi standard (unfilled bars) were spotted onto the origin of separate ITLC strips. After mobilization, the strips were cut into four pieces for gamma counting. Fraction 1 corresponds to the sample origin whereas fraction four corresponds to the solvent front. **(B)** Serum stability of α-PAI-2 incubated at 37°C in human serum for 0 min (unfilled bars) and 45 min (filled bars) and subjected to ITLC and analyzed as per (A).

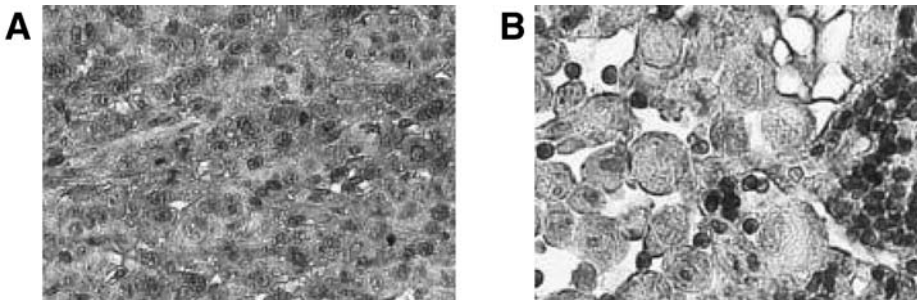


Fig. 3. Immunohistochemistry shows uPA expression in PC-3 xenografts and metastatic lymph nodes. PC-3 tumor xenograft cancer cells are strongly positive for uPA **(A)**; cancer cells from metastatic lymph nodes are positive for uPA (large cells, black color) whereas lymphocytes are negative for uPA (small cells, dark gray color) **(B)**. The sections were from different mice. (A): magnification ~× 200; (B): magnification ~×400.

### *3.3.2. Specificity*

Cell surface expression of FOLH1 on LN-3 cells and PAI-2 on PC-3 cells was assessed by flow cytometry and immunohistochemistry of cultured cells and/or xenograft tissues ***(70)*** using standard methodologies.

Some 95% of cultured PC-3 cells expressed uPA and were positive for the uPA MAb. Staining of tissues revealed strong uPA staining of cancer cells in the xenografts and in lymph node metastases (*see* **Fig. 3A,B**), but not in other organs. LN-3 cells stained strongly with J591, whereas the isotype control gave negative results (*see* **Fig. 4A,B**).

The flow cytometry assay is undertaken to determine whether the labeling process interferes with the binding characteristics of the protein. Similar high-fluorescence levels were observed when labeled and unlabeled proteins were used, indicating that the labeling did not interfere with the immunoreactivity of the preparations.

### *3.3.3. Stability*

1. Serum stability test: To estimate stability, the ACs were incubated with fresh human serum at 37°C for various times from 0 to 2 h for $^{213}$Bi-MAb. The percentage leaching/stability was calculated as a function of time.
2. DTPA challenge: Labeling may be specific or nonspecific, the latter being less stable. This was assessed by using DTPA to strip the nonspecific label from the protein. Three different concentrations of DTPA (1 µmol, 10 µmol, and 100 µmol) were incubated with the unchelated, labeled antibody, or with the AC for 0.5 and 1 h at 37°C and then analyzed by ITLC to determine specific and nonspecific labeling of the antibody.

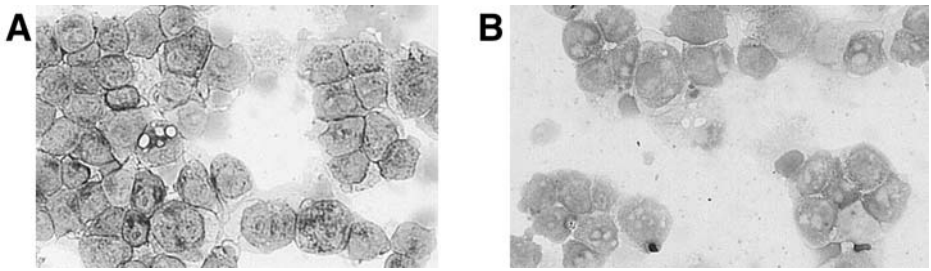


Fig. 4. Immunocytochemistry shows that LN-3 cells are strongly positive to J591 MAb **(A)** whereas the cells are negative to isotype control MAb **(B)**. Magnification ~×200.

### *3.3.4. In Vitro Cytotoxicity*

The cytotoxicity of ACs on prostate cancer cell growth was tested in vitro after treatment with cancer-specific or nonspecific ACs. Cell survival can be assessed by an established cytotoxicity assay, such as a clonogenic assay in agarose, MTT or MTS. We used the MTS assay ***(71)*** because it provides adequate accuracy, yet is faster and less costly in terms of operator time and consumables.

Briefly, after 48-h culture, cells are washed in PBS, harvested with 0.25% trypsin/0.02% EDTA, and diluted into 96-well plates at $2 \times 10^4$ cells/100 µL in RPMI-1640 plus 5% fetal bovine serum. To ensure equal activities, specific and nonspecific ACs are checked by radiation dose calibrator and set to the Gold-198 (198Au) setting for a gamma ray energy of 412 keV, compared with the 440 keV gamma ray emitted by Bi-213. The conjugate solutions are neutralized to pH 7.0, and four doses of specific and nonspecific AC are incubated with the cells overnight in 5% $CO_2$ in air at 37°C. As the half-life of $^{213}$Bi is only 46 min, the effective incubation period is ~2 h. After changing the medium in the wells to 100 µL of serum-free, phenol red-free RPMI-1640, 20 µL of Cell Titer 96 Aqueous One Solution reagent (Promega, WI) is added to each well and incubated for 3 h at 37°C followed by the addition of 10% sodium dodecyl sulphate (SDS) to stop the reaction. The absorbance of each well at 490 nm is measured using a plate reader. The absorbance reflects the number of surviving cells/well that retain metabolic activity. All results were analyzed using Prism software.

Both the alpha-J591 and alpha-PAI-2 were highly cytotoxic in vitro to LN-3 and PC-3 cells, respectively, in an activity concentration dependent fashion. For LN-3 cells, the 37% cell survival value $D^0 = 4.1 \pm 0.2$ µCi whereas control ACs showed negligible effects (*see* **Fig. 5A**). At the maximum dose of 10 µCi,

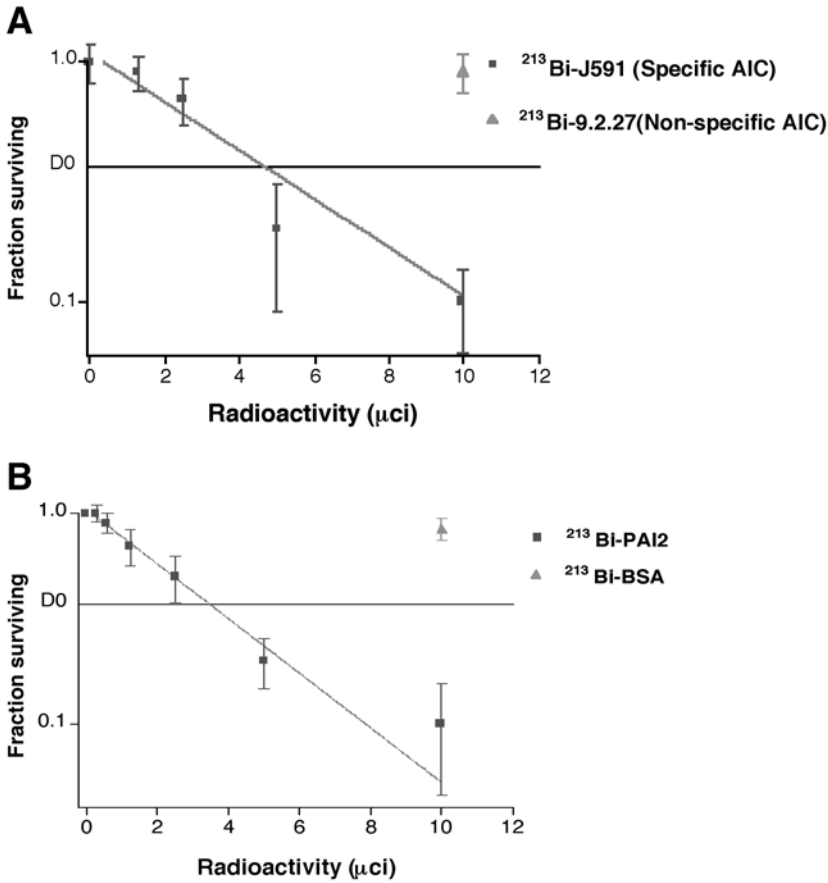


Fig. 5. Representative cytotoxicity study of **(A)** LN-3 and **(B)** PC-3 prostate cancer cells. 20,000 cells were seeded in 0.3-mL medium. Cells were treated with varying concentrations of $^{213}$Bi-J591 and $^{213}$Bi-PAI-2 (■) or nonspecific AIC (▲), respectively, incubated overnight and cell survival measured by MTS assay at 24 h and expressed as a percentage of cell survival of control cells. Results are expressed as a mean percentage ± SD of control plates containing nonspecific α conjugate. Each point represents a mean of three experiments with each experimental point having triplicate wells.

LN-3 cell survival was reduced to 12–14% by $^{213}$Bi-J591, whereas for the nonspecific AC, cell survival was 90%.

Bismuth-213-BSA showed only slight toxicity to PC-3 cells compared with $^{213}$Bi-PAI-2 at the maximum activity (7.5 μCi) used (92% and 10% cell survival, respectively) (*see* **Fig. 5B**). No significant toxicity was observed with either cDTPA-PAI-2 or PAI-2 (data not shown). The $D_0$ (37% cell survival)

value for $^{213}$Bi-PAI-2 was 3.4 μCi. At 15 μCi, $^{213}$Bi-PAI-2 killed only 10% of uPA-negative LN-3 cells, indicating that cytotoxicity was specific.

### 3.3.5. TUNEL Assay for Apoptotic Cells in Vitro

One possible mechanism responsible for the AC-induced cell death could be apoptosis. The following methodology was used to test this.

Cancer cells cultured in 12-well plates were treated with ACs with different activities (1, 2.5, 5, 10, and 25 μCi), with nonspecific AC (10 μCi), or without AC (media alone) at 37°C overnight. After treatment, cells were washed with Tris-buffered saline (TBS), harvested by treatment with 0.5% EDTA, and used for cytospins. Apoptotic cells were detected using standard TUNEL methodology ***(72)*** with the TdT-fragEL™ *in situ* apoptotic detection kit according to the manufacturer's instruction (Oncogene Research Products, Boston, MA) on paraformaldehyde-fixed LN-3 cells. The specificity of TUNEL reactivity was confirmed by undertaking in parallel appropriate negative (omitting TdT from the labeling mix) and positive (treated HL-60 slide) controls.

Patterns of TUNEL expression were as reported by Negoescu and colleagues ***(73)***. Cells with three or more nuclear chromatin fragments were considered positive for apoptosis. The free 3′ ends generated by apoptotic DNA cleavage were detected by TUNEL assay, in which the nonapoptotic cells stained green whereas apoptotic cells stained brown. They were examined using a Leica light microscope and the results were expressed as a percentage of total cells staining positive for apoptosis.

In the experiments described here, LN-3 and PC-3 cells were incubated with increasing concentrations of 213Bi-J591 (1-10 μCi for 24 h) or $^{213}$Bi-PAI-2, respectively. Treatment with specific ACs caused the cells to become apoptotic (*see* **Fig. 6A,B**), whereas treatment with nonspecific-ACs, chelator alone, or no treatment did not (*see* **Fig. 6C,D**). This indicates that the killing mediated by the ACs can be predominantly ascribed to the induction of apoptosis.

### 3.3.6. Immunohistochemistry and Apoptosis Immunolabeling

The expression of target antigens or the proliferative antigen Ki67 in cultured cells, frozen sections, or paraffin sections from mouse tissues was investigated using an indirect conjugated peroxidase method. Confluent cells were washed with sterile PBS, harvested with trypsin/EDTA, and used for cytospin preparations made with a Shando Cyto-centrifuge (Shando, Pittsburgh, PA). For these, $3 \times 10^4$ cells/60 μL were spun onto each glass slide. For PSMA staining, slides were fixed in acetone for 10 min at room temperature, treated with 3% hydrogen peroxidase in TBS (pH 7.5), incubated in normal rabbit serum for 10 min, and then incubated with mouse anti-human J591 (12.5 μg/mL) for 1 h at room temperature. They were then washed with TBS and subsequently incubated with

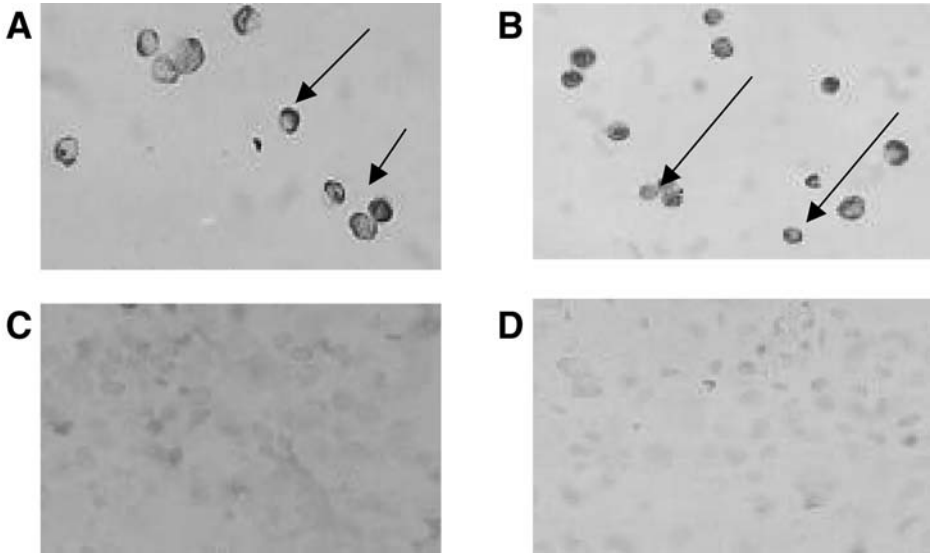


Fig. 6. TUNEL assay of LN-3 and PC-3, treated with $^{213}$Bi-J591 **(A)** or $^{213}$Bi-PAI-2 **(B)**. After 36 h, the treated and untreated cells were fixed and processed for TUNEL assay. The cells were then visualized by light microscopy. The arrows represent typical apoptotic cells with condensed or fragmented nuclei. Control cells show normal shape **(C, D)**. Magnification ~×200.

rabbit anti-mouse IgG-horseradish peroxidase (6.0 µg/mL) for 45 min and finally reacted with a freshly prepared solution of 10 mg of 3,3′diaminobenzidene tetrahydrochloride in 10 mL of Tris buffer (0.05 *M*, pH 7.6) containing 0.03% hydrogen peroxide. Positive cells appear brown.

For Ki67 staining, paraffin sections from tumors were deparaffinized in xylene, followed by a graded series of alcohols (100, 95, and 75%) and rehydrated in TBS (pH 7.5). They were subsequently immersed in boiling 0.01 *M* citric acid (pH 6.0) for 15 min to enhance antigen retrieval, treated with 3% hydrogen peroxidase, and then incubated with mouse anti-human Ki67 monoclonal antibody (1:50 dilution) overnight at 4°C. After that, the 3′diaminobenzidene tetrahydrochloride reaction was conducted as described above. The positive cells have brown nuclei. Sections were counterstained with hematoxylin for 4 min. Control slides were treated in an identical manner using an isotype monoclonal antibody or no primary antibody as a negative control.

Apoptotic cells in paraffin-embedded xenografted tissues taken 3 d after treatment of mice with specific or nonspecific ACs were detected using the

TUNEL method as described previously. After dewaxing, fixed sections (5 μm) were incubated with Proteinase K in 10 m*M* Tris-HCl, pH 7.4, for 20 min at room temperature before staining. The same controls were used as for in vitro TUNEL.

#### 3.3.7. Quantification of Proliferating and Apoptotic Cells

Sections were mounted with glycerol-gelatin solution (Sigma) for immunostained preparations or with DePex mounting medium (Sigma) for apoptotic cells and examined by two independent observers by light microscopy at 40× magnification. The number of Ki-67$^+$ (nuclear staining, regardless of intensity or pattern) or TUNEL$^+$ (apoptotic) cells was assessed among 500 to 1000 cells in randomly chosen fields. A cell is considered apoptotic when it shows cell shrinkage, nuclear pyknosis, chromatin condensation, and blebbing of the plasma membrane ***(74)***.

### 3.4. In Vivo TAT

A more stringent test of TAT is the effect of the therapy on the growth of human tumors grown in animals. In the following, we have outlined methods used when human PC cell lines were grown in immunodeficient BALB/c nu/nu (nude) mice. Other models would also be suitable for these tests, for example, the use of SCID mice.

#### 3.4.1. Animal Models

Male 8-wk-old nude mice, BALB/c (nu/nu), were used for prostate cancer animal models. To establish sc xenografts, $1.5 \times 10^6$ PC-3 cells were injected in the right shoulder region; LN-3 cells at $2 \times 10^6$ cells/100 μL in serum-free medium were similarly injected in the right flank together with 100 μL of Matrigel™ (Becton Dickinson, Bedford, MA).

First, nontoxic doses of ACs were established in a single-dose escalation schedule. Mice were followed for toxicity by monitoring body weight and performance status. Mice were treated with specific or nonspecific ACs either 2 d post-PC cell inoculation (considered to be comparable to effects which might occur with micrometastases) or 1 or 3 wk after the xenografts appeared (to test the effects of ACs on small but established tumors). Tumor progression was documented by measuring tumor volumes (length × width × depth × 0.52 in cubic millimeters) once weekly using calipers. Data points for both experiments were expressed as average tumor volume ± SD of mean based on 4–7 determinations. At sacrifice at 1, 3, and 5 wk post-tumor appearance, xenografts and other mouse tissues were OCT embedded for frozen sections or fixed in 10% neutral buffered formalin for paraffin embedding for histological assessment.

### *3.5. Discussion and Conclusions*

The use of monoclonal antibodies or proteins armed with toxins or radionuclides to specifically deliver these cytotoxic agents to tumor cells provides a valuable alternative approach for cancer therapy. Labeling MAbs with nuclides that emit α-particles is one approach for enhancing the selectivity of cancer cell irradiation. Other issues are to select the MAb that serves to carry the radionuclide to the tumor target and the type of malignancy chosen as the target for radioimmunotherapy. The radioisotope used here is $^{213}$Bi (half-life 45.6 min), which decays by the emission of alpha particles with high energy (8.35 MeV), high LET, and short range (~80 μm). As a consequence, the relative biological effectiveness is higher than that of the low-LET beta-particle emitters currently used in clinical radioimmunotherapy. Several review articles have recently summarized the applications of alpha-emitting radionuclides for the treatment of disease ***(15,75–77)***. Some earlier in vivo work with alpha particle emitters addressed leukemias, which are accessible to the circulation ***(78,79)***, and with injections of radiolabeled MAb directly to the tumor site ***(80)***, and with iv injection of $^{213}$Bi-labeled MAb to target micrometastases in lung ***(81)***. In this laboratory, we have reported successful intra-lesional TAT for sc melanoma ***(17)***.

#### *3.5.1. Alpha-J591*

PSMA is expressed in prostate cancer cells and the neovasculature of a wide variety of malignant neoplasms including lung, colon, breast, and others but not in normal vascular endothelium. The expression is further increased in higher-grade cancers, metastatic disease, and hormone-refractory prostate cancer. J591 is one of several MAbs to the extracellular domain of PSMA.

Alpha-J591 is an injectable AC to treat human prostate cancer. The antiproliferative effects of AC against prostate cancer have been reported by McDevitt and colleagues ***(82)*** and by Li and colleagues ***(22)*** using the methods described herein. These authors reported a very high density of PSMA in an androgen-dependent human PC cell line (LNCaP-LN-3) and in tumor xenografts in nude mice. The AC was found to extensively inhibit the growth of LN-3 cells in vitro in a concentration-dependent fashion, causing the cells to undergo apoptosis. In vivo studies showed that a local AC injection of 50 μCi at 2 d post-cell inoculation gave complete inhibition of tumor growth, whereas results for a nonspecific AC were similar to those for untreated mice. Furthermore, after 1 and 3 wk posttumor appearance, a single (100 μCi/100 μL) intralesional injection of AC inhibited the growth of LN-3 tumor xenografts (volume < 100 mm$^3$) in nude mice. Tumors treated with AC decreased in volume from a mean 46 ± 14 mm$^3$ in the first week or 71 ± 15 mm$^3$ in the third week to nonpalpable, whereas in control mice treated with a nonspecific AC using the same dose, tumor volume

increased from 42 to 590 $mm^3$. There were no observed side effects of the treatment. Because of its in vitro cytotoxicity and these anti-proliferative properties in vivo, the $^{213}$Bi-J591 conjugate has considerable potential as a new therapeutic agent for the treatment of prostate cancer.

### 3.5.2. Alpha-PAI-2

Li and colleagues ***(23)*** have reported the novel alpha-particle emitting ($^{213}$Bi) plasminogen activator inhibitor type 2 ($^{213}$Bi-PAI-2) construct, which targets the membrane-bound uPA on prostate cancer cells. The PC-3 prostate cancer cell line expresses uPA, which binds to its receptor (uPAR) on the cell membrane; PAI-2 is bound to uPA/uPAR to form stable complexes. The in vitro cytotoxicity of $^{213}$Bi-PAI-2 against prostate cancer cells was tested using the MTS assay, and apoptosis was documented using the TUNEL assay. In vivo, antiproliferative effects for tumors and prostate cancer lymph node metastasis were carried out in an athymic nude mouse model with an sc xenograft of PC-3 cells.

These authors found that $^{213}$Bi-PAI-2 was specifically cytotoxic to PC-3 cells in a concentration-dependent fashion, causing the cells to undergo apoptosis. A single local or ip injection of $^{213}$Bi-PAI-2 was able to completely regress the growth of tumors and lymph node metastases 2 d post-sc inoculation, and obvious tumor regression was achieved in the therapy groups compared with control groups with $^{213}$Bi-PAI-2 when the tumors measured 30–40 $mm^3$ and 85 to 100 $mm^3$. All control animals and one of five (20%) mice treated with 3 mCi/kg $^{213}$Bi-PAI-2 developed metastases in the lymph nodes whereas no lymphatic spread of cancer was found in the 6 mCi/kg-treated groups at 2 d and 2 wk post-cell inoculation. These results demonstrate that this novel $^{213}$Bi-PAI-2 conjugate selectively targets prostate cancer in vitro and in vivo and could be considered for further development for the therapy of prostate cancer, especially for the control of micrometastases or in minimal residual disease.

### 3.5.3. Conclusions

In this chapter we, have shown these alpha conjugates selectively kill human prostate cancer cells in vitro and can completely inhibit or regress tumor growth in vivo.

Specifically, TAT with $^{213}$Bi-labeled J591 and PAI-2 conjugates can do the following:

1. Kill prostate cancer cells (LN-3 and PC-3) in a dose-dependent manner, requiring approx 2 $^{213}$Bi decays per cell for 37% cell survival.
2. Completely regress tumor growth after local TAT at 2 d postinoculation using 2.5 mCi/kg or 6 mCi/kg for systemic TAT.

3. Delay tumor growth in a dose-dependent fashion.
4. Reduce lymph node metastases.

The mechanism of tumor regression involves targeting of tumor cells and vascular endothelium and induction of apoptotic regression. Small primary lesions or small preangiogenic lesions in prostate cancer should be considered to be the most suitable for TAT. However, although the control of the micrometastases by TAT for human prostate cancer remains problematic, TAT with $^{213}$Bi-labeled-J591 and PAI2 provides a potentially effective therapy for patients with micrometastases after primary treatment or patients with localized small tumors recurring after therapy or with minimal residual disease.

## Acknowledgments

The authors wish to acknowledge the ongoing support given by Professor J Kearsley, Director, Cancer Services Division.

## References

1. Landis, S. H., Murray, T., Bolden, S., and Wingo, P. A. (1998) Cancer statistics. *CA Cancer J. Clin.* **48,** 6–29.
2. Fowler, J. E. Jr., Braswell, N. T., Pandey, P., and Seaver, L. (1995) Experience with radical prostatectomy and radiation therapy for localized prostate cancer at a Veterans Affairs Medical Center. *J. Urol.* **153,** 1026–1031.
3. Wasson, J. H., Cushman, C. C., Bruskewitz, R. C., Littenberg, B., Mulley, A. G. Jr., and Wennberg, J. E. (1993) A structural literature review of treatment for localized prostate cancer. Prostate Disease Patient Outcome Research Team. *Arch. Family Med.* **2,** 487–493.
4. Litwin, M. S., Pasta, D. J., Stoddard, M. L., Henning, J. M., and Carroll, P. R. (1998) Epidemiological trends and financial outcomes in radical prostatectomy among Medicare beneficiaries, 1991 to 1993. *J. Urol.* **160,** 445–448.
5. Lepor, H., Ross, A., and Walsh, P. C. (1982) The influence of hormonal therapy on survival of men with advanced prostatic cancer. *J. Urol.* **128,** 335–340.
6. Blake, G. M., Zivanovic, M. A., McEwan, A. J., and Ackery, D. M. (1986) Sr-89 therapy: strontium kinetics in disseminated carcinoma of the prostate. *Eur. J. Nucl. Med.* **12,** 447–454.
7. Allen, B. J. and Blagojevic, N. (1996) Alpha- and beta-emitting radiolanthanides in targeted cancer therapy: the potential role of terbium-149. *Nucl. Med. Commun.* **17,** 40–47.
8. Vaughan. A. T., Bateman, W. J., Brown. G., and Cowan. J. (1982) The specific inhibition of cellular clonogenic proliferation using 211At labeled lectins and antibodies-1. *Int. J. Nucl. Med. Biol.* **9,** 167–171.
9. Goddu, S. M., Howell, R. W., and Rao, D. V. (1994) Cellular dosimetry: absorbed fractions for monoenergetic electron and alpha particle sources and S-values for radionuclides uniformly distributed in different cell compartments. *J. Nucl. Med.* **35,** 303–316.

10. Humm, J. L. (1987) A microdosimetric model of astatine-211 labeled antibodies for radioimmunotherapy. *Int. J. Radiat. Oncol. Biol. Phys.* **13,** 1767–1773.
11. Bloomer, W. D., McLaughlin, W. H., Lambrecht, R. M., Atcher, R. W., Mirzadeh, S., Madara, J. L., Milius, R. A., Zalutsky, M. R., Adelstein, S J. and Wolf, A. P. (1984) 211 At radiocolloid therapy: further observations and comparison with radiocolloids of 32P, 165Dy, and 90Y. *Int. J. Radiat. Oncol. Biol. Phys.* **10,** 341–348.
12. Macklis, R. M., Kinsey, B. M., Kassis, A. L., Ferrara, J. L. M., Atcher, R. W., Hines, J. J., et al. (1988) Radioimmunotherapy with alpha-particle-emitting immunoconjugates. *Science* **240,** 1024–1026.
13. Larsen, R. H., Akabani, G., Welsh, P., and Zalutsky, M. R. (1998) The cytotoxicity and microdosimetry of astatine-211-labeled chimeric monoclonal antibodies in human glioma and melanoma cells in vitro. *Radiat. Res.* **149,** 155–162.
14. McDevitt, M. R., Sgouros, G., Finn, R. D., Humm, J. L., Jurcic, J. G., Larson, S. M., et al. (1998) Radioimmunotherapy with alpha-emitting nuclides. *Eur. J. Nucl. Med.* **25,** 1341–1351.
15. Allen, B. J. (2000) Targeted alpha therapy: evidence for potential efficacy of alpha-immunoconjugates in the management of micrometastatic cancer. *Aus. Radiol.* **43,** 480–486.
16. Rizvi, S. M. A., Sarkar, S., Goozee, G., and Allen, B. J. (2000) Radio-immunoconjugates for targeted alpha therapy of malignant melanoma. *Melanoma Res.* **10,** 281–289.
17. Allen, B. J., Rizvi, S. M. A. and Tian, Z. (2001) Preclinical targeted alpha therapy for melanoma. *Melanoma Res.* **11,** 1–8.
18. Rizvi, S. M. A., Henniker, A. J., Goozee, G., and Allen, B. J. (2002) In vitro testing of the leukaemia monoclonal antibody WM-53 labeled with alpha and beta emitting radioisotopes. *Leukaemia Res.* **26,** 37–43.
19. Rizvi, S. M. A., Allen, B. J., Tian, Z., Li, Y., Goozee, G., and Sarkar, S. (2001) In vitro and preclinical studies of targeted alpha therapy (TAT) for colorectal cancer. *Colorectal Dis.* **3,** 345–353.
20. Allen, B. J., Tian, Z., Andronicos, N. M., Rizvi, S., and Ranson, M. (2001) Preclinical studies of targeted alpha therapy for human breast cancer using $^{213}$Bilabeled-PAI2. Breast Cancer 2001—Emerging Possibilities Conference, Monash Medical Center, March 18–21st.
21. Ranson, M., Tian, Z., Andronicos, N. M., Rizvi, S. M. A., and Allen, B. J. (2002) In vitro cytotoxicity study of human breast cancer cells using Bismuth213 ($^{213}$Bi)labeled plasminogen activator inhibitor type 2 (alphaPAI2). *Breast Cancer Res. Treatment* **71,** 149–159.
22. Li, Y., Tian, Z, Rizvi, S. M. A., Bander, N. H., and Allen, B. J. (2002) In vitro and prelinical targeted alpha therapy of human prostate cancer with Bi–213 labeled J591 antibody against the prostate specific membrane antigen. *Prostate Cancer Prostatic Dis.* **5,** 36–46.
23. Li, Y., Rizvi, S. M. A., Ranson, M., and Allen, B. J. (2002) 213BiPAI2 conjugate selectively induces apoptosis in PC3 metastatic prostate cancer line and shows anticancer activity in a xenograft animal model. *Br. J. Cancer* **86,** 1197–1203.

24. Beyer, G. J., Offord, R., Künzi, G., and Jones, R. (1995) Biokinetics of monoclonal antibodies labeled with radiolanthanides and 225 Ac in xenografted nude mice: preliminary results. *J. Lab. Compd. Radiopharm. (GENERIC)* **37,** 529–530.
25. Imam, S., Allen, B. J., Goozee, G., Sarkar, S., and Hersey P. (1997) In vitro and in vivo studies with terbium152 and samarium153 radioimmunoconjugates of the antimelanoma antibody 9.2.27. *Melanoma Res.* **7,** S35.
26. Allen, B J., Goozee, G., Imam, S., Sarkar, S., Leigh, J., and Beyer. G. (1996) Proceedings Of The International Conference On Dosimetry, Gatlinberg Tennessee, USA; CERNPPE/96127; Oak Ridge Associated Universities, **2,** 392–399.
27. Allen, B. J., Goozee, G., Sarkar, S., Beyer, G., Morel, C., and Byrne, A. (2000) Production of Terbium152 by heavy ion reactions and proton induced spallation. *Appl. Radiat. Isotopes* **54,** 53–58.
28. Corson, D. R., Mackenzie, K. R., and Segre, E. (1940) Artificially radioactive element 85. *Phys. Rev.* **58,** 672–678.
29. Larsen, R. H., Wieland, B. W., and Zalutsky, M. R. (1996) Evaluation of an internal cyclotron target for the production of $^{211}$At via the 209Bi ($\alpha$,2n)$^{211}$At reaction. *Appl. Radiat. Isotopes* **47,** 135–143.
30. Weinreich, R. (1997) Molecular radiotherapy with 211At, in *Advances In Hadron Therapy* (Almadi, U., Larsson B. and Lemoigne, Y., eds.), Elsevier Press, Amsterdam, pp. 359–382.
31. Doberenz, I., Doberenz, W., Wunderlich, G., Franke, W. G., Heidelbach, J. G., Fischer, S., et al. (1990) Case report. Endoarterielle therapie eines zungenkarzinoms mit 211Atmarkierten humanserumalbuminmikrospharen—erste klinische erfahrungen. *Nuc. Compact.* **21,** 124–127.
32. Zalutsky, M. R., Akabani, G, Cokgor, I., Friedman, H. S., Coleman, R. E., Friedman, A. H., et al. (1999) Astatine211 labeled chimeric antitenascin antibody: Phase 1 trial in brain tumor resection cavity patients. *Eur. J. Nucl. Med.* **26,** 1215: PS651.
33. Horak, E., Hartmann, F., Garmestani, K., Wu, C., Brechbiel, M., Gansow, O. A., et al. (1997). Radioimmunotherapy targeting the HER2/neu oncoprotein expressed on an ovarian tumour using the alphaemitting radionuclideconjugated monoclonal antibody $^{212}$PbDOTAAE1. *J. Nucl. Med.* **38,** 1944–1950.
34. McDevitt, M. R., Finn, R. D., Sgouros, G., Ma, D., and Scheinberg, D. A. (1999) An $^{225}$Ac/213Bi generator system for therapeutic clinical applications: construction and operation. *Appl. Radiat. Isotopes* **50,** 895–904.
35. Wynant, G. E., Murphy, G. P., Horoszewicz, J. S., Neal, C. E., Collier, B. D., Mitchell, E., et al. (1991) Immunoscintigraphy of prostatic cancer: preliminary results with $^{111}$Inlabeled monoclonal antibody 7E11C5.3 (CYT356). *Prostate* **18,** 229–241.
36. Kawakami, M. and Nakayama, J. (1997) Enhanced expression of prostatespecific membrane antigen gene in prostate cancer as revealed by in situ hybridization. *Cancer Res.* **57,** 2321–2324.
37. Watt, F., Martorana, A., Brookes, D. E., Ho, T., Kingsley, E., O'Keefe, D. S., et al. (2001) A tissuespecific enhancer of the prostatespecific membrane antigen gene, FOLH1. *Genomics* **73,** 243–254.

38. Israeli, R. S., Powell, C. T., Corr, J. G., Fair, W. R., and Heston, W. D. (1994) Expression of the prostatespecific membrane antigen. *Cancer Res.* **54,** 1807–1811.
39. Wright, G. L. Jr., Grob, B. M., Haley, C., Grossman, K., Newhall, K., Petrylak, D., et al. (1996) Upregulation of prostatespecific membrane antigen after androgendeprivation therapy. *Urology* **48,** 326–334.
40. Silver, D. A., Pellicer, I., Fair, W. R., Heston, W. D., and CordonCardo, C. (1997) Prostatespecific membrane antigen expression in normal and malignant human tissues. *Clin. Cancer Res.* **3,** 81–85.
41. Liu, H., Moy, P., Kim, S., Xia, Y., Rajasekaran, A., Navarro, V., et al. (1997) Monoclonal antibodies to the extracellular domain of prostatespecific membrane antigen also react with tumour vascular endothelium. *Cancer Res.* **57,** 3629–3634.
42. Lopes, A. D., Davis, W. L., Rosenstraus, M. J., Uveges, A. J., and Gilman, S. C. (1990) Immunohistochemical and pharmacokinetic characterization of the sitespecific immunoconjugate CYT356 derived from antiprostate monoclonal antibody 7E11C5. *Cancer Res.* **50,** 6423–6429.
43. Rosenstraus, M. J., Davis, W. J., Lopes, A. D., D'Aleo, C., and Gilman, S. (1990) In vitro and in vivo reactivity of antiprostate monoclonal antibody immunoconjugate 7E11C5.3GYKDTPA. *Antibody Immunoconj. Radiopharm.* **3,** 54–60.
44. Chang, S. S., Reuter, V. E., Heston, W. D., Bander, N. H., Grauer, L. S., and Gaudin, P. B. (1999) Five different antiprostatespecific membrane antigen (PSMA) antibodies confirm PSMA expression in tumourassociated neovasculature. *Cancer Res.* **59,** 3192–3198.
45. Murphy, G., Tjoa, B., Ragde, H., Kenny, G., and Boynton, A. (1996) Phase I clinical trial: Tcell therapy for prostate cancer using autologous dendritic cells pulsed with HLAA0201specific peptides from prostatespecific membrane antigen. *Prostate* **29,** 371–380.
46. Tjoa, B. A., Erickson, S. J., Bowes, V. A., Ragde, H., Kenny, G. M., Cobb, O. E., et al. (1997) Followup evaluation of prostate cancer patients infused with autologous dendritic cells pulsed with PSMA peptides. *Prostate* **32,** 272–278.
47. Dano, K., Andreasen, P. A., GrondahiHansen, J., Kristensen, P., Nielsen, L. S., and Skriver, L. (1985) Plasminogen activators, tissue degradation, and cancer. *Adv. Cancer Res.* **44,** 139–266.
48. Kwaan, H. C. (1992) The plasminogenplasmin system in malignancy. *Cancer Metast. Rev.* **11,** 291–311.
49. Andreasen, P. A., Kjoller, L., Christensen, L., and Duffy, M. (1997) The urokinasetype plasminogen activator system in cancer metastasis: A review. *Int. J. Cancer* **72,** 1–22.
50. Pollanen, J., Stephens, R., and Vaheri, A. (1991) Directed plasminogen activation at the surface of normal and malignant cells. *Adv. Cancer Res.* **57,** 273–328.
51. Schmitt, M., Wilhelm, O. G., Reuning, U., Kruger, A., Harbeck, N., Lengyel, E., et al. (2000) The urokinase plasminogen activation system as a novel target for tumour therapy. *Fibrinol. Proteol.* **14,** 114–132.
52. Kruithof, E. K. O., Baker, M. S., and Bunn, C. L. (1995) Biochemistry, cellular and molecular biology and clinical aspects of plasminogen activator inhibitor type2. *Blood* **86,** 4007–4024.

53. Miyake, H., Hara, I., Yamanaka, K., Gohji, K., Arakawa, S., and Kamidono, S. (1999) Elevation of serum levels of urokinasetype plasminogen activator and its receptor is associated with disease progression and prognosis in patients with prostate cancer. *Prostate* **39,** 123–129.
54. Foekens, J. A., Peters, H. A., Look, M. P., Portengen, H., Schmitt, M., Kramer, M. D., et al. (2000) The urokinase system of plasminogen activation and prognosis in 2780 breast cancer patients. *Cancer Res.* **60,** 636–643.
55. Pedersen, H., GrondahlHansen, J., Francis, D., Osterlind, K., Ronne, E., Hansen, H. H., et al. (1994) Urokinase and plasminogen activator inhibitor type1 in pulmonary adenocarcinoma. *Cancer Res.* **54,** 120–123.
56. Pedersen, H., Brunner, N., Francis, D., Osterlind, K., Ronne, E., Hansen, H. H., et al. (1994) Prognostic impact of urokinase, urokinase receptor, and type 1 plasminogen activator inhibitor in squamous and large cell lung cancer tissue. *Cancer Res.* **54,** 4671–4675.
57. Duggan, C., Maguire, T., McDermott, E., O'Higgins, N., Fennelly, J. J., and Duffy, M. J. (1995) Urokinase plasminogen activator and urokinase plasminogen activator receptor in breast cancer. *Int. J. Cancer* **61,** 597–600.
58. Stephens, R. W., Pedersen, A. N., Nielsen, H. J., Hamers, M. J. A. G., Hoyer-Hansen, G., Ronne, E., et al. (1997) ELISA determination of soluble urokinase receptor in blood from healthy donors and cancer patients. *Clin. Chem.* **43,** 1868–1876.
59. Brunner, N., Nielsen, H. J., Hamers, M., Christensen, I. J., ThorlaciusUssing, O., and Stephens, R. W. (1999) The urokinase plasminogen activator receptor in blood from healthy individuals and patients with cancer. *Acta Pathol. Microbiol. Immunol. Scand.* **107,** 160–167.
60. Bouchet, C., Spyratos, F., Martin, P. M., Hacene, K., Gentile, A., and Oglobine, J. (1994) Prognostic value of urokinasetype plasminogen activator (uPA) and plasminogen activator inhibitors PAI1 and PAI2 in breast carcinomas. *Br. J. Cancer* **69,** 398–405.
61. Foekens, J. A., Buessecker, F., Peters, H. A., Krainick, U., van Putten, W. L. J., Look, M. P., et al. (1995) Plasminogen activator inhibitor2: Prognostic relevance in 1012 patients with primary breast cancer. *Cancer Res.* **55,** 1423–1427.
62. Yoshino, H., Endo, Y., Watanabe, Y., and Sasaki, T. (1998) Significance of plasminogen activator inhibitor 2 as a prognostic marker in primary lung cancer: Association of decreased plasminogen activator inhibitor 2 with lymph node metastasis. *Br. J. Cancer* **78,** 833–839.
63. Hang, M. T. N., Ranson, M., Saunders, D. N., Liang, X. M., Bunn, C. L., and Baker, M. S. (1998) Pharmacokinetics and biodistribution of recombinant human plasminogen activator inhibitor type 2 (PAI2) in control and tumour xenograftbearing mice. *Fibrinol. Proteol.* **12,** 145–154.
64. Kozak, R. W., Raubitschek, A., Mirzadeh, S., Brechbiel, M. W., Junghans, R. P., Gansow, O. A., et al. (1989) Nature of the bifunctional chelating agent used for radioimmunotherapy with Y90 monoclonal antibodies: A critical factor in determining in vivo survival and organ toxicity. *Cancer Res.* **49,** 2639–2644.

65. Izard, M., Boniface, G. R., Hardiman, K. L., Brechbiel, M. W., Gansow, O. A., and Walker, K. Z. (1992) An improved method for labeling monoclonal antibodies with Sm153. *Bioconjug. Chem.* **3,** 346–350.
66. Pettaway, C. A., Pathak, S., Greene, G., Ramirez, E., Wilson, M. R., Killion, J. J., et al. (1996) Selection of highly metastatic variants of different human prostatic carcinomas using orthotopic implantation in nude mice. *Clin. Cancer Res.* **2,** 1627–1636.
67. Horoszewicz, J. S., Leong, S. S., Kawinski, E., Karr, J. P., Rosenthal, H., Chu, T. M., et al. (1983) LNCaP model of human prostatic carcinoma. *Cancer Res.* **43,** 1809–1818.
68. Montgomery, B. T., Young, C. Y., Bilhartz, D. L., Andrews, P. E., Prescott, J. L., Thompson, N. F., and Tindall, D. J. (1992) Hormonal regulation of prostatespecific antigen (PSA) glycoprotein in the human prostatic adenocarcinoma cell line, LNCaP. *Prostate* **21,** 63–73.
69. Veldscholte, J., RisStalpers, C., Kuiper, G. G., Jenster, G., Berrevoets, C., Claassen, E., et al. (1990) A mutation in the ligand binding domain of the androgen receptor of human LNCaP cells affects steroid binding characteristics and response to antiandrogens. *Biochem. Biophys. Rev. Commun.* **173,** 534–540.
70. Cordell, J. L., Falini, B., Erber, W. W., Ghosh, A. K., Abdulaziz, Z., MacDonald, S., et al. (1984) Immunoenzymatic labeling of monoclonal antibodies using immune complexes of alkaline phosphatase and monoclonal antialkaline phosphatase (APAAP complexes). *J. Histochem. Cytochem.* **32,** 219–229.
71. Mosmann, T. (1983) Rapid colorimetric assay for cellular growth and survival: application to proliferation and cytotoxicity assays. *J. Immunol. Meth.* **65,** 55–63.
72. Gavrieli, Y., Sherman, Y., and BenSasson, S. A. (1992) Identification of programmed cell death in situ via specific labeling of nuclear DNA fragmentation. *J. Cell. Biol.* **119,** 493–501.
73. Negoescu, A., Lorimier, P., LabatMoleur, F., Drouet, C., Robert, C., Guillermet, C., et al. (1996) In situ apoptotic cell labeling by the TUNEL method: Improvement and evaluation on cell preparation. *J. Histochem. Cytochem.* **44,** 959–968.
74. Kerr, J. F., Wyllie, A. H., and Currie, A. R. (1972) Apoptosis: A basic biological phenomenon with wideranging implications in tissue kinetics. *Br. J. Cancer* **26,** 239– 257.
75. Zalutsky, M R. and Bigner, D. D. (1996) Radioimmunotherapy with alphaparticleemitting radioimmunoconjugates. *Acta Oncol.* **35,** 373–379.
76. Vaidyanathan, G. and Zalutsky, M. R. (1996) Targeted therapy using alpha emitters. *Phys. Med. Biol.* **41,** 1915–1931.
77. McDevitt, M. R., Sgouros, G., Finn, R. D., Humm, J. L., Jurcic, J. G., Larson, S. M., and Scheinberg, D. A. (1998) Radioimmunotherapy with alphaemitting nuclides. *Eur. J. Nucl. Med.* **25,** 1341–1351.
78. Jurcic, J., McDevitt, M. R., Sgouros, G., Ballangrad, G., Finn, R. D., Ma, D., et al. (1999) Phase 1 trial of targetd (particle therapy for myeloid leukaemias with bismuth213HuM195 (antiCD33). *Proc. Am. Soc. Clin. Oncol.* 18, 7a.

79. Huneke, R. B., Pippin, C. G., Squire, R. A., Brechbiel, M. W., Gansow, O. A., and Strand, M. (1992) Effective alphaparticlemediated radioimmunotherapy of murine leukemia. *Cancer Res.* **52,** 5818–5820.
80. Zalutsky, M. R., McLendon, R. E., Garg, P. K., Archer, G. E., Schuster, J. M., and Bigner, D. D. (1994) Radioimmunotherapy of neoplastic meningitis in rats using an αparticleemitting immunoconjugate. *Cancer Res.* **54,** 4719–4725.
81. Kennel, S. J., Boll, R., Stabin, M., Schuller, H. M., and Mirzadeh, S. (1999) Radioimmunotherapy of micrometastases in lung with vascular targeted $^{213}$Bi. *Br. J. Cancer* **80,** 175–184.
82. McDevitt, M. R., Barendswaard, E., Ma, D., Lai, L., Curcio, M. J., Sgouros, G., et al. (2000) An alphaparticle emitter antibody ($^{213}$BiJ591) for radioimmunotherapy of prostate cancer. *Cancer Res.* **60,** 6095–6100.

# 21

# Phenotypic and Functional Differences of Dendritic Cells Generated Under Different In Vitro Conditions

**Stephanie E. B. McArdle, Selman A. Ali, Geng Li, Shahid Mian, and Robert C. Rees**

## 1. Introduction

The immune system is capable of recognizing and rejecting autologous tumor cells. This is suggested by reported cases of spontaneous remission of various cancers ***(1)*** and the presence of infiltrating leukocytes, the majority of which consist of T cells. However, the very existence of cancer and its inevitable progression without treatment demonstrates the inefficiency of the natural immune defense in combating tumors and the ability of neoplastic cells to evade immune-surveillance. Thus, the major objectives of immunotherapeutic approaches to the treatment of cancer rely on the ability to augment adaptive and natural immune responses against malignant cells.

During the last decade, a great deal of attention has been paid to the role of dendritic cells (DCs) in the development of immune responses;, with the ultimate aim being to provide a novel means of cancer therapy for patients. DCs directly isolated from patients' blood have already been shown to be effective in promoting antitumor immunity in pilot clinical trials ***(2)***, and such approaches are likely to be effective in patients who have completed conventional antitumor therapies (surgery, chemotherapy, radiotherapy) and who have minimal residual disease. By reducing tumor bulk before immunotherapy, the degree of tumor "fight back" will be reduced and the efficiency of the immune response most likely enhanced.

### *1.1. Prostate Cancer-Associated Antigens*

Defining the expression of tumor antigens on primary and metastatic prostate cancer is the crucial first step in selecting appropriate targets for

From: *Methods in Molecular Medicine, Vol. 81: Prostate Cancer Methods and Protocols*
Edited by: P. J. Russell, P. Jackson, and E. A. Kingsley © Humana Press Inc., Totowa, NJ

**Table 1**
**Antigens or Genes Overexpressed in the Prostate or Prostate Cancer Tissues**

| Antigen | Brief description |
|---|---|
| PSA | Prostate-specific antigen; 34 kDa glycoprotein |
| PSMA | Prostate-specific membrane antigen; 100 kDa membrane glycoprotein |
| PSCA | Prostate stem cell antigen; 123 amino acid protein |
| PAP | Prostate acid phosphatase; 343 amino acid, 41 kDa |
| PCTA-1 | Prostate carcinoma tumor antigen; 35 kDa |
| Ep-CAM | Transmembrane glycoprotein; 40 kDa |
| MUC-1 and 2 | Mucin antigens |
| GM-2 | Ganglioside antigen |
| Thy-1 | Transmembrane glycoprotein with 30% homology to PSCA; 110 kDa |
| Bcl-2 | Anti-apoptosis protein |
| Tn, sTn, TF | Blood group antigens |
| hCG beta | Human chorionic gonadotrophin |
| PAGE-1 | X chromosome-linked GAGE-like gene |
| NY-ESO-1 | CT antigen |
| p53 | Tumor suppressor protein |
| Survivin | Anti-apoptosis protein |

immune attack ***(3)***. **Table 1** summarizes the antigens or genes overexpressed in the prostate or prostatic cancer tissues. Unfortunately, not all of the antigens expressed in cancer tissues are suitable for the development of immunotherapy. They may, for instance, be poorly immunogenic or occur frequently in normal tissues, implying that these antigens could elicit harmful autoimmune reactions. However, some prostate cancer-associated antigens have been successfully used in DC-based immunotherapy of prostate cancer, for example, with cultured autologous DCs pulsed with HLA-A2 peptide derived from prostate-specific membrane antigen ***(4)***. The Phase I study used HLA-A2 peptide derived from prostate-specific membrane (PSM) antigens (PSM-P1 and PSM-P2) and autologous DCs; PSM-P1-, and -P2-pulsed autologous DCs were administered to 51 patients with advanced hormone refractory prostate cancer. Neither significant acute or chronic toxicity was observed at any of the doses used except for mild to moderate cases of hypotension without pulse change during the time of infusion. A total of 107 patients with either local recurrence of prostate cancer after primary treatment failure or with hormone-refractory metastasis prostate cancer were treated in a Phase II clinical trial. Patients

received six infusions of autologous DCs pulsed with PSM-P1 and -P2 every 6 wk. The treatment was well tolerated by all participants. Approximately 30% of the trial participants had clinical responses, as defined by the modified National Prostate Cancer Project criteria including a 50% reduction in prostate-specific antigen (PSA) ***(2,4,5)***. A population of peripheral blood-derived antigen-presenting cells, including DCs, pulsed with selected peptides from prostate acid phosphate have been shown to induce prostate cancer-specific cytotoxic T lymphocyte (CTL) in vitro ***(6)***. The use of PSA-specific peptides pulsed onto DCs to induce CTL has not been reported to date. However, Heiser and coworkers ***(7)*** observed that DCs transfected with mRNA encoding PSA could stimulate a primary PSA-specific CTL response in vitro.

### 1.2. DC Characteristics

DCs, first discovered in 1973 ***(8),*** originate from CD34+ progenitor cells in the bone marrow and migrate to the different lymphoid and nonlymphoid tissues. Upon exposure to inflammatory cytokines, DCs capture antigen and upregulate the expression of histocompatibility and costimulatory molecules ***(9)***. At this point DCs are able to migrate from peripheral tissues to regional lymph nodes, where they present antigen to and promote the clonal expansion of antigen-specific T lymphocytes. Final maturation is completed by the interaction of DCs with T helper cells recognizing the presented antigen ***(10)***. Indeed, evidence suggests that initial priming of cytotoxic T lymphocytes requires both presentation of antigen in the context of major histocompatibility complex class-I molecules together with an appropriate costimulatory signal provided by the antigen-presenting cell (APC). Most tumors do not express costimulatory molecules; therefore, transfer of tumor antigen from the tumor to an APC is required for the initiation of specific cytotoxic T lymphocyte responses. This transfer of antigen has been termed cross-priming, and evidence suggests that DCs play a central role in the process ***(11)***; the failure of the majority of naturally occurring tumors to initiate an effective immune response may, in large, be caused by the absence of cross-priming. However, despite the various mechanisms that tumors may possess to evade immune attack, there are significant data to show that DC-based immunotherapy can provide a real and measurable antitumor effect.

DCs are therefore antigen-presenting cells capable of initiating primary immune responses ***(10)***. They display different functional repertoires of cell surface markers at different stages of their development. In the immature state, DCs are very effective in processing native protein antigens via major histocompatibility complex (MHC) class-II-restricted as well as the MHC class-I pathways ***(12–14)***. Whole purified protein, necrotic cells, or apoptotic cells given to immature DCs are then able to elicit immune responses, which are

class-I and class-II restricted ***(13–16)***. Mature DCs are less able to capture new proteins for presentation but are much more efficient in presenting MHC-associated peptides, stimulating resting CD4+ and CD8+ T cells to grow and differentiate. Mature DCs pulsed with specific tumor peptide are also able to activate either $CD4^+$- or $CD8^+$-specific T-cell responses ***(17–19)***.

Difficulties in obtaining sufficient numbers of DCs have been solved, and methods have been developed to obtain substantial numbers of DCs from proliferating human bone marrow ***(20)*** and blood ***(21)***. This approach is less practical for small samples of human blood where the frequency of $CD34^+$ cells is very low (less than 1%). However, enrichment and isolation of $CD34^+$ stem cells is now a standard procedure for stem cell support after high-dose chemotherapy. Adequate numbers of $CD34^+$ cells can be positively selected from the blood of patients 3–4 d after treatment with G-CSF. However, the most widely used method to generate DCs to study their function and potential use in immunotherapy is to select monocytes present in human blood and culture them in vitro in medium containing granulocyte macrophage-colony stimulating factor (GM-CSF) and interleukin (IL)-4 ***(21–23)***. Cells generated in such a manner can be characterized according to their phenotypic and functional characteristics, including morphology, cell surface marker expression, phagocytosis, and ability to activate helper ($CD4^+$) and cytotoxic ($CD8^+$) T-lymphocytes. Here, we present a simple method to generate immature and mature DCs.

For clinical purposes, DCs have to be generated without the use of foreign proteins, in particular xenogenic proteins present in fetal calf serum (FCS). However we, along with Pietschmann and coworkers ***(24),*** have found that DCs generated in medium containing 1% autologous serum and GM-CSF and IL-4 for 6 d and tumor necrosis factor α (TNF-α) for another 2 d expressed significantly lower CD40, CD1a, and CD54 cell surface markers than DCs cultures in FCS-containing medium. Culturing DCs in autologous serum instead of 10% FCS induced morphological changes, including the absence of aggregate formation and a reduced activity in mixed lymphocyte reaction (MLR) assays. Their ability to phagocytose latex beads was comparable and both were capable of inducing T cells proliferation after incubation with 0.5 µg/mL of tetanus toxoid protein.

The following methods can be used to generate DCs and assess their phenotypic and functional properties.

## 2. Materials

### 2.1. Medium

The medium used throughout the study was RPMI 1640 supplemented with 200 mmol/L L-glutamine and with the addition of either 10% FCS or 1% autologous serum (heat inactivated 56°C for 30 min).

### 2.2. Other Reagents

1. Blocking buffer: 1X phosphate-buffered saline (PBS) + 0.1% bovine serum albumin and 0.02% sodium azide, stored at room temperature.
2. Sheath fluid: 6.38 g of NaCl + 1 g of boric acid + 0.2 g of EDTA-2K + 0.2 g of sodium tetraborate, made up to 1 L with distilled water and 0.5% formaldehyde added, and stored at room temperature.
3. Ficoll Hypaque, stored at room temperature.
4. Propidium Iodine, stored at 4°C.
5. Fluorescence Mounting Media (Dako, Cambridge, UK), stored at 4°C.
6. Tetanus Toxoid, *Clostridium tetani* (Calbiochem, Nottingham, UK), stored at –80°C in aliquots after reconstitution in sterile distilled water.
7. Tritium-labeled thymidine ($^3$H) (Amersham, Biotech, UK).
8. 1% Paraformaldehyde, stored at 4°C.
9. FITC-labeled latex beads (Sigma, UK), stored at room temperature.

### 2.3. Cytokines

All cytokines were aliquoted using PBS + 0.1% bovine serum albumin and stored at –80°C.

1. GM-CSF was obtained from R&D Systems (Oxon, UK) and was stored at $1 \times 10^7$ U/mL.
2. IL-4 was obtained from Prepotec (London, UK) and was stored at $1 \times 10^6$ U/mL.
3. TNF-α was obtained from Benderwein (Boehringer Ingelheim, Germany) and stored at 10 μg/mL.

### 2.4. Primary Antibodies

All antibodies were aliquoted and stored at –80°C.

CD14 was obtained from Harlan Sera Lab (Loughborough, UK); CD83*, CD86*, and CD1a* (nonconjugated antibodies) were bought from Pharmingen International (Oxford, UK), and CD11c, CD40, CD54, and isotype control IgG1 were bought from Diaclone (I.D.S, Tyne&Wear, UK). All antibodies were FITC-conjugated. MHC class-II an anti-DR antibody was generated from the cell line HB-55, which was obtained from the ATCC.

Secondary antibody consisted of a goat anti-mouse FITC-conjugated $F(ab)_2$ fragment and was obtained from Sigma.

Anti-tubulin antibody was obtained from Sigma. The secondary antibody consisted of an anti-IgG mouse antibody PE-conjugated and was obtained from Serotec (Oxford, UK).

## 3. Methods

### 3.1. Blood Separation

The blood packs used were obtained from the National Donor Centre at Sheffield, UK, as a leukophoresis pack containing 80 mL of concentrated

leukocytes obtained from 300 mL of blood. The cells were aspirated from the blood pack and mixed with 80 mL of sterile PBS in a sterile glass bottle.

The blood cells were separated using a density gradient on Ficoll Hypaque; 15 mL of diluted blood were carefully layered onto 7.5 mL of Ficoll Hypaque contained in a sterile universal. The universals were centrifuged at room temperature at 400*g* for 30 min without brake. The plasma layer was removed, placed in a centrifuge tube, and heat inactivated by incubation in a water bath at 56°C for 30 min and left to cool at 4°C for 1 h or until needed. Finally, the plasma sample was centrifuged at 600*g* for 10 min at 4°C and the supernatant carefully aspirated off and kept at -20°C in 5-mL aliquots.

The leukocyte layers were carefully removed with a wide-ended pipet and placed into separate prechilled plastic sterile universals. Cold PBS was then added to fill the tubes. The universals were centrifuged at 600*g* for 15 min at 4°C. The supernatant was centrifuged again under the same conditions and the pellet resuspended in 10 mL of medium. The original pellets were resuspended in 10 mL of cold PBS and centrifuged at 600*g* for 10 min at 4°C. The supernatant from all tubes was discarded and the cells resuspended in 10 mL of RPMI + glutamine. Cells from both tubes were pooled before counting (a total of 20 mL). Cell counts were performed using cells diluted first in 0.6% acetic acid to lyse any remaining red blood cells and subsequently diluted in trypan blue to exclude dead cells.

### 3.2. In Vitro Generation of Immature and Mature Dendritic Cells

This method was adapted from Thurner and coworkers ***(23)***. The generation of immature and mature DCs was obtained after 6 and 8 d in culture, respectively.

#### 3.2.1. Generation of Immature Dendritic cells

At day 0, peripheral blood mononuclear cells (PBMCs) were plated at 4–5 × $10^6$ cells/mL in medium containing either 10% FCS or 1% autologous serum in T75 flasks, with the volume not exceeding 40 mL. The cells were incubated at 37°C for 2 h. Nonadherent cells were then removed, concentrated by centrifugation at 600*g* for 10 min at 4°C, counted, and frozen at $1 \times 10^7$ cells/mL of freezing mixture, consisting of 60 to 70% FCS, 10% DMSO, and medium (designated T-lymphocyte fraction). The same volume of the same medium as used for the 2-h incubation was added to the adherent cells, which were incubated overnight at 37°C.

On day 1, the majority of the cells became nonadherent and were collected in a 50-mL tube, centrifuged at 400*g* for 5 min, resuspended in medium, and counted. The cell concentration was then adjusted to $1 \times 10^6$ cells/mL and 5 mL placed into each well of a 6-well plate and incubated for 45 min at 37°C. The

nonadherent cells were removed and discarded; the wells were washed very gently with medium, and then 5 mL of fresh medium containing the relevant serum, 1000 U/mL GM-CSF, and 500 U/mL IL-4 were added to each relevant well and the plates incubated at 37°C (*see* **Note 1**).

At day 6, immature DCs were apparent in each of the cultures (+FCS or autologous plasma), consisting of nonadherent cells showing long digits. The cells from replicate wells were pooled together and centrifuged at 400*g* and counted.

Some cells were then used for flow cytometric analysis ($2 \times 105$ cells for each cell surface marker to be studied) and used in functional assays as detailed below (*see* **Subheadings 3.4.** and **3.5.**). The concentration of the remaining cells was adjusted to $0.5 \times 106$ cells/mL and used for DC maturation.

#### *3.2.2. Generation of Mature DCs*

The immature DCs were replated at $0.5 \times 106$ cells/mL per well of a 24-well plate in fresh medium containing the relevant serum and 1000 U/mL GM-CSF, 500 U/mL IL-4, and 10 ng/mL of TNF-α (*see* **Note 2**).

The cells were incubated for a further 2 d at 37°C. The mature cells were then harvested from the cultures and the level of expression of different cell surface marker was analyzed by flow cytometry after staining with a panel of antibodies; cultured cells were also used in two functional assays (*see* **Subheadings 3.4.** and **3.5.**).

**Figures 1** and **2** show the morphologic and phenotypic differences between DCs generated in media containing 1% autologous plasma or 10% FCS, as demonstrated by confocal microscopy and flow cytometry.

### *3.3. Differential Expression of Cell Surface Markers by Dendritic Cells Generated After 6 or 8 d of Culture (Flow Cytometric Analysis)*

Immature or mature DCs ($2 \times 10^5$) were placed into individual plastic tubes and washed once in 2–3 mL of blocking buffer to block any unspecific sites. The cells were centrifuged for 5 min at 400*g* and the supernatant decanted off, then the tubes inverted onto a tissue to clear any remaining droplets. Primary antibodies were added to individual tubes and the cells placed on ice for 30 min.

The cells were washed twice in 2 mL of blocking buffer and centrifuged at 400*g* for 5 min at 4°C to remove the excess antibody. The secondary antibody was added (unless directly conjugated antibody was used) to the cells and the tubes put on ice for a further 30 min. Cells were then washed twice with 2 mL of blocking buffer. The supernatant was removed and 200 µL of sheath fluid added to each tube; the cells were analyzed by flow cytometry or covered with foil and stored at 4°C until analysis (*see* **Fig. 2**).

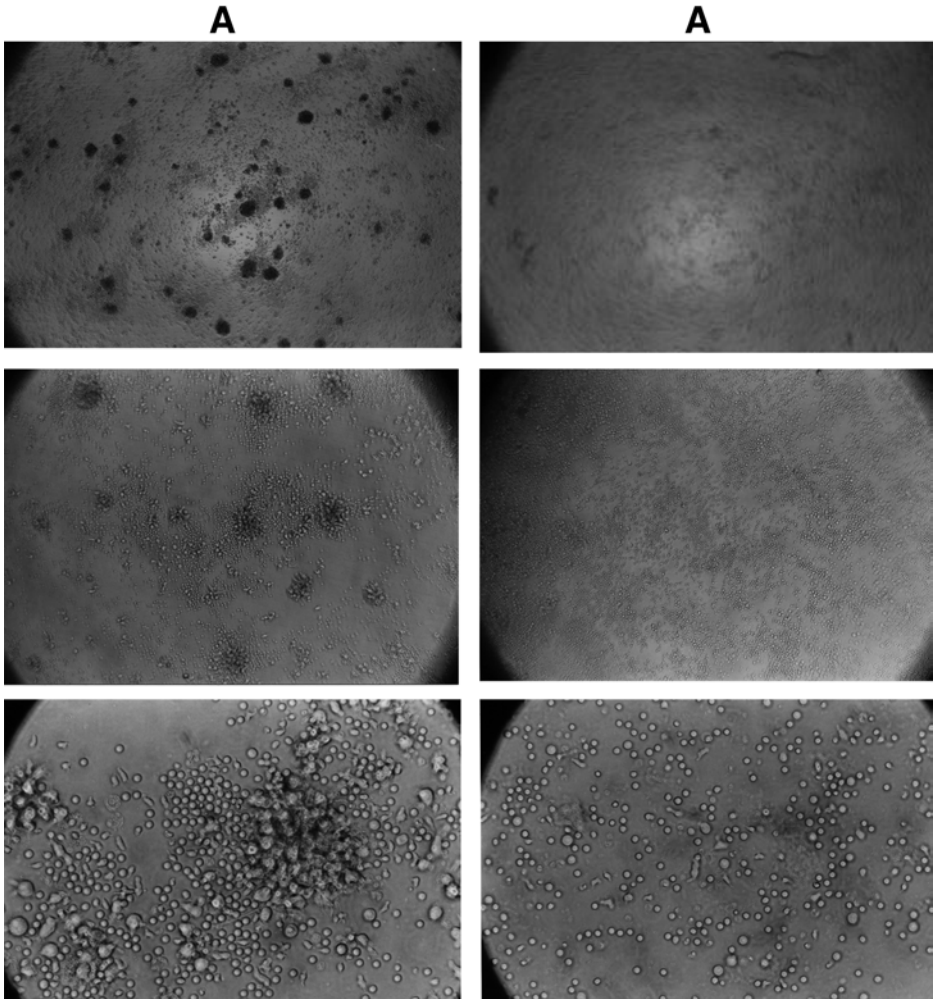


Fig. 1. DCs generated in media containing either 10% FCS **(A)** or autologous **(B)** serum. Adherent PBMCs were cultured for 6 d in RPMI containing 1000 U/mL of GM-CSF and 500 U/mL IL-4 with either 10% FCS (A) or 1% autologous serum (B). Cells are observed under different magnifications (10, 20, and 40×). Cells cultured with FCS show clear cluster formations.

### *3.4. Antigen Presentation Assay*

DCs were incubated for 24–48 h with or without tetanus toxoid (0.5 μg/mL) before coculture with autologous or allogeneic T cells. DCs were plated in triplicate in a 96-well plate (100 μL per well), starting at a concen-

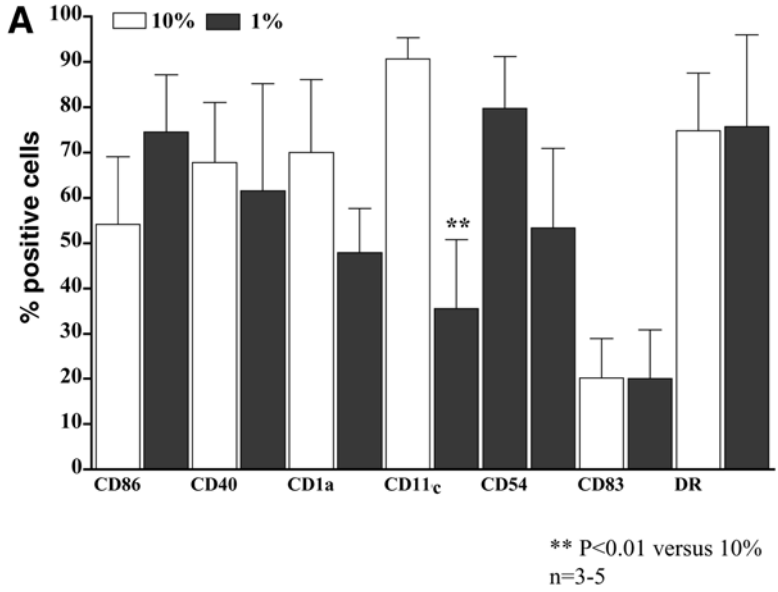


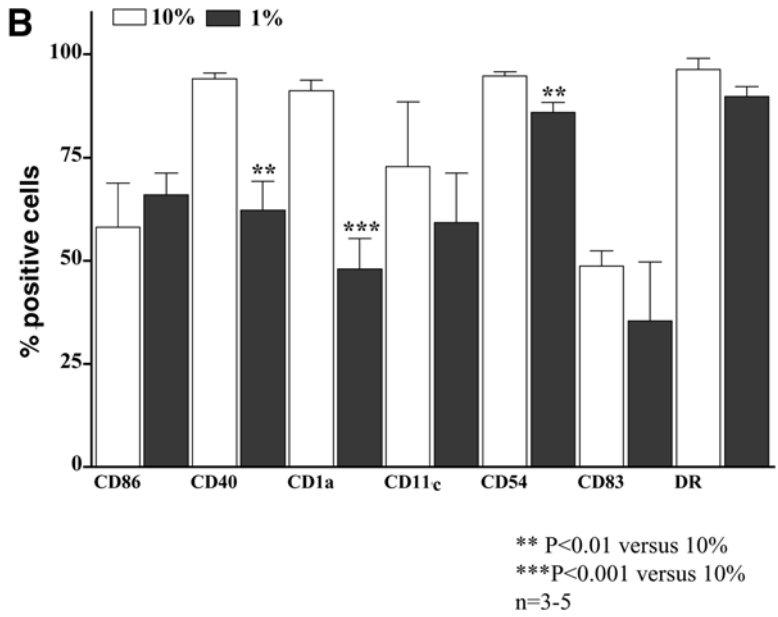


Fig. 2. Cell surface marker expression on immature DCs **(A)** and mature DCs **(B)**. Cell surface marker expression was detected on immature (A) or mature (B) DCs generated with either 10% FCS or 1% autologous serum using a FITC-conjugated antibody (CD11c, CD54) or nonconjugated antibody (CD1a, CD83, CD86, HLA-DR) followed by an FITC-conjugated goat anti-mouse F(ab)′ fragment. Analysis of the samples was by flow cytometry.

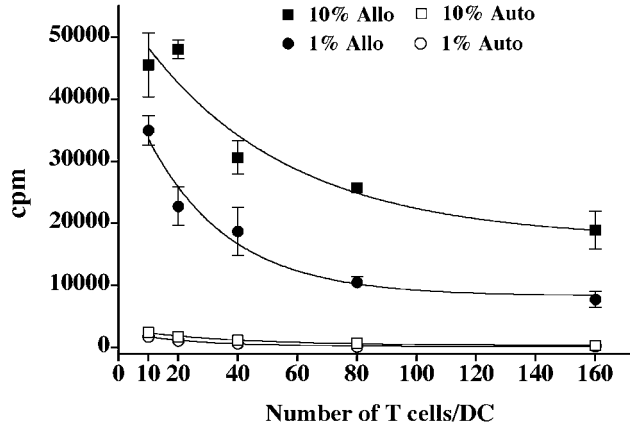


| | 10% Auto | 10% Allo |
|---|---|---|
| 10% Auto | / | ** P<0.01 |
| 1% Auto | NS | ** P<0.01 |
| 10% Allo | ** P<0.01 | / |
| 1% Allo | * P<0.05 | * P<0.05 |

Fig. 3. T cell proliferation in response to allogeneic and autologous DCs. DCs generated with either 10% FCS or 1% autologous serum were cocultured with autologous or allogeneic T cells for 6 d. Twenty microliters of 0.37 *M* bq/mL tritiated thymidine was then added to each well for the last 18 h. Both DC populations were able to induce an allogeneic T cell proliferation response but no or very little autologous T cell proliferation.

tration of $2 \times 10^5$ cells/mL and then diluted down. Autologous or allogeneic T-cells were removed from liquid nitrogen, washed twice with medium, counted, and made up to a concentration of $2 \times 106$ cells/mL in medium containing the relevant serum. Cells (100 µL) were added to relevant wells. Plates were incubated for 6 d at 37°C. Tritiated ($^3$H) thymidine was added for the last 18 h. The cells were harvested onto filter paper, which was transferred into scintillation tubes, followed by the addition of 2 mL of scintillation fluid. Counts per minute for each well were detected using a gamma spectrophotometer (*see* **Figs. 3 and 4**).

### 3.5. Phagocytosis Assay

For the phagocytosis assay, $0.5 \times 10^6$ cells/500 µL of immature or mature DCs were seeded into chamber slides in duplicate. FITC-labeled latex beads

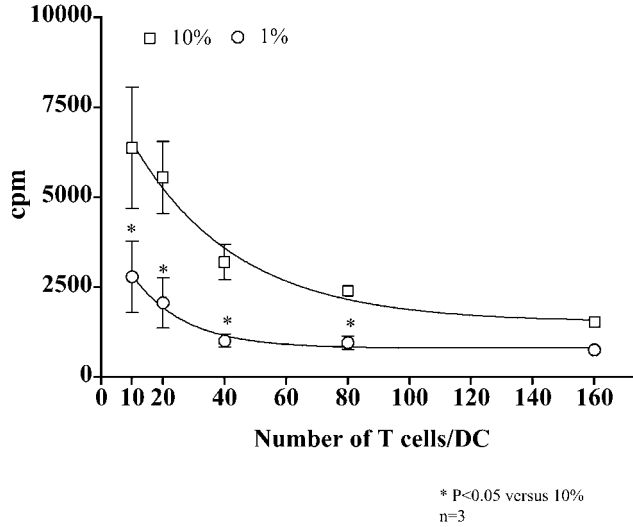


Fig. 4. T cell proliferation in response to dendritic cells incubated with 0.5 µg/mL tetanus toxoid. DCs generated with either 10% FCS or 1% autologous serum were incubated o/n with 0.5 µg/mL of tetanus toxoid protein and then cocultured with increasing numbers of autologous T cells for 6 d. Twenty microliters of 0.37 *M* bq/mL tritiated thymidine was then added to each well for the last 18 h. Both DC populations were able to induce autologous T cell proliferation when 0.5 µg/mL tetanus toxoid was used.

(10 µL of a 1/200 dilution) were added to each well, and the chamber was incubated at 37°C for 24 h. The medium was then removed and the cells gently washed with PBS. After removal of PBS from each well, the cells were fixed with 500 µL of 1% paraformaldehyde solution for 10 min at room temperature and then washed in PBS. Antitubulin (50 µL; 1/200 dilution) antibody was then added to each well for 30 min, and then the cells washed twice with PBS for 5 min to remove the excess of antibody. The cells were then stained with propidium iodine (10 µg/mL) for 1 min and the cells again washed twice with PBS. The plastic chambers on the slides were removed and Dako immunofluorescence mounting medium added to each slide. Coverslips were placed over the chambers, which were sealed with nail varnished (*see* **Fig. 5**).

### *3.6. Conclusions and Discussion*

The potential role of DCs in cancer immunotherapy has been firmly established in experimental tumor-therapy models and in a number of human clinical trials ***(25–28)***. DC-based cancer vaccines, formulated by loading DCs with antigenic peptides or tumor lysates or through genetically modifying DCs

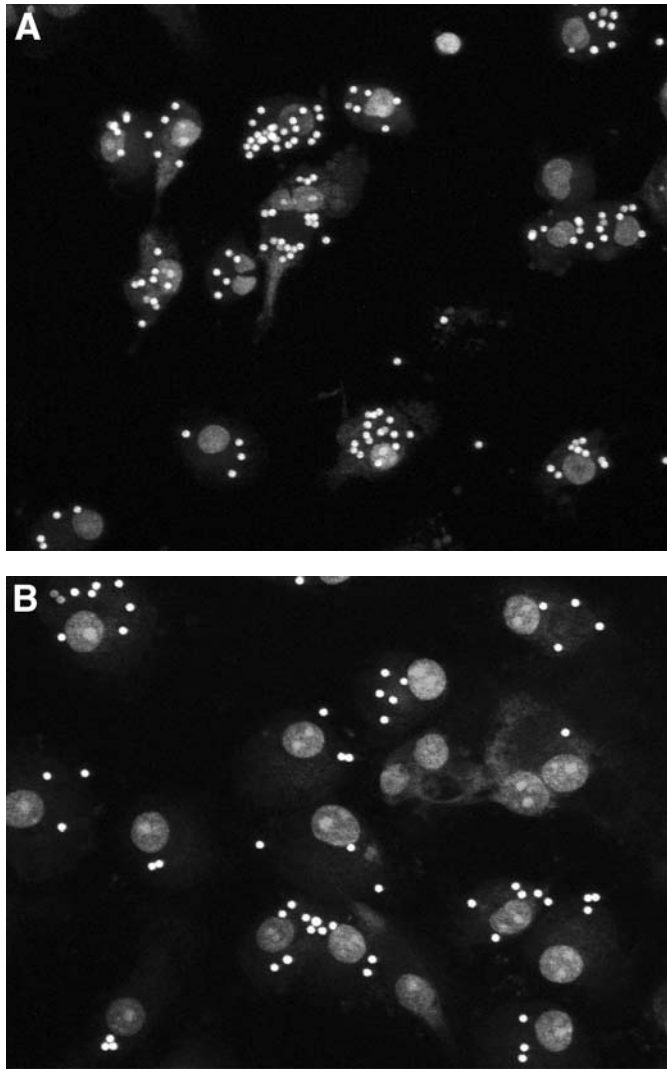


Fig. 5. Bead uptake by immature dendritic cells (**A** and **B**) or mature DCs **(C)**. DCs cultured for 6 d (A and B) or 10 d (C) were incubated overnight at 37°C with FITC-labeled latex beads (0.2 μm). Nuclei were stained with ethidium bromide and cytoskeleton with a mouse antitubulin antibody followed by a PE-conjugated anti-mouse antibody. When the cells were observed under confocal microscope, beads could be observed inside the immature DCs (A and B) but not or very little inside the matured DCs (C). *(Figure continues.)*

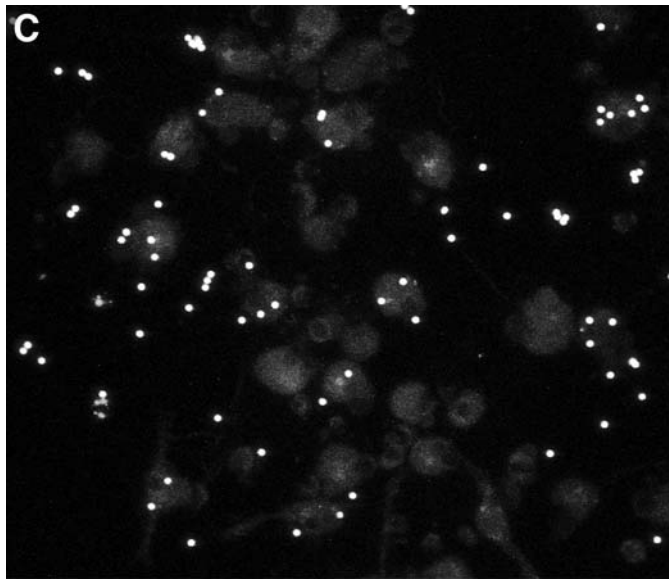


Fig. 5. *(Continued.)*

before in vivo administration represents a potentially powerful therapeutic strategy. Genetically modified or peptide pulsed DCs can generate effective immune responses to established tumors or subsequent tumor challenge. Autologous DCs from normal individuals or patients with prostate cancer transfected with RNA encoding PSA are effective in stimulating PSA-specific CTL in vitro, implying that neither natural tolerance to PSA antigens nor tumor-mediated T cell anergy represents a barriers for CTL generation against the self-antigen PSA ***(7)***. Delivering activated DCs (genetically modified or unmodified) directly into the tumor microenvironment was shown to enhance immunity and bypass the requirement for selective recruitment and local activation of DCs, which is usually disordered in tumors. DC inactivation has been clearly demonstrated in prostate cancer, where monocyte maturation to give rise to DCs is significantly inhibited, as assessed by the expression of DC markers CD1a and CD83 and T cell proliferation ***(29)***. We have recently shown, using a murine CT26 tumor model, that combined intratumor injection of disabled infectious single-cycle Herpes Simplex Virus (HSV) virus encoding mGM-CSF (DISC-mGM-CSF) and syngeneic bone marrow-derived DCs reduced the tumor growth of both primary and distant tumor implants ***(25)***. A period of 4–6 h between the injection of DISC-mGM-CSF virus and DCs was required to enhance the therapeutic effect. Similar therapeutic efficacy was also reported by others using intratumor injection of DCs engineered to secrete

IL-12 or modified to express CD40L ***(30–32)***. To select the appropriate conditions for DCs in therapy, the following criteria need to be addressed: antigen selection, methods for generation and activation of DCs, introducing (targeting) the antigen into either the MHC class-I or class-II processing pathways, and route of administration.

In the present study, culturing human adherent PBMC for 6 d in the presence of GM-CSF and IL-4 successfully generated DCs using media containing either FCS or autologous serum supplements. DCs have to be matured to become potent T-cell stimulators. During the maturation process a variety of different, specific genes are expressed, including genes encoding costimulatory molecules, MHC class-I and class-II antigens ***(9)***; in addition, maturation induces the rearrangement of cytoskeleton proteins, adhesion molecules and cytokine receptors ***(9)***. A series of tests was conducted to evaluate the phenotypic and functional status of the activated DCs, including MLR, cell surface markers expression, latex beads uptake, and antigen processing. DCs at day 6 were considered immature because they were efficient in taking up latex particles, necrotic cells, and tetanus protein; they expressed low levels of cell surface markers and induced a weak stimulation of allogeneic T cells in MLR (results not given). Culturing DCs for a further 2 d in the presence of TNF-α induced maturation, which was manifested by potent stimulation of allogeneic T-cells in MLR increased expression of CD86, CD40 and CD83, and downregulation of bead uptake.

Generation of DCs in medium containing human plasma (preferably autologous) is required if they are to be used for human therapy. Significant differences in the immunophenotype, macropinocytosis, endocytosis, and activity in MLR have, however, been reported between DCs generated in FCS vs human plasma ***(24)***. In our hands, high yields, increased expression of costimulatory molecules, and cell clustering during the first 3 d of culture were observed when PBMC were cultured in media supplemented with 10% FCS but not in 1% autologous plasma. A significant increase in the expression of CD1a, CD40, and CD54 was observed in DCs cultured in the presence of 10% FCS for 10 d in comparison with those cultured in autologous plasma; in addition, similar differences were noticed in functional assays using MLR.

## 4. Notes

1. All these steps of adherence were used to purify monocyte-derived DCs. Monocytes, macrophages, and B cells can all adhere to the plastic but with different intensity and longevity. Monocytes will adhere very quickly to the plastic and elute off after overnight incubation before finally adhering again very quickly to the plastic during the second stage of adherence. Macrophages will also adhere relatively quickly to the plastic but remain firmly adhered even after overnight incubation. B-cells may stick after the first adherence stage of 2 h but will elute off permanently after overnight incubation.

2. DCs can revert back to their original form when the cytokines are removed until they have fully matured; therefore, cytokines need to be replenished ***(36)***.

## Acknowledgments

We wish to acknowledge Steve Reeder for his technical assistance. This work was supported by the Dowager Eleanor Peel Trust, The Cancer and Polio Research Fund, The Medical Research Council, and The National Eye Research Centre.

## References

1. Krikorian, J., Portlock, C., Cooney, D., and Rosenberg, S. (1980) Spontaneous regression of non-Hodgkin's lymphoma. A report of nine cases. *Cancer* **46,** 2093–2099.
2. Lodge, P. A., Jones, L. A., Bader R. A., Murphy, G. P., and Salgaller, M. L. (2000) Dendritic cell-based immunotherapy of prostate cancer: Immune monitoring of a phase II clinical trial. *Cancer Res.* **60,** 829–833.
3. Zhang, S., Zhang, H. S., Reuter, V. E., Slovin, S. F., Scher, H. I., and Livington, P. O. (1998) Expression of potential target antigens for immunotherapy on primary and metastatic prostate cancers. *Clin. Cancer Res.* **4,** 295–302.
4. Murphy, G., Tjoa, B., Ragde, H., Kenny, G., and Boynton, A. (1996) Phase I clinical trial: T cell therapy for prostate cancer using autologous dendritic cells pulsed with HLA-A0201-specific peptides from prostate-specific membrane antigen. *Prostate* **29,** 371–380.
5. Tjoa, B. A., Simmons, S. J., Elgamal, A., Rogers, H., Kenny, G. M., Troychak, M. J., et al. (1999) Follow-up evaluation of a Phase II prostate cancer vaccine trial. *Prostate* **40,** 125–129.
6. Peshwa, M.V., Shi, J. D., Ruegg. C., Laus, R., and Schooten, W. C. (1998) Induction of prostate tumour-specific CD8+ cytotoxic T-lymphocytes in vitro using antigen-presenting cells pulsed with prostate acid phosphatase peptide. *Prostate* **36,** 129–138.
7. Heiser, A., Dahm, P., Yancey, D. R., Maurice, M. A., Boczkowski, D., Nair, S. K., et al. (2000) Human dendritic cells transfected with RNA encoding prostate-specific antigen stimulate prostate-specific CTL responses in vitro. *J. Immunol.* **164,** 5508–5514.
8. Steinman, M. R. (1991) The dendritic cell system and its role in immunogenicity. *Ann. Rev. Immunol.* **9,** 271–296.
9. Sallusto, F. and Lanzavecchia, A. (1994) Efficient presentation of soluble antigen by cultured human dendritic cells is maintained by granulocyte/macrophage colony-stimulating factor plus interleukin 4 and down regulated by tumour necrosis alpha. *J. Exp. Med.* **179,** 1109–1118.
10. Cella, M., Scheidegger, D., Plamer, L. K., Lane, P., Lanzavecchia, A., and Alber, G (1996) Ligation of CD40 on dendritic cells triggers production of high levels of interleukin-12 and enhances T cell stimulatory capacity: T-T help via APC activation. *J. Exp. Med.* **184,** 747–752.

11. Rodriguez, A., Regnault A., Kleijmeer, M., Ricciardi-Castagnoli, P., and Amigorena, S. (1999) Selective transport of internalized antigens to the cytosol for the MHC class I presentation in dendritic cells. *Nat. Cell. Biol.* **1,** 362–368.
12. Bachmann, M. F., Lutz, M. B., Layton, G. T., Harris, S. J., Fehr, T., Rescigno, M., and Ricciardi-Castagnoli, P. (1996) Dendritic cells process exogenous viral proteins and virus-like particles for class I presentation to CD8+ cytotoxic T lymphocytes. *Eur. J. Immunol.* **26,** 2595–2600.
13. Inaba, K., Metlay, J. P., Crowley, M. T., and Steinman, R. M. (1990) Dendritic cells pulsed with protein antigens in vitro can prime antigen-specific, MHC-restricted T cells in situ. *J. Exp. Med.* **172,** 631–640.
14. Shen, Z., Reznikoff, G., Dranoff, G., Kennteth, L., and Rock, L. (1997) Cloned dendritic cells can present exogenous antigens on both MHC class I and class II molecules. *J. Immunol.* **158,** 2723–2730.
15. Sauter, B., Albert, M. L., Francisco, L., Larsson, M., Somersan, S., and Bhardwaj, N. (2000) Consequences of cell death: Exposure to necrotic tumor cells, but not primary tissue cells or apoptotic cells, induces the maturation of immunostimulatory dendritic cells. *J. Exp. Med.* **191,** 423–433.
16. Rovere, P., Vallinoto, C., Bondanza, A., Crosti, M-A., Ricciardi-Castagnoli, P., Rugarli, C., and Manfredi, A. A. (1998) Cutting edge: Bystander apoptosis triggers dendritic cell maturation and antigen-presenting function. *J. Immunol.* **161,** 4467–4471.
17. Tsai, V., Southwood, S., Sidney, J., Sakaguchi, K., Kawakami, Y., Appella, E., et al. (1997) Identification of subdominant CTL epitopes of the GP100 melanoma-associated tumor antigen by primary in vitro immunization with peptide-pulsed dendritic cells. *J. Immunol.* **158,** 1796–1802.
18. Van Elsas, A., van der Burg, S. H., van der Minne, C. E., Borghi, M., Mourer, J. S., Melief, C. J. M., and Schrier, P. I. (1996) Peptide-pulsed dendritic cells induce tumoricidal cytotoxic T lymphocytes from healthy donors against stably HLA-A*0201-binding peptides from the Melan-A/Mart-1 self antigen. *Eur. J. Immunol.* **26,** 1683–1689.
19. Hsu, F., Benike, C., Fagnoni, F., Liles, T. M., Czerwinski, K., Taidi, B., et al. (1996) Vaccination of patients with B-cell lymphoma using autologous antigen pulsed dendritic cells. *Nat. Med.* **2,** 52–58.
20. Bender, A., Sapp, M., Schuler, G., Steinman, R. M., and Bhardwaj, N. (1996) Improved methods for the generation of dendritic cells from nonproliferating progenitors in human blood. *J. Immunol. Meth.* **196,** 121–135.
21. Romani, N. and Reider, D (1996) Generation of mature dendritic cells from human blood. An improved method with special regard to clinical applicability. *J. Immunol. Meth.* **196,** 137–151.
22. Caux, C., Dezutter-Dambuyant, D., Schmitt, D., and Banchereau, J. (1992) GM-CSF and TNF-alpha cooperate in the generation of dendritic Langerhans cells. *Nature* **360,** 258–261.
23. Thurnher, M., Papesh, C., Ramoner, R., Gastl, G., Bock, G., Radmayr, C., et al. (1997) In vitro generation of CD83+ human blood dendritic cells for active tumor immunotherapy. *Exp. Hematol.* **25,** 232–237.

24. Pietschmann, P., Stockl, J., Draxler, S., Majdic, O., and Knapp, W. (2000) Functional and phenotypic characteristics of dendritic cells generated in human plasma supplemented medium. *Scand. J. Immunol.* **52,** 377–383.
25. Ali, S. A., Lynam, J., McLean, C. S., Entwisle, C., Loudon, P., Rojas, J. M., et al. (2002) Tumor regression induced by intratumor therapy with a disabled infectious single cycle (DISC) Herpes Simplex Virus (HSV) vector, DISC/HSV/murine granulocyte-macrophage immunity. *J. Immunol.* **168,** 3512–3519.
26. Wang, L. R., Jeffery, F., Marty, G., Kuniyoshi, V., Bade, J., Ryback, E., et al. (2001) Phase I trial of intravenous peptide-pulsed dendritic cells in patients with metastatic melanoma. *J. Immunother.* **24,** 66–78.
27. Esche C., Shurin M. R., and Lotze MT. (1999) The use of dendritic cells for cancer vaccination. *Curr. Opin. Mol. Ther. **1,*** 72–81.
28. Morse M. A. and Lyerly H. K. (2000) Clinical applications of dendritic cell vaccines. *Curr. Opin. Mol. Ther.* **2,** 20–28.
29. Aalamian, M., Pirtskhalaishvili, G., Nunez, A., Esche, C., Shurin, G. V., Huland, E., et al. (2001) Human prostate cancer regulates generation and maturation of monocyte-derived dendritic cells. *Prostate* **46,** 68–75.
30. Nishioka, Y., Hirao, M., Robbins, P. D., Lotze, M. T., and Tahara, H. (1999) Induction of systemic and therapeutic antitumor immunity using intratumoral injection of dendritic cells genetically modified to express interleukin 12. *Cancer Res.* **59,** 4035–4041.
31. Melero, I., Duarte, M., Ruiz, J., Sangro, B., Galofre, J., Mazzolini, G., et al. (1999) Intratumoral injection of bone-marrow derived dendritic cells engineered to produce interleukin-12 induces complete regression of established murine transplantable colon adenocarcinomas. *Gene Ther.* **6,** 1779–1784.
32. Kikuchi, T. and Crystal, R. G. (1999) Anti-tumor immunity induced by in vivo adenovirus vector-mediated expression of CD40 ligand in tumor cells. *Human Gene Ther.* **10,** 1375–1387.

# 22

# Flavonoid Compounds in the Prevention and Treatment of Prostate Cancer

**Graham E. Kelly and Alan J. Husband**

## 1. Introduction

Compounds based on a flavonoid (di-phenolic) ring structure are emerging as a potentially important new class of pharmaceutical compounds with a broad range of biological activities, most prominent of which is their potential role as anticancer agents.

Flavonoids account for the single largest chemical class in the plant kingdom, with over 5000 different flavonoids described. Plant flavonoids appear on the whole to be biologically active compounds, as opposed to structural or nutritional compounds, participating in a wide range of fundamental biochemical processes within plant cells. Many of them are plant hormones, regulating important biological processes, such as plant growth and reproduction. This points to flavonoids playing key regulatory roles in cell cycle kinetics.

The mechanisms involved in the ability of these compounds to exert such a wide range of upregulating and downregulating effects on signal transduction processes within plant cells are largely unknown. But because flavonoids share the same basic di-phenolic steric structure as steroidal compounds, it is thought likely that they may operate, at least in part, through phenolic receptors similar to the steroid receptors found in plant and animal cells. Whatever the mechanism(s), the ubiquity of flavonoids in the plant kingdom and their broad range of important regulatory functions in plants, point to their being an important fundamental regulatory mechanism in cell biology involving phenolic compounds that to date has avoided description.

Interest in the potential role of plant flavonoids in prostate health was stimulated by epidemiological evidence of an inverse relationship between the incidence of both benign prostatic hyperplasia (BPH) and prostate cancer and the

From: *Methods in Molecular Medicine, Vol. 81: Prostate Cancer Methods and Protocols*
Edited by: P. J. Russell, P. Jackson, and E. A. Kingsley © Humana Press Inc., Totowa, NJ

dietary intake of foods rich in plant flavonoids ***(1)***. For example, BPH is more common in elderly men in Western countries than in men from the East ***(2),*** and the incidence of metastatic prostate cancer is approx 30 times higher in Western men than in age-matched men in China and eight times higher than in Japanese men ***(3)***. That these epidemiological differences are not associated with genetic or racial factors is evidenced by the following observations: (1) that Caucasian Seventh-Day Adventist men who maintain a traditional Adventist vegetarian diet suffer a much lower rate of prostate cancer compared to non-Adventist men ***(4),*** and (2) that Asian men who migrate to North America generally adopt the American prostate cancer incidence within one to two generations ***(5,6)***. The essential points of distinction between the typical Western diet vs the Asian or vegetarian diet are a greater reliance on meat for protein requirements and greater use of refined, fiber-free carbohydrates for energy requirements. Early interest in the link between diet and an increased risk of prostate cancer in Western men focused on dietary factors, such as animal fats, that might be actively promoting cancer development. The general lack of success in that area has led in recent years to an alternative view that the Asian (or vegetarian) diet contains factors that restrain the progression of latent prostatic disease into full-blown disease.

Most of the research into the potential role of flavonoids in prostate health has focused on the subset of these compounds known as isoflavones. Isoflavones are simple phenolic compounds that perform a wide variety of hormonal and growth factor functions in plants. There are over 1000 identified, the great majority of which are restricted to members of the *Leguminosae* family of plants. Of the large variety of isoflavones consumed daily by humans, four isoflavones are prominent because of their generally high levels in legumes commonly used as human foodstuffs: biochanin and formononetin and their respective demethylated derivatives, genistein and daidzein.

These four isoflavones are subjected to bacterial fermentation in the gut and demethylation by the liver to yield a variety of isoflavonoid compounds that circulate freely in the plasma and ultimately in the urine primarily as glucuronide conjugates and sulfates ***(7,8)***. The human prostate actively concentrates these dietary substances within the prostate tissue, further suggesting an evolutionary based role for these compounds in prostatic homeostasis. In a recent study comparing Chinese men in Hong Kong and Caucasian men in the United Kingdom, isoflavonoid levels in prostatic fluid were approx 7 times higher in the Chinese men ***(9)***.

## 2. Potential for Flavonoids to Reduce Incidence and Severity of BPH

With respect to BPH, there are a number of biological activities attributed to isoflavones that may have relevance in regulating the growth and function of

the prostate gland, contributing to a reduction in the incidence and severity of BPH in older men.

### 2.1. Effects on Androgen/Estrogen Activity

Androgens and estrogens play key roles in the development of prostatic proliferative diseases. Isoflavones may influence these roles through their influence on both the production of steroidal hormones and the interaction of these hormones with their specific receptors. Isoflavones exert both agonist and antagonist effects on the estrogen receptor (ER) depending on the relative proportion of steroidal and phenolic (isoflavonoid) estrogens. Isoflavones are able to bind to the human ER, to activate that receptor, and to initiate gene expression that is linked to the ER. However, compared with 17β-estradiol, these phenolics have considerably low receptor affinity and are weak estrogens, with estrogenic potencies between $10^{-2}$ and $10^{-4}$ compared with 17β-estradiol ***(10,11)***. The weak estrogenic effect of isoflavones means that they also display moderate anti-estrogenic activity. By binding to the ER and preventing the more potent steroidal estrogens, such as estradiol, reaching the receptor, their weaker estrogenic effect means that they are acting as competitive inhibitors ***(11,12)***. However, there is no evidence that isoflavones have any affinity for or ability to activate the androgen receptor ***(13)***.

Isoflavones also influence the production and metabolism of steroidal estrogens and androgens in a number of ways.

#### 2.1.1. Aromatase Inhibition

Biochanin is a moderate inhibitor of human estrogen synthetase (aromatase) activity ***(14)***; this appears to be a particular feature of biochanin because daidzein and genistein have little or no such activity. Aromatase is the enzyme in fat and muscle cells that is responsible for the conversion of androstenedione to estrone, and in men, this activity accounts for approximately two-thirds of estrogen produced. Declining testicular activity and increasing aromatization around midlife leading to a decrease in the androgen/estrogen balance is considered by some researchers to be a dominant factor in stromal hyperplasia ***(15)***.

#### 2.1.2. 5α-Reductase Inhibition

Genistein, daidzein, biochanin, and isoflavone metabolites, such as equol, are potent inhibitors of 5α-reductase activity, producing 80% inhibition at concentrations of 100 μ*M* ***(16)***. 5α-Reductase is located on the nuclear membrane of prostate cells and is responsible for the conversion of testosterone to 5α-dihydrotestosterone (DHT). DHT has about five times greater affinity compared with testosterone for the prostate androgen receptor and is the principal

androgen in the prostate *(17,18)*. Young Japanese men are reported to have lower 5-α-reductase activity compared with their Western counterparts *(19)*.

#### 2.1.3. 17β-Hydroxysteroid Dehydrogenase Inhibition

This enzyme is involved in the reversible interconversion of testosterone to androstenedione and plays an important role in the metabolism of both androgens and estrogens. Genistein, biochanin, daidzein, and isoflavonoid metabolites, such as equol, are potent inhibitors of this enzyme at concentrations as low as 10 μ*M* *(16,20)*.

#### 2.1.4. Sterol Sulfatase Inhibition

Daidzein is a potent inhibitor of sterol sulfatase, being effective at concentrations as low as 1 μ*M* *(21)*. Sterol sulfatase is an important enzyme in the metabolism of estrogens and androgens to the more biologically active sulfated forms.

#### 2.1.5. Increased UDP-Glucuronyltransferase Activity

Biochanin is a potent stimulator of this enzyme in human prostate cells, leading to the intracellular accumulation of testosterone as glucuronidated metabolites *(22)*. By increasing the intracellular glucuronidation of testosterone, biochanin successfully decreases the testosterone-stimulated release of prostate-specific antigen, pointing to a downregulation of the effect of androgen on the prostate *(23)*.

### 2.2. Effects on Cell Cycle and Cell Differentiation

The various growth factors that help to regulate the growth and function of prostate cells act via receptors in the cell membrane. Activation of those receptors requires the involvement of various enzyme systems that ultimately lead to the production of substances that affect DNA transcription and protein synthesis. The end result of this process may be to instruct the cell to divide or to differentiate or to perform a specialized function.

Isoflavones modulate a wide range of cytoplasmic and nuclear enzyme systems that are integral to these signal transductions regulating cell division and differentiation. Two particular enzyme systems that play key roles in cell proliferation and differentiation are the protein tyrosine kinases (PTKs) and the DNA topoisomerases. Although regulation of these nuclear enzymes may assist in maintaining normal prostate size, these actions of flavonoids are also relevant to their potential anticancer effects, which will be discussed in more detail below.

### 2.3. Role of Flavonoids in Prostate Cancer

In more recent times, intense interest has focused on the potential for plant flavonoids in the prevention and/or treatment of prostate cancer. The first

flavonoid to be extensively tested in this regard was quercetin, a flavone found in vegetables, such as onions and apples, and a common component of most human diets. Quercetin was found to be a relatively potent regulator of such fundamental biochemical processes as $NA^+K^+$ATPase ***(24)*** and $Ca^{2+}$ATPase ***(25)*** and reverse transcriptases ***(26)***. It also was the first inhibitor of PTKs to be described ***(27),*** and because many of the PTKs are oncogenes, this raised the possibility of quercetin being an effective anticancer compound. Quercetin also was found to be a potent inhibitor of phosphatidyl-3 kinase ***(28)*** and 1-phosphatidylinositol-4 kinase ***(29),*** important enzymes in proliferation-signaling pathways ***(30),*** suggesting a potential role in inhibiting cell proliferation. Subsequently, quercetin was found to cause cell cycle arrest in late G1 phase of human leukemic T cells and gastric, breast, and ovarian cancer cells ***(31,32)***. Quercetin also is reported to induce apoptosis in cancer cells through a pathway involving the heat shock proteins ***(33)*** as well as through downregulation of the mutant *p53* gene, which can block apoptosis ***(34)***.

Quercetin ultimately progressed to being tested as an intravenous agent in a Phase 1 study in cancer patients. It was shown to achieve inhibition of lymphocyte tyrosine kinase activity as well as providing some evidence of antitumor activity ***(33)***. Short-term administration of this compound in DMSO was found to be well tolerated; however, quercetin failed to progress to further clinical assessment, largely because it was recognized that there were other naturally occurring flavonoids with more potent anticancer activity.

Considerable attention has been focussed on the use of genistein for prostate cancer treatment. Genistein is a considerably more potent anticancer agent than quercetin and has been described as having anticancer activity in vitro against various types of human and animal cancers, including melanoma ***(35),*** leukemia ***(35–37),*** breast cancer ***(38–41),*** gastrointestinal cancers ***(42,43),*** prostate cancer ***(44)*** and neuroblastoma, Ewing's sarcoma, and rhabdomyosarcoma ***(45)***. Genistein, like quercetin, is a potent inhibitor of PTKs, preventing phosphorylation of PTKs at their receptor site; genistein inhibits most members of this large class of enzymes ***(23,46)***. Genistein also is a potent inhibitor of DNA topoisomerases I and II ***(47)***. The effect of these actions is to downregulate signal transduction mechanisms leading to mitotic arrest of cancer cells in the G2/M phase of mitosis ***(42),*** induction of terminal differentiation of cancer cells ***(35,37,48),*** and induction of apoptosis ***(49)***. Genistein also displays a range of other biological effects with potential anticancer outcomes, including inhibition of angiogenesis ***(50)*** and promotion of cancer cell adhesion ***(51)***.

Genistein was considered by the US National Cancer Institute in 1998 as an oral chemotherapeutic for prostate cancer particularly because of its high safety index and potent and novel anticancer mechanisms, making it an attractive potential anticancer agent. However, genistein failed to meet the NCI activ-

ity criteria when tested in xenograft animal models bearing human tumors, and Phase I studies did not proceed.

Another flavonoid to receive attention as a potential anticancer agent has been flavopiridol. This semisynthetic compound, an *N*-methylpiperinidyl, chlorophenyl flavone, based on a naturally occurring plant flavonoid, is a potent cyclin-dependent kinase inhibitor capable of mitotic arrest in either G1 or G2 ***(52)***. Flavopiridol exhibits antiproliferative activity in vitro against a broad range of human cancer cells, including nonsmall cell lung cancer cells ***(53)*** and prostate cancer and melanoma cells ***(54)***.

Flavopiridol underwent early stage clinical studies in 1998–1999 as an intravenous chemotherapeutic for gastric cancer and chronic myeloid leukemia in particular. Although those early studies (using flavopiridol administered by intravenous infusion dissolved in the carrier hydroxypropyl-β-cyclodextrin) revealed promising anticancer activity, flavopiridol was found also to have dose-limiting toxicity, the main side effects being nausea, diarrhea, fatigue, and fluid retention.

The conclusion from these various studies is that flavonoids as a chemical class offer a potentially important and novel approach to cancer therapy. The small number of flavonoids tested to date indicate that they exert a range of regulatory effects on human cells, in particular acting as regulators of dysfunctional cell cycle kinetics that are at the heart of carcinogenesis. They appear also to be relatively discriminating, acting predominantly on dysfunctional cells and thus pointing to a high level of safety.

### 2.4. Human Flavonoid Metabolites as Anticancer Agents

The potential for treatment of prostate cancer using flavonoid compounds has been rekindled by observations that although these compounds are moderately effective in native form, they form the substrate for a range of human metabolites. It is known that dietary isoflavones undergo variable degrees of metabolism within the body and that both the parent isoflavones and their metabolites are found in the body. This metabolism is thought to take place in two sites—through fermentation in the microflora of the gut and metabolism within the liver. A variety of metabolites of the isoflavones daidzein, genistein, formononetin, and biochanin are described. Those that have been identified in human fluid and characterized are as follows: equol (4′,7-dihydroxyisoflavan) ***(55)***; an isomer of equol (3′,7-dihydroxyisoflavan) ***(56)***; dihydrodaidzein (7,4′-dihydroxyisoflavone) ***(57)***; *cis* and *trans* isomers of tetrahydrodaidzein (7,4′-dihydroxyisoflavonol) ***(57)***; *O*-demethylangolensin [1-(2′,4′-dihydroxyphenol)-2-(4′′-hydroxyphenyl)-propan-1-one] ***(58)***; 6′-hydroxy-*O*-demethylangolensin [1-(2′,4′,6′-trihydroxyphenyl) -2-(4′′-hydroxyphenyl)-propan-1-one] ***(57)***; and 2-dehydro-*O*-demethylan-

golensin demethylangolensin [1-(2′,4′-trihydroxyphenyl)-2-(4″-hydroxyphenyl)-prop-2-1-one] ***(57)***. A further compound, 2H-1-benzopyran-7-ol, 3-(4-hydroxyphenyl), is a putative intermediate compound in the fermentation pathway from daidzein to equol ***(59)*** and has been given the common name dehydroequol ***(60)***. Recently, dehydroequol has been identified as a normal constituent of plants with the common name Haginin E ***(61)***.

The potential for each of these isoflavonoid metabolites to express anticancer properties and their potency relative to the parent isoflavones has not been previously described. However, a number of reports have noted considerable variation between individuals in their profile of isoflavonoid metabolites, leading to speculation on a possible link between metabolite profiles and differences in individual susceptibility to various diseases, including cancer ***(8,62)***. For instance, the lower rates of excretion of equol ***(63)*** and *O*-demethylangolensin ***(64)*** in the urine of women with breast cancer compared with women without breast cancer has been noted. However, the relative contributions of the parent isoflavones and their individual metabolites to the overall anticancer effect have not been established.

In pursuit of the pharmaceutical opportunities represented by these compounds, Novogen research has been focused on the synthesis of a panel of compounds based on the structure of selected metabolites for screening with regard to anticancer effect. This has produced a lead compound, phenoxodiol, which is a proprietary synthetic derivative of one of these compounds that, in preclinical screening, has produced potent anticancer activity against a range of cancer targets, including prostate cancer. In view of its potential to inhibit proliferation of prostate cancer cells, it has been further tested for anticancer properties as a potential prostate cancer therapeutic.

## 2.5. Preclinical Evaluation of Phenoxodiol as a Prostate Cancer Therapeutic Drug

### 2.5.1. Effects on Cancer Cell Proliferation

Phenoxodiol inhibits the proliferation of a variety of human cancer cell lines in vitro in a dose-dependent fashion and is between 5–20-fold more potent than genistein in its antiproliferative effects (*see* **Fig. 1**). The $IC_{50}$ values for phenoxodiol (*see* **Table 1**) range between 1 and 15 mg/mL (4.2–62.5 m*M*). No cancer type specificity is observed with the exception of the human colon cancer cell line HT29, where a higher $IC_{50}$ value of 15.0 (62.5 m*M*) mg/mL was recorded. This result is consistent with the known ability of the HT29 cell line to rapidly conjugate compounds to their β-glucuronides, rendering such compounds less bioactive ***(65)***. Flow cytometric analysis (*see* **Fig. 2**) shows that phenoxodiol arrests cells in G1 phase.

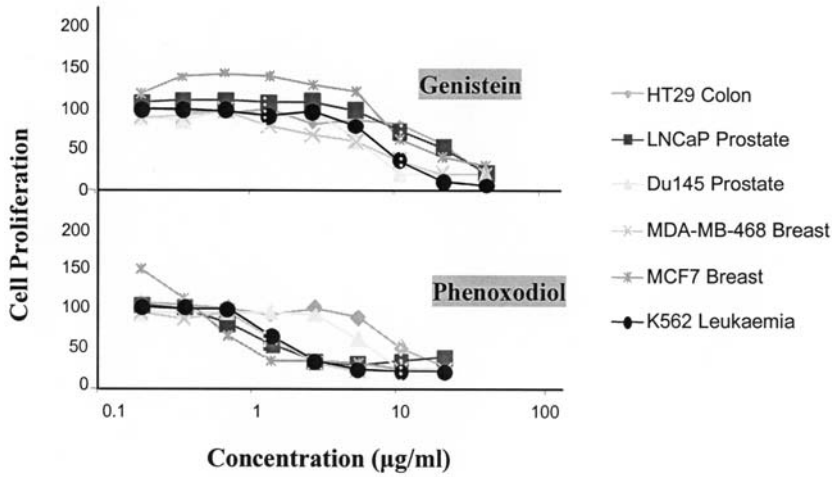


Fig. 1. Inhibitory effects of phenoxodiol compared with genistein on growth curves of a variety of cancer cell lines.

**Table 1**
**Phenoxodiol IC50 Values[a]**

| Cancer cell type | Cell line | $IC_{50}$ (µg/mL) |
|---|---|---|
| Human leukemia | K562 | 3.0 |
| | HL60 | 1.5 |
| Human breast cancer | MCF7 (ER+) | 1.5 |
| | MDA-MD-468 (ER–) | 1.0 |
| Human prostate cancer | DU-145 (AR–) | 3.0 |
| | PC-3 (AR–) | 2.0 |
| | LNCaP (AR+) | 1.5 |
| Human colon cancer | HT29 | 15.0 |
| | CaCo-2 | 1.0 |
| Human neuroglioma | Glioma | 7.0 |
| Human rhabdomyosarcoma | Kym | 0.2 |
| Human large cell lung cancer | H460 | 4.5 |

[a]Concentration at which 50% inhibition of target cell proliferation is achieved.

ER+, estrogen receptor positive; ER–, estrogen receptor negative; AR+, androgen receptor positive; AR–, androgen receptor negative.

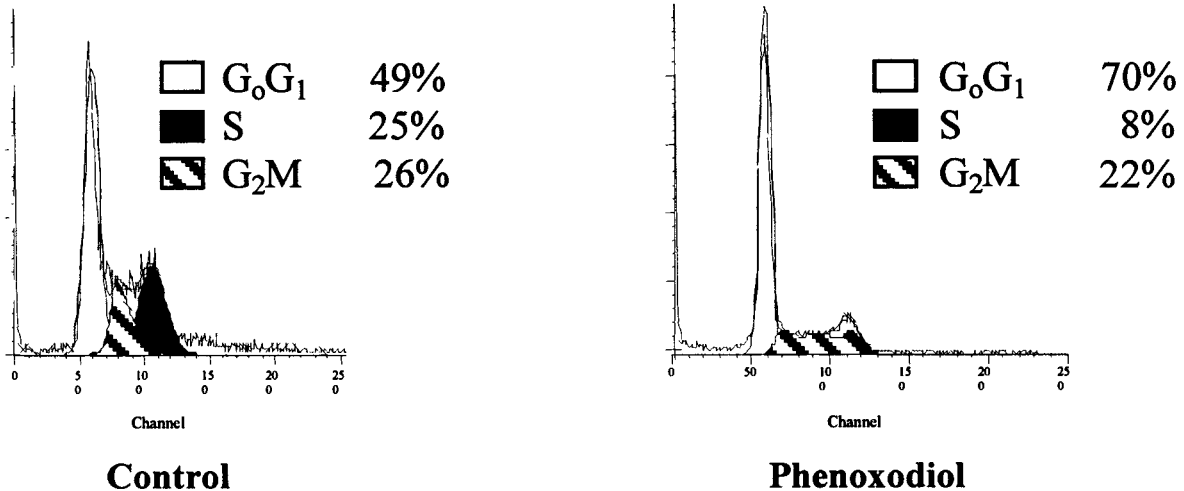


Fig. 2. Flow cytometric analysis shows that phenoxodiol arrests prostate cancer cells in the G1 phase.

**Table 2**
**Comparison of Activity of Phenoxodiol and Genistein Antagonize Estradiol Binding to Human ER**

| | ER-α | ER-β |
|---|---|---|
| Estradiol | 10 n*M* | 10 n*M* |
| Phenoxodiol | 2860 n*M* | 6090 n*M* |
| Genistein | 2450 n*M* | 100 n*M* |

[a]Concentration at which 50% inhibition of estradiol binding.

### 2.5.2. Clonogenic Assay

The effects of phenoxodiol on LNCaP and PC-3 tumor cell colonies growing in soft agar was tested at a range of concentrations and compared to the control (vehicle only) and positive control, etoposide. Phenoxodiol was highly effective at inhibiting both LNCaP and PC-3 colony formation. $IC_{50}$ concentrations were below 0.1 mg/mL for PC-3 and between 0.1 mg/mL and 1.5 mg/mL for the LNCaP cell line. Both $IC_{50}$ values are much lower than their corresponding values determined by the cell proliferation assay. While there are several differences between the two assays, the three-dimensional nature of the clonogenic assay is the most likely factor contributing to the lowering of $IC_{50}$ as a result of the extended exposure of the cells to phenoxodiol in this assay. This suggests that the antiproliferative effect of phenoxodiol, at least with rapidly dividing cells, is directly proportional to the length of time of exposure to the cancer cells.

### 2.5.3. ER Binding

Phenoxodiol exhibits weak agonism for the human ER. In an in vitro assay that measures antagonism of ligand binding to human ER, phenoxodiol was approx 280 times weaker than estradiol for ER-α and 600 times weaker than estradiol for ER-β (*see* **Table 2**).

### 2.5.4. Terminal Cell Differentiation

Phenoxodiol also has the capacity to induce differentiation of some cancer cells, potentially restoring them to a functionally normal state. After exposure of HL60 human leukemia cells to phenoxodiol, terminal differentiation was induced in a significant proportion of cells. After exposure to 100 μ*M* phenoxodiol, HL60 cells displayed (1) increased superoxide production (NBT) as a nonspecific indicator of cell differentiation and (2) increased expression of the surface marker, CD14, which is associated with monocytic differentiation. The results obtained for the functional differentiation and cell surface marker expression are illustrated in **Fig. 3**.

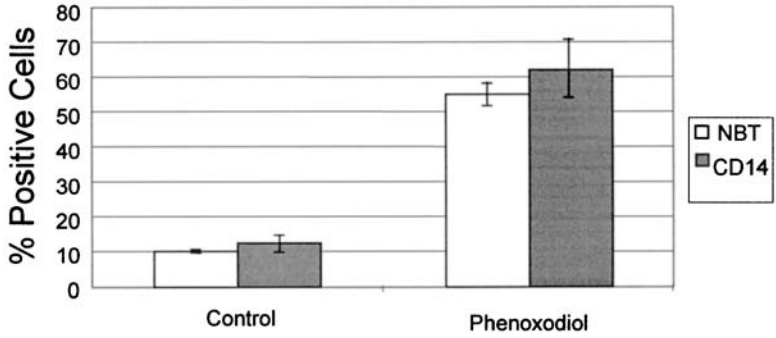


Fig. 3. Phenoxodiol (100 μ*M*) induces differentiation of HL60 leukemia cells.

**Table 3**
**Comparison of Estrogen Receptor (ER) Binding Activity of Phenoxodiol and Genistein Determined as Extent to Which the Compounds Antagonize Estradiol Binding to the Human ER[a]**

| Cancer cell type | Apoptotic effect | *p53* Functionality |
|---|---|---|
| HL60 human leukemia | 80% over 4 d | Wild-type |
| K562 human leukemia | 5% over 4 d | Mutant |
| LNCaP human prostate | 73% over 36 h | Wild-type |
| PC-3 human prostate | 4% over 36 h | Mutant |
| DU-145 human prostate | 8% over 36 h | Mutant |

[a]Concentration at which 50% inhibition of estradiol binding is achieved.

### *2.5.5. Apoptosis*

Human leukemia and human prostate cancer cells undergo apoptosis when exposed to phenoxodiol (*see* **Table 3**). Cancer cells progress from viable cells to an early apoptotic stage, where phosphatidylserine is exposed externally from the inner to the outer leaflet of the plasma membrane and then to a late apoptotic stage characterized by nuclear fragmentation. The degree of sensitivity appears to correlate with the functional state of the apoptotic regulatory gene *p53*. Cancer cells expressing the wild-type *p53* gene are sensitive to phenoxodiol, whereas those known to have a mutated nonfunctional *p53* gene remain resistant to apoptosis ***(66)***. However, these latter cancer cells still remain susceptible to the antitumor action of phenoxodiol through their susceptibility to mitotic arrest in the presence of the drug.

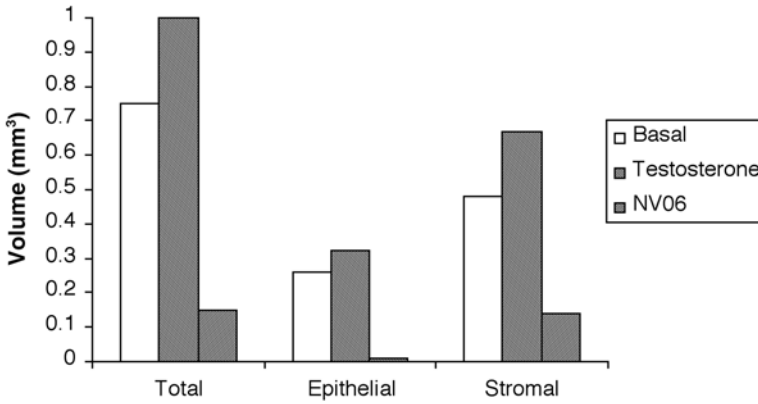


Fig. 4. Effect of phenoxodiol (50 μ*M*) and testosterone (10 n*M*) on the volume of neonatal rat prostate in organ culture.

### *2.5.6. Effects on Prostate Growth in Organ Cultures*

Phenoxodiol induces apoptosis of prostate smooth muscle cells and antagonizes the stimulatory effect of testosterone on these cells. Prostates incubated for 6 d with testosterone (10 n*M*) showed a marked increase in size and extent of terminal branching over prostate cultures incubated in the absence of testosterone. Stereological analysis permitted differences between individual compartments (epithelium, stroma, and lumen) to be determined (*see* **Fig. 4**). Whereas testosterone increased the volume of all compartments measured, the proliferative effect of testosterone was absent in cultures treated with phenoxodiol (50 μ*M*), but treatment with genistein (50 μ*M*) had no effect.

Using the terminal deoxynucleotidyl transferase (TdT)-mediated deoxyuracil triphosphate (dUTP) nick-end labeling staining technique that detects fragmented DNA, phenoxodiol induced a specific apoptotic effect in the mesenchymal cells of the prostate whereas the epithelial cells lining the ducts were unaffected. Further immunolocalization showed that phenoxodiol specifically targets the smooth muscle cells of the mesenchyme, which are key regulating cells of the growth of epithelium in both normal and carcinomatous prostate glands.

### *2.5.7. Effect on Cellular Enzymes*

$IC_{50}$ values for specific enzyme targets are presented in **Table 4**. Phenoxodiol is a potent inhibitor of topoisomerase II, the testosterone-metabolizing enzyme 5-α-reductase, and protein tyrosine kinases.

**Table 4**
**Downregulation of Enzymes by Phenoxodiol**

| Enzyme | $IC_{50}$ value (mg/mL) |
|---|---|
| Topo-isomerase I | >100 |
| Topo-isomerase II | 30 |
| Protein tyrosine kinases | 12 |
| 5α-Reductase | 2 |

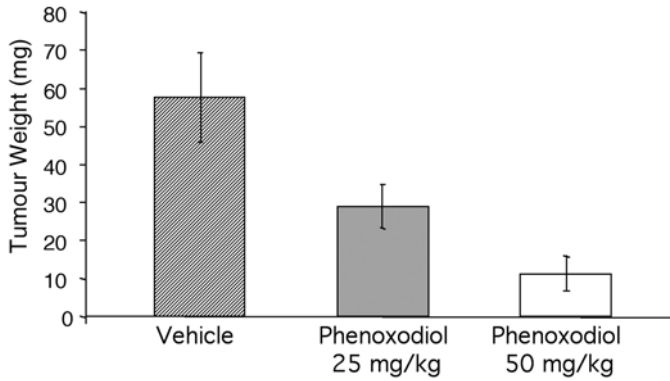


Fig. 5. Response of PC-3 tumors after treatment with phenoxodiol given by gavage.

### *2.5.8. Human Tumor Xenograft Studies*

By measurement of tumor weight, phenoxodiol has a significant anticancer effect on the growth of human prostate cancer cells (PC-3 cell line) implanted subcutaneously in male or female athymic mice and allowed to grow for 5 wk (*see* **Fig. 5**). Phenoxodiol was administered orally by gavage five times per week from the time of tumor implantation at two dosages—25 and 50 mg/kg. No studies have been conducted in this model using the intravenous route because of the impracticality of that route in mice.

### *2.5.9. Toxicology*

Phenoxodiol was administered by a single iv bolus injection to adult rats at one of seven dose levels (0, 5, 10, 20, 40, 60, and 80 mg/kg, respectively). There were two rats (one male, one female) used per dose. All animals were observed daily for 7 d posttreatment for clinical signs of toxicity. No clinical

abnormalities were observed over the 7-d observation period in any of the rats dosed with 0, 5, 10, 20, 40, or 60 mg/kg. Although animals in the 80 mg/kg group presented with subdued behavior, piloerection, slow respiration, depressed motor activity, and loss of balance for approx 2 h after dosing, they recovered after this time to remain normal for the remainder of the 7 d. Food consumption and body weights remained normal in all dosage groups over the 7-d observation period. At the end of the 7-d observation period, all rats were sacrificed and a gross necropsy performed. No gross abnormalities were observed in the liver, kidneys, adrenals, gonads, spleen, lungs, or heart of any animal in any group at necropsy.

## 3. Conclusions

The evidence for efficacy of flavonoid compounds, and in particular the synthetic flavonoid phenoxodiol, is sufficiently encouraging now to prompt the initiation of human clinical trials in cancer patients. Phase I/II trials are currently in progress for phenoxodiol, and it will be of considerable interest to determine the tolerability as well efficacy of this compound which may herald a new era of preventative and therapeutic options in the management of prostate disease.

## References

1. Adlercreutz, H., Fotsis, T., Heikkinen, R., Dwyer, J. T., Woods, M., Goldin, B. R., and Gorbach, S. L. (1982) Excretion of the lignans enterolactone and enterodiol and of equol in omnivorous and vegetarian postmenopausal women and in women with breast cancer. *Lancet* **2,** 1295–1299.
2. Ekman, P. (1989) BPH epidemiology and risk factors. *Prostate Suppl.* **2,** 23–31.
3. Dhom, G. (1991) Epidemiology of hormone-depending tumors, in *Endocrine Dependent Tumors* (Voigt, K. D. and Knabbe, C., eds.), Raven Press, New York, pp. 1–42.
4. Mills, P. K., Beeson, W. L., Phillips, R. L., and Fraser, G. E. (1989) Cohort study of diet, lifestyle, and prostate cancer in Adventist men. *Cancer* **64,** 598–604.
5. Dunn, J. E. (1975) Cancer epidemiology in populations of the United States—with emphasis on Hawaii and California—and Japan. *Cancer Res.* **35,** 3240–3245.
6. Kolonel, L. N., Hankin, J. H., and Nomura, A. M. Y. (1986) Multiethnic studies of diet, nutrition and cancer in Hawaii, in *Nutrition And Cancer* (Hayashi, Y., ed.), Japanese Science Society Press, Tokyo, pp. 29–40.
7. Setchell, K. D. R. and Adlercreutz, H. (1988) Mammalian lignans and phytooestrogens. Recent studies on their formation, metabolism and biological role in health and disease, in *Role of the Gut Flora in Toxicity and Cancer* (Rowland, I. R., ed.), Academic Press Ltd, San Diego, pp. 315–345.
8. Kelly, G. E., Nelson, C., Waring, M. A., Joannou, G. E., and Reeder, A.Y. (1993) Metabolites of dietary (soya) isoflavones in human urine. *Clin. Chim. Acta* **223,** 9–22.
9. Morton, M. S., Chan, P. S., Cheng, C., Blacklock, N., Matos-Ferreira, A., Abranches-Monteiro L., et al. (1997) Lignans and isoflavonoids in plasma and pro-

static fluid in men: Samples from Portugal, Hong Kong, and the United Kingdom. *Prostate* **32,** 122–128.
10. Miksicek, R. J. (1994) Interaction of naturally occurring nonsteroidal estrogens with expressed recombinant human estrogen receptor. *J. Steroid Biochem. Mol. Biol.* **49,** 153–160.
11. Collins, B. M., McLachlan, J. A., and Arnold, S. F. (1997) The estrogenic and antiestrogenic activities of phytochemicals with human estrogen receptor expressed in yeast. *Steroids* **62,** 365–372.
12. Miksicek, R. J. (1993) Commonly occurring plant flavonoids have estrogenic activity. *Mol. Pharmacol.* **44,** 37–43.
13. Cato, A. C., Miksicek, R., Schutz, G., Arnemann, J., and Beato, M. (1086) The hormone regulatory element of mouse mammary tumour virus mediates progesterone induction. *EMBO J.* **5,** 2237–2240.
14. Campbell, D. R. and Kurzer, M. S. (1993) Flavonoid inhibition of aromatase enzyme activity in human preadipocytes. *J. Steroid Biochem. Mol. Biol.* **46,** 381–388.
15. Morton, M. S., Griffiths, K., and Blacklock, N. (1996) The preventive role of diet in prostatic disease. *Br. J. Urol.* **77,** 481–493.
16. Evans, B. A., Griffiths, K., and Morton, M. S. (1995) Inhibition of 5 alpha-reductase in genital skin fibroblasts and prostate tissue by dietary lignans and isoflavonoids. *J. Endocrinol.* **147,** 295–302.
17. Bruchovsky, N. and Wilson, J. D. (1968) The conversion of testosterone to 5-alpha-androstan-17-beta-ol-3-one by rat prostate in vivo and in vitro. *J. Biol. Chem.* **243,** 2012–2021.
18. Anderson, K. M. and Liao, S. (1968) Selective retention of dihydrotestosterone by prostatic nuclei. *Nature* **219,** 277–279.
19. Ross, R. K., Bernstein, L., Lobo, R. A., Shimizu, H., Stanczyk, F. Z., Pike, M. C., and Henderson, B. E. (1992) 5-alpha-reductase activity and risk of prostate cancer among Japanese and US white and black males. *Lancet* **339,** 887–889.
20. Keung, W. M. (1995) Dietary estrogenic isoflavones are potent inhibitors of beta-hydroxysteroid dehydrogenase of P. testosteronii. *Biochem. Biophys. Res. Commun.* **215,** 1137–1144.
21. Wong, C. K. and Keung, W. M. (1997) Daidzein sulfoconjugates are potent inhibitors of sterol sulfatase (EC 3.1.6.2). *Biochem. Biophys. Res. Commun.* **233,** 579–583.
22. Sun, X.Y., Plouzek, C. A., Henry, J. P., Wang, T. T., and Phang, J. M. (1998) Increased UDP-glucuronosyltransferase activity and decreased prostate specific antigen production by biochanin A in prostate cancer cells. *Cancer Res.* **58,** 2379–2384.
23. Akiyama, T., Ishida, J., Nakagawa, S., Ogawara, H., Watanabe, S., Itoh, N., et al. (1987) Genistein, a specific inhibitor of tyrosine-specific protein kinases. *J. Biol. Chem.* **262,** 5592–5595.
24. Suolinna, E. M., Lang, D. R., and Racker, E. (1974) Quercetin, an artificial regulator of the high aerobic glycolysis of tumor cells. *J. Natl. Cancer Inst.* **53,** 1515–1519.

25. Shoshan, V. and MacLennan, D. H. (1981) Quercetin interaction with the ($Ca^{2++}$ $Mg^{2+}$)-ATPase of sarcoplasmic reticulum. *J. Biol. Chem.* **256,** 887–892.
26. Ono, K., Nakane, H., Fukushima, M., Chermann, J. C., and Barre-Sinoussi, F. (1990) Differential inhibitory effects of various flavonoids on the activities of reverse transcriptase and cellular DNA and RNA polymerases. *Eur. J. Biochem.* **190,** 469–476.
27. Glossmann, H., Presek, P., and Eigenbrodt, E. (1981) Quercetin inhibits tyrosine phosphorylation by the cyclic nucleotide-independent, transforming protein kinase, pp60src. *Naunyn Schmiedebergs Arch. Pharmacol.* **317,** 100–102.
28. Matter, W. F., Brown, R. F., and Vlahos, C. J. (1992) The inhibition of phosphatidylinositol 3-kinase by quercetin and analogs. *Biochem. Biophys. Res. Commun.* **186,** 624–631.
29. Prajda, N., Singhal, R. L., Yeh, Y. A., Olah, E., Look, K. Y., and Weber, G. (1995) Linkage of reduction in 1-phosphatidylinositol 4-kinase activity and inositol 1,4,5-trisphosphate concentration in human ovarian carcinoma cells treated with quercetin. *Life Sci.* **56,** 1587–1593.
30. Rizzo, M. T. and Weber, G. (1994) 1-Phosphatidylinositol 4-kinase: an enzyme linked with proliferation and malignancy. *Cancer Res.* **54,** 2611–2614.
31. Yoshida, M., Yamamoto, M., and Nikaido, T. (1992) Quercetin arrests human leukemic T-cells in late G1 phase of the cell cycle. *Cancer Res.* **52,** 6676–6681.
32. Scambia, G., Ranelletti, F. O., Panici, P. B., Piantelli, M., Bonanno, G., De Vincenzo, R., et al. (1990) Inhibitory effect of quercetin on OVCA 433 cells and presence of type II oestrogen binding sites in primary ovarian tumours and cultured cells. *Br. J. Cancer* **62,** 942–946.
33. Wei, Y. Q., Zhao, X., Kariya, Y., Fukata, H., Teshigawara, K., and Uchida, A. (1994) Induction of apoptosis by quercetin: involvement of heat shock protein. *Cancer Res.* **54,** 4952–4957.
34. Avila, M. A., Velasco, J. A., Cansado, J., and Notario, V. (1994) Quercetin mediates the down-regulation of mutant p53 in the human breast cancer cell line MDA-MB468. *Cancer Res.* **54,** 2424–2428.
35. Constantinou, A. and Huberman, E. (1995) Genistein as an inducer of tumor cell differentiation: Possible mechanisms of action. *Proc. Soc. Exp. Biol. Med.* **208,** 109–115.
36. Traganos, F., Ardelt, B., Halko, N., Bruno, S., and Darzynkiewicz, Z. (1992) Effects of genistein on the growth and cell cycle progression of normal human lymphocytes and human leukemic MOLT-4 and HL-60 cells. *Cancer Res.* **52,** 6200–6208.
37. Constantinou, A., Kiguchi, K., and Huberman, E. (1990) Induction of differentiation and DNA strand breakage in human HL-60 and K-562 leukemia cells by genistein. *Cancer Res.* **50,** 2618–2624.
38. Peterson, G. and Barnes, S. (1991) Genistein inhibition of the growth of human breast cancer cells: Independence from estrogen receptors and the multi-drug resistance gene. *Biochem. Biophys. Res. Commun.* **179,** 661–667.

39. Peterson, G. and Barnes, S. (1996) Genistein inhibits both estrogen and growth factor-stimulated proliferation of human breast cancer cells. *Cell Growth Differ.* **7,** 1345–1351.
40. Monti, E. and Sinha, B. K. (1994) Antiproliferative effect of genistein and adriamycin against estrogen-dependent and -independent human breast carcinoma cell lines. *Anticancer Res.* **14,** 1221–1226.
41. Pagliacci, M. C., Smacchia, M., Migliorati, G., Grignani, F., Riccardi, C., and Nicoletti, I. (1994) Growth-inhibitory effects of the natural phyto-oestrogen genistein in MCF-7 human breast cancer cells. *Eur. J. Cancer* **30A,** 1675–1682.
42. Matsukawa, Y., Marui, N., Sakai, T., Satomi, Y., Yoshida, M., Matsumoto, K., et al. (1993) Genistein arrests cell cycle progression at G2-M. *Cancer Res.* **53,** 1328–1331.
43. Yanagihara, K., Ito, A., Toge, T., and Numoto, M. (1993) Antiproliferative effects of isoflavones on human cancer cell lines established from the gastrointestinal tract. *Cancer Res.* **53,** 5815–5821.
44. Peterson, G. and Barnes, S. (1993) Genistein and biochanin A inhibit the growth of human prostate cancer cells but not epidermal growth factor receptor tyrosine autophosphorylation. *Prostate* **22,** 335–345.
45. Schweigerer, L., Christeleit, K., Fleischmann, G., Adlercreutz, H., Wahala, K., Hase, T., et al. (1992) Identification in human urine of a natural growth inhibitor for cells derived from solid paediatric tumours. *Eur. J. Clin. Invest.* **22,** 260–264.
46. Akiyama, T. and Ogawara, H. (1991) Use and specificity of genistein as inhibitor of protein-tyrosine kinases. *Methods Enzymol.* **201,** 362–370.
47. Constantinou, A., Mehta, R., Runyan, C., Rao, K., Vaughan, A., and Moon, R. (1995) Flavonoids as DNA topoisomerase antagonists and poisons: structure-activity relationships. *J. Natural Products* **58,** 217–225.
48. Watanabe, T., Kondo, K., and Oishi, M. (1991) Induction of in vitro differentiation of mouse erythroleukemia cells by genistein, an inhibitor of tyrosine protein kinases. *Cancer Res.* **51,** 764–768.
49. Uckun, F. M., Evans, W. E., Forsyth, C. J., Waddick, K. G., Ahlgren, L. T., Chelstrom, L. M., et al. (1995) Biotherapy of B-cell precursor leukemia by targeting genistein to CD19-associated tyrosine kinases. *Science* **267,** 886–891.
50. Fotsis, T., Pepper, M., Adlercreutz, H., Hase, T., Montesano, R., and Schweigerer, L. (1995) Genistein, a dietary ingested isoflavonoid, inhibits cell proliferation and in vitro angiogenesis. *J. Nutr.* **125 (3 Suppl),** 790S–797S.
51. Bergan, R., Kyle, E., Nguyen, P., Trepel, J., Ingui, C., and Neckers, L. (1996) Genistein-stimulated adherence of prostate cancer cells is associated with the binding of focal adhesion kinase to beta-1-integrin. *Clin. Exp. Metastasis* **14,** 389–398.
52. Carlson, B. A., Dubay, M. M., Sausville, E. A., Brizuela, L., and Worland, P. J. (1996) Flavopiridol induces G1 arrest with inhibition of cyclin-dependent kinase (CDK) 2 and CDK4 in human breast carcinoma cells. *Cancer Res.* **56,** 2973–2978.
53. Shapiro, G. I., Koestner, D. A., Matranga, C. B., and Rollins, B. J. (1999) Flavopiridol induces cell cycle arrest and p53-independent apoptosis in non-small cell lung cancer cell lines. *Clin. Cancer Res.* **5,** 2925–2938.

54. Drees, M., Dengler, W. A., Roth, T., Labonte, H., Mayo, J., Malspeis, L., et al. (1997) Flavopiridol (L86-8275): selective antitumor activity in vitro and activity in vivo for prostate carcinoma cells. *Clin. Cancer Res.* **3,** 273–279.
55. Axelson, M., Kirk, D. N., Farrant, R. D., Cooley, G., Lawson, A. M., and Setchell, K. D. (1982) The identification of the weak oestrogen equol [7-hydroxy-3-(4′-hydroxyphenyl)chroman] in human urine. *Biochem. J.* **201,** 353–357.
56. Bannwart, C., Adlercreutz, H., Wahala, K., Kotiaho, T., Hesso, A., Brunow, G., and Hase, T. (1988) Identification of the phyto-oestrogen 3′,7-dihydroxyisoflavan, an isomer of equol, in human urine and cow's milk. *Biomed. Environ. Mass Spectrom.* **17,** 1–6.
57. Joannou, G. E., Kelly, G. E., Reeder, A. Y., Waring, M., and Nelson, C. (1995) A urinary profile study of dietary phytoestrogens. The identification and mode of metabolism of new isoflavonoids. *J. Steroid Biochem. Mol. Biol.* **54,** 167–184.
58. Bannwart, C., Fotsis, T., Heikkinen, R., and Adlercreutz, H. (1984) Identification of the isoflavonic phytoestrogen daidzein in human urine. *Clin. Chim. Acta* **136,** 165–172.
59. Kok, J. W., Veldman, R. J., Klappe, K., Koning, H., Filipeanu, C. M., and Muller, M. (2000) Differential expression of sphingolipids in MRP1 overexpressing HT29 cells. *Int. J. Cancer* **87,** 172–178.
60. Makela, S., Davis, V. L., Tally, W. C., Korkman, J., Salo, L., Vihko, R., et al. (1994) Dietary estrogens act through estrogen receptor-mediated processes and show no antiestrogenicity in cultured breast cancer cells. *Environ. Health Perspect.* **102,** 572–578.
61. Wang, C. and Kurzer, M. S. (1997) Phytoestrogen concentration determines effects on DNA synthesis in human breast cancer cells. *Nutr. Cancer* **28,** 236–247.
62. Setchell, K. D., Borriello, S. P., Hulme, P., Kirk, D. N., and Axelson, M. (1984) Nonsteroidal estrogens of dietary origin: possible roles in hormone-dependent disease. *Am. J. Clin. Nutr.* **40,** 569–578.
63. Ingram, D., Sander, K., Kolybaba, M., and Lopez, D. (1998) Case-control study of phyto-oestrogens and breast cancer. *Lancet* **350,** 990–994.
64. Adlercreutz, H., Goldin, B. R., Gorbach, S. L., Hockerstedt, K. A., Watanabe, S., Hamalainen, E. K., et al. (1995) Soybean phytoestrogen intake and cancer risk. *J. Nutr.* **125 (3 Suppl),** 757S–-770S.
65. Martin, P. M., Horwitz, K. B., Ryan, D. S., and McGuire, W. L. (1978) Phytoestrogen interaction with estrogen receptors in human breast cancer cells. *Endocrinology* **103,** 1860–1867.
66. Zhou, H., Goldman, M., Wu, J., Woestenborghs, R., Hassell, A.E., Lee, P., et al. (1998) A pharmacokinetic study of intravenous itraconazole followed by oral administration of itraconazole capsules in patients with advanced human immunodeficiency virus infection. *J. Clin. Pharmacol.* **38,** 593–602.